ENGINEERING DIVISION LIBRARY

Property of
Flood Control District of MC Library
Please Return to
2801 W. Durango
Phoenix, AZ 85009

PREPRINTS OF THE INTERNATIONAL RIPRAP WORKSHOP

THEORY, POLICY AND PRACTICE OF EROSION CONTROL USING RIPRAP, ARMOUR STONE AND RUBBLE

FORT COLLINS
COLORADO
UNITED STATES
12 - 16 JULY 1993

VOLUME II

PRODUCED BY:
DELFT GEOTECHNICS
P.O. BOX 69
2600 AB DELFT
THE NETHERLANDS

Sponsored by

Colorado State University
Department of Civil Engineering
United States

Construction Industry Research and Information Association
United Kingdom

Delft Geotechnics
The Netherlands

Rijkswaterstaat
The Netherlands

University of Nottingham
Department of Geography
United Kingdom

Organizing committee

Colin R. Thorne
University of Nottingham
United Kingdom

Steven R. Abt
Colorado State University
United States

Frans B.J. Barends
Delft Geotechnics
The Netherlands

Krystian Pilarczyk
Rijkswaterstaat
The Netherlands

Stephen T. Maynord
US Army Corps of Engineers
United States

Garry Stephenson
Construction Industry
United Kingdom

ENGINEERING DIVISION LIBRARY

Property of
Flood Control District of MC Library
Please Return to
2801 W. Durango
Phoenix, AZ 85009

PREPRINTS OF THE INTERNATIONAL RIPRAP WORKSHOP

THEORY, POLICY AND PRACTICE OF EROSION CONTROL USING RIPRAP, ARMOUR STONE AND RUBBLE

FORT COLLINS
COLORADO
UNITED STATES
12 - 16 JULY 1993

VOLUME II

PRODUCED BY:
DELFT GEOTECHNICS
P.O. BOX 69
2600 AB DELFT
THE NETHERLANDS

Sponsored by

Colorado State University
Department of Civil Engineering
United States

Construction Industry Research and Information Association
United Kingdom

Delft Geotechnics
The Netherlands

Rijkswaterstaat
The Netherlands

University of Nottingham
Department of Geography
United Kingdom

Organizing committee

Colin R. Thorne
University of Nottingham
United Kingdom

Steven R. Abt
Colorado State University
United States

Frans B.J. Barends
Delft Geotechnics
The Netherlands

Krystian Pilarczyk
Rijkswaterstaat
The Netherlands

Stephen T. Maynord
US Army Corps of Engineers
United States

Garry Stephenson
Construction Industry
United Kingdom

CONTENT Page

W. Leeuwensteijn, A. Franke, V. Hombergen, J.K. Vrijling
Quarry based design of rock structures 552

G. Lefebvre, M. Ben Belfadhel, K. Rohan, O. Dascal
Field and laboratory investigation of steep riprap 570

D.A. Lienhart, H.H. Fisher, E.F. Robinson
The correlation of index tests with rock durability 588

D.B. Lister, B.J. Beniston, R. Kellerhals, M. Miles
Influence of bank material size on juvenile salmonid use of rearing habitat 601

J.S. Mani, H. Oumeraci, M. Muttray
Rundown velocity along the slope of a breakwater with an accropode cover layer 626

S.K. Martin
Riprap design for tow-induced waves 658

R.W.P. May, M. Escarameia
Riprap stability in highly turbulent flows 679

S.T. Maynord
Corps riprap design guidance for channel protection 692

J.W. van der Meer
A review of stability formulas for rock and riprap slopes under wave attack 712

J.W. van der Meer, K.W. Pilarczyk
Low-crested rubble mound structures 735

A.C. Parola
Boundary stress and stability of riprap at bridge piers 771

K.W. Pilarczyk
Design tools related to revetments including riprap 792

CONTENT Page

K.W. Pilarczyk
Simplified unification of stability formulae for rock and other revetments under current and wave attack 818

K.A. Sarker
Experience of using riprap works in Bangladesh 839

H. Schulz
Considerations regarding the experience and design of German inland waterways 862

F.D. Shields Jr, C.M. Cooper, S. Testa III
Towards greener riprap: Environmental considerations from micro- to macroscale 899

D.B. Simons
Fundamental concepts applied to the utilization of rock riprap to achieve channel stabilization 926

B. te Slaa
River training works for a bridge across the Brahmaputra river, Bangladesh 945

R.B. Sotir, N.R. Nunnally
Use of riprap in soil bioengineering streambank protection 969

C.R. Thorne, S.R. Abte, S.T. Maynord
Prediction of near bank velocity and scour depth in meander bends for design of riprap revetments 980

V.H. Torrey III
Flow slides in Mississippi riverbanks 1008

D.D. Ward
Numerical calculation of runup and overtopping on riprap revetments 1032

R.J. Wittler, S.R. Abt
Shields parameter in low submergence or steep flows 1051

K. Zen, H. Yamazaki
Slope instability due to wave-induced liquefaction in the seabed 1065

CONTENT

Page

M. Shafai-Bajestan, M.L. Alberston
Design of a riprap stilling basin for overhanging pipe 1100

K.R. Stank, M.M. Baig
Deterioration of carbonate breakwater stones on lake Michigan shoreline 1106

QUARRY BASED DESIGN OF ROCK STRUCTURES

W. Leeuwestein
CUR, P.O. Box 420, 2800 AK Gouda, The Netherlands
A. Franke, V. Hombergen and J.K. Vrijling
Rijkswaterstaat, Civil Engineering Division,
P.O. Box 20000, 3502 LA Utrecht, The Netherlands

1. Introduction

Rock is a widely used material for hydraulic structures in marine, estuarine and riverine environments. The reason for that is mainly that many types of rock can meet requirements with respect to density, size and strength and besides that this material is available in many places in the world.
A European initiative was taken by two research organisations, CUR[1] in the Netherlands and CIRIA[2] in England, to support an optimal use of rock in marine structures, by producing a Manual on the use of rock (CUR/CIRIA, 1991). Construction and material use are the two principal variables for design optimisation, of which material use is subject of this paper. Characteristic control parameters are stone size (D) and grading (D_{85}/D_{15}) of the rock.
In this paper it is demonstrated that there is a fair chance that by using conventional procedures of optimizing the design of a rock structure, the possibility of significant savings on material cost are overlooked.
First a conventional lifetime-cost optimisation is presented with respect to the size of the armour stone (demand-based design). This is done for two examples, a breakwater and a river bank protection. Subsequently, an optimisation is presented with respect to a given quarry production (supply-based design). For the breakwater this is done using a optimisation model developed in the Netherlands and described in this paper.

2. Materials, sources and production

Principal sources of stones are quarries and marine or river deposites of gravel. Quarries are located on land, often in mountaneous regions, and rock material is produced by blasting vertical slices from a rock or mountain. The result is often a more or less irregularly shaped material of different sizes (D) and weight (W). Unless defined otherwise, in this paper D is the nominal diameter, related to W by $D=(W/\rho_r)^{1/3}$ with ρ_r being the rock density. In practice, for D_n the 50% nominal value D_{n50} is used. The variety in size of the stones produced is characterized by a stone size distribution curve $F(X)=Pr(D<X)$, which is known as the production curve or so called Quarry Yield curve. In Figure 1 two examples are shown of which only type I produces the typical heavy armour stones. Alternatively, corresponding density curves can be used (eg. see Figs. 5 and 7).

By means of a blast design one may attempt to control the production. Depending on the demand by the structure, large size stones or large quantities of the smaller sizes may be wanted. The percentages of the various size categories needed are gouverned by stability requirements and filter rules discussed below. Blast design is mainly a matter of specific experience, but some guidance has been developed using placement and spacing of boreholes. Methods to assess the production by means of distribution functions, F(X), are presented by Rosin-Rammler and Schumann (CUR/CIRIA, 1991). The link with blasting practice is provided by parameters, which are taken from the blast design in the quarry.

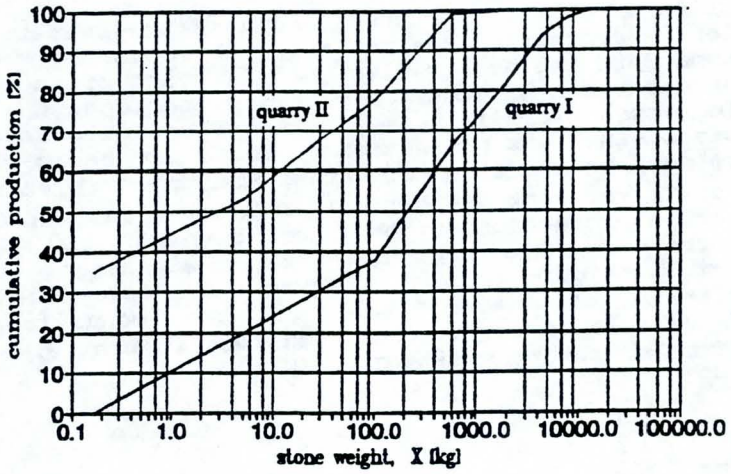

Figure 1 Example Quarry Yield curves

For practical reasons, quarry owners and contractors preferably use a set of standard gradings, defined by (at least) an upper and lower limiting weight (or size). In the following sections a set of gradings are used, which follow the standards presented by CUR/CIRIA.

3. Structure characteristics

The structures considered contain or consist entirely of rock material. At the wave and/or current exposed (usually sloping) face, this material extends from the crest down to the toe and sometimes even further.
At the crest, the rock material can be extended to a lee-side slope or (horizontally) over a backfill area.
In this paper a conventional rubble mound breakwater and a river bank protection are considered, with crest height and slope gradient being the main characteristic geometrical design parameters.
In general, armour layers (primary and secondary), filter layers and a core are distinguished, all mainly charaterized by a stone size (D). These stone sizes are determined by hydraulic stability. Regarding to wave attack, a structural porosity factor (P) is defined (see Appendix). A commonly used armour layer thickness (t_a) relates to D according to

$$t_a = 2\ D_{n50} \qquad (3)$$

The same relation is also used for other layers. The size of the material for filter and core are derived from requirements related to internal stability and filter functions (filter rules). The latter is commonly formulated in terms of a size ratio of the upper (armour) and the lower (filter) material (D_a/D_f), for example in the overall filter rule by Terzaghi (1922):

$$D_{50a}/D_{50f} = 5 \qquad (4)$$

The above, simplified, requirement is used in this paper. This is valid for uniformly sized material, whereas for wide graded rock values up to 20÷60 apply (CUR/CIRIA, 1991).

4. Functions and requirements

The function of rock in structures such as breakwaters and river bank protection is protection against external action by waves and/or currents. When extended to the sea or river bed in front of the toe, the function can be better described as scour or bottom protection. When extended on an inner slope or a backfill area, the function is to resist overtopping. In all cases, the rock protection supports the basic function of the structure such as reduction of wave disturbance (breakwater) and slope protection (river bank protection), whereby a certain accepted degree of damage to the protection may be inherent to an economic design aiming to minimize the cost of investment and expected damage.
As an example, Figure 2 shows a conventional optimisation with respect to armour size (D_a) under wave action, with wave conditions from section 5. Damage is calculated as the displaced rock volume (S_d) according to Van der Meer's formula, see appendix (CUR/CIRIA, 1991).

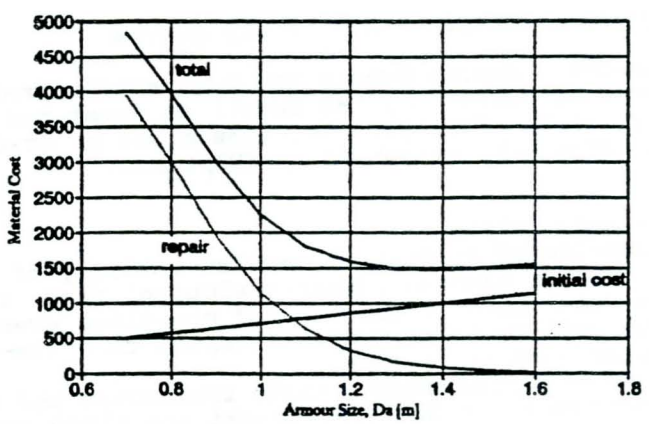

Figure 2 Conventional optimisation of breakwater armour investment vs. damage

lay-out

A variety of functions determines the alignment and length (breakwater) and and extent (toe, bottom protection) or situation (river bank protection) of rock structures. Also local bathymetry may play a role.
The bank protection discussed in this paper is designed for a braiding river. This implies that river channels and flood plains show a rather

irregular pattern, which changes from year to year under influence of flood waves. As a consequence, scour and the moving channels largely determine the lay-out of the bank protection.

cross section
Functional requirements play an important role in the design of the cross section of structures. Most important for breakwaters are wave transmission, wave run-up and overtopping. The crest height is largly determined by these parameters. Besides stability requirements (geotechic and hydraulic) often determine slope gradients and the extent of a toe protection. In this paper, the height of the transmitted wave (H_t) and the combined flood level (z_f) and run-up are the determining requirements for a breakwater and a bank protection respectively.

In this paper the crest level of the breakwater is determined by the requirement that the maximum wave height in the area protected by the breakwater be limited to H_{max} = 1 m. Construction further requires that the crest width be B = 5 m. The height of the river bank considered is determined by the requirement that crest is not overtopped during the design flood conditions. The slope is 1:3.5.
For both structures the depth of expected scour at the toe determines the construction (toe) depth.

hydraulic stability
Much emphasis has been put in the past on reduction of stone size for a cover or armour layer, given a design wave or current. Proven stability requirements are given by Shields (1936), based on shear stress and applicable for currents, waves or combinations of these and by Isbash (1959), based on velocity and applicable for currents only. On both requirements, roughly summarized here as the stability criteria ψ_{cr} = 0.03 (Shields) and $U_c/2g\Delta D$ = 1.4 (Isbash) reference can be found in Pilarczyk's paper. Here it is only useful to mention that experience has shown that in fact the above given threshold values are only common values. The observed variations can be indicated as 0.03 + 0.05 and 0.7 + 1.4 respectively, which can be partly explained as to be caused by differences in: a) exposure or b) probability of initial displacements (damage) or c) definitions.

current attack
The threshold velocity (U) can be written in terms of Shields' bottom shear stress (ψ) by:

$$\frac{U^2/2g}{\Delta D_{50}} = k_{sl}\frac{C^2}{2g}\psi_{cr} \qquad (3)$$

where C is Chezy's friction coefficient, note that C=f(D,..) and k_{sl} is the slope factor (see Appendix). An unambigious definition of damage for current attack is still not available. However, in this context damage may be roughly estimated by using ψ_{cr} as a damage parameter (a role comparable to Van der Meer's S_d, see appendix). By fitting of data by Gessler (1965) and interpreting his probability of displacement as a damage fraction (S_u), a practical relationship between ψ_{cr} and S_u has been found to be:

$$S_u = 3.5\ (\psi_{cr} - 0.0198)^{0.5} \qquad (4)$$

(In the range of ψ_{cr} between 0.02 and 0.10 the deviations from Gesslers' data in terms of damage are about 0.05).

wave attack
For stability of sloping rock under wave action Van der Meers' formulae have been gradually introduced since 1984 (CUR/CIRIA, 1991) as an alternative for the well known Hudson formula (1965). The main improvements are that account is given to wave period (T), storm duration (N) and structure porosity (P) and that a clear definition of damage (S_d) is provided.

5. Design conditions
breakwater
In this paper the design conditions for the breakwater are wave height (H) and period (T) and for the bank protection flood level (h), wave height (H) and current velocity (U). The design values are derived from fitting of prototype data into a suitable long-term wave height distribution function (Figures 3).

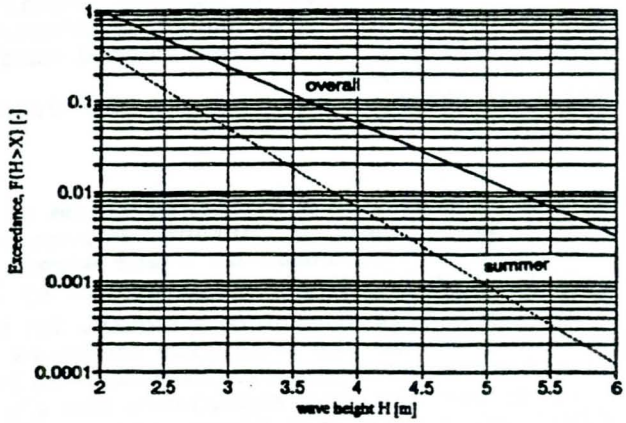

Figure 3 Example distributions of significant wave height

The breakwater is designed for the 1:50 wave conditions, which implies a significant wave height of H_s = 4.8 m and the corresponding mean wave period is assumed to be T_m = 9 s. The design wave height at the lee side is H_s = 1 m. The number of waves in the design storm is N = 5000 and the accepted damage (S_d) is based on a preliminary optimisation performed in section 4. Tides can be disregarded.

bank protection
For the bank protection, the 1:100 years design river discharge is Q = 20,300 m^3/s. Corresponding flood level and current velocity are z_f = 7.8 m and U = 2 m/s. The average water level is z_{av} = 1.6 m and the lowest water level is only slightly beneath this value. The stage curve with corresponding current velocities and the discharge distribution are shown in Figure 4.

Under 1:100 years wind conditions the wave height and period are H_s = 1.0 m and T_m = 3.5 s respectively. Due to (local) scour the bed level under design flood conditions is at z_b = -34 m.
The expected damage due to the current velocity (U), on the lower part of the slope, is evaluated using the Shields parameter (ψ_{cr}) as a damage parameter.

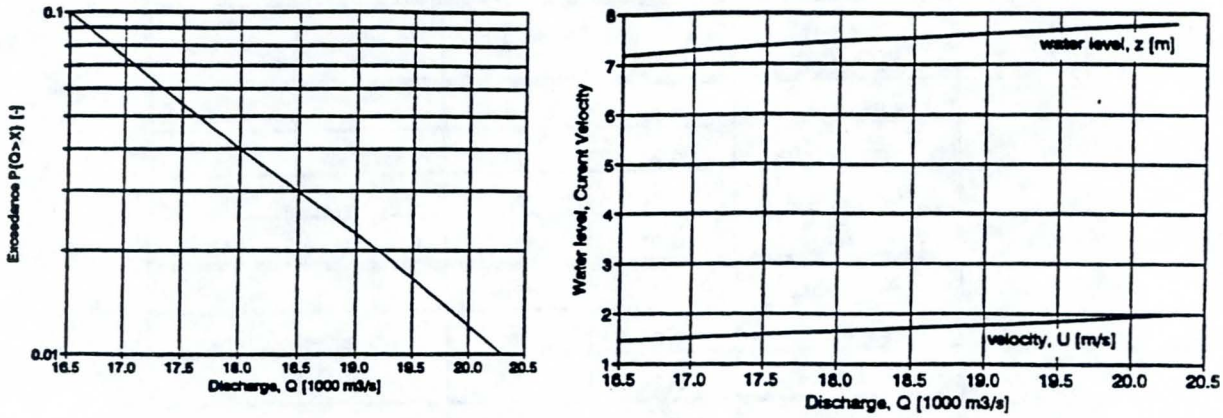

Figure 4 Example discharge distribution (left) and stage and velocity curves (right)

6. Demand-based design

The more conventional cross-sectional design can be characterized as a "demand design", which is basically described below. Lay-out and alignment are not further considered in this paper.

preliminary optimisation of breakwater armour size

Using a simplified approach for the wave transmission (CUR/CIRIA, 1991), it can be found that for a crest height of h_c = 15 m the relative freeboard is R_c/H_s = 1.04 with an associated transmission coefficient of C_t = 0.15 (see Appendix). The resulting transmitted wave height is H_t = 0.7 m, which remains well within the given requirement (H_{max}).
For the slope a preliminary gradient of 1:2 is chosen for both the front and lee side. However, in section 7 these slope angles are adjusted to optimise the design. Van der Meer's porosity factor is P = 0.4 (see appendix).

Expected damage (S_d) is used as a design criterion for which values exceeding S_d = 10 are not acceptable since these imply exposure and consequently (progressive) damage to the secondary and other layers.
Material cost rates for construction and repair are assumed as given in the appendix. The structure's lifetime (T_L) is T_L = 25 years.
Based upon these considerations and calculations for a series of (cover layer) stone diameters (D) a preliminary optimum armour size appears to be D_s = 1.5 m approximately (Figure 1). The corresponding damage during design conditions is S_d = 6 approximately. Applying a similar procedure to the lee side slope (with H_s = 1.0 m) an armour size of D_{sL} = 0.3 m is found.

evaluation of required stone volumes for breakwater

In order to facilitate the evaluation of stone volumes and a further iterative design of the breakwater cross section a design model has been used which is briefly described in section 9. This model enables evaluation of stone volumes associated with parameterized standard geometries, including toe structure.
The initial design was based upon the conditions described in section 5 with S_d=6 as the damage criterion. The results are summarized in Table 1, listing stone volumes (per running meter) needed for the primary and secondary armour layers and for the core. Evaluation of costs is done by using the material cost rates given in the Appendix.

part of breakwater	stone size D [m]	volume V [m^3]	grading [kg]	cost
prim. armour	1.52	90	6/10 t	1440
idem, leeside	0.34	3	10/200	12
sec. armour	0.30	95	10/200	380
core	0.06	120	50/150 mm	240
sub-totals		≈ 310		≈ 2070
prim. arm. toe	0.86	30	1/3 t	480
sec. arm. toe	0.29	7	10/200	28
filter toe	< 0.07	45	50/150 mm	90
totals		≈ 390		≈ 2670

Table 1 Required minimum stone volumes (per running m) for the breakwater obtained with the model

Armour stability together with filter requirements determine to a large extent the demand curve for the rock material to be used in the structure. Using the production from the quarry characterized by I in Figure 1, the actual approximate blasted rock volumes can be determined. The produced (Pr) and demanded (De) relative volumes (in %) are listed in Table 2.

								totals
	<10	10/200	0.2/1t	1/3t	3/6t	6/10t	>10t	
Pr	20	18	28	16	12	4	2	
De	45	26	0	7	0	22	0	
Pr/De	0.45	0.69	∞	2.27	∞	0.18	∞	
E	0	3.30	4.07	5.53	5.09	0	5.53	
R	5.00	4.50	7.00	4.00	3.00	1	0.50	
V	450	400	620	350	270	90	50	2230
C_m	900	1600	10000	5700	4300	1400	700	24600

Table 2 Quarry production and cost per running m for design-based breakwater, including toe as evaluated with the model

The results for the *matching ratio* (Pr/De) show that the heavy stones (6/10 t) have the lowest value of Pr/De and thus are the determining size. Defining the production multiplication factor as:

$$f_p = 1 \,/\, \min(Pr/De) \qquad (5)$$

this involves a production of f_p=22/4=5.5 times all grading volumes, to correspond to the determining volume, P_d = 90 m^3 of heavy stones (6/10 t). The relative excess production, defined for each grading as

$$E=(f_p\ Pr - De)/Pr, \qquad (6)$$

the *production ratio* (R) of each relative grading volume (Pr) with the *determining volume* (P_d), actual produced volumes (V, in m^3) and the the consequent material production cost (C_m) are shown in Table 2 from which it can be seen that the total cost amounts to 9.2 times the theoretical minimum cost of 2670 from Table 1. A practical measure for an economic design from, regarding material use, is the *cost (efficiency) ratio* (R_C) between the actual cost associated with a design and theoretical cost of the minimum design (here, R_C=9.2). Similarly, a *volume (efficiency) ratio* is defined as R_V (here R_V=5.7).

In this example case most of the excess production cost is made for the three successive gradings from 200 kg to 6 t. The (mis)match of demand and supply volumes for the considered gradings is shown in Figure 5 (left).

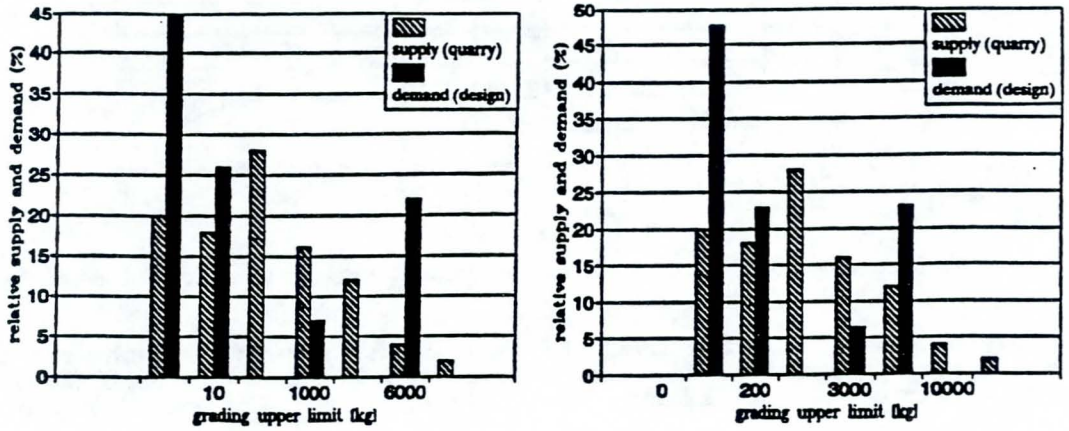

Figure 5 Matching of relative demand and production preliminary (left) and optimal (right) design

river bank protection
The crest level is primarily determined by the design flood level (z_f = 7.8 m, see section 5). Since serious wave action does not coincide with the flood season overtopping is no additional consideration with regard to the crest level. Provisionally it is assumed that the slope is 1:3.5 and that under design conditions the bottom level at the toe, including scour, is at z_b = -34 m. (disregarding other alternatives [3]).
For the upper part of the slope protection, waves are the determining loading while for the lower part the current velocities are. The design formulae used are Van der Meer's (Appendix) and eq.(3) respectively. In order to account for wave run-down, the transition is chosen at 1.5 m (=1.5 H_s) below the average water level (so at z_t = 0.1 m).

[3] An option is to provide the stone for the lowest part as a falling apron. Then usually a surplus of material is placed (CUR, 1993).

As a result, the upper part is designed against the wave (with H_s = 1 m) described in section 5, whereas for the lower part (from z_t = 0.1 m down to z_b = -34 m) the given velocity of U = 2 m/s is used with an average water depth for the slope, say h = 15 m.

With the material cost rates used in this paper (see Appendix) the cost of damage are small relative to the construction cost, at least for stone sizes D > 0.04 m. Using the above given design conditions and the damage curve according to eq.(4), any damage can be avoided by chosing D = 0.05 m (see Figure 6).

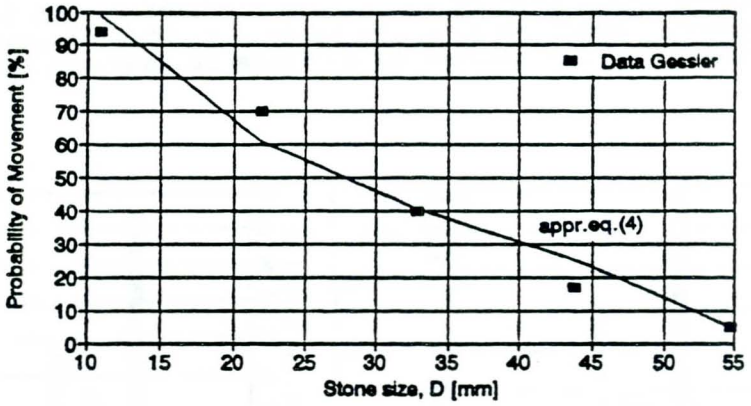

Figure 6 relative damage of bank protection due to the design flood

Applying eq.(1) for the layer thicknesses the material volumes and the associated cost can be calculated as listed in Table 3. Total required stone volume and cost of this minimum design are 34 m^3 and 88 respectively.

Grading	Diameter D [m]		Volume V[m^3]			Cost		
	upper	lower	upper	lower	Σ V	upper	lower	Σ C_m
30/60 mm		0.01		7	7		14	14
0.3/10 kg	0.04	0.05	8	9	17	16	18	34
10/200 kg	0.22		10		10	40		40
totals:			18	16	34	56	32	88

Table 3 Required stone volumes (per running m) for the minimum design bank protection

Produced volumes and associated costs are listed in Table 4. Comparing with the minimum design from Table 3, it becomes clear that this design for the bank protection does not match the given quarry yield curve at all. Volume and cost efficiency ratios are R_V = 4.7 and R_C = 20.2.

	stone class [kg]								totals
	<0.3	0.3/10	10/200	0.2/1t	1/3t	3/6t	6/10t	>10t	
Pr	10	10	18	28	16	12	4	2	
De	20	50	30	0	0	0	0	0	
Pr/De	0.50	0.20	0.60	∞	∞	∞	∞	∞	
E	3.00	0	3.33	5.00	5.00	5.00	5.00	5.00	
R	1.00	1.00	1.80	2.80	1.60	1.20	0.40	0.20	
V	16	16	29	45	26	20	6	3	161
C_m	30	30	120	720	420	310	100	50	1780

Table 4 Quarry production and cost (per running m) for design-based bank protection

The figures in this example show that the determining grading is 0.3/10 kg and that considerable excess volumes are blasted of all gradings above 200 kg.

7. Supply-based design

A basically different approach is to start with the quarry and to taylor the design to the size distribution of the supply. A striking example of this is the development of the concept of (dynamically stable) berm breakwaters, allowing a considerable reduction of armour size (see Figure 7). In this Figure demand and supply (of two alternative quarries) are shown as production densities, f(X). It is obvious that the production curves match the grading (1) better for the berm breakwater. However in this paper it is shown that also for conventional breakwaters this approach will often pay off.

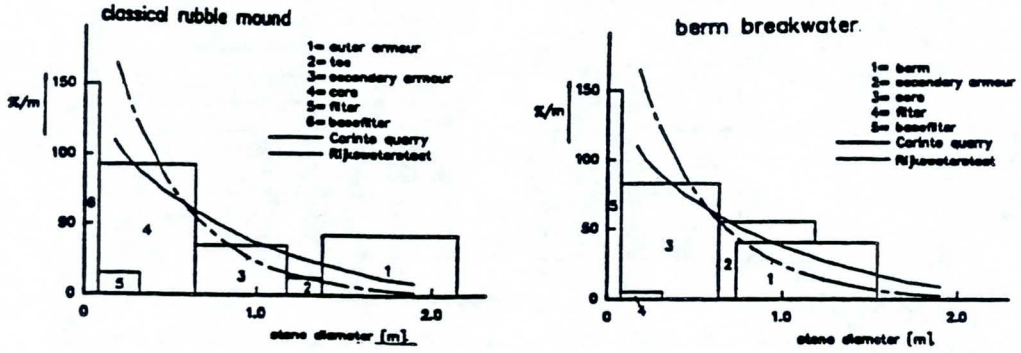

Figure 7 Rock demand and supply for a conventional vs. berm breakwater (Vrijling et.al. 1990)

breakwater

In order to facilitate a supply-based approach within an iterative design procedure for the breakwater cross section, a model has been developed in the Netherlands as a spinn off from the CUR/CIRIA Manual. This model includes the design of the toe and has been used to make the following evaluations of material costs. The model is briefly discussed in section 9.

Using the systematic design procedure of the model the breakwater design is further optimised to match the given quarry yield curve as good as possible. For this paper, optimisation of geometry have been sought in:

- front slope (cotg α_F)
- crest height (h_c)

By considering the calculated armour size (D_a) and transmission coefficient (C_t) is has been checked wheter the basic functional requirements stated in section 3 are still be met. Starting with the preliminary design from section 6 the cross section has been varied as shown in table 5.

cross-sectional parameter	minimum	reference	maximum
front slope, cotg α_F [-]	1:3	1:2	1:1.5
crest height, h_c [m]	14.0	15.0	15.0

Table 5 variation of cross-sectional parameters

Evaluation of the quarry yield curve and the required volumes (V) calculated with the model shows that still considerable savings can be achieved. The cost associated with a number of alternatives are indicated in Figure 8.

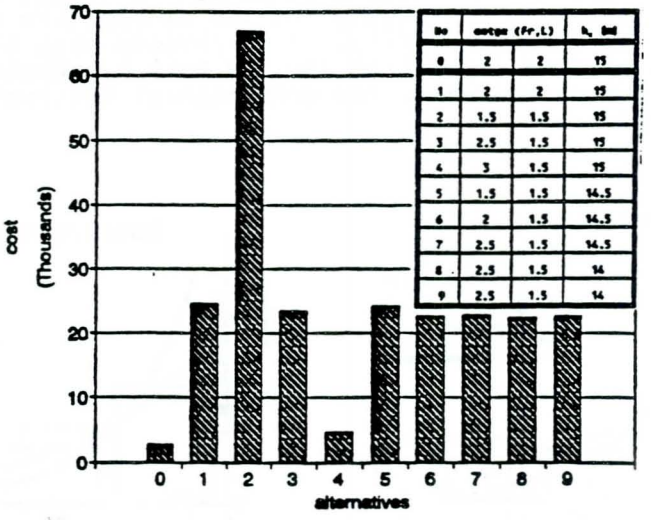

Figure 8 Cost comparison of alternative designs

It is obvious that application of a relatively mild front slope of cotg(α_F) = 3, while maintaining the preliminary lee-side slope with cotg(α_L) = 1.5, enables an optimum use of the quarry. The total volume of blasted rock is only 440 m^3 with associated cost of 4700. Relative to the minimum design (Table 1) the volume and cost ratios for this design are only R_V=1.1 and R_C=1.8. All of the other alternatives except one show cost ratios between R_V = 8.4 and 9.0. One exception is the one with a steep front slope of cotg(α_F) = 1.5. This design requires an armour size of D_a = 1.76 m, which is not produced in sufficient relative quantities (demand=23%, production=2%). To produce the armour stone, blasted volumes in excess of the needed result in a cost ratio of R_C = 25. For comparison, the production data of the optimum design are listed in Table 6 and placed next (right) to those of the preliminary design (left) in Figure 5.

For structures like the river bank protection the possibilities to vary the cross section are limited and practically confined to the slope gradient (stability) and crest width (overtopping). However, it has been demonstrated that for a type II quarry a supply-based design can be useful as well for structures as river bank protection for a final optimisation of the slope.

9. Model description

A brief description is given here on the model used to optimise wave exposed breakwater cross sections. The experience that an economic design of breakwaters and other rock structures is partly based upon efficient use of quarry output, was the reason to initiate the development of a computerized system for optimisation of the design of hydraulic structures like breakwaters, seawalls, dikes and bottom protection. In this context and as a spin off from the production of both CUR/CIRIA Manual on rock, the Dutch Department of Public Works and Transport (Rijkswaterstaat) has developed a model for a supply-based optimisation model for breakwaters. The model structure diagram is shown in Figure 9, which is largely self explaning.

describing the stone supply

Being a major materials design condition, a basic input for the model is the quarry production, schematized by a yield curve. Depending on whether an existing producing quarry is concerned (with a known yield curve) or rather that a dedicated quarry may be opened (with little information on the expected production) two options are presented to the user:

- provide the available quarry supply volumes;
- give the parameters for the theoretical prediction curves (eg. Rosin-Rammler, Schumann, section 2).

In both cases a series of production volumes can be provided, each concerning a grading or class, defined by lower and upper limiting weights. These gradings can be either standard gradings (usually cheaper) or specially defined gradings (usually more costly). In the latter case the model will generate the supply volumes for each defined grading. By providing a the length of the structure, the model evaluates the total volumes involved with the entire structure (instead of per running meter).

At the end of each iterative cycle, plots can be produced showing the breakwater cross section with principal results regarding required stone weights and a comparison (per grading or class) of quarry supply and demand of the design made so far (Figures 10 and 11).

determining the rock demand

Rock stability against waves is determined and used as a design criteria. This can be done for two optional design principles (Figure 12):

- both sides subject to the same design conditions (so basically a symmetric design);
- different wave exposure at both sides (leading to asymmetric design).

Additional options for the user concerning the basic initial cross-section are the crest width and the toe structure. With respect to the latter the user has two options, a standard toe or a "dredged" toe (Figure 12).

Principal hydraulic boundary conditions to be provided by the user are the design wave height and period and design high and low water levels (see section 5). Principal structural design input parameters (for definitions see sections 2 and 4 and Appendix) are porosity (P), slope angle ($tg\alpha$), damage (S_d), stone size ratio or filter rule (D_i/D_j) of successive layers, relative crest width (B/D_n) and transition levels. In each iterative design cycle the user may decide to adjust each of these parameters.

								totals
	0.3/10	10/200	0.2/1t	1/3t	3/6t	6/10t	>10t	
E	0	1.11	2.38	1.98	0.46	2.38	2.38	
R	1.00	0.90	1.40	0.80	0.60	0.20	0.10	
V	90	80	120	70	50	20	10	440
C_m	200	300	1900	1100	800	800	300	4700

Table 6 Production data of optimum breakwater design obtained with the model

river bank protection
Given the function of flood protection, the crest height is determined by the design flood level (z_f = 7.8 m) and the possibilities for variations in the cross section are confined to the revetment slope angle (cotgα). Using eq.(3) for the lower and and Van der Meer's formulae for the upper part of the protection, stability calculations have been made for slopes of 1:4 and 1:2 (which is assumed possible regarding geotechnical stability). The calculated stone sizes are D_s = 0.20 and 0.30 m respectively, but this hardly affects the demand per grading (appr. 20/50/30% for the three finest gradings). Regarding the required volumes, the indirect effect of an increase in layer thickness (1:2 comparing to a 1:4 slope) largely compensates for the direct effect of volume reduction, see Table 7. The figures show that savings achieved by the 1:2 slope are only 10%. In general the values for R_V and R_C emphasize that, to comply with th production of quarry I, these bank protection designs are highly inefficient. Further, by variation of the slope hardly any savings can be achieved for this type of rock structure, as long as the required volumes of the determining grading (here 10/200 kg) are not effected. However, if instead a quarry with yield curve II is available, in the first place the efficiency in general is improved considerably while, besides, possible savings achieved by slope optimisation become interesting (Table 7).

	quarry I		quarry II	
	1:4	1:2	1:4	1:2
V	170	150	95	84
C_m	1860	1680	540	460
R_V	5.0	4.4	2.8	2.5
R_C	21.1	19.1	6.1	5.2

Table 7 Effect of bank slope for two quarries

8. Comparison of demand vs. supply-based design
In contrast with the conventional demand-based design a supply-based design considerably reduces the excess cost of rock production in the quarry. This holds in particular for rock structures with many degrees of freedom with regard to the design of the cross section, such as for breakwaters. Applying the model to the example case of a breakwater the cost for materials could be roughly reduced down to 20% of those of the demand-type design. A practical criterion for comparison is the relative excess material loss (E), which is a measure for the amount of stone produced but not actually used in the structure. This loss (E) can be quickly reduced by adjusting the design by using the present model.

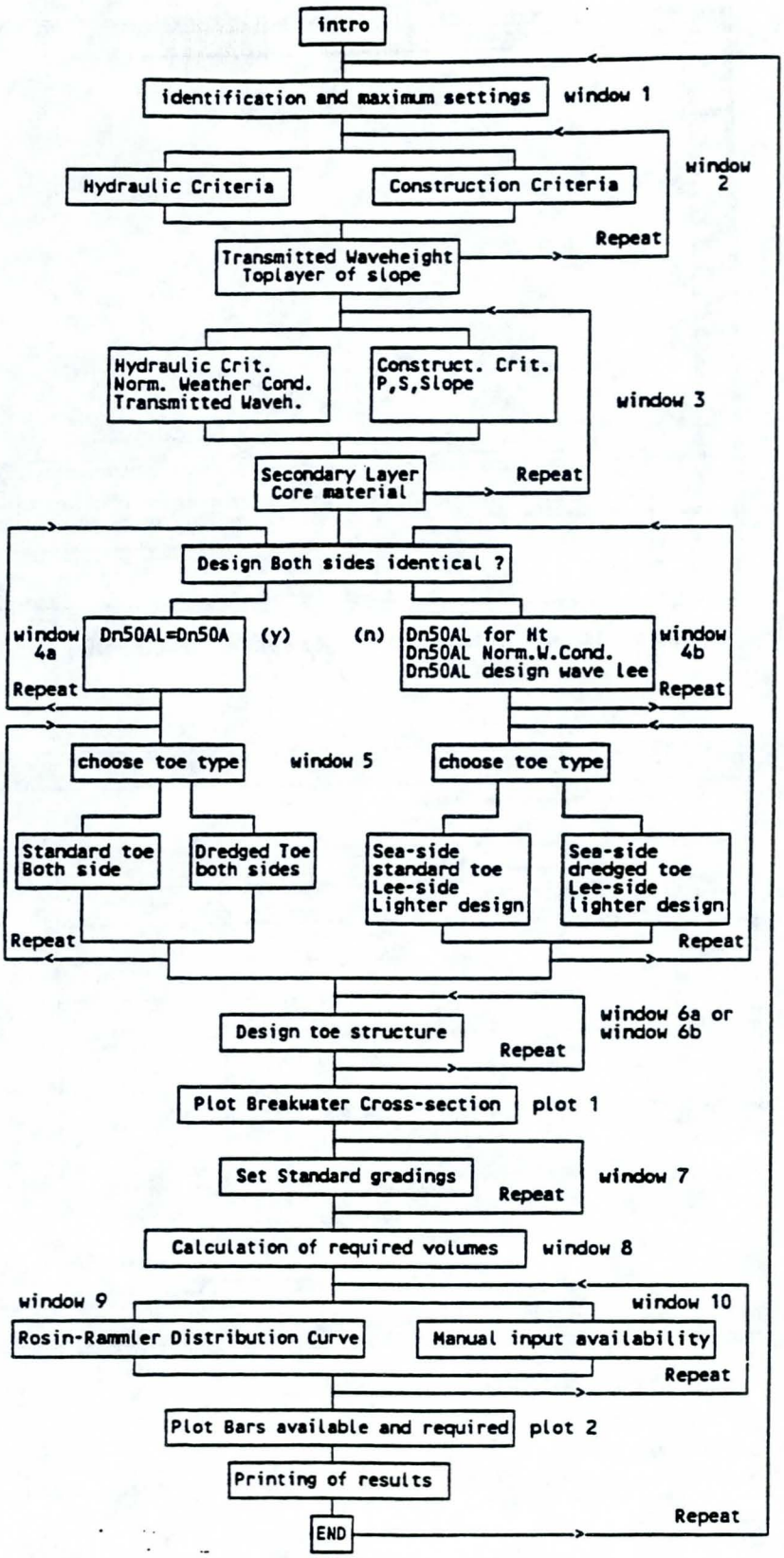

Figure 9 Model structure diagram

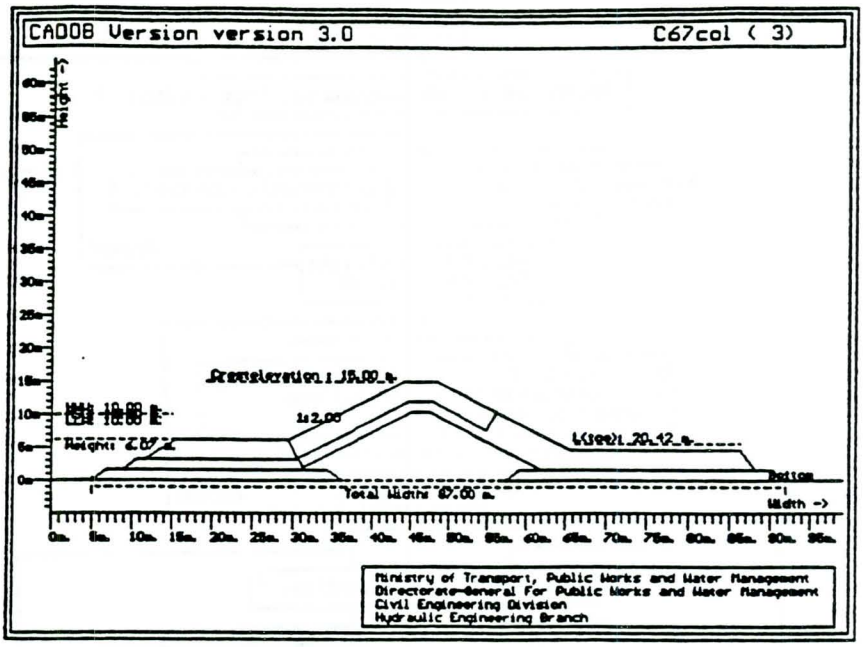

Figure 10 Example plot of breakwater cross section

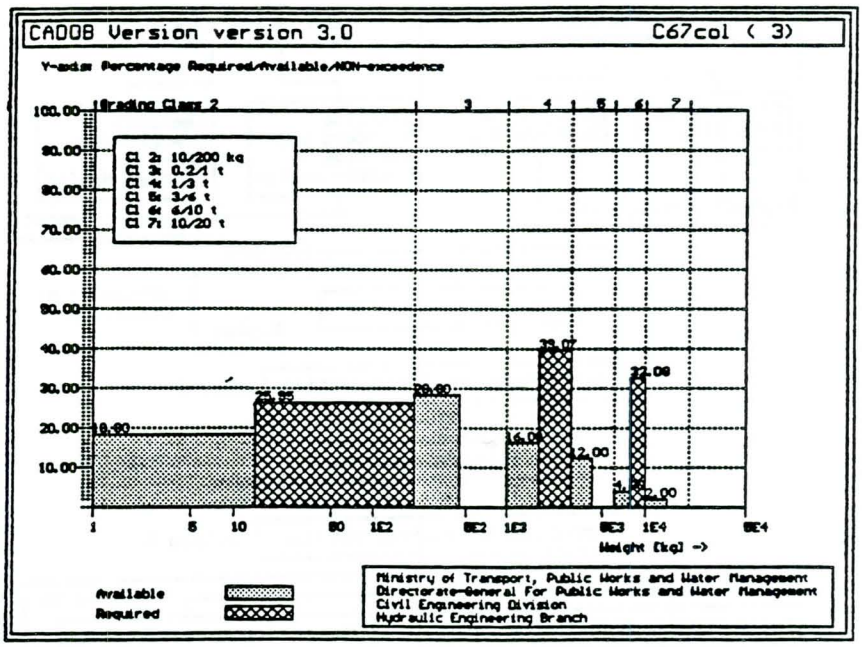

Figure 11 Example plot of stone supply vs. demand

construction stage
Besides, the model also includes an option to designing against damage during the construction stage.
Due to storm during construction serious damage may occur to the finer (non-armour) layers, leading to unacceptable delays and cost overrruns.

Since an exposed filter in this stage is particularly susceptible to wave action, the filter may be damaged. This can be avoided by proper dimensioning of the second layer (filter or secondary armour), using a second set of design conditions for construction. For construction stages reaching into known periods of increased storm frequency, these design conditions will be stronger (eg. than for construction in a quit "summer" season (see Figure 1).
Both, for the design of completed and construction stage the designer can adjust the accepted risk of damage through the damage parameter S_d (Appendix) by calculation of the cost associated with replacement of the lost stone volumes.

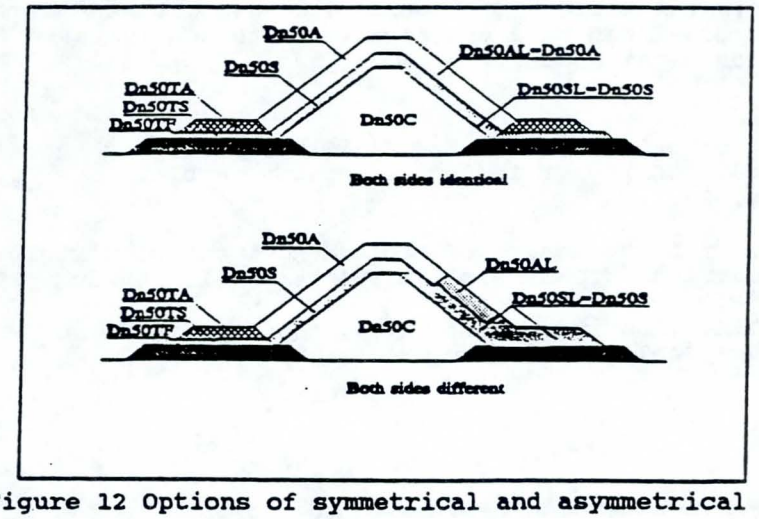

Figure 12 Options of symmetrical and asymmetrical cross section

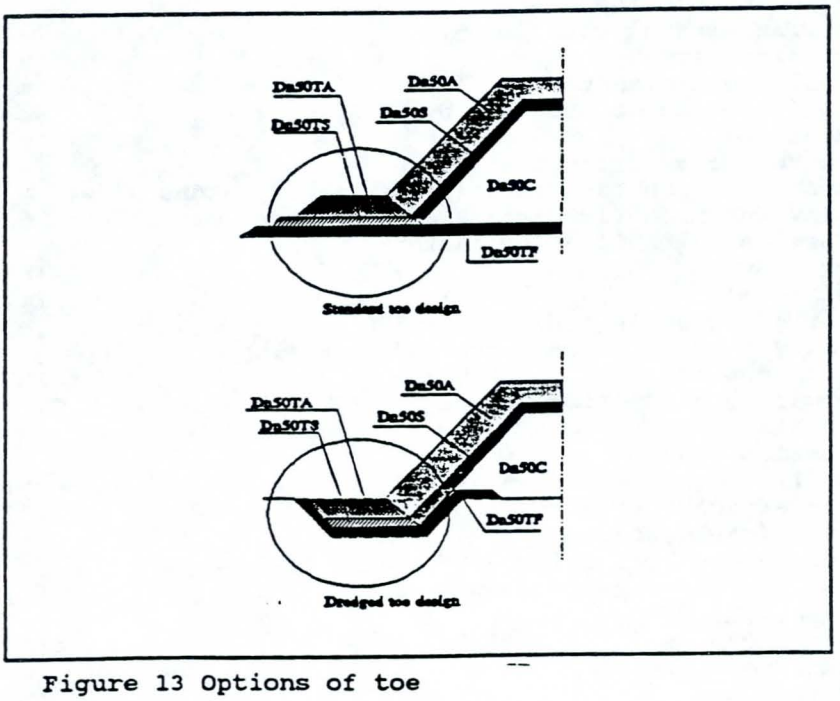

Figure 13 Options of toe

10. Summary and conclusions

It has been demonstrated that a supply-based design approach of rock structures will easily leads to significant savings of material cost. This holds in particular for breakwater, since this type of structure allows relatively many cross-sectional variations. Total investment costs of structures as far as they are related to material use may thus be reduced considerably.

The present state of the art of design methods for hydraulic structures built with rock allows for the development of routine design procedures, able to prevent already in the early stage of a project a too costly design. In this respect, the presented model developed in the Netherlands is a useful tool to arrive at a more economic use of rock in hydraulic engineering.

Allowing for further optimisation by considering replacement of determining gradings with substitutes (eg. earthfill, geotextiles or concrete units) the present model can be a practical tool to achieve even further reductions on material cost.

references

CUR/CIRIA, "Manual on the use of Rock in Coastal and Shoreline Engineering", CUR Report 154, CIRIA Special Publication 83, Gouda, The Netherlands, 1991.

Gessler, J., "The beginning of Bedload Movement of Mixture Investigated as Natural Armouring in Channels", Truninger Publ., Zürich, 1965.

Vrijling, J.K., Nooy vd. Kolff, A.H., "Quarry Yield and Breakwater Demand", IAEG, Balkema Publ., Rotterdam, 1990.

notation

A_e	Wave-induced erosion volume of rock slope	[m^2]
B	Berm width	[m]
C	Chezy friction coefficient	[$m^{\frac{1}{2}}/s$]
C_m	Material production cost	
C_t	Wave transmission coefficient	[-]
D	Stone diameter	[m]
D_n	Nominal stone diameter	[m]
D_i	Stone diameter not exceeded by i% by weight	[m]
De	Rock demand	[m^3]
E	Relative excess production	[-]
F	Distribution function (loading parameter, stone size)	
f	Density function (loading parameter, stone size)	
f_p	Production multiplication factor	[-]
h	Water depth	[m]
h_c	Crest level	[m]
N	Number of waves in design storm	[-]
P	Porosity factor for wave-exposed rock slopes	[-]
Pr	Rock production	[m^3]
P_d	Determining production volume	[m^3]
Q	River discharge	[m^3/s]
R	Production ratio	
R_c	Crest freeboard ($R_c = h_c - h$)	[-]
R_C	Volume efficiency factor	[-]
R_V	Cost efficiency factor	[-]
S_d	Damage parameter for wave-exposed rock slope	[-]
S_u	Damage parameter for current-exposed rock	[-]
T	Wave period	[s]
t	Layer thickness	[m]
U	Current velocity	[m/s]
V	Rock volume	[m^3]
W	Weight of stone	[kg]
z	Water level relative to datum	[m]
α	Slope angle of	[-]
Δ	Relative density of stone	[-]
ϕ	Friction angle (here chosen as 35°)	[-]

Ψ	Shields' bed shear parameter	[-]
ξ	Surf similarity parameter	[-]
ρ_r	Rock density	[kg/m^3]

Appendix

rock stability under wave action
Based on earlier work of Thompson and Shuttler (1975) an extensive series of model tests was conducted by Van der Meer (1988) on structures with covering wide ranges permeabilities and wave conditions. Two formulae were derived for plunging and surging waves respectively, describing the stability in terms of a ratio of wave height (H) over stone size (D) or H/ΔD. Note that for H and D the significant wave height (H_s) and 50% nominal diameter (D_{n50}) should be substituted:

$$H_s / \Delta D_{n50} = 6.2\ P^{0.18}\ (S_d/\sqrt{N})^{0.2}\ \xi_m^{-0.5}; \qquad \text{for plunging waves} \qquad (A1)$$

$$H_s / \Delta D_{n50} = 1.0\ P^{-0.13}\ (S_d/\sqrt{N})^{0.2}\ \sqrt{(\cot\alpha)}\ \xi_m^{P}; \qquad \text{for surging waves} \qquad (A2)$$

The transition from plunging to surging waves can be calculated using a critical value of ξ_m:

$$\xi_{mc} = [6.2\ P^{0.31}\ \sqrt{(\tan\alpha)}\ ]^{1/(P+0.5)} \qquad (A3)$$

In these formulae, α is the slope angle, Δ is the relative submerged rock density, ξ_m is the surf-similarity parameter (with respect to the mean wave period), N is the number of waves in the design storm, S_d is the damage parameter, defined as the dimensionless erosion volume A_e/D^2 and P is the notional permeability factor. Further details can be found in the CUR/CIRIA Manual (1991). Here it is only noted that S_d=2 to 3 and S_d=8 to 17 correspond to "no damage" and "failure" respectively (actual values depending on slope angle α) and that P varies from P=0.1 (stones on impermeable slope) to 0.6 (homogeneous rubble mound).

wave transmission
Based upon evaluation of a large data base performed for the Manual on Rock (CUR/CIRIA, 1991) wave transmission formulae has been found to answer approximatly the formula:

$$C_t = 0.46 - 0.3\ R_c/H_s \qquad (A4)$$

where R_c is the crest freeboard, defined as $R_c = h_c - h$.
The formulae is valid for a R_c/H_s range of -1.13 to 1.2, while for higher crests (R_c/H_s = 1.2 to 2.0) and lower crests (R_c/H_s = -1.13 to -2.0) the limiting values are C_t = 0.1 and C_t = 0.8 respectively.

slope factor for rock stability under current attack
For rock or stones on a river bank the following slope factor should be included in tha hydraulic stability analysis.

$$k_{sl} = \cos\alpha\ \sqrt{\left(1-\left(\frac{\tan\alpha}{\tan\phi}\right)^2\right)} \qquad (A5)$$

with ϕ being the friction angle of the rock (here assumed 35°).

material cost rates
With regard to overall material cost rates for armour, filter and core material the following figures are used:

weight class		cost rate [m^{-3}]
minimum	maximum	
	10 kg	2
10 kg	200 kg	4
200 kg		16

FIELD AND LABORATORY INVESTIGATION OF STEEP RIPRAP

G. Lefebvre, M.B. Belfadhel and K. Rohan
Université de Sherbrooke, Civil Engineering Department,
Sherbrooke, Quebec, Canada
O. Dascal
Hydo-Quebec, Div. Sécurité des Barrages,
Montreal, Quebec, Canada

INTRODUCTION

In 1986 the university of Sherbrooke and Hydro-Quebec jointly initiated an important research program to study riprap stability and repair at the La Grande hydro-electric complex in northern Quebec. With a 10,000 MW capacity, this complex has over 215 dikes and dams totaling more than 125 Km of riprap protection. The riprap generally performed well except at about ten sites where some damage was observed. The main purpose of the study was to examine in the field, the factors that are related to the damage and to propose long term and efficient repair techniques. However, before directly addressing the problem of repair, the research program was first oriented towards a better understanding of the damage mechanisms and the identification of the causes of damage so as to optimize the maintenance strategies. This was possible by conducting a detailed field investigation on fourteen riprap sites across the complex, completed by back analysis in which the theoretical riprap stability was compared to the maximum wave action that they experienced since reservoir filling (*Lefebvre et al, 1992*). An experimental investigation was then conducted to verify the main field conclusions under laboratory conditions as well as to appreciate the influence of different factors on the riprap stability and degradation mechanisms (*Rohan et al, 1992, Ben Belfadhel et al, 1993).*

TABLE 2. Riprap Gradation and Maximum Wave Experienced

Dam	Slope and Gradation					Maximum wave experienced
	Slope cot α	W_{50} min. (Kg)	W_{50}. ave. (kg)	W_{50} max. (kg)	Uniformity D_{85}/D_{15}	Hs (m)
CD-00	1.6	922	1,049	1,325	2.1	1.63
CD-05	1.7	1,037	1,729	2,688	1.7	1.31
CH-20	2.0	421	776	1,143	2.3	1.31
TA-BN	1.6	472	693	1,095	2.7	0.96
TA-10	2.2	639	982	1,622	2.1	1.03
TA-12	2.2	408	494	653	2.0	1.84
TA-13	2.3	429	513	1,053	2.0	1.87
TA-20	2.2	872	1,161	1,544	2.1	1.62
TA-32D	2.0	926	1,764	2,481	2.1	1.02
QA-00	1.5	476	974	1,581	2.6	0.80
QA-08	2.0	172	504	762	2.9	0.70
KA-03	1.37	1,086	1,488	2,272	1.9	1.80
KA-04	1.45	716	1,123	1,553	2.0	1.03
KA-05	1.56	399	625	723	2.3	0.98

In five of the investigated sites (TA-BN, QA-00, QA-08, KA-04, KA-05) a large fraction of fine material (0-30 cm) had been incorporated into the riprap during construction while measurements at the different sites indicated median diameters (D_{50}) between 63 and 100 cm. In the remaining sites the gradation was relatively regular without any fine material.

Damage Mechanisms and Classification

While the riprap slope and gradation have been found to greatly influence the riprap degradation mechanisms, the different types of damage and the overall performances have been classified according to the type of movement observed, the extent of damage and the severity of the degradation.

The major type of degradation mechanisms identified in the field are summarized and described in table 3.

TABLE 3. Description of the Different Damage Mechanisms Observed.

Damage mechanisms	Description	Remarks
Erosion	Progressive displacement of rocks from the surface	Facilitated when the riprap contains a large fraction of fine material
Spoonholes	Localized displacement of rocks leaving an easily identified impression in the riprap	Indication of strong wave action compared to the existing size of riprap
Bedding washout	Occurs when part of the bedding is washed away by wave action	Occurs generally after bedding exposure to wave action
Beaching	Formation of overlaying beaches generally covered with a deposit of fine material	Facilitated in the case of flat slopes and when the riprap contains a large fraction of fine material
Sliding	Sliding and loss of stability of the riprap near the crest following a damage near the water's edge	Observed exclusively in steep slopes and more frequently in riprap containing fine material
Rock fragmentation	Fragmentation and cracking of the riprap stones due to climate and the shocks imposed by waves	Observed only in a few instances and not considered a significant factor

The sliding mechanism was observed only in steep slopes and was much more pronounced in the case of riprap containing a large fraction of fine material. Sliding were noted mostly above the damaged area. For flatter slopes this mechanism was never observed even in heavily damaged areas. One should note that in many cases the damage resulted from the combination of several mechanisms listed in table 3.

Each damage was qualified as minor, partial or total. A minor damage corresponds to the erosion of only a few blocks from the surface of the riprap. The damage is considered partial when the bedding is apparent, and total when some bedding is washed away by waves.

Similarly in table 1 the observed riprap performance is classified as Excellent, Good, Moderate and Poor according to the following definitions:

Excellent performance: No damage has occurred at all;

Good performance: Only minor damage is visible;

Moderate performance: The dominant types of damage are minor and partial, total damage type are very few and localized;

Poor performance: Several total damages have been observed and substantial bedding washout has occurred at some locations.

Back analysis

The field observations and measurements have allowed a back analysis to be performed in which the theoretical stability of the riprap was compared to the maximum wave height that was experienced since reservoir filling (*Lefebvre et al, 1992*). Based on the in-situ gradation and slope, the theoretical stability was assessed using the Hudson formula associated with a stability coefficient K_{RT} of 2.2 and a design wave height H_D=1.27Hs. For each site it was then possible to calculate the maximum wave height that the riprap could withstand without damage or, in other words, a stability threshold. For each riprap three stability thresholds have been established based on the minimum, average and maximum gradation (W_{50}) measured.

The maximum waves heights experienced by the riprap in the field were estimated using the simplified wave prediction method recommended in the *Shore Protection Manual (1984)*. This procedure required the analysis of wind data recorded at five weather stations since the filling of the reservoirs, that is, between 1980 and 1987 depending of the site.

The back analysis along with the field observations have permitted to conclude that the two major causes of riprap damage across the La Grande complex seem to be either undersized riprap or the presence of a large fraction of fine material in some steep riprap. For regular riprap or riprap without fine material, the back analysis predicted behaviors which were in good agreement with the field observations. The riprap with excellent performance have not yet experienced a wave action

greater than their theoretical stability which is in contrast to the riprap which showed a poor performance. In the case of riprap containing a large fraction of fine material and particularly for steep slopes, the back analysis based on the actual W_{50} gave a contradictory performance picture. Many of these riprap have shown significant damage in the field while the theoretical calculations based on the in situ gradation (W_{50}) tended to predict an excellent performance.

Figures 1 to 3 show examples of the back analysis results for regular riprap presenting excellent and poor conditions (TA-10 and KA-03)and for riprap containing fine material in poor condition (TA-BN).

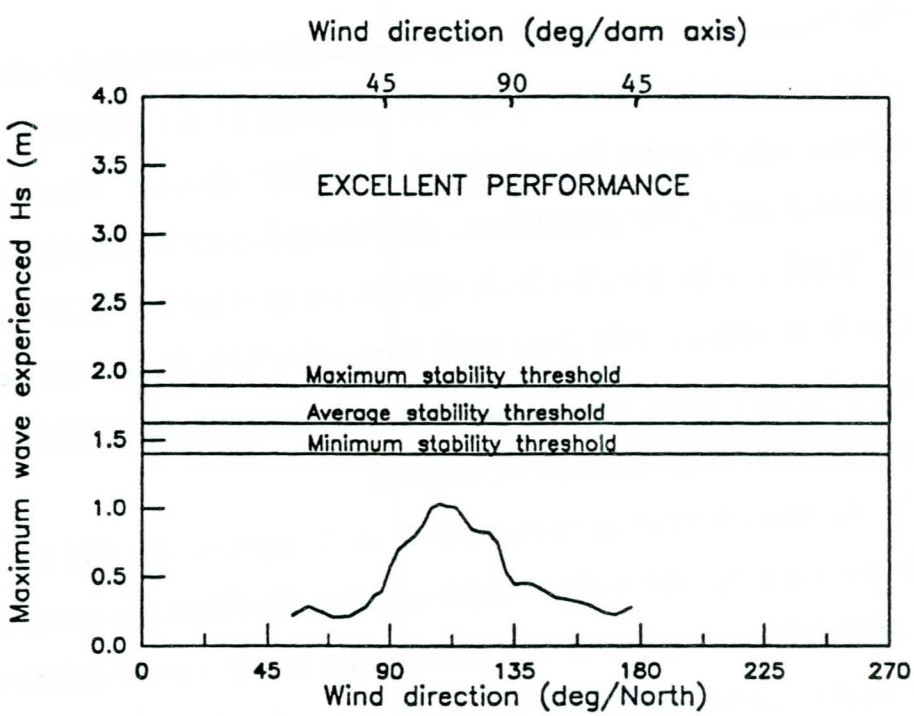

Figure 1. Regular Riprap in Excellent Condition (Site: TA-10, Slope: 2.2:1)

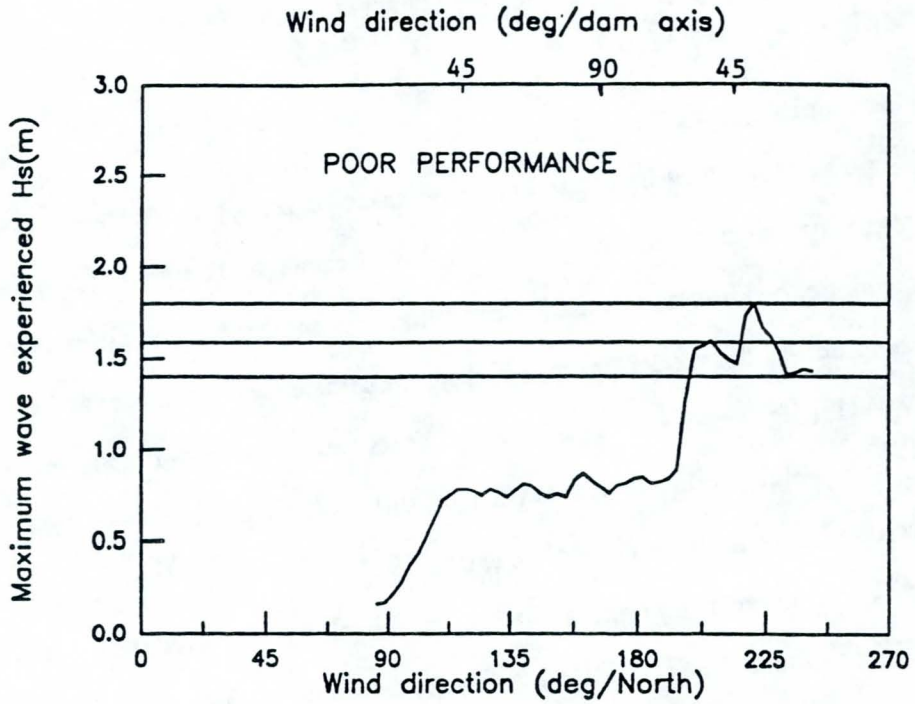

Figure 2. Regular Riprap in Poor Condition (Site: KA-03, Slope: 1.37:1)

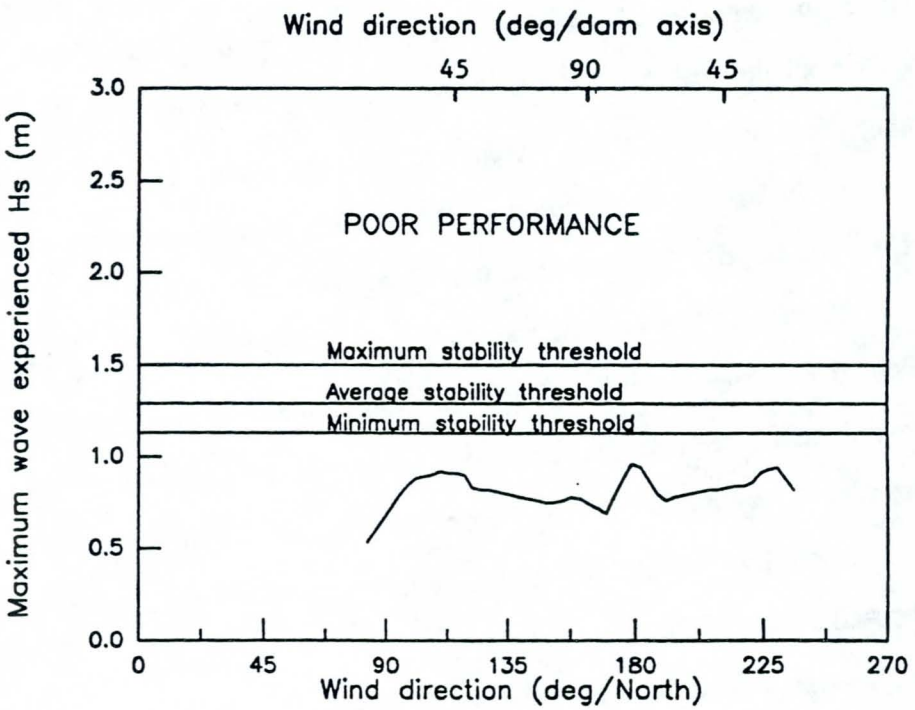

Figure 3. Riprap with Fine Material in Poor Condition (Site: TA-BN, Slope: 1.6:1)

LABORATORY INVESTIGATION

Testing Program

The laboratory investigation was conducted mainly to verify the conclusions of the field study regarding the mechanisms and the causes of damage. The testing conditions encompassed most of the slope, bedding and gradation conditions encountered in the different riprap across the La Grande complex. All the model riprap tested were characterized by the same median diameter D_{50} of 8.9 cm (W_{50}=1.1 kg) and a thickness of $2D_{50}$. Tests were carried out using regular waves with a period of 1.8 sec. which produced critical wave conditions (collapsible waves). The detailed testing procedures and conditions are given in *Rohan et al (1992)*.

For regular riprap the influence of the slope and gradation were investigated using three different gradations (D_{85}/D_{15}=1.2, 2 et 3) tested on both steep (1.5:1) and flat slopes (2.5:1) and a coarse bedding ($D_{50}/(D_{50})_b$=7.8) typical of rockfill embankment. Two other steep riprap were tested using a finer bedding ($D_{50}/(D_{50})_b$=2.8) corresponding to a sand and gravel bedding in the field. In all the cases the filter criteria between the riprap and their bedding were satisfied.

While all the tested riprap have were simply dumped on the slope with no or only slight rearrangement, in one test the riprap was carefully placed by hand in order to investigate the influence of the placing method on the stability. The riprap was characterized by a gradation D_{85}/D_{15} of 1.8, a steep slope (1.5:1) and a coarse bedding ($D_{50}/(D_{50})_b$=7.8).

The influence of fine material was investigated by testing the wide gradation riprap (D_{85}/D_{15}=3) to which 10% of fine material (0-2 cm) were added previous to testing. The percentage of fine was chosen arbitrarily since it was difficult to assess the real fine content from the field investigation. The purpose was to give an idea of the effect of the fine material rather than to quantify their influence. One should note that the addition of 10% of fine material did not significantly influence the median diameter value (D_{50}) of the riprap.

The damage evolution curves obtained for regular riprap and riprap containing fine material are presented in figures 4 to 8. The damage S is expressed by $S=A/(D_{n50})^2$ and represents the actual

number of cubical shape blocks eroded within a band width of one nominal diameter D_{n50} ($D_{n50}=(W_{50}/\rho r)^{1/3}$). The wave height is expressed addimentionnaly using the stability number Ns given by $Ns=H/(Sr-1).D_{n50}$ where H is the wave height and Sr the specific density of the riprap blocks ($Sr=\rho r/\rho w$).

In figures 4 to 8 failure is represented by shaded points and corresponds physically to bedding exposure through an opening of $D_{50}/2$

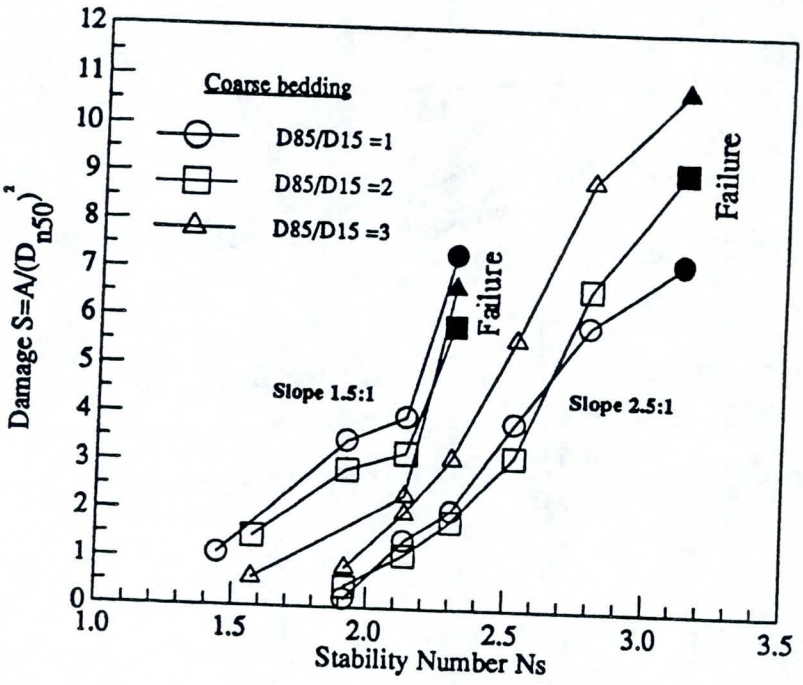

Figure 4. Influence of Slope and Gradation (Slope: 1.5:1 and 2.5:1)

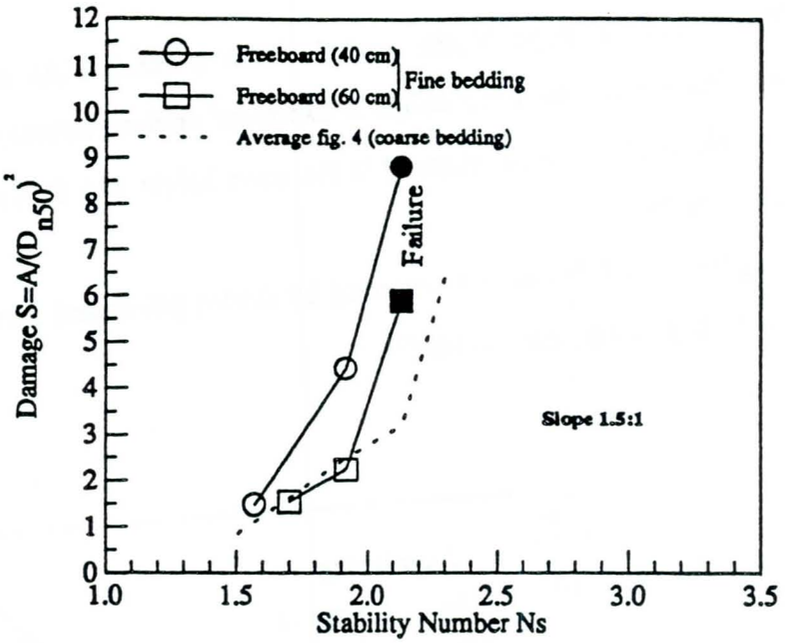

Figure 5. Influence of Riprap bedding (Slope: 1.5:1)

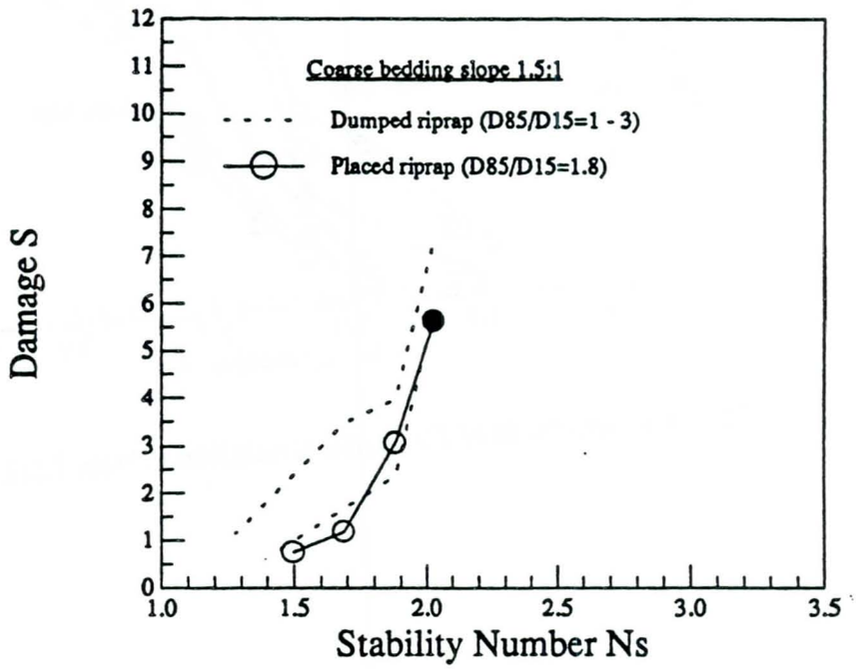

Figure 6. Influence of Placing Method (Slope: 1.5:1)

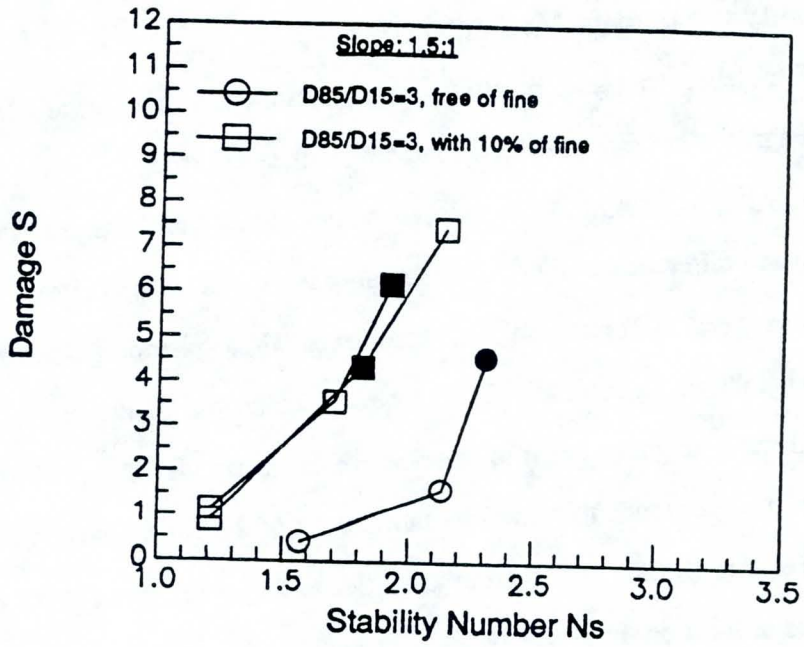

Figure 7. Influence of Fine Material on Steep Slope Riprap (Slope: 1.5:1)

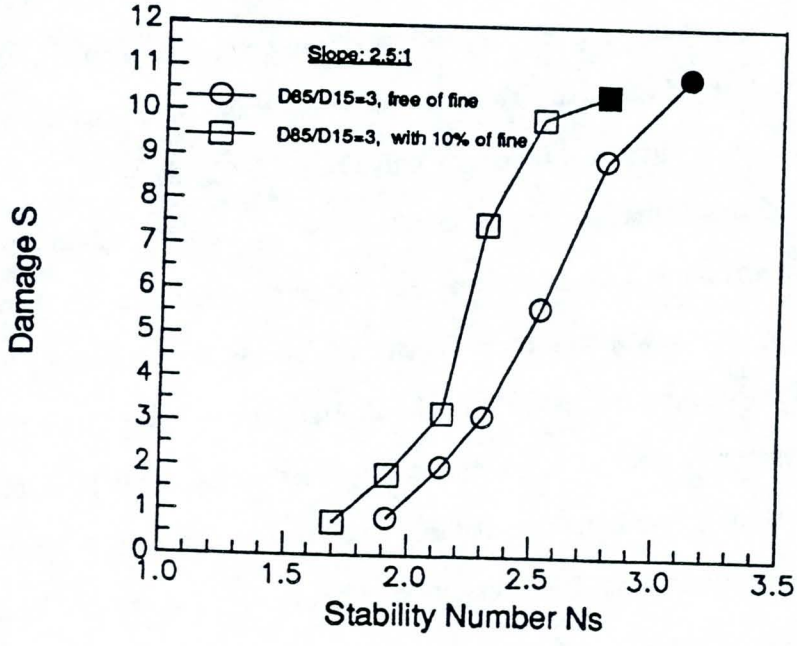

Figure 8. Influence of Fine Material on Flat Slope riprap (Slope: 2.5:1)

Stability and Damage Mechanisms

The laboratory tests results and observations have shown, in all cases, behaviors which were in good agreement with those anticipated from the field study.

For regular riprap, it was clearly observed that the damage mechanisms of steep and flat slope riprap are different mainly due to sliding phenomena occurring exclusively in the case of the steep slope between the crest and the water level. These phenomena always occurred beyond a critical wave height which corresponds to a rapid acceleration of the rate of damage towards failure. This critical wave height or point of acceleration is clearly identifiable on the damage curves of the steep riprap. It corresponds to a stability number Ns of 2.1 for the coarse bedding (fig. 4) and 1.9 for the finer bedding (fig.5). In the latter case the sliding phenomena were more pronounced near failure because of the more intensive bedding washout in this case.

In the case of the flat slope tested (2.5:1) no such sliding was observed and the damage curves show a relatively constant rate of damage (fig. 4).

For the two slopes tested, the gradation did not significantly influence the stability or the shape of the damage curve (fig. 4). The start of damage (S=1) and failure occurred approximately at the same wave heights respectively, regardless of the gradation. Similarly the two beddings tested, at least in the case of the steep slope, have only a minimal influence on the start of damage and influenced the wave height at failure by only about 8% (fig. 5).

Figure 6 shows that for the conditions tested, the riprap failure always occurred at the same wave height no matter if the riprap was dumped or carefully placed by hand. However, it seems that the stability is somehow increased at the start of damage when the riprap blocks are carefully placed. In terms of degradation mechanisms the hand placed riprap has shown a rigid behavior. Damage first started at apparently weak zones, then the local interlocking began to deteriorate rapidly leading to a rapid degradation towards failure. Although still present, the sliding phenomena were less frequent than for the dumped riprap. It seems that careful placing of riprap can lead to a certain reduction in the size of the riprap required by a design based on the start of damage criterion. However this

advantage should be associated to a reduced stability reserve when compared to dumped riprap, since a careful placing does not appear to affect the riprap resistance at failure.

For riprap containing fine material, the laboratory investigation has shown that the presence of fine material has a detrimental effect on the stability particularly in the case of steep slopes. For the 1.5:1 slope tested, figure 7 shows that when the fines are present the riprap stability is reduced by about 50% at failure and 30% at the start of damage (S=1). The loss of stability is however less important for the flat slope tested (fig. 8), being reduced to about 10% at failure as well as at the start of damage. The laboratory observations have shown that in the case of a steep slope the inclusion of fine material greatly reduces the internal stability of the riprap by creating a ball bearing effect. The sliding phenomena are then more pronounced and more rapidly affect the model's crest than for regular riprap. For the 2.5:1 slope, the presence of fine material did not clearly influenced the damage mechanisms

Verification of the Causes of Damage

The main causes of damage identified following the field investigation and the back analysis, may be verified by comparing the observed field performance to the laboratory performance of the tested riprap. Figure 9 et 10 compare the laboratory data obtained from regular riprap to the maximum significant wave height experienced in the field by regular riprap and by riprap containing fine material, respectively (table 3). For each riprap the maximum wave height is expressed by the stability number Ns calculated using the minimum W_{50} measured in the field ($N_s=H_s/(S_r-1).(D_{n50})_{min.}$), to represent the weakest zone of the riprap. The laboratory data are taken from figures 4 and 5 and expressed by the stability numbers corresponding to a start of damage criterion (S=1) and a stability limit (wave height before failure) criterion. For the 1.5:1 slope the stability numbers considered correspond to the average values obtained with the two bedding tested. In order to make the regular wave used in the laboratory comparable with the irregular natural waves, these stability numbers have been divided by 1.27 or 1.37. According to *Broderick (1984) and Ben*

Belfadhel et al (1993), regular waves will create the same amount of damage as irregular waves (Hs) as long as the regular waves height H is equal to 1.27Hs or 1.37Hs.

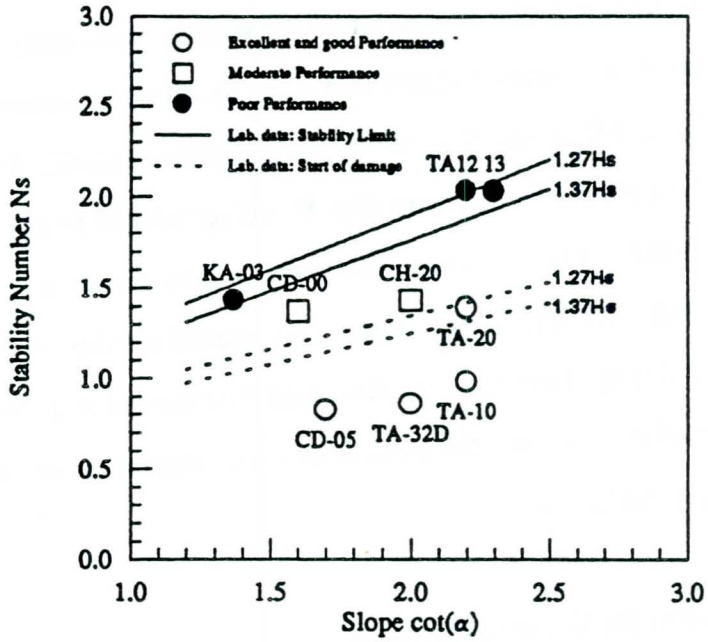

Figure 9. Comparison of Field Performance with Laboratory Data (Regular Riprap)

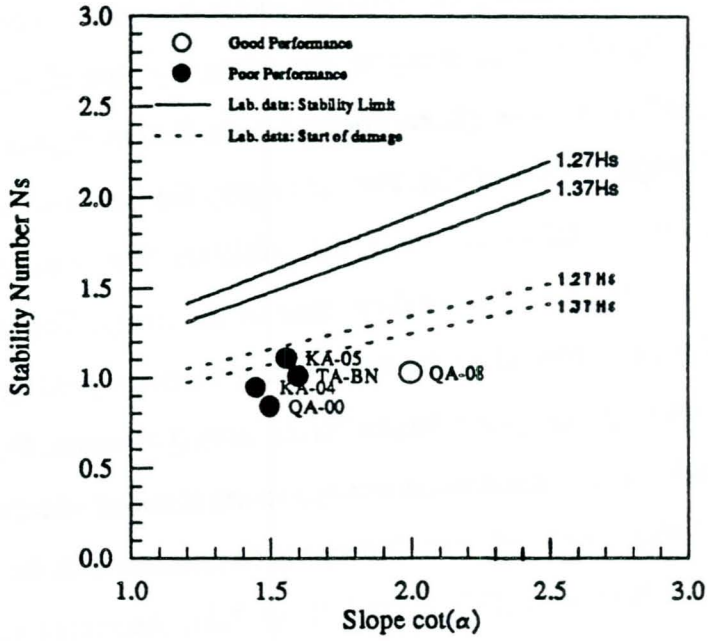

Figure 10. Comparison of Field Performance with Laboratory Data (Riprap with Fine)

For regular riprap the comparison shown in fig. 9 predicts behaviors which are in good agreement with the field observations. Riprap in excellent and good condition experienced waves heights corresponding to stability levels that were always below the start of damage conditions predicted from the experimental study. The maximum wave height experienced by the TA-20 dike reached the start of damage condition although the riprap performed very well. In this particular case the meticulous placement of the riprap during construction seems to have contributed to its stability, as suggested by the laboratory investigation (fig. 6). In the case of riprap with moderate performance the maximum waves heights experienced in the field lie between the start of damage and the stability limit conditions. In the case of the CD-00 riprap, minor damage was dominant and total damage was very localized. The CH-20 riprap performed very well except at two locations where very localized total damages were observed. Figure 9 shows that the maximum wave experienced by the riprap in poor condition have exceeded the stability limit obtained under laboratory conditions, confirming the field observations.

For riprap containing fine materials the behavior predicted in figure 10 differs from the in-situ observations except for the riprap on dike QA-08 which has a flatter slope of 2:1 and has shown a good performance. All steep riprap containing fine material have suffered significant damage even if subjected to maximum waves below the start of damage conditions defined in the laboratory on regular riprap. One can see from figure 10 that the presence of fines in the steep riprap has decreased the field stability by about 40%, which is roughly the reduction observed in the laboratory when incorporating 10% of fine material into the model riprap. The performance of steep riprap with fines cannot therefore be predicted by classical stability formulas in which the riprap gradation is characterized only by the D_{50}. It is also evident that even if the fines only slightly reduce the D_{50} they disproportionately affect the stability of the steep riprap.

CONCLUSION

A field investigation followed by a laboratory study have characterized the degradation mechanisms and assessed the performance of fourteen riprap sites across the La Grande Hydro-electric project in northern Quebec.

The field study has shown that the two main causes of damage were undersized riprap or the presence of fine material incorporated in certain steep riprap. The field investigation has also identified different degradation mechanisms depending of the slope. Degradation of steep riprap was in particular characterized by sliding phenomena observed above the damage zone.

The laboratory investigations have confirmed these observations and conclusions, and allowed some insights into the different factors which influence the stability and degradation mechanisms in riprap. As anticipated from the field study, the inclusion of fine materials in the riprap has been found to reduce the stability particularly in the case of steep slopes.

The riprap gradation and the type of bedding did not significantly affect the stability under test conditions. When compared to dumped riprap, individual placement of blocks does improve stability at the start of damage but not at failure.

REFERENCES

Ben Belfadhel, M., Lefebvre, G. and Rohan, K. (1993). "*Clarification on the use of Hudson Formula for Riprap Design.*", XXV IAHR Congress, September 1993, Tokyo, Japan.

Broderick, L.L. (1984). "*Riprap Stability Versus Monochromatic and Irregular Waves.*", Master Thesis, George Washington University, USA.

Lefebvre, G., Rohan, K., Ben Belfadhel, M. and Dascal, O. (1992). "*Field Performance and Analysis of Steep Riprap.*", American Society of Civil Engineers, Geotechnical Division, 1118(9), p. 1421-1448

Rohan, K., Ben Belfadhel, M. and Lefebvre, G. (1992). "*Damage Mechanisms and Influence of Gradation for Steep Riprap.*", Submitted to the American Society of Civil Engineers, Geotechnical Division.

Shore Protection Manual (1984). U.S.Army Corps of Engineers, Fort Belvoir, U.S.A.

ACKNOWLEDGMENT

The field and laboratory investigations were conducted in cooperation and with the financial support of Hydro-Quebec, Montreal, Canada. The support and the permission to publish this paper are greatly acknowledged.

THE CORRELATION OF INDEX TESTS WITH ROCK DURABILITY

D.A. Lienhart
US Army Corps of Engineers, Geotechnical Division,
P.O. Box 1159, Cincinnati, Ohio, USA
H.H. Fisher
US Department of Agriculture, Soil Conservation Service,
200 N. High Street, Columbus, Ohio, USA
E.F. Robinson
US Army Corps of Engineers, Ohio River Division Lab.,
11275 Sebring Drive, Forest Park, Ohio, USA

INTRODUCTION

Background

Rock used for erosion control (gabion-fill, riprap, armor and breakwater stone) must possess sufficient durability as provide sufficient protection throughout the expected life of the related engineering project. Attempts to predict the useful of life of such stone are generally performed through the use of laboratory accelerated weathering tests.

Several drawbacks exist with the accelerated weathering tests, however. For one, these tests generally have only an approximate 70 percent success rate. That is, the tests agree with the actual field exposure durability about 70 percent of the time. Secondly, the tests are time-consuming. The average freeze-thaw durability test requires a minimum of four weeks, not counting sample preparation, "before and after" photos and report preparation. The actual time requirement from receipt of the sample by the laboratory to receipt of the test report by the client approximates eight weeks minimum. Lastly, the tests are expensive. An entire suite of index tests can be performed on several samples for the same price of one accelerated weathering test on one sample and the information can be available within a matter of days.

Objectives

The objectives of this study are as follows:

1) determine if it is possible to use a few simple index tests to determine the suitability of rock quality for use as erosion protection;

2) determine the relationships between any index properties so identified and their relationship to durability;

3) determine what specification limits may be placed upon these properties such that most non-durable rock can be eliminated from use.

DURABILITY CONSIDERATIONS

In order to determine which properties should first be examined, the causes and severity of rock weathering and its relation to rock properties must first be identified.

Processes

The physical weathering processes which may affect the expected performance of rock used for riprap, armor or breakwater stone are:

1) frost weathering
2) wetting and drying (slaking)
3) stress relief
4) salt weathering

Processes such as freezing and thawing and wetting and drying are of significant concern the mechanics of the freeze-thaw process has been described by Lienhart, 1993). Stress relief has been found to be a particular factor in the glaciated north-central U.S. Salt weathering is of some concern for projects sited along the ocean shoreline.

Severity of Rock Deterioration

There are two types of deterioration. They may best be termed "rapid degradation" and "slow degradation." The "rapid" type results in particle fracturing and splitting while the "slow" type results in a gradual reduction in particle size through continual spalling

and/or sloughing of the particle surface or through gradual dissolution. Frost weathering and wetting and drying weathering can exhibit both types of degradation. Stress relief usually results in rapid degradation once the rock is quarried. Salt weathering usually results in slow degradation.

ROCK PROPERTIES

Properties Pertinent to Durability

When the actual conditions of exposure are considered there is one over-riding factor that controls rock quality and durability - mineralogic composition. Because the rocks made up of heavy minerals are, by historical observation, also the most durable, it follows that unit weight or density is also a factor.

Since the movement of moisture through rock appears to control the frost weathering, wetting and drying, and salt weathering, it can be concluded that porosity is the third factor.

Index Tests which Measure Pertinent Rock Properties

Petrographic analysis has already been determined by numerous studies to have the best success rate in prediction of rock durability and Dunn and Hudec (1965) have already shown the existence of the relationship between the presence of clay and durability. For carbonate rocks the volume of clay present in the rock may be cheaply, simply and quickly determined through the performance of acid insoluble residue analysis.

The determination of rock density may be performed by means of many standard test methods. Specific gravity was chosen simply because it is the standard method in use by both the USACE and the USDA SCS.

Index tests related to porosity are absorption and adsorption. Absorption is a measurement of the volume of larger pores while adsorption is a measurement of the volume of micropores. It is generally believed that the finer pores or micropores play a

significant role in rock durability.

INDEX PROPERTIES VERSUS DURABILITY

Durability Determination Procedure

Since there was no way to actually obtain fresh samples of non-durable stone (obviously, it is not known if a rock sample is non-durable until it has degraded and then it is no longer fresh), samples of varied durability were obtained and each sample was sawed into several pieces. One piece of each sample was subjected to the accelerated weathering test procedure described in ASTM D 5312 (Evaluation of Rock for Erosion Control Under Freezing and Thawing Conditions) and another piece to the accelerated weathering test procedure described in ASTM D 5313 (Evaluation of Rock for Erosion Control Under Wetting and Drying Conditions) (ASTM, 1993). The remaining pieces were subjected to additional testing procedures such as specific gravity, absorption, adsorption, sulfate soundness and various other tests.

The current database consists of approximately 125 samples from Indiana, Illinois, Kentucky, Michigan, Pennsylvania, Tennessee, Virginia, West Virginia, and Wisconsin. All index properties presented herein were not measured for all of the rock samples in the database. Almost all of the samples are limestones and dolomites. A few sandstones, and igneous rock types are also present but were excluded from this study because of their differing properties. This is not a large database but it is enough to provide an indication of possible relationships between durability and index properties.

Durability vs. Absorption and Specific Gravity

Originally, an attempt was made to chart durability test loss in percent versus each of the index properties but no obvious relationship was apparent. It was then realized that the percent loss was not a true measure of durability as some rocks exhibit "rapid degradation" and some exhibit "slow degradation." In either case however, the rock is non-durable.

The samples were then divided into durable and non-durable categories and the absorption value for each was plotted versus its specific gravity as shown in Figure 1. The two areas of this figure labeled as "Generally Not Durable" contain no data points for stone that suffered no change in the accelerated weathering tests (durable stone). The area labeled as "Generally Durable" however, contains a few data points for stone that suffered some minor changes during the accelerated weathering tests. These could be non-durable rocks but are generally thought to be durable with minor losses due to small spalls which originated during blasting.

Durability vs. Adsorption/Absorption Ratio and Specific Gravity

Figures 2 and 3 illustrate the relationship between adsorption:absorption ratio and specific gravity to durability. Like Figure 1, the area of these figures labeled as "Generally Not Durable" contain no data points for stone considered to be of durable quality. Also like Figure 1, the areas labeled as "Generally Durable" contain a few data points for stone that suffered some minor changes during the accelerated weathering tests. Again, this may be due to the harshness of the accelerated weathering test procedure which leads to only a 70 percent success rate when compared to actual exposure results. The difference between the limestone curve and the dolomite curve should be noted. This difference is probably related to the greater porosity and specific gravity values experienced with dolomites.

Durability vs. Adsorption/Absorption Ratio

The correlation of durability to the adsorption:absorption ratio is shown in Figure 4. Once again, there are no "durable" data points in the "Generally Not Durable" area but the presence of "non-durable" data points in the "Generally Durable" area. The explanation is the same as presented for figures 1 through 3.

Insoluble Residue Content vs. Sulphate Soundness Loss

The USDA SCS has a specification requirement for riprap that limits the rock of acceptable quality to a sulphate soundness loss of no more than 10 percent. For this

reason, the SCS database involves more soundness data than accelerated weathering test data. The insoluble residue test has been used by Fisher (1993) as a preliminary indicator of rock durability for a number of years. Figure 5 presents a graphical summary of some of the SCS data for limestones. An obvious relationship exists between the amount of insoluble residue in a limestone and the soundness loss experienced for that same limestone.

Proposed Specifications for Limestone and Dolomite

To summarize these preliminary correlations a set of proposed specifications is presented in Table 1. These proposed specifications, based on this study, are provided for comparison purposes and as a suggested means to judge rock quality for use as riprap.

SUMMARY AND RECOMMENDATIONS

The preliminary results of this study indicate a possible correlation of index rock properties with durability. This data also indicates that such a correlation must be performed by rock type and not as a single correlation for all rock types. This study has shown that the properties of adsorption, absorption and specific gravity are all interrelated and may be correlated with durability. This study has also shown that by using a series of simple index tests it is possible to establish specifications for various qualities of riprap.

Due to the small size of the database much additional work needs to be accomplished. Recommendations for further study include adding tensile strength and direct pore size measurement and size distribution using blue dye resin injected thin sections under petrographic examination. It is also recommended that a correlation be made using freshly quarried specimens from known non-durable geologic formations.

CONCLUSIONS

Based on this preliminary study, it is possible to develop a series of curves for each rock type such that through the performance of a series of index tests, questions

regarding rock quality and durability may be resolved in a matter of days rather than months. This study is just the introduction to the work needed in the future.

REFERENCES

American Society for Testing and Materials, 1993; ANNUAL BOOK OF ASTM STANDARDS; Volume 04.08; ASTM, 1916 Race St., Philadelphia, PA, 19103.

Dunn, James R. and Hudec, Peter P., 1965; THE INFLUENCE OF CLAYS ON WATER AND ICE IN ROCK PORES; State of New York Dept. of Public Works, Physical Research Report RR 65-5, 148 pp.

Fisher, Henry H., 1993; "Insoluble Residue of Carbonate Rock and Its Application to the Durability Assessment of Rock Riprap" in ROCK FOR EROSION CONTROL; ASTM Special Technical Publication 1177, edited by C.H. McElroy and D.A. Lienhart; ASTM, 1916 Race St., Philadelphia, PA, 19103; pp. 62-68.

Lienhart, David A., 1993; "The Mechanism of Freeze-Thaw Deterioration of Rock in the Great Lakes Region" in ROCK FOR EROSION CONTROL; ASTM Special Technical Publication 1177, edited by C.H. McElroy and D.A. Lienhart; ASTM, 1916 Race St., Philadelphia, PA, 19103; pp. 77-87.

INDEX PROPERTY	ROCK QUALITY		
	POOR	FAIR	GOOD
SPECIFIC GRAVITY	< 2.50	2.50 -2.65	> 2.65
ABSORPTION	> 1%, < 3%	1.25% - 2.5%	1% - 2%
ADSORPTION:ABSORPTION RATIO	< 0.03 (DOL) < 0.01 (LS)	< 0.06 (DOL) < 0.2 (LS)	< 0.1 (DOL) < 0.4 (LS)
INSOLUBLE RESIDUE	> 20%	15% - 20%	< 15%

TABLE 1 - PROPOSED SPECIFICATION FOR LIMESTONE & DOLOMITE

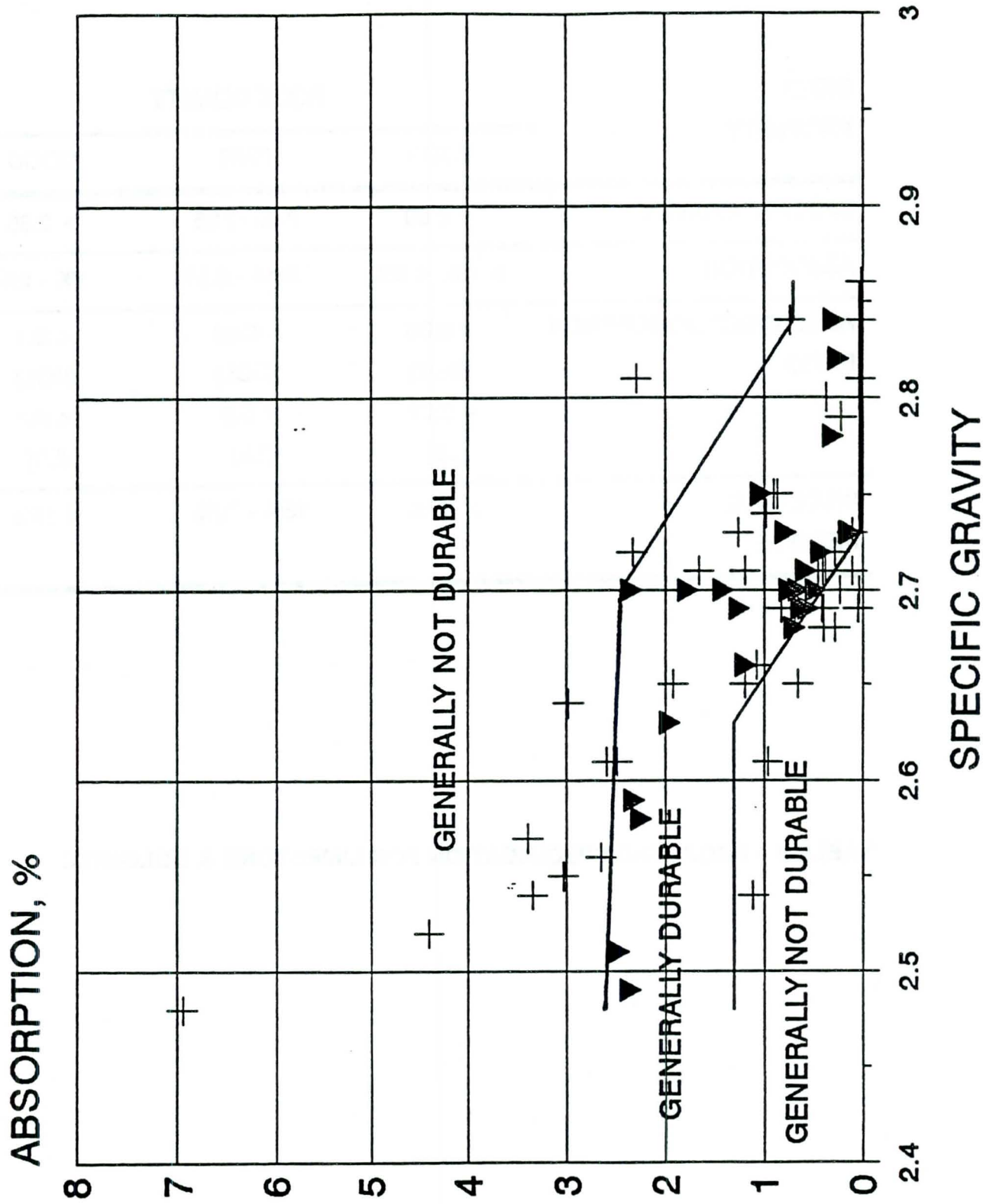

FIGURE 1 - Durability vs. Absorption and Specific Gravity for Limestones and Dolomites

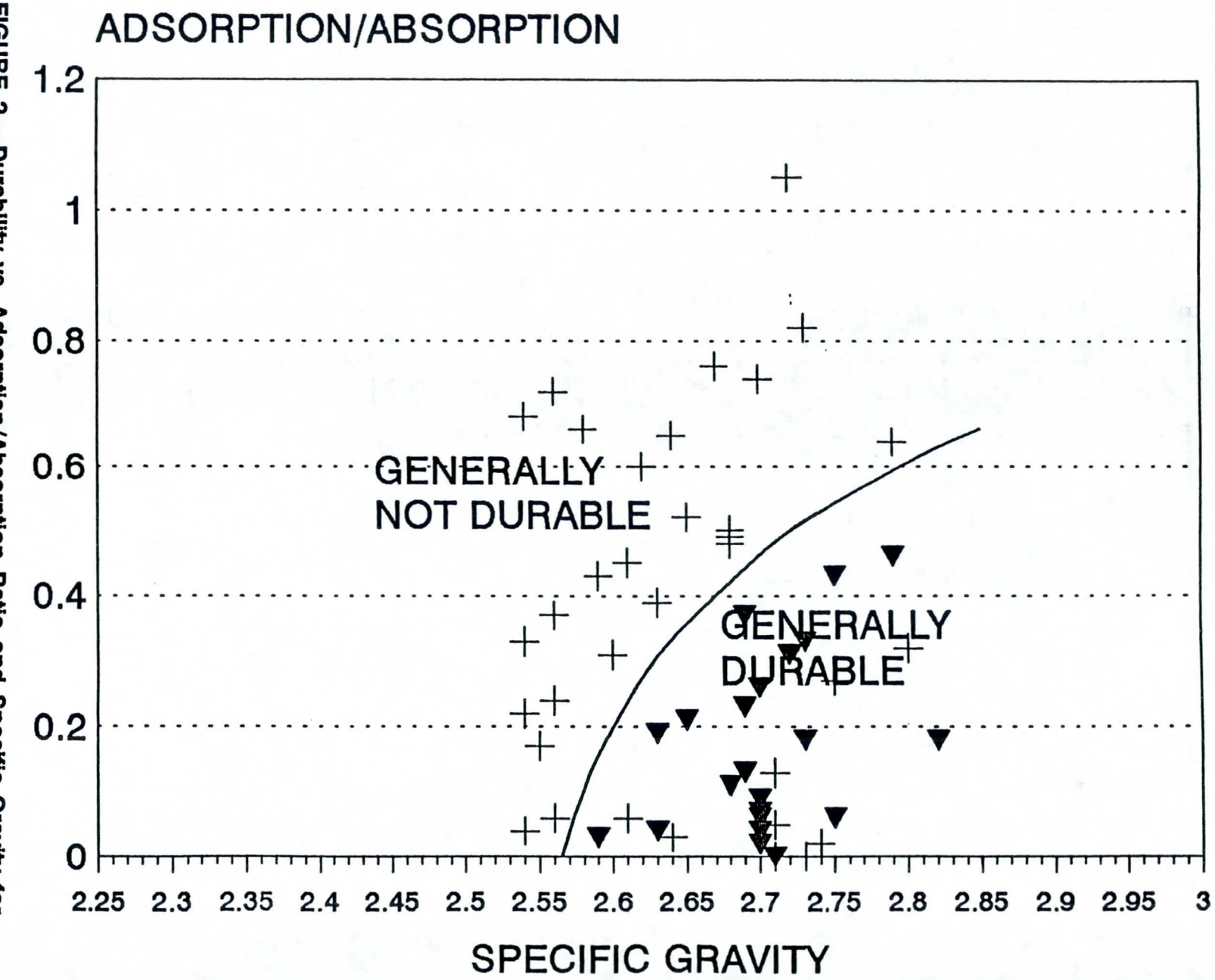

FIGURE 2 - Durability vs. Adsorption/Absorption Ratio and Specific Gravity for Limestones

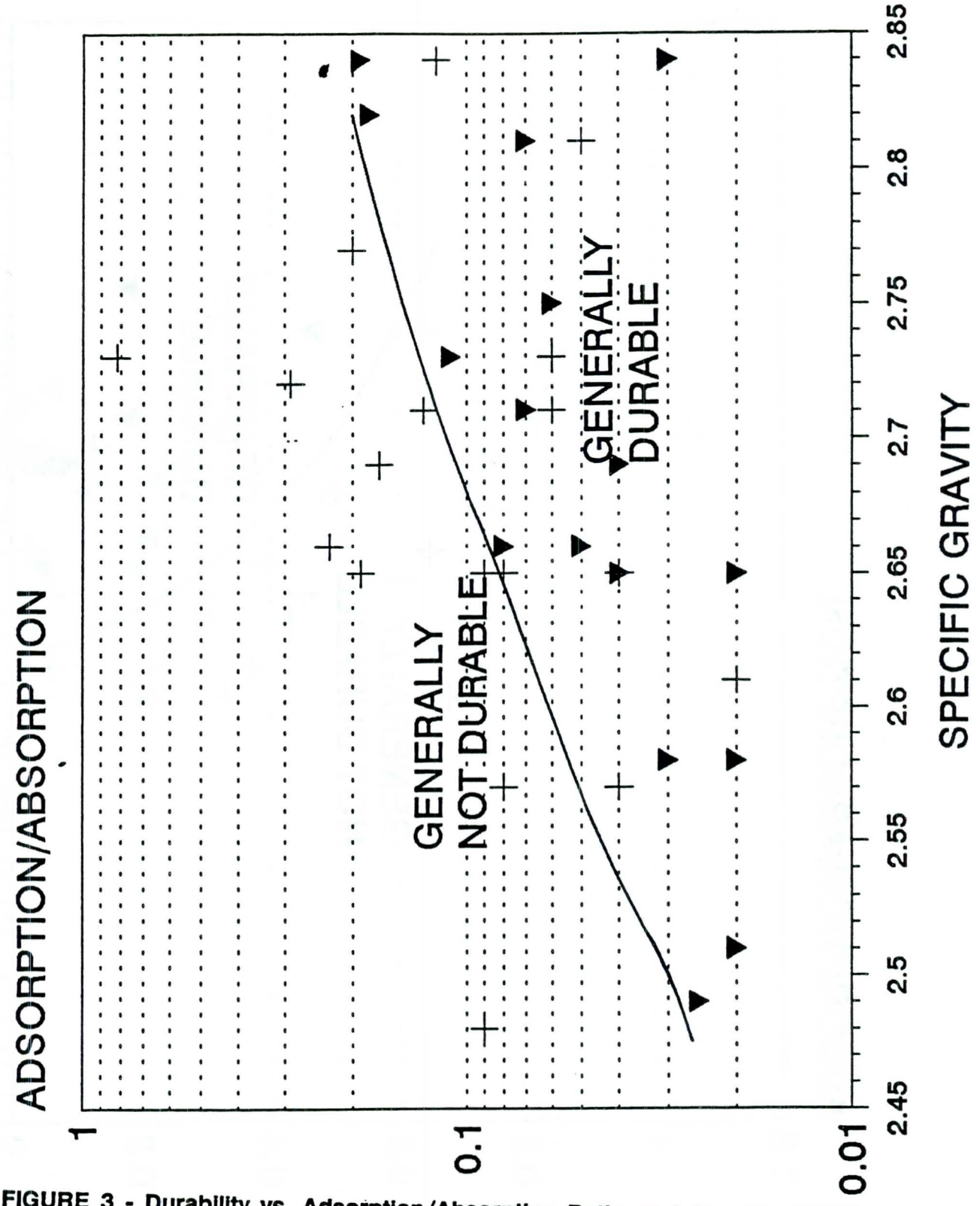

FIGURE 3 - Durability vs. Adsorption/Absorption Ratio and Specific Gravity for Dolomites

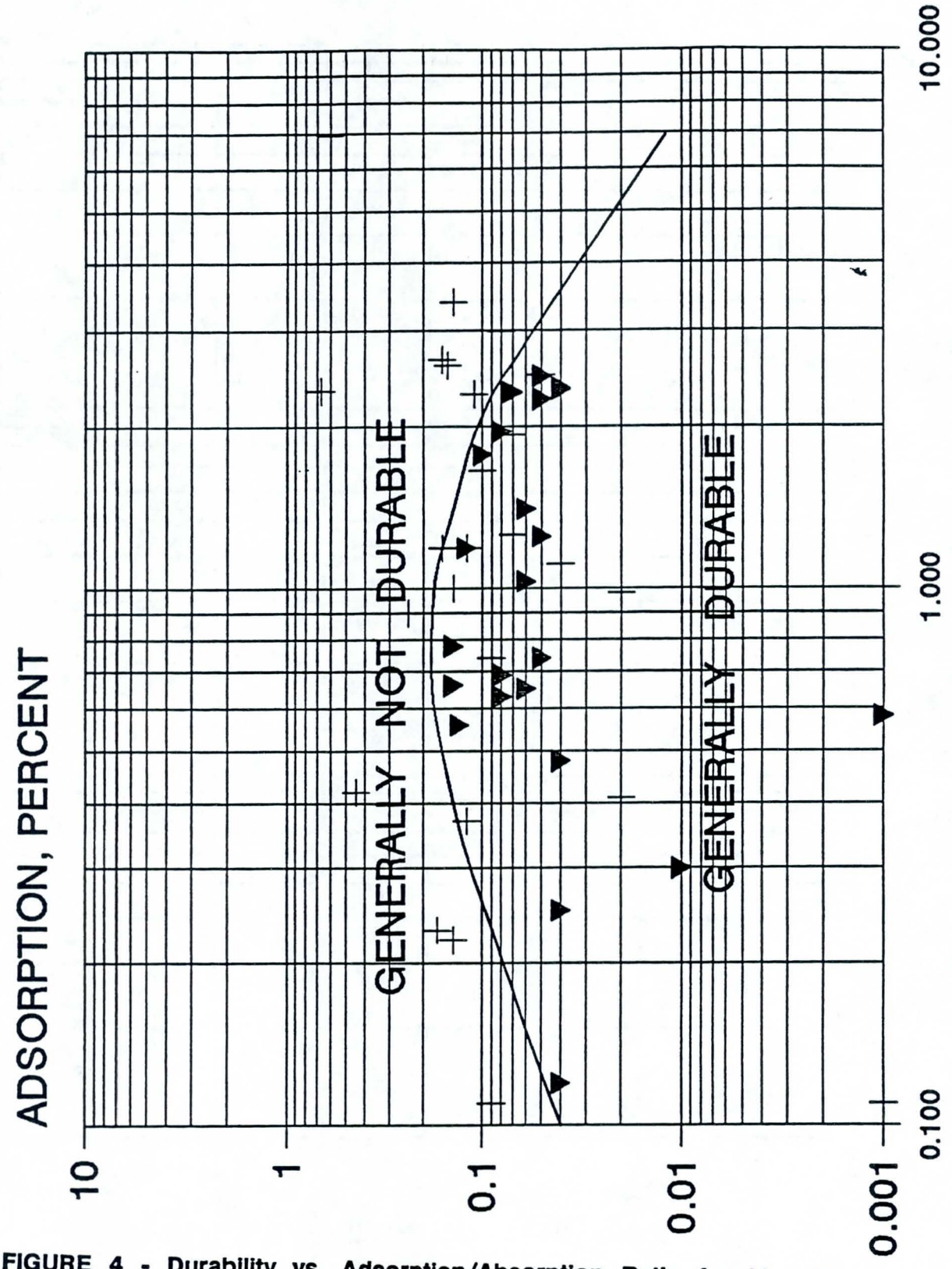

FIGURE 4 - Durability vs. Adsorption/Absorption Ratio for Limestones and Dolomites

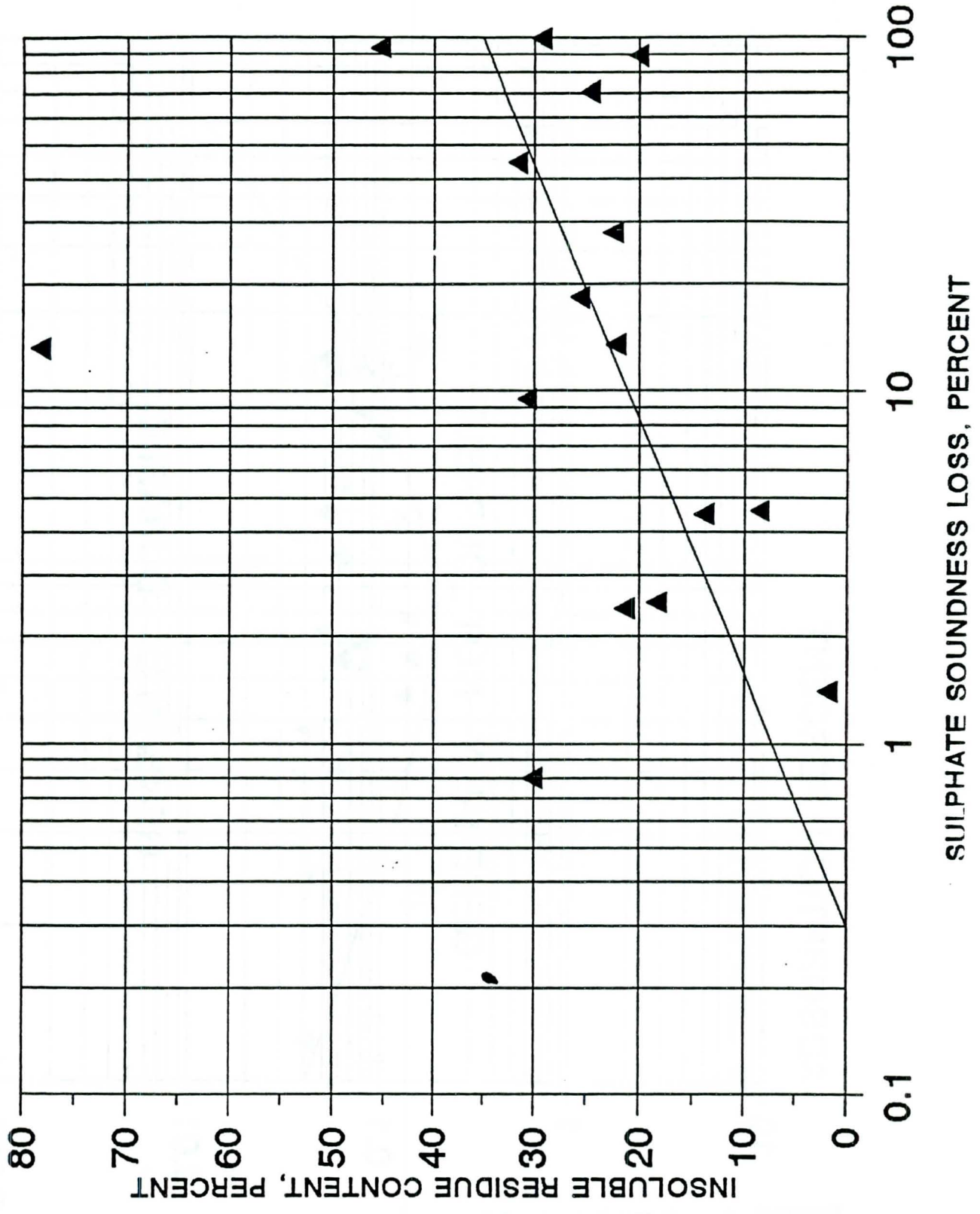

FIGURE 5 - Insoluble Residue Content vs. Sulphate Soundness Loss for Limestones

INFLUENCE OF BANK MATERIAL SIZE ON JUVENILE SALMONID USE OF REARING HABITAT

D.B. Lister
D.B. Lister & Associates Ltd, Sardis, Canada
R.J. Beniston
R.J. Beniston & Associates, Port Coquitlam, Canada
R. Kellerhals
Kellerhals Engineering Services Ltd, Heriot Bay, Canada
M. Miles
M. Miles and Associates Ltd, Victoria, Canada

ABSTRACT

Bank characteristics are an important determinant of habitat suitability for stream-rearing salmonid juveniles. Assessment of the effects of habitat alteration in two southern British Columbia streams, the Thompson and Coldwater rivers, included comparisons of juvenile salmonid densities along banks of large (> 30 cm mean diameter) and small (≤ 30 cm mean diameter) riprap, and natural cobble-boulder material. At Thompson River, large riprap supported higher chinook salmon (*Oncorhynchus tshawytscha*) and steelhead trout (*O. mykiss*) densities than small riprap and cobble-boulder banks during summer and winter. At Coldwater River in summer, chinook, steelhead and hatchery-reared coho salmon (*O. kisutch*) densities were greater along large riprap than small riprap banks, but wild coho exhibited no preference. Measures taken to roughen riprap banks at Coldwater River, by placing large (1-1.5 m diameter) boulders along the toe of the bank, appeared to increase rearing densities of all salmonids except underyearling steelhead. Underwater observations at Thompson River indicated the attractiveness of large riprap to salmonids resulted from the numerous eddies and shear zones created along the shoreline. The most suitable banks for juvenile salmonids were relatively steep, contained large material, and were constructed in a way that maximized roughness. Implications of these findings for design and construction of riprap banks are discussed.

INTRODUCTION

Bank characteristics are recognized as an important aspect of juvenile salmonid fish rearing habitat in streams (White and Brynildson, 1967; Murphy et al. 1986). Natural bank features such as vegetation provide cover, shading and insect food for stream-dwelling salmonids (Platts, 1991). Though man-made riprap bank protection is a common feature along streams, there has been limited quantitative assessment of either its impact on fish habitat suitability or methods to increase its value for fish rearing.

This paper describes the results of studies that examined salmonid fish rearing along essentially unvegetated banks of riprap and natural cobble-boulder material. While the focus is on the influence of bank material size, factors such as stream depth and velocity are also considered. These investigations were part of environmental impact assessments for two major linear development projects in British Columbia, the CN Rail twin tracking program (FEARO, 1985) and construction of the Coquihalla Highway (Andrew, 1991).

STUDY AREAS

The principal study area was the Thompson River, the largest tributary of the Fraser River, in the southwest interior of British Columbia. Studies were conducted in a 100 km section between Kamloops Lake and Spences Bridge, where the wetted channel is 100 - 200 m wide and carries a mean annual discharge of 775 m^3/s (Water Survey of Canada, 1989). Mean monthly discharge ranges from 215 m^3/s in February to 2350 m^3/s during the snow-melt freshet in June. The climate is arid in the study section and river bank vegetation is sparse. A 39 km section of the upper Coldwater River, a tributary in the Thompson River system, was also a study area. Mean annual discharge of the Coldwater River is 6.7 m^3/s and mean monthly flows range from 2 m^3/s in February to 24.8 m^3/s in June (Water Survey of Canada, 1989). Wetted width averages 12 m at a summer low flow of 1 m^3/s.

Both study streams support a variety of salmonid and non-salmonid fish species. Thompson River study sites were used for rearing and overwintering primarily by juvenile chinook salmon (*Oncorhynchus tshawytscha*) underyearlings (age 0) and rainbow-

steelhead trout (*O. mykiss*) parr (age 1-3). As the rainbow-steelhead population in the Thompson River is comprised of both freshwater resident rainbow trout and anadromous steelhead trout, which could not be readily separated in the field, the term *steelhead* is used here for simplification. In addition to chinook and steelhead, the Coldwater River supported a population of wild coho salmon (*O. kisutch*) and hatchery-reared coho salmon that had been planted in the river at the juvenile stage.

At Thompson River, the study compared fish use of riprap and natural cobble-boulder banks, both essentially unvegetated, along a railway embankment. Riprap protection of the embankment had been placed by side-dumping from railway cars. The original bank protection has been augmented over a period of approximately 70 years by side-dumped placements of larger riprap at eroding sites. As a result of these practises, riprap size varies greatly from site to site (Fig. 1), and vertical sorting has caused the larger material to occur at the toe of slope. Bank slopes are in the order of 1.5 h to 1 v or steeper. Bank height, measured from river surface to railway grade, averages approximately 8 m at low river flow.

At Coldwater River, riprap bank protection was placed at sites where the new highway embankment encroached on the stream channel or the channel had been diverted. Riprap pieces were placed individually with construction equipment. The riprap was keyed in to the stream bed to prevent undermining by scour. Measured D_{50} and D_{85} of the riprap averaged 59 cm and 99 cm respectively (M. Miles and Associates, 1992). Bank slopes approximated 1.5 h to 1 v. At two study sites, individual large (100 - 150 cm diameter) boulders were placed along the toe of the bank as part of a program to enhance fish habitat.

METHODS

The general study approach was to compare juvenile salmonid densities along unvegetated stream banks which differed in type and size of material. Field work at Thompson River was conducted in 1987 at high flow (mean discharge 600 m^3/s) during June 22 - July 2, at medium flow (mean discharge 450 m^3/s) during August 22 - September 10, and at low winter flow (175 m^3/s) during March 3-9, 1985.

Daytime water temperature ranges were recorded at 13 - 17°C, 17 - 19°C and 0.5 - 1°C during these respective periods. The Coldwater River field work concerning riprap size was conducted under summer low flow conditions (1 m^3/s) during August 22 - September 10, 1988. Recorded water temperatures ranged from 7.5 to 20.5°C. Additional data relating to boulder placements were obtained from field work during the same season in 1986, 1987, and 1988.

Fish densities were documented in the Thompson River along banks with no vegetative cover and composed of natural cobble-boulder material or protected with riprap classed as either small riprap, with median diameter (D_{50}) of 30 cm and less, or large riprap with D_{50} exceeding 30 cm. At Coldwater River, fish densities were compared at unvegetated banks of large and small riprap categorized in the same manner as at Thompson River. Bank material size (D_{50} and D_{90}) was estimated visually at individual study sites in both river systems. Size of material along the water line was estimated at the time of each fish population census, because estimated diameter varied with water level due to vertical sorting of material. Comparison of visual estimates with actual measurements of riprap size at individual sites indicated a positive bias in visual estimates at Thompson River (Kellerhals et al. 1989), but close correspondence between the two methods at Coldwater River (M. Miles and Associates, 1992). For this study, it was assumed that the visual method provided valid estimates of relative bank material size within a river.

Field surveys at Thompson River in 1987 involved paired comparisons of fish density at sites with banks of large riprap, small riprap and cobble-boulder material (Table 1). Sites in a given pair were generally situated within 3 km and sampled within the same 24 h period. As velocity was known to influence salmonid habitat selection in the Thompson River (Beniston et al. 1985), each site of a particular bank type was paired with one of another bank type in the same velocity category (Table 2). Fish were enumerated visually by a swimmer equipped with dry suit, mask and snorkel (Schill and Griffith, 1984). A single observer moved downstream and counted numbers of fish by species within 3 m of the river bank in the June survey, and within 5 m of the bank in the September survey (Fig. 2). Fish population estimates for a given site were based on the maximum number of fish observed in two passes along the site, which could vary from 25 to 110 m in length. Bank length surveyed in this manner totalled 3500 m and 5600 m in June

and September respectively. Water velocity and depth were also documented at a representative point along each enumeration site. Measurements taken at 1 m intervals between 1 and 5 m from shore were used to calculate mean depth and velocity for the site. Velocity at each measurement point was the average water column velocity estimated with a Marsh-McBirney Model 201 electromagnetic current meter set at 0.6 of the depth from the water surface.

The late winter study in the Thompson River involved 24 sites, including nine large riprap, four small riprap and 11 cobble-boulder sites totalling 430 m in bank length. As noted in previous winter studies (Edmundson et al. 1968), juvenile salmonids were hiding within the substrate during the day. A generator-powered DC electroshocker, without a net enclosure, was used to provide a fish population estimate for each site, based on the 2-step removal method (Seber and LeCren, 1967). Water velocity and depth were documented at each sampling site, but these factors were not included in this analysis.

Salmonid densities along 59 sites with large and small riprap banks were also compared during summer at Coldwater River. Fish were enumerated by DC electroshocker within a net enclosure, using the 2-step removal method (Seber and LeCren, 1967). Average water column velocity and depth were recorded at 1 m intervals along a single transect within each sampling unit. Another related study at Coldwater River involved assessment of juvenile salmonid use of two sites where large boulders had been distributed along the toe of a riprap bank to enhance fish rearing capability. Two pairs of sites, including test and reference sites, were studied in late summer of 1986, 1987 and 1988.

The detailed distribution of juvenile chinook and steelhead along 60 m of large riprap bank in the Thompson River was documented during September, 1987, to indicate how the fish were utilizing the hydraulic conditions created by individual pieces of riprap along the site. Locations of individual fish, or groups of fish, were recorded by a swimmer with mask and snorkel.

Statistical analyses were performed with the SPSS/PC+ computer program. The distributions of juvenile salmonid density estimates were non-normal, conforming more closely to a negative bimonial distribution, and included some zero values. Each density estimate was therefore log (x + 1) transformed to normalize variance

(Elliott, 1977). Mean fish densities cited in this paper are geometric means calculated from the log-transformed data. Analysis of variance (ANOVA) was used with the Student-Newman-Kuels test (Sokal and Rohlf, 1981) to compare differences between sample means. Relationships between fish density and physical habitat features were examined by multiple regression analysis. The non-parametric Wilcoxon signed-ranks test (Sokal and Rohlf, 1981) was used for all paired comparisons because of expected non-normal distributions.

HABITAT USE AND BANK TYPE

Thompson River

Juvenile chinook densities along banks in the Thompson River were positively related to bank material size, water depth and velocity in both June and September (Fig. 3). Steelhead parr exhibited a similar pattern (Fig. 4). Moderately strong and statistically significant ($P < 0.05$) correlations existed between fish density and the three physical variables, but there were also significant correlations ($P < 0.01$) between depth and velocity and bank size and velocity. The data were therefore subjected to multiple regression analysis to determine which physical variable had the most effect on habitat selection. Partial correlations between fish density and each physical parameter revealed that near-bank velocity had the most significant influence on chinook (partial $r = 0.26$; $P = 0.08$) and steelhead parr (partial $r = 0.38$; $P = 0.01$) density in June, and on steelhead parr density (partial $r = 0.67$; $P < 0.001$) in September. Chinook density in September was most strongly correlated with bank material size (partial $r = 0.58$; $P < 0.001$), and only secondarily with velocity (partial $r = 0.28$; $P < 0.05$).

Because of the predominant effect of velocity on habitat selection by chinook and steelhead, it was necessary to control for its effects in assessing the influence of bank type and material size on fish use of study sites. This was accomplished through paired comparisons of fish density at the three bank types (Tables 1 and 3), with each pair including only sites in the same velocity class (Table 2).

Considering the two species and study periods, seven of the eight paired comparisons between large riprap and the two other bank types showed large riprap to carry higher average salmonid densities (Fig. 5). The differences were greatest

in September, when large riprap supported significantly higher chinook densities than either cobble-boulder (Wilcoxon signed-ranks test; $P < 0.001$) or small riprap (Wilcoxon signed-ranks test; $P < 0.01$). Steelhead parr densities at large riprap in September were also significantly greater than at cobble-boulder sites (Wilcoxon signed-ranks test; $P < 0.01$). No consistent or significant differences in densities of the two species were evident in comparisons between small riprap and cobble-boulder banks, which were similar in material size (Table 3). The greater influence of bank size on habitat selection in September relative to June may have been related, at least in part, to an increase in bank material size along the water line (Table 3) due to the drop in river level and vertical sorting which results in the larger material concentrating at the toe of the bank.

A limited fish sampling effort in late winter indicated higher utilization of large riprap than either small riprap or cobble-boulder banks (Table 4). For chinook, large riprap supported a significantly higher density than the other bank types (ANOVA; $P < 0.05$). In the case of steelhead parr, however, the higher density at large riprap was not statistically significant (ANOVA; $P = 0.48$).

Coldwater River

Late summer densities of juvenile salmonids at Coldwater River were measured at sites with banks of either large or small riprap, but similar with respect to average water depth and velocity. Mean densities of chinook, hatchery coho and steelhead underyearlings and parr were greater at large than small riprap, but wild coho exhibited no apparent preference for bank type (Table 5). Differences in density of hatchery coho and steelhead parr at the two bank types were statistically significant ($P < 0.05$).

BOULDER PLACEMENTS ALONG RIPRAP

Large boulders, 1 - 1.5 m diameter, were placed along the toe of the riprap bank at two Coldwater River sites. These boulder placements were one of several instream structures used to enhance fish habitat at sites affected by highway construction (Miles et al. 1993). Six to eight boulders were spaced along 30 m of bank at each site to roughen the bank profile and increase habitat complexity for juvenile salmonids.

Mean densities of juvenile chinook, coho and steelhead parr were higher at the boulder placements than reference sites without boulders (Table 6). Only underyearling steelhead were unresponsive to the boulder placements. Differences in density at the two habitats were statistically significant ($P < 0.05$) for wild coho and steelhead underyearlings.

SALMONID BEHAVIOR AND STREAM BANK CHARACTER

In fast-flowing streams, drifting insects are usually the primary food source for salmonids (Chapman and Bjornn, 1969; Bachman, 1984). Rates of insect drift at a given point appear to be positively related to stream velocity (Everest and Chapman, 1972: Wankowski and Thorpe, 1979). Everest and Chapman (1972) observed that juvenile chinook salmon and steelhead trout selected stations that allowed them to hold in low or virtually zero velocity, usually near the stream bottom, but adjacent to a high-velocity flow. They postulated that such behavior maximized the quantity of drift food available to individual fish while minimizing energy expenditures needed to remain at the feeding station. Support for that hypothesis comes from artificial stream studies of juvenile coho salmon, brook trout (*Salvelinus fontinalis*) and brown trout (*Salmo trutta*) which showed that these species select feeding stations on the basis of water velocity characteristics and food supply, in a manner that tends to maximize net energy gain (Fausch, 1984).

In the present study, large riprap usually supported higher juvenile salmonid densities than banks composed of either natural cobble-boulder material or small riprap. Large riprap banks were distinguished by numerous small-scale irregularities resulting from the size of the material, its angular shape and, at Thompson River, the construction practise of side dumping which can cause some rocks to roll into positions several metres off the toe of fill. The associated bank irregularity or roughness produces numerous velocity shears and small eddies which can be exploited by salmonid juveniles. This was evident in a detailed study of one large riprap site in the Thompson River where juvenile chinook and steelhead parr occupied 20 separate locations along 60 m of bank (Fig. 6). The fish were associated with large pieces of riprap at every holding position, either within a downstream eddy or along the side or upstream face of a rock. Fish distribution

was also highly clumped, with 72% of all chinook observed at four locations including just 17% of total site length.

Juvenile chinook and steelhead in the Thompson River sought habitat with relatively high velocities. The river bank and bottom irregularities along large riprap apparently enabled these species to utilize high velocity sites, providing then with shelter from the strong flow (Shirvell, 1990) and, apparently, favourable conditions for exploiting insect drift food with a minimum of energy expenditure. The preference of Thompson River chinook and steelhead for large riprap in winter is consistent with the observed tendency of these species to seek relatively large boulder or rubble cover for overwintering in streams (Hartman, 1965; Edmundson et al. 1968; Bustard and Narver, 1975).

IMPLICATIONS FOR RIPRAP DESIGN

This study found that the most suitable river bank habitat for juvenile salmonids was relatively steep (1.5 h to 1 v), contained large rock, and had an irregular outside edge. The rough edge of riprap banks increased the complexity of local flow patterns and thus provided suitable micro-habitats for juvenile salmonids which preferentially reared in these ares. It should be stressed that the riprap investigated in this study had been either intentionally increased in size and irregularity in comparison to normal design practise (Coldwater River), or had been upgraded over time by side casting of large rock (Thompson River).

The above observations suggest that riprap embankments intended to provide habitat for juvenile salmonids should be constructed of coarser material than would be specified on the basis of commonly used design criteria (California Division of Highways, 1960; U.S. Army Corps of Engineers, 1969; RTAC, 1975). Also, the common practise of providing a smooth, hydraulically efficient riprap edge appears to be contrary to fish habitat requirements. The extensive placement of side-cast material or the construction of a *self launching apron* at the toe of a riprap slope may be beneficial to fish in deep water environments. In shallow water, however, this material can promote sediment accumulation and decrease effective bank material size. Our preference in these circumstances is to *key-in* riprap below the estimated scour level and place individual large rocks adjacent to the bank in a density and

configuration that minimizes the potential for near-bank sediment deposition. In high gradient rivers, the exposed rocks have to be very large to remain stable. Exposed rocks tend to collect debris which, while beneficial from a fish habitat perspective, may reduce hydraulic capacity unless the material dislodges at high flow.

CONCLUSIONS

It should be noted that replacement of vegetated natural stream banks with riprap can, in some cases, have a negative impact on habitat suitability for salmonids (Knudsen and Dilley, 1987). This study has indicated, however, that relatively inexpensive modifications to standard riprap specifications can significantly increase the fish habitat value of this material. Riprap designs for habitat enhancement must be carefully considered and based on both biological and hydraulic requirements. Investigation of rock sizes needed for stable placement of individually exposed boulders in various settings appears to be warranted. Patterns of habitat utilization by fish also need to be documented in different environments, as habitat requirements will vary from case to case, depending on species, life stage and other factors. No single design prescription will be appropriate for all situations.

ACKNOWLEGMENTS

The studies at Thompson River and Coldwater River were funded respectively by CN Rail, Edmonton, Alberta, and the British Columbia Ministry of Transportation and Highways, Victoria.

REFERENCES

Andrew, F.J. 1991. Cooperative efforts to protect salmonid habitat from potential effects of highway construction in British Columbia, p. 191-199. *In* J. Colt and R.J. White [ed.] Fisheries bioengineering symposium. Amer. Fish. Soc. Symposium 10.

Bachman, R.A. 1984. Foraging behavior of free-ranging wild and hatchery brown trout in a stream. Trans. Amer. Fish. Soc. 113: 1-32.

Beniston, R.J., D.B. Lister, and G.J. Naito. 1985. CN twin track project - juvenile salmonid rearing studies, Thompson River, 1984-85. Prepared for CN Rail, Edmonton, Alberta. 103 p.

Bustard, D.R., and D.W. Narver. 1975. Aspects of the winter ecology of juvenile coho salmon and steelhead trout. J. Fish. Res. Board Can. 32: 667 - 680.

California Division of Highways. 1960. Bank and shore protection in California highway practice. Documents Section, State of California, Sacramento.

Chapman, D.W., and T.C. Bjornn. 1969. Distribution of salmonids in streams, with special reference to food and feeding, p. 153-176. In T.G. Northcote [ed.] Symposium on salmon and trout in streams. H.R. MacMillan Lectures in Fisheries, Univ. of British Columbia, Vancouver.

Edmundson, E., F.H. Everest, and D.W. Chapman. 1968. Permanence of station in juvenile chinook salmon and steelhead trout. J. Fish. Res. Board Can. 25: 1453-1464.

Elliott, J.M. 1977. Statistical analysis of samples of benthic invertebrates. Freshwater Biol. Assoc. Sci. Publ. No. 25. Ambleside, Cumbria. 159 p.

Everest, F.H., and D.W. Chapman. 1972. Habitat selection and spatial interaction by juvenile chinook salmon and steelhead trout in two Idaho streams. J. Fish. Res. Board Can. 29: 91-100.

Fausch, K.D. 1984. Profitable stream positions for salmonids: relating specific growth rates to net energy gain. Can. J. Zool. 62: 441-451.

FEARO. 1985. CN Rail twin tracking program, British Columbia. Report of the Environmental Assessment Panel. Federal Environmental Assessment Review Office, Ottawa, Ontario. 51 p.

Hartman, G.F. 1965. The role of behavior in the ecology and interaction of underyearling coho salmon and steelhead trout. J. Fish. Res. Board Can. 22: 1035 - 1081.

Kellerhals, R., and D. I. Bray. 1971. Sampling procedures for coarse fluvial sediments. J. Hydraulics Div., Amer. Soc. Civil Engineers 97: 1165 - 1180.

Kellerhals Engineering Services, D.B. Lister & Associates and Sutek Services. 1989. A review of riprap measurements along the North Thompson, Thompson and Fraser rivers. Prepared for CN Rail, Edmonton, Alberta. 24 p.

Knudsen, E.E., and S.J. Dilley. 1987. Effects of riprap bank reinforcement on juvenile salmonids in four western Washington streams. N. Amer. J. Fish. Management 7: 351-356.

M. Miles and Associates. 1992. Coquihalla Highway: stability assessment of Coldwater River fisheries mitigation structures. Prepared for B.C. Ministry of Transportation and Highways, Victoria.

Miles, M., R. Kellerhals, and D.B. Lister. 1993. Stability of riprap structures to enhance fish habitat. Proceedings of the International Riprap Workshop. Fort Collins, Colorado.

Murphy, M.L., J. Heifetz, S.W. Johnson, K.V. Koski, and J.F. Thedinga. 1986. Effects of clear-cut logging with and without buffer strips on juvenile salmonids in Alaskan streams. Can. J. Fish. Aquat. Sci. 43: 1521 - 1533.

Platts, W.S. 1991. Livestock grazing, p. 387-423. *In* W.R. Meehan [ed.] Influences of forest and rangeland management on salmonid fishes and their habitat. Amer. Fish. Soc. Spec. Publ. 19.

RTAC. 1975. Guide to bridge hydraulics, C.R. Neill [ed.]. Road and Transportation Association of Canada. Univ. of Toronto Press, Toronto. 191 p.

Schill, D.J., and J.S. Griffith. 1984. Use of underwater observations to estimate cutthroat trout abundance in the Yellowstone River. N. Amer. J. Fish Management 4:479-487.

Seber, G.A.F., and E.D. LeCren. 1967. Estimating population parameters from catches large relative to the population. J. Anim. Ecol. 36: 631-643.

Shirvell, C.S. 1990. Role of instream rootwads as juvenile coho salmon and steelhead trout cover habitat under varying streamflows. Can. J. Fish. Aquat. Sci. 47: 852-861.

Sokal, R.R., and F.J. Rohlf. 1981. Biometry. 2nd ed. W.H. Freeman and Company, San Francisco. 859 p.

Wankowski, J.W.J., and J.E. Thorpe. 1979. Spatial distribution and feeding in Atlantic salmon juveniles. J. Fish Biol. 14: 239-247.

U.S. Army Corps of Engineers. 1969. State of knowledge of channel stabilization in major alluvial rivers. Committee on Channel Stabilization. Tech. Rep. No. 7, U.S. Army Engineer Waterways Experiment Station, Vicksburg, Mississippi.

Water Survey of Canada. 1989. Historical streamflow summary, British Columbia, to 1988. Environment Canada, Ottawa. 1056 p.

White, R.J., and O.M. Brynildson. 1967. Guidelines for management of trout stream habitat in Wisconsin. Wisconsin Dept. Nat. Resources Tech. Bull. 39. 64 p.

Table 1. Numbers of paired comparisons of juvenile salmonid density by bank type, Thompson River, 1987.

Survey period	Large riprap versus cobble	Large riprap versus small riprap	Small riprap versus cobble
June	10	9	8
September	17	12	10

Table 2. Water velocity criteria used in habitat classification for paired site comparisons, Thompson River, 1987.

Velocity Rating	Criteria
High	Surface water velocity of 50 cm/s less than 2 m from bank.
Moderate	Surface water velocity of 50 cm/s located 2 m or more from bank. Average velocity 1 - 5 m from bank is 10 - 47 cm/s.
Low	Surface water velocity of 50 cm/s located more than 5 m from bank. Average velocity 1 - 5 m from bank is less than 10 cm/s.

Table 3. Estimated bank material size at Thompson River study sites in June and September, expressed as the mean D_{50} and D_{90} for each category. Numbers of sites are given in Table 1.

	Bank D_{50} (cm)		
	Large Riprap	Small Riprap	Cobble-boulder
June	57	17	12
September	61	22	14
	Bank D_{90} (cm)		
	Large Riprap	Small Riprap	Cobble-boulder
June	79	27	17
September	102	61	22

Table 4. Mean density (number per 100 m) of chinook salmon yearlings and steelhead trout parr relative to Thompson River bank type in late winter. Ninety-five percent confidence intervals for the means are given in parentheses.[a]

	Large riprap (N = 9)	Small riprap (N = 4)	Cobble-boulder (N = 11)
Chinook	9.0 (2.4 - 33.8)	2.7 (0 - 17.4)	1.9 (1.0 - 3.6)
Steelhead	3.1 (1.3 - 12.9)	1.7 (3.1 - 8.8)	1.5 (1.2 - 2.8)

[a] Mean fork lengths of chinook and steelhead at study sites were 93 mm and 79 mm respectively.

Table 5. Comparison of juvenile salmonid densities and physical features at large (N = 39) and small (N = 20) riprap bank sites at Coldwater River. Asterisks denote a significant difference between large and small riprap (ANOVA; $P < 0.05$).

Bank Type	Mean number per 100 m[a]				
	Chinook	Coho		Steelhead	
		Wild	Hatchery	Underyearlings	Parr
Large riprap	100	6	27*	84	77*
Small riprap	68	8	4	52	40

	Physical features		
	Mean D_{50} (cm)	Mean depth at 3 m (cm)[b]	Mean velocity at 3 m (cm/s)[b]
Large riprap	55	49	20
Small riprap	26*	42	17

[a] Mean fork lengths of underyearlings were: chinook - 65 mm; wild coho - 48 mm; hatchery coho - 76 mm; and steelhead - 47 mm. Steelhead parr averaged 97 mm long.

[b] Measured at 3 m from bank.

Table 6. Comparative juvenile salmonid densities at Coldwater River riprap bank sites with and without nearshore boulder placements. Mean densities were derived from six paired comparisons of boulder placement and reference sites (without boulders). Asterisks denote significant differences between boulder placement and reference sites (Wilcoxon signed-ranks test; $P < 0.05$).

	Mean number per 100 m^2				
	Chinook	Coho		Steehead	
		Wild	Hatchery	Underyearlings	Parr
With boulder placement	44	14*	18	8*	20
Without boulder placement	34	8	4	14	15

Fig. 1. Riprap size distribution for railway embankment sites along the Thompson River system (N = 114). Sampling and measurement followed the grid by number technique described in Kellerhals and Bray (1971). Data are from Kellerhals et al. (1989).

Fig. 2. Swimmer with mask and snorkel enumerating juvenile salmonids along a riprap bank in the Thompson River.

Fig. 3. Juvenile chinook salmon density relative to bank material size, water depth and velocity at Thompson River study sites in June (N = 46) and September (N = 67). Mean fork length of chinook at study sites was 62 mm in June and 74 mm in September.

Fig. 4. Steelhead trout parr density relative to bank material size, water depth and velocity at Thompson River study sites in June (N = 46) and September (N = 67). Mean fork length of steelhead parr at study sites was 108 mm in June and 168 mm in September.

Fig. 5. Mean densities of juvenile chinook salmon and steelhead trout parr at large riprap, small riprap and cobble-boulder banks on the Thompson River in June and September, based on paired samples from the same velocity class.

Fig. 6. Distribution of juvenile chinook salmon and steelhead trout parr relative to individual pieces of riprap and current patterns along a Thompson River bank in September.

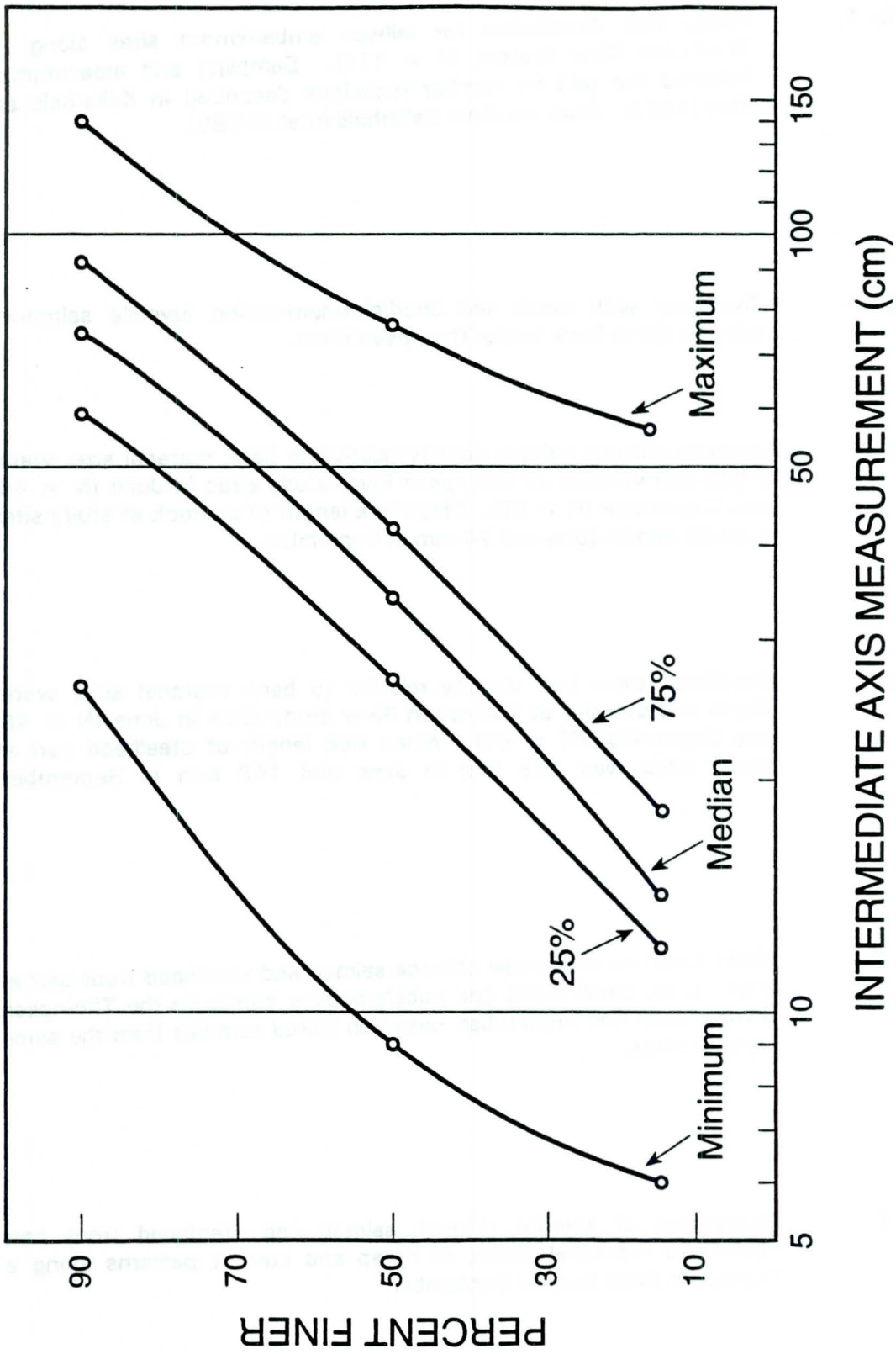
PERCENT FINER
90
70
50
30
10
5
10
50
100
150
INTERMEDIATE AXIS MEASUREMENT (cm)
Maximum
75%
Median
25%
Minimum

FIGURE 1

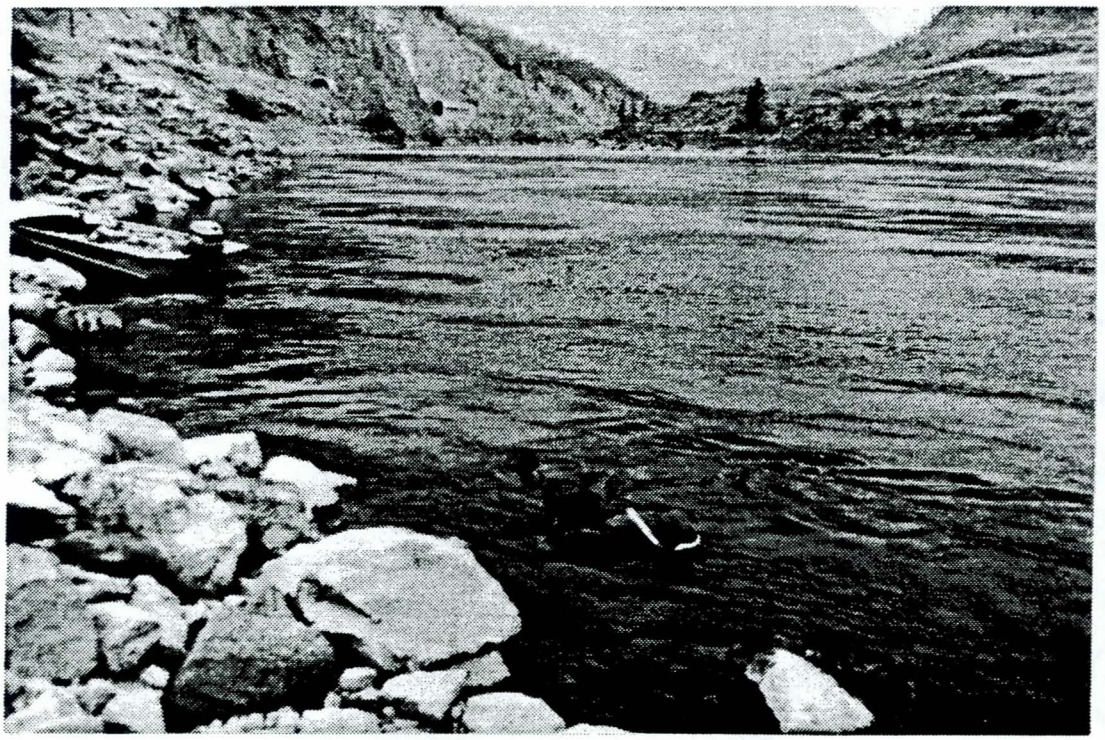

FIGURE 2

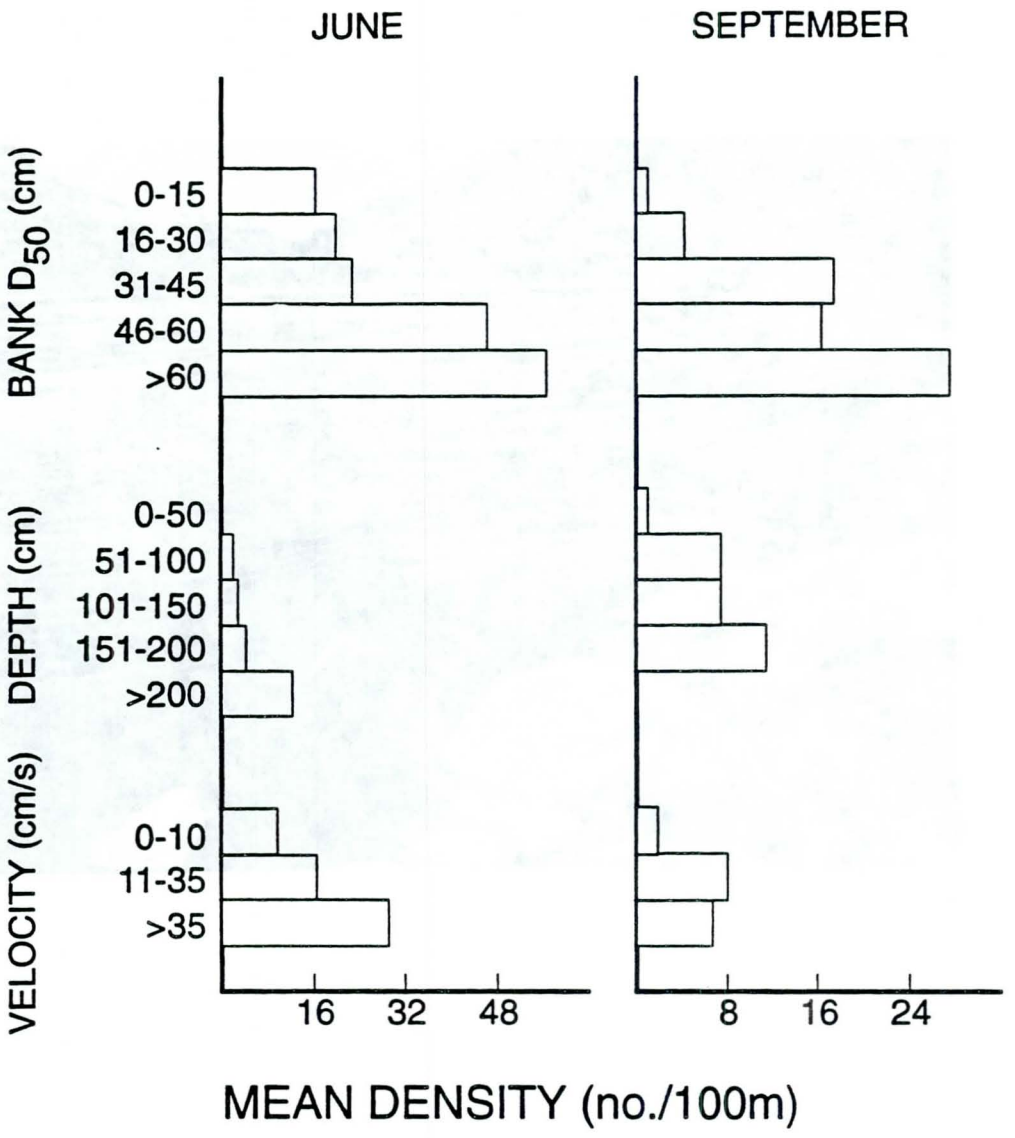
JUNE
SEPTEMBER
BANK D_{50} (cm)
0-15
16-30
31-45
46-60
>60
DEPTH (cm)
0-50
51-100
101-150
151-200
>200
VELOCITY (cm/s)
0-10
11-35
>35
16
32
48
8
16
24
MEAN DENSITY (no./100m)

FIGURE 3

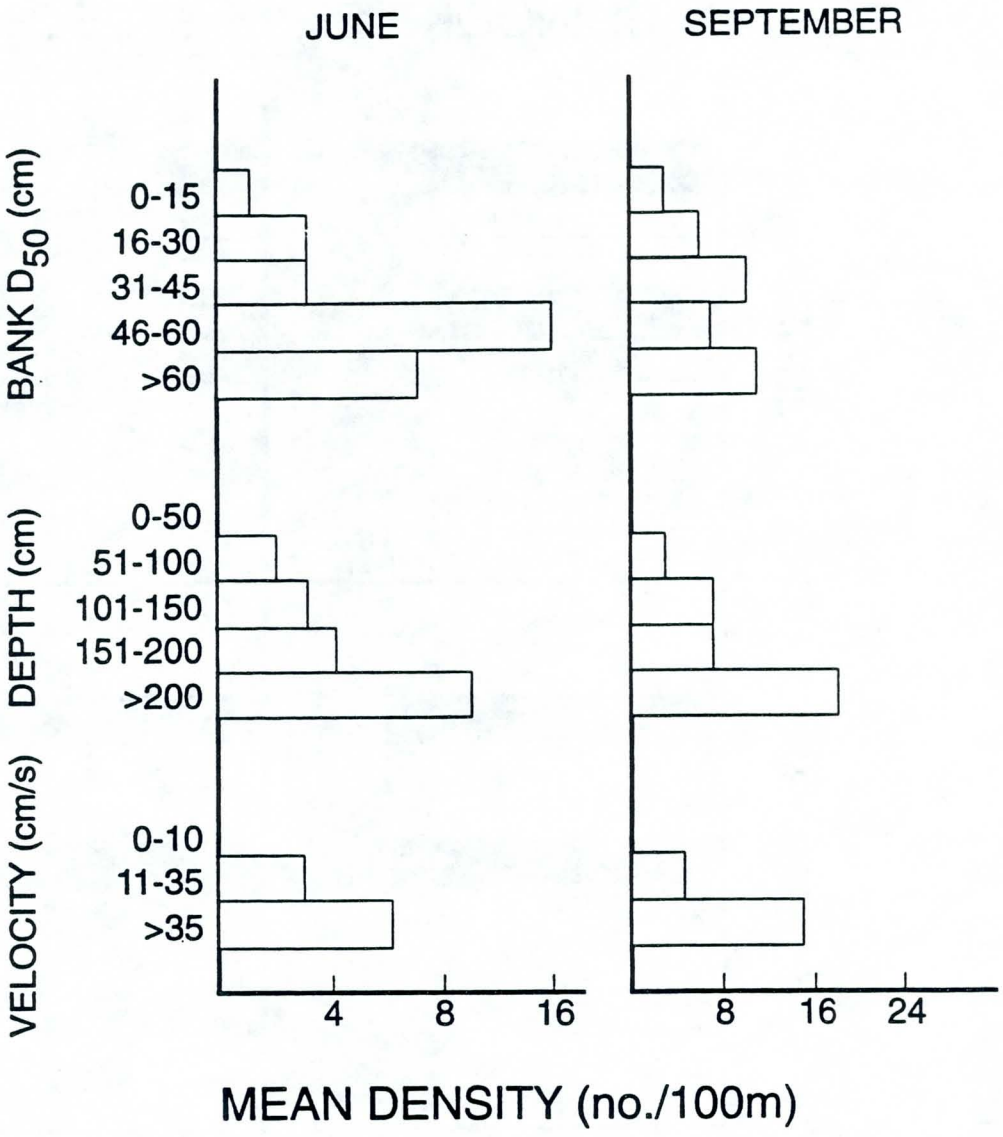
JUNE
SEPTEMBER
BANK D_{50} (cm)
0-15
16-30
31-45
46-60
>60
DEPTH (cm)
0-50
51-100
101-150
151-200
>200
VELOCITY (cm/s)
0-10
11-35
>35
4
8
16
8
16
24
MEAN DENSITY (no./100m)

FIGURE 4

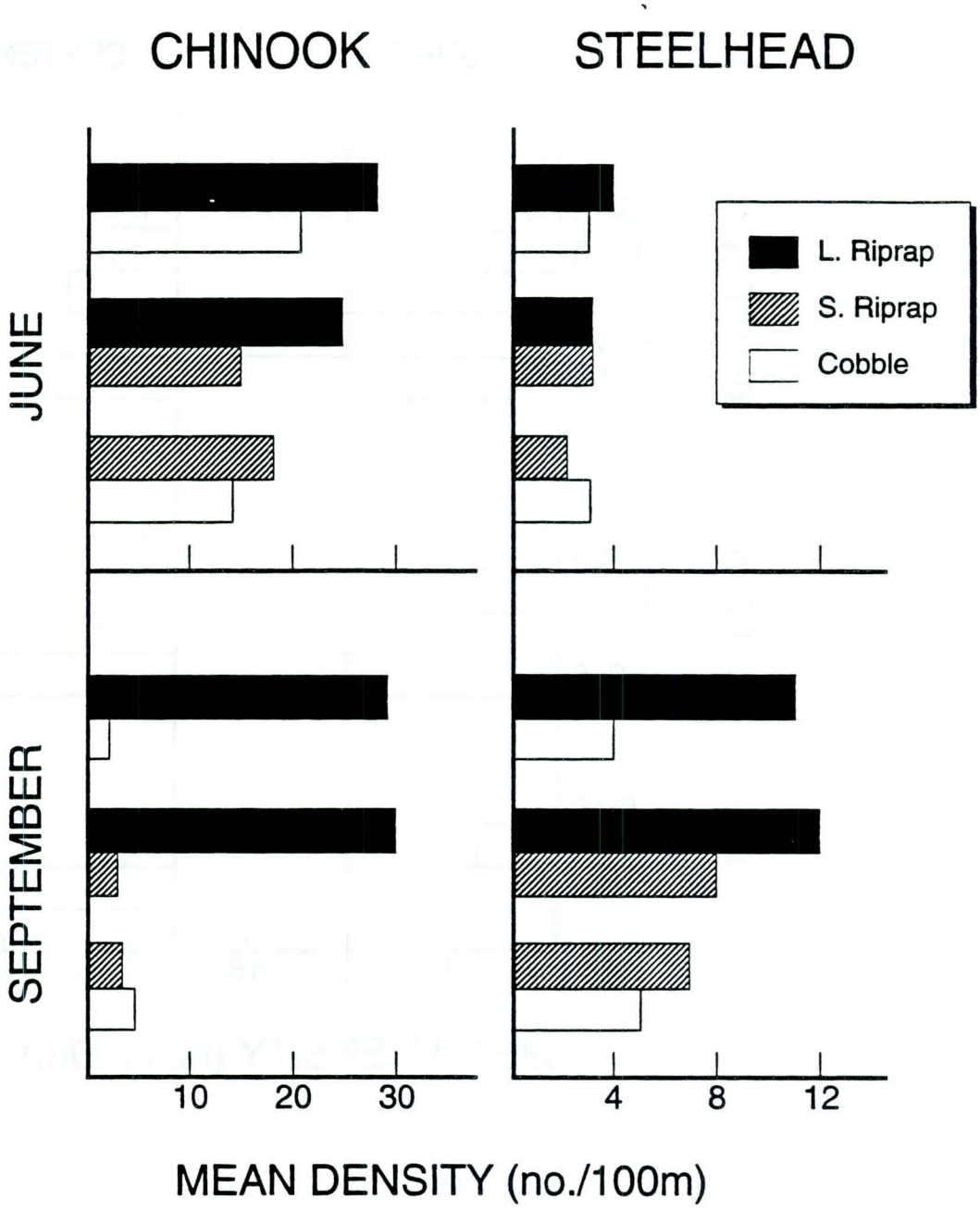
CHINOOK
STEELHEAD
L. Riprap
S. Riprap
Cobble
JUNE
SEPTEMBER
10
20
30
4
8
12
MEAN DENSITY (no./100m)

FIGURE 5

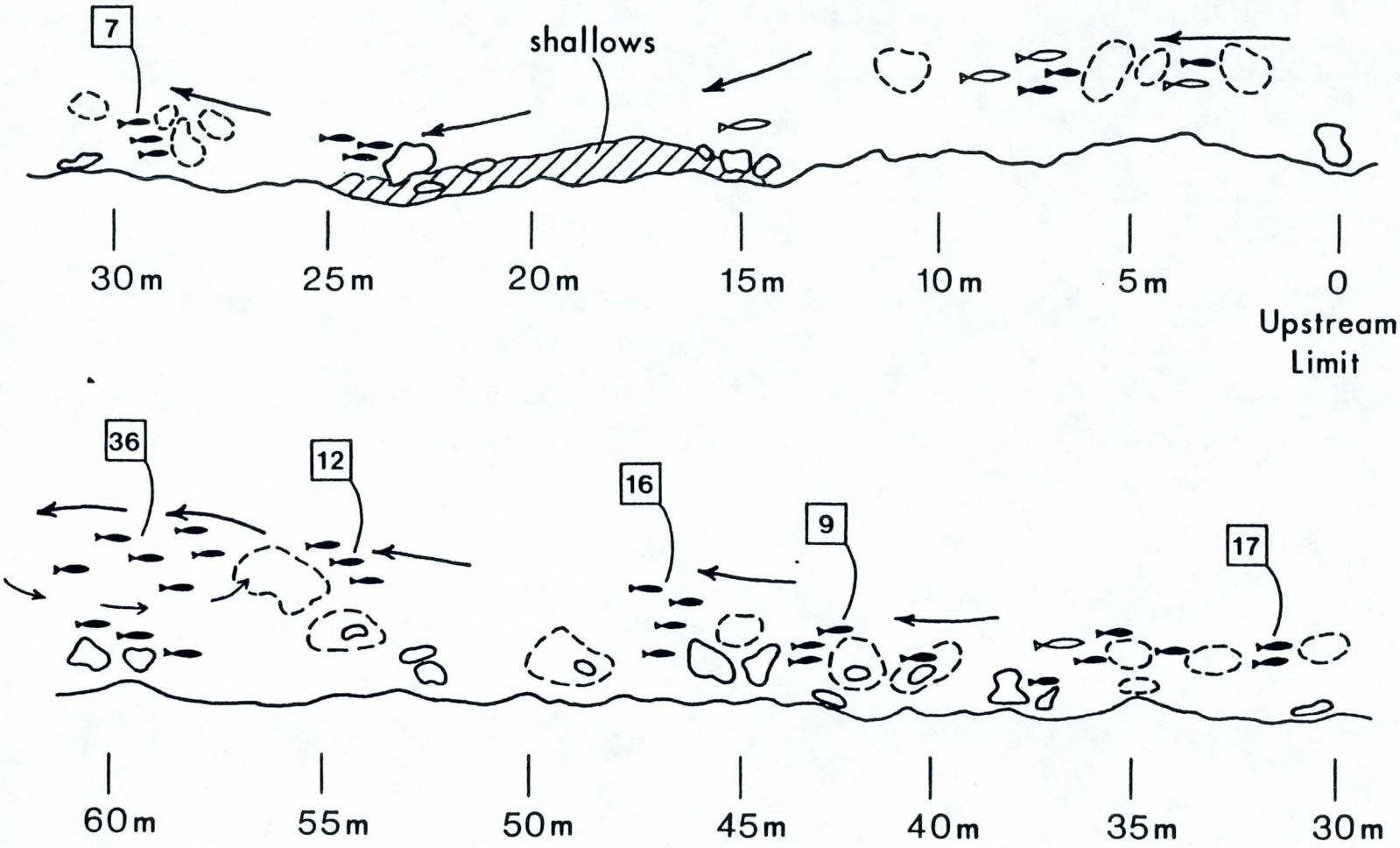

FIGURE 6

D.B. Lister

RUNDOWN VELOCITY ALONG THE SLOPE OF A BREAKWATER WITH AN ACCROPODE COVER LAYER

J.S. Mani
Ocean Engineering Centre, Madras, India
H. Oumeraci and M. Muttray
Franzius Institute, Hannover, Germany

ABSTRACT

Rundown velocity along the slope of a breakwater is one of the most important parameters in the design of the toe of the breakwater. Without adequate toe protection from erosion, the design of the breakwater is incomplete. Though a few small scale studies have reported about velocity measurements, unfortunately all of them were either for beaches or for surf zones. This paper details the experimental investigations conducted in regard to the rundown velocity along the slope of a breakwater at the large wave flume (GWK), Hannover, Germany.

The measurement on rundown velocity for the near prototype conditions was made possible because the wave flume facilitates generation of wave heights in the range of 0.20 to 2.0 m with wave period ranging between 3.0 and 12.0 seconds. The breakwater of interest was a rubble mound structure with an accropode armour layer. Two methods were adopted to determine the rundown velocity viz., (i) with a float and (ii) with a wave

gauge. the results on the variation of rundown velocity with Iribarren Number (ε) and wave steepness are presented in the form of non-dimensional graphs and discussed.

The studies indicated that the float method predicts a higher value of rundown velocity. (maximum velocity measured was of the order of 3.4 m/s) compared to the wave gauge method with a maximum value of 2.0 m/s. The experimental results strongly predicts the dependency of rundown velocity on wave period, in addition to wave steepness and Iribarren No. The trend curves of rundown velocity show a possible existence of an upper bound for the curves below which all trend curves lie irrespective of the wave period.

In addition a comparison between the present run-up results and that for rubble mound structure was made to support the applicability of results on rundown velocity for rubble mound structure.

Introduction

Rubble mound breakwaters are adopted for the protection of harbour basins, entrance channel to the harbour etc. These breakwaters were built in the world from ancient times, with the quarry stones of certain weight placed in a specific fashion to form a mound. With the advancement in the technology of development of harbours, navigation, shipping industry etc., it became inevitable to advance the techniques in the construction of rubble mound breakwaters. With the ever increasing demand for

the increase in draft by the ships calling at different ports, the construction of breakwaters in greater water depths became essential. The demand for increase in water depth warranted the design of the breakwater more critically, by considering all the disturbing forces that would challenge the stability of the breakwater.

In this context, various parameters which would destabilize the breakwater have been investigated by the scientists and engineers in the past. However, very few attempts have been made to determine the magnitude of the wave rundown velocity along the breakwater slopes which carry importance from the point of view of toe protection. A general formula for the determination of rundown velocity had been proposed by Brunn (1977) and referred by Jensen (1983) which are applicable for certain range of Iribarren number, there by limiting the applicability of the formula . A few small scale model studies have been reported (Kobayashi, et al, 1987; Battjes, Sakai, 1980; Stive, 1980; Nadaoka, Kondoh, 1982; Iwagaki et al., 1972; Iwagaki et al., 1974; Iwagaki et al., 1971) wherein the measurements related to vertical velocity variations either in the surf zone or along a beach slope are made and reported. A brief literature review suggested that the large scale measurement of rundown velocity along the breakwater slopes has not been attempted so far. As the rundown velocity is one of the critical parameters in the design of the toe of the breakwaters, large-scale tests have been conducted at the large wave flume, Hannover, Germany.

The study aimed at to determine the rundown velocity along a breakwater slope (1 : 1.5) comprising a layer of accropodes as armour blocks. Two methods were adopted to measure the rundown velocity viz., (i) with a float and (ii) with a wave gauge. As the waves were near similar to the prototype situation with wave heights from 0.2 to 2.0 m. and wave periods from 3.0 to 12.0 secs., it was possible to make a critical evaluation of rundown velocity. Non-dimensional graphs were made to study the variation of rundown velocity parameter ($Ruw/\sqrt{gh_t}$ or $Ruf/\sqrt{gh_t}$) with wave steepness, wave period and Iribarren No. (ε) and the results discussed.

EXPERIMENTAL SETUP AND FLUME CHARACTERISTICS

The experiments related to rundown velocity measurements were carried out in the large wave flume (measuring 320 m long, 5.0 m wide and 7.2 m. deep.), Hannover, Germany. Figure 1 shows the details of the wave flume. The wave flume is provided with a piston type wave generator capable of sensing the reflected wave amplitude and correct its stroke for the next incident wave so as to avoid multiple reflections in the flume. The details of the wave characteristics and the wave parameters that are possible with the wave generator and detailed in Table 1. The details of breakwaters for which the studies were conducted are shown in figure 2. The breakwater was made of rubble with the seaward side protected with an accropode armour layer. The front slope of the breakwater was 1 : 1.5. In order to avoid scouring during

the model tests, a geotextile had been provided in front of the toe of the breakwater with a slope of 1 : 50. The water depth at the toe of the breakwater was 3.10 m, and the water depth was 4.50 m. in the flume. Wave gauges were mounted in front and along the slopes of the breakwater for measurement of incident, reflected and transmitted wave heights, wave uprush and backwash. (Fig.2)

VELOCITY MEASUREMENT METHODS, ASSUMPTIONS AND LIMITATIONS

In order to measure rundown velocity, two approaches were adopted, the details of which are given below.

Velocity measurement by float:

To measure velocity, a spherical float 16 cm in diameter, light in weight (made out of thermocole) with eight compartments was fabricated to suit the breakwater. The details of the float are shown in figure 3. The measurement approach consisted of releasing the float at the instant when the rundown of wave was at its peak and recording the float path with the help of a camera (with shutter speed of 0.5 secs.) mounted on to a rigid platform fronting the breakwater. Figure 4a shows a usually observed flow field along the breakwater slope during wave rundown and the velocity vectors shown with figure give a relative magnitude of rundown velocity. Based on this flow field, an attempt has been made to derive the probable rundown

velocity variation along the breakwater slope (Fig.4b). With appropriate calibration (discussed later) both for the camera speed and measurement of travel distance of the float it was possible to determine the rundown velocity. For every input wave parameter, eight trials were conducted to check the correctness of the results.

Wave gauge method:

Simultaneous measurements were made using a wave gauge mounted along the seaward slope of the breakwater. From the time histories (Fig.5) of the wave uprush and backwash the rundown distance along the slope and the time difference between the crest and subsequent trough of the wave profile were obtained and velocity determined.

Calibration of camera speed and travel distance by float:

Camera speed:

The shutter speed for the camera was set to one half of a second, in order to measure peak rundown velocity. To check the camera speed photographs of a line marked on a strip chart paper were taken. The strip chart recorder was set to run at a speed of 60 cm/min. and the shutter speed for the camera set to one half of a second. The line marked on the strip chart produced a 5mm long black band in the photograph indicating correctness of the camera speed.

Calibration of travel distance by the float

As already indicated, the wave gauges were mounted on the seaward slope of the breakwater for measuring wave runup and rundown. One of the wave gauges was housed in a cage (mesh size 1 sq.in.) with every 50 cm. length painted alternately with yellow and blue colors. With the camera mounted on to a fixed platform and with parallax removed (so that the camera frame and cage are in the same plane)the photograph of the cage was taken. The distance of one yellow strip of the cage measured 9.07 mm in the photograph. This gave a calibration factor of 1 mm in the photo = 5.51 cm along the breakwater slope.

Assumptions

Following assumptions were made under the present studies:

1. Though, flow both during the rundown and runup of a wave cycle are unsteady, it is assumed that the flow is steady for a few seconds i.e 2 to 3 secs during rundown. A trapezoidal velocity-time history has been assumed for the rundown velocity (Fig. 4b).

2. The depth of flow (during rundown) along the breakwater slope remains constant, meaning that the water surface is parallel to the slope of the breakwater. (Fig 4a).

3. An uniform vertical velocity distribution prevails at any given point (between A and B) along the slope of the breakwater.

Limitations

Following are the limitations of the experimental results.

1. For very flat waves $\left((Hia/La) < 0.010\right)$ the measured rundown velocities are applicable near the still water level.
2. For steep waves $\left((Hia/La) > 0.010\right)$ the measured rundown velocities would provide a reasonable estimate, of the forces on the armour blocks in the vicinity of the toe of the breakwater.

3. It has been assumed that the velocity distribution over the depth of flow is constant (As the water depth along the breakwater slope is quite small ie.d <<< h (Fig.4a.)) during the rundown).

DATA MEASUREMENT AND ANALYSIS

Measurement of data:

For a given incident wave height and period the piston type wave generator was run to generate minimum of 150 waves. The wave heights sensed by the series of wave gauges (refer fig.2) and the wave gauges along the seaward slope of the breakwater were recorded on magnetic tapes using HP-2250 computer. The calibration factors for all the wave gauges were stored

separately on to an information file, for analysis. For each of the test run, the path traced by the float was photographed. A typical photograph showing the path traced by the float is given in photo 1.

Analysis:

Determination of incident and reflected wave heights:

Frequency and time domain analysis was carried out for the regular waves (to check the consistency of the results by changing the block size for the given set of data), using a programme called Analysis of Waves in Frequency and Time domain "ANWAFT". As the series of wave gauges in front of the break water recorded the incident plus the reflected wave heights, the incident and reflected wave heights were separated using the following procedure.

$$\text{Incident Wave Height } (H_{ia}) = (Hmax + Hmin)/2 \quad \text{-----(1)}$$

$$\text{Reflected Wave Height } (H_{ra}) = (Hmax - Hmin)/2 \quad \text{-----(2)}$$

Where Hmax and Hmin are the wave heights recorded in the region in which a series of wave gauges are positioned at an interval of 2 m.

Note:

The above procedure for determination of Hia and Hra was adopted when the wave length corresponding to water depth at the toe of the breakwater was less than or equal to 24m. (see fig.2 for the spacing of the wave gauges). For waves with wave lengths

larger than 24m, a separate set of data recorded by four wave gauges installed in front of the wave generator were adopted. Using a programme called ANIRW (Analysis of Incident and Reflected Waves), these data were analysed for determination of reflection coefficient.

Determination of run down velocities:

Rundown velocity with float:

From the photographs of flow path traced by the float the rundown velocity is obtained as follows.

Rundown velocity = ((Dfxcal) - D)/0.5 in cm/sec.

Where Df = Distance in mm traced by the float in the photo

Cal = calibration factor to determine actual distance.

Rundown velocity with wave gauge:

To determine rundown velocity with wave gauge mounted along the breakwater slope following expression was adopted.

Rundown velocity = [(Ru + Rd)/Sin (α)]/td in cm/sec.

Where Ru and Rd are wave runup and rundown height measured from still water level (fig.5).

α is the slope angle

td is the actual time taken by the water level to reach from its maximum to minimum (refer fig.4)

D = diameter of the float.

EXPERIMENTAL RESULTS

In the following paragraphs the findings of the experimental investigations are detailed and the discussions on the findings

are dealt with separately.

Variation of relative rundown velocity with wave steepness:

Figures 6 and 7 show the variation of relative rundown velocity with wave steepness (Hia / La) obtained under wave gauge and float measurements respectively. Based on data points, trend curves were drawn for actual wave periods ranging between 3 and 11.6 seconds. Non dimensionalising of wave period was not done intentionally as the wave periods generated in the channel match to the wave periods observed in the nature. This lead to a better interpretation of the results. Table 2 show a comparison of the magnitudes of relative rundown velocity obtained with float and wave gauge measurements.

In general both the figures and the table indicate the following:

1. Relative rundown velocity increases "exponentially" with an increase in wave steepness. For the range of wave steepness (0.004 - 0.007) the increase in relative rundown velocity is a function of wave period. For small wave periods (less than 5 secs.) a steady rise in relative rundown velocity is predicted, whereas for large wave periods (greater than 5 secs.) steep rise is observed. (Figures 6 & 7).
2. The relative rundown velocity obtained with floats consistently indicates a higher magnitude compared to those with wave gauge. The float predicts velocities which are 50 to 600 percent higher than the velocities with wave gauge (Table 2). This percentage increase is a function of wave steepness. For wave steepness less than 0.01 and T less than 5 sec., the percentage increase is of the order of 400

percent. For wave steepness greater than 0.01 and T greater than 3 secs. the percentage increase varies between 50 and 200 percent.

Variation of relative rundown velocity with Iribarren No.(ε):

Figures 8 and 9 show the variation of rundown velocity with Iribarren Number (ε) obtained with wave gauge and float respectively. Comparison of magnitude of relative velocities obtained with float and wave gauge for different ε values are given in Table 3.

Following are inferred from the above figures and the table.

1. Both methods of measuring velocities predict an "exponential decrease in relative rundown velocity with increase in ε 2.5 to 10.10.

2. The relative rundown velocity plot with wave gauge (fig 8) indicates that for ε greater than 8 there is no appreciable difference (of the order of 0.02, $\pm$ 0.005) in the magnitude of relative rundown irrespective of wave period. However this trend has not been indicated by the velocity plot (Fig 9) obtained with float.

3. Both the above plots indicate a substantial reduction in the magnitude of the relative rundown velocity (viz. of the order of 80 to 90%) for an increase in ε from 2.5 to 6.0. In addition, the trend curves appear to indicate that there is a possible upper bound beyond which further increase in

wave period does not influence the rundown velocity. In the present study the upper bound correspondto the wave period of T = 9 secs.

4. Table 3 indicates the magnitude of relative rundown velocity for different ε values obtained with both the methods discussed earlier. Comparison of magnitudes suggests that for small value of ε (less than 6), the float predicts a higher value of rundown velocity (by 70%) compared to wave gauge. For $6 < \varepsilon < 12$ the percentage increase is of the order of 50 to 100%. However when ε equal to 12, float predicts a lower magnitude for rundown velocity (by 60 to 90%) compared to wave gauge.

APPLICATION OF RESULTS FOR RUBBLE MOUND BREAKWATER

The run-up curve given in shore protection manual (1977) for a rubble mound structure with a slope of 1:1.5 was compared with that of present results for condition viz. $d_s/H_o' > 3.0$ (d_s : water depth at the toe of the structure and H_o' unrefracted wave height). The comparison is shown in figure 11. A fairly good agreement between the two trend curves suggests that the rubble mound structure with accropode cover layer would predict fairly the same run-up as that of rubble mound structure. As the slope of the structure is the same in both cases, it is quite reasonable to make an assumption that rundown would also be the same suggesting that rundown velocities determined in the present case can be applied for the rubble mound structures.

DISCUSSION ON THE RESULTS

The test results have shown consistently a higher value for the rundown velocity obtained with the float compared to that with wave gauge. Following are the probable reasons.

1. Peak velocities were measured by the float, as the float was released and its path recorded, when the rundown reaches its peak.

2. The top and bottom limits of the wave the rundown (recorded by the wave gauge) were considered in the calculation of rundown length along slope and corresponding duration was used to compute the rundown velocity. For certain incident wave climate the run down profile comprised of two portions viz.,
   a) a steep run down portion followed by
   b) a flat run down (Figure 10)

   Considering either (a) or (b) or both in the determination of rundown time makes the difference. As practicing engineers would be interested to know the peak rundown velocity which is quite important in the design aspect either for the armour block or for the blocks at the toe of the breakwater, it is recommended that the rundown velocities indicated by the float should be adopted as the velocities with wave gauges would give an average value.

This statement can be substantiated by the fact that for a given wave period of T = 3.9 secs. and wave steepness Hia/La of 0.063 figures 6 and 7 suggest that

a) With wave gauge a maximum $Ruw/\sqrt{gh_t}$ of 0.304 is obtained leading to a velocity of 1.67 m/s (Fig 6)

b) With float a maximum $Ruf/\sqrt{gh_t}$ of 0.570 is obtained giving a velocity of 3.14 m/s. (Fig 7)

PROTOTYPE APPLICATION OF THE RESULTS

Determine:

The run down velocity for a rubble mound breakwater for the following environmental conditions.

Wave height	= 3.0 m.
Wave period	=10.0 s.
Water depth	=12.0 m.
Seaward slope of the breakwater	= 1:1.5

Solution:

Determine the wave length La and Hia from Tables of functions given in the Shore Protection Manual (1977) for the deep water wave parameters. For the present case La is 99.6m and Hia is 2.88 m. For figure 7, for Hia/La = 0.029 and T = 10 secs the value of rundown velocity parameter is = $(Ruf/\sqrt{gh_t})$ = 0.545 and this leads to the rundown velocity of 5.90 m/s.

CONCLUSIONS

1. Relative rundown velocity increases exponentially with an

increase in wave steepness. For the range of wave steepness (0.004 to 0.077, the increase is a function of wave period. For small wave periods (less than 5 secs.) a steady rise in rundown velocity is predicted whereas for large wave periods (greater than 5 secs) a steep rise is predicted.

2. The relative rundown velocity obtained with floats consistently indicate a higher magnitude compared to those with wave gauge. For wave steepness less than 0.01 and T less than 5 secs., the percentage increase is of the order of 400 percent, however for wave steepness greater than or equal to 0.01 and T greater than 3 secs., the percentage increase varies between 50 and 200 percent.

3. A substantial reduction (of the order of 80 to 90%) in the magnitude of relative rundown velocity is predicted for an increase in ξ from 2.5 to 6.0. irrespective of the wave period.

4. The experimental trend curves for the variation of run down velocity either with Hia/La or ξ indicates that there is a possible upper bound below which all trend curves lie irrespective of the variation in wave period.

ACKNOWLEDGEMENTS

The study is part of an extensive research programme in breakwater within the Coastal Engineering Research Unit "SFB205" which is supported by the Germany Research council (DFG), Bonn.

The first author would like to express his sincere thanks to the authorities of IIT., Madras, and GTZ, Bonn for providing him an opportunity to visit Franzius Institute, Hannover. This enabled the author to conduct the experiments in Large Wave Flume at Hannover.

NOTATIONS:

Cal	: Calibration factor
D	: Diameter of the float
Df	: Distance traced by the float in photograph
d	: Depth of flow
d_s	: Water depth at the structure
g	: Acceleration due to gravity
H	: Wave height
Hia	: Actual incident wave height in front of the breakwater
Hra	: Reflected wave height
Hmax	: Maximum wave elevation corresponding to antinode
Hmin	: Minimum wave elevation corresponding to node
H_o'	: Unrefracted wave height
h	: Water depth
La	: Actual wave length in front of the breakwater
R	: Wave run-up
Rd	: Wave rundown
Ru (or)R	: Wave runup
Ruf	: Wave rundown velocity with float
Ruw	: Wave rundown velocity with wave gauge
T	: Wave period
Um	: Maximum rundown velocity
ξ	: Iribarren No. = $\tan\alpha / \sqrt{Hia/La}$
tan α	: Breakwater slope

REFERENCES:

Battjes, J.A., Sakai, T. (1980) : Velocity field in a steady breaker, 17th Coastal Engineering Conference Vol I, Australia pp 499-511

Brunn, P., Gunbak, A.R., (1977) : Stability of sloping structures in relation to tanβ/H/Lo. Risk criteria in design., Coastal Engineering1, pp 287-322.

Iwagaki, Y., Sakai, T., Kainuma, J., Kawashima, T. (1971) : Experiments on horizontal water particle velocity at water surface near breaking waves, Coastal Engineering in Japan, Vol 14, pp 15-23.

Iwagaki, Y., Sakai, T., Kawashima, T. (1972) : On the vertical distribution of water particle velocity induced by waves on beach. Coastal Engineering in Japan Vol 15, pp 35-41.

Iwagaki, Y., Sakai, T., Tsukioka, K., Sawai, N. (1974) : Relationship between vertical distribution of water particle velocity and type of breakers on beaches. Coastal Engineering in Japan, Vol 17, pp 51-58.

Jensen, O.J. (1983) : A monograph on rubble mound break waters. Published by Danish Hydraulic Institute, Denmark, Nov, pp 41.

Kobayashi,N., Otta,A.K., Roy,I (1987) : Wave reflection and run up on rough slopes. Jl. of .waterway, port, Coastal and Ocean Engineering., Vol 113, No.3 pp 282-298.

Nadaoka,K., Kondoh,T (1982) : Laboratory measurements of velocity field structure in the surf zone by LDV. Coastal Engineering in Japan Vol 25, pp 125-145.

Stive,M.J.F. (1980) : Velocity and pressure field of spilling breakers. Coastal Engineering Conference, Vol I, Australia pp 547-566.

Shore Protection Manual (1977): Published by U.S. Army Coastal Engineering Research Centre, U.S. Government Printing Office, Washington, D.C.

Table 1

CHARACTERISTICS OF THE WAVE FLUME

Sl.No.	Parameter	Range
1.	Length of channel	320 m
2.	Width	5 m
3.	Depth	7.2 m
4.	Water depth (max)	5 m
5.	Wave height	0.20 - 2.00
6.	Wave period	3.0 - 12.0
7.	Wave length $L_{4.5}$	12.7 - 69.0 m
8.	Wave length $L_{3.1}$	12.0 - 63.00 m
9.	Wave steepness H/L	0.0027- 0.077 m
10.	Iribarren No.(ε)	2.47 - 10.12 m

Table 2

RUN DOWN VELOCITIES WITH FLOAT AND WAVE GAUGE
FOR DIFFERENT WAVE STEEPNESSES

Hia/La	T sec	Ruw/$\sqrt{ght}$	Ruf/$\sqrt{ght}$	Ruw m/s	Ruf m/s	% increase
0.005	3.9	0.009	0.060	0.049	0.331	575
	4.8	0.020	0.095	0.110	0.524	376
	5.8	0.036	0.055	0.198	0.303	53
	7.6	0.030	0.045	0.165	0.248	50
	9.6	0.042	0.100	0.232	0.551	58
	11.6	0.041	0.090	0.226	0.496	119
0.01	3.0	0.022	0.065	0.121	0.358	196
	3.9	0.044	0.130	0.243	0.717	195
	4.8	0.058	0.150	0.319	0.827	159
	5.8	0.100	0.140	0.551	0.772	40
	7.6	0.092	0.150	0.507	0.827	63
	9.6	0.106	0.225	0.584	1.241	112
	11.6	0.085	0.205	0.468	1.130	141
0.025	3.0	0.093	0.160	0.513	0.882	72
	3.9	0.145	0.260	0.799	1.434	79
	4.8	0.197	0.310	1.086	1.710	57
	5.8	0.245	0.380	1.35'	2.096	55
	7.6	0.233	0.450	1.285	2.48	93
	9.6	0.271	0.505	1.494	2.78	86
	11.6	0.163	0.440	0.899	2.43	170
0.050	3.0	0.169	0.285	0.932	1.572	69
	3.9	0.267	0.455	1.472	2.510	70
	4.8	0.396	>1.000	2.184	>5.0	—
	5.8	0.435	0.650	2.399	3.58	49
	7.6	0.338	0.690	1.864	3.80	104
	9.6	0.470	0.730	2.592	4.03	55
	11.6	0.206	0.720	1.136	3.97	248

Table 3

RUNDOWN VELOCITIES WITH FLOAT AND WAVE GAUGES

FOR DIFFERENT ε VALUES

$\frac{\tan\alpha}{\sqrt{Hia/La}}$	T Sec.	$Ruw/\sqrt{ght}$	$Ruf/\sqrt{ght}$	Ruw m/s	Ruf m/s	% + or -
3.0	3.0	0.171	0.279	0.943	1.540	63
	3.9	0.260	0.470	1.43	2.59	81
	4.8	0.365	>1.0	2.01	>5.0	
	5.8	0.400	0.645	2.206	3.56	61
	7.6	0.298	>1.0	1.643	>5.0	
	9.6	0.362	>1.0	1.996	>5.0	
	11.6	0.270	>1.0	1.49	>5.0	
6.0	3.0	0.036	0.071	0.198	0.391	97
	3.9	0.066	0.158	0.364	0.871	139
	4.8	0.094	0.145	0.518	0.799	54
	5.8	0.128	0.212	0.706	1.169	65
	7.6	0.116	0.196	0.639	1.081	69
	9.6	0.141	0.292	0.777	1.610	107
	11.6	0.120	0.271	0.661	1.494	126
9.0	3.0	0.014	0.005	0.077	0.027	-65
	3.9	0.021	0.060	0.116	0.331	185
	4.8	0.031	0.045	0.171	0.248	45
	5.8	0.043	0.050	0.237	0.275	16
	7.6	0.041	0.062	0.226	0.342	51
	9.6	0.056	0.110	0.309	0.607	96
	11.6	0.044	0.106	0.243	0.584	140
12.0	3.0	0.006	0.002	0.033	0.011	-67
	3.9	0.011	0.014	0.061	0.077	26
	4.8	0.018	0.006	0.099	0.033	-66
	5.8	0.020	0.002	0.110	0.011	-90
	7.6	0.030	0.002	0.165	0.011	-93
	9.6	0.022	0.010	0.121	0.055	-54
	11.6	0.023	0.049	0.127	0.270	113

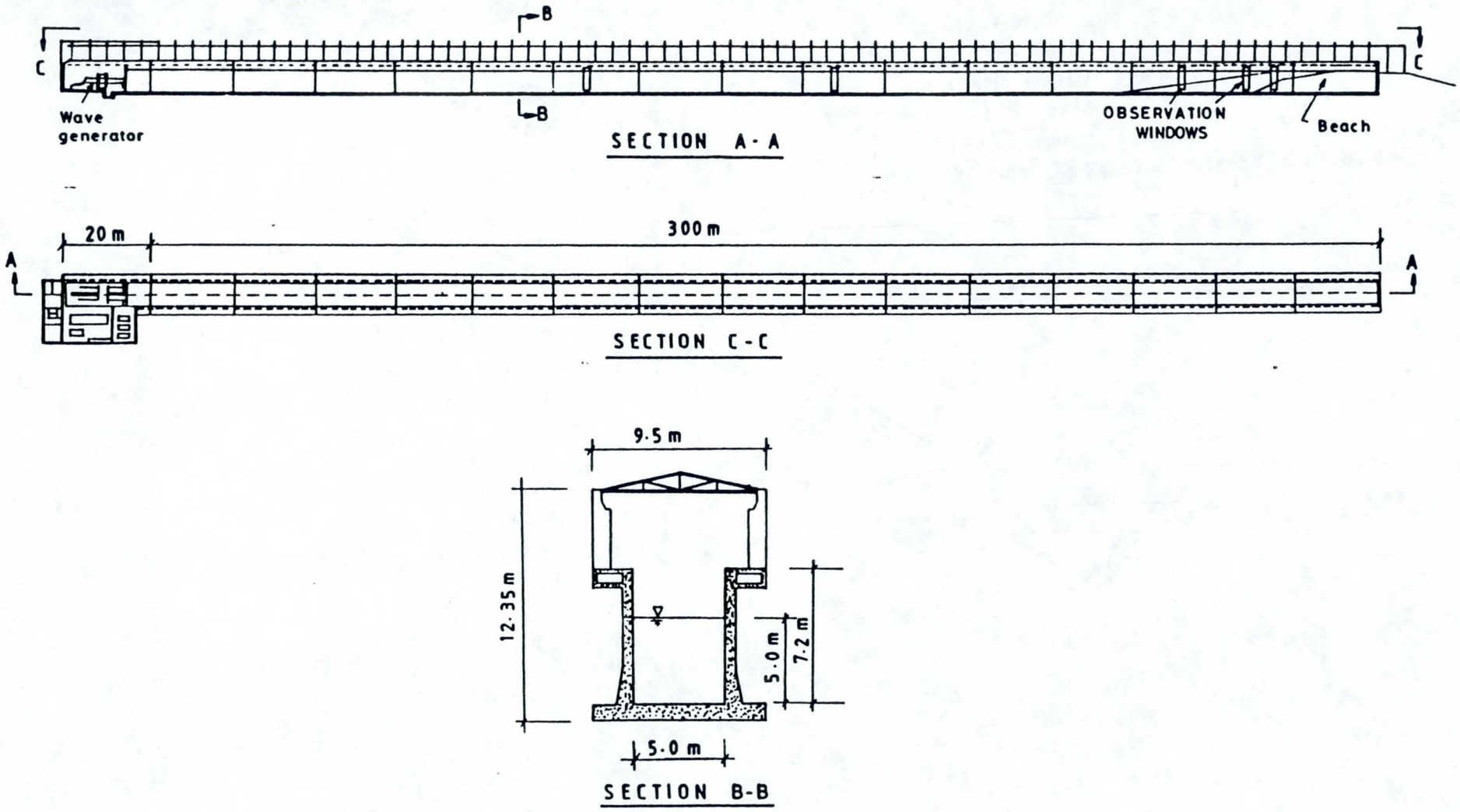

FIG. 1. DETAILS OF LARGE WAVE FLUME (GWK) AT HANNOVER GERMANY

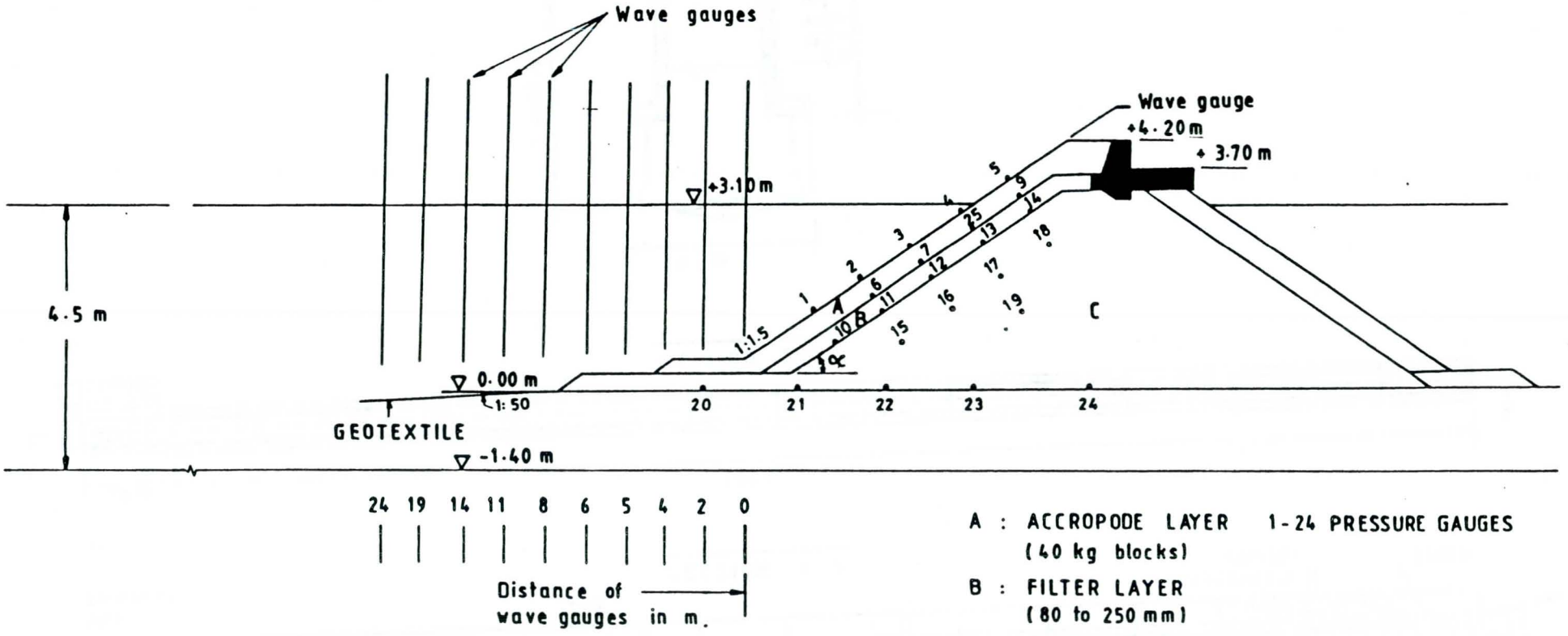

FIG. 2. SCHEMATIC DIAGRAM OF THE BREAKWATER AND WAVE GAUGE POSITIONS

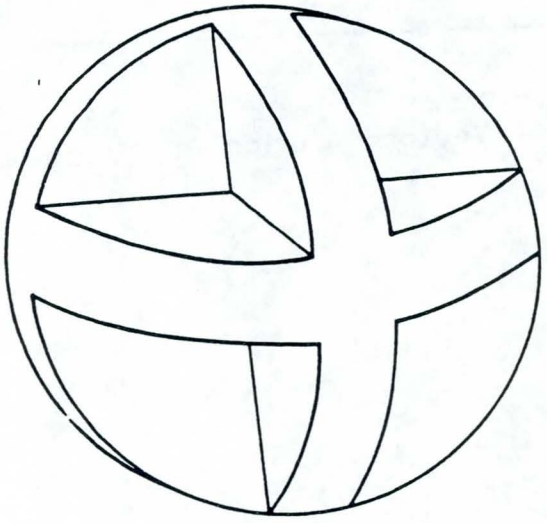

DIAMETER = 16 cm
WALL THICKNESS= 3 cm

FIG. 3. A VIEW OF THE FLOAT

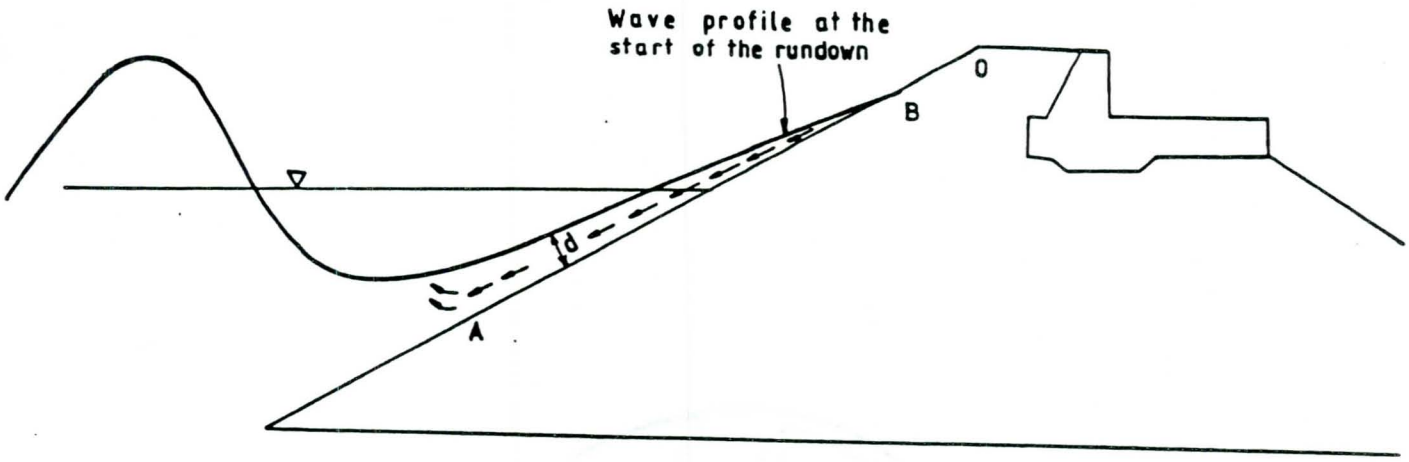

Fig. 4a. Velocity Vectors during a rundown

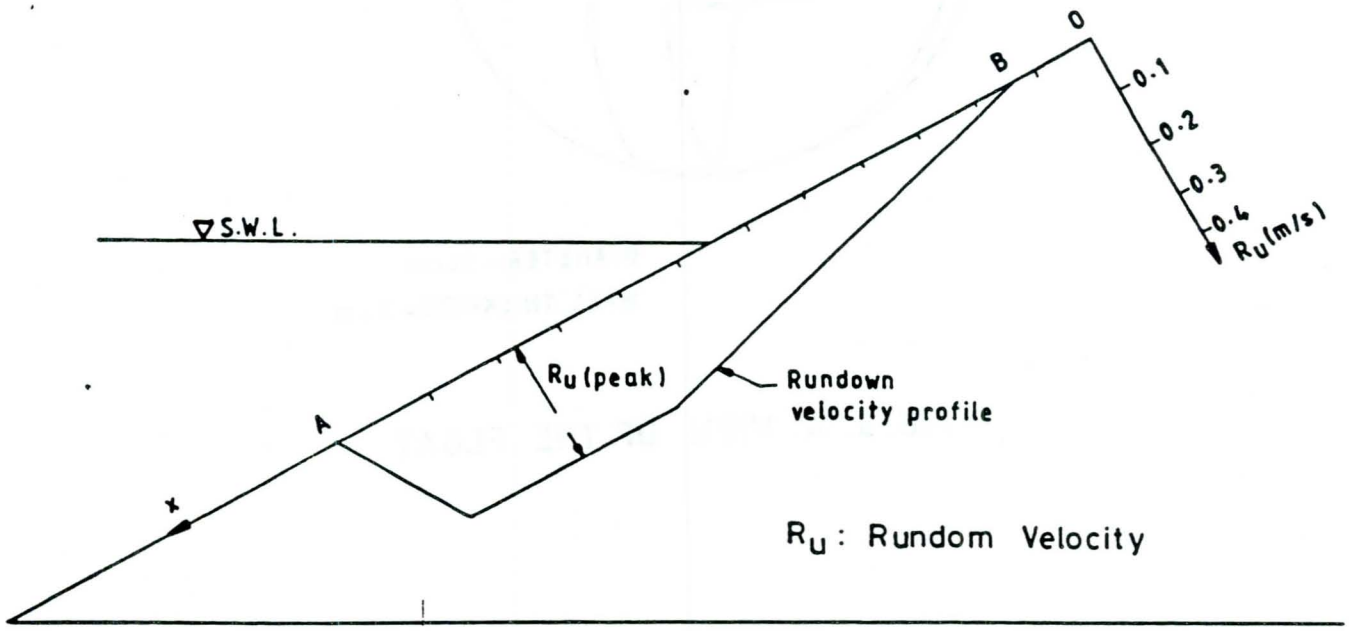

Fig. 4 b. Horizontal Velocity variation along the breakwater slope

FIG. 4. TYPICAL RUNDOWN VELOCITY PROFILE FOR STEEP WAVES

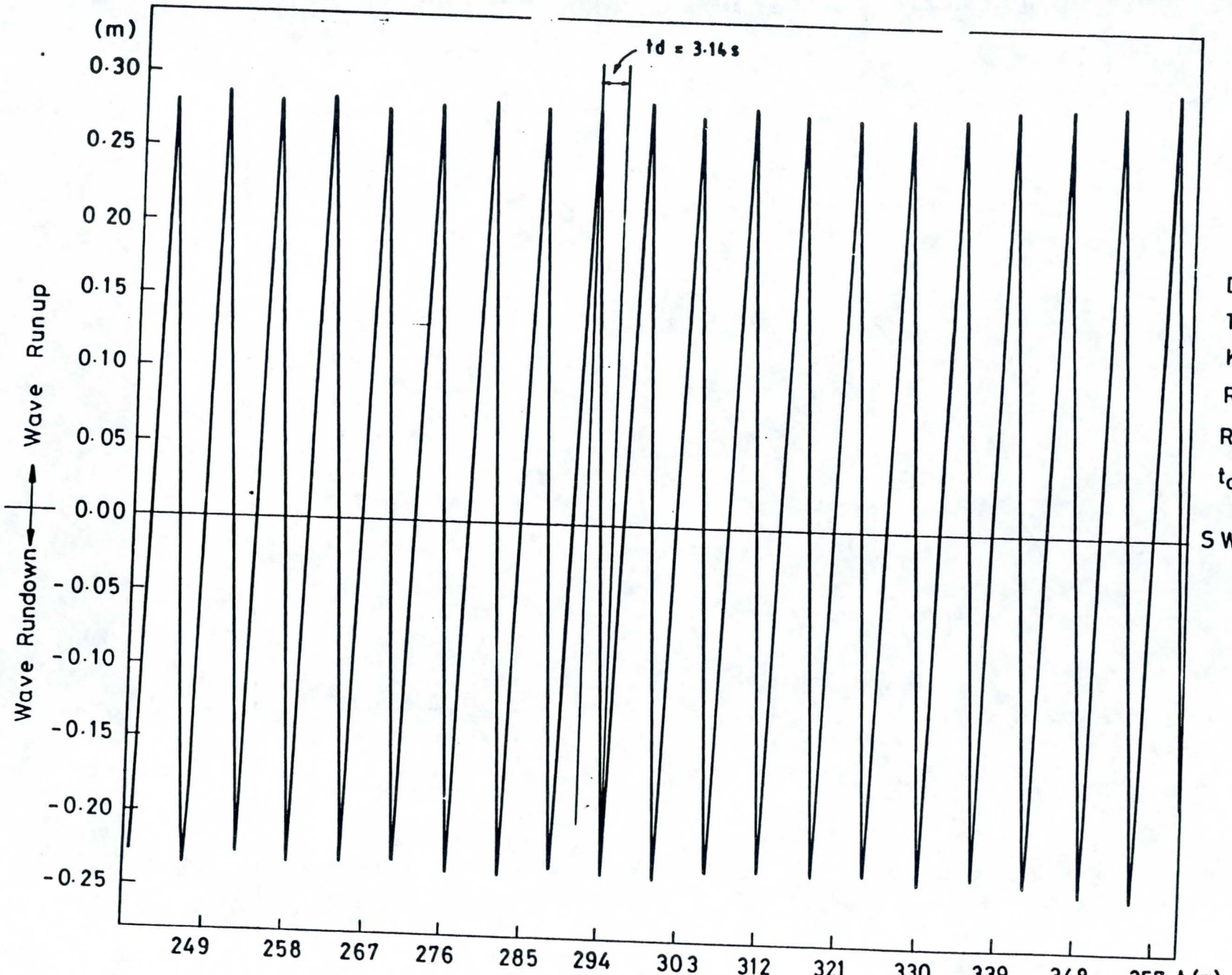

FIG. 5. TIME HISTORY OF WAVE RUNUP AND RUNDOWN

Preprints International Riprap Workshop 1993

J.S. Mani

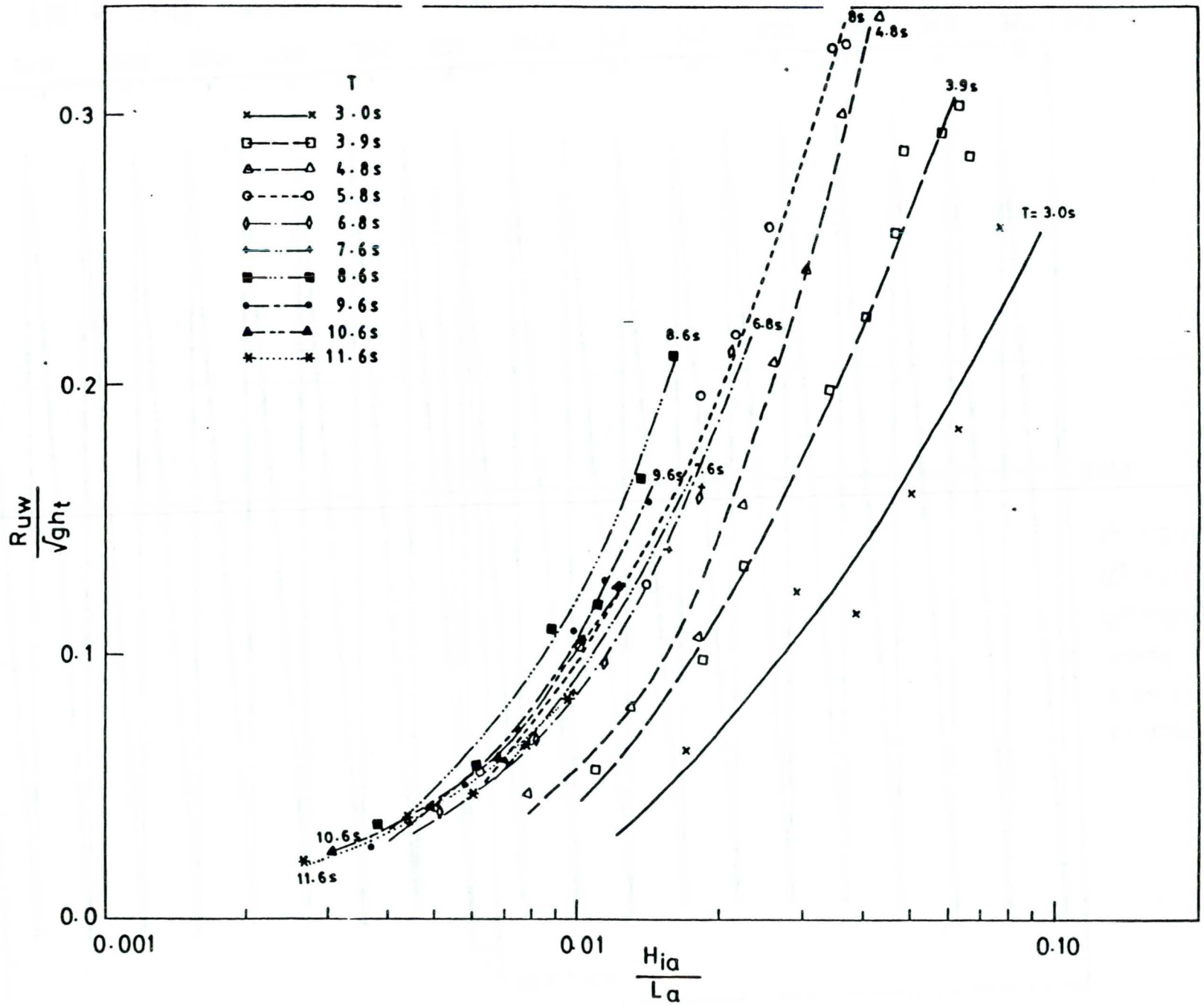

FIG. 6. VARIATION OF RUNDOWN VELOCITY WITH WAVE STEPNESS (WAVE GAUGE MEASUREM

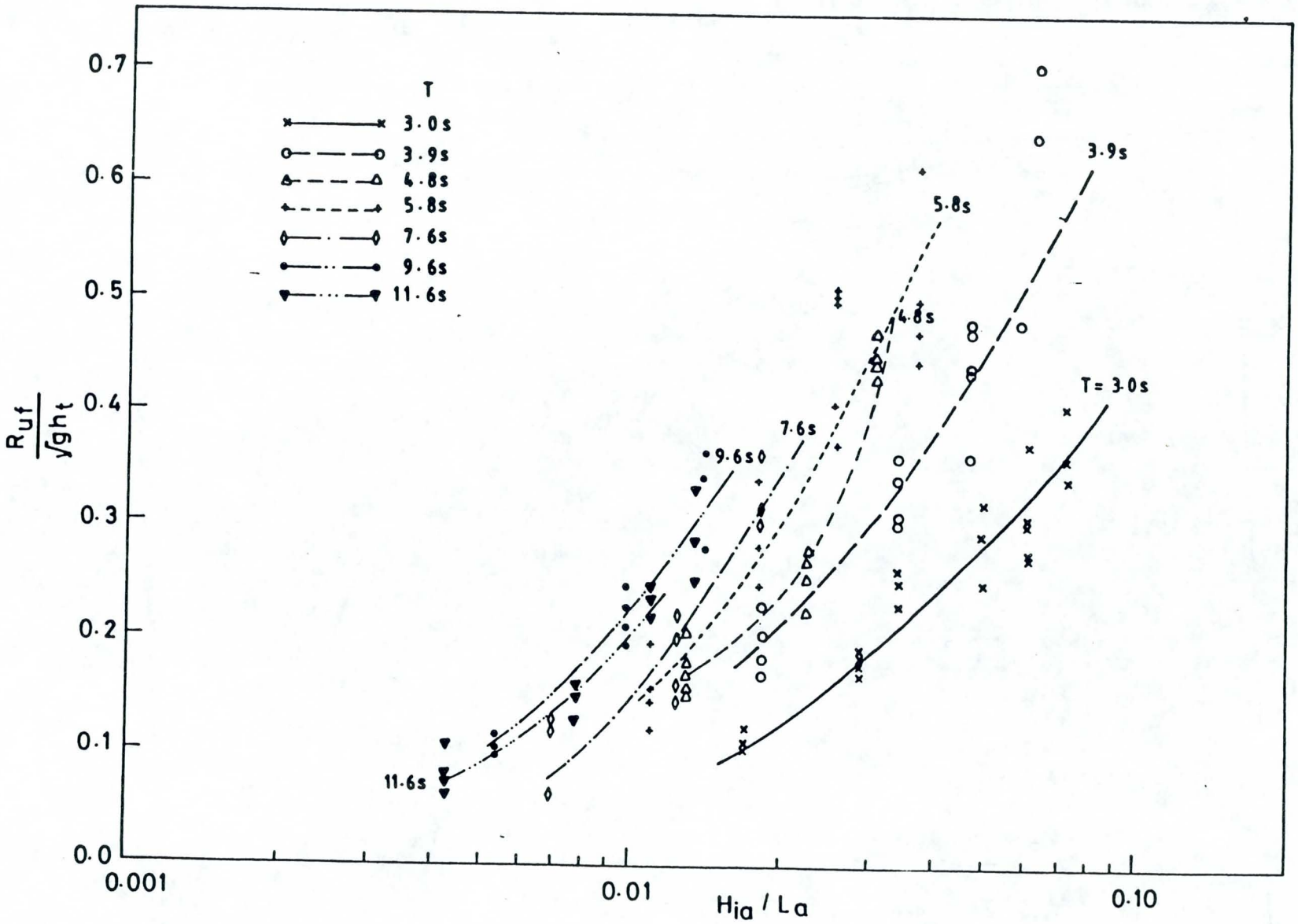

FIG. 7. VARIATION OF RUNDOWN VELOCITY WITH WAVE STEEPNESS (FLOAT MEASUREMENTS)

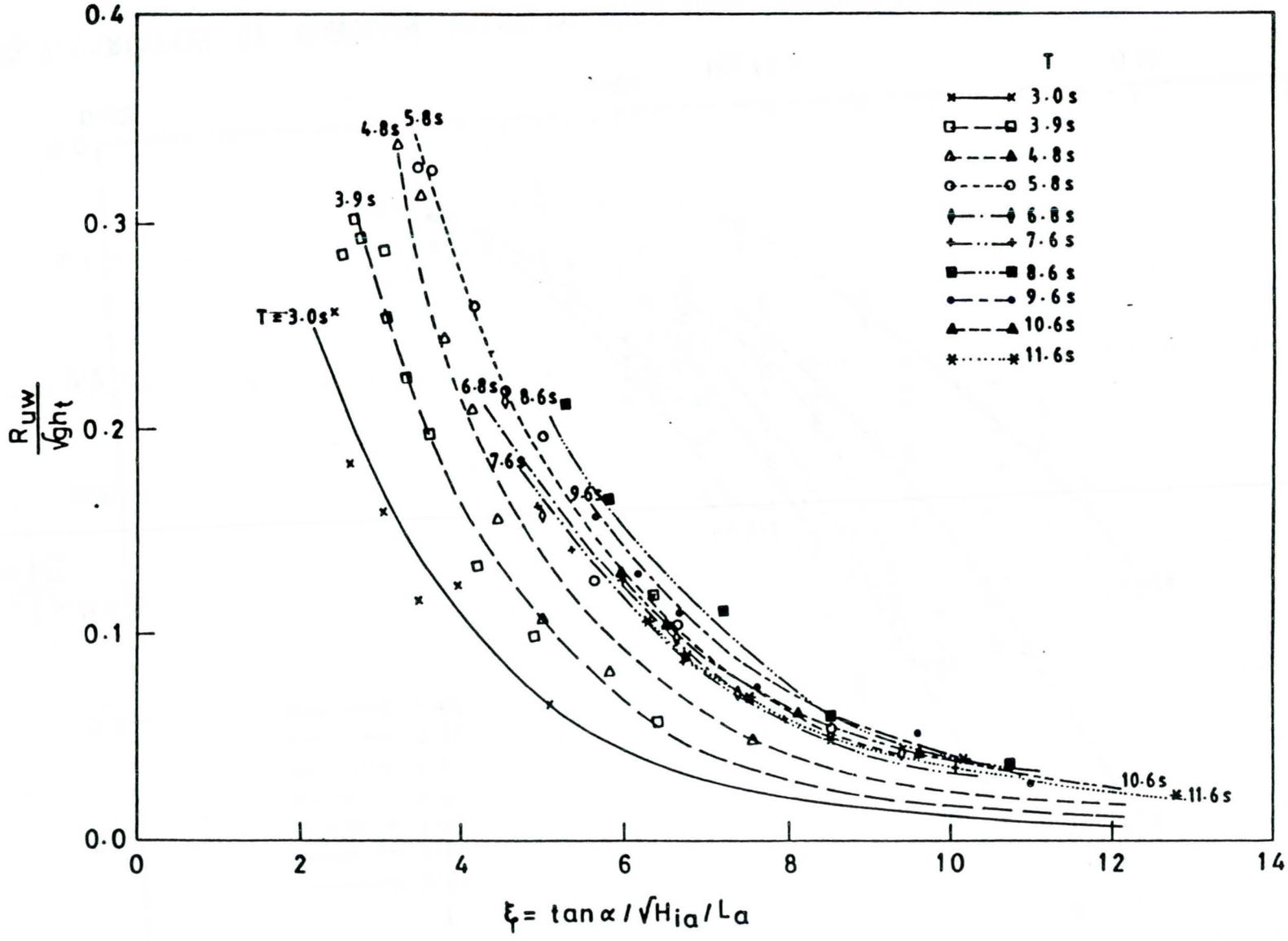

FIG. 8. VARIATION OF RUNDOWN VELOCITY WITH ξ_t (WAVE GAUGE MEASUREMENTS)

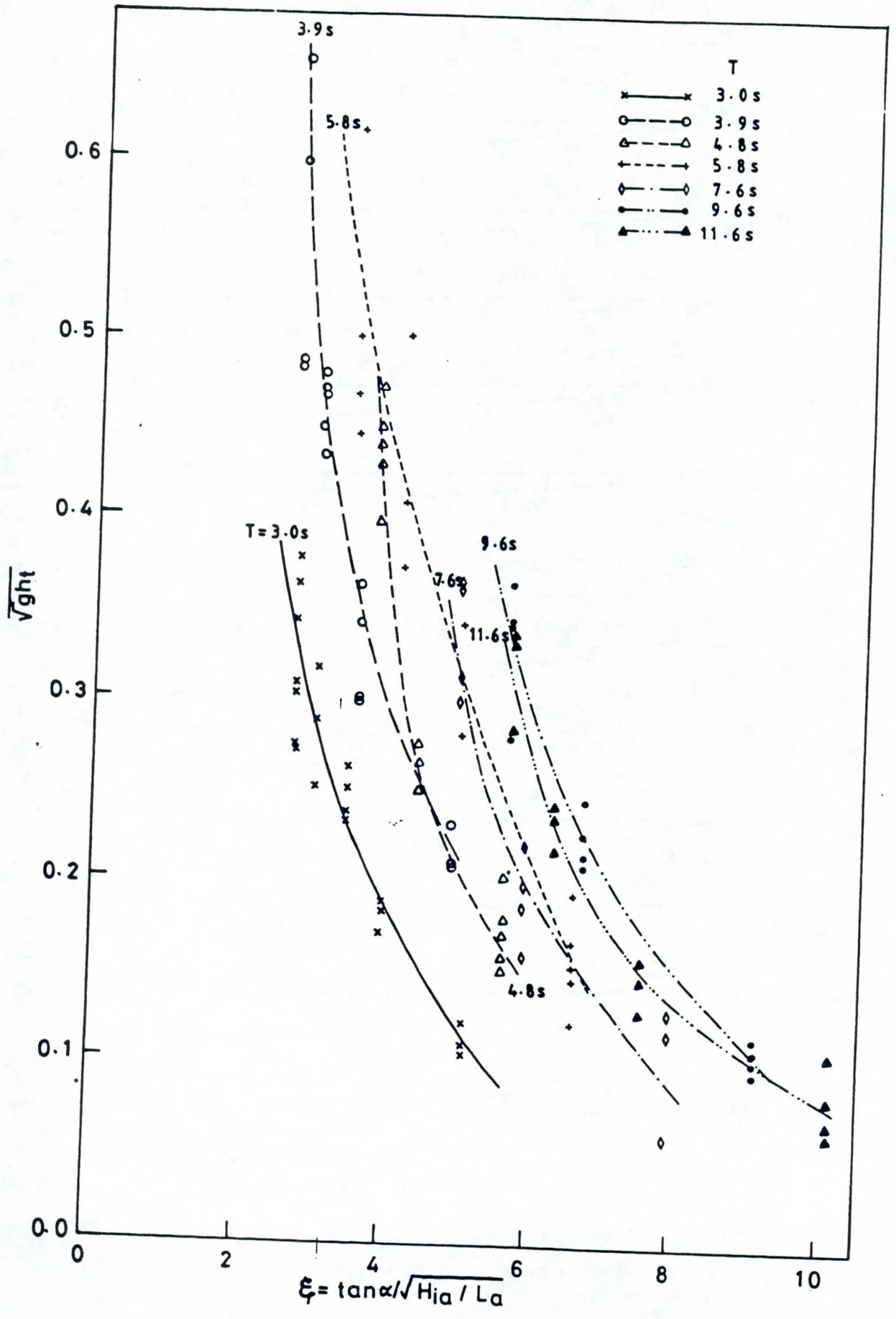

FIG.9. VARIATION OF RUNDOWN VELOCITY WITH ξ (FLOAT MEASUREMENTS)

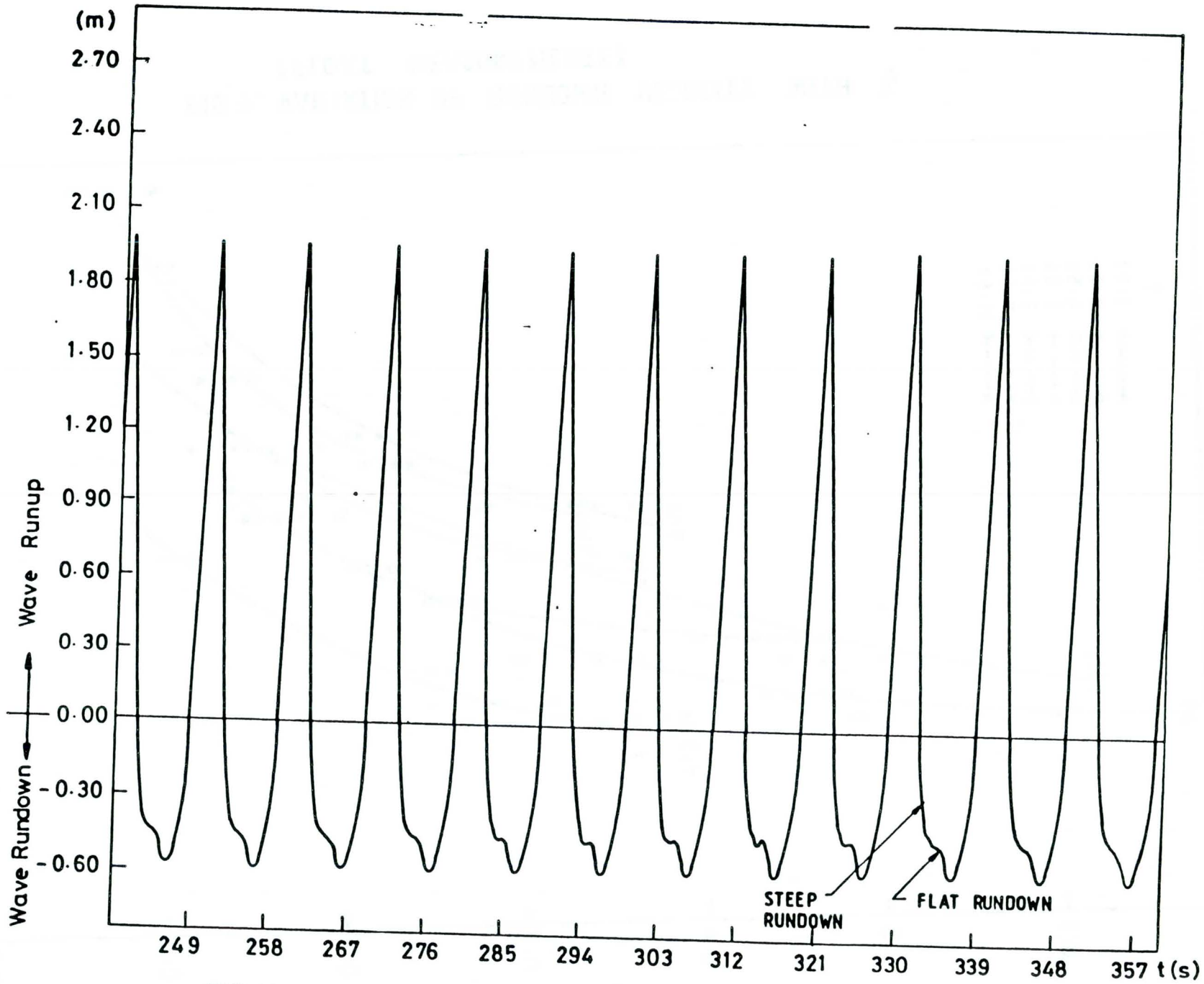

FIG.10. WAVE RUNUP AND RUNDOWN FOR H_{in} = 0.83 m, T = 10.0 s

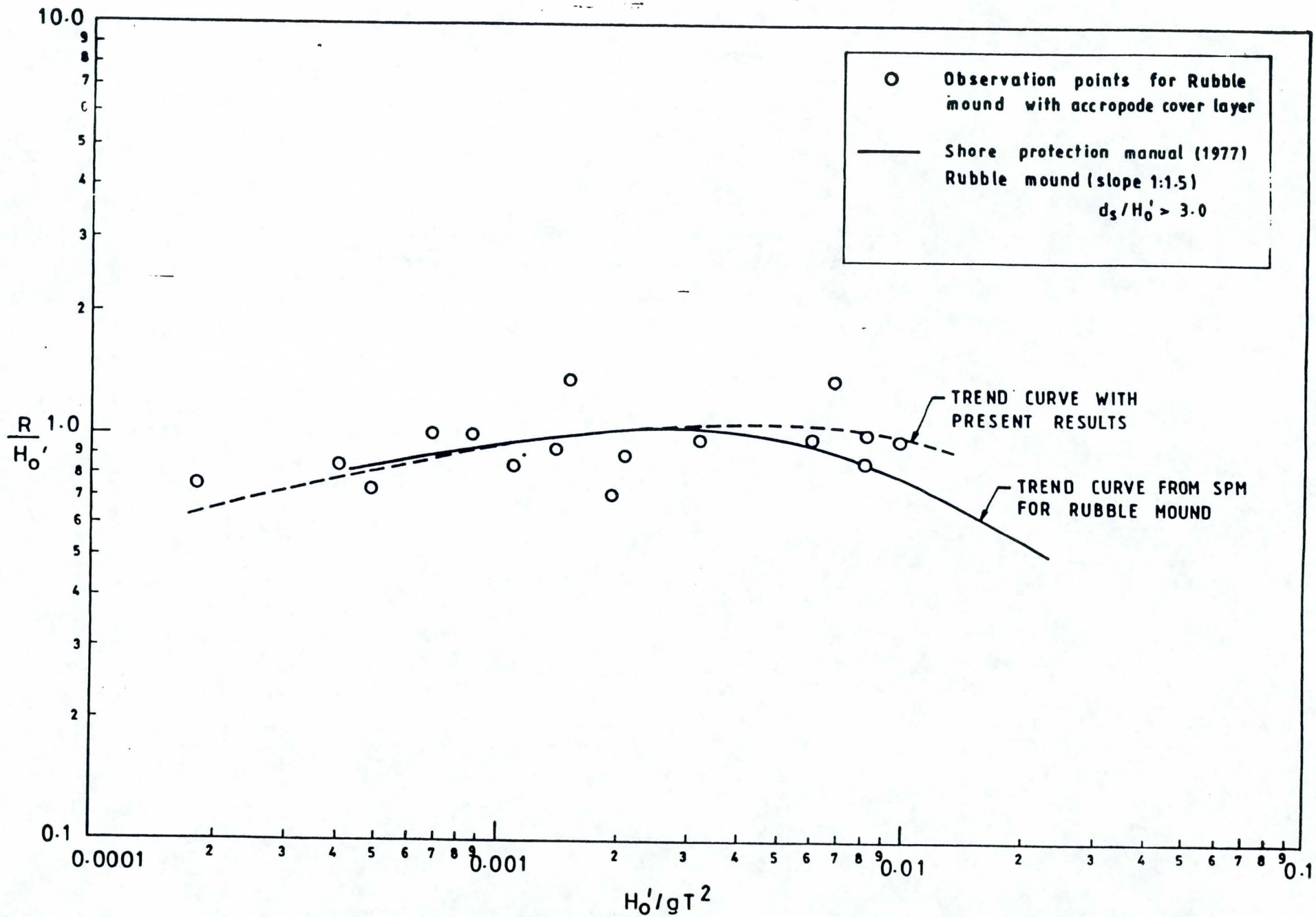

FIG.11. RUN-UP COMPARISON FOR ACCROPODE AND RUBBLE

RIPRAP DESIGN FOR TOW-INDUCED WAVES

S.K. Martin
US Army Engineers, Waterways Experiment Station,
Vicksburg, Mississippi

Abstract

As commercial towboats navigate our inland waterways, they generate physical forces in the form of waves and currents. As the tow moves, waves form at the bow and stern sometimes converging to create secondary waves. In confined channels, the moving tow generates a drawdown alongside the barge train and a transverse wave at its stern which propagates perpendicular to the shoreline at the speed of the boat. The characteristics and magnitude of the tow-induced waves are primarily a function of the speed of the tow, the geometry of the waterway, the shape and draft of the barges, and the sailing line of the tow. These waves have some characteristics that are similar to wind-induced and tidally produced waves, but are unique in several ways. The angle at which they attack the shore line; the combination of both long period and short period waves; and the duration and frequency characteristics are a few of the characteristics which can vary.

Riprap is a classical solution to bank stability problems related to wave-induced forces. Design guidance related to riprap design for waves was originally developed for protection of coastal shorelines. Numerous variations exist of the equation derived by Robert Hudson (1957) which relates weight of the stone to the wave height. This paper will present some of these equations and identify the equation and/or coefficients which results in the best stable rock size for waves produced by commercial towboats in inland waterways.

1. INTRODUCTION

Waves, formed by any of several mechanisms, naturally contribute to the erosion of the shore lines and banks. There are numerous causes of this erosional (groundwater seepage, local runoff, pool lowering, etc.). This paper deals only with protection of banks from erosion caused by waves. In coastal regions, wind drives the creation of these waves, and also governs the design of breakwaters and shore protection. In estuaries, tidally created waves coupled with offshore waves contribute to failure mechanisms. And certainly, waves produced by catastrophic floods (i.e. failed dam) or tectonically-generated waves (i.e. tsunami) produce infrequent, but energy-intensive conditions which can devastate the waters edge. There remains, however, yet another wave-producing device which can and does contribute to the erosion of the waters edge and deserves ample investigation... boats.

In the US, our inland waterway system can be described as a complex series of locks and dams, navigable open rivers and navigation channels. While the fetch across some of the navigation pools can cause significant wave setup, and the subject of recreation craft are a topic of their own, more often than not, commercial towboats are the predominant wave producers on our inland waterways. It is important, therefore, to understand the characteristics of the waves formed by these vessels and identify the mechanisms which cause bank erosion.

The characteristics and magnitude of the tow-induced waves

are highly dependent on a number of variables including the speed of the tow, the geometry of the waterway, the shape and draft of the barges, and the sailing line of the tow. The angle at which they attack the shore line; the combination of both long period and short period waves; and the duration and frequency are a few of the wave characteristics which can vary from wind-induced waves.

Waves and drawdown produced by a moving tow have the most impact on the upper portion of the slope. The magnitude, angle of propagation, and period affect the run-up characteristics of the waves, and consequently determine the extent of protection required on the upper embankments.

Riprap is a classical solution to bank stability problems related to wave-induced forces. Design guidance related to riprap design for waves was originally developed for protection of coastal shorelines. Numerous variations exist of the equation derived by Robert Hudson (1957) which relates weight of the stone to the wave height. This paper will present some of these equations and identify the equation(s) and/or coefficients which results in the stable rock size for waves produced by commercial towboats in inland waterways.

2. BOAT WAVES

2.1 Typical Commercial Tow

Every navigable waterway has a unique set of vessels which are common to that particular navigation system. The actual dimensions, horsepower and payload are a function of the navigation channel's own unique characteristics. Beyond the general limitations of width, depth and capacity, particular physical constraints may include the size of the locks, the height of bridges, the radius of the bendway, or some other authorized navigable constraint such as depth.

Unlike the deep draft channels which contain self-propelled ships and tankers, towboats pushing non-motorized barges are

common to the shallow draft waterways in the US. Even within the inland navigation system in the US, the nominal dimensions and characteristics of the commercial tows vary from waterway to waterway. Figure 1 (US Army Corps of Engineers 1980) shows some of the typical barge types and towboats. The individual barge sizes are fairly standard for all the US inland waterways except the Columbia/Snake system where the vessels are uniquely designed to accommodate the lock sizes of approximately 86 ft by 675 ft. The number of barges in each tow and their configurations are a function of the size of the system and its locks. On the Upper Mississippi, tows typically contain six jumbo barges, three wide by two long, but can push as many as 15. On the Lower Mississippi, the tows are often made up of over 40 barges. Some small rivers may only be able to accommodate a few barges (Haunchey and Grier 1985).

2.2 Tow-Induced Waves

The waves generated by a moving tow include the bow wave, the transverse stern wave, diverging waves, drawdown, and secondary waves. The bow wave, also known as the front wave, is generated at the front of the lead barges as the tow pushes the water ahead. In a confined channel, the magnitude of the bow wave is generally of a lesser magnitude than the transverse stern wave. Beginning at the corners of the lead barges waves diverge from the sides of the tow and propagate away from the tow at an angle (See photo, Figure 2). In larger channels, the diverging waves may coincide with the stern wave, forming incidental peaks with amplified wave heights known as secondary waves.

The transverse stern wave is the resulting wave formed as water displaced by the tow flows around the vessel to the stern. In a narrow channel, near a bank, the transverse wave moves in the same direction as the vessel, is generally perpendicular to the bank slope, and can resemble a moving hydraulic jump. This wave is related to the drawdown. Drawdown, also called water level depression, is the drop in water level alongside the barges

caused as the tow moves forward and water is displaced from bow to stern. Drawdown is accompanied by a strong current moving opposite to the tow direction, the return current. (See Figure 3, schematic of front wave, drawdown, etc. from PIANC (1987)).

2.3 Wave Characteristics

The waves produced by tows in shallow water differ from their wind driven counterparts. The wave magnitudes, periods, frequency, and direction of propagation are unique due not only to the type of wave (bow, stern, drawdown, etc.), but also the conditions in which they are produced (boat speed, channel geometry, etc.). Both long and short period waves are generated by the moving tow.

The drawdown begins near the bow and rebounds near the stern producing a single wave with a duration on the order of 40-120 seconds. The waves following the stern diminish in magnitude with distance from the stern and have a period on the order of 2-5 seconds. Secondary waves along side the barges maintain a rather consistent amplitude over the length of the bargetrain and also have short periods of approximately 1-5 seconds. See Figure 4, a time history plot of experimental data (Maynord and Oswalt 1986).

These waves propagate to the shoreline at varying angles depending upon the geometry of the channel and the vessel Froude number, $V_s / (\sqrt{gd})$. Under some conditions the waves exhibit a pattern similar to that derived by Lord Kelvin's theory of ship waves in deep water (Verhey and Bogaerts 1989); but unlike ships, the drawdown behaves like a shallow water wave and can form waves traveling perpendicular to banks. This is demonstrated when the transverse stern wave moves as a hydraulic jump at high Froude numbers.

2.4 Complications

The prediction of wave heights and the design of bank

protection is further complicated by the waterway geometry and flow conditions, the tow's characteristics, and the specific operating conditions of the vessel.

2.4.1 Waterway Characteristics

Quantification of the navigation effects in a uniform channel is complicated in and of itself, but in natural riverine environment the complexity is increased by a multitude of factors. The irregular channel shapes, side channels, backwaters, moveable bed materials, flow conditions near structures, secondary currents in bends, and irregularity of bank slopes and materials must be considered.

2.4.2 Vessel Characteristics

Add to the above variables, specific vessel characteristics, conditions while passing or with multiple tows, and operating conditions, and the ability to predict wave heights and characteristics becomes overwhelming. Although commercial tows can be found with a rather typical range of towboat power and with standard barge arrangements as seen in Figure 1, the actual configuration, draft and towboat characteristics can vary from tow to tow. For instance, you may find "mixed" barge arrangements containing both empty and full barges, some barges with "raked" ends and some with square, some towboats with twin propellers, some with kortnozzles, etc.

2.4.3 Operating conditions

The tow's operating conditions have an effect on the tow-induced forces. These conditions include whether it is maneuvering or underway, it's speed, and it's sailing line (the lateral location, or path, of the tow in the navigation channel).

Maneuvering tows have the greatest impact in close quarters such as near structures, through river bendways, or in marine terminals, where the vessel must power up, make sharp turns, or maneuver such that its propeller jets can scour the bed or

embankment. Tows underway have reached a constant sailing speed, with a constant propeller speed, and are traveling in a generally straight course parallel with the bank requiring only minor adjustments to the rudders. In this case, either the return current or the waves typically dominate the forces.

For tows underway, the speed is the most critical element in defining the magnitude of the waves. As a tow approaches its limiting speed (the maximum obtainable speed regardless of available power in which a given size vessel can move through a given cross-sectional area of the channel), the wave heights exponentially increase such that a small increase in boat speed produces a dramatic difference in wave height. Finally, the location of the sailing line or path of the tow with respect to the bank can effect the magnitude of the wave height.

2.5 Prediction of Wave Height

Since the equations for riprap design are based on a "design" wave height, it is important to be able to understand and quantify this value. The exact definition of design wave height may be vague at best, and varies from formulation to formulation. In spite of the many complications heretofore described, numerous equations exist that predict wave height. Some are related to the bow wave, the transverse stern wave, drawdown, or secondary waves. Some regard maximum values and some average. In the interest of space, only one such example of a predictive equation follows for secondary waves, presented by Verhey and Bogaert (1989) which relates the wave height to the sailing line, vessel speed and water depth. The coefficient, α_1, regards the type of vessel and it's draft. The equation given for estimating wave height, H, is:

$$H = \alpha_1 h \left(\frac{S}{h}\right)^{-0.33} F_h^{4.0}$$

where:

h = water depth

S = distance between ship's side and bank

$$F_h = \frac{V_s}{\sqrt{gh}}$$

3. EQUATIONS FOR RIPRAP DESIGN

3.1 Original Hudson Equation

Previous recommendations for stone slope protection from waves have been based on variations of the general equation relating wave height to stone size presented by Hudson (1957). Hudson used the stability number, N_s, a dimensionless parameter, to evaluate the condition at the start of damage.

$$N_s = \frac{\gamma_r^{1/3} H}{\left(\frac{\gamma_r}{\gamma_w} - 1\right) W_r^{1/3}}$$

where

W_r = weight of individual rock, lb

γ_r = specific weight of rock, lb/ft^3

γ_w = specific weight of water, lb/ft^3

H = wave height, ft

Hudson found through his testing that the stability number was a function of the slope of the embankment. For a 2H:1V slope, N_s was experimentally found for non-breaking waves on a rubble-mound breakwater to be 1.8, and for a 3H:1V slope, it was 2.1. Solving this equation for the weight of the rock, W_r, and substituting the weight of rock for which 50 percent is lighter by weight, W_{50}, as the representative rock size, the equation is as follows:

$$W_{50} = K_1 \frac{\gamma_r H^3}{\left(\frac{\gamma_r}{\gamma_w} - 1\right)^3}$$

where

K_1 = coefficient replacing N_s^{-3}

3.2 Forms of the Equation

Many researchers have developed a version of this equation by including more variables in the evaluation of their coefficients. Most modifications have been made regarding armour design in coastal regions due to waves on a breakwater structure; some have been developed for ship-induced waves. While the basic form of the equation is the same, the coefficients are radically different as a result of the parameters and conditions tested. Some of these conditions regard wave characteristics and the bank conditions, such as whether the waves were breaking or non-breaking, angle of attack of the waves, wave period, number of waves, slope of the embankment, etc.

A thorough literature review was conducted and the various forms of the equations were put in the form of equation 2 so that a comparison could be made regarding the values of K_1. Table 1 summarizes the general forms of the coefficients according to these different researchers for design of armour units non-related to ship-induced waves and lists pertinent information regarding the test conditions. Table 2 contains those formulas developed for ship waves. Not all forms of the equations, nor researchers reviewed, are listed in this summary and furthermore, some interpretation by the author was used to extract the information from the original literature. Often different stability criteria and incorporation of a safety factor have been used in the determination of the coefficients regarding the design stone weight. Also the selection of the representative or design wave height used in the formulas often varies from study

to study (peak, average, "significant"). The type of armour protection tested was, likewise, variable so that specifics regarding gradation, stone shape (smooth quarry, rough quarry, tetrapods, quadripods, etc.), filter conditions were not always inherent to the formulation.

3.3 Variability in Riprap Size Resulting from Equations

As might be expected, the wide array of form and parameters in the coefficient K_1 produce a design rock weight that is highly variable. To compare the formulas, typical values of the data collected from the Tennessee-Tombigbee study of riprap protection for tow-induced forces were used (Maynord and Oswalt 1986). The following were made to determine the "design" W_{50}:

1. Two values of wave height were used, H_1 = 3.1 ft and H_2 = 1.5 ft. The values resulted in both a failed and a stable condition in the testing of three different riprap gradations. These values are representative of both a large wave and an average wave, respectively of those typically generated by moving tows in confined waterways.

2. Two bank conditions were used in the Tennessee-Tombigbee study, $\alpha = 26.57°$ was selected for this comparison. A bank slope of 2H:1V makes an angle measured from the horizontal of 26.57°. Riprap protection is generally not placed on a steeper slope than this but often is placed on 2.5:1 or 3:1.

3. A wave period T_z, of 3 seconds was selected. While this is not representative of the drawdown wave it is appropriate for the secondary waves.

4. According to the literature a deep water wave length, L equals $(gT^2/2\pi)$. This computes to an L = 46 for these examples, except in the Verhey and Bogaert's (1989) equation where L is a function of the ship speed, V. (See Table 2).

5. The specific weight of the stone, γ_r, was assumed to be 165 lb/ft^3 and the specific weight of water, γ_w, 62.4 lb/ft^3.

6. According to Ahrens (1989) a value of 7000 for the

number of waves, N, was used to determine the stability number of the van der Meer and Pilarczyk equation.

7. Also, unlike the practice in the Hydraulics Laboratory at WES of relating W_{50} to the spherical diameter of the stone, most of the equations presented here assumed a nominal diameter of the stone based on a cube.

8. While many of the coefficients seemed to be conservatively determined at the initiation of motion of the riprap, some may have been intended to have a safety factor added, as in the case of coefficients determined when the filter was exposed. Where available, the criteria were mentioned in the tables.

Table 3 shows the results of the calculations and compares the riprap weights for both wave heights and all equations in Tables 1 and 2. The last value shows how the results from the Tennessee-Tombigbee study compare to the formulations. After reviewing the variability of the design rock, 27 lb to 1231 lb for H = 3.1 ft, it is obvious the design engineer is left with a rather serious decision regarding the selection of the correct rock size. The question must be asked, which equation is more appropriate for the protection of embankments due to tow-induced waves?

4. OTHER DESIGN GUIDANCE

4.1 Design Guidance

The most thorough design guidance is found in the PIANC guidelines. A very systematic method is presented for evaluating the hydrodynamic forces and determining the appropriate rock size. The Delft Hydraulics Laboratory has likewise published numerous articles and reports regarding the design of bank protection. In the Hydraulics Laboratory at WES, several site-specific studies, along with research conducted to date, have resulted in a more thorough understanding of navigation-induced

forces and provided more guidance regarding riprap design specifically for protection against tow-induced forces. Some of the WES reports regarding this guidance are Maynord (1984), Maynord and Oswalt (1986) and Martin (1992). At this date however, a specific formula has not been developed.

Based on the author's evaluation of the formulas and procedures in this paper, and the results of the testing she has conducted, the method presented by Verhey and Bogaerts and the secondary wave formula in PIANC (1987) appear to correlate the closest with the testing conducted at WES. Some caution should be taken, particularly in the Verhey and Bogaerts approach, regarding the angle of wave attack. As stated before in a confined waterway where the vessel Froude numbers are higher, the transverse stern wave can form as a moving hydraulic jump. It is also unconfirmed that even at lower Froude numbers that the waves form at the angles prescribed by Lord Kelvins theory. The photo in Figure 2 shows the wave patterns near the bow of a moving tow in a channel with an island from tests recently conducted for the Louisville District Corps of Engineers by the WES. Furthermore, in the tests conducted at WES for riprap protection the separation of specific wave types and drawdown are indiscernible in the apparent stability or failure of the rock embankment. Consequently, the total effect of the navigation-induced forces (including any current effects) is reflected in the test results.

4.2 Current Research

Current research at the Waterways Experiment Station is focussed on determining the most economical stable rock design for navigation-induced forces. Current testing expands on the previous research to include more variations in blockage ratio, sailing lines, vessel speeds, bank slopes, and rock sizes. The main product of this research will be a design equation for riprap specifically suited to the tows and waterway systems found in the US. A by-product of this research will be methods of quantifying the hydrodynamic forces.

5. SUMMARY

In summary, this paper has presented the existing guidance regarding the determination of riprap size for protection against waves, and the appropriateness of this guidance for protection from tow-induced waves. Additionally, specific characteristics of the tow-induced forces are presented along with the parameters which shape these characteristics.

6. ACKNOWLEDGMENTS

The views presented in this paper reflect the opinions of the author and not necessarily those of the US Army Corps of Engineers. Permission has been granted by the Chief of Engineers to publish this paper.

7. REFERENCES

Ahrens, John 1989. "Recommendations for Updating EM1110-2-1614, design of coastal revetments, seawall, and bulkheads," Draft report, US Army Waterways Experiment Station, Vicksburg, MS.

Bhowmik, Nani G. 1976. "Development of Criteria for shore protection against wind-generated waves for lakes and ponds in Illinois," Research Report No. 107, University of Illinois at Urbana-Champaign, Water Resources Center, Urbana, IL.

Fuehrer, M., Romisch, K., and Engelke, G. 1981. "Criteria for dimensioning the bottom and slope protections applying the new methods of protecting the navigation canals," 25th Permanent International Association of Navigation Congresses, Edinburgh, Section 1.

Hanchey, James R. and Grier, David V. 1985. "The United States navigation system," Bulletin No. 51, Permanent International Association of Navigation Congresses, Brussels, Belgium.

Hudson, Robert Y., 1957. "Laboratory investigation of rubble-mound breakwaters," Presented at June 1957 meeting of the American Society of Civil Engineers, Buffalo, NY. Also issued as paper 2171, ASCE Journal WW3, V.83, P.93-121, Sept. 1959.

Martin, Sandra K. 1992. "Riprap design for towboat-induced forces in lock approaches," Miscellaneous Paper HL-92-3, US Army Engineer Waterways Experiment Station, Vicksburg, MS.

Maynord, Stephen T. 1984. "Riprap protection on navigable waterways," Technical Report HL-84-3, US Army Engineer Waterways Experiment Station, Vicksburg, MS.

Maynord, Stephen T., and Oswalt, Noel R. 1986. "Riprap stability and navigation tests for the divide-cut section Tennessee-Tombigbee Waterway," Technical Report HL-86-3, US Army Engineer Waterways Experiment Station, Vicksburg, MS.

Permanent International Association of Navigation Congresses. 1987. "Guidelines for the design and construction of flexible revetments incorporating geotextiles for inland waterways," Report of Working Group 4 of the Permanent Technical Committee 1, Supplement to Bulletin No. 56, Brussels, Belgium.

US Army Corps of Engineers, 1980. "Layout and design of shallow-draft waterways, Engineer Manual 1110-2-1611, Department of the Army, Washington, DC.

van der Meer, J.W. and Pilarczyk, K.W. 1987. "Stability of breakwater armour layers, deterministic and probabilistic design," Publication No. 378, Delft Hydraulics Laboratory, The Netherlands.

Verhey, H.J. and Bogaerts, M.P. (1989). "Ship waves and the stability of armour layers protecting slopes." Publication No. 428, Delft Hydraulics Laboratory, The Netherlands.

Table 1
Summary of Equations (Non-related to Ships)

Source	Conditions	Form of the Coefficient, K_l
1) Hudson (1957)	Breakwaters No damage	$0.3125\ (\cot \alpha)^{-1}$
2) Bhowmik (1976) (after Hedar and Saville)	Wind waves "stable weight"	$0.388\ \gamma_w^{-1}\ (\cos \alpha - \sin \alpha)^{-3}$
3) Ahren (1989)	Breakwaters Zero damage	$0.675(\cot \alpha)^{-0.5}$
4) van der Meer and Pilarczyk (1987)	Breakwaters Start of damage	
	a) Plunging waves (L = deep water wave length)	$0.1367\ (\tan \alpha)^{1.5}\ (H/L)^{-0.75}$
	b) Surging waves	$3.8275\ (\cot \alpha)^{-1.5}\ (H/L)^{0.15}\ (\tan \alpha)^{-0.3}$
5) PIANC (1987) (after Pilarczyk)	Wind Waves	$0.0878\ (\tan \alpha)^{1.5}\ (H/L)^{-0.75}$

Table 2
Summary of Equations (Related to Ships)

Source	Conditions	Form of the Coefficient, K_l
6) Verhey and Bogaerts (1989)	Secondary ship waves $L' = 0.67(2\pi)(V^2/g)$ $\beta = 55°$	$\frac{0.0878\ (\cos\beta)^{1.5}\ (\tan\alpha)^{1.5}}{(\cos\alpha + \sin\alpha)^3\ (H/L')^{0.75}}$
7) Fuehrer, Romisch, Engelke (1981)	Ship waves with safety factor	$0.8638\ (\tan\alpha)$
8) PIANC (1987) after LaBoyrie	Transverse Stern wave (max drawdown)	$0.2963\ (\tan\alpha)$
9) PIANC (1987) after Verhey and Pilarczyk	Secondary ship waves $\beta = 55°$	$0.1715\ (\cos\beta)^{1.5}$

Table 3

Source	H_1 = 3.1 ft		H_2 = 1.5 ft	
	K_1	W_{50}	K_1	W_{50}
1) Hudson	0.1563	173	0.1563	20
2) Bhowmik	0.0686	77	0.0696	9
3) Ahren	0.4773	528	0.4773	60
4) van der Meer and Pilarczyk				
a) plunging	0.3654	404	0.6298	79
b) surging	1.1128	1231	0.9973	125
5) PIANC (wind waves)	0.2347	260	0.4045	51
6) Verhey and Bogaerts	0.0241	27	0.0395	5
7) Fuehrer, et. al.	0.4319	478	0.4319	54
8) PIANC (transverse stern wave)	0.5926	655	0.5926	74
9) PIANC (secondary waves)	0.0745	82	0.0745	9
10) Tennessee-Tombigbee (No safety factor)	N/A	>68	N/A	13

OPEN HOPPER BARGES

TYPE	LENGTH FEET	BREADTH FEET	DRAFT FEET	CAPACITY TONS
STANDARD	175	26	9	1000
JUMBO	195	35	9	1500
SUPER JUMBO	250-290	40-52	9	2500-3000

COVERED HOPPER BARGES

TYPE	LENGTH FEET	BREADTH FEET	DRAFT FEET	CAPACITY TONS
STANDARD	175	26	9	1000
JUMBO	195	35	9	1500

INTEGRATED CHEMICAL AND PETROLEUM BARGES

LENGTH FEET	BREADTH FEET	DRAFT FEET	CAPACITY TONS
150-300	50-54	9	1900-3000

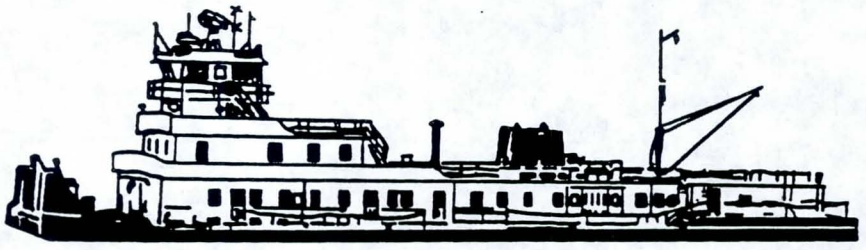

TOWBOATS

LENGTH FEET	BREADTH FEET	DRAFT FEET	HORSEPOWER
65-160	24-50	5-9	300-7000

Figure 1.: Predominant barge and tow types

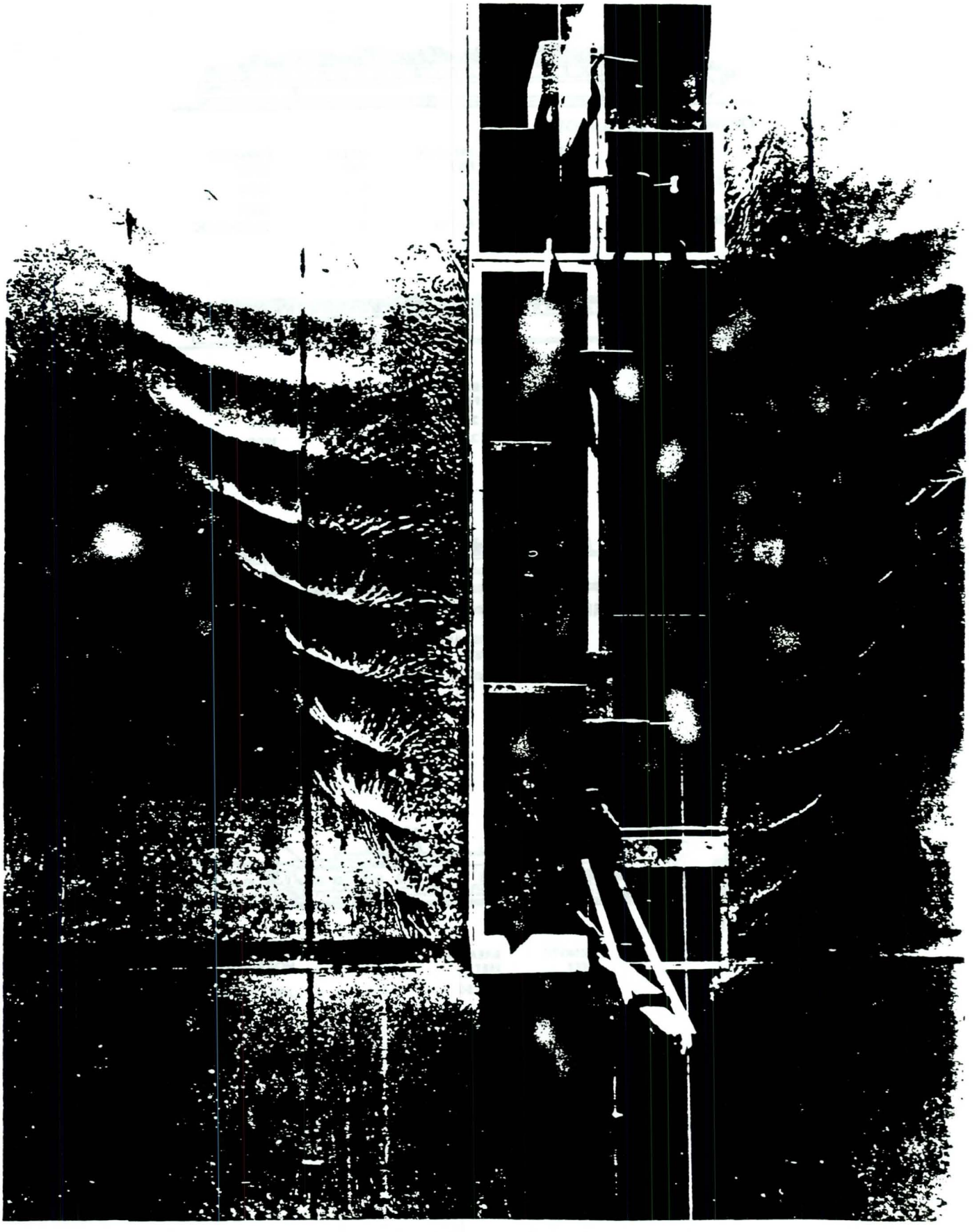

Figure 2

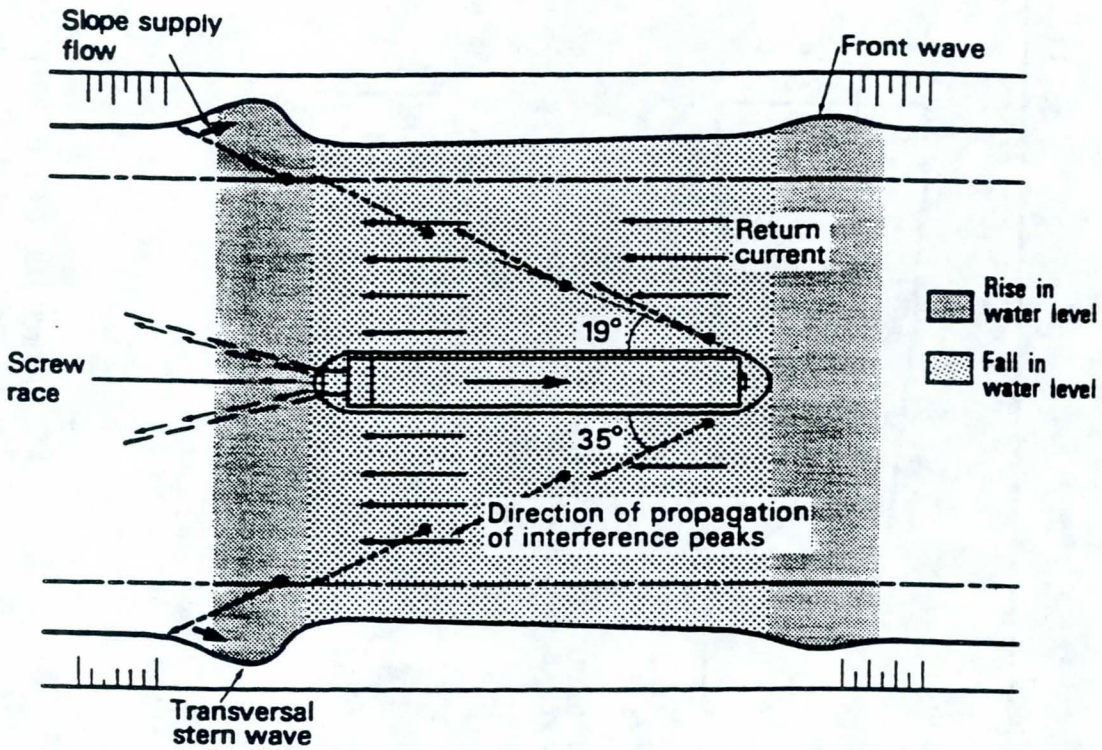

Figure 3: Components of ship induced water motion

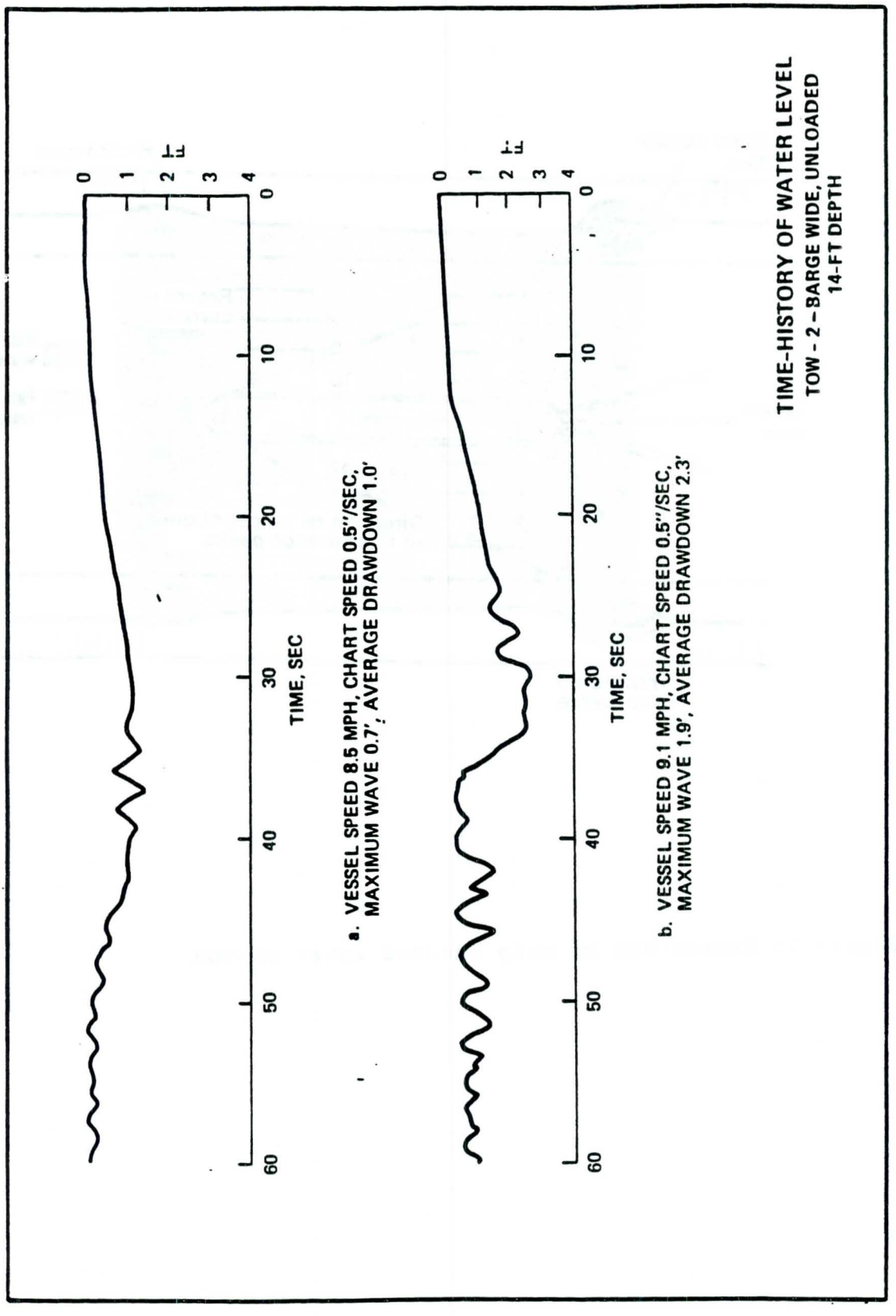
TIME-HISTORY OF WATER LEVEL
TOW - 2 - BARGE WIDE, UNLOADED
14-FT DEPTH
FT
0
1
2
3
4
0
10
20
30
40
50
60
TIME, SEC
a. VESSEL SPEED 8.5 MPH, CHART SPEED 0.5"/SEC,
MAXIMUM WAVE 0.7', AVERAGE DRAWDOWN 1.0'
b. VESSEL SPEED 9.1 MPH, CHART SPEED 0.5"/SEC,
MAXIMUM WAVE 1.9', AVERAGE DRAWDOWN 2.3'

Figure 4

RIPRAP STABILITY IN HIGHLY TURBULENT FLOWS

R.W.P. May and M. Escarameia
HR Wallingford, Research Department, UK

1. INTRODUCTION

Flows downstream of hydraulic structures can be highly turbulent and the velocity distributions very non-uniform. Channel protection is normally required to prevent, or at least limit, the extent of scour produced by the flow on the bed and banks. Riprap is one of the most widely used forms of flexible protection for natural and artificial watercourses. However, despite a considerable amount of past research, many of the available design methods give widely-varying predictions of stable stone sizes. Such uncertainties can have major economic consequences ; a typical difference of 30% in predicted stone size can increase the weight of the stone by a factor of 2.2. Furthermore, existing equations do not take quantitative account of the effect of turbulence on stability.

An experimental study, funded by the UK Department of the Environment, was therefore carried out at HR Wallingford to study the effects of current velocity and turbulence level on the stability of riprap placed on horizonal channel beds and sloping banks.

2. INITIATION OF PARTICLE MOVEMENT

The initiation of particle movement can be taken as the beginning of the failure process for a river protection revetment. The velocity of the water and the surface roughness of the riprap determine the value of mean shear stress acting on the protective layer; in turn, the shear stress also influences the shape of the vertical velocity profile above the protection. Individual stones are subject to lift and drag forces, with random fluctuations in magnitude and direction caused by the turbulence in the flow. 'Failure' is therefore, to a certain extent, a probabilistic event because movement occurs when the mean force combines with a sufficiently large random component to exceed the resistance exerted by other particles in the bed.

A number of factors can influence the initiation of particle movement. Some are associated with the geotechnical characteristics of the rock, some with the layout of the revetment (eg existence of filters) and others with the hydraulic features of the flow. Included in the first group are the size, the specific weight, the surface roughness, the gradation and the porosity of the rockfill. The particle shape, defined by a suitable shape factor, may also be included in this group. Some test studies have shown that flatter stones have a lower threshold velocity than standard quarry stone. However, tests performed at the Delft Hydraulics Laboratory, The Netherlands, with coarse particles showed no direct relationship between shape and threshold velocity for particles with the same nominal size (Pilarczyk (1984) in The Closure of Tidal Basins). The effect of the gradation seems to be small for the gradations usually recommended for riprap, and the D_{50} size of the stone is usually accepted as a good measure of the stone size. Associated with the gradation is the range of porosities that can be achieved for a particular rockfill. It seems probable that the higher the degree of compaction (ie the lower the porosity), the higher is the rock stability. However, no systematic studies are known to have been carried out on this topic.

3. PREVIOUS STUDIES

Many formulae are available for determining the size of riprap needed for stability against current attack. However, comparison is not always easy because of the use of different definitions of stone size and flow velocity. Some equations are also dimensional and implicitly include values of stone density (ρ_s) and gravitational acceleration (g).

Most of the available formulae can be expressed in the non-dimensional form:

$$\frac{D}{y_o} = \left[\frac{C_m V^2}{2g(s-1)\, y_o \Omega} \right]^m \qquad (1)$$

where D is the stone size, y_o is the flow depth, V is a representative velocity, s is the relative density of the stone in water ($= \rho_s/\rho$) and Ω is a factor that takes account of bank slope (by definition, $\Omega = 1$ for a flat bed). C_m is a non-dimensional coefficient that can be expected to vary with the turbulence level.

The well-established Izbash type of formula (see, for example, Izbash & Khaldre, 1970) has a value of m = 1 and, when applied to channel protection problems, is normally expressed in terms of the near-bed velocity V_k. Equating the fluid drag force acting on a stone with the frictional resistance due to its immersed weight leads to an equation of the form:

$$D_s = C_1 \frac{V_k^2}{2g(s-1)} \qquad (2)$$

where D_s is the size of the equivalent sphere corresponding to the W_{50} weight of the riprap grading. Izbash's formulae have values of $C_1 = 0.70$ for normal turbulence and $C_1 = 1.36$ for higher turbulence. Peterka (1958) suggested a design curve for riprap downstream of stilling basins which is equivalent to a value of $C_1 = 1.22$. Campbell (1966) also produced design curves for small stilling basins which correspond to values of $C_1 = 2.0$ for normal conditions and $C_1 = 2.74$ for higher turbulence. These results are expressed in terms of the near-bed velocity but most references do not specify the height above the bed at which V_k should be determined.

The more general form of equation (1) can be obtained by equating the fluid shear stress exerted on the bed with the critical shear stress given by the Shields curve for the threshold of movement. The value of the exponent m depends on the relationship assumed between the friction factor of the flow and the relative roughness of the bed. The Manning-Strickler equation, for example, leads to a value of m = 1.5. However, two recent studies have obtained better agreement with a value of m = 1.25. Maynord et al (1989) developed the following equation from experiments on streambank protection with normal levels of channel turbulence:

$$\frac{D_{30}}{y_o} = 0.71\, S_f \left[\frac{U_d^2}{2g(s-1)y_o}\right]^{1.25} \qquad (3)$$

where y_o is the flow depth and U_d is the local depth-averaged velocity of the flow. Incipient failure corresponds to a value of $S_f = 1.0$ but a safety factor of $S_f = 1.2$ is recommended for design. This equation is valid for flat beds and bank slopes not exceeding 1V : 2H. Pilarczyk (1990) derived a general formula for revetments that in the case of localised sections of riprap is equivalent to:

$$\frac{D_n}{y_o} = 1.32 \left[\frac{K_T}{\Omega} \left(\frac{U_d^2}{2g(s-1)y_o} \right) \right]^{1.25} \quad (4)$$

D_n is the size of the equivalent cube corresponding to the W_{50} weight, and K_T is a turbulence factor with values of 1.0 for normal turbulence in rivers, 1.5 for increased turbulence and 2.0 for high turbulence. Values of K_T = 1.5 or 2.0 should only be used when, due to difficulties in finding U_d, the mean cross-sectional velocity is substituted. The slope factor Ω is given by

$$\Omega = \left[1 - \frac{\sin^2\alpha}{\sin^2\phi} \right]^{0.5} \quad (5)$$

where α is the angle of the bank to the horizontal and ϕ is the friction angle of the riprap.

Some of the formulae mentioned above are compared in Figure 1 in terms of the parameter D_n/y_o and the Froude number $F_r = U_d/\sqrt{(gy_o)}$ of the flow (assuming a flat bed Ω = 1, s = 2.65, D_s/D_n = 1.24, D_{30}/D_n = 0.70 and K_T = 1.0). For the Izbash-type equations, the relationship between V_K and U_d was estimated using Rouse's (1950) formula for the velocity against the stone:

$$\frac{U_d}{V_k} = 0.68 \log_{10} (y_o/k_s) + 0.71 \quad (6)$$

with the roughness k_s assumed equal to D_n. Although the curves in Figure 1 are fairly similar in shape, they still give significantly different predictions of stone size. These differences are most likely due to the effect of turbulence on stability.

4. EXPERIMENTAL RIG AND MATERIALS

The tests were carried out in a large flume with a test channel measuring 1.21m wide by 16.4m long and fitted with three pumps having a total capacity of 0.5m^3/s (Figure 2). An adjustable sluice gate was installed in the flume to produce a hydraulic jump with associated turbulence upstream of the test section. The model materials were placed in this test section which was 2.60m long and started 2.88m downstream of the gate. Tailwater depths were controlled by means of a flap gate and a valve at the downstream end of the flume.

The transition between the smooth invert of the flume and the mobile bed of the test section was achieved by roughening a 1.74m length with wooden boards to which stone particles were glued. This transition reach also prevented excessive scour due to high turbulence levels immediately downstream of the jump.

A different arrangement of the flume was required for the tests on bank stability : a sloping bank was introduced on one side of the 1.21m wide test section, with the vertical wall of the flume on the opposite side. This simulated half a symmetrical trapezoidal channel, and allowed observations through the perspex windows of the flume. Two banks with slopes of 1:2 and 1:2.5 (V : H) were studied separately in the flume, and a transition was included to allow a gradual change between the rectangular section at the sluice gate and the trapezoidal section at the test section. The banks were formed using wooden boards ; wire mesh was fixed to the boards to increase their roughness and prevent the whole layer of riprap sliding down the slope.

Three different angular stones with D_{50} sizes between 4.6 and 11.8mm were used in the tests as well as three different rounded stones with D_{50} sizes between 7.3 and 9.3mm ; the specific gravities of the stones were in the range s = 2.57 to 2.74. Full details of the gradings and shape factors for the six stone types are given by Escarameia & May (1992). The gradings of the model materials broadly conformed with the usual guidelines for riprap (see, for example, Hemphill & Bramley, 1989).

5. TEST PROCEDURE

The stability of the riprap was investigated for two different conditions : 'normal' channel turbulence, and a range of higher turbulence levels produced by a hydraulic jump. In the normal turbulence tests, the sluice gate upstream of the test section was kept fully open so that it would not interfere with the flow. The initiation of stone movement was obtained by either increasing the flow discharge or lowering the tailwater level. The procedure adopted in the tests with higher turbulence was first to adjust the sluice gate opening so that the resulting hydraulic jump always formed well upstream of the test section. The tailwater level was then gradually lowered until initiation of particle movement was observed. The test rig was not intended to reproduce any particular prototype configuration ; the jump was used purely to generate required levels of turbulence in the test section.

The tests were principally carried out to identify the threshold of stone movement. An objective criterion for the threshold was established by counting the number of stones that moved during a certain specified time within a rectangular area marked out on the bed. The motion of the stones was easily observed through the transparent window on one side of the flume.

The total discharge in the flume was measured by means of a Crump weir installed at the downstream end. The water level in the test section was recorded using a micrometer point gauge. The mean and fluctuating velocities in the test section were measured by a Minilab ultrasonic current meter. This recorded instantaneous velocities in three orthogonal directions and was moved vertically to obtain velocity profiles above the area of bed marked out for observations of the threshold of movement. The relative bulk of the instrument prevented measurements being made very close to the bed or the free surface of the flow. The signals were recorded digitally at a frequency of 12.5Hz and checked to remove occasional spikes caused by the passage of air bubbles between the prongs of the probe. The data were then analysed to determine statistical and spectral properties of the turbulence.

For the experiments with a horizontal bed, the riprap was placed in a layer with a thickness of approximately 4-6 D_{50} and levelled carefully before each test. The vertical velocity profiles were measured on the centreline of the channel within the rectangular area used for observing the threshold of movement.

For the experiments with a sloping bank, velocities were measured at three verticals within the cross-section of the flow : on the centreline of the horizontal part of the bed, at the toe of the bank and half-way up the bank between the toe and the water surface. According to the flow conditions, the position where stones first started to move varied between the bank, the toe and the horizontal bed.

6. DATA ANALYSIS

The experimental results for the stability of riprap on a flat bed with higher levels of turbulence are compared in Figure 1 with some of the equations described in Section 3. The considerable amount of scatter is due to the range of turbulence levels produced in the tests and demonstrates that a design equation with a fixed coefficient for 'turbulent' conditions is unlikely to prove satisfactory.

The relationship between the stone size and the flow conditions causing movement can be analysed in terms of either the local depth-averaged velocity U_d or a suitable definition of the near-bed velocity. The value of U_d is usually easier to assess and can be a sufficient parameter for the case of continuous streambank protection where a fully-developed boundary layer produces a consistent relationship between the mean velocity and the flow conditions near the bed. In the case of localised areas of protection around hydraulic structures, the boundary layer may be only partially developed so the velocity and turbulence near the bed can vary independently of the mean velocity. The results of the

present experiments were therefore analysed in terms of the near-bed velocity V_b which was defined as the longitudinal velocity at a height above the bed equal to 10% of the local water depth. This level was considered to be close enough to the bed to be representative while avoiding measurement errors due to high velocity gradients occurring nearer the bed. The measurements were therefore compared with the following Izbash-type equation:

$$D_n = C \frac{V_b^2}{2g(s-1)} \tag{7}$$

The turbulence intensity T_i was also determined at the 10% level and defined as:

$$T_i = \frac{V_{rms}}{V_b} \tag{8}$$

where V_{rms} is the root-mean-square fluctuation in velocity about the mean value V_b.

The variation of the coefficient C in equation (7) with the turbulence intensity T_i is shown in Figure 3. It can be seen that the results for the two bank slopes (1V : 2.5H and 1V : 2H) are mixed in with those for the flat bed. It does not therefore appear necessary to include a slope parameter such as Ω, see equation (5). The following best-fit equations for C were fitted to the data:

$$C = 0.36 \qquad \text{for } T_i \leq 0.10 \tag{9}$$

$$C = 12.3\, T_i - 0.87 \qquad \text{for } 0.10 < T_i \leq 0.30 \tag{10}$$

Equation (9) can be considered as applying to the case of normal channel flow without externally-generated turbulence. If Izbash's equation (2) for normal turbulence is made equivalent to equation (7) (by using D_n and by estimating V_b at 0.10 y_o above the bed) it gives a value of about C = 0.33 which agrees well with the present figure of 0.36.

Equation (10) demonstrates the strong destabilizing effect of turbulence. Increasing the value of T_i from 10% to 20% increases the size of stone needed by a factor of 4.4 and its weight by a factor of 85. In order to ensure safe design, it is advisable to adopt a design curve that is safe compared with all the experimental data. It is therefore recommended to use the upper-envelope line shown in Figure 3 which has the equation:

$$C = 12.3\, T_i - 0.20 \qquad \text{for } T_i \geq 0.05 \tag{11}$$

This result is valid for riprap on a flat bed or on banks with slopes up to 1V : 2H. In the case of banks, the values of V_b and T_i should be determined at a height of 0.10 y_o above the toe.

As mentioned previously, the local depth-averaged velocity U_d may sometimes be easier to estimate than V_b. Analysis of the experimental data for the flat bed and the bank slope of 1V : 2.5H showed that the two velocities could be related by the best-fit equation:

$$\frac{V_b}{U_d} = 0.52 \left(\frac{y_o}{D_n}\right)^{0.14} \tag{12}$$

Substitution of equation (12) into equation (7) gives the following type of formula based on depth-averaged velocity:

$$\left(\frac{D_n}{y_o}\right) = \left[\frac{K\, U_d^2}{2g(s-1)y_o}\right]^{0.78} \tag{13}$$

Re-analysis of the data in this format gave the following best-fit equations for the dependence of the coefficient K on the turbulence intensity:

$K = 0.075$ for $T_i \leq 0.10$ (14)

$K = 3.75\, T_i - 0.30$ for $0.1 < T_i \leq 0.30$ (15)

For safe design it is recommended to use the corresponding envelope line to the data:

$K = 3.75\, T_i - 0.09$ for $T_i \geq 5\%$ (16)

These last three equations are only valid for flat beds and banks not steeper than 1V : 2.5H. The values of V_b/U_d for the slope of 1V : 2H did not fit equation (12) satisfactorily and showed more variability.

Overall, equation (7) is preferred to equation (13) as a method of sizing riprap because it fits the results more closely and is valid for all the slopes that were tested. A full listing of the experimental data, including the three-axis turbulent velocity profiles, is given in Escarameia & May (1992).

7. UNDERLAYERS

Tests were also carried out to investigate the effect of a granular underlayer on the stability of the riprap in the armour layer. The underlayer consisted of a 20mm thick layer of medium sand (D_{50} = 0.72mm) beneath a 25mm thick layer of riprap (D_{50} = 4.6mm, angular stone). The grading of the sand was chosen so as to conform with the widely-used Terzaghi criteria for granular filters.
The effect of the underlayer was found to vary with the level of turbulence in the flow. At lower intensities, the armour layer remained stable to higher discharges than in the tests carried out with a single 25mm thick layer of the same riprap. However, at higher intensities, the opposite was found to occur. Scour holes formed at the upstream end of the test section and increased the turbulence levels further downstream ; as a result, more scour holes developed throughout the test section until complete failure of the protective blanket took place. It appeared that uplift pressures generated by the turbulence enabled the sand to migrate upwards into the armour layer ; the sand then destabilised the stones by reducing the interstitial contacts between them.

Comparative tests were also carried out with a non-woven filter fabric between the sand and riprap layers. The filter fabric used was Terram NP4 (0_{90} = 0.05mm) with characteristics compatible with the granular and armour layers on either side. The geotextile prevented the upward migration of the sand particles and under turbulent conditions increased the stability of the armour layer to approximately the same level as that of a single 25mm thick layer of riprap. However, when failure did occur it was more sudden because the geotextile lifted and disrupted the armour layer.

8. CONCLUSIONS

The experiments have demonstrated that quantitative account needs to be taken of the turbulence intensity as well as the flow velocity when determining the size of riprap needed for stability. Turbulent flows downstream of hydraulic structures can have a wide variety of velocity profiles so it is best to relate stone sizes to the flow conditions near the bed that cause movement. The suggested design equations (7) and (11) therefore use the values of mean velocity and root-mean-square fluctuation at a height equal to 10% of the flow depth above the bed or the toe of the bank.

In the case of trapezoidal channels, first movement of the stone could occur on the sloping bank, at the toe or on the horizontal bed, depending on the flow conditions. The slope of the bank did not affect the value of the stability coefficient C in equation (7) for slopes between horizontal and 1V : 2H.

The standard Terzaghi criteria for the design of granular underlayers may not be appropriate for armour layers that are subjected to high-turbulence flows. The turbulence appears to cause upward migration of the granular material which then destabilizes the rock layer. Use of a suitable filter fabric between the riprap and the underlayer prevented this loss of stability.

ACKNOWLEDGEMENTS

Funding for this research study was provided by the UK Department of the Environment and HR Wallingford. The authors would also like to thank the assistance given by Mr I R Willoughby and Mr R Atkins, and by Mr S Mambretti of the Politecnico di Milano.

REFERENCES

Campbell F B (1966). Hydraulic design of rock riprap. Miscellaneous Paper No. 2-777. US Army Engineer WES, USA.

Escarameia M and May R W P (1992). Channel protection ; turbulence downstream of structures. HR Report SR 313.

Hemphill R W and Bramley M E (1989). Protection of river and canal banks. CIRIA, Butterworths, London.

Izbash S V and Khaldre Kh Yu (1970). Hydraulics of river channel closure. Butterworths, London.

Maynord S T, Ruff J F and Abt S R (1989). Riprap design. J. of Hydr. Eng, ASCE, Vol. 115, No. 7, pp937-49.

Peterka A J (1958). Hydraulic design of stilling basins and energy dissipators. US Dept. of the Int., Bureau of Reclamation, Eng. Monograph No. 25.

Pilarczyk K W (1984), in The closure of tidal basins ; closing of estuaries, tidal inlets and dike breaches. Delft University Press, The Netherlands.

Pilarczyk K W (1990). Stability criteria for revetments. Proc. of the 1990 National Conf. on Hyd. Eng., ASCE, eds Chang H H and Hill J C, San Diego, USA, pp245-50.

Rouse H (ed) (1950). Engineering hydraulics. Proc. of the 4th Hyd. Conf., Iowa Inst. of Hydr. Res., June 1949, John Wiley & Sons Inc, New York.

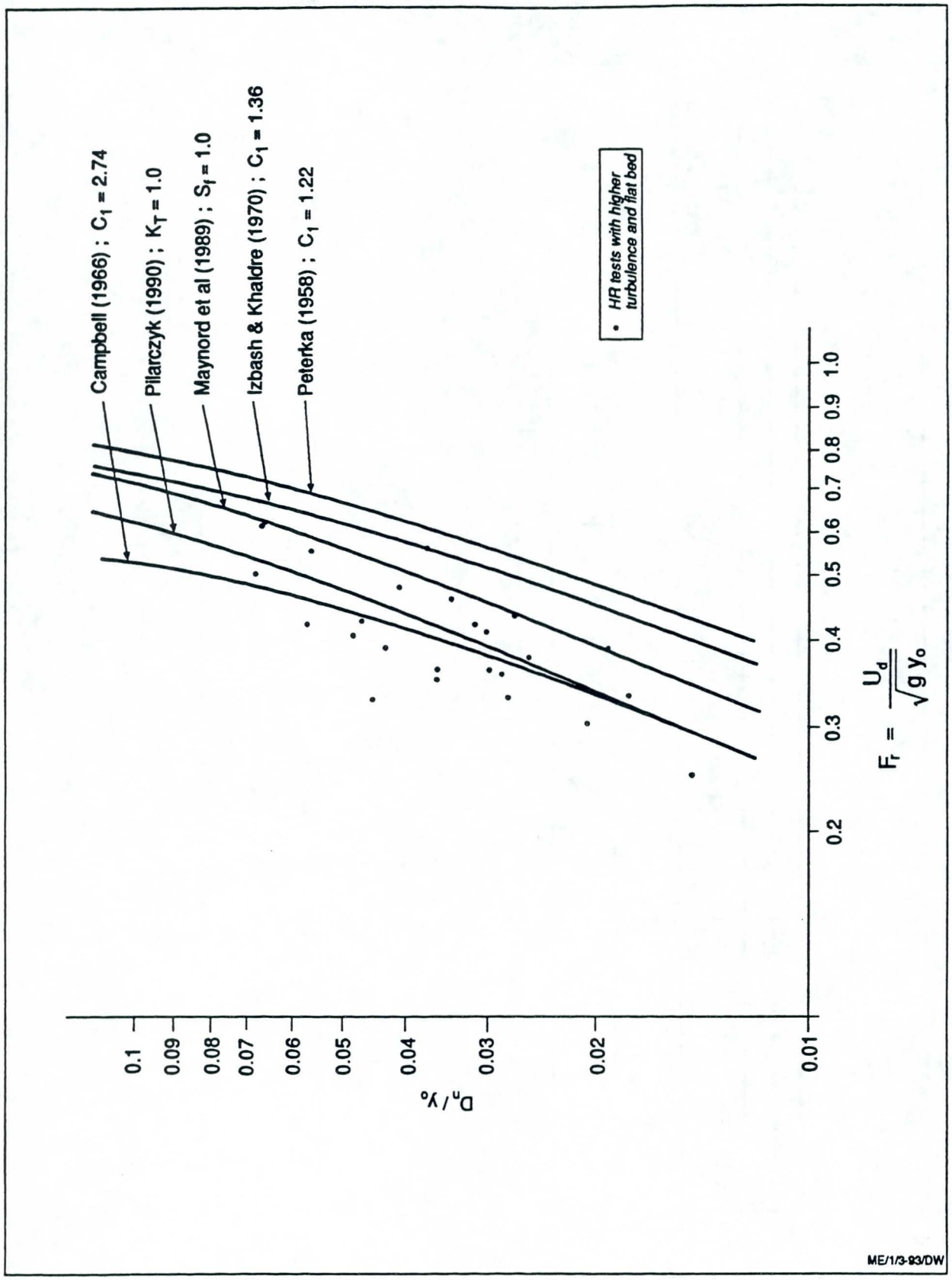

Figure 1 **Comparison of design equations for riprap and experimental data for higher turbulence on flat bed**

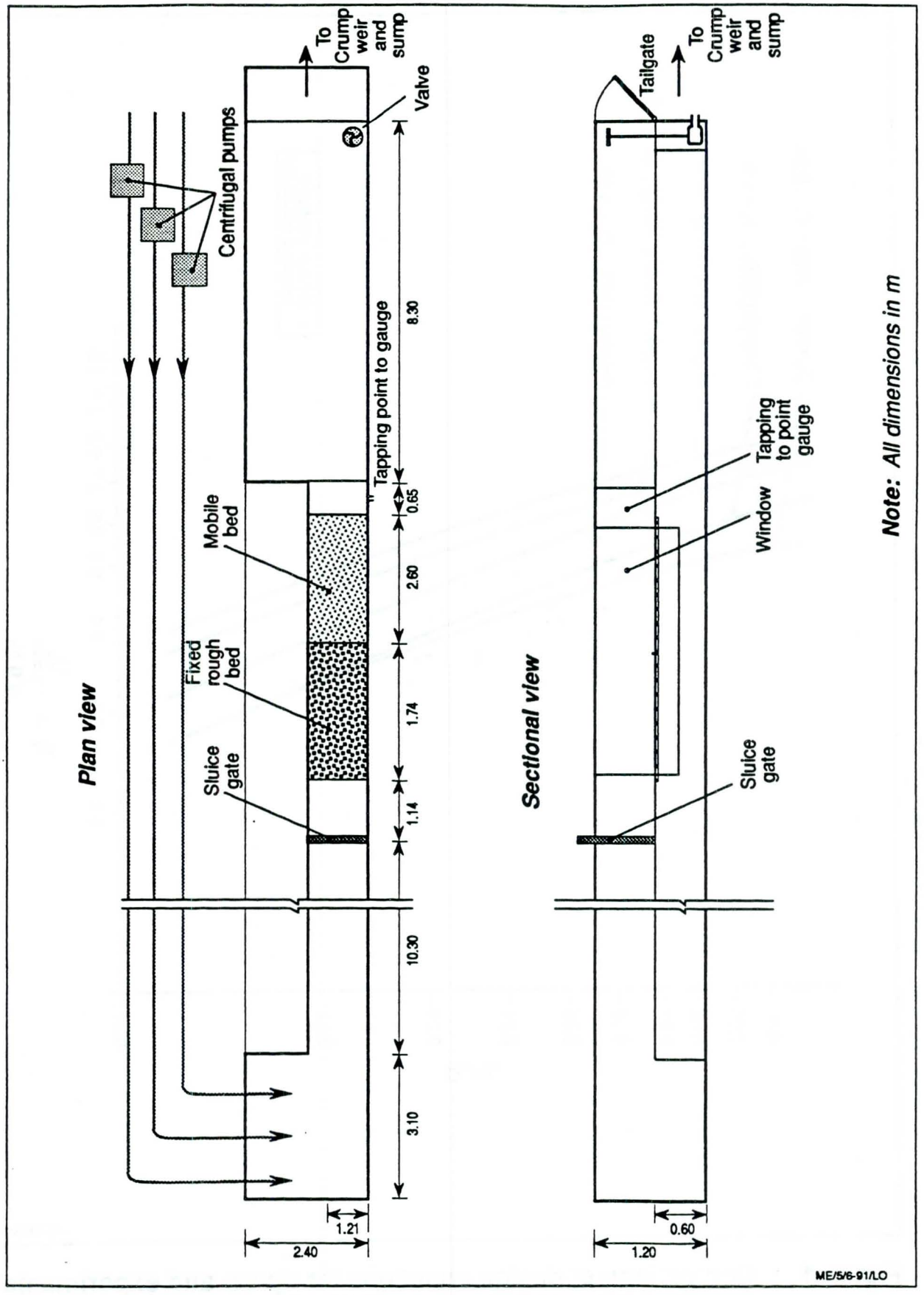

Figure 2 General layout of test rig

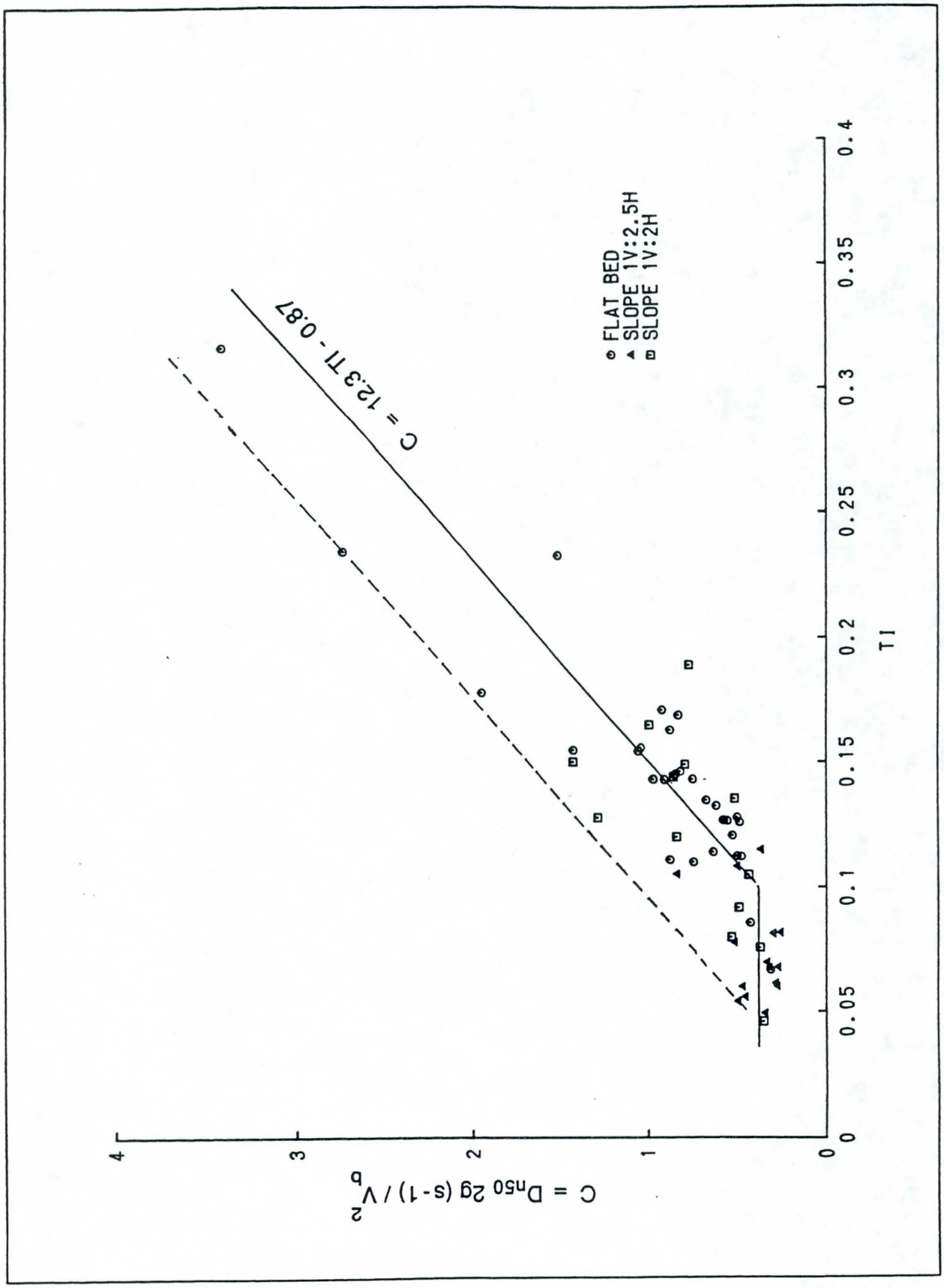

Figure 3 Relationship between C and the turbulence intensity

CORPS RIPRAP DESIGN GUIDANCE FOR CHANNEL PROTECTION

S.T. Maynord
US Army Waterways Experiment Station,
Vicksburg, Mississippi

INTRODUCTION

Determining stable riprap size continues to be an area of considerable interest because significant cost savings can be realized with improved design guidance. This report addresses guidance for sizing riprap in open channels having slopes less than 2 percent and excludes areas immediately downstream of hydraulic jumps. This includes riprap used in any form of channel protection including bank protection, river training structures, toe protection, and any other configuration of launchable riprap.

Various methods have been used to quantify the forces imposed on the riprap and to determine the stable riprap size. Based on the authors experience, the vast majority of riprap design procedures currently in use for open channel stability problems addressed herein can be derived from the following methods.

Method 1-Isbash method

Isbash(1935) developed guidance for sizing stones in river closures based on the velocity against the stone V_s and formulated

$$D_c = C_I \left(\frac{\gamma_w}{\gamma_s - \gamma_w}\right) \frac{V_s^2}{2g} \quad (1)$$

where D_c = characteristic size, C_I = 1.35 for isolated stone, C_I = 0.69 for embedded stone, γ_w = unit weight of water, γ_s = unit weight of stone, and g = acceleration of gravity. Note that there is no dependence on depth in the Isbash equation. Numerous design

approaches use the Isbash equation with average velocity instead of V_s. The California Division of Highways (1970) approach is a typical example of method 1.

Shields(1936) proposed a parameter for defining stability of non-cohesive particles using shear stress which is also referred to as tractive force. The Shields parameter τ^* is defined as

$$\tau^* = \frac{\tau}{(\gamma_s - \gamma_w) D_c} \quad (2)$$

where τ = average shear stress exerted by fluid on boundary when particle begins to move and τ^* = 0.047 - 0.060 commonly used for fully developed rough turbulent flow.

Method 2- Shear stress,slope method

The shear stress in Equation 2 is determined from

$$\tau = \gamma_w d S_e \quad (3)$$

where d = flow depth and S_e = slope of energy gradeline. Slope can be a difficult parameter to accurately measure or compute. The Anderson et al (1970) approach is a typical example of method 2.

Method 3- Shear stress, log velocity profile

The shear stress in equation 2 is determined from the Keulegan(1938) mean velocity logarithmic velocity equation that can be rearranged into

$$\tau = \frac{\rho V^2}{(5.75 Log \frac{11.1 d}{K_s})^2} \quad (4)$$

where ρ = water density = γ_w/g and K_s = equivalent sand grain roughness, K_s = 2-3 D_{90} or 3-6 D_{50} for riprap. The appropriate value of K_s, the origin of the velocity profile, and the applicability of the log profile to high relative roughness (D_c/d) are some of the problems associated with using equation 4. The Stevens and Simons (1976) method is a typical example of method 3.

Method 4- Shear stress, Manning-Strickler equation

The shear stress in equation 2 is determined by the Manning-Strickler equation as

$$\tau = \frac{C\rho V^2}{(d/D_c)^{1/3}} \quad (5)$$

Where C = coefficient. Using the power or monomial velocity profile with equation 2 is equivalent to using the Manning-Strickler approach above. Methods 3 and 4 provide similar results over a wide range of D_c/d. The Federal Highway Administration HEC-11 (1989) is a typical example of method 4.

Method 5- Velocity, dimensional analysis

Neill(1967) used average velocity instead of shear stress in a dimensional analysis to define

$$\frac{\gamma_w V^2}{g(\gamma_s-\gamma_w)D_c} = f\left(\frac{D_c}{d}\right) \quad (6)$$

This approach allows the use of experimental data to define the form of the equation rather than forcing the equation to assume a form that agrees with existing velocity profile equations. Neill's experimental data defined

$$\frac{\gamma_w V^2}{g(\gamma_s-\gamma_w)D_c} = 2.5\left(\frac{D_c}{d}\right)^{-0.2} \quad (7)$$

Equation 7 transforms to the Isbash equation 1 if the exponent is 0 instead -0.2 and transforms to the shear stress, Manning-Strickler method (equations 2 and 5) if the exponent is -0.333 instead of -0.2. Pilarcyk(1987) and Maynord(1988) present equations identical to equation 7 (except for small changes in the coefficient) that can be solved directly for D_c as follows

$$\frac{D_c}{d} = C\left[\left(\frac{\gamma_w}{\gamma_s-\gamma_w}\right)^{1/2}\frac{V}{\sqrt{gd}}\right]^{2.5} \quad (8)$$

The Corps of Engineers EM 1110-2-1601 (1991) method is a typical example of method 5.

Pilarcyk(1990) developed a general equation for rock sizing that incorporates methods 1 and 3 through 5.

The objective of this report is to discuss the development of the Corps of Engineers (1991) method.

CORPS OF ENGINEERS DESIGN PROCEDURE

General

In the late 1970's and 1980's, the Corps of Engineers conducted a research program with the goal to develop improved riprap design guidance applicable to a wide range of rock characteristics, channel alignments, channel cross-sections, and hydraulic conditions. During this research, almost every aspect of riprap design was questioned and tested if possible. During this process, it became apparent that designers prefer methods based on velocity rather shear stress. Depth-averaged velocity was chosen as the characteristic velocity because it can be estimated by the designer by a variety of methods and it is representative of local hydraulic conditions. The basic equation was developed using the Method 5- velocity and dimensional analysis with the addition of several empirical coefficients(see Maynord 1988 and 1992). From EM 1110-2-1601 (1991) the equation for stone size is

FOR MAYNORD: GOOD EQN TO USE FOR PRACTICING ENGRS (GOOD, EASY FORM OF EQN.)

$$D_{30}=S_f C_S C_v C_T d\left[\left(\frac{\gamma_w}{\gamma_s-\gamma_w}\right)^{1/2}\frac{V}{\sqrt{K_1 g d}}\right]^{2.5} \quad (9)$$

where

D_{30} = characteristic riprap size of which 30 percent is finer by weight.

S_f = safety factor, minimum = 1.1

C_s = stability coefficient for incipient failure, thickness = $1D_{100}$(max) or $1.5D_{50}$(max), whichever is greater, D_{85}/D_{15} = 1.7 to 5.2

= 0.30 for angular rock

= 0.375 for rounded rock(EM 1110-2-1601 incorrect, gives 0.36)

D_{85}/D_{15} = gradation uniformity coefficient
C_V = velocity distribution coefficient
= 1.0 for straight channels, inside of bends
= 1.283-.2log(R/W) for outside of bends (1 for R/W > 26)
= 1.25 downstream of concrete channels
= 1.25 at end of dikes
R = centerline radius of bend
W = water surface width at upstream end of bend
C_T = blanket thickness coefficient
K_1 = side slope correction factor
d = local depth, use depth at 20 percent upslope from toe for side slopes

The exponent of 2.5 in this equation was based on laboratory data from straight, tilting flumes. The extreme values of the exponent in Equation 9 are from 2 to 3. An exponent of 2 results in the Isbash equation (no dependence on depth) and is generally used when there is no boundary layer development such as areas downstream of hydraulic jumps or in the propellor wash behind vessels. Most channel protection problems have some degree of boundary layer development. An exponent of 3 results from application of the shear stress and Manning-Strickler equations and only occurs when a) completely developed boundary layer and b) relative roughness is low enough to yield a constant Shields coefficient. Channel protection projects are designed for the location where the imposed force is the highest such as the highest velocity in a bendway. In most cases, the boundary layer at these points of maximum stress is not close to reaching a completely developed state. The second requirement, low relative roughness, is not satisfied in many of shallow, relatively steep flood control channels which means that the assumption of a constant Shields coefficient is questionable because several investigators have found increasing τ^* with increasing D_c/d.

Consequently, most bank and channel riprap protection problems fall somewhere between the two extreme exponents of 2 and 3. This led to the adoption of the 2.5 exponent for all bank and channel riprap protection problems, not just the straight, tilting flumes from which it was derived. The major advantage of adopting a single power is that the riprap designer is not faced with making a decision regarding velocity profile and constancy of Shields coefficient that is a difficult problem even for people who have researched the topic for years.

Data used in the development of this method were limited to slopes less than or equal to 2 percent. Data are also limited to $D_{30}/d \geq 0.02$, which means the method has not been verified for relatively deep flows.

The basis for each of the coefficients and parameters in Equation 9 and methods for their determination will be discussed in the next part of this paper.

Design Conditions

Riprap should be designed for the combination of velocity and depth that gives the largest rock size. This combination is not always the design discharge. In many cases bank-full discharge produces the combination of velocity and depth that results in the largest rock size.

D_{30}, Characteristic Particle Size for Gradation

One of the most controversial changes from traditional guidance to the new guidance has been the adoption of a characteristic particle size of D_{30}. A gradation plot in Figure 1 illustrates concepts such as the lower and upper gradation limits (also referred to as minimum and maximum) as well as D_{100}(max), D_{30}(min), etc. Stability tests conducted at a thickness of $1D_{100}$, which is the most commonly used thickness for bank protection, showed that gradations ranging from uniform to highly nonuniform exhibited the same stability if they had the same D_{30}. Maynord *(1988)* documents other investigators who found a characteristic size less than the commonly used D_{50}. One of the results of the D_{30} finding is that

uniform gradations use the least volume of rock to achieve the same stability because the thickness is equal to the maximum stone size. One of the troubling aspects of these results is that an investigator of riprap subjected to channel flow has not yet been found who has been able to confirm the commonly held notion that a range of sizes gives increased stability due to better interlock. The poor performance of highly non-uniform gradations is probably related to their high potential for size segregation that results in locally weak spots in the revetment. The use of D_{30} instead of D_{50} requires that the designer determine which of the available gradations has a D_{30}(min) greater than or equal to the computed D_{30} rather than to D_{50}. If the designer prefers to work in terms of D_{50}, the approximate relation to D_{30} is

$$D_{50}=D_{30}(D_{85}/D_{15})^{0.32} \qquad (10)$$

The use of a single particle size to characterize a gradation, whether D_{30}(min) or D_{50}(min), does not reflect all the characteristics of that gradation. The following equation can be used to determine if D_{30}(min) is representative or if D_r(min) should be used as the characteristic particle size:

$$D_r(\text{min}) = \sqrt[3]{D_{85}(\text{min})\,[D_{15}(\text{min})^2]} \qquad (11)$$

S_f, Safety Factor

The minimum safety factor to account for nonhydraulic factors and other uncertainties is 1.1. The general tendency in riprap design is to conservatively estimate velocity, which adds in a safety factor. Having to select an available gradation having D_{30}(min) greater than or equal to the computed D_{30} often adds another safety factor. For these reasons, the minimum safety factor is set low at 1.1.

C_s, Stability Coefficient

Stability coefficients defining the onset of unacceptable rock movement were determined from large-scale laboratory tests. These laboratory tests attempted to simulate mechanically placed riprap on a filter fabric without tamping or smoothing after placement. For thickness = $1D_{100}$(max) or $1.5D_{50}$(max), whichever is greater, C_s = 0.30 for angular rock. Limited tests show that C_s = 0.375 for rounded rock.

C_v, Velocity Profile Correction

An evaluation of the velocity profile over bottom riprap in straight channels resulted in the following equation:

$$\frac{V(y)}{V} = (1 + N)\left(\frac{y}{d}\right)^N \qquad (12)$$

where V(y) = velocity at y, N = 0.25 for d/D_{90} from 3 to 20, and y = distance from the top of the riprap. The velocity profile given by Equation 12 is the profile for which the stability coefficient for angular rock was found to be 0.30. At the point of major attack in bendways and just downstream of concrete channels, the profile is more nearly vertical with velocity in the upper zone (near the surface) less than Equation 12 and velocity in the lower zone (near the bottom) greater than Equation 12. For the same depth-averaged velocity, the vertical velocity profile in bends and just downstream of concrete channels tends to have a greater capacity to move the riprap because the velocities near the riprap and the shear stress are larger. In the case of riprap just downstream of concrete channels, the velocity profile has not adjusted from the smooth concrete surface to the rough riprap. In the case of bendways, secondary currents are suspected of causing the change in velocity profile.

In either case, an increased stone size is required. Two choices are available for making this increase. The first of these would involve going back to the basic shear stress equations; developing a velocity profile relationship for the bend or the area downstream of the concrete channel; and determining a new

relationship between the shear stress, relative roughness, Shield's coefficient, and the applicable velocity profile. Because this is a formidable task and would have made the design procedure difficult to use, the second choice, a completely empirical approach to velocity profile effects, was selected. For riprap just downstream of concrete channels, an empirical velocity profile correction C_v of 1.25 should be used in Equation 9. For riprap in channel bends, the velocity profile correction is dependant on the strength of the secondary currents, which is generally related to the parameter R/W. From stability tests reported in Maynord (1992), the empirical velocity profile correction coefficient C_v was found to be 1.2 for R/W = 2.5. The relationship used for the velocity profile correction given in EM 1110-2-1601 *(1991)* is

$$C_v = 1.283 - 0.2 \log \left(\frac{R}{W}\right) \qquad (13)$$

where C_v is equal to 1 for $R/W \geq 26$.

A third area where the velocity profile departs significantly from Equation 12 is riprap on the nose of a rock dike. Due to the constricting effect of the dike, flow rapidly accelerates around the dike. Due to the short distance the flow is affected by the dike, the boundary layer has no chance to grow and is continually being reduced by the flow acceleration. Limited tests show that the velocity profile correction to be multiplied by the rock size should be 1.25 for riprap on the nose of a dike.

C_T, Riprap Blanket Thickness

Blanket thickness is generally measured in terms of the maximum stone size D_{100}. The minimum allowable blanket thickness is $1D_{100}$, and many streambank protection projects use this thickness. Only for uniform gradations ($D_{85}/D_{15} \leq 2$) must the thickness also be at least $1.5D_{50}$ for equivalent stability. Stability tests have shown that thickness greater than T* , where T* is the greater of $1.5D_{50}$ or $1.0D_{100}$, results in increased stability. Figure 2 shows guidance given in EM 1110-2-1601 *(1991)* for thickness effects. The interpolated curve having $D_{85}/D_{15} = 1.7$ is applicable to the gradations in Table 1 *(USACE 1971)*. (This curve was interpolated

between the curve for D_{85}/D_{15} = 2.5 and D_{85}/D_{15} = 1 which was conservatively assumed to have no increase in stability for increased thickness.) Gradations having $D_{85}/D_{15} \geq 5.2$ should use the curve for 5.2. When greater blanket thickness is used to increase stability, it must be realized that some rock movement will occur prior to the revetment becoming stable.

V. Depth Averaged Velocity

One of the primary reasons for adopting a design procedure based on depth-averaged velocity is because several techniques exist for estimation of this velocity. Velocity is also easy to visualize and measure compared to shear stress. Any riprap design problem has two parts. The first part is to estimate the imposed force. The second part is to use the imposed force and determine riprap size. The most difficult and most uncertain part of riprap design lies in estimating the imposed force whether it be local depth-averaged velocity or shear stress. When riprap is designed for a channel bottom, local depth-averaged velocity is a straightforward concept even if it may be difficult to determine. When side slope riprap is designed, local depth-averaged velocity varies greatly from toe of slope to waterline and near-bank velocity is meaningless unless the position is specified. The EM 1110-2-1601 (1991) method uses depth-averaged velocity at a point 20 percent upslope from the toe V_{ss} for side slope riprap design. The 20 percent point was selected because straight channel side slope stability tests resulted in the same stability coefficient C_s as straight channel bottom stability tests with this position on the side slope and the appropriate adjustment for side slope angle. This point is consistent with the location of maximum side slope shear stress from straight channel studies.

Various tools exist to estimate depth-averaged velocity for use in riprap design and include the following with some of their limitations:

1. Numerical models: two-dimensional (2D) depth-averaged numerical models have been shown to be unconservative in prismatic bends. Bernard *(1992)* has developed a correction method for 2D

depth-averaged models, and a version is available that can be used with 386 personal computers (PC's). This model has compared well with data from trapezoidal channels and is presently being tested against data from natural channels.

2. Physical models: rarely available for bank protection projects due to cost. If available, near bank velocity distributions should be measured to obtain V_{ss}.

3. Empirical methods: must be applied only to cases similar to the data from which they were derived.

4. Analytical methods: methods based on conveyance such as the ALPHA method given in EM 1110-2-1601 *(1991)* should be limited to straight channels because secondary currents can cause the ALPHA method to be unconservative. Thorne and Abt (unpublished data) discuss additional analytical methods that incorporate the effects of secondary currents.

5. Prototype data: normally require extrapolation to design conditions but usually not available. EM 1110-2-1601 provides a method for extrapolating observed velocities.

This paper focuses on the application of the empirical method given in EM 1110-2-1601 *(1991)*, presented in Figure 3. Figure 3 is applicable only for estimating characteristic side slope velocity V_{ss} in straight or curved channels. Figure 3 was derived from velocity data taken in physical models and prototypes. The amount of scatter in this type of data is large and the curves were drawn on the conservative side of the data. In the case of bendways, Figure 3 is based on bends having fully developed bend flow, which means the bend angle is sufficiently large to develop close to the maximum velocity for that value of R/W. To use the minimum V_{ss}/V_{avg} on Figure 3 for straight channels requires that the channel be far enough downstream of bends, constrictions, or other devices that might create an imbalance of flow across the channel. Consequently one should be very cautious about specifying a straight channel and rarely should V_{ss}/V_{avg} be less than 1. Figure 3 estimates V_{ss} from only average channel velocity V_{avg}, R, W, and channel type (natural or trapezoidal). The effects of other factors such as bend angle, bank angle, and bed/bank rough-

ness have not been determined. It is important to note that V_{ss}/V_{avg} has rarely been found to exceed 1.6 in any alluvial or man-made fixed bed channel. Thus for the outer bank of bendways, the designer is simply defining where in the range of V_{ss}/V_{avg} = 1 to 1.6 to design the protection. Figure 3 assists in that determination and generally provides a conservative estimate. Since Figure 3 is valid only for estimating side slope velocity, velocity estimation for all problems other than bank protection (such as channel bottom protection) must use some other technique to determine local depth-averaged velocity, such as the numerical model described previously.

Average channel velocity is used in the EM method *(1991)* only in conjunction with the empirical velocity estimation technique and is determined from discharge/channel area (Q/A). Area and discharge should be restricted to the main channel and should not include overbank areas.

Bend Radius and Water-Surface Width

Center-line radius of curvature of the bend and the water-surface width at the upstream end of the bend are used to characterize the bendway in the EM rock sizing techniques. The center-line radius and the width should be based on flow in the main channel and should not include overbank areas.

Natural versus Trapezoidal Channel

In the empirical velocity estimation technique shown in Figure 3, two channel types, natural and trapezoidal, are used. Trapezoidal channels are often man-made with a smooth alignment; and sediment transport is not sufficient to build point bars, which can concentrate flow against the outer bank. The data used in developing the trapezoidal channel curve were from clear-water channel models having riprap bottom and banks and aspect ratios (top width/average depth) ranging from 11 to 22. While many trapezoidal channels have aspect ratios greater than 22, secondary currents in the lower aspect ratio channels will provide more velocity concentration along the outer bank than the higher aspect ratio channels. In contrast, the natural channel curve in Figure

3 is applicable to channels having irregular alignment with sediment transport leading to point bars and toe scour that concentrate the flow along the outer bank.

K_1, Side Slope Angle

Stability studies have shown that the decrease in stability that occurs from placing a revetment on a side slope is not as significant as suggested in some of the previous guidance. This is likely due to the fact that the angle of repose of a revetment is greater than the angle of repose of a rock dike(Maynord 1988). The relation of K_1 versus side slope angle from EM 1110-2-1601 *(1991)* is shown in Figure 4. The solid line should be used for revetments and is described by the empirical relation

$$K_1 = -0.672 + 1.492Cot(\theta) - 0.449Cot^2(\theta) + 0.045Cot^3(\theta) \quad (14)$$

The least volume of riprap per foot of bank line is used when revetments are placed on slopes between 1V:1.5H and 1V:2H. For slopes flatter than 1V:4H, rock stability is not affected by the slope angle for revetments subject to channel flow. Slopes steeper than 1V:1.5H are not recommended.

Example Problems

The following examples demonstrate application of the EM 1110-2-1601 procedures *(1991)*. Gradations shown in Table 1 are used for demonstration in some of the examples, but these gradations should not be taken as a recommendation.

Example 1: Bank Protection Only

Problem. Determine stable riprap size for the outer bank side slope of a natural channel bend in which the maximum velocity occurs at bank-full flow. Water-surface profile computations at bank-full flow show an average channel velocity of 2.2 m/sec (7.1 ft/sec) and a depth at the toe of the outer bank of 4.6 m (15 ft). The channel is sufficiently wide so that the added resistance will not

significantly affect the computed average channel velocity. A nearby quarry has rock weighing 2643 kg/m^3 (165 lb/ft^3) and can produce the 0.30-, 0.38-, 0.46-, 0.53-, and 0.61-m (12-, 15-, 18-, 21-, and 24-in.) D_{100}(max) gradations shown in Table 1. A bank slope of 1V:2H has been selected based on geotechnical analysis. A typical blanket thickness of $1D_{100}$(max) will be used in this design with the minimum safety factor of 1.1. Center-line bend radius is 189 m (620 ft) and water-surface width is 61.0 m (200 ft).

Solution. Using Figure 3 with R/W = 189/61 = 3.1 results in V_{ss}/V_{avg} = 1.48 for a natural channel bend. The resulting V_{ss} = 1.48(2.2) = 3.2 m/sec (10.5 ft/sec). Using Equation 9 with C_t = 1 , C_v = 1.18 (from Equation 13), K_1 = 0.88 , and d = 0.8(4.6) = 3.7 m (12 ft) results in a computed D_{30} = 0.19 m (0.63 ft). Table 1 shows that of the available gradations, the 0.46-m (18-in.) D_{100}(max) gradation is the smallest gradation having D_{30}(min) $\geq$ the computed D_{30}. This gradation should be placed to a thickness of $1D_{100}$(max) or 0.46 m (18 in.). This example demonstrates that the actual safety factor is often larger than 1.1 because available gradations are used. In this case the actual safety factor is (0.73)/(0.63/1.1) = 1.27.

Example 2: Design For Thickness Greater Than $1D_{100}$

If a thickness greater than $1D_{100}$(max) is specified, smaller gradations can be used if available. This option frequently (but not always) requires that the blanket thickness be larger than the thickness for rock placed to $1D_{100}$(max). Using Example 1 and specifying a thickness parameter N of 1.2 in Figure 2 (determined by trial and error), results in a computed D_{30} = 0.18 m (0.59 ft) and an 0.46-m (18-in.) blanket thickness of the Table 1 gradation having a D_{100}(max) = 0.38 m (15 in.). Although both the gradations from Example 1 and this example will remain stable for the design conditions of Example 1, the two gradations are not equal in stability because the real safety factor for the D_{100}(max) = 0.38m (15 in.) gradation placed to a thickness of 0.46 m (18 in.) is (0.61)/(0.59/1.1) = 1.14.

Using Example 1 again, suppose a gradation has a unit weight = 2643 kg/m^3 (165 lb/ft^3), D_{85}/D_{15} = 5.2, D_{30}(min) = 0.12 m (0.40 ft), and D_{100}(max) = 0.43 m (17 in.). Since D_{30}(min) = 0.12 m (0.4 ft) is less than the required D_{30} = 0.19 m (0.63 ft), a thickness of $1D_{100}$(max) will not be stable. What thickness would be required to remain stable for the conditions of Example 1? Try various thickness parameters N from Figure 2 to determine the minimum stable thickness. The following table gives the results of this trial and error analysis.

$N = \frac{\text{Thickness}}{D_{100}\text{ (max)}}$	Thickness, (in[a])	C_T from Figure 2	Required D_{30} (ft)
1.5	26	0.76	0.48
1.75	30	0.64	0.40
2.0	34	0.53	0.33

[a]1 in. = 25.4 mm.
1 ft = 0.305 m.

Use of this alternate gradation for Example 1 would require a blanket thickness of 0.76 m (30 in.) because the D_{30}(min) = 0.12 m (0.4 ft) is equal to or greater than the required D_{30} = 0.12 m (0.40 ft). This gradation placed to a 0.76-m (30-in.) thickness satisfies the requirements of Example 1 but is not exactly equal in stability to the previously determined gradations in Table 1 because the actual safety factor is different.

PC PROGRAM

A PC program "RIPRAP15" incorporating these procedures has been developed and is available from the author.

SUMMARY AND CONCLUSIONS

The Corps of Engineers riprap design procedure presented herein is applicable to bank and channel protection in low-turbulence environments. While shear stress and other characteristic velocities have been used, local depth-averaged velocity was selected as the basis for this procedure because methods are available for estimating depth-averaged velocity and because many designers will not use shear-stress-based procedures.

This method has several empirical coefficients analogous to the Shields coefficient that take into account the effects of rock shape, blanket thickness, and side slope angle. The traditional Carter, Carlson, and Lane *(1953)* relationship is more conservative than the empirical curve presented herein for side slope effects. Another empirical coefficient is used to account for changes in the vertical velocity profile such as that occurring in bendways or downstream of concrete channels. This empirical approach was chosen because a theoretical approach would have been unfriendly to most users of riprap design guidance.

Gradation effects are addressed by using D_{30} as the characteristic particle size in lieu of the commonly used D_{50}. Equation (10) relates D_{50} to D_{30} and D_{85}/D_{15} for designers preferring to use D_{50}.

Blanket thickness and gradation must both be specified to define the stability of a revetment. A uniform riprap can be placed to a large thickness with only a small increase in stability compared to the minimum blanket thickness. However a nonuniform riprap placed to a large thickness will be much more stable than the minimum thickness of the same gradation. The method presented herein defines the stability of a wide range of gradation and thickness.

Design examples show how the method is applied to several different cases.

ACKNOWLEDGEMENT

The tests described and the resulting data presented herein, unless otherwise noted, were obtained from research conducted under the Civil Works Investigation, "Riprap Design and Cost Reduction: Studies in Near-Prototype Size Laboratory Size Channel," of the US Army Corps of Engineers by the US Army Engineer Waterways Experiment Station. Permission was granted by the Chief of Engineers to publish this information.

REFERENCES

Anderson, A.G., Paintal, A.S., and Davenport, J.T. 1970. *Tentative Design Procedure For Riprap-Lined Channels*, National Cooperative Highway Research Program Report 108, University of Minnesota, Minneapolis, Minn.

Bernard, R.S. and Schneider, M.L.. 1992. *Depth-Averaged Numerical Modeling for Curved Channels*, US Army Engineer Waterways Experiment Station,Technical Report HL-92-9, Vicksburg, MS.

California Division of Highways. 1970. *Bank and Shore Protection in California Highway Practice*, State of California, Department of Public Works, Sacramento, Ca.

Carter, A.C.,Carlson, E.J., and Lane, E.W. 1953. *Critical Tractive Forces on Channel Side Slopes in Coarse, Non-Cohesive Material*. Hydraulic Laboratory Report No. HYD-366, US Bureau of Reclamation.

Federal Highway Administration. 1989. *Design of Riprap Revetments*, HEC-11, Turner-Fairbank Highway Research Center,Va.

Isbash, S.V. 1935. *Construction of Dams by Dumping Stones in Flowing Water*, Translated by A. Dorijikov, US Army Engineer District, Eastport, Me.

Maynord, S.T.1988. *Stable Riprap Size For Open Channel Flows*. Technical Report HL-88-4. US Army Engineer Waterways Experiment Station, Vicksburg MS.

Maynord, S.T. 1992. *Riprap Stability: Studies in Near-Prototype Size Laboratory Channel*, Technical Report HL-92-5. US Army Engineer Waterways Experiment Station, Vicksburg, MS.

Neill, C.R. 1967. *Mean-velocity Criterion for Scour of Coarse, Uniform Bed-material*,IAHR, 12th Congress, Paper C6,3,c6.1-c6.9.

Pilarczyk, K. 1987. in *Guidelines for the Design and Construction of Flexible Revetments Incorporating Geotextiles for Inland Waterways*, PIANC, supplement to Bulletin no 57.

Pilarczyk, K. 1990. *Coastal Protection*, Proceeding of short course on Coastal Protection, Delft University of Technology.

Shields, A. 1936. *Application of Similarity Principles and Turbulence Research to Bed-load Movement*, English Translation by W.P. Ott and J.C. van Uchelon, California Institute of Technology, Publication 167.

Stevens, M.A. and Simons, D.B. 1976. *Safety Factors for Riprap Protection*, Hyd Division, ASCE, Vol 102, No HY5, pp 637-655.

US Army Corps of Engineers. 1971. *Additional Guidance for Riprap Channel Protection*, Ch 1. ETL 1110-2-120, US Government Printing Office, Washington, DC, 14 May.

US Army Corps of Engineers.1991. *Hydraulic Design of Flood Control Channels*. EM 1110-2-1601. US Government Printing Office, Washington, DC, 1 July.

TABLE 1. GRADATIONS FOR SPECIFIC STONE WEIGHT OF 165 LB/FT^3,[a] FROM USACE(1971)

D_{100} (max)	Limits of Stone Weight (lb) for Percent Lighter by Weight[b]						D_{30} (min)	D_{90} (min)
	100		50		15			
(in.)	Max	Min	Max	Min	Max	Min	(ft)	(ft)
12	86	35	26	17	13	5	0.48	0.70
15	169	67	50	34	25	11	0.61	0.88
18	292	117	86	58	43	18	0.73	1.06
21	463	185	137	93	69	29	0.85	1.23
24	691	276	205	138	102	43	0.97	1.40

[a] 1 lb/ft^3 = 16.018 kg/m^3

[b] Stone weight limit data from USACE(1971). Relationship between diameter and weight is based on the shape of a sphere.

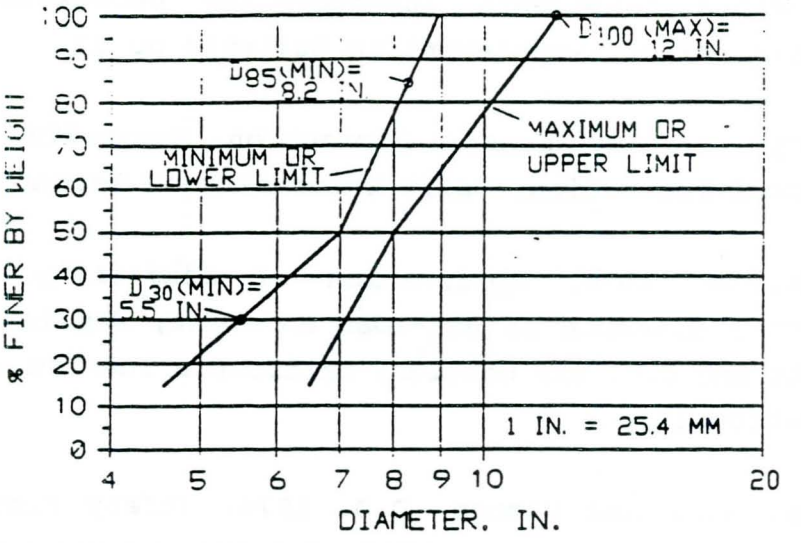

FIGURE 1. EXPLANATION OF GRADATION TERMINOLOGY

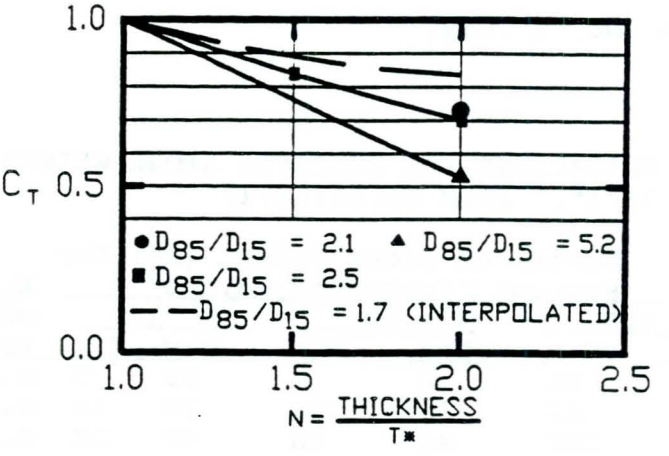

$$C_T = \frac{D_{30} \text{ FOR THICKNESS OF } NT*}{D_{30} \text{ FOR THICKNESS OF } T*}$$

$T* = 1D_{100}$ OR $1.5D_{50}$, WHICHEVER IS GREATER

FIGURE 2. CORRECTION FOR RIPRAP BLANKET THICKNESS

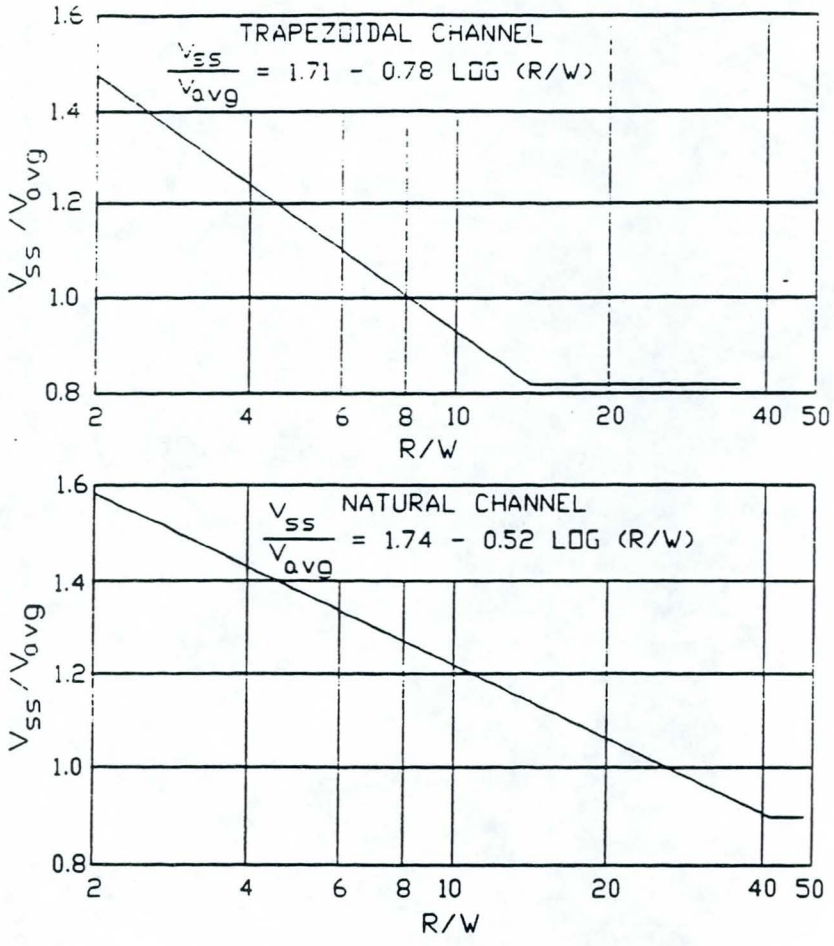

FIGURE 3. VELOCITY ESTIMATION BASED ON EM 1110-2-1601 (1991)

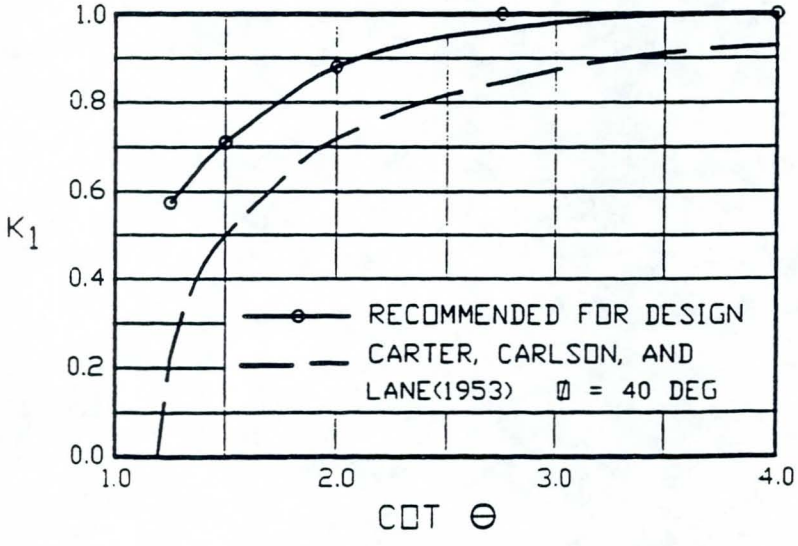

FIGURE 4. SIDE SLOPE CORRECTION COEFFICIENT

A REVIEW OF STABILITY FOR ROCK AND RIPRAP SLOPES UNDER WAVE ATTACK

J.W. van der Meer
Delft Hydraulics, P.O. Box 152,
8300 AD Emmeloord, The Netherlands

ABSTRACT

The Hudson formula (CERC, 1984) is an ancient well known stability formula for armor layers of rubble mound structures. The main reason for its success was the simplicity of the formula in combination with an engineering judgement through the stablity factor K_D.

The paper first summarizes how some of the old stability formulas are related by assuming incipient instability of an armor unit. A more basic formula that then can be developed has already been described by Sigurdsson (1962). By making assumptions on the direction of the wave force (parallel or perpendicular to the slope) and on the natural angle of wave attack the formula of Iribarren (1950), the same formula modified by Hudson (1959) and the well known formula of Hudson (1959) simply follow from the more basic formula.

Based on the work of Thompson and Shuttler (1976) an extensive series of model tests with random waves was performed by Van der Meer (1988a and b) on rock and riprap slopes. A large number of possible influences on stability was checked. The analysis of more than 400 tests resulted in two new design formulas.

One formula describes the stability for plunging waves $\xi_m < 2$-4, where ξ_m is the surf similarity parameter) and the other for surging waves (larger ξ_m). Minimum stability is found for the collapsing waves, according to the findings of Ahrens (1975), Losada and Gimenez-Curto (1979) and Bruun (1985). Other influences on stability, besides the wave period and slope angle that are combined in ξ_m, were the duration of the storm and the permeability of the structure (breakwater, revetment or seawall). Finally a clear defined damage level was introduced.

REVIEW ON REGULAR WAVE FORMULAS

The International Commission for the study of Waves (PIANC, 1976) gave an overview of existing stability formulas for static stability of rock slopes. Generally, a stability formula can be developed by assuming incipient instability of an armour unit, subjected to certain wave forces. Depending on the schematisation of resisting forces and wave forces, numerous formulas can be developed, as shown by the Commission mentioned above.

Most stability formulas, however, have a common part. And this part can be regarded as very important for stability of rock slopes, but also for stability of artificial armour units and for stability of placed block revetments. A general development of a stability formula will be given first.

Figure 1 shows a part of an amour layer. The slope angle is given by α, the natural angle of repose by ϕ and the boyant mass of the stone by W', where

$$W' = (\rho_a - \rho_w) D_{n50}^3$$

where:

ρ_a = mass density of rock

ρ_w = mass density of water

D_{n50} = nominal diameter $D_{n50} = (W_{50}/\rho_a)^{1/3}$

W_{50} = average weight of stone (50% value on mass distribution curve)

The wave forces are schematized by two forces, one parallel to the slope, F_P, and the other normal to the slope, F_N. The same assumptions were made by Sigurdsson (1962). Assuming incipient instability the momentum equation for the point A gives:

$$F_N \sin\phi\ D/2 + F_P \cos\phi\ D/2 = g\ W'\ \sin(\phi-\alpha)\ D/2 \qquad (1)$$

Generally, wave forces as F_P and F_N are related to the wave height (Hudson (1959)) by the following equation:

$$F = \rho_w\ g\ C\ D^2H \qquad (2)$$

where:
F = wave force
C = coefficient
D = diameter of the stone

Assuming a coefficient C_1 for the normal wave force, F_N, a coefficient C_2 for the parallel wave force, F_P, and assuming $D = KD_{n50}$, (K = coefficient), Equation 1 becomes with 2:

$$\rho_w g\ C_1 D_{n50}^3\ H \sin\phi\ K^3/2 + \rho_w g\ C_2 D_{n50}^3\ H \cos\phi\ K^3/2 = g(\rho_a-\rho_w) D_{n50}^4 \sin(\phi-\alpha) K^4/2 \qquad (3)$$

Equation 3 can be elaborated to:

$$H/\Delta D_{n50} = K \sin(\phi - \alpha)/(C_1 \sin\phi + C_2 \cos\phi) \qquad (4)$$

with:

$$\Delta = (\rho_a - \rho_w)/\rho_w \qquad (5)$$

Defining the friction coefficient, μ, (Iribarren (1950)) as $\mu = \tan\phi$, Equation 4 can finally be rewritten to:

$$H/\Delta D_{n50} = K(\mu\cos\alpha - \sin\alpha)/(\mu C_1 + C_2) \qquad (6)$$

Equation 6 was already developed by Sigurdsson (1962). The $H/\Delta D_{n50}$ is the same as the often used stability number, N_s, (Hudson, (1959)). In fact $H/\Delta D_{n50}$ is a combination of two dimensionless variables, the H/D_{n50} and the relative mass density, Δ. The $H/\Delta D_{n50}$ appears in a lot of stability formulas.

In fact the $H/\Delta D_{n50}$ determines the stability of a stone under wave action. Statically stable structures have $H/\Delta D_{n50}$ values between 1 and 4, and dynamically stable structures between 6 and 500.

Artifical armour units can be described by the nominal diameter, D_n, where $D_n = (W/\rho_a)^{1/3}$. In that case $H/\Delta D_n$ can be used. An important design parameter for placed block revetments is the thickness of the blocks, D. With this definition of D, the parameter becomes $H/\Delta D$. It is obvious that by using a nominal diameter for a mass and a thickness for a block, the stability of different structures under wave attack can be compared by using the parameter $H/\Delta D$ as a reference. Moreover, structures under steady flow regimes are often described by the Shields parameter, $u^2/g\Delta D_{n50}$. Assuming $H :: u^2/g$, the agreement between $H/\Delta D_{n50}$ and the Shields parameter becomes clear.

Equation 6 can be rewritten to some well known formulas. Assuming that only a parallel force exists, ($C_1 = 0$), Equation 6 becomes Iribarren's formula:

$$H/\Delta D_{n50} = K_1(\mu\cos\alpha - \sin\alpha) \qquad (7)$$

with:
$K_1 = K/C_2$

Assuming only a normal force ($C_2 = 0$), Equation 6 becomes Iribarren's formula, modified by Hudson (1959):

$$H/\Delta D_{n50} = K_2(\mu\cos\alpha - \sin\alpha)/\mu \qquad (8)$$

with:
$K_2 = K/C_1$

Hudson (1959) assumed for rubble structures $\phi = 1$, which reduces Equation 6 to:

$$H/\Delta D_{n50} = K(\cos\alpha - \sin\alpha)/(C_1 + C_2) \quad (9)$$

Hudson combined all coefficients to one coefficient, K_D, and replaced the term $\cos\alpha - \sin\alpha$ by $(\cot\alpha)^{1/3}$. This reduces Equation 9 to the well-known Hudson formula, although written in a more simple equation:

$$H/\Delta D_{n50} = (K_D \cot\alpha)^{1/3} \quad (10)$$

Summarizing, $H/\Delta D_{n50}$ is an important variable in a stability formula. Different types of structures can be compared using this variable.

K_D is a stability coefficient taking into account all not mentioned variables. K_D-values suggested for design correspond to a "no damage" condition where up to 5% of the armour units may be displaced. In the 1973 edition of the Shore Protection Manual the values given for K_D for rough, angular stones in two layers on a breakwater trunk were:
$K_D = 3.5$ for breaking waves,
$K_D = 4.0$ for non-breaking waves.

The definition of breaking and non-breaking waves is different from plunging and surging waves on a structure slope. A breaking wave in Formula 10 means that the wave breaks due to the foreshore in front of the structure directly on the armour layer. It does not describe the type of breaking due to the slope of the structure itself.

No tests with random waves had been conducted, it was suggested to use H_s in Eq. 10. By 1984 the advice given was more cautious. The SPM now recommends $H = H_{10}$, being the average of the highest 10 percent of all waves. For the case considered above the value of K_D for breaking waves was revised downward from 3.5 to 2.0 (for non-breaking waves it remained 4.0). The effect of these two changes is equivalent to an increase in the unit stone mass required by a factor of about 3.5!

The main advantages of the Hudson formula are its simplicity, and the wide range of armour units and configurations for which values of K_D have been derived. The Hudson formula also has many limitations. Briefly they include:

- Potential scale effects due to the small scales at which most of the tests were conducted,
- The use of regular waves only,
- No account taken in the formula of wave period or storm duration,
- No description of the damage level in the formula,
- The use of non-overtopped and permeable core structures only.

Based on earlier work of Thompson and Shuttler (1975) an extensive series of model tests was conducted at Delft Hydraulics (Van der Meer (9188a), Van der Meer (1987), Van der Meer (1988b)). The tests included structures with a wide range of core/underlayer permeabilities and a wider range of wave conditions.

Wave conditions are given principally by the incident wave height at the toe of the structure, H_i, usually as the significant wave height, H_s (average of the highest 1/3 of the waves) or H_{m0} ($4\sqrt{m_0}$, based on the spectrum); the mean or peak wave periods, T_m or T_p; the angle of wave attack, β, and the local water depth, h. The mean period T_m is used in this paper. The wave period is often written as a wave length and related to the wave height, resulting in a wave steepness. The wave steepness, s_{om}, can be defined by using the deep water wave length, $L_{om} = gT_m^2/2\pi$:

$$s_{om} = 2\pi H_s/gT_m^2 \qquad (11)$$

If the wave height in front of the structure is used in Eq. 11, a fictitious wave steepness is obtained. This steepness is fictitious because H_s is the wave height in front of the structure and L_{om} is the wave length on deep water. The most useful parameter describing wave action on a slope, and some of its effects, is the surf similarity or breaker parameter, ξ_m:

$$\xi_m = \tan\alpha/\sqrt{s_{om}} \qquad (12)$$

The surf similarity parameter has often been used to describe the form of wave breaking on a beach or structure. Small values (< 0.5) give spilling waves on a beach, intermediate values (0.5-2) give plunging (breaking) waves and larger values give surging (non-breaking) waves. The transition from plunging to surging ($\xi_m \approx 2$) is called collapsing waves.

The acceptable limits of S depend mainly on the slope angle of the structure. For a two diameter thick armour layer the values in Table 1 can be used. The initial damage of S = 2-3 is according to the criterion of the Hudson formula which gives 0-5% damage. Failure is defined as exposure of the filter layer. For S values higher than 15-20 the deformation of the structure results in an S-shaped profile and should be called dynamically stable.

The behaviour of the structure can be described by a few parameters. Statically stable structures are described by the development of damage. This can be the amount of rock that is displaced or the displaced distance of a crown wall. Dynamically stable structures are described by a developed profile. The damage to the armour layer can be given as a percentage of displaced stones related to a certain area (the whole or a part of the layer). In ths case, however, it is difficult to compare various structures as the damage figures are related to different totals for each structure. Another possibility is to describe the damage by the erosion area around swl. When this erosion area is related to the size of the stones, a dimensionless damage level is presented which is independent of the size (slope angle and height) of the structure. This damage level is defined by:

$$S = A_e / D_{n50}^2 \qquad (13)$$

where:

S = damage level

A_e = erosion area around swl

A plot of a structure with damage is shown in Fig. 2. The damage level takes into account settlement and displacement. A physical description of the damage, S, is the number of squares with a side D_{n50} which fit into the erosion

area. Another description of S is the number of cubic stones with a side of D_{n50} eroded within a D_{n50} wide strip of the structure. The actual number of stones eroded within this strip can be more or less than S, depending on the porosity, the grading of the armour stones and the shape of the stones. Generally the actual number of stones eroded in a D_{n50} wide strip is equal to 0.7 to 1 times the damage S.

The permeability of the structure has influence on the stability of the armour layer. The permeability depends on the size of filter layers and core and can be given by a notional permeability factor, P. Examples of P are shown in Fig. 3, based on the work of Van der Meer (1988a). The lower limit of P is an armour layer with a thickness of two diameters on an impermeable core (sand or clay) and with only a thin filter layer. This lower boundary is given by P = 0.1. The upper limit of P is given by a homogeneous structure which consists only of armour stones. In that case P = 0.6. Two other values are shown in Fig. 3 and each particular structure should be compared with the given structures in order to make an estimation of the P factor. It should be noted that P is not a measure of porosity!

Two formulas were derived by Van der Meer (1988) for plunging and surging waves respectively. These formulas may be written as:

for plunging waves:

$$H_s/\Delta D_{n50} = 6.2\ P^{0.18}\ (S/\sqrt{N})^{0.2}\ \xi_m^{-0.5} \qquad (14)$$

and for surging waves:

$$H_s/\Delta D_{n50} = 1.0\ P^{-0.13}\ (S/\sqrt{N})^{0.2}\ \sqrt{\cot\alpha}\ \xi_m^{P} \qquad (15)$$

The transition from plunging to surging waves can be calculated using a critical value of ξ_m:

$$\xi_{mc} = [6.2\ P^{0.31}\ \sqrt{\tan\alpha}]^{1/(P+0.5)} \qquad (16)$$

For $\cot\alpha \geq 4.0$ the transition from plunging to surging does not exist and for these slope angles only Eq. 14 should be used. The notional permeability factor P is shown in Fig. 3. The factor P should lie between 0.1 and 0.6. Design values for the damage level S are shown in Table 1. The level "start" of damage, S = 2 - 3, is equal to the definition of "no damage" in the Hudson formula, Eq. 10. The maximum number of waves N which should be used in Eqs. 14 and 15 is 7500. After this number of waves the structure more or less has reached an equilibrium. The wave steepness should lie between $0.005 < s_{om} < 0.06$ (almost the complete possible range). The relative mass density varied in the tests between 2000 kg/m^3 and 3100 kg/m^3, which is also the possible range of application.

The reliability of the formulas depends on the differences due to random behaviour of rock slopes, accuracy of measuring damage and curve fitting of the test results. The reliability of the Formulas 14 and 15 can be expressed by giving the coefficients 6.2 and 1.0 in the equations a normal distribution with a certain standard deviation. The coefficient 6.2 can be described by a standard deviation of 0.8 (variation coefficient 6.5%) and the coefficient 1.0 by a standard deviation of 0.8 (8%). These values are significantly lower than that for the Hudson formula at 18% for K_D (with mean K_D of 4.5). With these standard deviations it is simple to include 90% or other confidence bands.

Equations 14 - 16 are more complex than the Hudson formula 10. They include also the effect of the wave period, the storm duration, the permeability of the structure and a clearly defined damage level. This may cause differences between the Hudson formula and Eqs. 14 - 16, which has been described in the next section. Nevertheless, it is more difficult to work with Eqs. 14 - 15. For a good design it is required to perform a sensitivity analysis for all parameters in the equations, as described hereafter.

COMPARISON OF HUDSON AND NEW FORMULAS

The $H_s/\Delta D_{n50}$ in the Hudson formula is only related to the slope angle $\cot\alpha$. Therefore a plot of $H_s/\Delta D_{n50}$ or N_s versus $\cot\alpha$ shows one curve for the Hudson

formula. Formulas 14 - 16 take into account the wave period (or steepness), the permeability of the structure and the storm duration. The effect of these parameters are shown in Fig. 4.

The upper graph shows the curves for a permeable structure after a storm duration of 1000 waves (a little more than the number used by Hudson). The lower graph gives the stability of an impermeable revetment after wave attack of 5000 waves (equivalent to 5 - 10 hours in nature). Curves are shown for various wave steepnesses. Depending on the structure and wave parameters the Hudson formula under or overpredicts the actual stability. Only for some cases (s_{om} = 0.01 in upper graph and s_{om} = 0.05 in lower graph) both formulas give the same stability.

DESIGN GRAPHS

Design graphs can be drawn using Formulas 14 and 15. In order to demonstrate the influence of the different parameters the graphs are given for an assumed structure. The properties of this structure are:

Nominal diameter	D_{n50}	= 1.0 m
Mass density stone	ρ_s	= 2,600 kg/m^3, that is W_{50} = 2,600 kg.
Mass density water	ρ_w	= 1,000 kg/m^3, equivalent to a relative mass density, Δ, of 1.6
Slope angle	$\cot\alpha$	= 3.0
Damage level	S	= 5 (tolerable damage in 50 years)
Permeability	P	= 0.5 (permeable core, see Fig. 3c)
Storm duration	N	= 3000 waves

Influence of wave height, period and damage level

Most of the design graphs are shown on H_s - ξ_m plots. The wave height is plotted on the vertical axis and the surf similarity or breaker parameter on the horizontal. The breaker parameter takes into account the influence of the wave period and slope angle. The damage levels S = 2 (start of damage),

S = 5 and 8 (tolerable damage) and S = 12 (filter layer visible, failure) have been plotted in Fig. 5. Formula 14 is plotted on the left side of the Figure (plunging waves) and formula 15 on the right side (surging waves).

By using the assumed parameters for the structure given above, the plunging wave curve for S = 5 can be found from Formula 14:

$$H_s = 5.43\ \xi_m^{0.5} \qquad (16)$$

and the surging wave curve from Formula 15:

$$H_s = 1.88\ \xi_m^{0.5} \qquad (17)$$

The transition from plunging to surging waves is described by Equation 16. This transition (collapsing waves) gives the minimum stability. In the plunging region wave run-up is decisive for stability and in the surging region wave run-down. In the collapsing region both run-up and run-down forces are high which causes the minimum of stability.

Influence of slope angle

Figure 6 shows the stability formulas for slope angles with $\cot\alpha$ = 1.5, 2.0, 3.0, 4.0 and 6.0. The left side (plunging waves) is given by one curve which means that the breaker parameter is an excellent parameter in the breaking wave region. For slopes gentler than 1:4 surging waves do not occur. For steeper slopes the minimum decreases, i.e. a lower wave height causes instability, and the transition from plunging to surging waves shifts to the right.

Influence of permeability

Figure 7 shows the curves for values of the permeability coefficient. The value of P = 0.1 (impermeable structure) gives the lower boundary and the value of P = 0.6 (homogeneous structure) gives the upper boundary. The influence of the wave period for plunging waves (left side of Figure) shows the same trend for all four structures, although a more permeable structure is

more stable. A more permeable structure is also more stable for surging waves ($\xi_m > 3.5$), but the stability increases with larger wave periods. The curves are steeper for larger permeability.

This phenomena can be explained in physical terms by the difference in water motion on the slope. For a slope with an impermeable core, the flow is concentrated in the armor layer causing large forces on the stones during rundown. For a slope with a permeable core, the water dissipates into the core, and the flow becomes less violent. With lower wave periods (larger ξ_m), more water can percolate and flow down through the core. This reduces the forces and stabilizes the slope.

The stability increases by moe than 35% as P shifts from 0.1-0.6 in relation to the wave height. This means a difference of a factor of 2.5 in mass of stone for the same design wave height. This is only caused by a difference in permeability. This aspect is taken into account in the berm breakwater concept (Baird and Hall, 1984) where a permeable berm is applied.

Influence of storm duration

Figure 8 shows the damage level of S = 5 for different storm durations, i.e. different numbers of waves. For $\xi_m = 2$ and N = 1000 this damage level is reached with a wave height of $H_s = 4.3$ m. For a very long storm (N > 7000) it is reached with $H_s = 3.5$ m. The storm duration is a parameter which only becomes obvious when testing with random waves. For monochromatic waves equilibrium is found within 1000 waves. This means that it is not so easy to use stablity formulas developed with monochromatic waves for prototype conditions where the waves are random. It is not simply a matter of replacing H by the significant wave height H_s or even a higher wave height.

Damage curves

Another graph which can be calculated from the formulas is the damage curve in which the damage is plotted as a function of the wave height. Figure 9 gives the damage curves for two different values of wave steepness, $s_{om} = 0.02$ ($S = 0.00907\ H_s^5$, from Equation 14) and 0.05 ($S = 0.00289\ H_s^5$, also from Equation 14).

CONCLUSIONS

Old stability formulas have been developed from a general stability formula described in Sigurdsson (1962), including the Hudson formula.

New stability formulas have been developed, based on an extensive number of random wave tests. These formulas have been compared with the Hudson formula and give a more accurate description of stability of rock and riprap slopes.

The graphs in Figures 5 to 9 give a good impression of the influence of all the governing parameters on stability. Formulas and graph plotting have been programmed on a personal computer. This makes it very easy for the designer to design the armor layer of a rubble mound breakwater or revetment and to look into the effects of various changes on stability and possibilities for improving design.

REFERENCES

Ahrens, J.P., 1975. Large wave tank tests of riprap stability. CERC, Technical Memorandum No. 51.

Baird, W.F. and Hall, K.R., 1984. The design of berm breakwaters using quarried stones. Proc. 19th ICCE, Houston, Tex. 2580-2591.

Bruun, P., 1985. Design and construction of mounds for breakwaters and coastal protection. Developments in geotechnical engineering, 37, Elsevier, Amsterdam.

Coastal Engineering Research Center, 1984. Shore Protection Manual. U.S. Army Corps of Engineers.

Hudson, R.Y., 1959. Laboratory investigations of rubble mound breakwaters. WES Report, Vicksburg.

Iribarren, R.C., 1950. Generalizacion de la formula para el calculo de los diques de escollera y comprobacion de sus coeficientes. (Generalization of the formula for calculation of rock fill dikes and verification of its coefficients). Revista de Obras Publicas, Madrid. Translated by A. Haritos, WES Translation N. 51-4, 1951.

Losada, M.A. and Gimenez-Curto, L.A., 1979. The joint effect of the wave height and period on the stability of rubble mound breakwater using Iribarren's number. Coastal Eng., 3, pp. 77-96.

PIANC, 1976. Final Report of the International Commission for the study of waves, second part. Annex to bulletin No. 25, Vol. III/1976.

Siggurdson, G., 1962. Wave forces on breakwater capstones. proc. ASCE, WW3.

Thompson, D.M. and Shuttler, R.M., 1975. Riprap design for wind wave attack. A laboratory study in random waves. HRS, Wallingford, Report Ex 707.

Van der Meer, J.W., 1987. Stability of breakwater around layers - Design formulae. Elsevier Coastal Engeneering, 11, 219-239.

Van der Meer, J.W., 1988a. Rock slopes and gravel beaches under wave attack. PhD-thesis, Delft University of Technology. Also Delft Hydraulics Publication No. 396.

Van der Meer, J.W., 1988b. Deterministic and probabilistic design of breakwater armor layers. Proc. ASCE, Journal of WPC and OE, Vol. 114, No. 1

Slope	Initial damage	Intermediate damage	Failure
1:1.5	2	3-5	8
1:2	2	4-6	8
1:3	2	6-9	12
1:4	3	8-12	17
1:6	3	8-12	17

Table 1 Design values of S for a two diameter thick armor layer

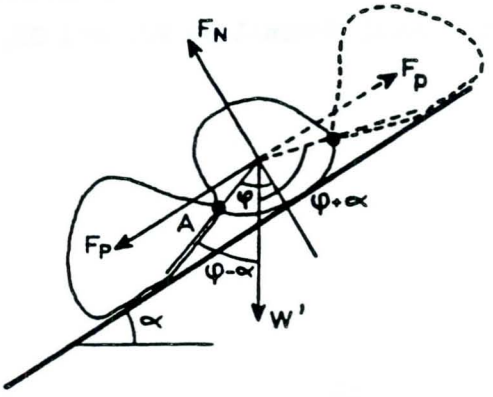

Fig. 1 Schematisation of incipient instability

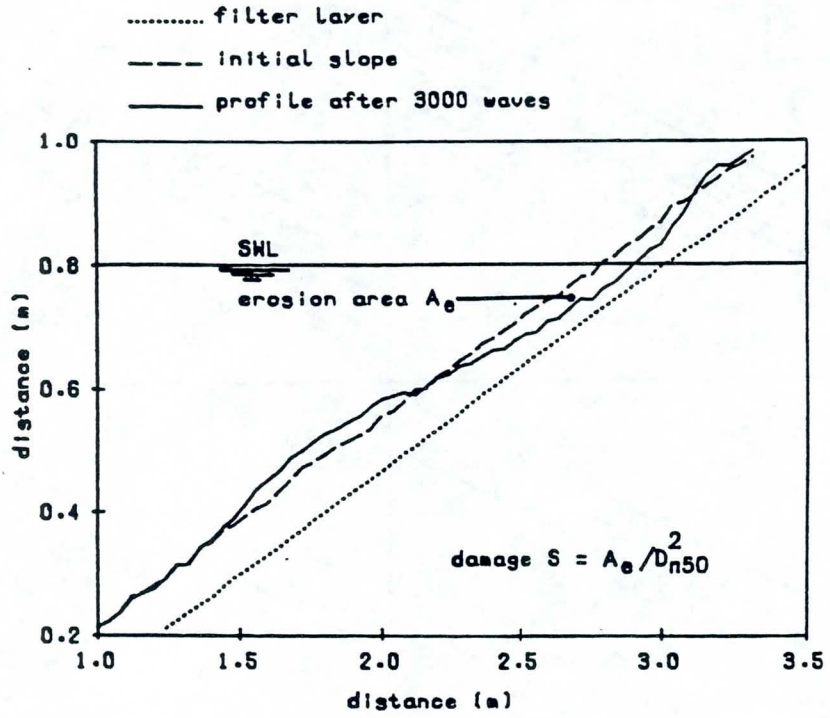

Fig. 2 Damage S based on erosion area A_e

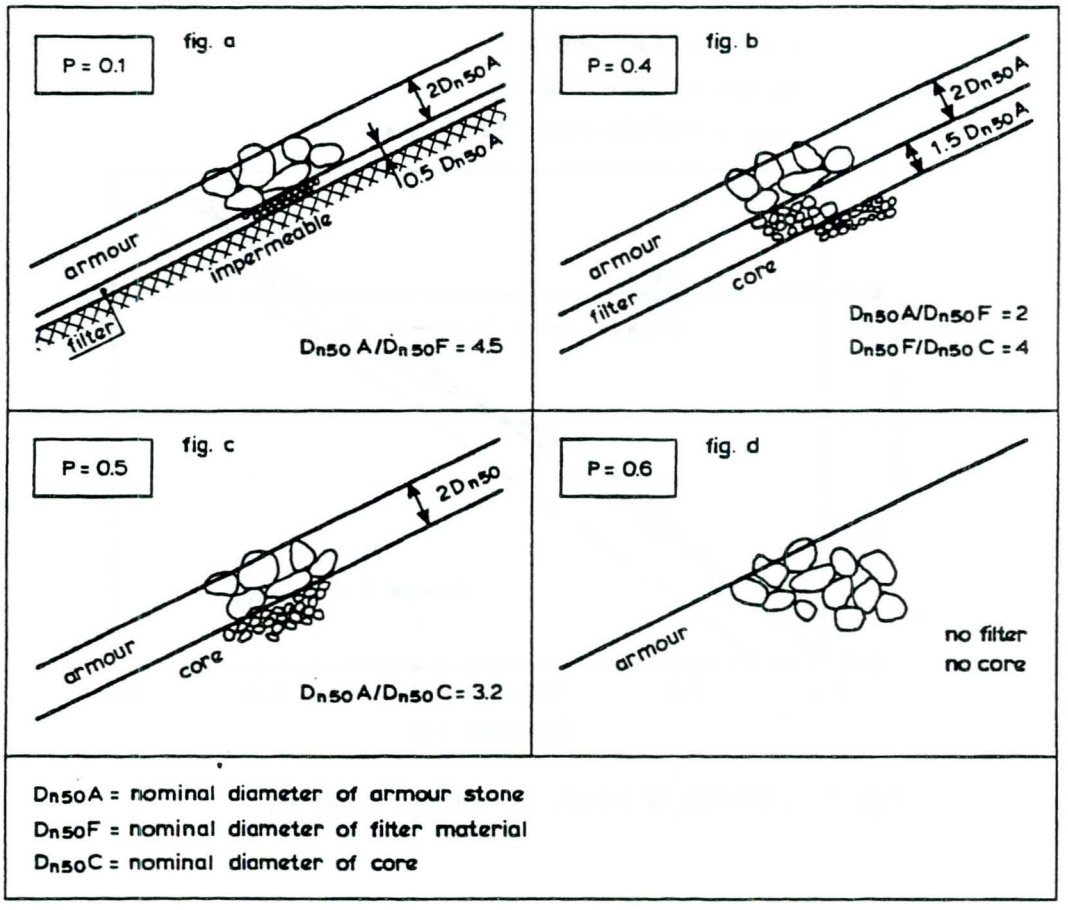

Fig. 3 Notional permeability factor P for various structures

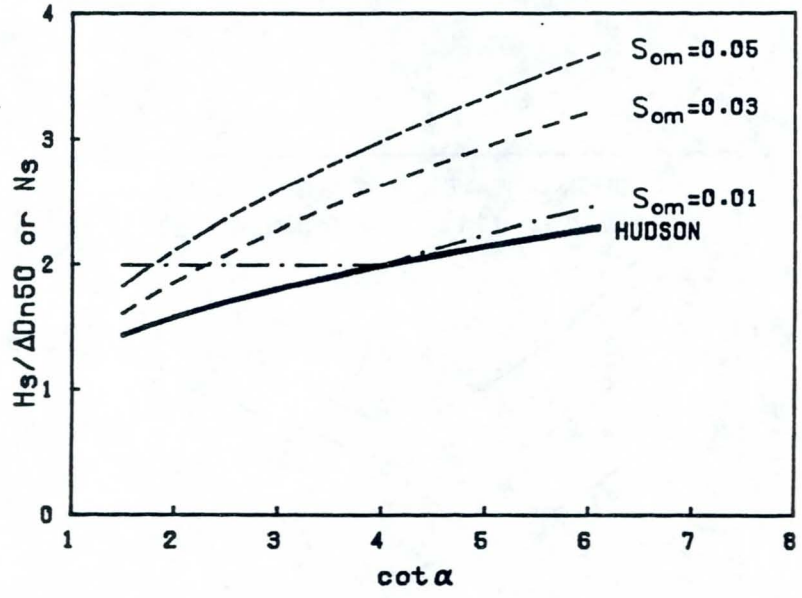

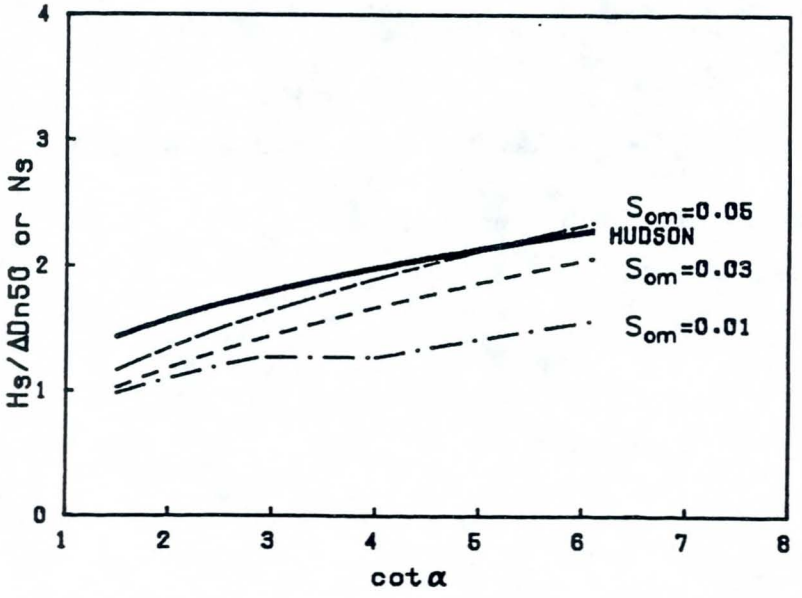

Fig. 4 Comparison of Hudson (Eq.10) and new formulas (Eq.14–16)

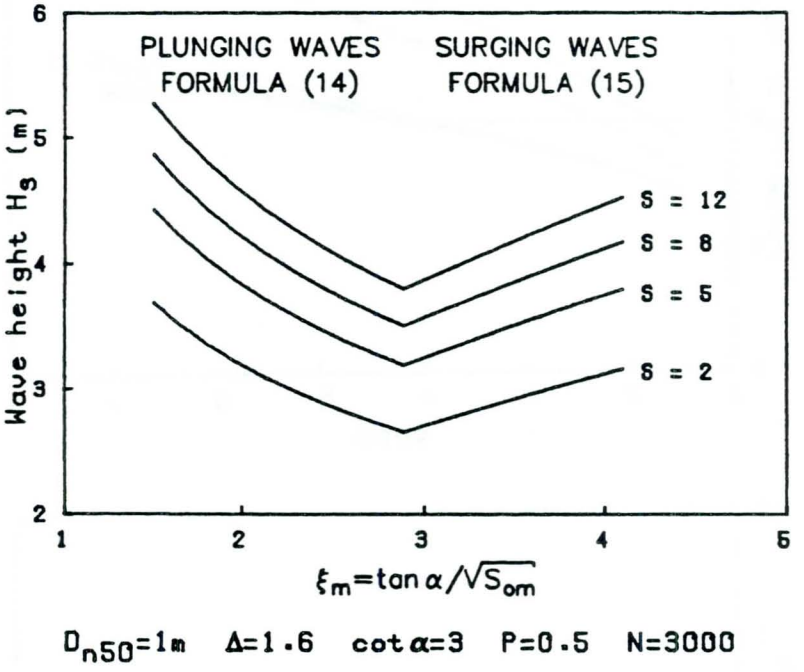

Fig. 5 Influence of damage level

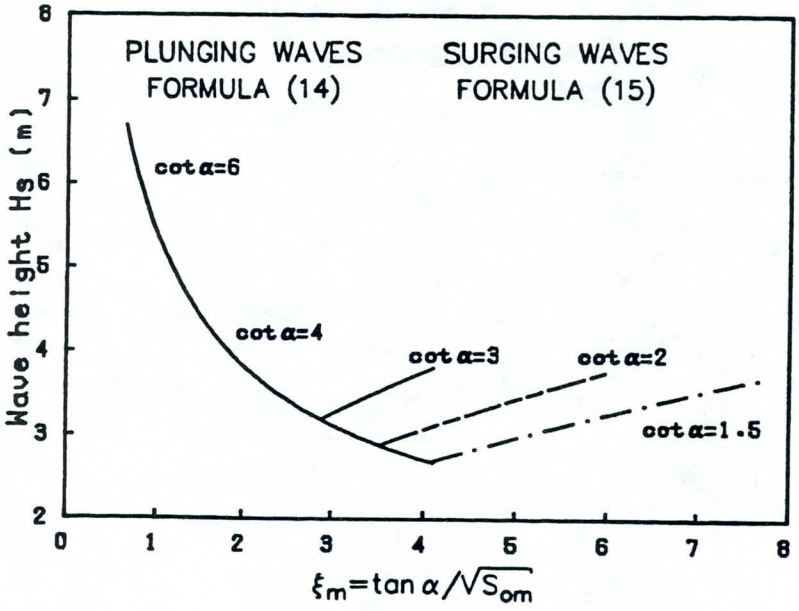

Fig. 6 Influence of slope angle

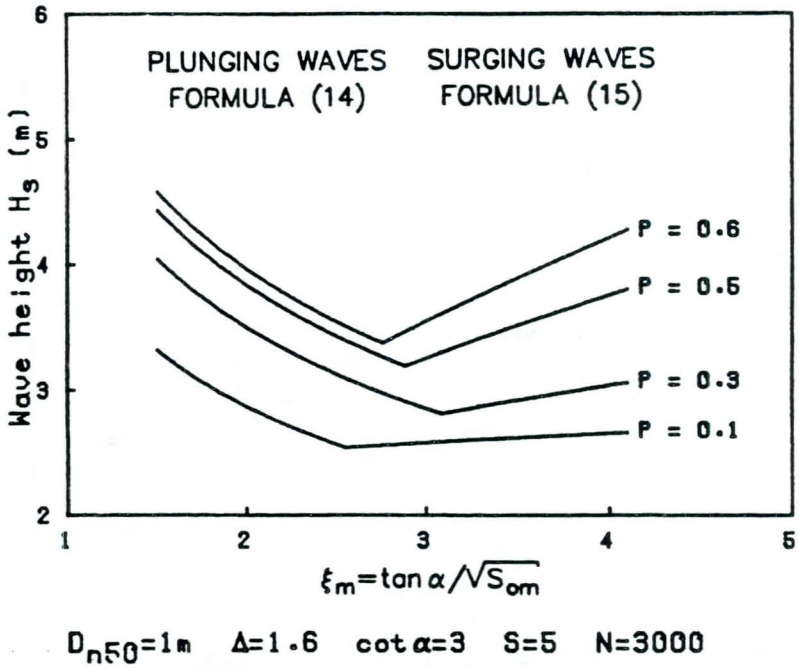

Fig. 7 Influence of permeability

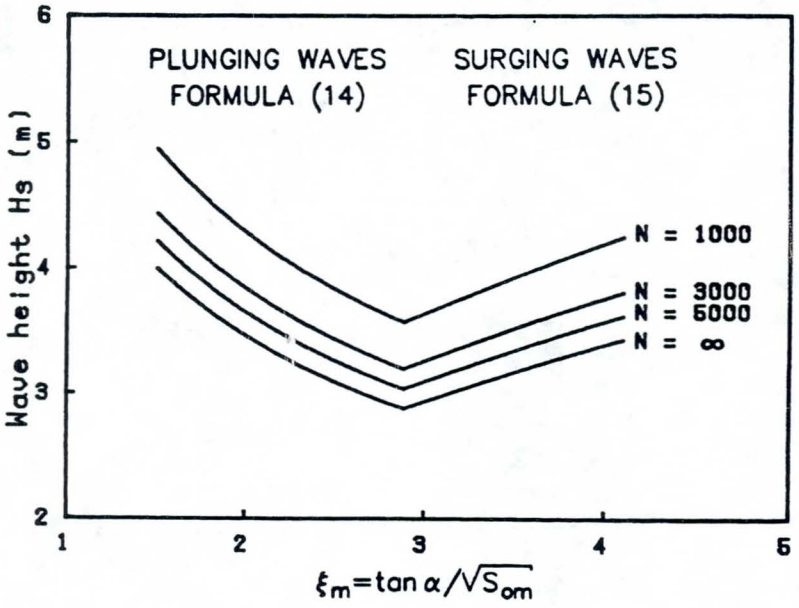

Fig. 8 Influence of storm duration

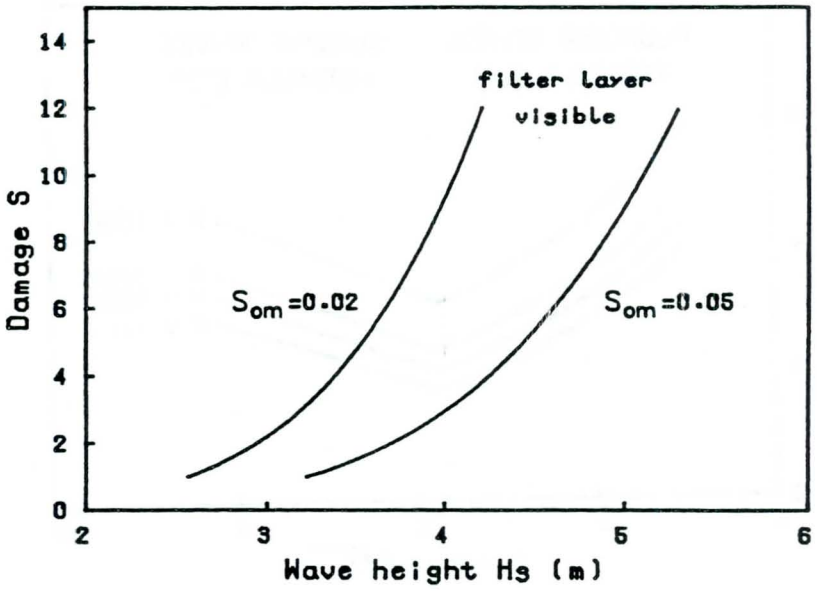

Fig. 9 Damage curves

LOW-CRESTED RUBBLE MOUND STRUCTURES

J.W. van der Meer
Delft Hydraulics, P.O. Box 152,
8300 AD Emmeloord, The Netherlands
K.W. Pilarczyk
Rijkswaterstaat, P.O. Box 5044
2600 GA Delft, The Netherlands

ABSTRACT

Low-crested structures can be classified into three categories: dynamically stable reef breakwaters, statically stable low-crested structures with the crest above SWL and statically stable submerged structures. This paper presents practical design formulas and graphs with respect to the stability for each of the three classes mentioned above. In addition, formulas were developed to predict wave transmission over low-crested rubble mound structures, taking into account the crest height and width, wave height and wave steepness. Most available data sets of various investigations from all over the world were re-analysed in order to produce the design formulas. The reliability of each formula was described.

INTRODUCTION

In many cases of rubble mound structure design a certain degree of overtopping is acceptable leading to considerable savings on the quantity of material being used. Other structures are so low that also under daily conditions the structure is overtopped. Structures with the crest level around SWL and sometimes far below SWL will always allow overtopping and transmission.

It is obvious that if the crest level of a structure is low, wave energy can pass over it. This brings about two effects. Firstly the armour on the front side can be made less heavy compared with a non or marginally overtopped structure, due to the fact that part of the energy is lost caused by overtopping.
The second effect is that both the crest and rear should be armoured in such a way that it can withstand the attack by overtopping waves. For rock structures often the same armour is applied on front face, crest and rear. The methods to establish the rock armour size for these structures will be given first. These methods, however, do not hold for structures with an armour layer of concrete units. In those cases it may even be possible that heavier armour units are required on the rear than on the front side. For those structures physical model investigations may give an acceptable solution. Next, the other design aspect, wave transmission, will be dealt with in this paper.

The complete re-analysis of the data on stability can be found in Van der Meer (1990a). A summary was presented by Van der Meer and Pilarczyk (1990). The data sets on wave transmission are described in Van der Meer (1990b), the analysis leading to practical formulas in Daemen (1991). A summary on transmission was presented by Van der Meer and d´Angremond (1991).

This paper summarizes both the stability and the transmission. The analysis of data has not been described, but only the final results such as design graphs and formulas, including their reliability.

CLASSIFICATION OF LOW-CRESTED STRUCTURES

Low-crested rock structures can be divided into three categories: dynamically stable reef breakwaters, statically stable low-crested structures (with the crest above the still water level, SWL) and statically stable submerged breakwaters.

A reef breakwater is a low-crested homogeneous pile of stones without a filter layer or core which is allowed to be reshaped by wave attack (Fig. 1). The initial crest height is just above the water level. Under severe wave conditions it is allowed that the crest height subsides to a certain equilibrium crest height. The equilibrium crest height and corresponding wave transmission are the main design parameters.

Statically stable low-crested breakwaters are close to non or marginally overtopped structures, but are more stable due to the fact that a (large) part of the wave energy can pass over the breakwater (Fig. 2).
All waves overtop statically stable submerged breakwaters and the stability increases remarkably as the crest height decreases (Fig. 3). It is obvious that the wave transmission is substantial at these structures.

DESCRIPTION OF DATA SETS

A number of studies on stability and wave transmission has been published with enough details to make a comparison with other studies useful and possible. All data selected, except for one, were obtained with random-wave testing. Data and references based on monochromatic waves were not taken into account as they were found to be too far from reality were random waves are present. A short description of the data sets will be given in the following.

A very extensive investigation on stability of rock slopes and gravel beaches was performed at Delft Hydraulics between 1983 and 1987. The (basic) background and all test data were described in Van der Meer (1988). A part of the study aimed at stability and transmission at low-crested breakwaters. These tests cover all three structure types described above (reef type, low-crested above SWL and submerged).

Ahrens (1987) described the stability and transmission at reef type breakwaters, see Fig. 1. During his tests on wave transmission it may well be possible that the crest height had changed, which makes it difficult to choose the correct crest height for that test. The crest height from Ahrens´ tests used in this paper is the height measured after the test.

Ahrens performed a large number of tests on stability and transmission at these structures and presented a formula for the equilibrium crest height. Hearn (1987) gives a more extensive analysis of Ahrens' data, and she developed a design formula for wave transmission.

Powell and Allsop (1985) describe the hydraulic performance of low-crested breakwaters with the crest above SWL, including transmission. Only a small damage, namely displacement of some rocks was allowed during design conditions.

Givler and Sørensen (1986) described about 45 tests on the stability of submerged breakwaters. The tests were performed with periodic waves and included both a large range of wave heights and wave periods. This was the reason to select this case as other datasets with random waves were not available. The damage at the crest was measured and the damage criteria for design are similar to conventional breakwaters (no or only little damage allowed). Only the results on stability are re-analysed in this paper.

Seelig (1980) has measured wave transmission for a large number of structure cross-sections, mostly with periodic waves, but also with random waves. For the reason described above only the random wave data have been considered. This data set was only used for wave transmission.

Three types of structures were tested by Daemrich and Kahle (1985), all with the crest at or below the water level. Only wave transmission was observed during the tests.

Finally, Daemen (1991) described tests on wave transmission at statically stable structures with the crest around SWL. Tests were performed with constant wave steepness and various crest levels and wave heights.

STABILITY OF LOW-CRESTED STRUCTURES

Reef breakwaters

The analyses on stability by Ahrens (1987, 1989) and Van der Meer (1990a) were concentrated on the change in crest height due to wave attack, see

Fig. 1. Ahrens defined a number of dimensionless parameters which described the behaviour of the structure. The main one being the relative crest height reduction factor h_c/h_c'. The crest height reduction factor h_c/h_c' is the ratio of the crest height at completion of a test, h_c, to the height at the beginning of the test, h_c'. The natural limiting values of h_c/h_c' are 1.0 (no deformation) and 0.0 (structure not present anymore) respectively.

The wave height can be characterised by $H_s/\Delta D_{n50}$ (Van der Meer (1988)) or N_s (stability number: Ahrens (1987, 1989)).

$$H_s/\Delta D_{n50} = N_s \qquad (1)$$

where:

H_s = significant wave height, H_s or H_{m0} ($H_{m0} = \sqrt{4m_0}$ was used in this study)

Δ = relative mass density; $\Delta = \rho_a/\rho_w - 1$

ρ_a = mass density of armour rock

ρ_w = mass density of water

D_{n50} = nominal diameter of rock; $D_{n50} = (M_{50}/\rho_a)^{1/3}$

M_{50} = average mass (50% value on mass distribution curve)

m_0 = zeroth moment of wave energy density spectrum

For the reef breakwater Ahrens found that a longer wave period caused more displacement of the material than a shorter period. Therefore, he introduced the spectral (or modified) stability number, N_s^*, defined by:

$$N_s^* = H_s^{2/3} L_p^{1/3}/\Delta D_{n50} \qquad (2)$$

where: L_p = the Airy wave length calculated using the peak period of the wave energy density spectrum, T_p and the water depth at the toe of the structure h. In fact, a local wave steepness is introduced in Eq. 2 and the relationship between the stability number N_s and the spectral stability number N_s^* can simply be given by:

$$N_s^* = N_s \times s_p^{-1/3} = H_s/\Delta D_{n50} \times s_p^{-1/3} \qquad (3)$$

where: s_p = the local wave steepness; $s_p = H_s/L_p$

That a longer wave period should give more damage than a shorter period is not always true. Ahrens concluded that it was true for reef breakwaters where the crest height lowered substantially during the test. It is, however, not true for non or marginally overtopped breakwaters (Van der Meer (1987 or 1988)). The influence of the wave period in that case is much more complex than suggested by Eq. 3.

The crest height (reduction) of a reef type breakwater can be described by:

$$h_c = \sqrt{A_t / \exp(aN_s^*)} \qquad (4)$$

where "a" = a coefficient and A_t = area of structure cross-section.

Ahrens presented various equations for the coefficient a. The most recent and refined one is given by Ahrens (1989):

$$\text{"a"} = 0.046(h_c'-h_c)/h + 0.2083(h_c/h)^{1.5} - 0.144(h_c/h)^2 + 0.4317/\sqrt{B_n} \qquad (5)$$

where:
h = water depth at structure toe and
$B_n = A_t/D_{n50}^2$ (bulk number)

The structures of Van der Meer (1988) had other crest heights, water depths, bulk numbers and slope angles than Ahrens' structures. A fit of Eqs. 4 and 5 with these data showed that they could not describe these additional data. The difference was large and results were presented in Van der Meer (1990a). Eqs. 4 and 5, therefore, can only be used for reef type breakwaters that are similar to Ahrens' cross-sections.

Therefore all the data of Ahrens (1987) were re-analysed together with the data of Van der Meer (1988). The complete analysis is given by Van der Meer (1990a). The analysis showed that the breakwater response slopes C' (as initially built) and C (after the test) had to be included. The breakwater response slope is defined by:

$$C' = A_t/h'^2_c \text{ and } C = A_t/h_c^2 \qquad (6)$$

The final equation that was derived from the analysis is given by:

$$h_c = \sqrt{A_t / \exp(aN_s^*)} \qquad (4)$$

$$\text{with "a"} = -0.028 + 0.045C' + 0.034h_c'/h - 6.10^{-9}\, B_n^{\,2} \qquad (7)$$

and $h_c = h_c'$ if h_c in Eq. 4 $> h_c'$.

The lowering of the crest height of reef type structures as shown in Fig. 1, can be calculated with Eqs. 4 and 7. It is possible to draw design curves from these equations which give the crest height as a function of N_s^* or even H_s. An example of h_c versus H_s is shown in Fig. 4. The reliability of Eq. 4 can be described by giving the 90% confidence bands given by $h_c \pm 10\%$ and is shown in Fig. 4.

Statically stable low-crested breakwaters above SWL

The stability of a low-crested conventional breakwater can be related to the stability of a non or marginally overtopped structure. Stability formulas as the Hudson formula or more advanced formulas (Van der Meer (1987, 1988)) can be used for example. The required rock armour diameter for an overtopped breakwater can then be determined by application of a reduction factor for the mass of the armour.

Data sets that could be used for analysis were a part of Ahrens' data (with small damage to the crest), Powell and Allsop (1985) and Van der Meer (1988). Fig. 5 gives the damage curves of a part of Van der Meer's tests with four crest heights, R_c, and for a constant wave period of 1.7 s. From this figure it is obvious that a decrease in structure crest height results in an increase in stability, although the difference between no overtopping and little overtopping (R_c = 0.125 m) is small.

Furthermore, from the tests it could be concluded that the wave period had influence on the maximum relative crest level R_c/H_s. For higher values of this R_c/H_s the structure behaved as a non-overtopping one. This can also be explained in a physical way. A long period gives higher run-up on a slope than a short period. Therefore more energy is lost by overtopping for a long period at the same crest level as for a short period.

The transition crest height where the increase in stability begins (given as a R_c/H_s value) should in fact also be a function of the wave period (or wave steepness). In Powell and Allsop (1985) a dimensionless crest height R_p^* was introduced which was used to describe wave transmission and which included the wave steepness. The definition is given by:

$$R_p^* = R_c/H_s \sqrt{s_{op}/2\pi} \qquad (8)$$

where: s_{op} = fictious wave steepness = $2\pi H_{m0}/gT_p^2$.

Curve fitting showed that the transition crest height, where for lower values the stability increases, can simply be described by:

$$R_p^* = 0.052 \text{ or } R_c/H_s = 0.13/\sqrt{s_{op}} \qquad (9)$$

The average increase in stability ($H_s/\Delta D_{n50}$ or N_s^*) for a structure with the crest at SWL, in comparison with a non-overtopped structure, is of the order of 20-30 per cent. If the increase in stability is set at 25 per cent, independent of wave steepness, and when a linear increase in stability is assumed between $R_p^* = 0.052$ and $R_p^* = 0$, the increase in stability can be described as a function of R_p^* only (or R_c/H_s and s_{op}), see Fig. 6. In addition, if the increase in $H_s/\Delta D_{n50}$ is not taken as a measure but the reduction in required nominal diameter D_{n50}, the final equation becomes:

$$\text{Reduction factor for } D_{n50} = 1/(1.25 - 4.8\ R_p^*) \qquad (10)$$

$$\text{for } 0 < R_p^* < 0.052$$

This final equation 10 describes the stability of a statically stable low-crested breakwater with the crest above SWL simply by application of a reduction factor on the required mass of a non-overtopped structure. Eq. 10 is shown in Fig. 6, for various wave steepnesses, and can be used as a design graph. The reduction factor to be applied for the required nominal diameter can be read from this graph (or calculated by Eq. 10).

An average reduction of 0.8 in diameter is obtained for a structure with the crest height at the water level. The required mass in that case is a factor $0.8^3 = 0.51$ of that required for a non-overtopped structure.

It is not really required to describe the reliability of the reduction factor in Eq. 10. The reliability of D_{n50} is about the same as for a non-overtopped structure, i.e. the reliability depends on the stability formula that is used to calculate the D_{n50} for a non-overtopped structure. These reliabilities are described in Van der Meer (1988).

SUBMERGED BREAKWATERS

Ahrens (1987, 1989), Allsop (1983) and Powell and Allsop (1985) had always during their tests an initial crest level at or above SWL. Only Van der Meer (1988) and Givler and Sørensen (1986) had initial crest heights below SWL. The total amount of data is limited, however. Van der Meer (1988) tested only a slope angle of 1:2 and Givler and Sørensen (1986) tested only a slope of 1:1.5. The seaward slope angle may have some influence on the stability of the submerged structure. Therefore the description of submerged structures here will be only valid for rather steep slopes, say about 1:1.5 to 1:2.5.

The slope angle has large influence on non-overtopped structures. In the case of submerged structures the wave attack is concentrated on the crest and less on the seaward slope. Therefore, excluding the slope angle of submerged structures, being a governing parameter for stability, may be legitimate.

The stability of submerged breakwaters appeared only to be a function of the relative crest height h_c'/h, the damage level S and the spectral stability number N_s^*. The damage level S is defined by Van der Meer (1988). Shortly, S = 2 means start of damage, S = 5 is moderate damage and S = 8-12 means severe damage (filter layer visible; not acceptable). Figs. 2 and 3 give examples of large S-values of 14.5 and 17.0. The final design formula is given by:

$$h_c'/h = (2.1 + 0.1\ S)\ \exp(-0.14\ N_s^*) \qquad (11)$$

For fixed crest height, water level, damage level, and wave height and period, the required ΔD_{n50} can be calculated from Eq. 11, finally yielding the required rock weight. Also wave height versus damage curves can be derived from Eq. 11. Eq. 11 is shown as a design graph in Fig. 7 for four

damage levels. The reliability of Eq. 11 can be described when the factor 2.1 is considered as a stochastic variable. The data gave a standard deviation of 0.35. With this standard deviation it is possible to calculate the 90% confidence bands, using 2.1 ± 1.64 * 0.35 in Eq. 11. Fig. 7 gives the 90% confidence bands for S = 2. The scatter is quite large and this should be considered during design of submerged structures.

WAVE TRANSMISSION AT LOW-CRESTED STRUCTURES

Governing variables

The most important variables with respect to wave transmission are summarized here and explained in Fig. 8.

The crest height related to SWL, i.e. the crest freeboard is given by R_c. In particular, if the size of the armour rock is large and the crest level is close to SWL (i.e. R_c close to 0), the definition of the crest level is crucial. From the existing data sets, it could not be verified in what way the crest level was defined. For the test series of Daemen (1991), the crest has been defined as the plane through the upper edges of the armour units. The height of the structure is defined by h_c. The crest width is defined by B. The water depth in front of the structure is given by h. The relationship between the parameters is: $R_c = h_c - h$.

The size of the armour rock is introduced as the nominal diameter D_{n50}. The wave heights are given by H_i and H_t, representing the incoming and transmitted wave height respectively. Both values are expressed as H_s (mean of highest one third of the waves), or H_{m0} (based on spectrum, $4\sqrt{m_0}$). It must be emphasized here, that H_t is not always Rayleigh-distributed. The wave period, T_p, is used throughout this part on wave transmission, being the peak period of the spectrum; the wave steepness s_{op} is defined as $2\pi H_s/gT_p^2$, with H_s defined at the toe of the structure. The transmission coefficient K_t is given by $K_t = H_t/H_i$. Finally, when discussing transmission of wave energy, it may be necessary to account for the permeability of the structure.

Important references on wave transmission are Seelig (1980) and Madsen and White (1976). Seelig (1980) describes a model for wave transmission, supported by many tests. Most of the tests were performed with monochromatic

waves and the model was based only on these tests. Random wave tests showed fairly good agreement when the mean wave height and the peak period were used, but the model was not based on these random wave tests. Seelig (1980) used the results of Madsen and White (1976) to describe the transmission through a breakwater. These results were only based on monochromatic waves and basically for (very) long waves. Comparison with short waves gave large overpredictions in transmission coefficients (K_t = 0.16 versus 0.04).

The model of Seelig (1980) may be useful for design. In this paper it was not used as it was too much based on monochromatic and long waves. However, the tests with random waves of Seelig (1980) were part of the total data set that was re-analysed (see for example Fig. 10).

Analysis with R_c/H_i as main parameter

Van der Meer (1990b) attempted to analyse the existing data starting from the assumption that the transmission coefficient K_t would largely depend on a dimensionless crest height. The dimensionless crest height, was defined in two ways, as: R_c/H_i, namely only related to the wave height, and as the parameter R_p^* (Eq. 8), which includes both wave height and steepness, used by Powell and Allsop (1985). However, they used the mean wave period T_m instead of T_p, in calculating the wave steepness. It is stressed again that in this part on wave transmission only the peak period is used.

From the analysis with R_c/H_i and R_p^* versus K_t it could in general be concluded that the parameter R_p^* is not better than R_c/H_i as long as the whole range of relative crest levels is considered. Only for positive values of R_p^* (≥ 0.025) the results are better than with R_c/H_s.

Another phenomenon was found from Ahrens' (1987) data. Plotting all data of Ahrens obtained for one particular wave period against the relative crest height, a wide scatter of K_t was observed for high values of R_c/H_i (see Fig. 9). A closer analysis shows that this scatter is mainly due to the occurrence of low wave heights, having roughly the same dimensions as the rock. Apparently low (and relatively long) waves travel easily through the top of the structure.

Combining all data, and plotting the transmission coefficient against the relative crest height, Fig. 10 is obtained. As expected, the result shows

considerable scatter, but a clear trend can be observed. Part of the scatter can be attributed to the influence of the wave period and part to the influence of extremely small waves, while crest width and permeability may also have some influence.

The average value of K_t for $-2 < R_c/H_i < -1$ is about 0.8. Except for the triangles (Ahrens' data, small wave heights), the average value of K_t for $1 < R_c/H_i < 2$ is about 0.1. Between these ranges the value of K_t decreases almost linearly with R_c/H_i. Based on this simple analysis the following formula for wave transmission can be proposed:

$$\begin{aligned} &\text{For: } -2.0 < R_c/H_i < -1.13 && K_t = 0.80 \\ &\text{For: } -1.13 < R_c/H_i < 1.2 && K_t = 0.46 - 0.3R_c/H_i \\ &\text{For: } 1.2 < R_c/H_i < 2.0 && K_t = 0.10 \end{aligned} \qquad (12)$$

This curve is shown in Fig. 10 as well. The scatter is large which means that the formula can be simple. It means also that for application this large scatter should be taken into account. The standard deviation of K_t amounted to $\sigma(K_t) = 0.09$ and was assessed from the graph, assuming a normal distribution. This means that the 90 per cent confidence levels are given by $K_t \pm 0.15$. It is evident that for large negative values of R_c/H_i, K_t should approach 1, and for large positive values of R_c/H_i a value close to 0. The 90 percent confidence levels are given in Fig. 10.

For design purposes, however, the scatter is a serious drawback. After all, an accurate forecast of wave transmission may lead to considerable savings by reducing the total height of the structure. Therefore, it was decided to perform additional tests and to continue the efforts towards a better expression for wave transmission.

Analysis with R_c, s_{op} and D_{n50} as main parameter

In order to study the wave transmission process further, additional tests were carried out by Daemen (1991). The results of the tests are presented in Fig. 11 where a distinction has been made between the two wave steepness values of $S_{op} = 0.02$ (long waves) and 0.04 (short waves).

Until now, wave transmission is being described in the conventional way as a function of R_c/H_i. It is not clear, however, that the use of this combi-

nation of crest freeboard and wave height produces similar results with, on the one hand constant R_c and variable H_i, and on the other variable R_c and constant H_i. Moreover, when R_c becomes zero, all influence of the wave height is lost, leading to a large scatter in the graph at $R_c = 0$. Therefore, it was decided to separate R_c and H_i.

There is a direct relationship between the design wave height and the size of armour rock, which is often given as the stability factor $H_s/\Delta D_{n50}$. It can be concluded that the nominal diameter of the armour rock will characterise the rubble mound structure. It is, therefore, also a good parameter to characterise both the wave height and the crest height in a dimensionless way.

The relative wave height can then be given as H_i/D_{n50}, in accordance with the stability factor, and the relative crest height as R_c/D_{n50}, being the number of rocks that the crest level is above or below SWL. Moreover, a separation into H_i/D_{n50} and R_c/D_{n50} enables a distinction between various cases. For example low H_i/D_{n50} values (smaller than 1 to 2) produce low waves travelling trough the crest and high H_i/D_{n50} values (3 to 5) yield situations under extreme wave attack. Finally, D_{n50} can be used to describe other breakwater properties such as the crest width B. This yields the parameter B/D_{n50}.

The primary parameters for wave transmission can now be given as:

Relative crest height : R_c/D_{n50}
Relative wave height : H_i/D_{n50}
Fictitious wave steepness: s_{op}
and possibly : B/D_{n50}

Fig. 12 shows the wave transmission versus R_c/D_{n50} for the data of Van der Meer (1990b) and the tests of Daemen (1991). The data are grouped by constant wave steepness, s_{op}. Straight lines are drawn through the points with the same wave steepness. Fig. 12 makes clearly visible that a lower wave steepness (or a longer period) results in a larger transmission coefficient. This is true for the whole area of R_c/D_{n50}, except for large positive and negative values. Furthermore, the lines in Fig. 12 are parallel to each other.

The general trend of the wave transmission coefficient, going from high positive values of R_c/D_{n50} to high negative values, is that the transmission coefficient first remains low, then increases in the area of R_c/D_{n50} between +2 and -2 and finally remains high. Theoretically, the increasing wave transmission coefficient will be expressed by a smooth curve from 0 for very high crest heights to 1 for very low crest heights. The most important area, however, is the area where the transmission increases rapidly. For the sake of simplicity it is assumed that this area can be described by straight lines as shown in Fig. 12.

This means that a linear relationship is assumed in the area of R_c/D_{n50} roughly between +2 and -2. The wave transmission can now be described as:

$$K_t = aR_c/D_{n50} + b \qquad (13)$$

In this equation "a" determines the slope of the line and "b" gives the value of K_t at $R_c/D_{n50} = 0$. From Fig. 12 it can already be concluded that the wave steepness s_{op} is only present in the coefficient "b" and not in the coefficient "a" (the lines in Fig. 12 are parallel).

Fig. 13 shows the data of Daemen (1991) with a constant wave steepness of $s_{op} = 0.02$ and various classes of relative wave heights. In fact, Fig. 13 shows the influence of the relative wave height H_i/D_{n50} on wave transmission. From this Fig. 13 it can be concluded that for $R_c/D_{n50} < -1$ a larger H_i/D_{n50} produces smaller wave transmission. For $R_c/D_{n50} > -1$ the opposite occurs: a larger H_i/D_{n50} gives larger wave transmission.

This phenomenon can be explained in a physical way. On a low-crested breakwater, where R_c/D_{n50} is positive, the transmission is primarily determined by overtopping and thus by wave runup. In this area of R_c/D_{n50} a larger relative wave height yields a higher runup, thus more overtopping and hence a larger transmission coefficient. On a submerged breakwater, where R_c/D_{n50} is negative, higher waves will be more affected by the structure whereas small waves pass unhindered. In this case a larger relative wave height results in a smaller transmission coefficient.

Fig. 14 gives the values of the transmission coefficient which holds for high (above SWL) and low (submerged) relative crest heights, outside the

range given by the curve of Eq. 13. Fig. 14 shows that both the maximum and minimum transmission are independent of the relative wave height H_i/D_{n50}. Based on Fig. 14 the following minimum and maximum values were derived:

Conventional breakwaters:

Minimum: $K_t = 0.075$; maximum: $K_t = 0.75$ (14)

Reef type breakwaters:

Minimum: $K_t = 0.15$; maximum: $K_t = 0.60$ for $R_c/D_{n50} > -2$ (15)
linearly increasing to
$K_t = 0.80$ for $R_c/D_{n50} = -6$

Final results on wave transmission

The final outcome of the analysis on wave transmission, including the data of Daemen (1991), was a linear relationship between the wave transmission coefficient K_t and the relative crest height R_c/D_{n50}, which is valid between minimum and maximum values of K_t. In Fig. 15 the basic graph is shown. The linearly increasing curves are presented by:

$$K_t = a\, R_c/D_{n50} + b \quad (13)$$

with: $$a = 0.031\, H_i/D_{n50} - 0.24 \quad (16)$$

Eq. 14 is applicable for conventional and reef type breakwaters. The coefficient "b" for conventional breakwaters is described by:

$$b = -5.42\, s_{op} + 0.0323\, H_i/D_{n50} - 0.0017\, (B/D_{n50})^{1.84} + 0.51 \quad (17)$$

and for reef type breakwaters by:

$$b = -2.6\, s_{op} - 0.05\, H_i/D_{n50} + 0.85 \quad (18)$$

Permeability of the structure (underneath the armour layer) did not show significant influence. In the cases described in this paper most wave transmission is caused by overtopping or by waves travelling through the armour layer on the crest. The minimum and maximum values are described by Eqs. 14 and 15.

Validation and reliability of formula on wave transmission

The analysis was based on various groups with constant wave steepness and a constant relative wave height. The validity of the wave transmission formula (Eq. 13) corresponds, of course, with the ranges of these groups. The formula is valid for:

$$1 < H_i/D_{n50} < 6 \text{ and } 0.01 < s_{op} < 0.05$$

Both upper boundaries can be regarded as physically bound. Values of $H_i/D_{n50} > 6$ will cause instability of the structure and values of $s_{op} > 0.05$ will cause waves breaking because of steepness. In fact, boundaries are only given for wave heights which are too low relative to the rock diameter and for very low wave steepnesses (low swell waves).

The formula is applicable outside the range given above, but its reliability is lower. Fig. 16 shows the measured wave transmission coefficient versus the calculated one from Eq. 13, for various data sets of conventional breakwaters. The reliability of the formula can be described by assuming a normal distribution around the line in Fig. 16. With the restriction of the range of application given above, the standard deviation amounted to $\sigma(K_t) = 0.05$, which means that the 90 per cent confidence levels can be given by $K_t \pm 0.08$. This is a remarkable increase in reliability compared with the simple formula given by Eq. 12 and Fig. 10, where a standard deviation of $\sigma(K_t) = 0.09$ was given. The 90 percent confidence levels are also given in Fig. 15.

The reliability of the formula for reef-type breakwaters is more difficult to describe. If only tests are taken where the crest height had been lowered less than 10 per cent of the initial height h_c, and the test conditions lie within the range of application, the standard deviation amounts to $\sigma(K_t) = 0.031$. If the restriction about the crest height is not taken into account the standard deviation amounts to $\sigma(K_t) = 0.054$.

CONCLUSIONS

Low-crested rubble mound structures can be divided into three categories: dynamically stable reef breakwaters; statically stable low-crested breakwaters ($R_c/H_s > 0$) and statically stable submerged breakwaters. Waves overtop these structures and the stability increases remarkably if the crest height decreases.

The stability of reef breakwaters is described by Eqs. 4 and 7. Design curves can be drawn with the aid of these equations. An example is given in Fig. 4.

The stability of a low-crested breakwater with the crest above SWL is first established as a non-overtopped structure. Stability formulas derived by Van der Meer (1987, 1988) can be used. The required rock diameter for an overtopped breakwater can then be determined by application of a reduction factor, given by Eq. 10. Design curves are shown in Fig. 6.

The stability of submerged breakwaters depends on the relative crest height, the damage level and the spectral stability number. The stability is described by Eq. 11 and a design graph is given in Fig. 7.

A formula was described for wave transmission at low-crested structures. The outcome of this formula was a linear relationship between the wave transmission coefficient K_t and the relative crest height R_c/D_{n50}, which is valid between minimum and maximum values of K_t. In Fig. 15 the basic graph is shown. The linearly increasing curves are presented by Eqs. 13, 16 and 17 (conventional breakwaters) or 18 (reef type). The minimum and maximum values of K_t are given by Eqs. 14 and 15.

ACKNOWLEDGEMENTS

The Rijkswaterstaat (Dutch Public Works Department), is gratefully acknowledged for their financial support of various studies that have led to this paper.

APPENDIX I. REFERENCES

Ahrens, J.P., 1987. Characteristics of reef breakwaters. CERC, Vicksburg, Technical Report CERC-87-17.

Ahrens, J.P., 1989. Stability of reef breakwaters. ASCE, Journal of WPC and OE, Vol. 115, No. 2.

Allsop, N.W.H., 1983. Low-crest breakwaters, studies in random waves. Proc. of Coastal Structures ´83, Arlington

Daemen, I.F.R. Wave transmission at low-crested breakwaters. Delft University of Technology, Faculty of Civil Engineering, Delft, 1991, Master´s Thesis.

Daemrich, K.F. and Kahle, W., 1985. Schutzwirkung von Unterwasserwellenbrechern unter dem einfluss unregelmässiger Seegangswellen. Eigenverlag des Franzius-Instituts für Wasserbau und Küsteningenieurwesen, Heft 61.

Givler, L.D. and Sørensen, R.M., 1986. An investigation of the stability of submerged homogeneous rubble-mound structures under wave attack. Lehigh University, H.R. IMBT Hydraulics, Report #IHL-110-86.

Hearn, J.K., 1987. An analysis of stability of a wave field modification due to low-crested, sacrificial breakwaters. University of Florida, Miami, MSc-thesis.

Madsen, O.S. and White, S.M., 1976. Reflection and transmission characteristics of porous rubble-mound breakwaters. MR 76-5, U.S. Army Corps of Engineers, Coastal Engineering Research Center, Fort Belvoir, Va., USA.

Powell, K.A. and Allsop, N.W.H., 1985. Low-crest breakwaters, hydraulic performance and stability. Hydraulics Research, Wallingford. Report SR 57.

Seelig, W.N., 1980. Two-dimensional tests of wave transmission and reflection characteristics of laboratory breakwaters. WES, CERC, Vicksburg, Technical Report NO. 80-1.

Van der Meer, J.W., 1987. Stability of breakwater armour layers - Design formulae. Coastal Eng., 11, p 219 - 239.

Van der Meer, J.W., 1988. Rock slopes and gravel beaches under wave attack. Doctoral thesis, Delft University of Technology. Also: Delft Hydraulics Communication No. 396

Van der Meer, J.W., 1990a. Low-crested and reef breakwaters. Delft Hydraulics Report H 986.

Van der Meer, J.W., 1990b. Data on wave transmission due to overtopping. Delft Hydraulics Report H 986.

Van der Meer, J.W. and Pilarczyk, K.W., 1990. Stability of low-crested and reef breakwaters. ASCE. Proc. 22th ICCE, Delft, The Netherlands.

Van der Meer, J.W. and d´Angremond, K., 1991. Wave transmission at low-crested structures. ICE, Thomas Telford. In: Coastal structures and breakwaters. London, United Kingdom, p. 25 - 42

APPENDIX II NOTATION

a, b	=	coefficients
A_t	=	area of structure cross-section
B	=	width of structure crest
B_n	=	bulk number, $B_n = A_t/D^2_{n50}$
C, C'	=	breakwater response slope, after and before a test, Eq. 6
D_{n50}	=	nominal diameter, $D_{n50} = (M_{50}/\rho_a)^{1/3}$
g	=	gravitational acceleration
h	=	water depth at toe of structure
h_c, h_c'	=	structure height, after and before a test
H_i	=	incident wave height, H_{m0} of H_s
H_{m0}	=	significant wave height, $4\sqrt{m_0}$
H_s	=	significant wave height, mean of highest one third of the waves
H_t	=	transmitted wave height, H_{m0} or H_s
K_t	=	transmission coefficient, $K_t = H_t/H_i$
L_p	=	local wave length
M_{50}	=	50% value on mass distribution curve
m_0	=	zeroth moment of wave energy density spectrum
N_s	=	stability number, $N_s = H_s/\Delta D_{n50}$
N^*_s	=	spectral stability number
P	=	notional permeability factor
R_c	=	crest height above SWL
R^*_p	=	dimensionless crest height
s_{op}	=	wave steepness, $s_{op} = 2\pi H_s/gT_p^2$
s_p	=	local wave steepness
S	=	damage level
T_p	=	peak wave period
α	=	slope angle
Δ	=	buoyant mass density, $\Delta = \rho_a/\rho_w - 1$
ρ_a, ρ_w	=	mass density rock, water
σ	=	standard deviation of normal distribution

REPRINT SALES SUMMARY

The stability of low-crested structures such as dynamically stable reef breakwaters, low-crested structures with the crest above SWL and submerged structures has been described. Wave transmission at low-crested structures is given in design formulas. The reliability of all formulas has been described.

KEYWORDS

Waves, transmission, stability, rubble structures, reef, armour, submerged.

FIGURE LEGENDS

1 Example of reef type breakwater
2 Example of low-crested breakwater
3 Example of submerged breakwater
4 Design graph of reef type breakwater
5 Influence of crest height on damage curves (from Van der Meer (1988))
6 Design graph with the reduction factor for the rock diameter of a low-crested structure ($R_c < 0$) as a function of relative crest height and wave steepness
7 Design curves for a submerged structure with 90% confidence bands for S = 2
8 Governing variables related to wave transmission
9 Influence of wave height on transmission. Data of Ahrens (1987), T_p = 1.45 s
10 Wave transmission versus relative crest height. All data with 90% confidence bands
11 Wave transmission data of Daemen (1991)
12 Wave transmission versus R_c/D_{n50}. Data of Van der Meer (1990b) and Daemen (1991)
13 Influence of relative wave height on wave transmission for constant wave steepness of s_{op} = 0.02
14 Minimum and maximum wave transmission
15 Basic graph for wave transmission with 90% confidence bands
16 Calculated versus measured wave transmission for conventional breakwaters

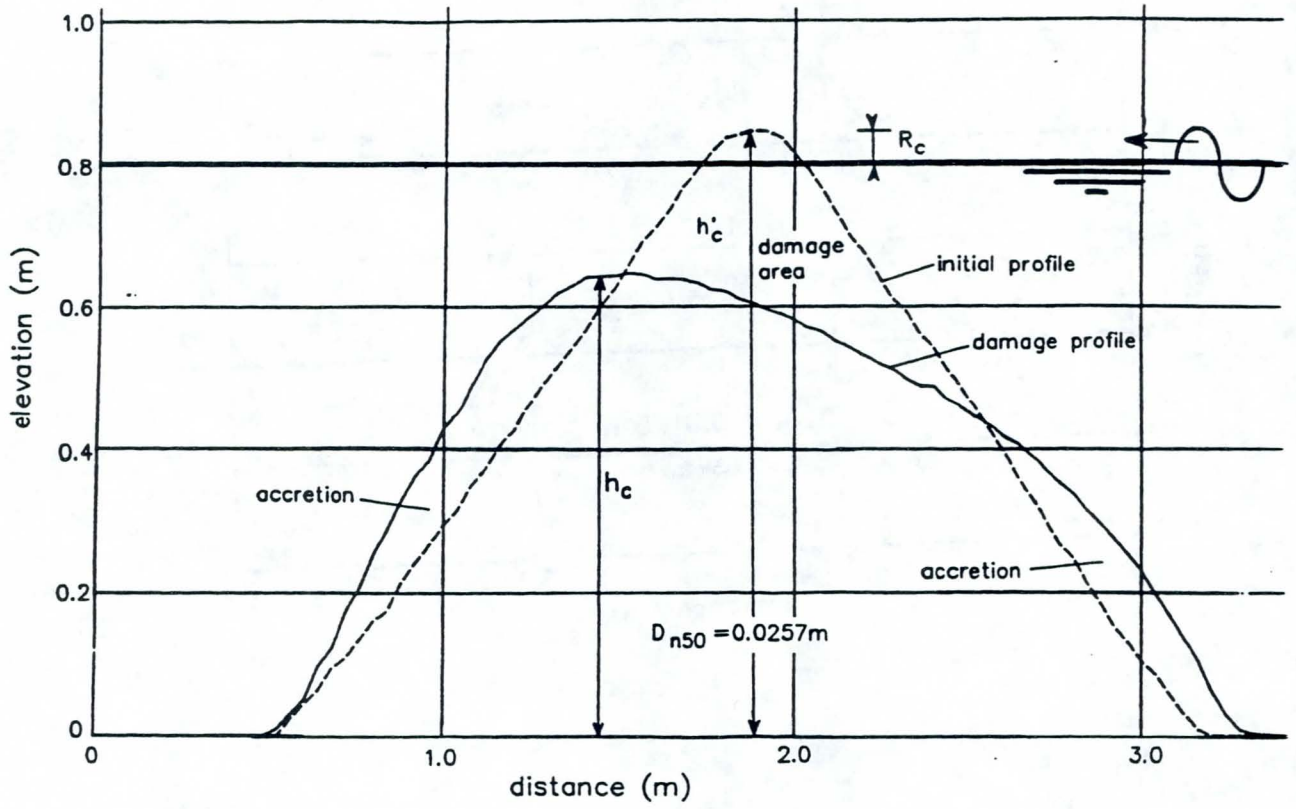
1.0
0.8
0.6
0.4
0.2
0
elevation (m)
0
1.0
2.0
3.0
distance (m)
R_c
h'_c
damage area
initial profile
damage profile
h_c
accretion
accretion
D_{n50} =0.0257m

Figure 1

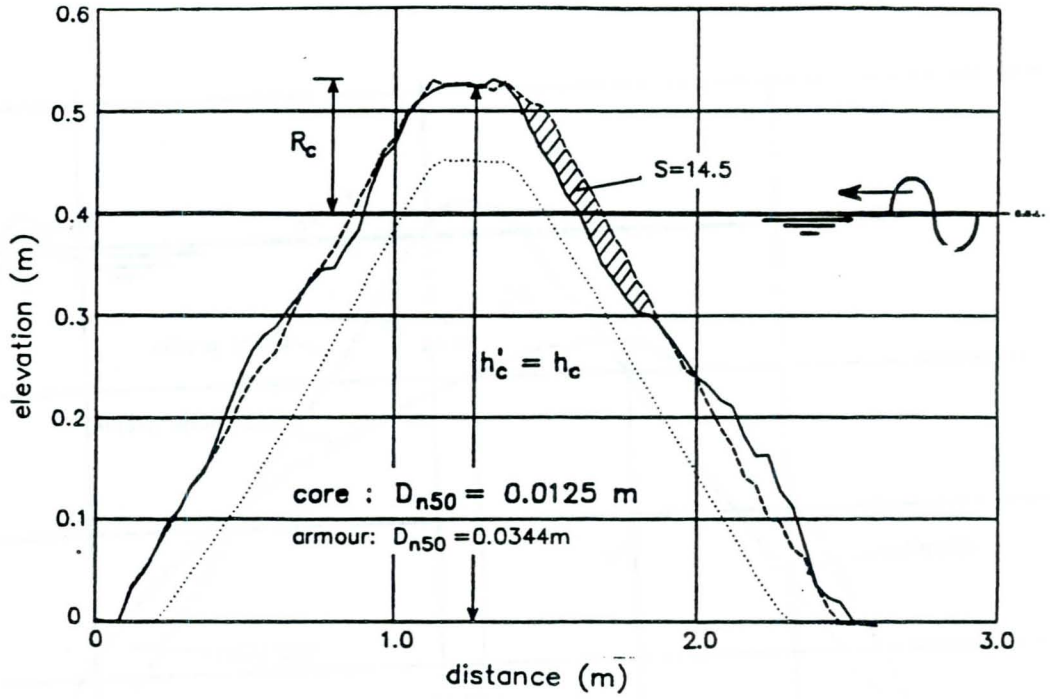
0.6
0.5
0.4
0.3
0.2
0.1
0
elevation (m)
R_c
S=14.5
$h'_c = h_c$
core : D_{n50} = 0.0125 m
armour: D_{n50} =0.0344m
0
1.0
2.0
3.0
distance (m)

Figure 2

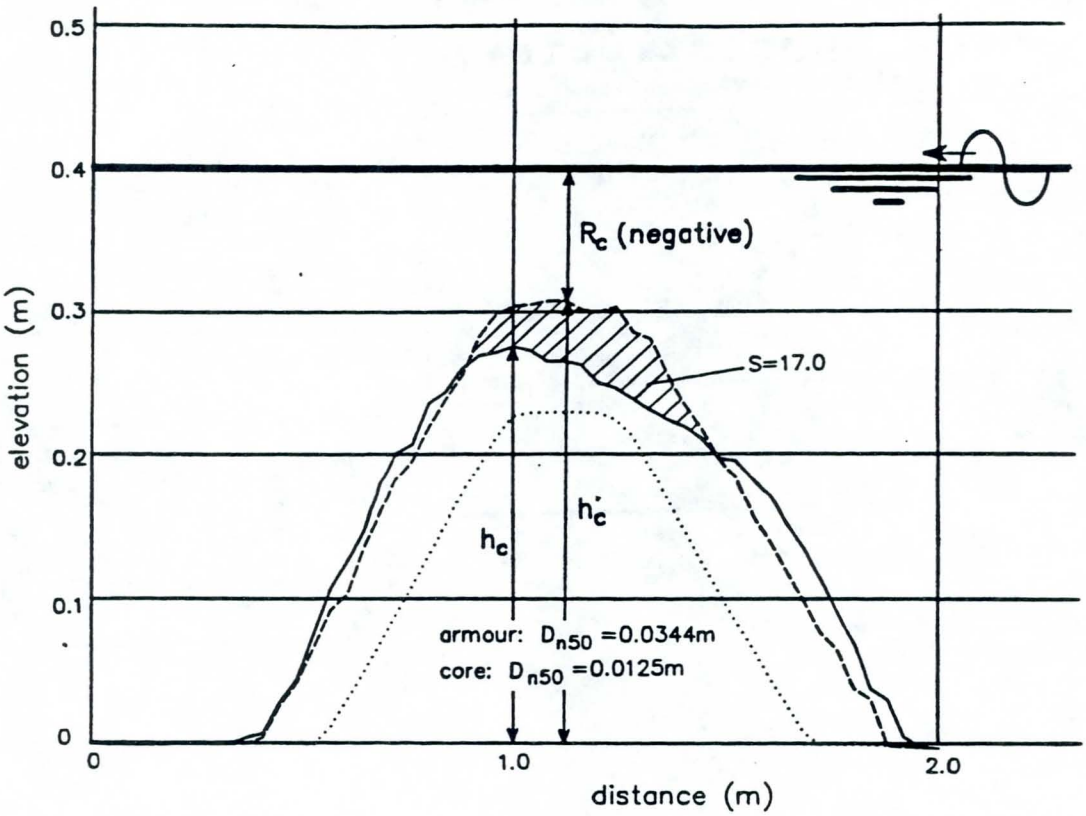
0.5
0.4
0.3
0.2
0.1
0
elevation (m)
R_c (negative)
S=17.0
h_c
h_c^*
armour: D_{n50} =0.0344m
core: D_{n50} =0.0125m
0
1.0
2.0
distance (m)

Figure 3

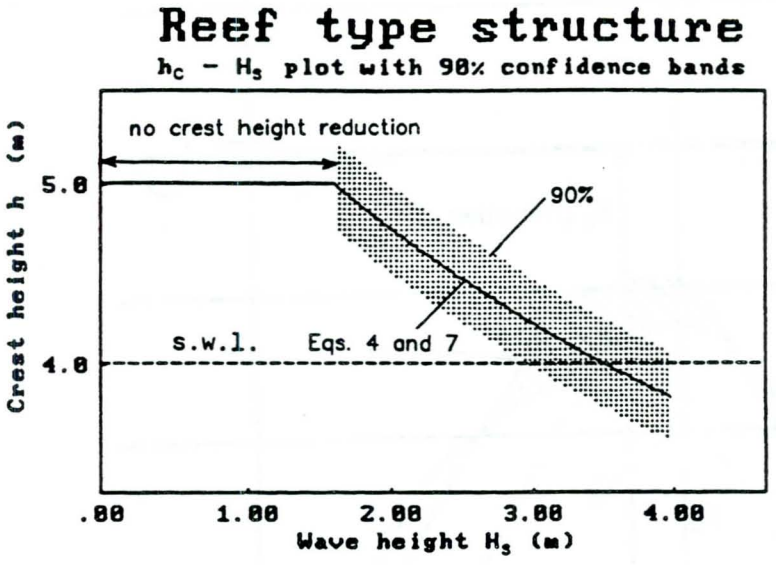

D_{n50} = .484 (m)
B_n = 205.1 (-)
C = 1.92 (-)

For H_s = 2.000
H_s/h = 0.5
depth limitation

M_{50}	-	300.000 (kg)
ρa	-	2650 (kg/m^3)
ρw	-	1025 (kg/m^3)
h'_c	-	5.000 (m)
h	-	4.000 (m)
A_t	-	48.00 (m^2)
T_p	-	8.00 (s)

Figure 4

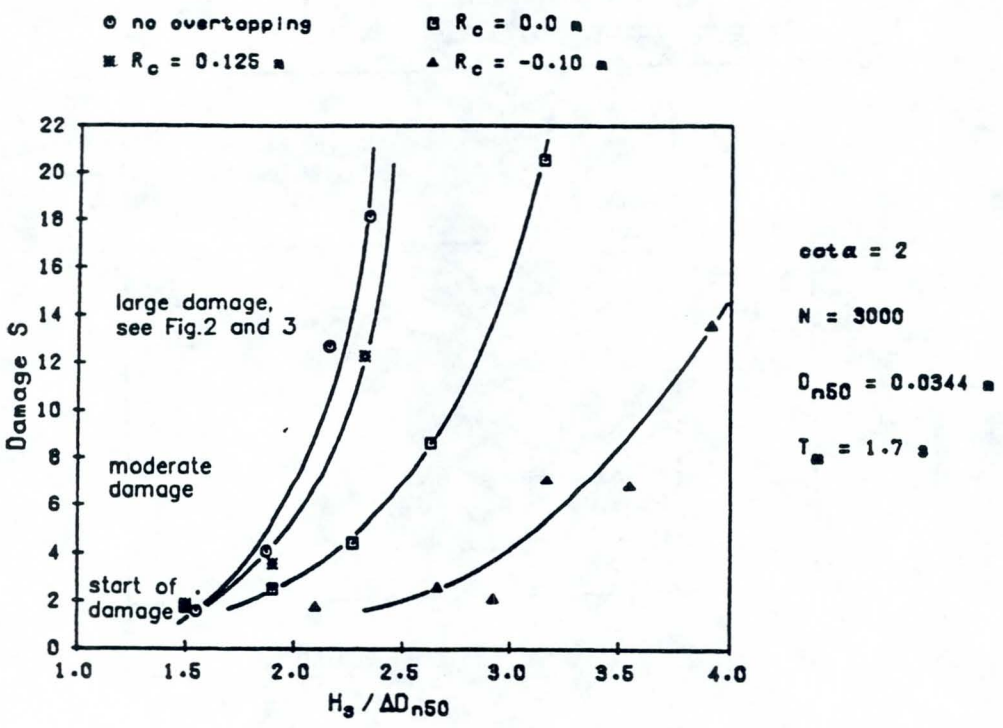
no overtopping
R_c = 0.0 m
R_c = 0.125 m
R_c = -0.10 m
Damage S
large damage, see Fig.2 and 3
moderate damage
start of damage
$H_s / \Delta D_{n50}$
cotα = 2
N = 3000
D_{n50} = 0.0344 m
T_m = 1.7 s

Figure 5

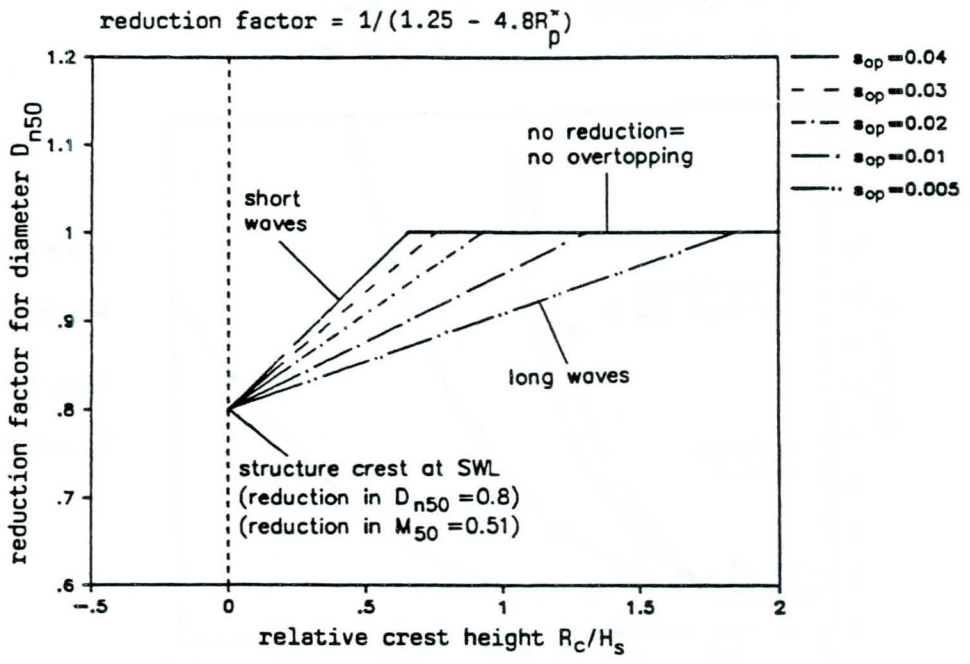
reduction factor = 1/(1.25 - 4.8R*p)
reduction factor for diameter Dn50
relative crest height Rc/Hs
1.2
1.1
1
.9
.8
.7
.6
-.5
0
.5
1
1.5
2
sop=0.04
sop=0.03
sop=0.02
sop=0.01
sop=0.005
no reduction=
no overtopping
short
waves
long waves
structure crest at SWL
(reduction in Dn50 =0.8)
(reduction in M50 =0.51)

Figure 6

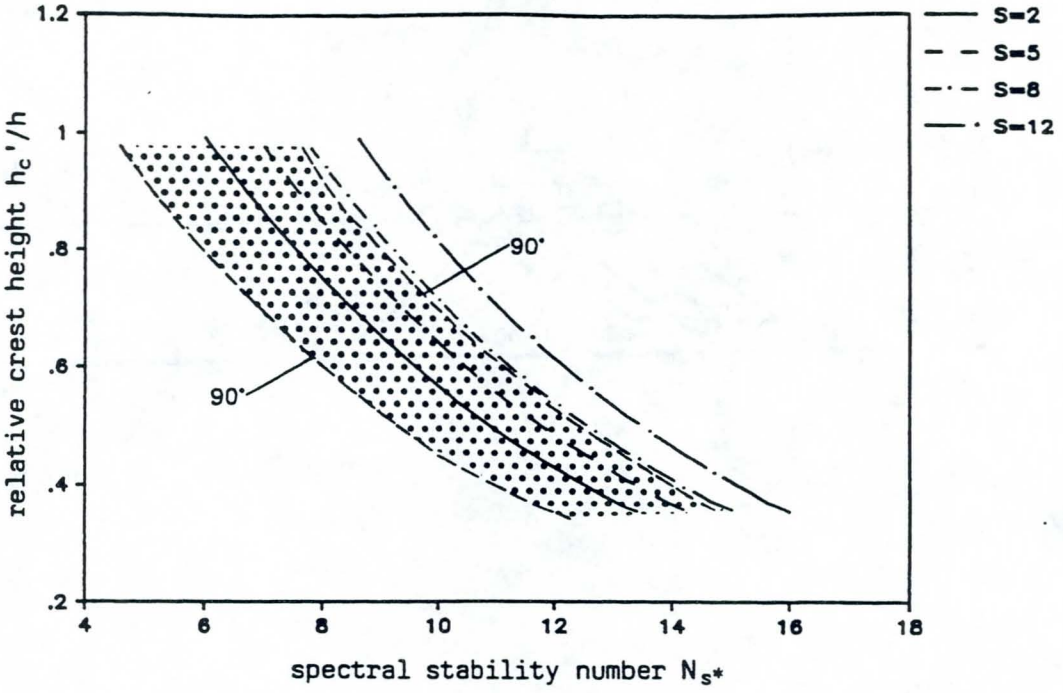
1.2
1
.8
.6
.4
.2
4
6
8
10
12
14
16
18
relative crest height h_c'/h
spectral stability number N_{s*}
90°
90°
S=2
S=5
S=8
S=12

Figure 7

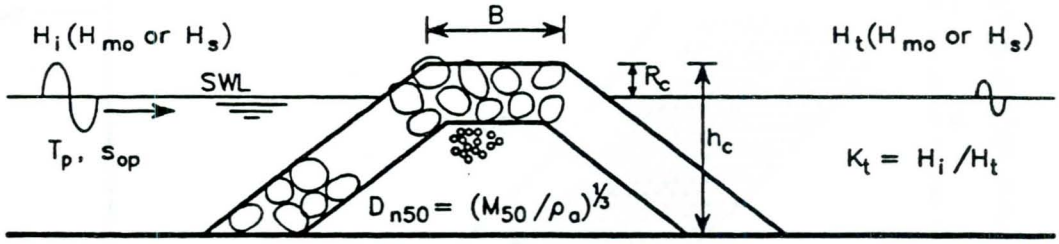
B
H_i (H_{mo} or H_s)
SWL
T_p, s_{op}
R_c
h_c
H_t (H_{mo} or H_s)
$K_t = H_i / H_t$
$D_{n50} = (M_{50} / \rho_a)^{1/3}$

Figure 8

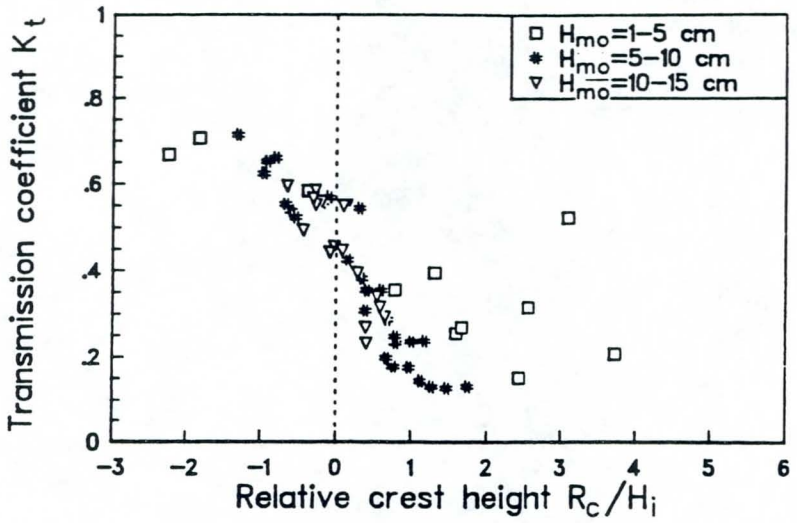
Transmission coefficient K_t
1
.8
.6
.4
.2
0
−3
−2
−1
0
1
2
3
4
5
6
Relative crest height R_c/H_i
H_{mo}=1–5 cm
H_{mo}=5–10 cm
H_{mo}=10–15 cm

Figure 9

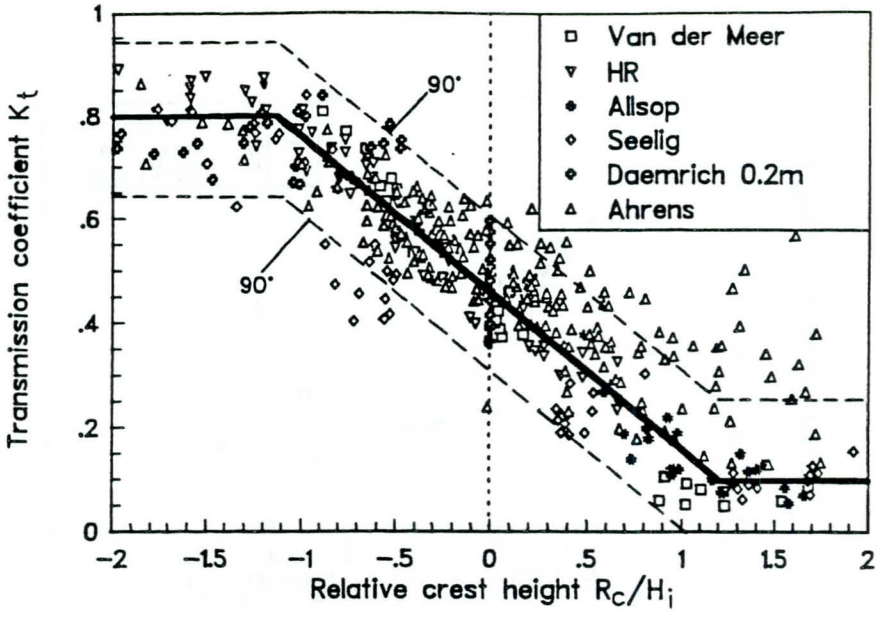
Transmission coefficient K_t
1
.8
.6
.4
.2
0
−2
−1.5
−1
−.5
0
.5
1
1.5
2
Relative crest height R_C/H_i
90°
90°
Van der Meer
HR
Allsop
Seelig
Daemrich 0.2m
Ahrens

Figure 10

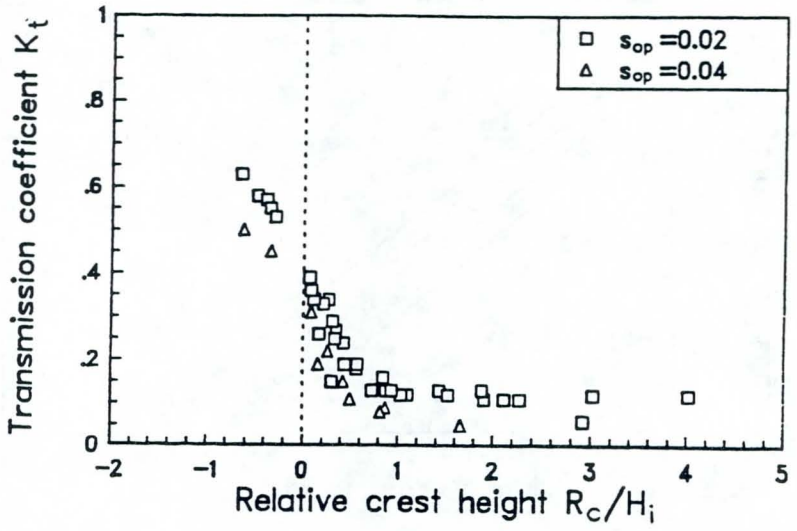
Transmission coefficient K_t
1
.8
.6
.4
.2
0
−2
−1
0
1
2
3
4
5
Relative crest height R_c/H_i
s_{op} =0.02
s_{op} =0.04

Figure 11

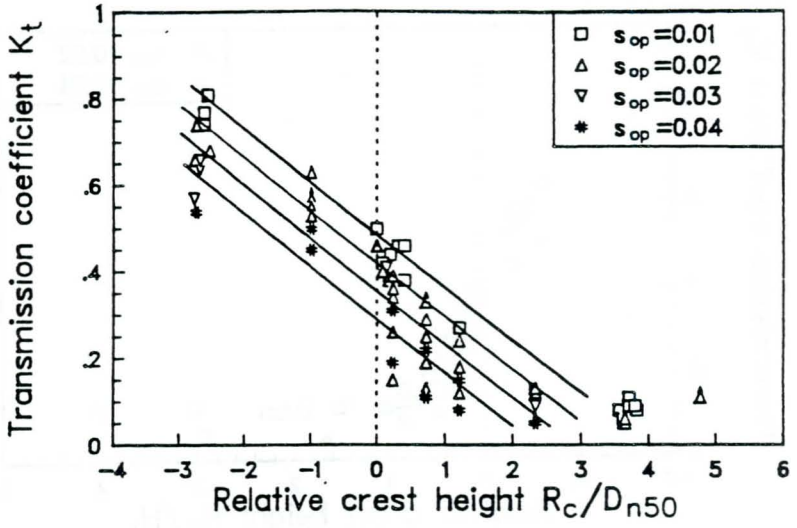
Transmission coefficient K_t
Relative crest height R_c/D_{n50}
s_{op}=0.01
s_{op}=0.02
s_{op}=0.03
s_{op}=0.04
0
.2
.4
.6
.8
1
−4
−3
−2
−1
0
1
2
3
4
5
6

Figure 12

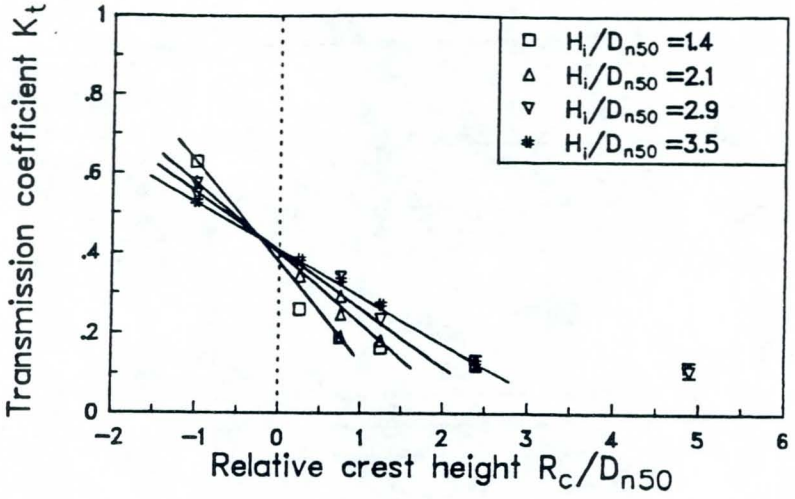
Transmission coefficient K_t
1
.8
.6
.4
.2
0
−2
−1
0
1
2
3
4
5
6
Relative crest height R_c/D_{n50}
H_i/D_{n50} =1.4
H_i/D_{n50} =2.1
H_i/D_{n50} =2.9
H_i/D_{n50} =3.5

Figure 13

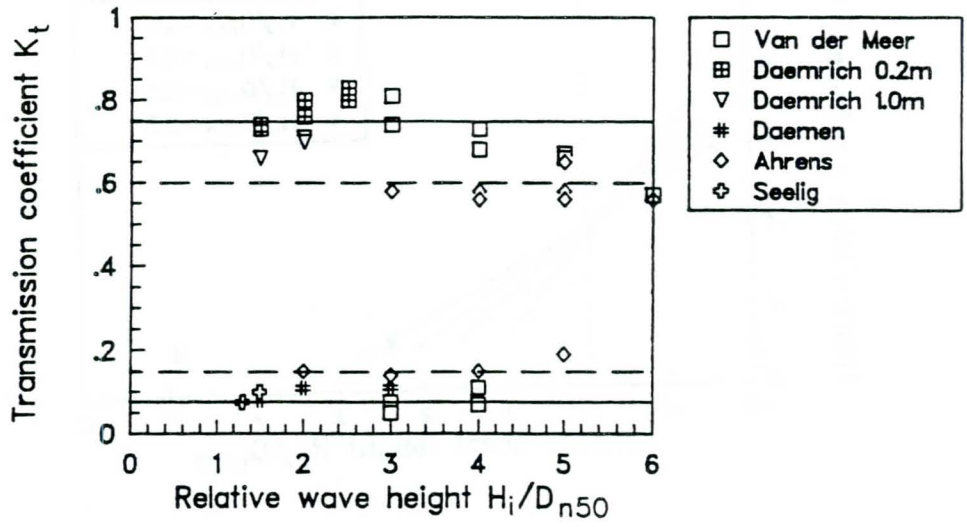
Transmission coefficient K_t
1
.8
.6
.4
.2
0
0 1 2 3 4 5 6
Relative wave height H_i/D_{n50}
Van der Meer
Daemrich 0.2m
Daemrich 1.0m
Daemen
Ahrens
Seelig

Figure 14

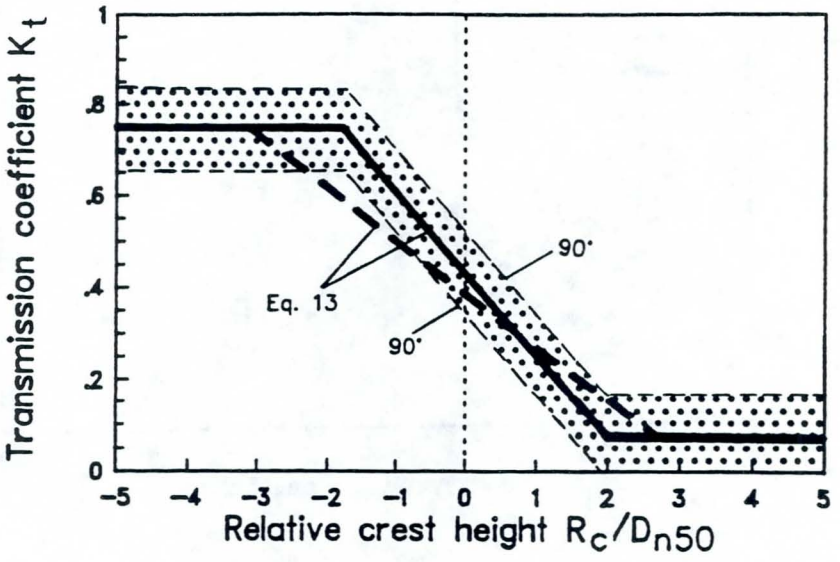
Transmission coefficient K_t
1
.8
.6
.4
.2
0
−5 −4 −3 −2 −1 0 1 2 3 4 5
Relative crest height R_c/D_{n50}
90°
Eq. 13
90°

Figure 15

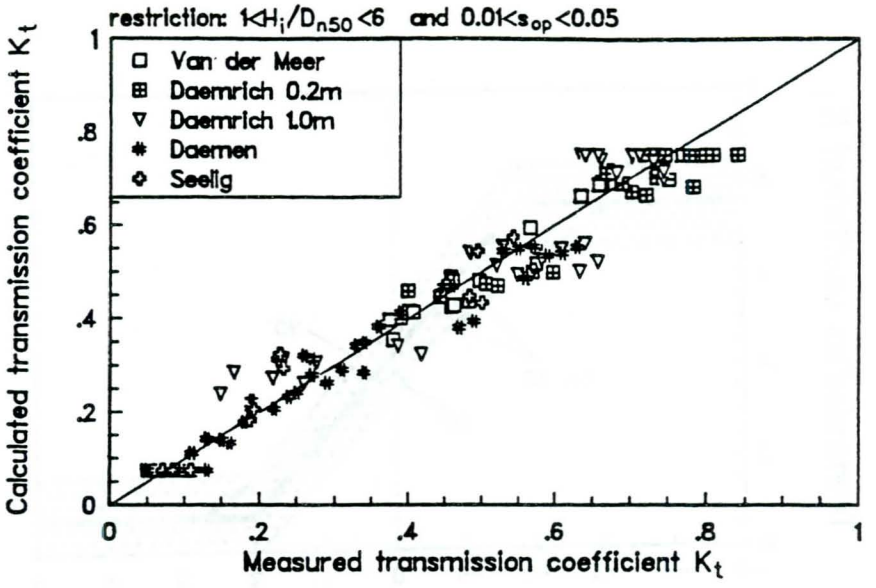
restriction: 1<H$_i$/D$_{n50}$<6 and 0.01<s$_{op}$<0.05
Van der Meer
Daemrich 0.2m
Daemrich 1.0m
Daemen
Seelig
Calculated transmission coefficient K$_t$
Measured transmission coefficient K$_t$
0
.2
.4
.6
.8
1

Figure 16

BOUNDARY STRESS AND STABILITY OF RIPRAP AT BRIDGE PIERS

A.C. Parola
University of Louisville, Civil Engineering Dept.
Louisville, Kentucky, USA

Introduction

Erosion of foundation material by flood waters is the most frequent cause of catastrophical bridge failure in the United States (Makowski et al. 1990). Bridge piers induce strong secondary currents that increase local boundary stress. Consequently, erosion and sediment transport capacity of the secondary currents are substantially larger than in unobstructed flow resulting in the formation of local scour holes in streambeds surrounding pier foundations. Often local scour in combination with general and constriction scour degrade the streambed to the extent that foundations are undermined causing settlement and, in some cases, collapse of supported bridge spans.

Riprap commonly is placed on the streambed surrounding piers to protect the streambed from the local secondary currents induced by piers. The placement of riprap significantly changes the local flow conditions and resulting boundary stresses. The size of the riprap must be substantially larger than the riprap used to protect streambeds in unobstructed flow due to the locally high boundary stresses around piers.

Flow Field Induced by Bridge Piers

Local scour of the streambed around a pier results from 1) locally high boundary stresses, 2) locally high seepage gradients, and 3) diversion of bedload sediment (Hjorth 1975). These effects are produced by a combination of flow constriction, downflow in front of the pier and the associated horseshoe vortex system, and wake vortex systems as shown in Figure 1. The constriction of streamlines, principally two-dimensional except in a region close to the pier, causes convective flow acceleration. The flow acceleration is enhanced by the lowering of

pressure in the wake region of the pier by wake vortices. Near the streambed, the convective acceleration is further enhanced by the presence of the downflow on the upstream face of the pier. The approach flow limiting streamlines, shown in Figure 1, are pushed upstream and away from the pier by the momentum of the downflow fluid.

The dov..flow, resembling half of a vertical jet, occurs on the upstream face of piers. This downflow results from the vertical velocity gradient of the approaching flow (Moore and Masch 1963) and the curvature of streamlines (Tison 1937, from Hjorth 1975). The impingement of the downflow on the streambed can form an area of relatively high boundary stress compared to boundary stress of the surrounding streambed. The downflow rolls up into a complex vortex system upstream of the pier. The vortex system was explained qualitatively in terms of the change in circulation caused by piers in shear flows by Shen et al. (1966). The jet is deflected upstream by the pier and streambed, causing an upstream flow separation and a forced vortex system.

Another effect of the downflow jet and the consequential separation of flow on the bed upstream of piers is the deflection of approach flow limiting streamlines. The fluid near the streambed of the approaching flow is diverted around the region of the horseshoe vortex system and the bedload sediments transported by this fluid are also diverted (Hjorth 1975), as shown by the hypothetical trajectory of sediment particles in Figure 1. Hypothetically, even if the boundary stress under the vortex system is equal to the boundary stress on the surrounding bed, net erosion still would occur because any sediment removed from under the vortex could not be replaced by inflowing sediment.

The wake vortex systems form in the separation regions on the sides of an downstream from rectangular foundations and piers as shown in Figure 1. Similar wake vortices are generated downstream of flow separations from cylindrical and round-nosed piers. At Reynolds numbers (based on pier diameter) typical of flood flows, these wake vortices are unstable, are shed alternately, and are convected downstream. Hjorth (1975) measured pressure variations in the bed near flow separation points that were sufficient to cause local liquefaction of the

streambed. Melville (1975) observed bursts of sediment particles exploding from the streambed as wake vortices passed over those sediments. Melville (1975) hypothesized that the wake vortices and horseshoe vortices are connected; although Dargahi (1987) found in his experiments that wake vortices are shed at different frequencies than horseshoe vortices.

Boundary Stress at Bridge Piers

As a result of the flow field complexity around bridge piers, analytical and numerical attempts to determine time-averaged boundary stresses have relied on a series of assumptions that simplify the flow field considerably. Since direct measurement of boundary stresses in three-dimensional boundary layers with a substantial adverse pressure gradient is extremely difficult, simplifying assumptions are required to enable the use of velocity or pressure measurements to estimate boundary stresses. Consequently, the accuracy of the boundary stresses reported is qualitative, as stated by the investigators reporting boundary stresses measurements.

Breusers et al. (1977) and others analytically determined the maximum flow velocity for the design of riprap protection as the two-dimensional approximation to inviscid flow perpendicular to the axis of an infinitely long circular cylinder. The maximum velocity is located on the cylinder surface along radii perpendicular to the undisturbed velocity direction and is 2 times the undisturbed velocity. Nicollet and Ramette (1971) observed that sediment particles at the sides of model piers began to move at approach flow velocities equal to about 50% of the velocities required to cause incipient motion of the streambed in the approach flow. As in most experiments to determine scour depth, the experiments by Nicollet and Ramette (1971) were conducted with the same bed material in the approaching flow as around the pier; therefore, the effects of increased roughness caused by riprap on the flow field and resulting boundary stress were not investigated. Other investigators (Ettema 1980) obtained similar results for the initial erosion at cylindrical piers in similar experiments.

Melville (1975), Hjorth (1975), and Dargahi (1987) have attempted to estimate the spatial distribution of average boundary stresses on the bed surrounding piers from velocity measurements or preston tube measurements. The basic assumptions in these estimations were that 1) the velocity profiles in the flow with pressure gradients near the pier were similar to those in the approaching flow and 2) the approaching flow streambed roughness was essentially the same as that of the streambeds surrounding piers. Melville (1975) found that under plane bed conditions, the maximum boundary stress was located on the streambed under the edge of the wake zone downstream of the flow separation line and was approximately 3.5 times the boundary stress far upstream of the pier. Melville's measurements showed that boundary stresses under the horseshoe vortex region of flow were small until a scour hole developed. Melville conducted similar experiments on scour holes of various depths. These measurements showed that the location of maximum boundary stress shifted from downstream of the flow separation line on the pier sides to the region under the horseshoe vortex as the scour hole depth was increased from the plane bed condition.

Hjorth (1975) used preston tube measurements to approximate average boundary stresses around circular cylinders and square cylinders of various widths on a fixed plane bed of homogeneous roughness. He reported average spatial distributions of boundary stresses that varied considerably in magnitude from those reported by Melville (1975). In one case, he reported boundary stresses on the bed around a circular cylinder nearly 12 times those of the approaching flow. Other measurements showed that rectangular piers with sides oriented parallel to the approaching flow direction caused boundary stresses to increase by a factor of about 3 over the undisturbed flow conditions. Square cylinders with the sides rotated 45 degrees to the approach flow induced boundary stresses as high as 11 times those of the undisturbed flow.

Dargahi (1987) also used preston tube measurements to approximate the boundary stresses around a model circular cylinder. He obtained mean boundary stresses of approximately 3.5 times those of the approaching flow in a zone extending upstream and downstream from the region of flow separation. The boundary stress investigations by Hjorth (1975), Melville (1975), and Dargahi (1987) did not include the effects of the variation in bed roughness from the

approach flow to the region surrounding the pier. Because riprap substantially alters the roughness and flow field and because the boundary stresses are very dependent on roughness in high Reynolds number flow, the effect must be considered. Measurements required to estimate boundary stresses in flows with high roughness are extremely difficult.

Parola (1990) measured the approach flow conditions that caused failure of model riprap placed around piers on a plane bed and within scour holes for an approach flow streambed that ranged in relative roughness from 0.004 to 0.4. With this information the maximum boundary stress on the bed surrounding the pier was approximated assuming the maximum boundary stress was equal to the critical boundary stress for incipient motion of the particles in uniform flow. The critical stress was estimated from Shields equation

$$\tau_c = C_s (\rho_s - \rho) g D_p \qquad (1)$$

where τc = critical shear stress, Cs = the Shields parameter, ρs = density of sediment, ρ = density of water, g = gravitational acceleration, Dp = equivalent particle diameter around the pier. The value of Cs=0.06 was chosen for the model riprap.

The approaching flow boundary stress was approximated from the log velocity equation

$$\tau_o = \frac{\rho U_o^2}{[5.75 \log(5.53 \frac{Y}{D_o})]^2} \qquad (2)$$

Using the data of Parola (1990) and assuming $\tau_{max} = \tau c$, the ratio of maximum boundary stress to approach flow boundary stress was plotted in Figure 2. Figure 2 shows that τ_{max} / τ_o varies considerably from about 1 to 18. The minimum increase in boundary stress was found under conditions with very high approach flow relative roughness. The maximum increase in boundary stress was found in the case of a relatively smooth approach flow roughness. The 18 fold change in τ_{max} / τ_o shows the variability of this quantity.

The ratio of maximum boundary stress computed above was plotted against the average stagnation pressure of the approaching flow, ρU^2, in Figure 3. The boundary stress ranges from 0.01 ρU^2 to 0.07 ρU^2. This analysis shows that the maximum boundary stress at the pier is

dependent on the average velocity of the approach flow and is relatively independent of the approach flow boundary stress.

Seepage Gradients

On the streambed near vertical separation lines, the local pressure variation on the streambed can be substantial. Hjorth (1975) showed that the change in pressure along the streambed can vary as much as ρU^2 from the front corner of a pier to the side of the pier. Posey (1973) realized that such seepage gradients would result in the removal of fine grain material from beneath riprap protection and that a filter should be provided to prevent removal of the fine grain materials

Stability of Riprap Around Rectangular Piers

Parola (accepted 1993) considered the effect of several dimensionless parameters on riprap stability around rectangular piers aligned with flow. A demonsionless equation was written as

$$N_c = f\left(\frac{d}{b}, \frac{Y_o}{b}, \frac{D_p}{b}, \frac{D_o}{Y_o}\right) \tag{3}$$

where N_c was defined as

$$N_c = \frac{\rho\, U_o^2}{(\gamma_s - \gamma)\, D_p} \tag{4}$$

Small-scale laboratory data for rectangular piers are shown in Figure 4 with the uniform flow data of Neill (1967), the equation representing the conditions of "first movement" of gravel given as

$$\frac{\rho\, U_o^2}{(\gamma_s - \gamma)\, D_o} = 2.5\left(\frac{D_o}{Y_o}\right)^{-0.20} \tag{5}$$

and the relation provided by Maynord et al. (1989) expressed as

$$\frac{\rho\ U_o^2}{(\gamma_s-\gamma)\ D_{30}} = 2.62\ (\frac{D_{30}}{Y_o})^{-0.20} \qquad (6)$$

for riprap placed in straight channels. Figure 4 shows that riprap sizes must be 4 to 8 times larger around the base of a rectangular pier than that required in uniform undisturbed flow.

Figure 5 shows the variation in N_c with the relative depth of placement, d/b, and for various values of relative rock size, b/D_p. Negative values of d/b represent material mounded around the pier and positive values of d/b represent cases where the riprap top surface was below the streambed for riprap placed within scour holes. The increase in N_c with scour depth was expected; however, the increase in N_c with increase in mound height was unexpected. The mound of riprap may disturb the formation of vortices and the associated downflow by disrupting the approach flow velocity gradient. The lowest value of N_c occurred for material placed slightly below the surrounding streambed and for rocks in the smallest size range.

In Figure 5, three ranges of b/D_p are shown. The lowest values of N_c are obtained at each elevation within the scour hole for constant value of d/b. Lower bound lines are shown in Figure 5 for each range of b/D_p. These lines show that smaller rocks relative to the pier size are moved at lower values of N_c than are larger rocks. One explanation of this behavior is that the larger rocks tend to dissipate the energy of the vortices and downflow. A similar explanation was provided by Ettema (1980) concerning the effect of relatively large bed material on the formation of scour holes. In addition, the size of vortices induced by a pier are a fraction of the pier width; therefore, as riprap size approaches the pier width, the effectiveness of the pier-induced vortices at dislodging riprap is diminished. Equations representing the minimum value of N_c throughout the range of d/b values are

$$N_c = 0.8 \quad for\ 20 < \frac{b}{D_p} < 33 \qquad (7)$$

$$N_c = 1.0 \quad for\ 7 < \frac{b}{D_p} < 14 \qquad (8)$$

$$N_c = 1.2 \quad for\ 4 < \frac{b}{D_p} < 7 \tag{9}$$

The effect of relative flow depth and relative roughness of the approaching flow was not found to be significant in the range of flow depths and roughness tested.

Stability of Riprap Around Cylindrical Piers

Breusers, Nicollet, and Shen (1977) recommended an equation for the size of riprap placed around cylindrical piers that can be expressed as

$$D_p = 2.83 \frac{\rho U_o^2}{(\gamma_s - \gamma)} \tag{10}$$

Equation 10 was developed from the equation proposed by Isbash (1935) for predicting riprap size given velocity and by using the observation of Hancu (1971) and Nicollet and Ramette (1971), that erosion at a circular pier was initiated at a flow velocity equal to half the critical velocity upstream of the pier irrespective of the diameter of the pier.

Bonasoundas (1973) recommended a relation for determining stone size for riprap aroundcylindrical piers given by

$$D_p(cm) = 6 - 3.3U_o + 4U_o^2 \tag{11}$$

Quazi and Peterson (1973) conducted a small-scale model study using a cylindrical pier model and model riprap placed flush with the approach flow bed. Based on experimental results, they presented the equation

$$\frac{\rho\ U_o^2}{(\gamma_s - \gamma)\ D_p} = 1.14 \left(\frac{D_p}{Y_o}\right)^{-0.20} \tag{12}$$

The cylindrical pier data are shown in Figure 6. The data span a region bounded by the values of N_c obtained by Neill (1967) for uniform unobstructed flow, and by a line defined by a minimum value of N_c of 1.4 . Equation 5 (N_c= 1.6 for velocities above 1 m/s) provides a good estimation of the lower limit of N_c except for two data points collected by Quazi and Peterson (1973). Equation 10, however, overpredicts rock size by a factor of at least four. Figure 6 shows that the critical conditions for a round-nosed pier and those for a cylindrical pier are not significantly different.

Figure 6 also shows that the size of rocks placed around cylindrical or round-nosed piers must be 2 to 3.6 times larger than that required for stability in uniform undisturbed flow for the same flow conditions. These values correspond well to the maximum stress values measured by Melville (1975) and Dargahi (1987).

Extent of Riprap Protection

The extent of riprap protection required is dependent on the overall conditions at the bridge crossing and local factors. If the entire channel is expected to degrade, then the riprap at the pier should be designed with this in mind. Local factors that should be considered are 1) the extent of the high boundary stress region near the pier and 2) the extent to which sediment is diverted around the pier.

Hjorth (1975) conducted experiments in which a thin layer of sediment was placed over a plane bed on which a cylindrical pier was attached. Flow conditions in which the boundary stresses were in excess of that required for ripples to form on the bed were established. In the region of the streambed affected by the presence of the pier, the layer of sediment was removed. He suggested that the area of which the plane bed was exposed should be protected. The minimum region suggested for a cylindrical pier was given as shown in Figure 7.

Similar experiments were conducted by the author on a rectangular pier in which the angle between the approach flow direction and the long axis of the pier was varied as shown in Figure 8. This figure shows that the riprap protection should extend upstream about 2 times the projected length, L, of the pier normal to the flow direction, horizontally about $2L$, and downstream about 7 L. Protection of the region downstream of the pier is required if scour holes downstream of the pier are unacceptable. The placement of riprap around the front of the pier

prevents sediment from entering the wake zone. The wake vortices then become effective in forming scour holes on the bed downstream of the pier if unprotected (Hjorth 1975).

Design Equations

Equations 7, 8, and 9 are recommended for use in determining the size of riprap to provide protection to the streambed around rectangular piers, round-nosed piers with significant skew to the approaching flow, or piers that have rectangular foundations that are located near or above the streambed. A value of N_c=1.4 is recommended for cylindrical piers in which the rectangular foundation is located well below the streambed, and for round-nosed piers that are expected to remain aligned with flow and that have rectangular foundations located well below the streambed. Additional research is required to determine the effect of b/D_p on size to reduce riprap sizes required. The velocity used in these equations should be the vertically averaged velocity of the flow approaching the pier. Riprap stability is sensitive to velocity increases, and therefore, caution should be used when selecting a design safety factor. Rather than using a safety factor, the author recommends that the rock size should be selected for that flood level which is acceptable as causing riprap instability. Although the elevation of placement of the riprap was found to affect the riprap stability significantly, riprap size should not be reduced to account for the placement elevation because the future elevation of the streambed may change with time, causing a reduction in resistive capacity.

When riprap is in place around a pier, pressure fluctuations may still be adequate to displace soil particles, especially fine sands or silty sands. The stability of those particles must be considered. Bed particles can be retained if a geotextile filter is placed over the bed. Applying the usual filter criteria (higher permeability than the protected soil as well as retention of particles) may be impractical because the primary purpose of the filter is bed retention. A filter should be selected to retain bed particles and then stability of the system should be checked considering the stabilizing weight of the riprap over the filter. Sufficiently large uplift forces to displace the overlying rock are unlikely to be mobilized under even completely clogged filters, but an analysis of such uplift should be done to confirm stability.

To protect the streambed from the secondary currents caused by a pier, the riprap must be extended from the pier surface as shown in Figures 7 and 8. Because the extent of the pier influence on the flow is sensitive to the projected length of the pier perpendicular to the flow direction, all possible skew angles should be considered in determining the extent of protection.

Conclusions and Recommendations

Secondary currents induced by bridge piers cause high local boundary stresses, high local seepage gradients, and sediment diversion from the streambed surrounding the pier. These effects result in an increase in erosion capacity of the flow over unobstructed conditions. Riprap placed around the pier to armor the streambed must be selected such that it can remain stable under the boundary stresses created by the secondary currents. Riprap placed around a pier significantly changes the roughness of the bed surrounding a pier and as a result changes the boundary stress from those of the unprotected condition. Equations that relate riprap size to flow conditions were presented.

Pressure fluctuations on the streambed near separation zones and under wake vortices could cause streambed material to migrate through riprap protection. A properly designed filter should be placed below riprap protection, especially near corners of rectangular piers and in the region of wake vortices.

Riprap should be extended to cover regions of high boundary stresses and regions where sediment is diverted from the streambed. The extent of the riprap required is sensitive to the angle at which the approach flow makes with the axis of the pier; therefore, all likely angles of attack should be considered when designing riprap protection.

Additional data are needed to more accurately describe the relation between relative rock size and riprap stability, especially for rocks that are large relative to the pier. Also, the effect of mounding riprap around a pier should be further investigated. Additional research should be conducted on riprap placed around cylindrical piers to determine the effect of the parameters investigated in this study for rectangular piers. Although the experiments of this study were conducted without a bed load, the effects of bed load on riprap stability are envisioned to be minor. Further studies are required to determine the effect of various factors such as bed materials on which the riprap is placed, riprap gradation, placement methods, general lowering of the streambed, ice, and debris. The equations presented should be used considering the unknown effects of these factors.

References

Bonasoundas, M. (1973). "Flow structure and problem at circular bridge piers," Report No. 28, Oskar V. Miller Institute, Munich Technical University, Munich, West Germany.

Breusers, H. N. C., Nicollet, G., and Shen, H. W. (1977). "Local scour around cylindrical piers," Journal of Hydraulic Research, 15(3), 211-252.

Dargahi, B. (1987) . "Flow field and local scouring around a cylinder," Bulletin No. TRITA-VBI-137, Hydraulics Laboratory, The Royal Institute of Technology, Stockholm, Sweden.

Ettema, R. (1980). "Scour at bridge piers," dissertation presented to the University of Auckland, Auckland, New Zealand, in partial fulfillment of the requirements for the degree of Doctor of Philosophy.

Hancu, S. (1971). "Sur le calcul des affouillements locaux dans la zones piles du ponts," Proceedings, 3, 14th IAHR Congress, Paris, France.

Hjorth, P. (1975). "Studies on the nature of local scour," Bulletin Series A, No. 46, Department of Water Resources Engineering, University of Lund, Sweden.

Isbash, S. V. (1935). "Construction of dams by dumping stones in flowing water," Translated by A. Dorijikow, US Army Engineer District, Eastport, ME.

Makowski, D. B., Thompson, P. L., and Yew, C. P. (1989). "Scour assessment at bridges," Proceedings, ASCE National Conference on Hydraulic Engineering, New Orleans, LA.

Maynord, S. T., Ruff, J. F., and Abt, S. R. (1989). "Riprap Design," Journal of Hydraulic Engineering, 115(7), 937-949.

Melville, B. W. (1975) "Local scour at bridge sites," Ph. D. Thesis, University of Auckland, Auckland, New Zealand.

Moore, W. L. and Masch, F. D. (1963). "The influence of secondary flows on local scourat obstructions in a channel," Proceedings, Federal Interagency Sedimentation Conference, Miscellaneous Publication No. 970, Agricultural Research Service, U.S. Department of Agriculture, Washington, DC, No. 36.

Neill, C. R. (1967). "Mean velocity criterion for scour of coarse uniform bed material," Proceedings, 12th IAHR Congress, Ft. Collins, CO, No. C-6, Vol. 3, C6.1-C6.9.

Nicollet, G. and Ramette, M. (1971). "Affouillements au voisinage de piles de pont cylindriques circulaires," Proceedings, 3, 14th IAHR Congress, Paris, France, 315-322.

Parola, A. C. (1990). "Stability of riprap used to protect bridge piers," Ph.D. Thesis, The Pennsylvania State University, University Park, PA.

Posey, C. J. (1981). "Test of scour protection for bridge piers," Journal of the Hydraulics Division, ASCE, 100(HY12), 1773-1783.

Quazi, M. E. and Peterson, A. W. (1973). "A method for bridge pier riprap design," Proceedings, First Canadian Hydraulics Conference, University of Alberta, Edmonton, Canada, 96-106.

Shen, H. W., Schneider, V. R., and Karaki, S. S. (1966). "Mechanics of local scour," Report CER66HWS22, Colorado State University, Fort Collins, CO.

Notation

U_o	=	average velocity of the approach flow at critical conditions (m/s)
Y_o	=	depth of the approach flow (m)
k_o	=	roughness of the approach flow bed (m)
SH	=	pier shape and orientation factor
b	=	pier width perpendicular to the direction of the approach flow (m)
k_p	=	roughness of bed in the around pier (m)
D_o	=	characteristic rock size in the approach flow bed (m)
D_{30}	=	rock size for which 30% by weight is finer (m)
d	=	maximum depth of riprap top surface below stream bed (m)
D_p	=	characteristic rock size around pier (m)
g	=	gravitational acceleration (9.81 m/s^2)
ρ	=	fluid density (kg/m^3)
ρ_s	=	rock density (kg/m^3)
μ	=	dynamic viscosity of fluid (kg/m s)
N_c	=	stability number
L	=	Project length of pier perpendicular to the direction of the upstream flow

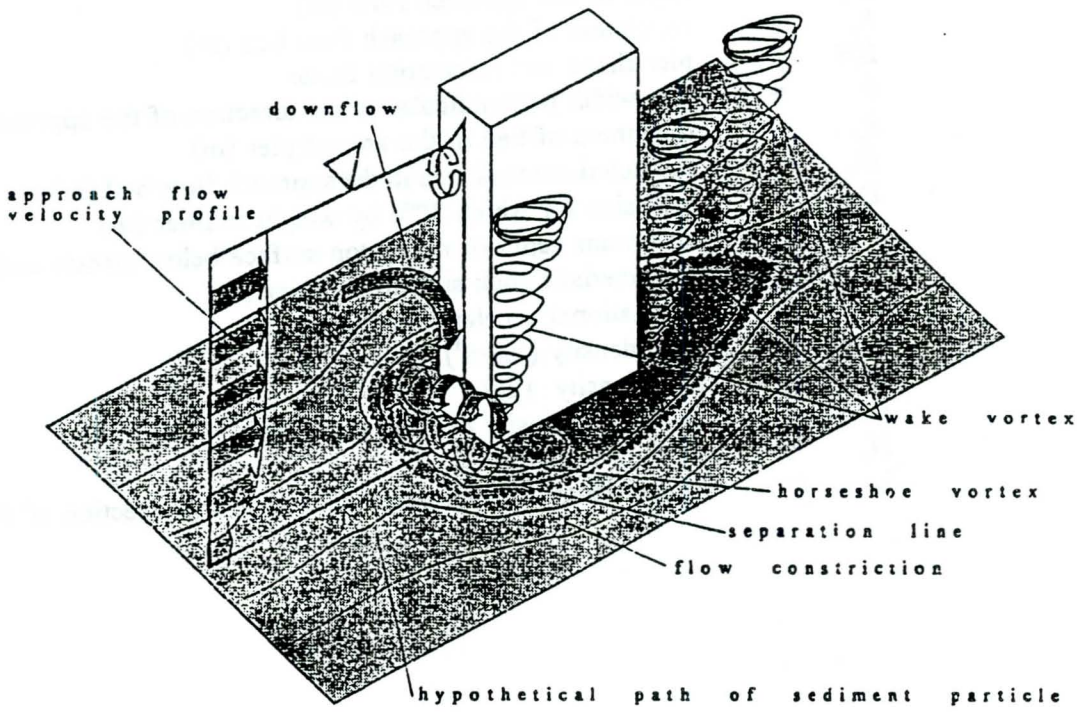

Figure 1. Flow Around a Rectangular Bridge Pier

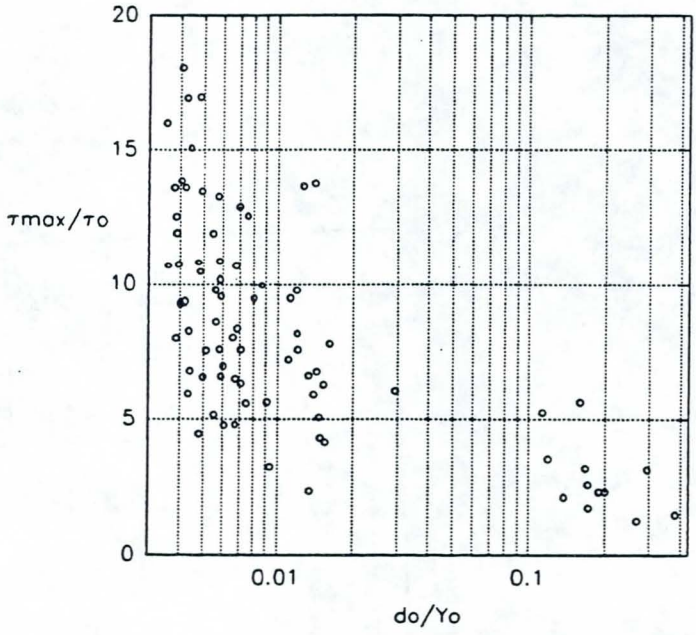

Figure 2. Maximum Boundary Stress Around a Rectangular Pier

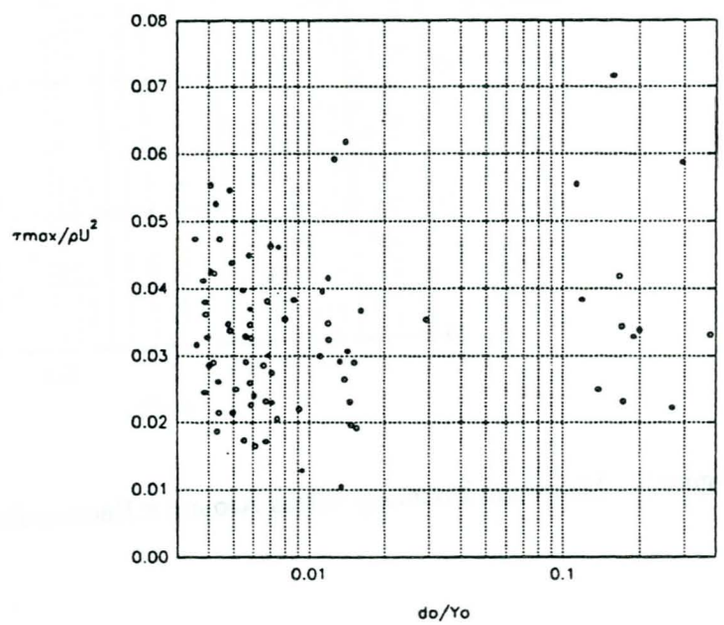

Figure 3. Maximum Boundary Stress Around a Rectangular Pier

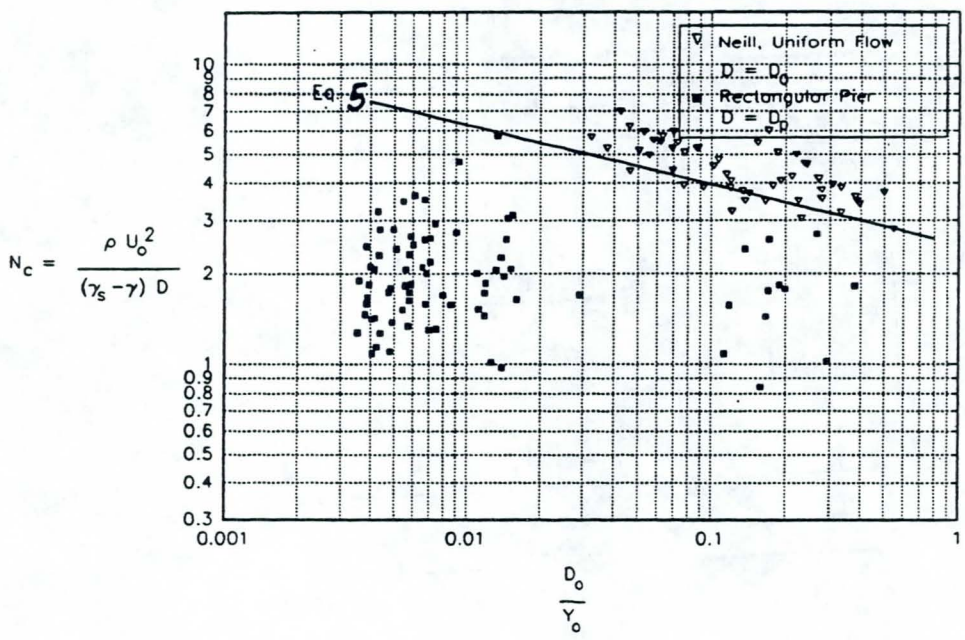

Figure 4. Comparison of Riprap Failure Conditions in Uniform Flow and Around a Rectangular Pier

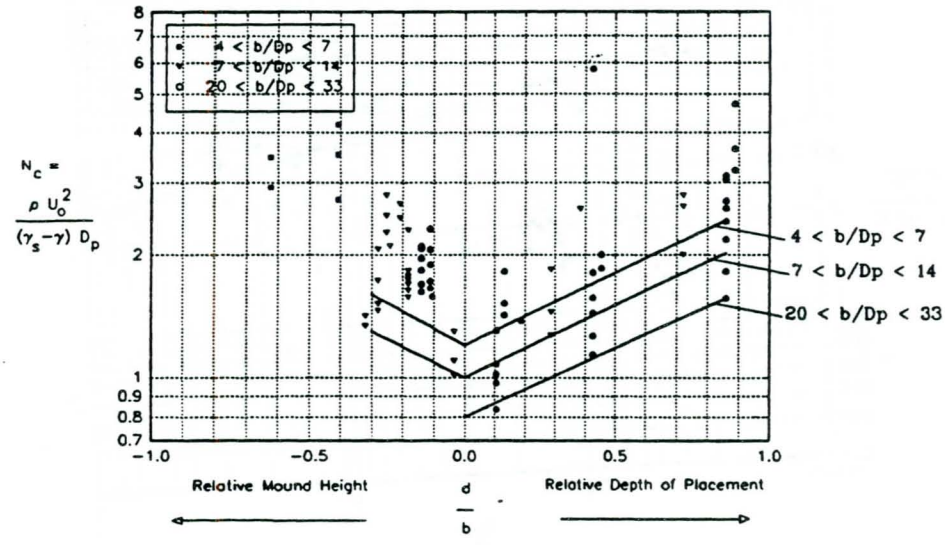

Figure 5. Influence of Relative Placement Depth on Stability of Riprap Around Rectangular Piers

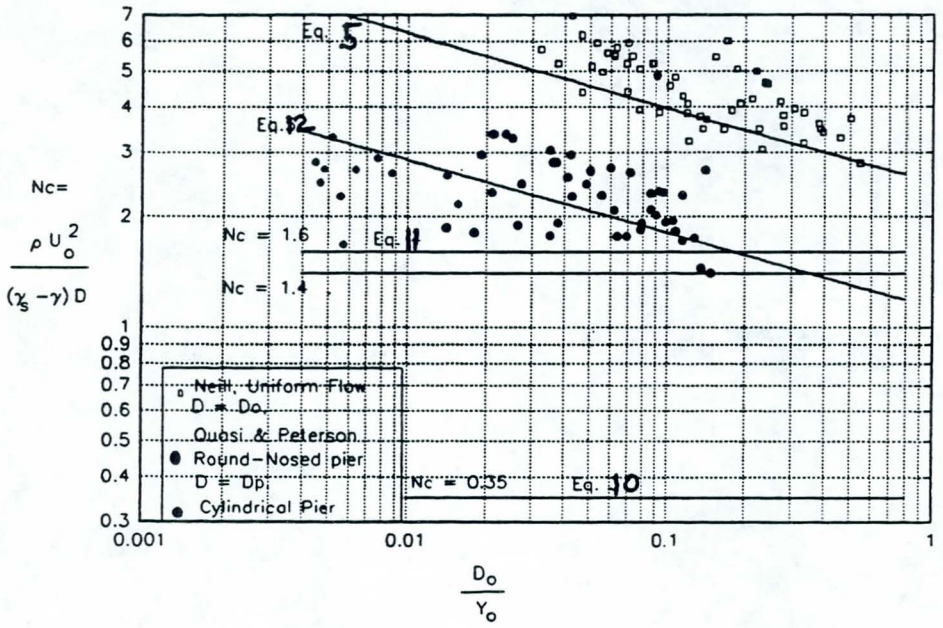

Figure 6. Stability of Riprap Around Circular and Round-Nosed Piers

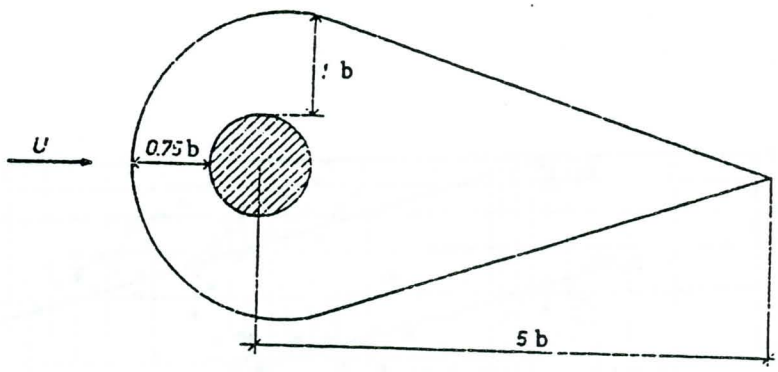

Figure 7. Minimum Extent of Riprap Protection Suggested for a Cylindrical Pier (Hjorth 1975)

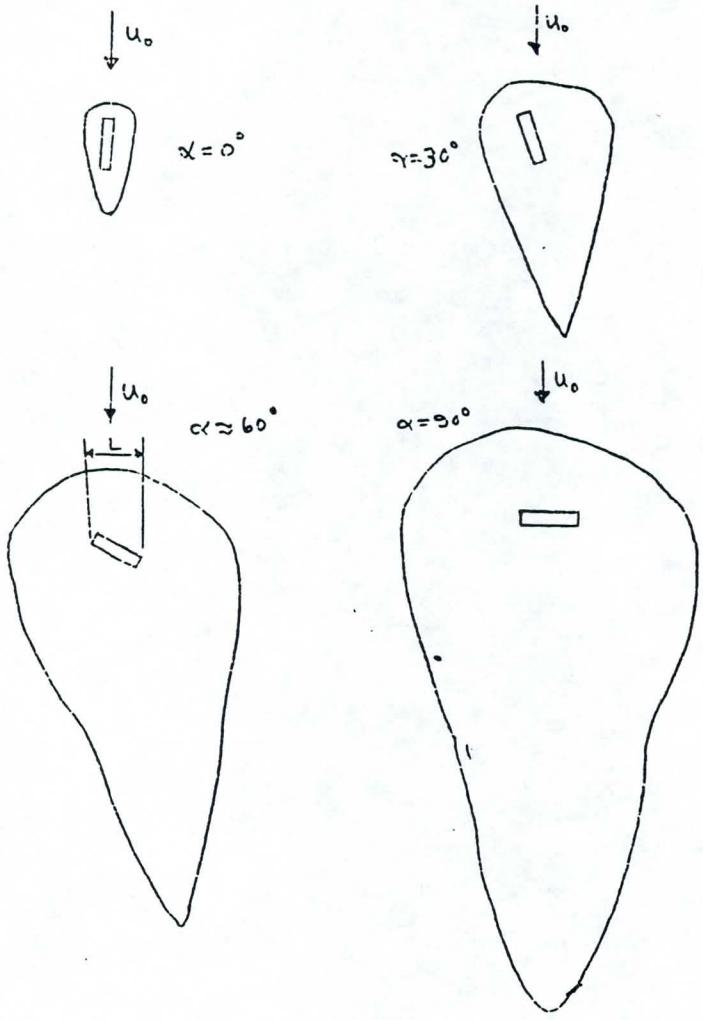

Figure 8. Extent of Plane Bed Exposed by Secondary Currents at a Rectangular Pier

DESIGN TOOLS RELATED TO REVETMENTS INCLUDING RIPRAP

K.W. Pilarczyk
Rijkswaterstaat, Road and Hydraulic Engineering Div.,
P.O. Box 5044, 2600 GA Delft, The Netherlands

Abstract

The increased world-wide demand for relatively low-cost and reliable design methods for protective structures has resulted in preparing a set of national and international guidelines for design, construction and maintenance of hydraulic structures (dams, dikes, breakwaters, banks and revetments). Because the riprap belongs mostly to the low-cost solutions, this continued demand has also resulted in development of better design criteria and measures to improve the stability of rock materials. Although existing knowledge on this subject has still some limitations, it is useful to systematize this knowledge and to make it available for international community (designers and managers).
The paper reviews the basic design metodology and the existing (available) international design documents related to riprap.

Introduction

The use of coarse materials, such as gravel and rubble, in civil engineering practice is very common. There has been an increasing need in recent years for reliable information on design methodology and stability criteria of coarse materials exposed to wave and current action. This need arises partly from an increase in the number and size of (closure-)earth dams and the maintanance of old dams which have to be protected accordingly to the higher safety standards, and partly from constructing of structures at specific locations where they are exposed to more severe wave and current attack (artificial islands, offshore breakwaters, waterways with increased intensity and loading due to developments in navigation, etc.)
For countries where gravel or quarrystone is available these materials usually are more economic for protection works than artificial materials like concrete. However, the shortage of natural materials in certain geographical regions and/or limited dimensions of natural rock have led to the application of other types of protections such as concrete units, gabions, nylon fabrics, sand/concrete bags or mattresses, etc.

The stability of protective structures subject to currents and wave attack is a complex problem. The understanding of hydraulic processes/interactions and various failure mechanisms is still in rudimentary stage, and it is not yet possible to describe many important phenomena and their interactions by theory. We are still in the phase of formulating general concepts and trying to test their validity and practical applicability.
While laboratory investigations provide a means for gaining further understanding of interaction processes between external factors and the protective components, the solution of many practical engineering problems cannot wait until complete understanding of these processes is obtained. Therefore, existing knowledge on this subject (though limited) should be systematized and made available for designers.

The present paper presents a short review of design (national and international) documents, design methodology and criteria. The relevant additional literature is mentioned in references. Special attention is paid to the developments in the Netherlands where, due to the specific circumstances (protection of low-lying country against water), the high safety standards and high quality of the design codes are required. Most of these developments are already included in the international documents (ie.PIANC).

Design philosophy and methodology

General design methodology

When designing structures, the following aspects have to be considered:
- the function of the structure,
- the physical environment,
- the construction method,
- operation and maintenance.

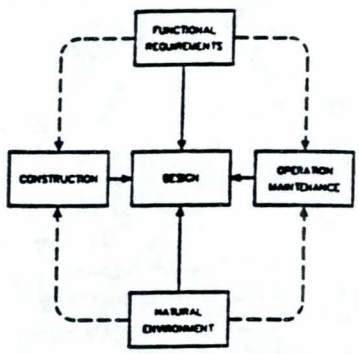

The main stages which can be identified during the design process are shown in Figure 1. The designer should be aware of the possible constructional and maintenance constrains (Pilarczyk, 1990).

Based on the main functional objectives of the hydraulic structure a set of technical requirements has to be assessed. When designing a structure, the following requirements to be met can be formulated:
1. the structure should offer the required extent of protection against hydraulic loading/flooding at an acceptable risk,
2. events at the structure should be interpreted with a regional perspective of the area involved,
3. it must be possible to manage and maintain the structure,
4. requirements resulting from landscape, recreational and ecological viewpoints should also be met when possible,
5. the construction cost should be minimized to an acceptable level,
6. legal restrictions.

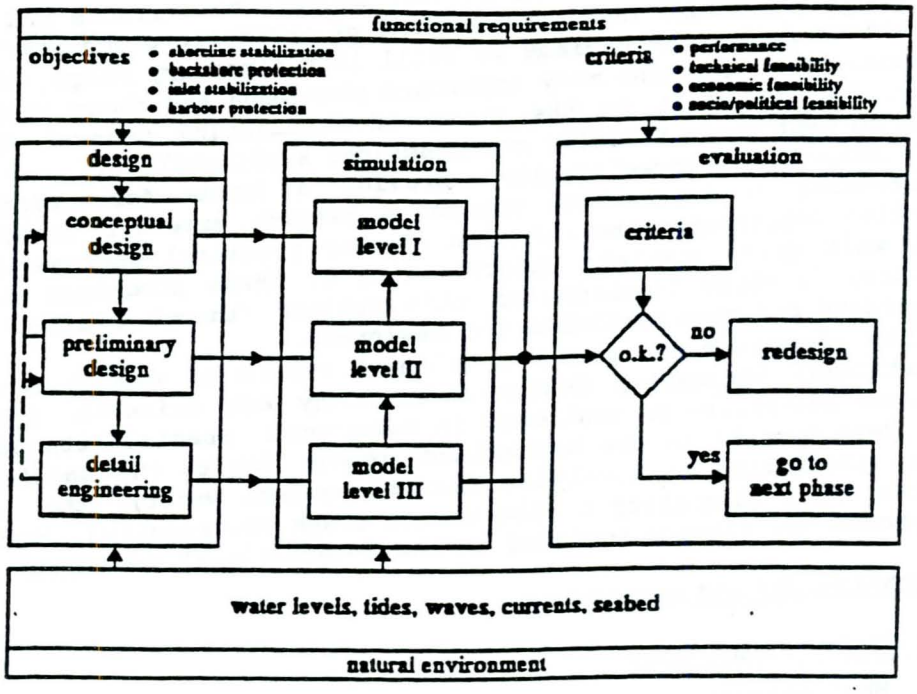

Figure 1 The design methodology

Elaboration of these points depends on specific local circumstances as a type of upland (low-land or not) and its development (economical value), availability of equipment, manpower and materials, etc. For example, the high dikes/seawalls are needed for protection of low-lands against inundation while lower dikes/seawalls are often sufficient in other cases. The cost of construction and maintenance is generally a controlling factor in determining the type of structure to be used. The starting points for the design should be carefully examined in cooperation with the client or future manager of the project.

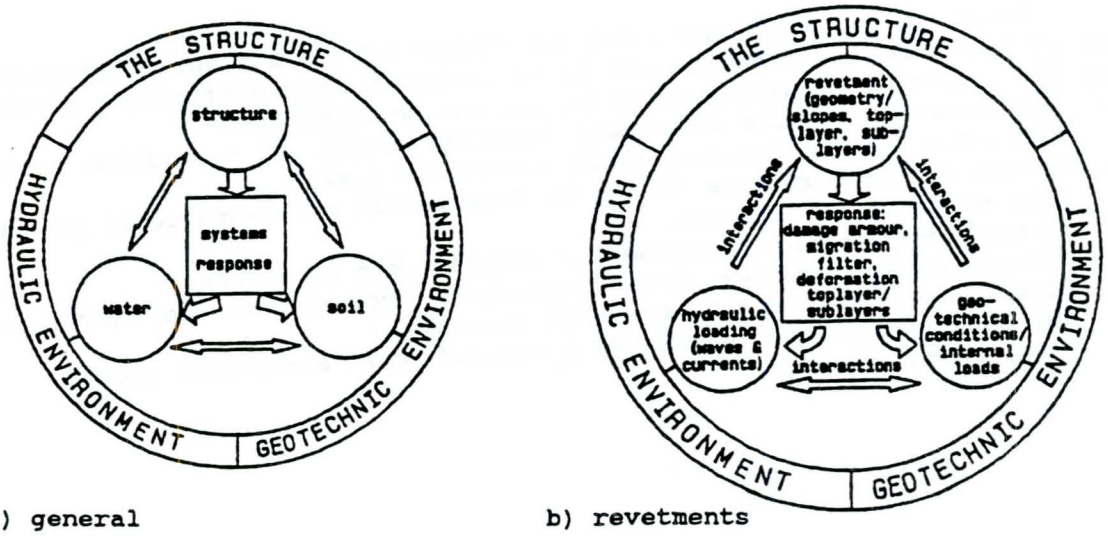

a) general b) revetments

Figure 2 Soil-Water-Structure Interactions (SOWAS-concept)

Most research problems on water defences have multidisciplinary character, specifically, in the technical sense. This is characterized by all relevant interactions between the element soil, water and structure (so-called SOWAS-concept), and may lead to combined hydraulic-, geotechnical- and structural research (Van der Weide,1988). The interactions described above may be brought together in the diagrams shown on Figure 2. The outer circle represents the environmental or human activities, responsible for loads on the system. The different elements of this system - soil, water, structure - are represented by the inner circles. The external interactions between the elements, soil, water structure, are shown by arrows, connecting the respective elements.

Because the traditional research takes place within the respective disciplines (hydraulic, geotechnic, structural, material technology, environmental, etc.), it is not always easy to organize the combined (multidisciplinary) research. The separate disciplines are often faced by separate institutions (laboratories, institutes, departments, etc.) with a different research culture and different management policy.

The objective of SOWAS is to bring together engineers and scientists with different backgrounds to stimulate exchange of experience at and between various levels.

The Dutch practice has learned that the best way to perform an integrated research is by organizing the working-groups or project-teams with independent chairmans where the all institutions involved are able to participate. The working group defines the total program and the involvement of specific disciplines and institutions. It is evident that the concept of soil-water-structure interaction (SOWAS) plays a very important role in the Dutch Research Strategy on Water Defences.

Design philosophy in the Netherlands

The chosen national design/safety policy determines in a certain way the required level/quality of design documents (design standards/codes, process simulation/dimensioning techniques,materials/products specifications and the execution techniques).

The low-lying countries as the Netherlands are strongly dependent on good (safe) water defences (sea/river-dikes , dams and/or banks). In the past the design of dikes/dams and revetments was mostly based on rather vague experience than on the general valid calculation methods.

The increased demand for reliable design methods for protective structures has resulted in the Netherlands in preparing an adeqate design policy, especially regarding the safety aspects, and in reliable technical design methods and design codes.The backgrounds of this policy are briefly overviewd below. For a treatment of these matters in greater depth the reader is referred to the original reports and publications.

Dams, dikes, seawalls and banks are functioning to protect upland (population and economical values) against erosion or inundation due to storm surges. There is still much misunderstanding on the use of dikes and seawalls and their possible disadvantages related to the disturbance of the environment and natural processes. However, it should be said that in many cases when the upland becomes endangered by inundation (as in The Netherlands) or by high-rate erosion (think also of possible increase of sea-level rise) leading to high economical or ecological losses, whether one likes it or not, the dike or seawall can even be a 'must'for surviving.

The proper engineering strategy to be followed should always be based on the total balance of the possible effects of the counter measures for the area considered, including the environmental issues and the economical effects or possibilities. It is an 'engineering-art' to minimize the negative effects of the solution chosen.

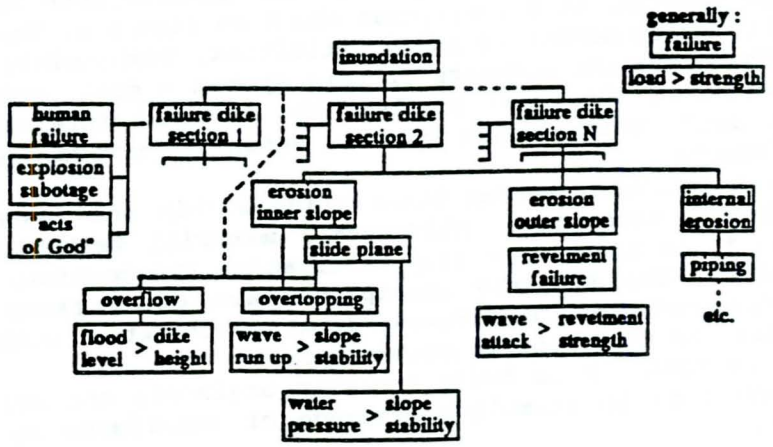

Figure 3 Simplified Fault Tree for a Dike/Bank

Absolute safety against storm surges is nearly impossible to realize. Therefore, it is much better to speak about the probability of failure of a certain defence system. The ultimate potential threat for the Dutch sea defences is derived from extreme storm surge levels with a very low probability of exceedance (1% per century for sea-dikes) and equated with the average resistance of the dike (or dune). Under these ultimate loadconditions, probability of failure of the dike (seawall) should not exceed 10%. To apply this method, all possible causes of failure have to be analyzed and consequences determined. This method is actually under development in the Netherlands for dike and dune design (TAW 1984, 1985, CUR/TAW 1990). The 'Fault tree' is a good tool for this aim (Figure 3). In the fault tree, all possible modes of failure of elements can eventually lead to the failure of structure.

The probabilistic approach to sea defences as developed in The Netherlands is briefly summarized in (Pilarczyk, 1992) and is treated more extensively in CUR/TAW-report (1990).

National organization and cooperation in the Netherlands

The design documents are prepared by special workings groups (i.e. Fig.4) acting under supervision of the Technical Advisory Committee on Water Defences (TAW), Rijkswaterstaat (RWS=Public Works Dpt.) and the Dutch Center for Civil Engineering Research and Codes (CUR). The working groups and/or project-teams have mostly a multidisciplinary character and consist not only of researchers but also of designers, contractors and coastal managers. This form of cooperation helps to identify and to define thr problems, to create understanding for the chosen strategy and to implement the results. This is a very efficient way to build a bridge between the research (new developments) and the practice.

The important role in the transfer of technology in civil engineering in the Netherlands plays the Centre for Civil Engineering Research and Codes.

Collective research of national interest as well as work in connection with codes and specifications for concrete and civil engineering (incl. water defence structures in cooperation with TAW and RWS) are the main activities of this centre (CUR). Among others the activities concentrate on design methods, execution, maintenance and management of hydraulic structures, and on codes and specifications for hydraulic engineering. The major hydraulic engineering projects especially are characterized by broad-based multidisciplinary studies and a lot of research. Therefore, the integral approach to projects and new developments is stimulated by the CUR.
In the CUR, experts from public authorities, contractors, industry, engineering consultants, research institutions, and educational establishments are acting in co-operation with one another on the same (collective) basis.
Finance is provided partly by industry, partly by individual members and partly by government contributions. The procedure for each research subject and for each code to be drafted consists in setting up a committee composed of experts in the field concerned.
Experimental research and special study projects are entrusted to various Dutch laboratories and consultant firm commissioned to carry out these investigations. New developments in technology for which there already exists substantial practical interest, but which are not yet considered ready for specification in codes of standards, are the subject of CUR recommendations. Since these are established through the existing committee structure and under the responsibility of the CUR, they carry a certain authoritative weight.This form of diffusion of technical information appears to be appreciated in practice.

The transfer of (new) know-how into the potential users take place through the publications, Symposiums, Workshops and, in more direct way, through the advisory branch assisting the client in solving his problems and the more or less regular Post-academial Courses.

Example of integrated research on revetments

Numerous types of revetments have been developed in the Netherlands for shore and bank protection of navigation channels against erosion by waves and currents (i.e., rip-rap, blocks, asphalt, etc.). The reason for this is the increase of the problem with respect to the defence of the shores (i.e. more rigid safety requirements for sea-dikes) and banks of

navigation channels (i.e., increase of size and speed of motorvessels), as well as the high cost and shortage of natural materials.
The fact that design rules are still limited in quantity has stimulated investigations in the area of rip-rap, artificial blocks and bituminous revetments as well, in the area of geotextiles. Problems which arise due to these developments require solutions which often only can be found by in-depth specific multidisciplinary studies (Figures 2, 3, 4 and 5).

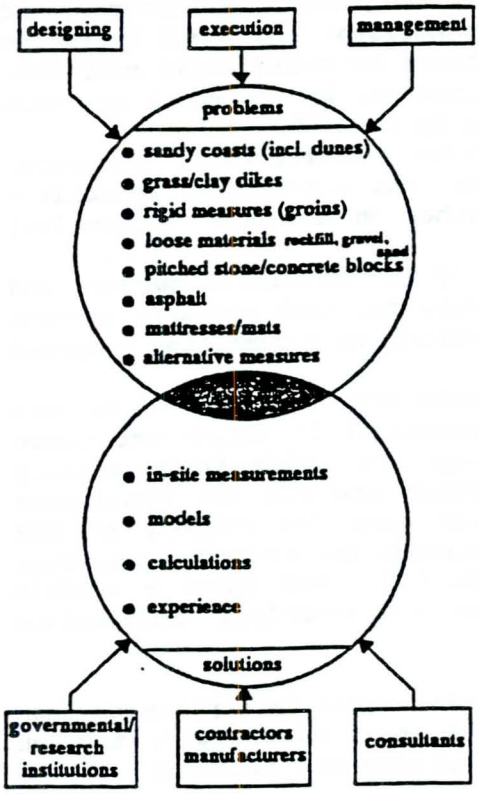

Fig.4 Integrated approach

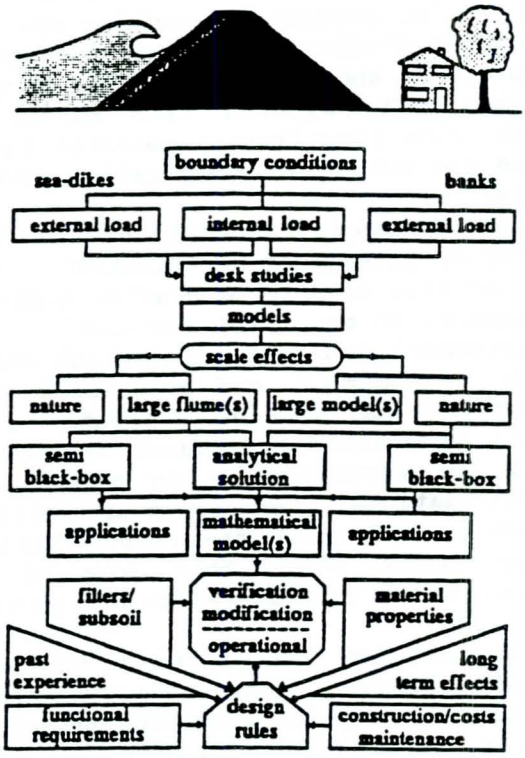

Fig.5 Sea-dikes and banks research approach

In order to control the future sea-dikes and bank-protection problems, the Dutch Ministry of Transport and Public Works (Rijkswaterstaat) assigned the Delft Hydraulic Laboratory and Delft Soil Mechanics Laboratory to carry out systematic research into these areas. The research on sea-dikes and revetments was carried-out under the joint responsibility of the Rijkswaterstaat and the Technical Advisory Committee for Water Defences. The project was guided by two working groups with the common chairmanship. In this way it was possible to agree on the common integrated research program. On the basis of the analysis of practical design problems and the gaps in the existing knowledge, the required research programmes had been determined (Figure 5).

This program follows the general SOWAS-concept as it is outlined in Figure 2; it includes the integration between two fields (banks and dikes) as well interdisciplinary integration (soil-water-structure).
The basic programmes have been carried out by means of small-scale models. However, it must be pointed out that a small-scale hydraulic model for navigation purposes still needs a lot of space. For example, in the scope

of bank protection research programme, the hydraulic model of an inland navigation fairway in scale 1:25 has been built in a 40 x 90 m shed to observe the induced water motions and their erosive effects on the banks.

Since model research has certain inherent technical restrictions known as scale effects, required additional information has been obtained by means of prototype investigations, i.e., the Delta-Flume at the Delft Hydraulics and some prototype locations in respect to the sea-dikes problems and the Hartel Canal (Rotterdam area) with test embankments with respect to bank- protection of navigation channels (Pilarczyk, 1984).
The result of the prototype tests, in combination with the model results and the calculation methods (incl. mathematical model) developed in the framework of the systematic research on dike protection (Delft Hydraulics and Delft Geotechnics 1989) and systematic research on bank protection (Delft Hydraulics 1988) extended with knowledge gained from practical experience, led to preparation of guidelines for reliable dike and bank protection designs (CUR/TAW, 1992).
The aim of the total research was to develop such design criteria to minimize the amount of maintenance and construction costs of new revetments. Actually, this research program is extended into the environmental friendly solutions for banks and dikes (Pilarczyk et al,1990).

Design principles and verfication of design

Based on some international design documents (PIANC,1987,1992, Pilarczyk,1990, CUR/CIRIA,1991) one may formulate the following design items for revetments. However, the similar design items can also be, in a similar way, formulated for other hydraulic structures.

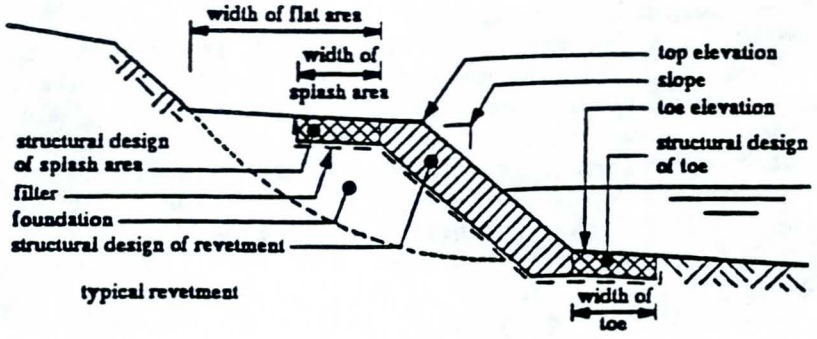

Figure 6 Design components of typical revetment structure

1. Designer's checklist

The review of the key elements that must be considered in the design (dimensioning) of revetment structure is illustrated Figure 6.
The most critical structural design elements are: 1) the stability of the coverlayer, 2) the security of the foundation, 3) the minimization of settlement and sliding and 4) the toe protection to prevent undermining. All of these are potential causes of failure of coastal structures. The usual steps needed to develop an adequate structure design are:

1.1 General aspects
-Formulate purpose of the project
-Formulate functional requirements

-Formulate project restraints/material/labour/equipment/time/finance
-Formulate global description of boundary conditions.

1.2 Prepare alternative general solutions

1.3 Determine boundary conditions
-hydraulic: water levels, wave climate, currents, morphology, etc.
-geotechnical: soil types and relevant parameters
-other relevant conditions and loads: ice, earthquake, vegetation

1.4 Feasibility studies for generated
-Detect suitable structure configurations (geometry)
-Review the possible failure mechanisms
-Select a suitable armor alternative and size of armor units
-Make a preliminary feasibility analysis of alternatives
* develop cost estimate for each alternative
* evaluate construction requirements and limitations of alternatives
-Select the final solution

1.5 Final design
-Consider the use of models (improving boundary conditions)
-Consider the probabilistic approach
-Make final estimation and evaluation of the structure geometry
-Design the final dimensions of the structure incl. prediction of scour and design toe protection and transitions
-Check for possible failure mechanisms of the final design incl. risk
-Go through the overall project and checklist for final control
-Prepare specifications for materials/equipment/cost/quality control

2. Design considerations (an example of modern design approach)

When using the content of the PIANC-report (Flexible Revetments, 1992) the following design considerations can be used during the design process:

1° Steeper or milder slope gradient
- Steeper slope makes the protective length (revetment) shorter; as a first approximation, the slope length (L) is related to the height of slope to be protected (h) by $L = h/\sin \alpha$.
- For breaking waves the run-up (Ru) on the steeper slope will increase proportionally to tan α, namely: Ru::tan α; this yields a higher crest position and ev., a larger volume of the dike.
- The run-down on the steeper slopes also increases, possibly leading to higher overpressures and thus, thicker protective elements.
- For steeper slopes the necessary thickness of protective elements increases additionally inverse with cos α, due to a reduction of the effective (vertical) weigth component of the elements.
- For steeper slopes the friction between the protective elements increases with sin α, however, it is difficult to quantify the concequences of this effect exactly.
- For steeper slopes the internal gradients increase, leading to more severe requirements concerning the sublayers.
- A steeper slope imposes more severe requirements for the support by a toe-protection.
- The damage progress after an initial damage is more rapid for the steep slopes, thus providing more danger for scouring.
- Steep slopes are more easily damaged by ice.

Especially when using slopes steeper than 1 on 3, the above considerations should be taken into account for a proper design.

2° Berm or no berm
- Application of a berm reduces the run-up, making possible a lower crest elevation, but it may lead to a larger volume of a dike; cost optimization is necessary.
- A berm can serve as a maintenance road.
- A berm creates a discontinuity in a protection (weak point).
- A berm reduces the phreatic level in a dike with a positive effect in case of low permeable or impermeable revetments.
- A berm reduces ice ride-up.

3° High or small permeability of a toplayer.
- High permeability reduces the uplift pressure and leads to a thinner units.
- When the high permeability is created by large openings washing out of the sublayers can take place; to avoid this the following measures can be taken:
  a. coarser filter; however thus leads to increase of the hydraulic gradients across the toplayer and thus to the thicker units,
  b. geotextile underneath the blocks; if not sufficiently open this may increase the uplift pressure,
  c. a good solution can be the use of bounded filters (sand-bitumen, sand-cement etc.).
  To reduce these disadvantages the permeability should be distributed over the units instead of being concentrated (i.e. in one big hole).
- High permeability of a toplayer may increase the hydraulic gradients at the sublayer-subsoil interface; a proper design of a filter possibly in combination with a geotextile is needed.
- High permeability of a toplayer reduces somewhat the run-up.
- In the case of a very high permeability created by large holes the drag forces along the slope may increase considerably, leading to large forces on the units and thus larger dimensions.

4° Rough or smooth surface
- A rough surface (can also be obtained by using blocks of various height) reduces the run-up and thus it reduces the crest elevation and eventually the volume of a dike. This effect is evident mainly when the whole run-up zone is equipped with roughness elements. When the upper slope is protected by a grass-mat the application of the roughness elements on the lower part of a slope will have a limited effect.
- The high roughness elements introduce high drag-forces which should be incorporated in the stability calculations.
- Rough surface is unfavourable under ice conditions.

5° High or low permeability of sublayers (filter)
- Decreasing of sublayer-permeability reduce the up-lift forces on the toplayer leading to reduction of the thickness of the protective units.
- For non-cohesive (granular) materials a decrease of the permeability can be obtained by:
  . finer granular material (however, washing out through the toplayer should be avoided and the geotechnical (in-)stability should be checked),
  . wide-graded material (the internal stability should be examined)

- Applying clay as a cohesive sublayer need formulation of proper specifications on clay properties to avoid erosion, piping or shringkage.
- Lower permeability of sublayer/filter reduces the hydraulic gradients at the interface with a subsoil en abling a reduction of the thickness of the sublayer/filter.

6° Shape of sublayer/filter-material
- Rounded material is often cheaper than broken material; however, the lower angle of repose may lead to geotechnical instability, more settlement, and forces on the toe-structure.

7° Thick or thin sublayer/filter
- Reduction of the thickness of sublayer/filter leads to reduction of the up-lift forces but simultanieously it leads to increase of the hydraulic gradients along the interface with the subsoil.

N.B. As a compensation for this effect a less permeable filter, or a geotextile can be applied at the interface with subsoil.

8° Shape of blocks

- Rectangular blocks	- Colums of irregular shape
. good alignment/joining	. mostly nicer appearance
. low permeability	. higher permeability
. easy mechanical placing	. less easy mechanical placing
. problems in bends	. easier with bends
. difficult to repair	. easier repair
. washing in/grouting quite difficult	. washing in/grouting possible
. often cheaper	. often more expensive
. more rapid progress of damage	. slower progress of damage

N.B. In the case of blocks, the self-healing tendency as for riprap is absent; therefore the stability of blocks should be guaran teed under all design conditions.

9° Concrete (or other artificial material) or natural stone
- Natural stone, if available in respect to the required quality and quantity can often be a favourite solution.
- Concrete blocks (or asphaltic revetments) can often be a good alternative (especially when the natural stone is not locally available) because of:
  . often lower cost
  . good/constant quality
  . uniform size
  . mechanical execution
  . more choice regarding composition, size etc.

N.B. The economical optimization including the availability of materials,equipment and skills is mostly decisive for the choice.

10° Effect of aging and/or wearing/fatigue

During the life-time of revetment structures their original specifications can change due to the climatological effects (wind, rain, frost, abrasion, sedimentation due to waves, marine growth etc.). As far as possible the course of time should be

taken into account in the design process. However, it is not easy to quantify these effects. Some qualitative description is given below:

- Aging of the toplayer
  - Due to the wave attack at various water levels the permeability and the interlocking may change with time. For small interspaces between the blocks the permeability can decrease due to siltation of sediment while the friction between the blocks may increase.
  - Vegetation in the interspaces may also increase the friction/interlocking; however, it is possible that in the case of a heavy wave attack, the silted and/or vegetated interspaces will be cleaned-up earlier, thus providing no additional strenght at the moment of design loading on the protective units.
- Aging of the sublayers
  - In the case of alternative materials used as sublayers (minestone, slags, silex etc.) special attention should be paid to the changes of the physical properties of these materials under influence of air, wave shocks, variing humidity, frost etc.
  - In the case of geotextiles special attention should be paid to the possibility of clogging and/or blocking (leading to drastic change of permeabilities and increase of uplift pressures).
  - The siltation of the sublayers/filter has in general a positive effect; due to the decrease of permeability the up-lift forces decrease.

11° Residual strength of revetments

Revetments should be designed in such a way that the chance of failure is acceptably low. The quantification of a risk is related to the type of revetment, especially regarding the progress of damage, for example:

- the grouted (washed-in/blinded) polygonal system (i.e. basalt, basalton) is less sensitive to progressive damage than a system with rectangular blocks;
- a very rough surface is more sensitive to damage than a smooth surface;
- application of a strong geotextile retards the extension of damage to the subsoil;
- cohesive-(clay) or bounded-sublayers are primary measures to increase the secoundary strength of revetment-structures.

12° Cost optimization

- The total costs of a revetment are related to:
  - capital costs (execution)
  - yearly maintenance
  - large/periodic maintenance
  - repair of damage
  - demolition (after a life-time)

A total capitalization of the cost gives mostly the optimal result.

- In general, the revetments with a lower capital costs will be damaged more frequently damaged and will need more maintenance. Local subsidy-regulations may influence the choice. However, in case of sea-defences, especially along low shores, higher capital costs (stronger protection) should be preferred. In the case of

land reclamation or bank protection the results of the capitalization of the costs can be applied directly.

3. Overall (project-)checklist

For practical design work, besides the environmental boundary conditions (water levels, waves, currents) some additional conditions have to be considered. These conditions are mainly of political, economical or practical nature.

Known conditions relevant to the particular job should be listed at the beginning of the design procedure. This list should be supplemented as the work progresses. A number of design examples can than be chosen for further evaluation. The final checklist should then be used for the verification of the final design.

In the following a number of relevant points for the checklist have been summarired. When selecting the design parameters the following main points should always be considered:
- The quality of the boundary conditions, e.g. wave statistics.
- The quality of the design approach, e.g.is a model study required.

- The development of failure. Some types of cover layer develop nearly instant failure when design conditions are exceeded. Other types fails gradually. For a particular type of coverlayer which fail instantly the design parameters should be on the safe side.
- Consequences of failure:loss of life, damage to property, economy.
- The possibility and probability of regular inspection/maintenance.

Usually the design of a revetment is also influenced by political considerations for instance:
- The possibility of employing local labour and equipment. This may be a wish of the client, or economically attractive for the contractor.
- The possibility of using labour intensive methods in construction.
- The possibility of using domestic materials and equipment. This may be a wish of the client but may also give better availability and service.
- Special time consuming import routines or decision making.

When selecting structure type, building method and tolerances the following points should be considered:
- Difficult working conditions for instance below waterlevel.
- The skill and experience of the labour and the contractors.
- The possibility of providing special materials, machines and labour with special skills.
- The tender method (invited or public).
- Acces to the construction site during the building period and after completion of the work.
- Limitations to construction period for instance set by the client or by the weather conditions.
- Weather risk during the construction period.
- Possibility of measures against weather risk.
- Quality of infrastructure. For instance the strength of roads and

depth of ports necessary for the transportation of materials and machines.
- Easy to maintain including sustained availability of repair materials, spare parts etc.
- Possibility of maintenance from the beach (sensitive to weather conditions) or from the crest.
- The possibility of instant repairs of damage occurred or only in certain periods of the year (freezing, thawing, rainy season).

The revetment will influence the environment in general and besides it will cause certain morphological changes. Therefore the following points should be considered:
- Use of the beach during the construction period (recreational use, fishing).
- Use of the beach and the revetment after completion of the work (recreational use, fishing, shore protection works).
- Regards to the surrounding nature (colour, surface structure, slope height, possibility of planting).
- Positioning of the revetment in the beach profile and design of the edges of the structure in relation to the long term trend of the coastline.
- The clients plans and possibilities to maintain beach level in relation to level and design of the foot.

The design check-points should be carefully examined in cooperation with the client and/or future manager of the structure.
The cost of construction and maintaining, and often the environmental requirements, are generally a controlling factor in determining the type of the structure to be used.

Review international design documents related to riprap

The review on design methods and approaches related to riprap is mainly based on (but not limited to) the following technical documents:

1. US Shore Protection Manual (US Army Corps of Engineers)
2. US Design of Small Dams (Dpt.of the Interior, Bureau of Reclamation)
3. US Hydraulic Design of Flood Control Channels; Engineer Manual
4. PIANC Guidelines on Risk Consideration when Determining Bank Protection Requirements
5. PIANC Guidelines for the Design and Construction of Flexible Revetments incorporating Geotextiles for Inland Waterways
6. PIANC Guidelines on Flexible Revetments in Marine Environment
7. PIANC Guidelines on Analysis of Rubble Mound Breakwaters
8. CUR/CIRIA Manual on use of Rock in Coastal and Shoreline Engineering
9. CUR/RWS Manual on use of Rock in Hydraulic Engineering
10. Advances in Rockfill Structures, Proceedings NATO Workshop
11. Technical Standards for Port and Harbour Facilities in Japan.

The overview of content of these documents and the comment on application related to revetments/riprap is given below.

ad 1. US Shore Protection Manual (ed. 1973, 1975, 1977, 1984)

The Shore Protection Manual (SPM), produced by the Coastal Engineering Research Center (CERC) of the U.S. Army Engineer Waterways Experimental

Station (WES), is so famous that it does not need a special recommendation; it can be treated as a kind of a "bible" in coastal engineering.
The Manual is restricted mainly to the coastal problems. However, the design methodology and structural design of some structures (ie. revetments) can be applied elsewhere (Ch.7). The aspect of coastal boundary conditions (waves, water levels, littoral processes) is treated very extensively allowing to determine the design boundary conditions for the most practical cases (at least for preliminary design).
The structural design (Ch.7) is mainly directed to the design of seawalls and breakwaters against wave forces. All design aspects are treated in details. However, the design of protective units is based only on the Hudson stability formula which, as it is commonly known, has a number of practical limitations (Van der Meer in 'Coastal Protection', 1990, Pilarczyk, ed.).
The design against velocity forces, ie. stability of channel revetments, is treated very briefly with reference only to the stability formula based on the Isbash data. In respect to the newly developed dimensioning criteria becomes SPM a little bit obsolete. However, it should be mentioned that the complete updating of the SPM is planned by the CERC for the coming years.

ad 2. US Design of Small Dams (Dpt.of the Interior, Bureau of Reclamation)

The manual on Design of Small Dams, produced by the Bureau of Reclamation of the US Department of the Interior (the last revised reprint in 1977), can also be treated as a "bible", but this time , in dam engineering. Although the dimensioning techniques are not updated acc. to recent developments (i.e. see ICOLD publications), this manual still remains of a great value as an overall technical design document, especially in respect to the project planning, design requirements, boundary conditions, materials (incl. extensive treatment of rock) and construction techniques.
Main Chapters:

I. Project Planning (purpose of development and project studies)
II. Ecological and Environmental Considerations
III. Flood Studies
IV. Selection of Type Dam (classification and factors for selection)
V. Foundations and Construction Materials (soil/rock clas. and testing)
VI. Earthfill dams (design principles, foundation, embankments, examples)
VII. Rockfill Dams (types and requirements, embankment design, membrane)
VIII Concrete Gravity Dams
IX. Spillways (incl. hydraulics and structural design)
X. Outlet Works (incl. hydraulic and structural design)
XI. Diversion during Construction
XII. Maintenance and Operation

(additionally, a number of appendices for specific items are included).

ad 3. US Hydraulic Design of Flood Control Channels; Engineer Manual (1991)

Purpose. This Manual presents procedures for the design analysis and criteria of design for improved channels that carry rapid and/or tranquil flows.
Applicability. This Manual applies to major organizations and laboratories having responsibility for the design of civil works projects.
General. Procedures recommended herein are considered appropriate for design of features which are usable under most field conditions encountered in Corps of Engineers projects. Basic theory is presented as required to clarify presentation and where the state of the art, as found in standard textbooks, is limited. In the design guidance, where possible, both

laboratory and prototype experimental test results have been correlated with current theory.
Contents:
- Introduction: channel classification, preliminary investigation/selection
- Open channel hydraulic theory incl. design aspects and various situations
- Riprap protection (10 pages): riprap characteristics, channel characteristics, design guidance for stone size, revetment toe scour estimation and protection, ice/debris/vegetation, quality control
- Special features and considerations (sediment control, channel junctions)

Appendix F: Standarization of Riprap gradations.
Additionally, a number of design charts are included.
Comment: despite of the announcement that this report represents the state of the art, only US references are included. Even the PIANC reports (1987) where US representatives were involved are not mentioned. The stone stability formula is based on the extensive research by Maynord (1988). This formula is very similar to the formulae included in (PIANC,1987,1992). It would be useful (for the users) to make a comparison between these formulae and to draw final conclusions on their applications.

ad 4. PIANC Guidelines on Risk Consideration when Determining Bank Protection Requirements (1987)

The PIANC Working Group no. 3 (PTC I) was requested to elaborate a statement concerning the possibilities of introducing probabilistics into design of bank protections and, to indicate whether the use of probabilistic methods could lead to appreciable savings in bank protection design and maintenance.
Current practice is usually to consider the protection of the banks only from the technical point of view: to define the size of structure and to design a reliable/durable protection (incl. a certain safety margin). However, from the economic point of view, the designer often has to design the "cheapest" protection, even though other predetermined criteria should be observed such as the maximum safety, or minimum maintenance costs. Obviously the technical and economic considerations must be inter-related, and the risk aspects should be included. This integration can be obtained by applying a probabilistic approach.
In the report the all steps of project realization are analysed in the context of the probabilistic approach incl. the necessary input parameters and interpretation of output. The following items are discussed:
- The project realization philosophy incl. the modelling of interactions.
- The methods of reliability analysis incl. limit states and fault trees,
- The probabilistic description of load and strength of the structure,
- The cost, decision-making and project evaluation.

Risk is considered to be the expected value of a cost function with respect to the probabilistic distribution of possible events. This expected value can be considered as a weighted average of the consequences of each situation as a failure mode by taking into account the probability of occurrence of each. The acceptable risk level is related to the total initial cost of the structure and the maintenance to be carried out in the future. Construction and maintenance are based on a certain criteria one of which is cost. Using economic considerations, all costs can be expressed in terms of money. An optimum can be reached by minimizing the total costs of all the elements involved.
An illustration of probabilistic calculations is presented for a hypothetical case of a navigation canal acc. to European standards.

This report can be recommended to the all designers of protective structures as an excellent introduction to the modern design techniques in civil engineering.

ad 5. PIANC Guidelines for the Design and Construction of Flexible Revetments incorporating Geotextiles for Inland Waterways

Inland waterway embankments in general consist of easily erodible material requiring protection against water motion and other forces.
The rapid growth of shipping on inland waterways after 1945 has stimulated, especially in the Netherlands, small- and large scale research programmes together with the development of new materials, design methods and execution techniques. Along with these technical developments there has been an increasing general awareness of the social, environmental and economic aspects of civil engineering projects, so much so that it is often necessary to consider these factors at the initial design stage.

The PIANC report of the Working Group no.4 (PTC I) discusses in a systematic and practical way the all design steps including the actual design methods and practical applications. Special attention is paid to the items:
- systematic design methodology,
- materials: geotextiles (properties and testing), riprap, concrete blocks, fabric and other containers, bituminous systems, and other systems,
- design techniques:
  * boundary conditions (hydraulic, geotechnical and others),
  * determination of hydraulic load (o.a. ship induced load),
  * revetment and subsoil interaction (integrated approach),
  * dimensioning of the revetment (coverlayer/sublayers) incl. transitions,
  * verfication of design,
- practical considerations: specifications, construction techniques, maintenance and quality assurance.

This report can be treated as a good example of the practical design guide.

ad 6. PIANC Guidelines on Flexible Revetments in Marine Environment (1992)

The PIANC Working Group no. 21 (PTC II) has produced an extensive guideline report aimed at assisting Engineers in the design, construction and maintenance of flexible revetment systems in the marine environment.

The report, as an extension of the Report of PTC I Working Group no.4, records the current state of the art based on a wide range of international sources, and a better understanding of the function and performance of this type of engineering structures. With it the Design Engineer will have a better understanding of the complex forces acting on and within the revetment structure. He will know where the current limits of qualitative analysis lie and he will have some guidance on how best to deal with situations which at the moment are beyond normal design calculations. For the Construction Engineer and the Maintenance Engineer the report should give a better understanding of the way in which the revetment structure will perform its function in an active marine environment, and from the practical advice given in the Report they should be able to avoid many of the pitfalls and problems that have occurred in the past.
Contents (200 pages):
1°. Introduction

2°. Systems and Materials: Introduction, Flexible revetment systems, Specifications of materials, Regional considerations, Environmental impact of systems and materials
3°. Design philosophy: Functional requirements, Structural and design concepts, Failure modes and response models, Design approach
4°. Design conditions: Coastal morphology, Hydraulic boundary conditions, Geotechnical boundary conditions, Other boundary conditions
5°. Design Procedures: Design methods and modelling, Geometrical design, Hydraulic and ice loading, Sublayers and filters, Cover layers, Composite slopes, transitions, splash area and toe protection, Geotechnical instability, Examples of probabilistic approach
6°. Other design considerations: Practical considerations, Economic considerations, Verification of design
- Appendices: I Case study; II Inventory of experience; III Recommendations

ad 7. PIANC Guidelines on Analysis of Rubble Mound Breakwaters (1992)

After a considerable number of large breakwaters had failed or suffered severe damage, a Working Group established by PIANC's Permanent Technical Committee II (PTC II) produced a report published as a supplement to Bulletin no. 48 (1985) on the stability of rubble mound breakwaters. This report summarised important details of a large number of rubble mound breakwaters and highlighted areas of risk and uncertainty in the analysis, design and construction of such structures. However, it concluded, inter alia, that "it is not possible at the present time to determine risk with a satisfactory degree of accuracy". Therefore, the PIANC Working Group no. 12 of PTC II was set up to consider the analysis of rubble mound breakwaters with a view to achieving a better understanding of safety aspects.
This working group has developed the method of practical application of risk analysis in the design of rubble mound breakwaters by using partial coefficients. Six subgroups, A-F, were established to carry out different aspects of the study. The reports of these subgroups are available in full at the PIANC General Secretariat. The Main Report summarises the subgroup reports and presents the overall view of the results of the Working Group.

A procedure is outlined for using partial coefficients to prepare and optimise preliminary designs. The value of the new system has been demonstrated by some examples based on collected data. The proposals included in this report should not be regarded as a recommended code for design. They may, however, be useful as guidelines for the development of a new/better way of improving safety of designs by using a more rational method of evaluating probabilities of failure during the life-time of a breakwater.

The publications are on sale exclusively at the PIANC General Secretariat, WTC-Tour 3- 26th floor, Boulevard S. Bolivar 30- B- 1210 Brussels, Belgium.

ad 8. CUR/CIRIA Manual on use of Rock in Coastal and Shoreline Engineering

Introduction and objective of the Manual:
The Netherlands and the UK have taken the initiative to produce the first European guidelines on the use of rock in Coastal and Shoreline Engineering (CUR Report 154, CIRIA Special Publication 83, 1991, 600 pages).
The design guidelines are contained in a Manual (1991) resulting from a joint project of CIRIA (*) and CUR (**), on behalf of the U.K. and the Netherlands respectively.

The manual is intended for applications where protection against wind generated waves is one of the dominant design considerations. The manual is written for appraising civil engineer with some coastal experience.

*) Construction Industry Research and Information Association

**) Centre for Civil Engineering Research, Codes and Specifications

Contents of the Manual:

The manual sets out an integrated approach to the planning and design process by considering a range of related parameters (e.g. availability and durability of materials, environmental implications, methods of construction, future maintenance, economic factors) alongside the engineering requirements.

Main categories of rock structures are treated as breakwaters, dams, seawalls and offshore bottom protection.

Chapters

- Introduction
- Planning and design
- Materials
- Boundary conditions and data collection
- Design tools
- Structures
- Maintenance

Appendices

* Model specifications and material standards
* Model method of measurement
* Instruments for hydraulic and geotechnical data collection
* Structure monitoring techniques

Materials:

A system of standard grading specifications is given in the manual together with a new model for assessing rock degradation. This is an important step to enable quarry producers, designers and contractors to make optimal use of rock materials in armour and filter layers. The Manual recommends to designers and producers what they should ask for and what they may economically produce or stockpile.

Environmental assessment:

The designer is faced with an increasing demand to indicate and account for the environmental impact of his project. Guidelines are given to the designer for inclusion of relevant environmental assessments in design process.

State of the art in design of rock structures:

Recent developments in design methods arising from the project are incorporated as well as traditional methods. These new tools help the designer to produce a more economic structure. Emphasis is placed on the life cycle costing when devising the most appropriate solutions.

Static stability and dynamic profile development of rock are described, based upon research at Delft Hydraulics Laboratory.

Improvements of the Manual, compared to traditional design methods, concern formulae for influences on rock stability of wave period, rock grading, shape and porosity.

Construction:

Boundary conditions set by commonly used equipment are given (draught, maximum wave during operation). Practical aspects of transport and placement of rock are treated in the context of progress of construction and project optimisation.

Maintenance and repair:

Those responsible for the management of marine structures have an increasing need for information on the cost involved with exploitation, maintainance, repair and possible future rehabilitation of their structures. The Manual provides the designer with a range of tools to assess the inevitable damage to the rock structure and the consequent costs.

Quality Assurance:
A list is provided of elements that can be subject to quality assurance systems. Leading objectives are control of construction schedule and cost and to assure proper functioning of the structure according to the requirements for the design.

ad 9. CUR/RWS Manual on use of Rock in Hydraulic Engineering

Objective of the Manual:
The Manual is produced by CUR (*) in the Netherlands to provide the designer with the necessary information and design methods for Rock-based structures in Marine, Coastal, River and Dam Engineering.
This 2nd Manual extends the 1st European Manual on "Use of Rock in Coastal and Shoreline Engineering" into the fields of river and dam engineering.
Users of the Manual:
The manuals is written for civil engineers, involved in:
coastal and river management and those working at the design and construction of hydraulic structures in these fields in particular when using rock.
Contents of the Manual:
The manual presents an integrated design approach covering materials, quality assurance, environmental assessment, methods of construction and implications for maintenance and economy.
Categories of rock structures discussed are breakwaters, seawalls, offshore bottom and scour protection, reservoir and estuary dams, river dams and bank protections, barriers, sills and weirs.
The latest developments in the field of design, construction and maintenance of rockfill structures are included.
Publication of the 2nd Manual: end of 1993

(*) Centre for Civil Engineering Research, Codes and Specifications,
address: CUR, PO Box 420, 2800 AK Gouda, The Netherlands,
Phone/Fax: -31-(0)1820-39600/30046

ad 10. Advances in Rockfill Structures, Proceedings NATO Workshop, (1990)

The Proceedings of the NATO Workshop on Advances in Rockfill Structures (650 pages) presents the individual contributions of the outstanding experts in the whole field of rock applications. It is a very valueable supplement to the already existing literature on this subject.
Contents:
1° Rockfill structures: the present and the future
2° Physical characterization and assessment of rock durability through index properties (types, properties, laboratory characterization)
3° Rockfill modelling (in place, triaxial testing, oedometer test)
4° Laboratory shear strength tests and the stability of rockfill slopes
5° Laboratory compression tests and the deformation of rockfill structures
6° Collapse: its importance, fundamentals and modelling
7° Test fills and in situ tests(plate loading,density,permeability,tension)
8° Laboratory testing and quality control of rockfill - German practice
9° Creep of rockfill (rate method appl. to settlement, crest settlement)
10°Filters and drains (filter criteria, recent investigations, drains)
11°Stress-strain laws and parameter values incl. critical state model
12°Finite element methods for fills and embankment dams
13°Concrete face rockfill dams (design practice, construction, monitoring)
14°Static behaviour of earth-rockfill dams incl. modelling and safety eval.
15°Dynamic behaviour of rockfill dam (earthquakes, response, liquefaction)

16°Monitoring and safety evaluation of rockfill dams incl. data processing
17°Principles of rockfill hydraulics (characterization, friction losses, stability of rockfill subject to flow, seepage flow)
18°Through and overflow rockfill dams incl. mesh-protected rockfills
19°Specifications and control of natural rockfills inc. control of supplies
20°Asphaltic concrete face dams (revetments, deformability, performance).

ad 11. Technical Standards for Port and Harbour Facilities in Japan (1980)

The original "Technical Standards for Port and Harbour Facilities with Commentary" (published in 1979 in Japanese) compiled all the advanced Japanese port and harbour engineering techniques into one book.
The present publication contains the main parts of the above document excluding the official procedures, for the purpose of introducing the Japanese system of port and harbour engineering to overseas countries.
Contents (317 pages):
Part I Design conditions
1° General 2° Ships 3° Wind and wind pressure
4° Waves 5° Wave forces 6° Tide
7° Current and c. forces 8° Estuary hydraulics 9° Littoral drift
10°Soil characteristics 11°Earthquake and seismic force
12°Earth pressure and water pressure 13°Surcharge (deadweight and load)
14°Coefficient of friction
Part II Materials
1° General 2° Steel 3° Concrete
4° Bituminous materials 5° Stones 6° Timber
Part III Precast reinforced concrete members
1° Box caissons 2° L-shaped blocks 3° Cellular blocks
PartIV Foundations
1° General 2° Bearing capacity of shallow foundations
3° Bearing capacity of deep foundations 4° Bearing capacity of pile found.
5° Settlement of found. 6° Stability of slopes 7° Soil stabilization
Part V Waterways and basins
1° General 2° waterways 3°Basins
4° Basin for small crafts
Part VI Protective facilities for harbour
1° General 2° Breakwaters 3° Special type breakwat.
4° Jetties and groins 5° Training jetties 6° Locks
7° Other protective facilities for harbour
Part VII Mooring facilities
Part VIII Other facilities
Part IX Special purpose quays
The standards are (per definition) written in a very compact form and they are limited to the headlines of design of various harbour structures. In part I 'Design Conditions' the main informations are based on the US Shore Protection Manual. For calculation of the weight of armor stones and blocks the Hudson's formula is recommended. There is no formula recommended against current attack. For the coefficient of static friction used in stability calculation against sliding the value of 0.8 for rubble against rubble, and 0.6 for concrete against rubble is recommended. The information on stones in Part II (Materials) is only limited to some general statements and the specifications on internal friction and the unit weight for various coarse materials.
N.B.
There is a number of original Japanese design manuals going much deeply into the dimensioning problems. Some of them are partly translated by CERC.

Conclusions

1. The limitation of this paper does not allow to prepare a fully (detailed) evaluation of the available Worldwide experience on application of rock and design(methodology) of various rock(fill) structures. However, the background information can be found in the reports and manuals as mentioned in the references.
2. The informations presented in the design documents can be of use in solving the typical problems of the choice of protective structure in respect to design hydraulic load, the ability of materials, and desired function of structure (i.e. Chapter on design principles and verification of design).
   It should be rememberd that rock and rockfill structures are only one option for defence works and must be considered in conjunction with, or as an alternative to other options in the scope of project optimization and fulfilling the functional and environmental requirements.
   The modern design approach (metodology) can be found in the respective PIANC guidelines and in the CUR/CIRIA Manual on use of rock.
3. The event or fault tree can be a useful tool for a proper design and for programming the necessary research. Because of the multidisciplinary character of the most problems to be solved the application of the integrated SOWAS-concept and the probabilistc approach should be further stimulated.
4. Not all failure modes are sufficiently recognized and described. The proper design of toe protection (against scouring), slope protection (against wave and current forces, and against internal forces as seepage etc.) incl. proper filter construction, and protection against overtopping can be decisive for the total stability of a defence structure. Although definitive design methods are still lacking, the already existing design rules can be of use in particular cases.
5. Industrial waste products (minestone, slags, silex, clay from consolidation of polluted dragged silt, etc.) often create a great problem regarding their storage (dumping). In the Netherlands considerable experience has been gained with the application of industrial waste products as alternative materials in hydraulic engineering (i.e. bank and bed protection, filter constructions, fill material of closure structures). When using these materials special attention should be paid to the environmental implications. The technical dimensioning criteria can be derived from the existing knowledge on natural materials (Pilarczyk, 1987).
6. There is still a need for international unification and/or standarization of design methodology/criteria. Further research on failure modes and prototype verification of developed dimensioning criteria is still needed. Careful evaluation of prototype failure-cases may provide useful information/data for verification purposes.
   In all cases, experience and sound engineering judgement play an important role in applying these design rules, or else mathematical or physical testing can provide an optimum solution.
7. Because of the shortage of national research-funds and complexity of problems, international cooperation, especially in the common fields of problems (research, design codes), and the technology transfer, especially to developing countries, should be further stimulated.

References

Anonymous (1980), Technical Standards for Port and Harbour Facilities in Japan, Port and Harbour Institute, Yokosuka, Min. of Transport.

Anonymous (1984), Flexible armoured revetments incorporating geotextiles, Proceedings of the international conference organized by The Institution of Civil Engineers, London, 29-30 March 1984, Publ. Thomas Telford Ltd.

ASCE, (1967), closure to "Sediment Transportation Mechanics: Initiation of Motion", by the Task Committee on preparation of Sedimentation Manual, J. Hydraulic Division, ASCE, 93 (HY5), september.

Bezuijen, A., et al (1987), Design criteria for placed block revetments and granular filters, 2nd COPEDEC Conference, Beijing.

Blaauw, H.G., et al (1984), Design of bank protection of inland navigation fairways, Conf. on Flexible Armoured Revetments inc. Geotextiles, London

Breusers, H and A. Raudkivi (1991), Scouring, IAHR Hydraulic Structures Design Manual, Published by A. Balkema, Rotterdam.

Burger, A., et al (1988), Design method for block revetment, 21st Intern. Conf. on Coastal Engineering, Torremolinos, Spain.

Chang Howard, H.(1988), Fluvial Processes in River Engineering, Wiley&Sons.

Chen Andrie,T. and C.B.Leidersdorf (editors),(1988), Arctic Coastal Processes and Slope Protection Design, (ASCE), New York.

Christensen, B.A. (1972), Incipient motion on cohesionless channel banks, in Sedimentation (Hsieh Wen Shen, ed.), Fort Collins, Colorado.

CUR (1987), Manual on artificial beach nourishment, report 130, Centre for Civil Engineering Research and Codes(CUR), P.O.Box 420, 2800 AK Gouda,NL

CUR/TAW, (1989), Guide to the assesment of the safety of dunes as a sea defence, Centre for Civil Engineering Research and Codes/Technical Advisory Committee on Water Defences, Report 140, Gouda, Netherlands.

CUR/TAW, (1989), Guide to concrete dike revetments, Report 119, Gouda, NL.

CUR/CIRIA (1991), Manual on use of rock in coastal engineering, Centre for Civil Engineering Research and Codes (CUR), Gouda, The Netherlands.

CUR (1992), Artificial sand fills in water, CUR-report 152

CUR (1992), Sand Closures, CUR-report 157

CUR/RWS (1993), Manual on rock in hydraulic engineering (in preparation).

Delft Hydraulics and Delft Geotechnics (1989). Technical Guidelines: End report on systematic research on block revetments for dikes, R. M 1881.

Delft Hydraulics (1988). Technical Guidelines: End report on systematic research on bank protection, Report M 1115 (in Dutch).

Flexible armoured revetments inc.geotextiles (1984), T.Telford Ltd, London.

Graaff, J. van de (1986), Probabilistic design of dunes; an example from the Netherlands, Coastal Engineering, Vol.9.

Graaff, J. van de and M.J. Koster (1990), Dune and beach erosion and nourishment, in 'Coastal Protection' (Pilarczyk, ed.), Balkema Publ.

Graauw, A.F. and K.W. Pilarczyk (1981), Model-prototype conformity of local scour in non-cohesive sediments beneath overflow-dam,XIX IAHR, New Delhi

Graf, W.H. (1984), Hydraulics of sediment transport.

Groot, M.B. de, et al (1988), The interaction between soil, water and bed or slope protection, Proc. Inter. Symp. on Modelling Soil-WaterStructure Interactions, SOWAS '88, IAHR/ISSMFE/IUTAM, Delft (Ed. P.Kolkman et al).

Hales, L.Z. and J.R. Houston (1983), Erosion control of scour during construction, Technical Report HL-80-3, Rep.4, US Army, Vicksburg.

Hewlett, H.W.M., Boorman, L.A., and Bramley, M.E. (1987), Guide to the design of reinforced grass waterways, CIRIA Report 116, London, U.K.

Highway Research Board (1970/73), Tentative Design Procedure for Riprap-lined Channels, Rep.108 (1970), Washington, and Univ. of Minnesota/St.

Anthony Falls Hydraulic Lab., Project rep.no.146/field evaluation (1973)
Hjulström, F. (1935), The morfological activity of rivers as illustrated by river Fyris, Bull.Geol.Inst. Uppsala, vol. 25 (chap.III).
Hoekstra, A. and Pilarczyk, K.W. (1992), Coastal Engineering Design Codes in The Netherlands, Coastal Engineering Practice '92, ASCE, Long Beach.
ICCE (1990), Part IV: The Dutch Coast (special session), 22nd Coastal Engineering Conference, Vol. 2, Delft.
ICOLD (1980), Dams and the environment, Bulletin no. 35 and no. 50 (1985) and no. 66 (1989).
ICOLD (1986), Geotextiles as Filters and Transitions in Fill Dams, Bull. 55
ICOLD (1991), Watertight Geomembranes for Dams, Bulletin 78.
Isbash, S.V. (1935), Construction of dams by dumping stone in running water, Moscow-Leningrad.
Isbash, S.V. and K.Y. Khaldre, (1970,1976), Hydraulics of river channel closures, Butterworths, London.
Jansen, P. Ph., L. van Benegom, J. van den Berg, M. de Vries and A. Zanen (1979), Principles of River Engineering, Pitman, London.
Knauss, J. (1979), Computation of maximum discharge at overflow rockfill dams, 13th Congr. des Grands Barrages, New Delhi, Q50, R.9.
Kobayashi, N. and B.K.Jacobs (1985), Riprap stability under wave action, J.Waterway, Port, Coastal and Ocean Engineering, ASCE, vol.111, WW3.
Kobayashi, N. and A. Wurjanto (1990), Numerical model for waves on rough permeable slopes, J. Coastal Research, SI(7),(also 23rd ICCE, Venice).
Kolkman P.A.,J.Lindenberg en K.W.Pilarczyk (editors),(1988), Modelling Soil-Water-Structure Interactions,Proc.SOWAS'88,A.A.Balkema,Rotterdam
Kraus, N.C. and O.H. Pilkey, eds. (1988), The effect of seawalls on the beach, Journal of Coastal Research, Special issue no. 4.
Maranha das Neves, E. (ed.), (1991), Advances in Rockfill Structures, NATO Workshop, Lisabon, 1990; Kluwer Academic Publishers, Dordrecht/London.
Maynord, S.T. (1988), Stable Riprap Size for Open Channel Flow, Technical Report HL-88-4, US Army Engineer Waterways Experiment Station, Vicksburg
Meer van der, J.W. and Pilarczyk, K.W. (1984), Stability of rubble mound slopes under random waves, 19th Int. Conf. on Coastal Eng., Houston (also DELFT HYDRAULICS Publ. no. 332 and 396, and Proc. ASCE, Journal of WPC and OE, Vol. 114, no. 1, 1988).
Meer, J.W. van der (1988), Rock Slopes and gravel beaches under wave attack, Doctoral Thesis, Technical Univ. Delft (Delft Hydraulics N°396).
Neill, C.R. (1967), Stability of course bed material in open channel flow, Edmonton/ also, IAHR Congress, Fort Collins.
Neill, C.R. (1973), A guide to bridge hydraulics, Univ. of Toronto Press.
Paintal, A.S. (1971), Concept of critical shear stresses in loose boundary open channels, Journal of Hydraulic Research, 9, no.1.
PIANC (1985), The Stability of Rubble Mound Breakwaters in Deeper Water, PIANC Bulletin no. 48
PIANC (1987a), Guidelines for the design and construction of flexible revetments incorporating geotextiles for inland waterways, PIANC Bull. no. 57, Secretariat: Boulevard S. Bolivar 30, B-1210 Brussels, Belgium
PIANC (1987b), Risk consideration when determining bank protection requirements, Bulletin nr. 58
PIANC (1989), Economic Methods of Channel Maintenance, Bulletin no. 67
PIANC (1990), Inspection, Maintenance and Repair of Maritime Structures Exposed to Material Degradation caused by a Salt Water Environment, Bulletin no. 71
PIANC, (1987), Guidelines for design and construction of flexible revetments incorp. geotextiles for inland waterways, Supplement to PIANC Bulletin no. 57, Brussels.

PIANC (1992), Flexible revetments in marine environment, Supplement to PIANC Bulletin no. 78-79, Brussels.
PIANC (1992), Analysis of Rubble Mound Breakwaters, Suppl. Bulletin 78/79
PIANC (1993), Vegetation for bank protection (in preparation)
Pilarczyk, K.W. (1984), Prototype tests of slope protection systems, Inter. Conf. on Flexible Armoured Revetments inc. Geotextiles, London.
Pilarczyk, K.W.,J. van Overeem and W.T. Bakker (1986), Design of beach nourishment scheme, Proc. 20th Int. Conf. on Coastal Engineering.
Pilarczyk, K.W. et al (1987), Application of some waste materials in hydraulic engineering, 2nd European Conference on Environmental Technology, Amsterdam, The Netherlands.
Pilarczyk, K.W. (1987), Sea Defences: Dutch Guidelines on Dike Protection, Rijkswaterstaat, Road and Hydraulic Engineering Division, Report WB-NO-87110, April 1987, the Netherlands (also: 2nd COPEDEC, Beijing).
Pilarczyk, K.W. (1989), Design of coastal protection structures. Short Course. Asian Institute of Technology, Bangkok.
Pilarczyk, K.W. ed. (1990), Coastal Protection, Balkema Publ., Rotterdam.
Pilarczyk, K.W., H.J. Verhey, and G.J. Akkerman (1991), Rockfill Design Criteria for Overflow Dams, 17th ICOLD Congress, Vienna.
Pilarczyk, K.W. (1992), Dutch experience on design of dikes and revetments, Coastal Practice '92 (ASCE), Long Beach, CA.
Rijkswaterstaat (1987), The Closure of Tidal Basins; closing of estuaries, tidal inlets and dike breaches, Delft University Press, Delft, NL.
Rijkswaterstaat (1990), A new coastal defence policy for the Netherlands, Rijkswaterstaat, Tidal Water Division, The Hague.
RWS/DWW (1991), Nature Engineering and Civil Engineering Works,RWS/Road and Hydraulic Engineering Division, Delft.
Simons, D.B., Y.H. Chen and L.J. Swenson (1984), Hydraulic test to develop design criteria for the use of Reno mattresses, Colorado State University, Fort Collins Colorado.
SPM (1984), Shore Protection Manual, U.S. Army Corps of Engineers.
Steetzel, H.J. (1987), a Model for beach and dune profile changes near dune revetment, Proc. Coastal Sediments '87, New Orleans.
Stephenson, D. (1979), Rockfill in Hydraulic Engineering, Elsevier, vol.27.
Technical Advisory Committee for Water Defences (TAW),
a. Guide to the assessment of the safety of dunes in a sea defence (1984), CUR report 140 (1989)
b. Probabilistic design of flood defences, (1985), CUR report 141 (1990) (both publications available at the CUR Centre, P.O.Box 420, Gouda,NL
TAW/Rijkswaterstaat (1985), The use of asphalt in hydraulic engineering, Rijkswaterstaat Communications no. 35
TAW (1991), Guidelines on design of river dikes, Technical Advisory Committee on Water Defences (TAW), Published by the Centre for Civil Engineering Research and Codes (CUR), Gouda, The Netherlands.
US Army Corps of Engineers (1991), Hydraulic Design of Flood Control Channels, Engineer Manual, EM 1110-2-1601, Washington
Veldhuijzen van Zanten, R., editor (1986), Geotextiles and Geomembranes in Civil Engineering (Handbook), A.A. Balkema Publ., Rotterdam
Vellinga, P. (1986), Beach and dune erosion during storm surges, Ph.D. Thesis Delft University of Technology (also: Delft Hydraulics Publication No. 131, Delft, The Netherlands).
Ven te Chow, (1959), Open-channel Hydraulics, McGraw-Hill Book Co.
Weide, J. van der (1988), An introduction of the SOWAS-concept, Proc. Inter. Symp. on Modelling Soil-Water-Structure Interaction, SOWAS '88, IAHR/ISSMFE/IUTAM, Delft, (Editor P. Kolkman et al).
Willis D.K.,W.F.Baird & O.T.Magoon (eds)(1988), Berm breakwaters, ASCE, NY.

APPENDIX: Software related to rock applications

BREAKWAT: PC-model for breakwaters applications developed by the Delft Hydraulics and the Rijkswaterstaat in the Netherlands. The program incorporates the design formulae by Van der Meer on static and dynamic stability of rock under wave attack. The progress of damage in function of wave conditions, storm duration and composition of structure can be calculated. Also, the profile development, stability/reshaping of berm breakwaters, and stability of toe and transitions are incorporated. The basic stability relationships were verified by the prototype tests in the large Delta-flume (waves up to 2.5m).

DIPRO: PC-model on **DI**mensioning **PRO**tections developed by the Delft Hydraulics and the Rijkswaterstaat in the Netherlands. The program is applicable for dimensioning of bank protections of navigational channels and natural rivers. The program incorporates the formulae on prediction of ship-induced water motion and the response functions for slope protection (riprap, blocks, filters, etc.) as established through the systematic research incl. prototype verfication. Some environmental friendly solution incorporating vegetation are also included. The program is being continuously updated in respect to the current developments. The separate Handbook on Environmental Friendly Solution will be published in 1994.

CLODES: PC-model on **CLO**sure **DES**ign developed by the Rijkswaterstaat (in cooperation with Delft Hydraulics) in the scope of large program of closure works in 80's in the Netherlands. The program relates to rockfill closure dams in tidal estuaries, however, it is also applicable under other conditions. The horizontal, vertical and combined closure methods incl.bed protection are treated in details. The superposition of current and wave attack is included. The design relationships are based on an extensive model research and prototype verification.

IBREAK: PC-model originally developed by Kobayashi (Univ. of Delaware) for reproduction of water movement (runup/rundown and overtopping) and structural response of riprap slopes. This model is actually being further developed/improved at the Delft Hydraulics into more practical/operational model for coastal engineering applications.

For more information on the Dutch computer programs contact:
Delft Hydraulics, P.O.Box 177, 2600 MH Delft, The Netherlands

WES/CERC: Waterways Experiment Station and Coastal Engineering Research Center have developed a system of computer programs on various hydraulic and coastal engineering applications where the rock/riprap are often implicitely included.
An example of such program is the Automated Coastal Engineering System (ACES,1992) developed by CERC. The general goal of the ACES is to provide state- of -the -art computer based tools with application to the coastal engineering problems such as, for example: wave prediction, wave transformation, runup, transmission, overtopping, and structural design (breakwaters, toe protection, rubble- mound revetments).

For more information contact:
CEWES-IM-MI-C, 3909 Halls Ferry Road, Vicksburg, MS 39180-6199, USA.

SIMPLIFIED UNIFICATION OF STABILITY FORMULAE FOR ROCK AND OTHER REVETMENTS UNDER CURRENT AND WAVE ATTACK

K.W. Pilarczyk
Rijkswaterstaat, Road and Hydraulic Engineering Div.,
P.O. Box 5044, 2600 GA Delft, The Netherlands

Abstract

A simplified "black box" approach is presented for a number of revetment systems for banks and shore protection. The design criteria, based on the physical similarity with rip-rap and block revetments, are defined for wave and current attack.

Introduction

There is a great number of formulae available on the stability of various protection systems against currents and waves. Most of them are developed on the base of limited number of parameters involved and within a restricted range of variability of these parameters, or juist as a fitting of these restricted expetimental data, and often missing any physical background. Due to all these imperfections the comparison between the formulae is also or often even impossible.
Moreover there is no link made between the current- and wave- attack criteria. This situation is very confusing for the potential users.

In the following, an attempt is made into somewhat simplified unification of the existing approach with reference to the basic physical principles including such elements as the velocity and the friction-, drag-, lift- forces, shear-stress, submerged weight, and the basic relationships between currents and waves.
A simplified "black box" approach is presented for some of these systems leading to a more consistent stability approach in practical applications.
The types of revetments which have been studied in the last years are shown in Table 1. In this figure the critical modes of failure, the corresponding determinant loads and the required strength are summarized qualitatively.
Based on the physical similarity with the placed-block revetments and rip-rap, for which the recent research has provided new stability relations, the similar relationships can be derived for other systems as grouted systems, gabions, geotextile mattresses and open stone-asphalt.
Finally, a brief discussion on the applicability of proposed criteria is presented.

Initiation of particle motion. Basic concepts.

The equilibrium of particle on the bed of a stream is disturbed if the resultant effect of the disturbing forces (drag force, lift force, viscous forces on the particle surface) becomes greater than the stabilising forces as gravity and cohesion (i.e. clayey soil). The acting forces have to be expressed in known quantities such as velocities or bottom shear stress. They will have a strongly fluctuating character sothat the initiation of motion also has a statistical aspect.

type of coverlayer	critical failure mode	determinant wave loading	strength
sand / gravel	• inition of motion • transport of material • profile formation	• velocity field in waves	• weight, friction • dynamic 'stability'
clay / grass	• erosion • deformation	• max. velocity • impact	• cohaesion • grass-roots • quality of clay
rip-rap	• inition of motion • deformation	• max. velocity • seepage	• weight, friction • permeability of sublayer / core
gabions / (sand-, stone-, cement-) mattresses incl. geotextiles	• inition of motion • deformation • rocking • abrasion / corrosion of wires • u.v.	• max. velocity • wave impact • climate • vandalism	• weight • blocking • wires • large unit • permeability incl. sublayer
placed blocks incl. block mats	• lifting • bending • deformation • sliding	• overpressure • impact	• thickness, friction, interlocking • permeability incl. sublayer / geotextile • cabling / pins
asphalt	• erosion • deformation • lifting	• max. velocity • impact • overpressure	• mechanical strength • weight

Table 1. General characteristics of revetments

Most of the older relations (the 18th century) have the form:

$$U_{bottom,crit.} = (4.5 \text{ to } 5)\sqrt{D} \quad (D \text{ in m, } U \text{ in m/s}) \qquad (1)$$

It can be rewritten in a dimensionless-form as:

$$U^2_{bank}/(2g\Delta D) = 0.62 \text{ to } 0.77 \cong 0.70 \qquad (2)$$

A well known example of a velocity-type stability criterion has been presented by Isbash (1935,1970). His empirically derived formulae for embedded and exposed stones on a sill read:

for exposed stones on a sill: $U^2/(2g\Delta D_{50}) = \varphi = 0.7$ (3)

for embedded stones on a sill: $U^2/(2g\Delta D_{50}) = \varphi = 1.4$ (4)

The Isbashs' formulae can be used directly when instead of the depth mean velocity U the near-bed velocity (say at 1 m above the bed) is known/used.

Erosion,transportation, and deposition of loosely materials were also studied by Hjulström (1935), see also ASCE (1967) and Graf (1984). He has presented very useful diagram showing the limiting zone at which incipient motion starts. Because the more correct bottom velocity is seldom available, Hjulstrom decided to use the average flow velocity as a reference. For this reason it was presumed that the average velocity is about 40 percent greater than the bottom velocity for a flow depth exceeding 1 m.
The ASCE Task Committee (1967) has elaborated the Hjulström's data toegether with other data into the form as presented in figure 1.
The diagram indicates that loose, fine sand is the easiest to erode, and that the great reasistance to erosion in the smallest particle range must depend on the cohesion and adhesion forces. This diagram can serve for quick orientation/first approximation of necessary grain sizes.

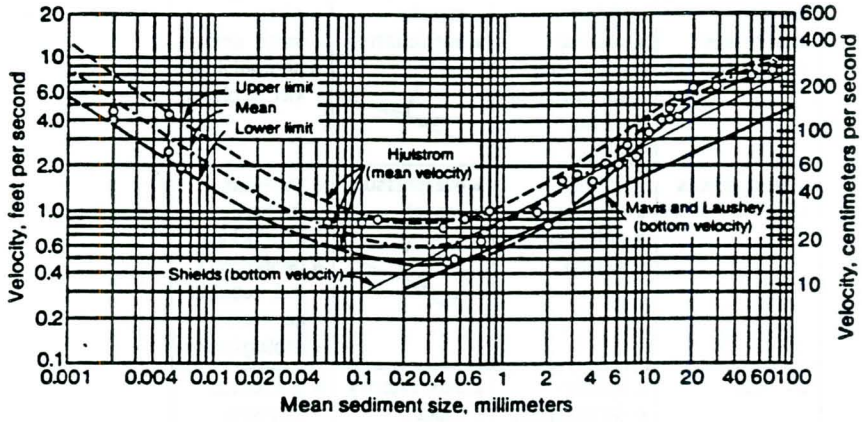

Figure 1 Critical water velocity vs. mean grain size (after ASCE,1967)

1° Basic approach on equilibrium of an (exposed-) grain on the bed under current attack.

The disturbing force F (resultant of drag force 'K' and lift force 'L') will be proportional to the bottom velocity U_b or to the bottom shear stress τ_o, and the particle surface area (D^2).

The stabilising gravity force is proportional to the submerged weight G and the bottom friction 'f' (f=tanθ, where θ= angle of repose).
The condition for equilibrium can be expressed by the relations:

(a) $K = f\,G$, or

$$\tfrac{1}{2}C_D\rho U^2\pi D^2/4 = f\pi D^3/6(\rho_s-\rho)g$$

$$U^2/(2g\,\Delta\,D) = (2/3)f/C_D = \varphi \qquad (5)$$

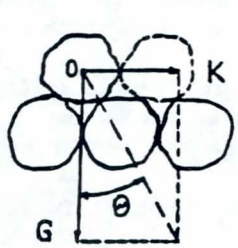

where f=tanθ, θ=angle of repose,
C_D=drag coef., U=bottom velocity,
D=nominal diameter, $\Delta=(\rho_s-\rho)/\rho$=relative density.

Assuming θ= 42°(for rock), f= tan 42°= 0.90, C_D= 0.4 to 1.0 (Fig.2), one obtains:

$$U^2/(2g\,\Delta\,D) = \varphi = 0.60 \text{ to } 1.5$$

Acc.to Isbash , φ = 0.7 for exposed stones and φ = 1.4 for embedded stones.

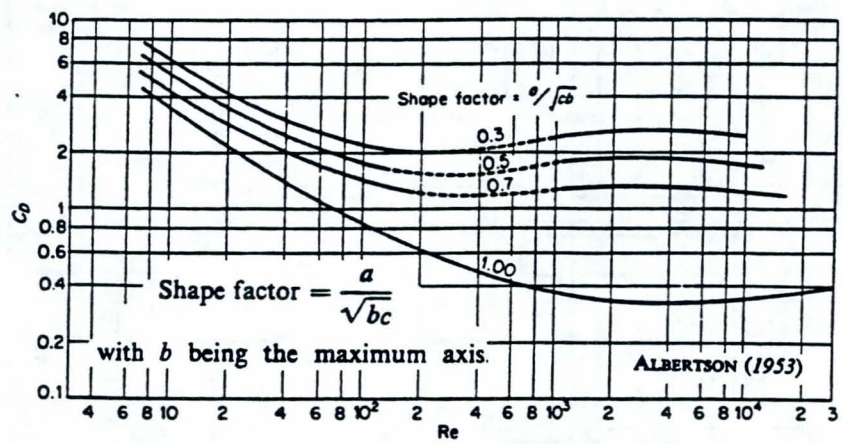

Figure 2 Drag coefficient vs. Reynolds number and shape factor (Graf,1984)

(b) The moment with respect to the turning point S gives the equation:

$$F\,b = G\,a \text{ , or}$$

$$(\tfrac{1}{2}C_F\rho U^2\pi D^2/4)\,b=(\pi D^3/6(\rho_s-\rho)g)\,a$$

$$U^2/(2g\,\Delta\,D) = (2/3)(a/b)/C_F = \varphi \qquad (6)$$

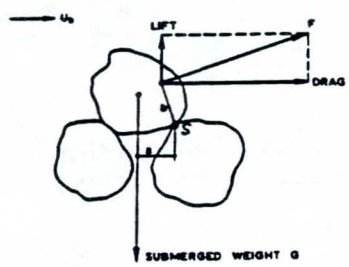

Assuming a=b and C_F= 0.4 to 1.0, then φ= 0.67 to 1.67.
C_F is a combination of coefficients for drag- and lift-forces.

The both cases ((a) and (b)) indicate that even such simple static-equilibrium approach provides reasonable results close to the reality. It also indicates the main governing parameters involved and the general (physically justyfied) structure of the possible stability criterion.

(c) By applying in the case (a) or (b) the bottom shear stress τ_o instead of velocity U, and replacing C_F ,'f'and other numerical coefficients by Ψ, one may obtain the following equation:

$$\alpha_1 \tau_o D^2 > \alpha_2 (\rho_s-\rho) g D^3 , \text{ or}$$

$$\tau_o > \Psi (\rho_s-\rho) g D \qquad (7)$$

where $\Psi = \alpha_2/\alpha_1 = F(f, C_F, R_*)$ is a combined factor depending on the flow conditions near the bed, particle shape and roughness, the position of the particle relative to other particles and the Reynolds number; $\Psi = \Psi_{cr}$ for critical conditions of inception of movement.

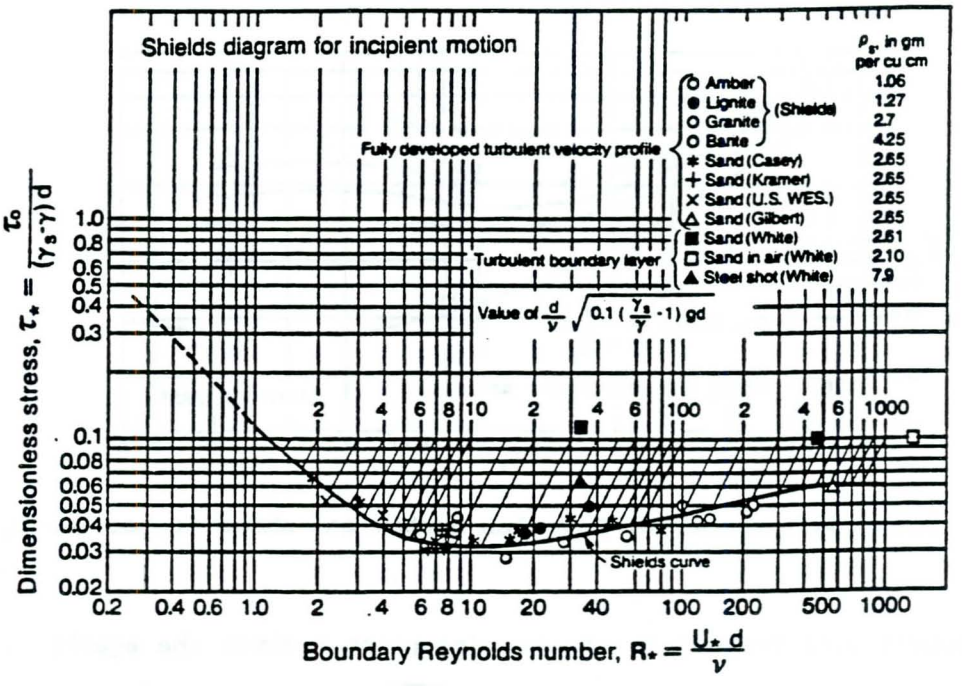

Figure 3. Shields' diagram; dimensionless critical shear stress vs. shear Reynolds number

Because U is proportional to shear velocity, $u_* = \sqrt{\tau/\rho_w}$, all other theoretical considerations based for example on drag force due to velocity will give the same result that (see also Figure 3):

$$\psi_{cr} = \frac{\tau_{cr}}{(\rho_r - \rho_w)\ g\ D} = \frac{u_{*cr}^2}{\Delta\ g\ D} = f(Re_*) \qquad (8)$$

and,

$$u_* = \sqrt{\tau/\rho_w} = \sqrt{\ g\ R\ I} = U\sqrt{g}/\ C$$

where ψ_{cr} = critical dimensionless shear stress parameter (Shields)
τ_{cr} = critical value of bed shear stress induced by the fluid at which the stones first begin to move
ρ_r = mass density of the rock material
ρ_w = mass density of sea water
D = grain size
u_* = shear velocity, $u_* = \sqrt{\tau/\rho_w}$
τ = bed shear stress
ν = kinematic fluid viscosity
Re_* = Reynolds number for based on shear velocity defined as $Re_* = u_{*cr}\ D/\nu$
R = hydraulic radius or water-depth
I = slope of energy level
U = mean velocity
C = Chezy coefficient (in $m^{1/2}/s$)

2° Derivation of design criteria

In steady flow the shear stress τ acting on the bed can be computed as:

$$\tau_c = \rho_w\ g\ \frac{U^2}{C^2} \qquad (9)$$

in which U is the depth-averaged current velocity and C is the Chezy coefficient. When the bed is hydraulically rough the Chezy coefficient depends only on water depth (R or h) and bed-roughness parameter, k_s:

$$C = 18\ \log\ (1+12h/k_s) \quad \text{(based on: Christensen,1972)} \qquad (10a)$$

or,

$$C = 18\ \log\ (12h/k_s) \quad \text{(usual form)} \qquad (10b)$$

Introduction of Ψ into the Chezy equation provides a general form of a stability criterion in terms of mean (depth-average) velocity:

$$\frac{U^2/2g}{\Delta\ D_{50}} = \frac{C^2}{2g}\psi_{cr} \qquad (11)$$

Accordingly to Shields, for sediments coarser than 4 mm ($R_* > 200$) the value of ψ_{cr} is nearly constant (see Figure 3).

After introducing the C-relation, one obtains the well-known equation (criterion) for fully developed logarithmic-velocity profile on a horizontal bed:

$$\frac{U}{\sqrt{(\Delta\ D)}} = C\sqrt{\psi_{cr}} = 18\ \log(1+12\ h/k_s)\ \sqrt{\psi_{cr}} \qquad (12)$$

This formulae is mostly presented in the following form (eq.13):

$$\frac{U}{\sqrt{\Delta\, g\, D}} = \frac{18}{\sqrt{g}} \log\left(\frac{12h}{k_s}\right) \sqrt{\Psi_{cr}}$$

The roughness-value can roughly be estimated as follows:

- for fine sediment: k_s = (1 to 2) D_{50} , i.e. $k_s = 2\ D_{50}$;

- for coarse materials: k_s = (1 to 2) D_{90} , i.e. $k_s = 2\ D_{90} \approx 4\ D_{50}$;

Assuming these roughness-values, one may obtain the practical stability criteria for incipient of motion in the following form:

- for fine sediment (eq.14a)

$$\frac{U_{cr}}{\sqrt{\Delta\, D_{50}\, g}} = 5.75 \log\left(\frac{6h}{D_{50}}\right) \sqrt{\Psi_{cr}}$$

- for coarse materials (eq.14b)

$$\frac{U_{cr}}{\sqrt{\Delta\, D_{50}\, g}} = 5.75 \log\left(\frac{3h}{D_{50}}\right) \sqrt{\Psi_{cr}}$$

Alternatively, a more general factor Λ_h can be used instead of $C^2/2g$, expressing the influence of the relative water depth (h/D_{50}). Since h/D_{50} largely determines the velocity profile, Λ_h may be regarded as a depth or velocity profile factor. The velocity criterion then reads:

$$\frac{U^2/2g}{\Delta\, D_{50}} = \Lambda_h\ \psi_{cr} \qquad (15)$$

Returning to C in terms of the roughness k_s gives:

$$\Lambda_h = (18^2/2g)\ \log^2(1+12h/k_s) = (18^2/2g)\ \log^2(12h/k_s) \qquad (16)$$

Subsequently, a relationship between k_s and grain size can be introduced. A reasonable approximation for coarse material is $k_s = 2\ D_{90} \approx 4\ D_{50}$, which after substitition into eq.(16) leads to:

$$\Lambda_h = (18^2/2g)\ \log^2(3h/D_{50})$$

In fact, these relations can be used directly as a velocity criterion by substituting a priori a value for ψ_{cr}, which then plays the role of a "damage parameter".

The transfer of Isbash (eq.4), with ψ=0.04 as a damage parameter, into Shields (eq.15) provides: $\Lambda_h = 35$.

Pilarczyk (1989) proposes for non-developed velocity profile:

$$\Lambda_h = 32\ (h/k_s)^{0.2} \cong 32\ (h/D_{50})^{0.2} \cong 32\ (h/D_n)^{0.2}$$

This may be compared to an approach using Strickler's resistance formula, which gives (for a developed profile):

$$\Lambda_h = (625/2g)\ (h/k_s)^{0.33}$$

Since it can be assumed that for say $h/D_n \leq 5$, the water flowing through the upper part of the rock layer can not be neglected anymore, an additional imaginary depth of, depending on the porosity, h_{im} = about 1 times D, might be added to h in the formulae given for Λ_h. Moreover, D_{50} can be replaced by D_{n50}.

The various forms of the depth factor for various velocity distributions are summarized below:

developed profile (Chezy): $\Lambda_h = (18^2/2g)\ \log^2(1+12(h + D_n)/k_s)$
developed profile (Strickler): $\Lambda_h = (625/2g)\ ((h + D_n)/k_s))^{0.33}$
non-developed profile(Pilarczyk): $\Lambda_h = 32\ (h/D_n + 1)^{0.2}$
non-developed profile (Isbash): $\Lambda_h = 35$

The bed roughness of rock can be assumed equal to: k_s = (2 to 3) D_n,
where D_n=equivalent diameter; $D_n=(M_{50}/\rho_s)^{1/3} = 0.84\ D_{50}$.
It should be noted that the effect of the additional imaginary depth practically vanishes for h/D > 2 but is most practical for h/D < 1.

The formulas given above do not take into account the influence of (high) **turbulence** generated by specific obstacles or constructions such as spillways with a hydraulic jump, sills, sharp bends etc.. In that case, the magnitude of acting velocity or shear stress will increase by a factor φ_t or $K_t=\varphi_t^2$ respectively, and the stone diameter has to be reduced by a factor:

$$K_t = \varphi_t^2 = ((1 + 3\ r)\ /\ 1.45)^2 \qquad (17)$$

in which r is the relative turbulence intensity; a value of r = 0.10 has been normally assumed in a uniform flow in rivers and r = 0.15 for flow over a rough bed.
Directly downstream from a hydraulic jump (stilling basin), values of r in order of 0.5 (at the end of hydraulic jump) to 0.35 (at the distance of about 5 times of waterdepth from the end of hydraulic jump). These give the values for K_t of about 3 and 2 respectively. The level of turbulence diminish to the normal level (K_t = 1) at the distance of about 10 to 15 times of the water depth.

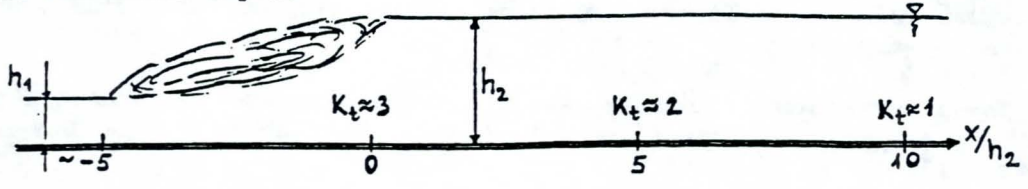

Now adding the various correction factors (turbulence factor, slope reduction factor and, eventually needed, numerical coefficient) gives the following generally applicable formula for the critical depth-mean velocity:

$$\frac{U^2/2g}{\Delta D} = \Phi^{-1} K_s K_t^{-1} \Lambda_h \psi_{cr} \qquad (18)$$

where:

K_s = slope reduction factor ($K_s \leq 1$),
Λ_h = depth or velocity profile factor,
K_t = turbulence factor ($K_t \geq 1$),
Φ_c = stability factor; $\Phi_c = 1$ for 'normal' conditions and $D = D_{50}$.

It should be noted that K_s ($K_s<1$) is a strength reduction factor whereas Φ_c and K_t >1 are the loading amplification factor. For example, when flow is passing from the smooth bed (i.e. concrete apron) into the rough bed (i.e. rock bottom protection), the acting shear stress at the transition can be twice the normal shear stress for rock, which will be developed at certain distance below the transition. The similar situation is created when multidirectional flow is present (i.e. tidal conditions); in that case the edge of bottom protection will be also attacked by flow coming from the sandy bed with necessity of a drastic adjustment of the shear stress at the edge of the rocky protection. This explains why in the final design formula the various Φ_c-values are introduced for various practical situations.

For practical purposes, the final stability criterion for riprap and other protective units under current attack has a form:

$$\Delta D_n = \Phi_c K_t 0.03 \Psi_{cr}^{-1} K_h K_s^{-1} U^2/2g \qquad (19a)$$

or,

$$U^2/(2g \Delta D_n) = (\Psi_{cr}/0.03) (\Phi_c K_t K_h)^{-1} K_s \qquad (19b)$$

where: Φ_c=stability factor (all numerical coefficients are combined to one factor), 0.03=reference value of shear-stress parameter, Ψ_{cr}=critical value of shear-stress parameter, K_t=parameter of turbulence, K_h=parameter describing velocity profile (logarithmic,exponential), K_s=parameter of slope, U=mean velocity.
The interelationship between K_h en Λ_h is given by:

$$K_h = 33/\Lambda_h \qquad (20)$$

NB. Factor '33' is compensated in eq.19 by the explicite reference value of the critical shear stress parameter equal to 0.03. It makes the practical use of the design formula more easier.

Based on these backgrounds the general design formula for current attack has been established for broad application in the wide range of various revetment-types.

N.B. The information on another design concept nl. based on tractive forces (bottom shear stress) instead of velocity can be find in Ven te Chow (1959) and Graf (1984).

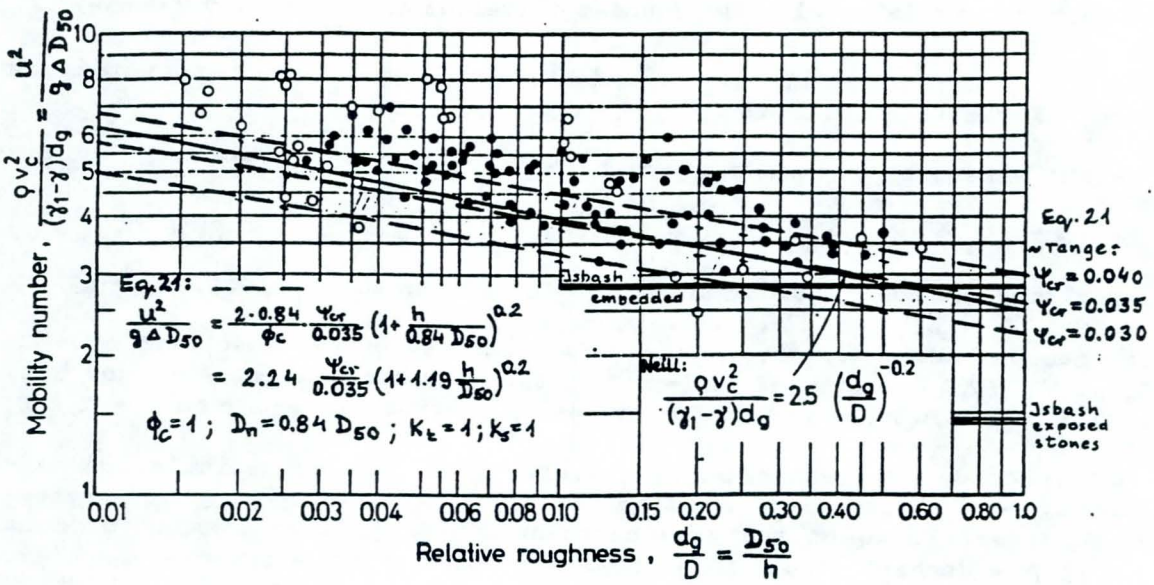

Figure 4. Comparison eq.21 with experimental data collected by Neill (1967)

Application of general design formula for current attack

General applications

An alternative for the use of threshold values for stress or velocity is the application of empirical formulae. Pilarczyk (1989,1990) presented the overview of some practical design formulae for rock and rock related units against current attack in various civil engineering applications. He has combined these formulae to one general form:

$$\Delta_m D_n = \phi_c K_t \cdot \frac{0.035}{\psi_c} \cdot K_h \cdot K_s^{-1} \cdot \frac{\bar{u}^2}{2g} \qquad (21)$$

in which:

D_n	= thickness of protection unit	[m]
Δ_m	= relative density of protection system	[-]
ϕ_c	= stability factor for current	[-]
K_t	= turbulence and/or shear stress adjustment factor	[-]
K_h	= depth (or velocity profile-) factor	[-]
K_s	= slope factor	[-]
ψ_c	= critical shear stress parameter	[-]
u	= mean velocity (depth averag	[m/s]
g	= acceleration of gravity	[m.s^{-2}]

The value of 0.035 instead of 0.03 is chosen as a reference value for a critical shear stress parameter (mostly between 0.03 and 0.04), which

also better correlates with the rounded values of the stability factor.

The same formula can be used for rock related units or systems as blocks, blockmats and gabions.

The strength parameters Δ_m and D_n can be calculated with:

- for rock: $D_n = (M_{50}/\rho_s)^{0.33}$ or $D_n \cong 0.84\ D_{50}$ and $\Delta_m = \Delta = (\rho_s - \rho)/\rho$

- for placed blocks and blockmats: $D_n = D$ = thickness of block, $\Delta_m = \Delta$

- for gabions and mattresses: $D_n = d$ (= thickness of mattress) [m] and $\Delta_m = (1-n)\ \Delta$; the size of fill-rock D_n can be calculated as for rock but with a higher ψ_c. The minimum thickness of mattress is equal to $d = 1.8\ D_n$

in which: D_n = equivalent diameter [m], D_{50} = 50% passing median stone diameter [m], d = thickness of a system [m], Δ_m = relative density of a system [-], M_{50} = 50% value of the mass distribution [kg], ρ_s = density of rock [kg.m^{-3}], ρ = density of water [kg.m^{-3}], n = porosity of stones [-], approx. n = 0,4.

The values of the critical shear stress parameter ψ_c can be assumed equal to $\psi_c = 0.035$ for rock (0.025 when absolutely stability is required, see also Paintal 1971, and 0.05 when some limited displacement of stones,i.e. in a case of temporary situation, is acceptable), $\psi_c = 0.05$ for free blocks, $\psi_c = 0.05$ to 0.070 for blockmats/mattresses, and equal to $\psi_c \leq 0.10$ for fill-rock in gabions/mattresses (acceptable motion of stones).

The various correction factors K are estimated as follows:

K_h = $2/(\log(1 + 12\ h/k_s))^2$ for a logarithmic velocity profile, or
K_h = $(1 + h/D_n)^{-0.2}$ for a not-fully developed velocity profile
K_s = $\cos\alpha\ (1-\tan^2\alpha/\tan^2\theta)^{0.5} = (1-\sin^2\alpha/\sin^2\theta)^{0.5}$
K_t = 1.0 (normal turbulence, rivers);
K_t = 1.5 (very common case: non-uniform flow with increased turbulence as below stilling basins, outer bends, r/B > 2, etc.)
K_t = 2.0 (high turbulence as below hydraulic jump, local disturbances, sharp outer bends, r/B ≤ 2)
K_t = 3.0 (jet impact, screw race velocity, hydraulic jump)

with: h = water depth [m], r = center-line radius of bend, B = watersurface width at upstream end of bend, k_s = bed roughness given approximately by: $k_s = D$ (smooth units,i.e. concrete blocks $D_n = D$ = thickness of block), and $k_s = (1 \text{ to } 3)D_n$ (rough units, i.e. rock), α = slope angle [°], and θ = angle of internal friction [°].
The following remarks can be made.

- Firstly, the factor K_t only holds for bank and shore slopes. For a bed slope in the flow direction with angle β a different value should be used (K_t): $K_t = \sin(\theta-\beta)/\sin\beta$
where θ = angle of internal friction of protecting materials. Generally, $\theta >> \beta$ and the reduction in flow direction can be neglected.

- Secondly, the value of K_t = 1.5 or 2 for (sharp) outer bends should only be applied if due to the difficulties in defining the local mean velocity, the average mean velocity in the cross-section is applied.

The following values of the stability factor ϕ_c are recommended: ϕ_c = 1.0 to 1.50 for exposed edges and/or transitions (depending also on flow direction) and ϕ_c = 0.50 to 0.75 for continuous protection; ϕ_c = 0.75 can be treated as a common reference value for rock.

The values of stability factor are strongly affected by composition of the system and execution. In general, the upper figures of ϕ_c are recommended as safe values. The lower ϕ_c-values refer to the systems with higher integrity (i.e. (grouted-) cabled blockmats, gabions/stone mattresses, grouted blocks etc.), proper choice of permeabilities of the toplayer, and/or when a certain (limited) movement is allowed. For a continuous protection with blocks laying on properly equalized bed the ϕ_c = 0.5 can be used while ϕ_c = 0.75, usually applied for rock, is also a proper ϕ_c-value for blocks on unequal bed. Stability of free placed blocks can be improved by washing in the interspaces between the blocks by a granular grout. The washing out of this material can be prevented when D (grout) > 0.3 d_i (interspace). In such case the stability can be similar to the cabled blockmat. The blocks should be placed in a chess-pattern to limit the length of interspaces. For the exposed edge with rock on fascine mattress the ϕ_c = 1.0 can be used while for the rock direct on geotextile ϕ_c = 1.50 is recommended.

Examples of exposed edges are: bed protection at scour holes(particularly in the case of two-directional current i.e. ebb and flood), edges of a toe protection, transitions between adjacent revetment systems, connections between mats or mattresses. When the edges can be adversely attacked, for example, from the direction of the scour hole (i.e. during ebb) the more conservative (higer-) ϕ_c-values are recommended. Because of practical problems with edges and transitions, very often the whole protective system is designed based on stability criteria for edges. In other cases special measures should be taken to avoid overturning the mats at edges and transitions.

Due to all these uncertainties it is difficult to give a more sharp indication on ϕ_c-values. The best engineering judgement will always be a decisive factor in each particular case. For example, because of various practical reasons the minimum thickness of protective elements is defined as 0.08 m for blockmats and prefabricated open stone asphalt mats (in situ 0.10 m), 0.10 m for free blocks, 0.15 for (basket-) stone mattresses and sand mattresses.

Additional information can be found in Flexible Armoured Revetments (1984), The Closure of Tidal Basins (1987), PIANC-reports (1987 and 1992), and in the Manuals on Rock (CUR/CIRIA, 1991 and CUR/RWS, 1993).

Criterion for closure works

Replacing U in (eq.21) by $U=\mu\sqrt{2g(H_u-h_B)}$, where H_u and h_B represent the upstream and downstream water level above the crest respectively, the criterion becomes (eq.22a):

$$\frac{H_u}{\Delta D_n} = \frac{1}{\phi_c K_t} \frac{\psi_{cr}}{0.035} \left(\frac{h_B}{D_n} + 1\right)^{0.2} + \frac{h_B}{\Delta D_n}$$

or (eq.22b):

$$\frac{H_u}{\Delta D_n} = \frac{1.1}{\phi_c K_t} \frac{\psi_{cr}}{0.035} \left(\frac{h_B}{\Delta D_n} + 0.6\right)^{0.2} + \frac{h_B}{\Delta D_n}$$

where K_h , for not fully-developed velocity profile and permeable toplayer, is defined as:

$$Kh = (h_B / D_n + 1)^{0.2}$$

Applying Φ_c=0.75 (see further in the text above), K_t=1, Ψ_{cr}=0.035 and μ = 1, the stability criterion reeds:

$$H_u/(\Delta D_n) \cong 1.5 \ (h_B/\Delta D_n + 0.6)^{0.2} + h_B/\Delta D_n \qquad \text{for } h_B/\Delta D_n > 0 \qquad (22c)$$

This equation fits reasonably the experimental data (Pilarczyk et al, 1991) in figure 5. If some limited movement of rock is acceptable, Ψ_{cr}=0.035 can be replaced by 0.04 or even 0.05. For more conservative (more safe) approach, or when the over-flow-structure must be functioning permanently, especially in the case of supercritical flow, Ψ_{cr}=0.03 and K_t=1.25 to 1.5 can be applied. For $-5<h_B/\Delta D_n<0$ the value calculated at $h_B/\Delta D_n=0$ can be of use as a first approximation.

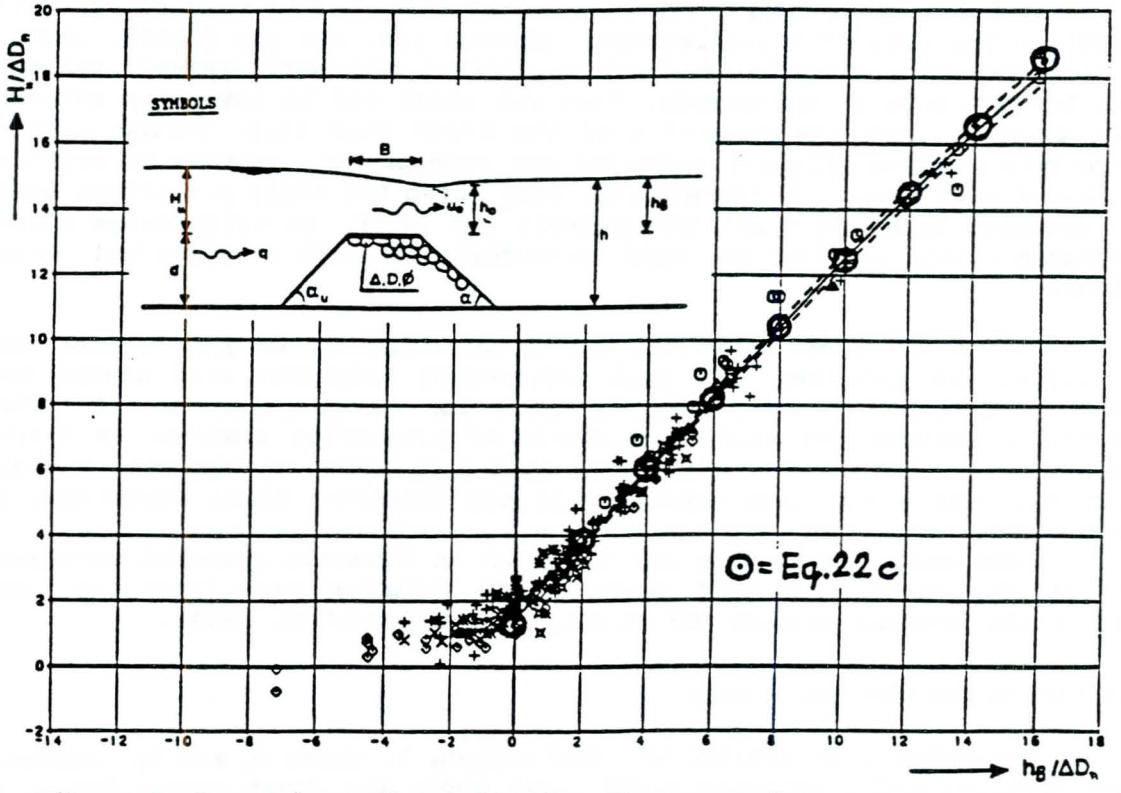

Figure 5. Comparison of results for closure works

Further (practical) simplification

In the most practical cases of hydraulic engineering the not-fully developed velocity profile will take place, and the formula (21) can be further simplified in the following way:

For $K_h=(\frac{h}{D_n})^{-0.2}$ *and* $\frac{h}{D_n}>2$,

$$\frac{\Delta D_n}{h}=\left(\sqrt{\frac{0.035\Phi_c K_t}{2\Psi_{cr}K_s}}\frac{u}{\sqrt{gh}}\right)^{2.5}=\left(\frac{1}{7.5}\sqrt{\frac{\Phi_c K_t}{\Psi_{cr}K_s}}\frac{u}{\sqrt{gh}}\right)^{2.5}$$

Or, for $\Psi_{cr}=0.035$

$$\frac{\Delta D_n}{h}=\left(\sqrt{\frac{\frac{1}{2}\Phi_c K_t}{K_s}}\frac{u}{\sqrt{gh}}\right)^{2.5}$$

For more standard applications, $K_t=1$ *and* $\phi_c=0.75$, *the formula reeds*:

$$\frac{\Delta D_n}{h}=0.6\left(\frac{u}{\sqrt{ghK_s}}\right)^{2.5}$$

Basic approach on stability of rock under wave attack

The stability of rock on a slope under wave attack is related mainly to the forces exerted by the run-up and the run-down, wave impact, and the induced lift-forces. The breaker hight (position of the wave-crest just before breaking) is strongly affected by the roughness and the permeability of revetment, and the geometry of slope (a.o. composite slopes, berms, etc.). The breaker height, H_b, is mostly expressed in terms:

$$H_b = a_\alpha H \xi^b \qquad (23)$$

where: a_α= numerical factor depending also on slope gradient, H= wave height, ξ= surf-similarity parameter; $\xi=tg\alpha(H/Lo)^{-0.5}$, T=wave period, L_o=wave length; $L_o=gT^2/2\pi$, α=slope angle, and 'b'= exponent depending of roughness and permeabilty of revetment. The equilibrium condition in respect to the lift-force,L,(L :: H_b :: U_j/2g), reads:

$$C_L \rho g H_b = (1+f)(\rho_s-\rho) g D \cos\alpha$$

or $$H_b/\Delta D = \cos\alpha / C_F$$

and $$H/\Delta D = [(1+f)/(a_\alpha C_L)](\cos\alpha/\xi^b) \qquad (24a)$$

$$H/\Delta D = \Phi_T \cos\alpha/\xi^b \qquad (24b)$$

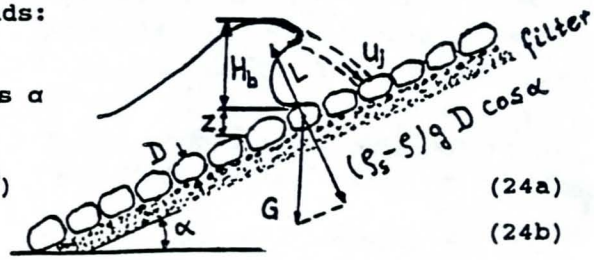

where C_L= lift-transfer function, f= friction factor between stones/blocks, U_j= velocity in a jet (wave impact), and Φ_T= cumulative stability factor for a given geometry of slope.

Eq.24 provides the general structure of stability criterion for wave attack

The experiments provide also that Φ_T is equal to about 2 for loosely coarse materials and $\Phi_T > 3$ for pitched stones and placed-block revetments on permeable sublayer, while $\Phi_T > 6$ for placed blocks on relatively smooth clay-surface of proper quality.(NB.: because of possibility of washing out of clay particles through the interspaces between the blocks, the proper geotextile on the clay-surface is recommended). On the other side, the analysis of the physical structure of the total stability factor (eq.24) allows to explains these differences. The total stability factor is equal to:

$$\Phi_T = [(1+f)/(a_u C_L)] \qquad (25)$$

For the further analyse we will assume a_u=1.
* For the first layer of riprap the friction factor f will be relatively small (assume $0<f<0.25$) and the high permeability resulting in a relatively high C_L-values (assume $0.5<C_L<1$), then $1<\Phi_T<2.5$.
* For pitched stones/placed blocks contacting at least with a one side the neighbouring block, laying on permeable sublayer, one may assume f=0.25 to 0.5 and $0.4<C_L<0.5$ providing $2.5<\Phi_T<4$.
* For placed blocks on clay and geotextile one may assume f=0.5 and low permeability of such sublayer with C_L=0.25, resulting in Φ_T=6.
This analyse should be interpreted only in qualitative sense.

On the other side, the maximum velocity on the slope due to the run-down can roughly be given by:

$$U = \varphi_r (2g H_b)^{0.5} = \varphi_r (2g a_u H \xi^b)^{0.5} \quad \text{for} \quad \xi < 3 \quad \text{(breaking waves)} \qquad (26)$$

where φ_r= correction factor for slope roughness and permeability (close to 1), $UT/\pi H$ remains nearly constant for non-breaking waves ($\xi > 3$). The expected range of a_u for steep slopes is between 0.5 and 1.0 (using $H=H_s$= significant wave height); however, the experimental data are rather scarce. The direct comparison of eqs.3 and 4 (φ = 0.7 and 1.4), after substituting D by D_n (=equivalent diameter; $D_n=(M_{50}/\rho_s)^{1/3}$ = 0.84 D), and eq. 24b (or eq.28) with $\Phi_T = \Phi_r = 2$ (assuming cosα=1) provides:

- for φ = 0.7, $U = (0.42\ 2g\ H_s \sqrt{\xi/\cos\alpha})^{0.5} = 0.91 \sqrt{(g\ H_s)}\ \xi^{0.25}$
- for φ = 1.4, $U = (0.83\ 2g\ H_s \sqrt{\xi/\cos\alpha})^{0.5} = 1.29 \sqrt{(g\ H_s)}\ \xi^{0.25}$

The coincidance of predicted and measured values seems to be not too bad, however, for real comparison more experimental (systematic) data on the breaker height and the breaking process, and the resulting water movement on slopes of various composition are needed.

Applying the slope factor (K_s) for run-down forces as equal to cosα, and replacing H by H_s (significant wave height) the final criterion becomes:

$$H_s / (\Delta D_n) = \Phi_T * \cos\alpha\ \xi^{-b} \quad \text{or,} \qquad (27)$$

$$H_s / (\Delta D_n) = \psi_u * \Phi_r * \cos\alpha\ \xi^{-b} \qquad (28)$$

where: α= slope angle and b= exponent related to type of structure; b= 0.5 for rock and b= 1.0 for smooth revetments with low permeability, Φ_r= total stability factor, Φ_r= stability parameter for rock equal to 2.25 and ψ_u= upgrading parameter (table 2) for systems other than rock (ψ_u= 1 for rock).

Criterion		Limits	
$\frac{H_s}{\Delta_m D} = \Psi_u \cdot \phi_r \frac{\cos\alpha}{\sqrt{\xi_p}} = \psi_u \, 2.25 \frac{\cos\alpha}{\sqrt{\xi_p}}$		$\phi_{(rock)} = 2.25$ $ctg\alpha \geq 2$ $\xi_p < 3$	
System	ψ_u	Description	Sublayer
Ref. Rock	1.0	Riprap (2 layers)	Granular
	1.33	Riprap (tolerable damage)	Granular
Pitched Stone	1.00	Poor quality (irregular-)stone	Granular
	1.33	Good quality (regular-)stone	Granular
	1.50	Natural basalt	Granular
Blocks/ Block-mats	1.50	Loose closed blocks; H_s < 1.5 m	Geotextile on sand Ganular
	1.50	Loose (closed-)blocks	
	1.50	Blocks connected to geotextile	Granular
	2.00	Loose closed blocks	Geotextile on clay Granular
	2.00	Cabled blocks/Open blocks (> 10%)	
	≥2.50	Grouted (cabled-)blocks/Interlocked blocks adequately designed	Granular
Grout	1.50	Surface grouting (30% of voids)	Granular
	1.50	Pattern grouting (60% of voids)	Granular
Open Stone Asphalt	2.00	Open stone asphalt; $U_p \leq 6$ m/s	Geotexile on clay Sandasphalt
	2.50	Open stone asphalt; H_s < 4 m	
Gabions	2+3.0	gabion/mattress as a unit, H_s < 1.5	Geotextile on sand or Geotextile on clay
	2+2.5	stone-fill in a basket; $d_{min} = 1.8 D_n$	
Fabric Con-tainers	1.00	P_m < 1 less permeable mattress	Sand or Clay and ev. Geotextile
	1.50	$P_m \approx 1$ (P_m=ratio permeab.top/sublayer)	
	2.00	$P_m \geq 2$ permeable mattress of special design	
Grass	-	Grass-mat on poor clay; U_p < 2 m/s	Clay (U_p= permiss. velocity)
		Grass-mat on proper clay; U_p < 3 m/s /s	

Table 2 Indicative categories for protective systems

Application of general design formula for wave attack

General

In the past only local usage and experience have determined the selection of the type and dimensions of the coastal protection. Often designs were conservative and too costly or were inadequate. The technical feasibility and dimensioning of coastal structures can be actually determined on a more founded basis and supported by a better experience than in the past. Often, however, the solution being considered should still be veryfied in a scale models and/or in prototype since no generally accepted design rules exist for all possible solutions and circumstances.
Referring to the revetments of dikes/seawalls, a summary of the key elements that must be considered in the design (dimensioning) are illustrated in Figure 6. The existing design rules for some (selected) structural elements (shape, height, cover-layer etc.) are briefly reviewed in the subsequent sections. For detail engineering 'Coastal Protection'(Pilarczyk, 1990), the Manual on Rock (CUR/CIRIA 1991) and SPM (1984), can be of use.

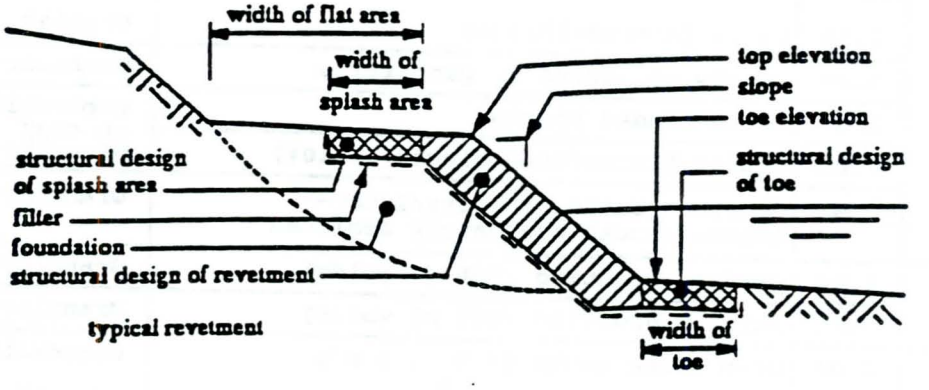

Figure 6 Design components of dike/seawall-revetment

Stability (or threshold conditions) for loose materials, from sand to rock, is investigated rather extensively, and the proper design criteria are availbale. However, the stability of randomly dumped quarried rock can often be substantially improved by taking special measures (= composite systems, i.e., grouting, pitched stone, mattresses, etc.). On the other hand there are a number of protective systems related to artificial materials such as concrete (i.e., block-mats) and asphalt. Also grassmats serve as slope protection. For most of these systems it is possible to give some rough, indicative stability criteria which allow the engineer to make a comparison with a random placed rock, and thus, to make a proper choice of protection. The following systems will be considered: riprap, placed or pitched blocks/stones, grouted (bound) stones, bituminous systems, gabions/stone mattresses, fabric containers (bags/mats), and clay/grass-mats.

Because of the great variety of the possible composition of protective systems it is not possible to present a generally valid stability formulation for these systems. Therefore, only some principles and examples will be given here. For comparison of all these systems, the stability of dumped rock will serve as a reference.

Slope protection.Stability criteria for wave attack.

The general empirical (approximate) formula derived by Pilarczyk (1990) and supported by large scale tests is (eq.28):

$$\frac{H_s}{\Delta_m D} \leq \psi_u \phi_r \frac{\cos\alpha}{\xi_p^b} \quad ; \quad (\mathrm{ctg}\alpha \geq 2)$$

or

$$\Delta_m D = \psi_u^{-1} \phi_r^{-1} \cos\alpha^{-1} H_s \xi_p^b \quad ; \quad (\text{strength}) = (\text{load})$$

with: ξ_p = breaker similarity index on a slope,

$$\xi_p = \tan\alpha \, (H_s/L_o)^{-0.5} = 1.25 \, T_p . H_s^{-0.5} . \tan\alpha$$

in which:

ψ_u = system-determined (empirical) stability upgrading factor (ψ_u = 1.0 for riprap as a reference and $\psi_u \geq 1$ for other revetment systems) [-],

ϕ_r = stability factor or stability function for incipient of motion, defined at ξ_p = 1 [-],

H_s = significant wave height [m],

T_p = peak wave period [s],

L_o = wave length [m]; $L_o = gT_p^2/2\pi$

D = specific size or thickness of protection unit [m],

α = slope angle [°],

Δ_m = relative density of a system-unit [-],

b = exponent related to the interaction process between waves and revetment type (roughness, porosity/permeability etc.), $0.5 \leq b \leq 1$. For rough and permeable revetments as riprap, b = 0.5.
For smooth and less permeable placed-block revetments it can be closed to b = 1. The value b = 2/3 can be treated as a common representative value for other systems (i.e. more open blocks and block-mats, mattresses of special design etc.).

The formula (eq.28) is applicable till ξ_p = 3 (breaking waves); for ξ_p > 3, the sizes calculated at ξ_p = 3 can still be applied.

D and Δ_m are defined for specific systems such as:

- rock ; $D = D_n = (M_{50}/\rho_s)^{1/3}$ and $\Delta_m = \Delta = (\rho_s - \rho_w)/\rho_w$
- blocks ; D = thickness of block and $\Delta_m = \Delta$
- mattresses; D = d = average thickness of mattress and $\Delta_m = (1-n)\Delta$, where n = bulk-porosity of fill material and Δ = relative density of fill material. For common quarry stone $(1-n)\,\Delta \approx 1$.

In the case of relatively impermeable core (i.e. sand/clay) and number of waves N ≈ 3000, the following ϕ_r-values for rock can be recommended:

ϕ_r = 2.0 for the rest of stones (lower limit of incipient of motion),

ϕ_r = 2.25 average value for incipient motion (motion 1 to 3 stones over the width of slope equal to D_n), and

ϕ_r = 3.0 as a first approximation for maximum tolerable damage for 2-layer system on granular filter (damage-depth less or equal to $2D_n$); ϕ_r = 3 can also be applied for incipient motion of rock placed on permeable core (rockfill core or thick granular filter).

The ϕ-value equal to 2.25 will be used as a reference value for the stability comparison with other alternative systems. The difference with stability of rock due to the improving measures will be expressed by the upgrading of the factor ψ_u.

The important difference between the loose rock and the alternative systems concerns the behaviour of the systems after the initiated movement (damage). Due to the self-healing effect of the loose rock a certain displacement of rock units can be often accepted (up to $\phi \leq 3$). In the case of alternative systems, i.e., block revetment, the initial damage (i.e. removing of one block) can easily lead to a progressive damage; there is no reserve-stability.
The comparison of stability of various systems (parameter ψ_u) and the necessary parameters for calculation purposes are contained in Table 2. Other structural requirements and design rules concerning revetments are given by Pilarczyk (1990).

Protection against overtopping

If a structure (revetment) is overtopped, even by minor splash, the stability can be affected. Overtopping can: (a) erode the area above or behind the revetment, negating the structure's purpose; (b) remove soil supporting the top of the revetment, leading to the unraveling of the structure from the top down; and (c) increase the volume of water in the soil beneath the structure, contributing to drainage problems. The effects of overtopping can be limited by choosing a higher crest-level or by armouring the bank above or behind the revetment with a splashapron. For a small amount of overtopping a grass-mat on clay can be adequate. The splash apron can be a filter blanket covered by a bedding layer and, if necessary to prevent scour by splash, riprap or pavement of concrete units or asphalt.

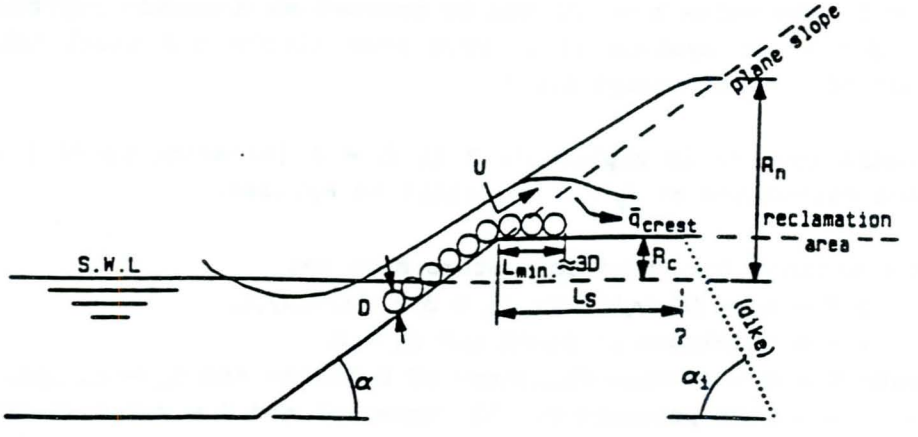

Figure 7 Definition of splash area

No definite method for designing against overtopping is known due to the lack of the proper method on estimating the hydraulic loading. Pilarczyk (1990) proposes the following, indicative way of design of the splash area, eq. 29, (Figure 7):

$$\frac{H_s}{\Delta D_n} = \frac{2\cos\alpha_i}{\Phi_T \xi^{2b}\left(1 - \frac{R_c}{R_n}\right)}$$

where:
H_s = significant wave height,
ξ = breaker index; $\xi = \tan\alpha (H_s/L_o)^{-0.5}$,
α = slope angle,
α_i = angle of crest or inner-slope,
L_o = wave length,
b = coefficient equal to 0.5 for smooth slopes and 0.25 for riprap,
R_c = crest-height above still water level,
R_n = wave run-up on plane slope,
D = thickness of protective unit ($D = D_n$ for rock), and
ϕ_T = total stability factor equal to 1.0 for rock, 0.5 for placed blocks and 0.4 for blockmats.

The width of protection in the splash-area, which is related to the energy decay, can be roughly assumed as equal to:

$$L_s = \frac{\Psi}{5} T \sqrt{g(R_n - R_c)} \geq L_{min}$$

with a practical minimum (L_{min}) equal to total thickness of revetment (incl. sublayers) as used on the slope (= a minimum length of transition from the slope into the crest). ψ is an engineering-judgement factor related to the local conditions (importancy of structure), $\psi \geq 1$.

Stability of rockfill-protection of crest and rear slope of an overtopped or overflowed dam or dike can also be approached with the Knauss formula (Knauss, 1979). The advantage of this approach is that the overtopping-discharge, q, can be used directly as an input parameter for calculation. Knauss analysed steep shute flow hydraulics for the assessment of stone stability in overflow rockfill dams (impervious barrages with a rockfill spillway arrangement). This kind of flow seems to be rather similar to that during high overtopping.His (simplified) stability relationship can be re-written in the following form, eq.30:

$$q = 0.625 \sqrt{g}\ (\Delta D_n)^{1.5}\ (1.9 + 0.8\ \Phi_p - 3\sin\alpha_i)$$

in which:
q = maximum admissible discharge ($m^3/s/m$)
g = gravitational acceleration (9.81 m/s^2)
D_n = equivalent stone diameter, $D_n = (M_{50}/\rho_s)^{1/3}$
Δ = relative density; $\Delta = (\rho_s - \rho_w)/\rho_w$
α_i = inner or crest slope angle
ϕ_p = stone arrangement packing-factor, ranging from 0.6 for natural dumped rock-fill to 1.1 for optimal manually placed rock; it seems to be reasonable to assume $\phi_p = 1.25$ for placed blocks.

Conclusions

The practical stability criteria for various revetments under wave and current attack are defined. By using the same reference formulae the direct comparison and/or choice of revetment is possible. The accuracy of the

formulae is sufficient for the most practical calculations.

Further verification of developed dimensioning criteria is still needed. Prototype measurements/tests and careful evaluation of failure cases may provide useful information/data for verification purposes.

In all cases, experience and sound engineering judgement play an important role in applying these design rules. For specific problems, the original reports on specific revetments (see References), or else mathematical or physical testing can provide a better solution.

References

ASCE, (1967), closure to "Sediment Transportation Mechanics: Initiation of Motion", by the Task Committee on preparation of Sedimentation Manual, J. Hydraulic Division, ASCE, 93 (HY%), september.

Chang Howard, H. (1988), Fluvial Processes in River Engineering, John Wiley & Sons, New York.

Christensen, B.A. (1972), Incipient motion on cohesionless channel banks, in Sedimentation (Hsieh Wen Shen, ed.), Fort Collins, Colorado.

CUR/CIRIA (1991), Manual on use of rock in coastal engineering, Centre for Civil Engineering Research and Codes (CUR), Gouda, The Netherlands.

CUR/RWS (1993), Manual on rock in hydraulic engineering (in preparation).

Flexible armoured revetments inc.geotextiles (1984), T.Telford Ltd, London.

Graf, W.H. (1984), Hydraulics of sediment transport.

Hjulström, F. (1935), The morfological activity of rivers as illustrated by river Fyris, Bull.Geol.Inst. Uppsala,vol. 25(chap.III).

Isbash, S.V. (1935), Construction of dams by dumping stone in running water, Moscow-Leningrad.

Isbash, S.V. and K.Y. Khaldre, (1970,1976), Hydraulics of river channel closures, Butterworths, London.

Knauss, J. (1979), Computation of maximum discharge at overflow rockfill dams, 13th Congr. des Grands Barrages, New Delhi, Q50, R.9.

Meer van der, J.W. and Pilarczyk, K.W. (1984), Stability of rubble mound slopes under random waves, 19th Int. Conf. on Coastal Eng., Houston (also DELFT HYDRAULICS Publ. no. 332 and 396, and Proc. ASCE, Journal of WPC and OE, Vol. 114, no. 1, 1988).

Neill, C.R. (1967), Stability of course bed material in open channel flow, Edmonton/ also, IAHR Congress, Fort Collins.

Paintal, A.S. (1971), Concept of critical shear stresses in loose boundary open channels, Journal of Hydraulic Research, 9, no.1.

PIANC, (1987), Guidelines for design and construction of flexible revetments incorp. geotextiles for inland waterways, Supplement to PIANC Bulletin no. 57, Brussels.

PIANC (1991/92), Flexible revetments in marine environment, Supplement to PIANC Bulletin no. 78-79, Brussels.

Pilarczyk, K.W. (1989), Design of coastal protection structures. Short Course. Asian Institute of Technology, Bangkok.

Pilarczyk, K.W. ed. (1990), Coastal Protection, Balkema Publ., Rotterdam.

SPM (1984), Shore Protection Manual, U.S. Army Corps of Engineers.

Pilarczyk, K.W., H.J. Verhey, and G.J. Akkerman (1991), Rockfill Design Criteria for Overflow Dams, 17th ICOLD Congress, Vienna.

The Closure of Tidal Basins (1987), Delft University Press/The Netherlands.

Ven te Chow, (1959), Open-channel Hydraulics, McGraw-Hill Book Co.

EXPERIENCE OF USING RIPRAP WORKS IN BANGLADESH

K.A. Sarker
Dhaka, Bangladesh

1. INTRODUCTION

This paper on 'experience of using riprap works in Bangladesh' has been prepared to deliver in an international workshop considering all aspects of the Theory, Policy and Practice of erosion control using Riprap, Armour Stone and Rubble. The workshop will be held in Fort Collins, Colorado during July 12-16 1993.

Bangladesh lies between 20°30' and 26°45' north latitude and 88°and 92°50'east longitude and has an area of about 144000 square kilo metres. It is one of the largest delta in the world. The delta has been created by three mighty rivers viz: The Ganges-Padma, Bhramaputra-Jamuna and Meghna with their numerous tributaries and distributaries (See Figure 1). A total of 250 rivers criss cross the country having a total length of about 24,000 Km (BWDB, 1988). Almost all the rivers are alluvial in nature, characterised by soft and unstable bed and bank that are changing their position and shape continuously. This instability in river geometry coupled with huge discharge and sediment load causes scouring and erosion and a chain of reaction starts. The changes are both rapid and slow. Apart from natural factors, man-induced changes may also set in motion river response that can propagate over a long distance. Riprap is considered as an integral part of River Training Works. Bangladesh has many river erosion problems and those erosions are being countered by riprap. Therefore, Bangladesh has many experiences of successes and failures on riprap works.

Chapter 2 will discuss the history of major rivers erosion and shifting. Chapter 3 will list some existing rip-rap works in connection with major rivers, medium and border rivers. Chapter 4 will summarize the experiences whereas Chapter 5 is conclusion.

2 HISTORY OF EROSION AND SHIFTING BEHAVIOUR OF THREE MAJOR RIVERS

Unlike their present courses, during Rennel's Survey (1767-1776) the Padma and the Meghna flowed through independent channels until they joined near the coast a little north of Dakshin Shahbazpur island. The Brahmaputra used to flow through the present day Old Brahmaputra channel and had its confluence with the Meghna near Bajitpur. Combined flow of the Brahmaputra and the Meghna known as the Lower Meghna used to drain into the Bay past Shahbazpur island. The Ganges used to flow from approximately present Goalunda to south for about 24.14 Km past Faridpur town, then took south- easterly course up to Rajnagar and then took southerly course east of Gournadi and finally joined Meghna north of Dakshin Shabazpur island.

An extraordinary flood or earthquake occurred in 1789. This caused the Jenai (present Brahmaputra-Jamuna river), a distributary of the Brahmaputra, to develop gradually into the current main channel of Brahmaputra which joined the Ganges at Goalunda. The change increased the Padma flow. The combined flow of Brahmaputra and Padma found an easier course to the sea through the Kirtinasa channel south of Dhaka district, to bring about the mighty junction with the Meghna river above Chandpur. This is evidenced by comparison of the map prepared by Major Rennel with those prepared in later years. The medium and small rivers are also being shifted with respect to the Major rivers. Figure 1 will also show the courses of three major rivers during 1770s (Rennel's Survey).

3 RIPRAP WORKS IN BANGLADESH

3.1 Objectives of riprap works along with related bank protection works in Table 1 were:

- to protect adjacent population, land, industry of a township (Chandpur, Bhairab Bazar, Sirajganj, Rajshahi, Moulvibazar etc.);
- to protect important structures (Highway bridge across Meghna, Railway bridges across the Ganges at Hardinge bridge and across the Meghna at Bhairab Bazar, Teesta Barrage across Teesta River at Guddimari); and
- to protect viable agriculture land.

3.2 List of seven riprap works in Major and Medium Rivers and experiences are summarized in Table 1 and locations are shown in Figure 1.

3.2.1 Mahipur/Godownerhat, Teesta River. These are two small towns along Teesta River. The river is flashy, wide and shallow. Bank material is sandy. It caused erosion on concave banks near these two towns. In early 1970s, protection works in the form of bamboo spurs; and fencing have been tried by Bangladesh Water Development Board (BWDB) but such works could not stand the erosion. In 1986, about 1000 metres (m) riprap works with sand cement blocks were constructed. The combination of spurs with riprap was found successful.

3.2.2 Sirajganj Town Protection. About 2600 metres (m) strip of right bank of Bhramaputra river at Sirajganj Town has been protected by riprap works in several phases. Some brick matressing works were done by BWDB once in 1964 which were washed away in 1968; then in 1969 which again washed away in 1970. A cheaper material of sand cement (S.C) blocks of different sizes (0.15 m to 0.60 m cubes) were then introduced and dumped during 1971-74. They were found successful. In late 1980s, some repair of existing works was done. Additional S.C blocks were dumped to strengthen the same riprap works to bring the bank at natural slope. A groyne was constructed in 1968. The combination of groyne and riprap was found effective.

3.2.3 Rajshahi Town Protection. From 1960 and onward, Rajshahi Town continued to be threatened seriously from the Ganges erosion. The bank erosion was then checked by brick matressing with wire mesh and wooden pegs by BWDB. Heavier cement concrete (C.C) blocks were placed in the toe. The river continued to hit the town and then in 1970, it became a major problem. Between 1971-77, series of brick crates spur along with T-head groyne were constructed near the police line. Thus the town near the police line was saved but the erosion point hit tne court building. A physical model study was carried out with spurs and riprap. In order to control caving due to eddy formation as well as secondary current, the protection was by groynes which was supported by C.C blocks/ brick mattressing. However, the works have not yet been fully successful as zones of active erosion has oscillated from time to time.

3.2.4 Hardinge Railway Bridge across the Ganges. The riprap protection with Indian Pakur stones for Hardinge bridge is the one of the oldest works in Bangladesh which was undertaken by Railway Department in early 1930s (British Time). The performance of the riprap works was found good. The stones carried from Pakur was famous for size and shape.

3.2.5 Chandpur Town Protection in detail. A detail study of maps shown that the lower Meghna river both upstream and downstream of Chandpur town has shifted its position gradually to the east (Figure 2). But this shifting process seems halted at Chandpur town due to presence of rip-rap and other bank protection works. The protected bank acts as a control point in the river reach of lower Meghna. The erosion increases as the Meghna proceeds towards south.

a) Various hydraulic parameters contribution to erosion at Chandpur Town are given below:

Meghna Maximum discharge:147,000 cum/sec. (29.8.88)

Water Levels:	Maximum 5.35 m PWD (29.8.88)
(50 yrs return period)	Minimum 0.19 m PWD (1955)
Maximum tidal fluctuation:	1.22 m
Velocity during flood:	3.5 - 4.5 m/sec.

b) **Past Efforts for Protection of Chandpur town**

Railway: To protect the railway station, the Railway Engineers started dumping big size rocks along the bank of the Meghna since the beginning of the century. The protection works continued until Bangladesh Water Development Board (BWDB) took over in 1972.

BWDB: In 1972, the then Prime Minister visited Chandpur town to see himself a serious erosion and asked for the town protection on priority basis. Accordingly, about 732 metres of rip-rap works were done on the basis of a study done by one local consultant. The manual methods were used for dumping boulders along the eroding bank near Puran Bazar. The entire work was done during August-September of 1972 when the river velocity was more than 3 m/sec.

The past studies and recommendations on riprap for Chandpur Town Protection is given briefly in Table 2.

3.2.6 Bhairab Bazar (Upper Meghna). To protect the railway bridge and the town, massive riprap works were undertaken by BWDB during 1987-88 and 1989-90 (see photo 1). The works stopped further extension of the bank erosion.

C.C Riprap blocks near Patenga in Chittagong were displaced due to April 1991 Cylone (See photo 2).

3.3 River Training with riprap works across Border Rivers. Bangladesh has about 180 km fluctuated and 325 km undemarcated river boundary with India. These rivers and their protection are politically important. According to BWDB, border towns, villages and land in Bangladesh are subjected to an accelerated rate of erosion due to some bank protection activities in other countries. However the Indo-bangla Joint River Commission (JRC) have been discussing the issues since 1974, although the progress is very slow. Some examples are given below:

3.3.1 Horoddah and Sankara Villages Protection (Ichamati River), along west Bengal, India. Due to construction of some protective measures by India, the above Bangladesh villages were under erosion from Ichamati River. Bangladesh successfully protected their land by placing of percupines in that coastal belt.

3.3.2 Hasanpur and Mohanpur (Ganges left bank) about 24 Km of down stream of Farraka Barrage. India constructed spur and riprap at Nimtia, Jagtai villages which diverted the flow to erode Bangladeshi villages. The matter was discussed in a local level expert committee and agreed not to extend further construction of bank protection work.

3.3.3 Zakiganj Town (Bangladesh) and Karimganj Town (Assam, India) Protection. Zakiganj Town is located in convex face of Kushyara river while Karimganj in the concave side. To save Karimganj town, India has constructed a large number of deflected spurs with riprap during 1960s and has continued upto 1992. One spur extended beyond the mid-stream of the river. It caused erosion in Bangladesh side. To protect Zakiganj Town, Bangladesh also constructed several spurs followed by riprap. The river is constricted between the towns and formed a deep channel.

3.3.4 Ballah Railway Station (Khowai River). To save Indian Ballah town, they took several protective measures since 1948 which caused erosion to a Bangladesh railway station. Indo-Bangladesh Joint River Commission (JRC) discussed the matter and recommendations are being implemented.

3.4 Small Scale Water Projects. Upto December 1990, about 8000 hydraulic structures were constructed by BWDB for Flood Control, Drainage and Irrigation purposes to raise agriculture production. All structures have protecive/flexible aprons both at upstream and downstream. The materials commonly used are brick blocks/mattress, C.C blocks above sand-khoa filter. The performance of these riprap were found good where operation of the gates were done properly. See photo 3 for a typical protective works of a small scale hydraulic structure.

4 EXPERIENCES OF RIPRAP WORKS

Like elsewhere in the World, the riprap in Bangladesh are also auxiliary to bank protection works (spur, groyne etc.). They are expensive on account of their bulk. Because of high cost involved, all available materials are used. The most ideal materials should be stone/boulders. According to Table 1 and 2, riprap experiences are described below:

4.1 Attainment of objectives. Many riprap works constructed for bank protection are being severely damaged during big floods. Some have sustained the loadings or require only minor repairs. A few have never been exposed to river attack due to morphological changes. Overall achievement however, is found satisfactory.

4.2 Department responsible for riprap works. BWDB is the leading agency in riprap implementation. Railway Department, Roads and Highways Directorate and Inland Water Transport Authority (IWTA) are also responsible for minor river bank protection works related to their properties; but their major works are referred to BWDB.

4.2 Boulder size, availability and alternate materials. In Bangladesh, boulders are available in a limited areas across the border near Sylhet; but the sizes and weights (less than 100 lbs) are in many cases not adequate. Neighbouring country India has a plenty collection of boulders. For political reason, they are not brought from India.

The common types of riprap materials used in Bangladesh are as follows:

- Graded boulder or stone riprap over brick khoa filters or graded filter. These are being used in important locations like, Chandpur and Bhairabbazar towns on the bank of river Meghna, Manu River Bank Protection near Moulvibazar Town Protection, near Chringa bridge on the bank of Matamuhuri River. The boulder riprap has a long history. It was used to protect Hardinge bridge from the Ganges erosion in 1934 and to protect the Chandpur railway station in a small scale since beginning of the century.

- Sand Cement (S. C) blocks over filter layer. Used in Mahipur and Godownerhat in connection with Teesta River bank protection.
- Cement Concrete (C. C) block over filter layer. Used as Sirajganj Town Protection from Jamuna River erosion. Also used in Chittagong Shore protection (see photo 2).
- Herringbone brick mattresses laid over brick khoa filters. The brick mattresses are enclosed in galvanized wire mesh. Widely used for Rajshahi Town Protection from the Ganges erosion.

The following materials, other than in Table 1 are also being used:

- Brick Blocks over filter layer of sand and brick khoa are mostly used for the protection of loose apron at both ends.
- Combination of brick gabion at upper section and C.C or S.C blocks at falling apron.
- Articulated concrete slab over filter layer.
- Iron slags were used in Patenga Town Protection but found ineffective due to salinity problem.

Presently, geotextile layers are being used as filter in stead of the previously used 15 cm to 30 cm brick chips.

It appeared from above discussion that the stone availability of adequate size and shape is a great constraint. Bangladesh has only a few stone quarries near Indo-Bangla border at Sylhet but they are smaller in size and weight than most riprap requirments. Cement concrete blocks are expensive, brick mattressing is good only in a limited region. Despite its high cost, C.C blocks are used as the major material for Bangladesh existing riprap works as shown in Table 1. Sand cement blocks are cheaper but not adequately heavy. Synthetic bags filled with a mixture of sand and other suitable ingredients are found suitable but not durable. However, studies are going on to find out appropriate materials for different locations. See Figure 3 for typical riprap materials and construction.

4.3 Design Considerations. The riprap design must satisfy the minimum permissible design criteria and practicalities of construction. According to BWDB, they faced tremendous construction problems with the specified designs for the works in Table 1.

The bank stabilization unit or hard point has three elements for the most works in Table 1 (see figure 4). I. Armour protection layer on slope, slope protection above Low Water Level (LWL) up to the crest level; slope protection below LWL down to toe. II. Toe/Falling aprons and III. Upstream and downstream terminations. The third element is composed of first two but has a distinct function, is exposed to more adverse hydraulic conditions and involves different construction techniques.

Armour protection layer above LWL can be placed in the dry and it is easy to construct. In most cases of Table 1, two layers of materials (S.C. cubes, C.C cubes, boulders) were used. The two layers conception were taken from old Indian practice and found to be conservative. The upper layer normally were displaced and played no clear role.

The slope protection below LWL is always submerged in turbid water. In some cases, this portion went under sediment after construction. This section is difficult in terms of construction and maintenance. The design must give due consideration to both these aspects. Graded rocks offered better performance than a mixture of block cubes. Due to shape, the mix cubes usually segregated during dumping and added difficulty over distribution monitoring. In future the choice of materials may be made on the basis of cost and scope of the protection works in terms of materials procurement, contractor's capability and manpower. The two layers design is found effective as at least one would be achieved in practice over the whole face. This is the minimum functional requirement.

The primary function of toe or falling apron is to prevent the toe scour undermining the slope and initiating progressive geotechnical scope failure. As a secondary function it provides a toe weight which improves the slope stability. It also acts as a flexible apron. The design followed in Bangladesh riprap are mostly from Indian practice of launching apron. The most difficult part is construction of the falling apron when dumping can not be controlled as per specification. According to Table 1, both blocks and boulders were used in the construction of falling apron. There are also arguments for and against the use of dumped boulder in toe/apron in place of cubes. Both materials can result in uneven displacement during deformation process. See Photo 4 for a riprap work with short launching apron located near Chittagong but has been surviving well.

The terminations were exposed to most severe hydraulic conditions. It is very difficult to hold the blocks/boulders in the slopes due to the geometry. The larger size of blocks/boulders at lower slope have proven hydraulically more suitable.

Slopes are designed with respect to natural slope (1:2 to 1:2.5 in Table 1). The natural slopes considered in Chandpur was 1:4. But there is a big question whether the specified slope was actually maintained during construction.

It is easy to design filter but difficult to construct as specified. The use of geotextile layer has proven to be a successful filter.

During assessing experiences, it was difficult to know the exact cause of some past failures. In case of severe damages particularly occurring during the floods. The damages start at invisible locations and surveys are not carried out during periods of severe condition. It thus becomes difficult to explore the cause of failure and also to propose improvement in design and construction.

4.4 Budgetary Implications. Like other development works in Bangladesh, the budget for riprap is available most from foreign aid. Bangladesh can not finance her timely, portion of the budget for establishment, land acquisition etc. to cope with the aid and the execution suffers. The work scheduled for completion in one season, can not be completed in time. It is also difficult to arrange fund during emergency need during flood time. After 1988 flood, the World Bank provided some repair fund as a flood damage repair of riprap works.

4.5 Construction Management, River condition and Time of construction. Ideally, the riprap works both physically and financially should be constructed when the mean Low Water Level (LWL) remain below the most of the working zone. According to BWDB Engineers, most of the works are done during the flood time because of late Contractor selection and late site possession. The LWL of most rivers in Bangladesh begin to rise in April and remain higher during May to September. Working during High Water Level (HWL) is difficult, not only because of poor visibility- but also due to relatively high velocities, turbulence and rapid sediment transport. Temporary current deflectors, and cofferdams are liable to undermine or simply wash away. Placing riprap materials/filters become a hazardous and impracticable task, no matter how sophisticated equipment are utilized. At low flows, bulk materials and equipment can not be brought to sites by big vessel. Most blocks are casted at site and are dumped/placed manually due to lack of equipment availability. To carry a 100/120 lbs block manually is a difficult job.

There is a low risk of damage of construction in one season. If the construction can be completed in one season, no down-time payment for plant and equipment and one for mobilisation/demobilisation is necessary. The contractor establishment as well as risk of loss of materials /equipment from site are low. It is apparent that one season construction offers a potentially lower cost, if the Contractor has the

resources and expertise to complete the task. To construct some major riprap works within one season- one has to be well organized to consider the exceptional weather, the site possession should be available before the working season. A well organized construction management with materials, equipment and manpower can make a program successful.

4.6 Selection of working Contractor. The Engineer-in-Charge has to subdivide the works into: material supply; equipment supply; blocks casting; block placement/ dumping etc. to involve many Contractors. There are too many Contractors with respect to availablity of work, particularly in the area of bank protection. It becomes very difficult to manage the progress and quality of works with so many Contractors. It is reported by Engineers-in-charge that many Contractors (mostly politically affiliated) do not follow the BWDB procedural requirements. On the other hand, Engineers in many construction works are biased in favour of the Contractors. All these factors delay the work commencement. There is again a tendency to dump the boulders or blocks during high flood flow when actual measurement of quantity is under question.

4.7 Monitoring and Maintenance Expenses. Due to importance of riprap works, BWDB has been monitoring the existing works during the flood periods. There was a lack of maintenance fund before 1988 flood. After that, the World Bank and other donors provided fund under Flood Damage Repair (FDR) and the maintenance of riprap works is progressing well.

5.0 CONCLUSION

Most rivers in Bangladesh are affected by significant bank erosion due to their physical and hydraulic characteristics. The problem of erosion continues to attract the public attention as evident from wide coverage in national dailies specially during flood period. River training including riprap works are therefore considered as a very important tool to protect properties and lives from such erosion.

Despite many constraints in the design, implementation and operation of riprap works, the performance of many existing works are found good.

The planning and design of riprap works depend largely upon the judgement of experienced engineers. At the same time model tests have proved very helpful. Further systematic experimentation on the behaviour of rivers by means both physical and numerical models should be resorted to as far as possible. Historical behaviour of river erosion, reason of failures etc. should be found out which could be used in future riprap development.

On materials, sand-cement blocks have proven to be an alternate materials to boulders. The use of indigenous materials and method were found very effective in minor and medium rivers bank protection. More studies for the development of these traditional methods of bank protection should continue. For these works materials like boulders can be procured from India at a reasonable price.

Due to poor construction management, the cost and hazard occurrences increased in many existing riprap locations. There is scope of development in managing a good construction sequence that all the works can be completed -both repair and new in one season.

Implementation capability in handling the immense and concentrated quantities of riprap works, design, tendering, construction equipment and materials, manpower, electricity should be well organized well ahead of taking the riprap works.

Contractors are mostly politically affiliated. They like more profits illegally but by doing less works; engineers/officials are getting involved in misappropriation. Everybody involved in riprap works should do their duties professionally.

Indo-Bangla Joint River Commission (JRC) can develop a good strategy of river bank protection in cases of border rivers.

Maintenance and Monitoring after construction of riprap works should be further improved. There is a need of good inventory of all riprap and river training works for monitoring purpose. Special studies are however going in pilot basis under Flood Action Plan 21/22.

6 REFERENCES:

1. Ainun Nishat 1986, "Control of Erosion and Deposition in Rivers" paper presented at Dhaka Regional Workshop on Erosion and Sediment Transport Processes.

2. Bangladesh Water Development Board (BWDB), 1976 "Comprehensive Plan on resuscitation and training of rivers and town protection of Bangladesh."

3. BWDB 1988, "Report of the National Committee on Protection of Chandpur Town."

4. Central Board of Irrigation and Power, India, 1971, Manual on "River behaviour Control and Training."

5. Consulting Consortium FAP 21/22 1992, "Interim Draft report on Bank protection and river training pilot project."

6. Galay and Pegg 1974, "Report on the stabilization of Meghna River-Chandpur Irrigation Project."

7. Hossain, Akram GM 1988, " Term paper on river Training Works in Bangladesh."

8. Islam, Zahurul Md. 1991, "Failure of flood embankments: Care studies of some selected projects in Bangladesh."

TABLE 1
MAJOR RIPRAP WORKS IN BANGLADESH

	Location (Length of Revetment)	Construction Year	Levels	Bank Slope	Structural Features of Revetments (Riprap)									Experience/Comments
					Bank Mats.	Type of filter layer		Armour Layer on slope		Toe	Falling Apron			
1.	Kashipur (Teesta)	1966	Crest+35.12 RWL+35.05 LWL+33.56	1:2.5	fine sands	8cm coarse Sand 8cm khoa	-	0.55m	S.C. blocks 0.45m (2 layers)	-	10.7m	1.65/1.4	S.C. blocks	Materials quantity= 30m³/lin.m Revetment cost = Tk. 45.000/-m Bank erosion/sliding during past years
2.	Godowaerhat (Teesta)	1969	Crest+43.8 RWL+39.3 LWL+35.15	1:2	fine sands	8cm coarse Sand 8cm khoa	Propex 6064	0.30m 0.65m	S.C.blocks placed above 37 S.C. blocks 0.30 to 0.39m of random	-	10.6m	1.25/2.12	S.C. blocks 0.3 to 0.36m	Materials quantity = 30m³/lin. m Revetment cost = Tk. 40.000/- m No visible damage so far
3.	Sirajganj Town River (Jamuna)	1964-69	-	-		-	-	-	Brick mattressing /dumping	-	-	-	-	Brick mattressing placed in 1964 and 1969 washed away after 4 and 1 year respectively contingent on seriousness of attack.
	Section (1) = 1710m Section (2) = 830m	1971-74	Crest+16.15 RWL+14.60 LWL+6.70	1.3	fine/medium sands	-	-	-	S.C. blocks (size 0.15 to 0.60m)	-	-	-	-	By annual dumping of S.C/C.C. blocks the revetment could be maintenance till 1955 in 1955 serious sliding and damages occurred at various places over a length of 1160m
	Repair and strength-ening works	1986 and after works		natural		-	-	1.21m	C.C. blocks and railway waggon	-	14 to 50m	1.52/3.0	C.C. blocks	Repair costs 1986-89 Tk. 27m
4.	Rajshahi Town Protection work (Ganges)	1960	Crest+29.50 RWL+19.20 LWL+3.52	1:2	silty soil	7.5 cm 15 cm	-	0.15m	Brick Mattressing with wire mesh and wooden pegs	0.30x0.30x0.45m C.C.block with bamboo and bamboo pins	-	-	-	Damage occurred at many places
	-do-	1988-92	Crest+26.50 RWL+19.20 LWL+8.55	1:2	silty soil	7.5 cm 15 cm	Geotextile 230G/m²	0.15m	Brick Mattressing with wire mesh and wooden pegs	0.50x0.30x0.45m C.C. block with bamboo and bamboo pins	-	-	C.C. blocks	Good after 1990 Geotextile are being used as filter below brick mattressing
5.	Baraigram Bridge (Ganges)	1952 1955		natural	silty soil	-	-	Various	Boulders dumped at random on the slope	Not known (N.K)	N.K.	N.K.	N.K.	Working well for a long time. Railway Dept. occasionally dump boulders to the damaged areas.
6.	Chandpur Town (2550m) (Meghna)	1972 onward	RWL+5.35 LWL+0.15	natural	silty soil		-	Various	Boulder dumping on slope 1:1	Dumped boulder	-	-	-	Protection by will dumping of boulders did not work and the township is threatened to be eroded
	Chandpur Town (1200m), -do-	1989-90	-do-		silty soil	30 cm Khoa above LWL	3 layers geotextile bags dumped	0.30m	C.C. Block Boulder		15m	3 layers geotextile bags	Geotextile bags filled with sand	Work at two places at Puran Bazar and Baitul Bazar executed as per recommendation of National Committee.
	Chandpur Town (445m), -do-	1991	-do-	natural	silty soil	-do-	-	0.6x0.6x0.45m wire crates filled with boulders	Boulders in crates to the damaged area	Dumped wire crates				The boulder crates have been dumped on emergency basis to stop the erosion during end of 1991
7.	Shahrab Bazar (Upper Meghna)	86-87 & 89-90	G.L + 6.70 LWL + 1.80	1:2	silty soil	30 cm Khoa over 15 cm sand	-	0.70m	Boulders	Falling apron	15m	1.0/2.5	Boulders	Severe erosion occurred upstream of Railway bridge during 1988. Work undertaken by Railway Dept. for protecting the bank by boulders pitching.

Source: PAP 21/22, INTERIM REPORT 1992

Table 2
Past studies and recommendations
in connection with Chandpur Town Protection

	Studies done by	Causes of Erosion	Scour depth	Recommended Protective Works	Total Est.	Recommended Riprap Works
1.	International Engineering Company (IECO, 1966)	• Strong current of Meghna and Padma • Strong wave action	29.7 m	• No definite Recommendation is given	Not Available	Not Available
2.	Netherlands Engineering Company (NEDECO, 1967)	• Strong current of Meghna & Padma	Not stated	• Shift Chandpur port at south of Puran Bazar • Protect river bank	Unknown	Several km (not specific)
3.	Leedshill Deleuw (LDL, 1969)	• Main Meghna flow hitting bank along Chandpur Irrigat. project	Not stated	• Protect Meghna Bank with - Rock+bamboo to a mattress in-addition to 3 groynes	$ 23.5 M Tk.176M	7.2km beyond Dakatia mouth 1:4 slope with Indian rock local rock small
4.	Prokoushali Sangsad Ltd (PSL, 1973)	• Strong rollers and eddies formation due to join left and right courses of Meghna.	31 m	• Connect Chirirchar (Island) with main-land with a x-band with revetment works • riprap	$14.0 M Tk.140 M	731.5
5.	Dr. V.J. Galay Brig. Pegg (April 1974)	• Shifting Meghna Thalweg toward the town coupled with scour of Dakatia river • Ineffectiveness of existing river training works for small boulder size and steep slope.	51 m	• Extend riprap work 3.2 km at u/s and 2.4 km at d/s of old works with 100 lbs boulders at 1:4 slope.	Not khown	5.6 km
6.	Emdad Ali (BWDB, 1975)	• Strong current of Meghna and Padma	24.4 m	• Only riprap to protect both Town & Chandpur Project	Not known	8.0 km
7.	National Committee 1988	• Same as sl. 5 • Imbalance hydra-ulic condition due to Dakatia flow.	54 m	• Concrete blocks riprap works in 3 categories for 638 m Slope 1:2,Block size 38 cm to 53 cm cubes. Heavier at toe.	Not known	0.7 km

Source: Report of National Committee 1988

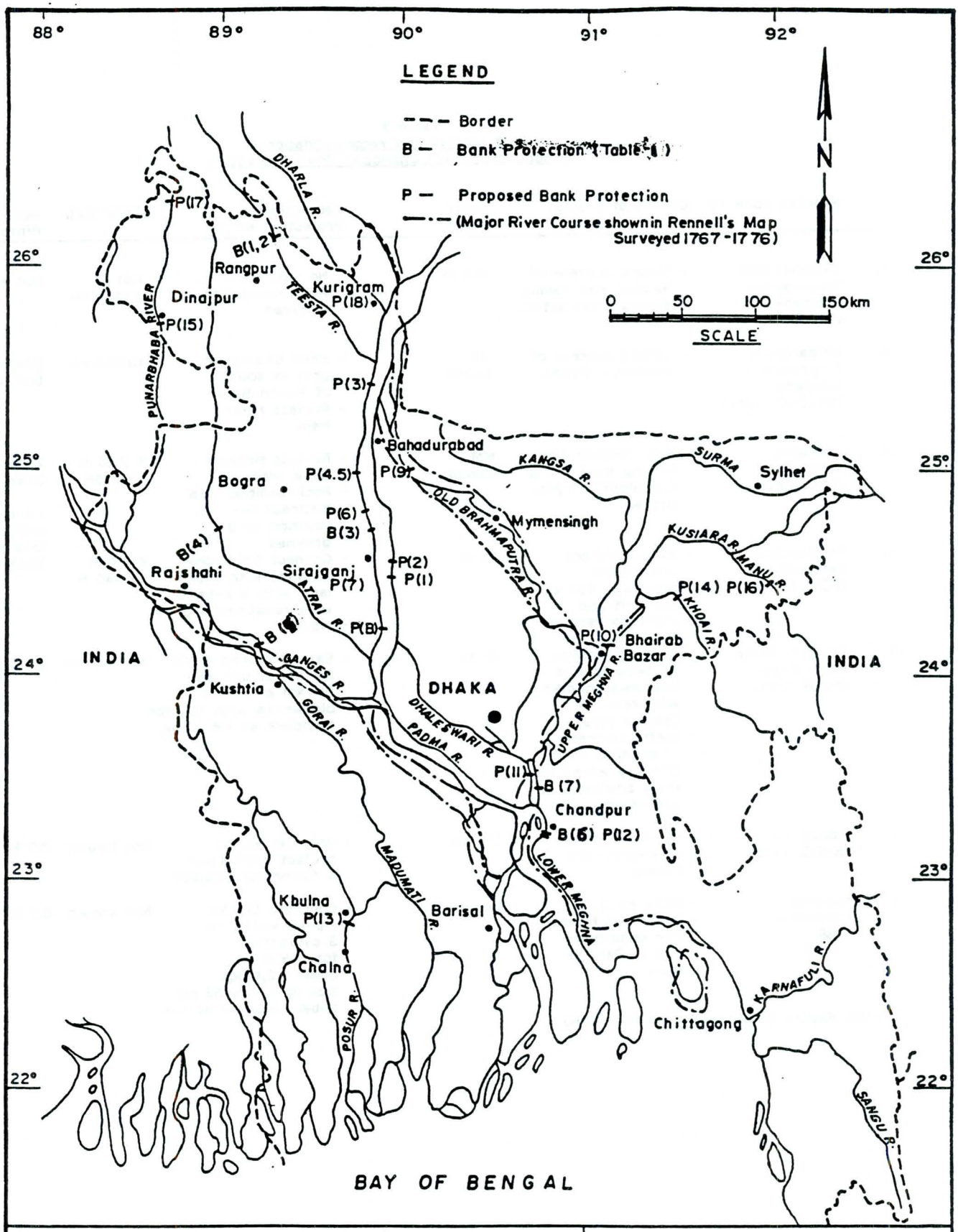

LOCATION MAP OF EXISTING/PROPOSED RIPRAP WORKS IN BANGLADESH

DATE :- MARCH, 1993

FIGURE :- 1

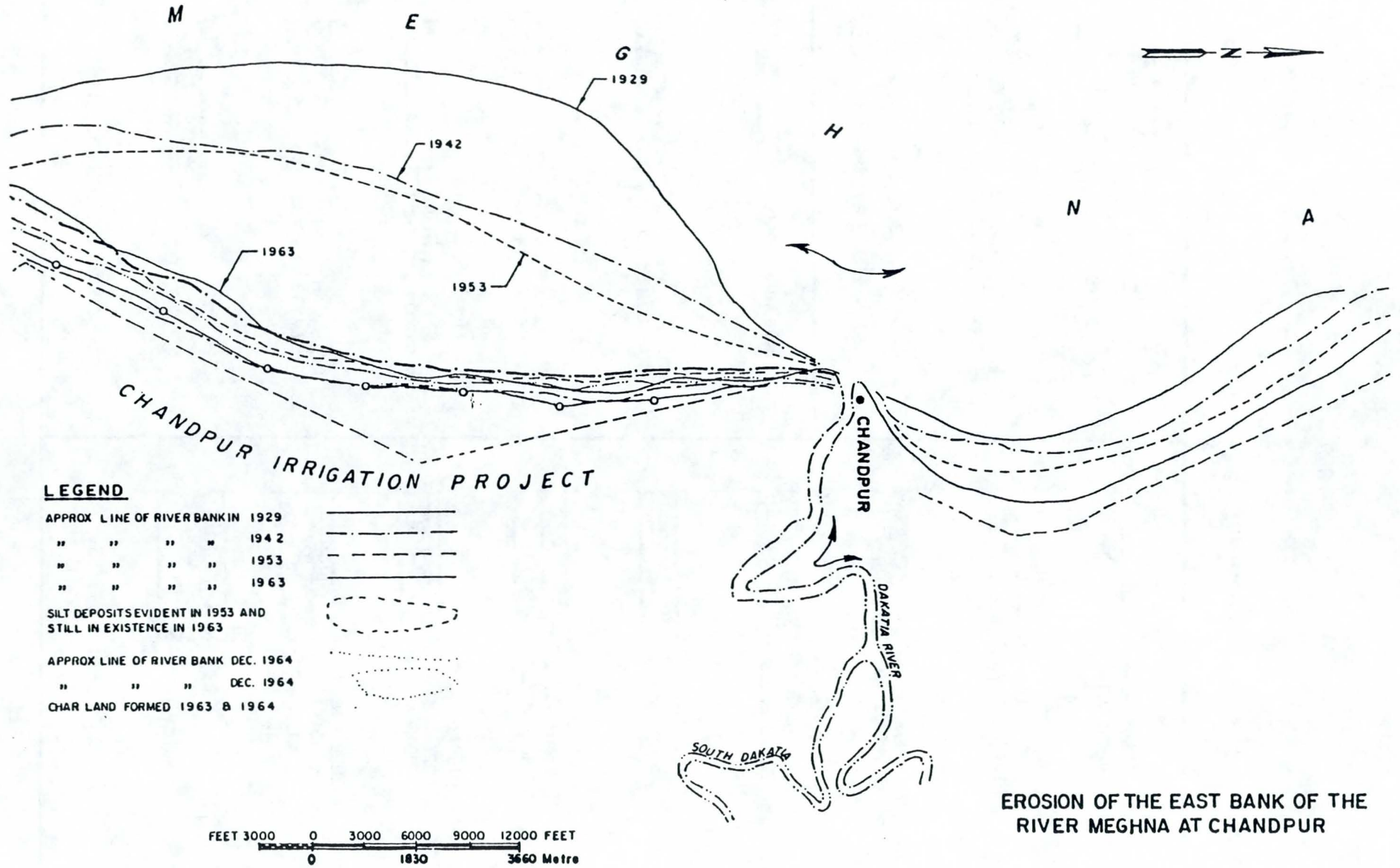

EROSION OF THE EAST BANK OF THE RIVER MEGHNA AT CHANDPUR

FIGURE : 2

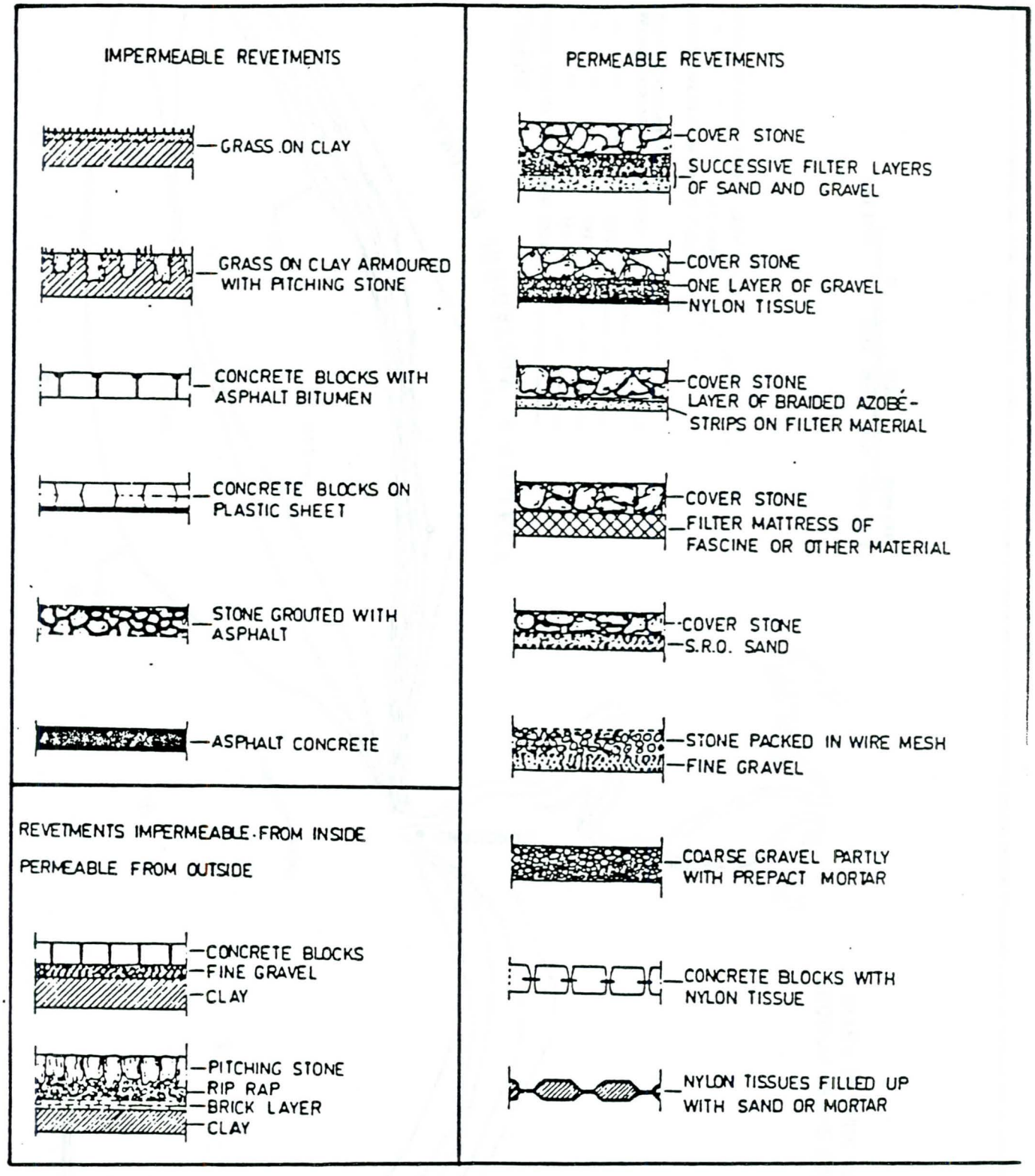

Figure 3 Examples of riprap constructions

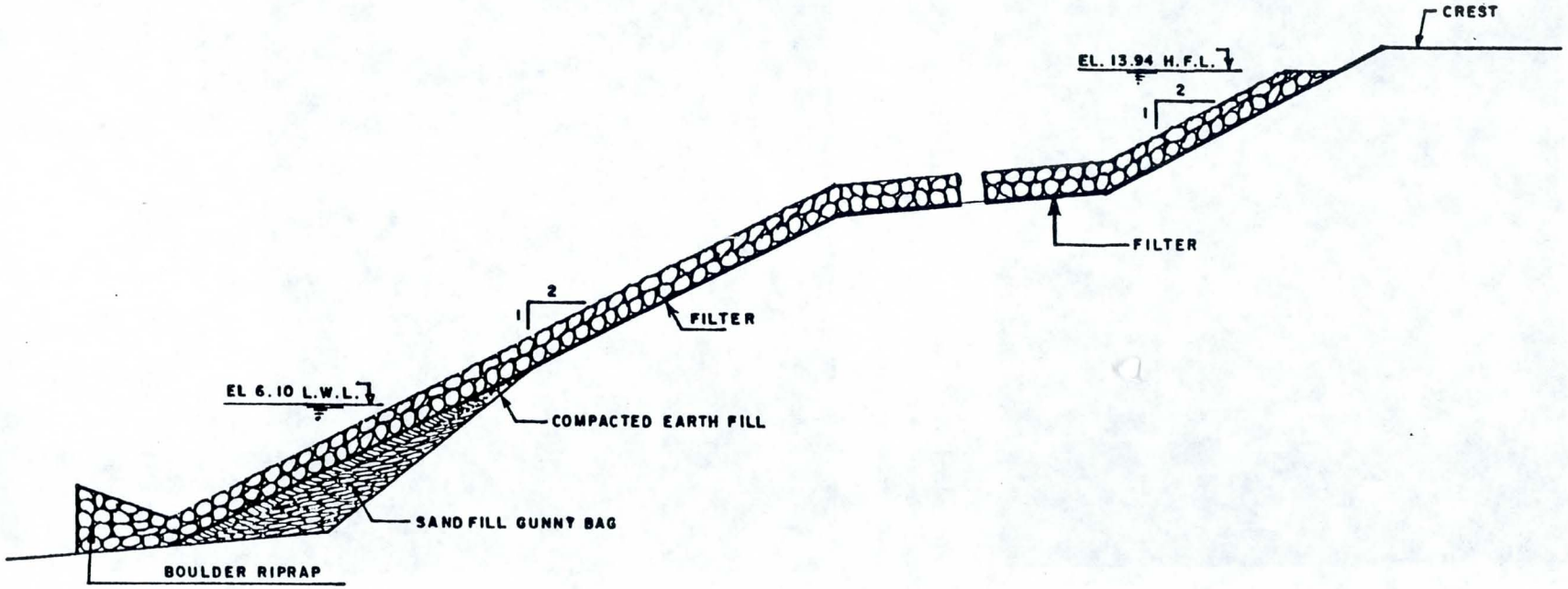

FIGURE-4 TYPICAL RIPRAP WORKS IN MANU RIVER BANK PROTECTION.

December, 1992

Photo 1 • Boulder Riprap works to protect the Bhairab Bazar Town on the right bank of Meghna River. The old railway bridge, built in early 20th century, is also now saved.

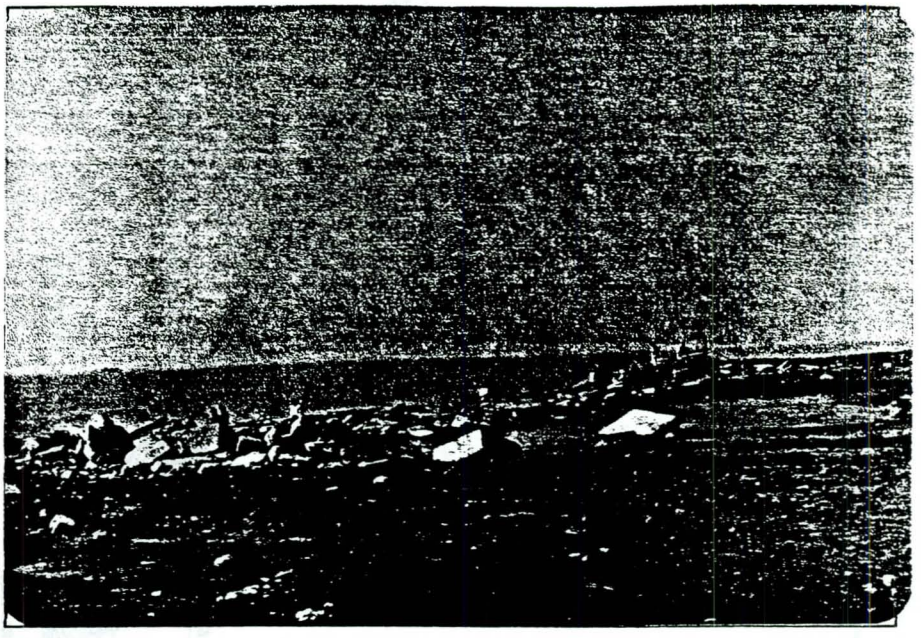

December, 1992

Photo 2 • Riprap works with cc blocks used along Patenga town protection as shore protection, were severely damaged during the April 1991 cyclone. The industries and the airport remain vulnerable till todate. However, a special Cyclone Protection Project is under implementation under IDA/JICA finance to be completed by June, 1994.

December, 1992

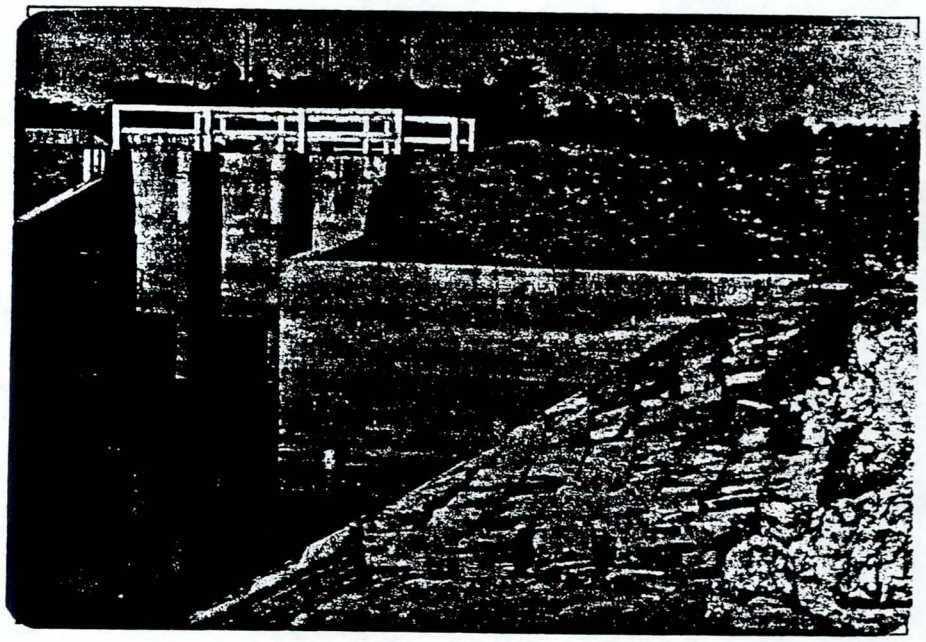

Photo 3 · Brick Blocks are used in most of the hydraulic structures. There are about 8000 hydraulic structures built todate in Bangladesh.

January, 1993

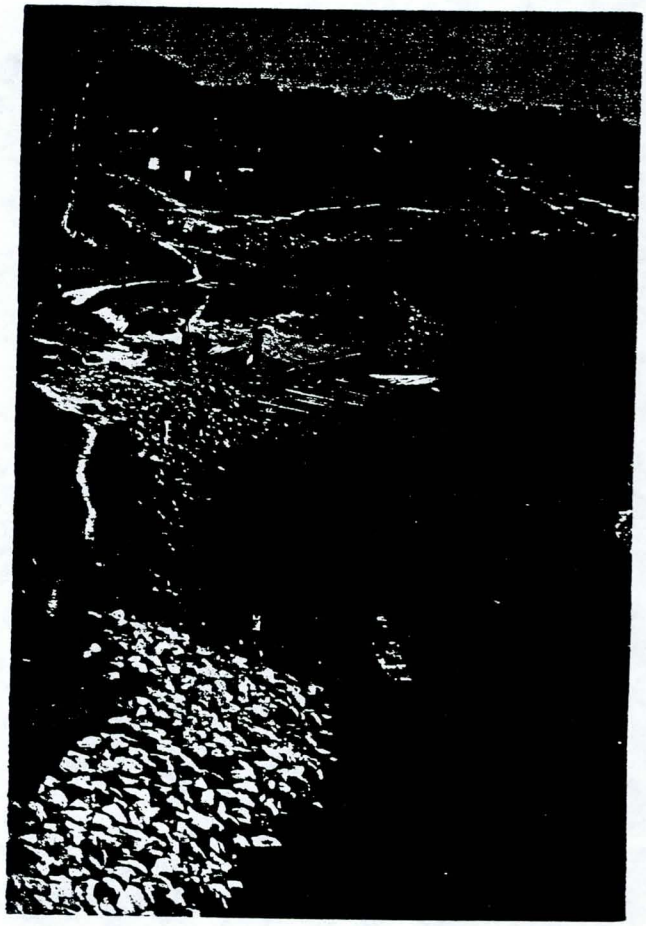

Photo 4 · Upstream, Sangu River, Chiringa Bridge near Chittagong. Riprap with a short Launching apron.

CONSIDERATIONS REGARDING THE EXPERIENCE AND DESIGN OF GERMAN INLAND WATERWAYS

H. Schulz
Federal Waterways Engineering and Research Institute

Introduction

During the last two to three decades German inland waterways have been rebuilt into PIANC-class IV waterways during continuous shipping traffic. These activities were accompanied by the introduction of geotextiles as filter layers. Due to the damage and increased maintenance, research activities have been increased to investigate the stability of revetments. These research efforts, including aspects regarding the geotechnical stability of the subsoil and in-situ measurements, as well as laboratory and flume measurements, have been carried to investigate and understand the failure mechanisms. In addition engineers have been successful in developing different kinds of stable revetments by trial and error.

The following presentation of theory and practice, as well as of examples and practical questions regarding construction, will be confined to a small section of the whole spectrum of problems regarding 'revetments', that is to say to permeable revetments, and here again to non-grouted or partly grouted riprap revetments along the man-made inland waterways of the Federal Republic of Germany, mainly concerning the north and north-west German canals.

Cross sections of waterways and constructional forms of permeable revetments

Fig. 1 shows the normal cross sections of the western and northern German waterways and the cross sections of the ships, which travel along them, which have been stipulated as being standard. The ratio of the cross section of a canal (wet cross section) to that of a ship amounts to at least n = 7.

Due to the requirements of the dynamics of vehicle movement, at the present time, a somewhat larger cross section for waterways for large engined freight ships is under discussion, in order to improve the meeting safety (Söhngen, Zöllner [5]).

A revetment is a structure, through which a stable sloping of the bank should be produced, which is more steep than would be possible under natural influences and subsoil conditions. It consists of a cover layer, which is resistant to hydraulic loads from waves and current, and of one or several filter layers between the protective layer and the subsoil. In the German waterways authorities various standard construction forms for permeable revetments have developed, on which an information sheet has been drawn up, in which fig. 2 shows the basic design of a permeable revetment. According to this, we mainly differentiate between four construction forms, where, in each case, the permeability is greater near the water as opposed to the subsoil, the four forms being loose riprap, partially grouted riprap, fully grouted riprap and coatings or cover layers of concrete blocks. In fig. 2 the filter shown is a geotextile filter, which must fulfill the requirements of the 'Loaflet for the Application of Geotextile Filters for the Federal Waterways'. Grain filters are not excluded, however, they must conform with the 'Loaflet for the Application of Grain Filters'. These loaflet and the corresponding additional technical requirements or Technical Delivery Terms complement one another and provide a unified set of rules for invitations of tenders, awards of contracts, the construction and cost calculations of revetments.

Hydraulic loads

The hydraulic loads (fig. 3) consist of a bow wave in the form of a slight raising of the water level, followed by a great lowering of the water level, which occurs in a short space of time and is caused by the return current of the water displaced by the ship's hull. Then follows the transversal stern wave, which runs with the ship and, then, starting at particular speeds, breaks, when approaching the flattening bank. The breaking stern cross waves are the main loads for the cover or protective layer. It must withstand these wave loads and must consist of suitably heavy elements with positional stability. The dimensioning of this protective layer is a classic task for hydraulic engineering. In the same way, the dimensioning of the bed in relation to the return current speed from the passage of ships and in relation to the screw race is also a classic task for hydraulic engineering, since the beds are, as a rule, not fortified in the waterways of the Federal Republic of Germany, except along stretches with sealing.

Geotechnical considerations

The water level draw down represents the main load for the subsoil. In this connection, it can be seen in the net of iso-potential and streamlines in fig. 4, which arises as a result of a speedy draw down of the water level by 70 cm in 10 s with a permeable revetment of non-grouted riprap. For those concerned with soil mechanics, the section of the network of iso-potential lines, which lies below the lowered water level, appears unusual, since it is normally assumed, that the water is fully incompressible and thus a pressure change in the outer water level produces no excess pressure of the pore water at all, because no change in the effective pressures occurs and thus no changes in the volume in the grain skeleton. With the conditions along the waterways, we cannot, however, assume that there is an incompressible pore fluid, since, due to shipping, a great deal of air is brought into the canal water and also into the pore water, so that the medium here is a compressible pore medium. We must imagine, that fine air bubbles adhere to the pores in the subsoil and with every

pressure change in the outer water their volume decreases or increases. When the water level is drawn down, the water pressure is reduced and thus the volume of the small air bubbles becomes greater. They thus displace the water from the pores and, so that it can flow out, there must be a gradient, i.e. an excess pressure of the pore water must arise. The iso-potential field here shows a situation calculated for a compressible pore fluid using the FE-programme Steenzet 2 by Delft/Geotechnics (Hjortnaes-Pedersen et.al. [1]). The excess pressure required for the displacement of the water by the additional volume of air leads to a flow of pore water in the outer water and thus to a gradient, which is directed against the gravitational force.

Let us now take a look at the stability of an element of a revetment consisting of one cover layer and a filter, which might be found in the area of the lowered water level. We place a slip line, as is customary in soil mechanics, at any depth z parallel to the surface of the slope going into the soil (fig. 5). The condition of equilibrium means that the revetment element described must not move on the slip line parallel to the slope. Sliding occurs, when the descending force of the slope H is greater than the frictional force T. The frictional force is the product of the normal force on the base and the frictional coefficient, so that the following can be stated:

$$\sigma' \cos\vartheta \cdot \tan\varphi \geq \sigma' \sin\vartheta \qquad (1)$$

Up to now the discussion here has applied to the case, where there is absolutely no water, or where there is a volume element completely under water without a any flow of water. Let us now consider the whole situation taking the flow into account, which is directed outwards as a result of the draw down. For this purpose, I shall use pore water pressure, which has an effect on the lower side of the volume element of the revetment being examined (fig. 6). It results from the remaining potential at the depth of the slip line, which represents a portion of the whole potential difference between the steady state water level and the lowered water level. We have become accustomed to describing this pore water pressure as excess pore water pressure, although it is not an excess pore water pressure in the classic sense of soil mechanics.

The reason for this is, that this excess pore water pressure does not result from compressing the grain skeleton due to an outside load, but from a change in the volume of the fluid phase, which, due to the potential produced, can lead to a volume change in the grain skeleton. However, this expression very vividly describes, that, when excess pore water pressure occurs, it is also associated with a consequence regarding the stability. Due to the excess pore water pressure, the normal force on the sliding plane is reduced by the amount of the pore water pressure, without the component sliding down the slope being also reduced at the same time. In this connection fig. 7 shows a free polygon, from which it becomes clear, that for the same geometry under the influence of excess pore water pressure an additional supporting force is necessary, in order to produce an equilibrium.

Where can this additional supporting force for a revetment come from? Since no excess pore water pressure arises in the riprap, because the permeability is very great and thus the water can flow very easily out of the pores of the stones, and since the excess pore pressure in the filters is also very small, it can be seen, that by increasing the surcharge, principally in the form of riprap, this holding force can be made available for the additional friction, which is linked with the surcharge. We can illustrate this in the classic Coulomb diagram (fig. 8), in which we increase the surcharge until, taking the excess pore water pressure into account, the stress point is below the rupture line. The proof of this mechanism has been obtained from 1:1 model tests in a test pit (fig. 9), where we produced a draw down of the water level, similar to that during the passage of shipps. After the successive reduction of the thickness of the cover layer of riprap deformations in the subsoil had occurred, which we discovered by the fact that the water pressures registered during steady state conditions increased by several centimeters in the pore water pressure transducers. From this it can be concluded, that, if the thickness of the cover layer is insufficient, movements in the subsoil can occur. In the test described a complete rupture could not occur, because, after the activation of a displacement path of several centimeters, a foot support became active.

As we have seen, it is important to have a knowledge of the excess pore water pressure, which arises in the subsoil, when the water level is drawn down. Since this excess pore water pressure is mainly due to the fact that the pore medium is compressible due to small trappings of air, and that the compressibility cannot be directly measured, the only possibility of determining this influence is by measuring the pore water pressure in-situ. For this reason, a pore water pressure measuring system has been developed (Köhler, Feddersen [3]), which is simple to carry out and is suitable for very quick changes in the water level and thus also for pore water pressure changes. For this purpose, first of all pipes with a closed tip and with openings closed by filter stones, which are positioned suitable in relation to the height of the pore water pressure transducer used later, are rammed in. The pipes are staggered according to the depth, so that the course of the excess pore water pressure can be recorded as a function of the depth. The pore water pressure transducer (fig. 10) is then inserted into the pipe, locked into place and with the help of a packer is sealed off from above. Thus the pore water pressure transducers can be recovered at any time and can be recalibrated, when used on a permanent basis.

The evaluation of measurements of this kind is carried out for one individual water draw down, whereby the evaluations and calculations are based on an exponential function depending on the depth. The theoretical solution to the differential equation for the elastic storability of the soil consists of a product formulation with an exponential function and a trigonometrical function. The exponential function describes the change of the excess pore water pressure depending on the depth, whilst the trigonometrical function mainly represents the load influence depending on time and location. When the water level is drawn down due to shipping, we belief that a fairly accurate one-dimensional observation can be made. All characteristics of the soil and the water, such as permeability and compressibility of the soil, the bulk modulus of the water and the speed of the draw down can be combined into one value, which in Dutch literature is described as the elastic storage length L_{es}. In the Federal Waterways Engineering and Research Institute, we have simply combined them into one parameter b and the hydraulic load is represented by parameter a (Köhler, Schulz [2]). Both parameters are then only functions of time. Thus the

excess pore water pressure can be shown according to the following equation:

$$\Delta p(z', t) = z_A \cdot \varphi_W \cdot g \cdot (1 - a(t)\exp(-b(t) \cdot z')) \quad (2)$$

with
Δp excess pore water pressure
z' depth ordinates, normal towards the slope level, positive inwards
t time
z_A draw down of the outer water level
ρ_W density of the water
g earth acceleration
a parameter, dimension 1
b parameter, dimension 1/length.

An example for the evaluation of a fast draw down is shown in fig. 11. Here a water level draw down of 85 cm in 10 s was given in a model experiment in a glass tube. The soil used was sand with a uniformity coefficient of approximately U = 6 and a d_{10} of 0,12 mm. The resulting b-value was > 7 and thus very high. The influence of the permeability of the material can be seen in another test (fig. 12), where a draw down of 65 cm also in 10 s was produced, however, the grain diameter was d_{10}=0,34 mm and the uniformity coefficient had only a value of 1,5. It can be seen, how quickly the excess pore water pressure is reduced here, since after just 10 s, i.e. at the point in time where the draw down is at its maximum, the greater part of the water level draw down has also already been dispersed in the subsoil. To make another comparison with the previous experiment (fig. 11): here the full excess pore water pressure is still present after 10 s at a depth of 50 cm. This means that at this depth the soil has not yet absorbed the effects of the outer draw down of the water level. The water used for the experiment was tap water with compressed air on the reservoir water table in order to produce an adequate amount of pressure. It should also be mentioned, that the tests were carried in such a way, that the water pressure on the lower side of the tube was kept constant.

The measurements in natural surroundings are far more complex, and the non-homogeneities of the subsoil play a decisive role in the evaluation and interpretations.

However, they are indispensable, since the natural conditions of air saturation of the pore water and the non-linearity of the whole process cannot be adequately reproduced, either theoretically or in tube experiments. The aim of our measurements is to establish a simple connection between the b-value and the permeability for each point in time, when a maximum draw down is reached, i.e. for the most disadvantageous situation, which gives a safe reference value to those concerned with planning.

Conditions regarding geotextiles as filters

The concept presented here provides a set of instruments, with the help of which it is possible to make a prognosis on the consequences, when traffic conditions on the waterways change. At the moment, we are in a period of transition from Rhine-Herne canal ships to large-engined ships and to a pushed tow system. The water draw down in the waterways involved with these vessels is outside the range of experience with traffic up to now, with regard to the northern and western German waterways and the revetments, which, according to experience, have had the stability to withstand the required range of loads with the construction methods up to now. However, we know, that in most cases the safety factor only has a value of slightly greater than 1, so that under large hydraulic loads extensive damage to the revetments would be unavoidable. A situation of this kind arose once at the beginning of the 70's, when geotextile filters began to be used in constructions. You can all well imagine, that the effect of mineral filters does not only consist of preventing the migration of fines out of the subsoil, but also that mineral filters reduce pressure too, i.e. subdue it, and due to their surcharge contribute to the stability of the subsoil. The pressure reduction could be clearly seen in the picture of the potential field. If a grain filter layer of this kind with a thickness of 30 - 40 cm is replaced by an almost weightless geotextile only a few millimeters in thickness, it can be observed, that the surcharge is no longer adequate to guarantee the stability of the revetment. The consequences of this construction method at that time were, that migration of material below the geotextile and deformations in the revetment (fig. 13) occurred, which led to the production of a two-layered geotextile filter with a so-called 'roughness' or

'clawing layer', which today is generally described as an 'additional layer'. At that time, the reduced stability of the cover layer, due to the absence of stability of the subsoil, was compensated by the development of 'grouting'. Through grouting the loose riprap is connected making greater units and a disk effect is produced, through which longitudinal forces can be lead to the bed of the waterway. This has a positive effect on the stability of a revetment, but the revetment loses its flexibility. The grouting can, however, only increase the weight on the subsoil to an insignificant extent, so that, as before, it is still possible for the soil to migrate under the geotextile, which has actually been observed. From this it was deduced that revetments must be flexible. In my opinion, the flexibility is, however, no longer a compelling criterium, if the stability of the subsoil is guaranteed at each point, where the hydraulic loads occur, assuming of course, that stability exists at each point.

Comparison calculations

Taking the above geotechnical aspects regarding the stability of revetments, I have carried out several model calculations for a waterway with a trapezoidal cross section, where the width of the water surface was varied (Schulz [6]). A ship was selected, corresponding in size to the large-engined freight ships, and it was assumed that the subsoil conditions had certain characteristics, which I will mention later. For 90% and 95% of the critical speed and for the critical speed itself, I selected the required stone size, according to the supplement of the PIANC-bulletin of the working group no. 4 (PIANC [4]). In fig. 14 we can see, that assuming a bulk density of 2,75 g/cm^3 the stone sizes, which are necessary during a passage at 90% or 95% of the critical speed, correspond to categories 2 and 3 (fig. 15) of the stone sizes for hydraulic structures. If the ship's speed increases further, the size of stone required increases overproportionally (fig. 14).

If we take a look at the second criterium, necessary for the overall stability of the thickness of the cover layer, then we have a similar situation (fig. 16). At 90% and 95% of the critical speed of a large engined freight ship, in almost all cross sections

we can manage with the normal thickness of the cover layer, which is as a rule between 40 and 60 cm, even in the selected standard cross section with a water surface width of 52 m. Thus no failure is to be expected with subsoil 1. However, if the ship's speed increases above the amount of 95% of the critical speed, then a limit state occurs with a standard revetment, due to liquefaction of the subsoil.

We will now make a brief comparison again with the Rhine-Herne canal ship (fig. 17), which sails the same cross section. We can see, that, at 95% of the critical speed, the cover layers are in no way endangered, but that, if the speed is increased up to the critical range, stability problems also arise here. This is of significance, in that we know from the maintenance of older significance, in that we know from the maintenance of older canals, such as for example the Mittelland Canal, that partly the stone sizes and the thickness of the covering layers being nongrouted are not adequate to guarantee stability. In addition to other reasons, the speeds too, which are greater than those usual in West German canals, are made responsible for this.

Subsoil 1, which I referred to above, corresponds to soil type 2 of the Federal Waterways Engineering and Research Institute (fig. 18), as defined for the dimensioning of geotextiles. It represents a type of soil, which as a rule contains little fine sand, is mainly in the medium sand range, and which basically can be described as being non-critical.

If our design is based on a concept, which includes the observation of the stability of the base of a cover layer, then we must also concern ourselves with the weights of the filter layers needed. The illustrations, which I have shown you up to now, all referred to a grain filter with a thickness of 40 cm as a base and the thicknesses of the revetments were adapted to this.

The grain filter naturally subdues the excess pore water pressure, and, due to its much greater permeability, it contributes a great deal to the surcharge, which affects the subsoil stability. In contrast, a geotextile filter has practically no bulk. Consequently, it is not surprising, when in a design concept for geotextiles a greater

revetment thickness is given. The increase in thickness, which is shown in fig. 19, is based on the fact, that the weight of the grain filter was fully included, which is not quite correct, but was used for reasons of simplification, and that a geotextile has no weight to apply to the subsoil. You can recognise a considerable increase in the required thickness of the cover layer for large engined freight ships travelling at 0,9 times the critical speed.

Of course, the permeability of the subsoil is still a very important factor, since, if excess pore water pressures play a role, then, as already described, the permeability plays a considerable role. The smaller it is, the more difficult it is for the water to flow out of the soil, and the greater the required hydraulic gradients become, and accordingly the excess pore water pressure becomes greater and the necessary thicknesses of cover layers must increase. You can see in fig. 20, that, where the permeability is smaller by twice the power of ten, for large-engined freight ships sailing on the centreline of the canal, the required cover layer thickness for a waterway width of 55 m increases to approximately 90 cm.

These comparisons are based on subsoil 2, which corresponds to soil type 4 (fig. 21) of the Federal Waterways Engineering and Research Institute. It is a soil, with a substantial portion of silt and very low permeability, but still without cohesion, which would increase the stability.

In the design concept, the shear strength of the subsoil is an important parameter in the form of a friction angle. In fig. 22, where the angle of internal friction was varied, it can be seen that the required revetment thickness decreases as the angle of internal friction increases. As soon as the friction angle reaches values, which can be achieved naturally with sand and gravel, there is a point, at which the thickness of the cover layer is no longer determined by the stability criteria of the subsoil, but by pure interlocking criteria of the revetment stones. It may not be reduced any further below these values necessary for proper interlocking.

Constructional problems

Structural engineering difficulties occur, when the enlargement of the waterways has to be carried out in water, i.e. during continuous shipping traffic. How is the enlargement basically carried out in this case?

The enlargement of the waterways during continuous shipping traffic is carried out in a longitudinal direction. The new cross section is produced by widening and deepening it by means of underwater dredging. In order to obtain a most accurate profile as possible, it has become customary to carry out the earth excavations using hydraulic excavators on stilted pontoons, where the excavator driver can as a rule control the position of the shovel via a monitor. Pontoons held by wires and anchors have proved to have an inadequate positional stability.

The accuracy of the profile, when forming the subgrade, is an important precondition for producing a good filter. When geotextile filters were first introduced, it was thought, that the problems with the placement of grain filters regarding the positional accuracy, the danger of segregation and the constant layer thickness had been solved. However, the installation technique at the time was not at all suitable for laying down a geotextile without folds and for covering the subgrade completly. The latter effect is, however, a further precondition for avoiding soil migration under the geotextile as far as possible. Further problems arose with placing geotextiles, when lowering them down to the bed of the waterway from the pontoons and, subsequently, covering them with riprap, because the geotextiles act as a 4 m high sail in the water and the hydrodynamic forces from the return current of passing ships had considerable consequences. The pontoons anchored by wires moved by meters while other ships passed and it is easy to imagine, that both the geotextile and the seams had to tolerate considerable tensile forces. Furthermore, the laying is not very exact and as the riprap is poured on, any movement of the loosely layed geotextile cannot be controlled. Findings of divers in the 80's have also confirmed, that considerable transverse shortening accured and the overlappings of 1 m had thus not been maintained, that through the passing ships the edges in the overlapping areas, where the

geotextile was not covered by riprap, had become folded over, and that the planned status had not been achieved at all.

In the second half of the 80's new impulses were set and a system of placing the geotextiles to the ground with a big roller which moves on the subgrade with own excititation was introduced (fig. 23). Today, practically no geotextile is placed without a roll, unless it is self-rolling, or it merely acts as a deflection roller close to the ground.

The negative experiences with the application of geotextiles, after the initial euphoria, have caused more attention to be paid once more to the grain filter constructional method, and the problems regarding falling down through the water were examined more closely. In the mideighties fall tests in West German canals showed, that grain filters, which are placed correctly by falling down from the water surface, are found orderly even at a depth of 4 m. Tests with large crates anchored at various points on the subgrade have shown this. More recent investigations in the Mittelland Canal with a lowerable feeding structure, whereby the laminae are not opened until it is immediately above the subgrade, have shown that by shortening the free fall distance of the filter material it can be distributed more evenly, but especially, where the exactness of the subgrade does not come up to standard, it is difficult to guarantee the regularity of the filter construction. However, the difficulty in controlling the complete process from a technical point of view plays a very large role here.

Up to now little has been invested in the sector of control. A very wide gap exists here between the design, tender and contract stages and the monitoring and controlling of the work carried out on the construction site. This gap must be closed, in order to obtain more stable and especially durable revetments.

The positional stability of a bank-lining is a necessary precondition for a naturally wide variety of plants to grow along a canal bank. Only where this condition has been fulfilled, can a canal bank also be set out using technical means, which, under the given assumptions resulting from the waves from shipping, allow an ecologically attractive solution to be found for the bank slope and the subsoil.

Literature

[1] Hjortnaes-Pedersen, A.G.I., Bezuijen, A. and Best, H. (1987): Non-steady flow under revetments using the Finite Element Method, 9th Europ. Conference Soil Mech. and Found. Eng., Dublin

[2] Köhler, H.-J. and Schulz, H. (1986): Use of geotextiles in hydraulic constructions in the design of revetments. In: Proc. 3rd Int. Conf. on Geotextiles. Viene, Austria, p. 1185-90

[3] Köhler, H.-J. and Feddersen, I. (1991): In situ measurements of pore water pressure in soils and concrete constructions. In: Proc. 3rd International Symposium on Field Measurements in Geomechanics, Oslo

[4] PIANC (1987): Guidelines for the Design and Construction of Flexible Revetments Incorperating Geotextiles for Inland Waterways. In: Report of Working Group No. 4 of the Permanent Technical Committee I, Supplement to Bulletin No. 57

[5] Söhngen, B. and Zöllner, J. (1992): Schiffahrtsversuche auf dem Dortmund-Ems-Kanal. In: Binnensschiffahrt - ZfB - Nr. 8

[6] Schulz, H. (1993): Auskleidung der Wasserstraßen - Grenzen der Nutzung. In: Binnenschiffahrt - ZfB - Nr. 5

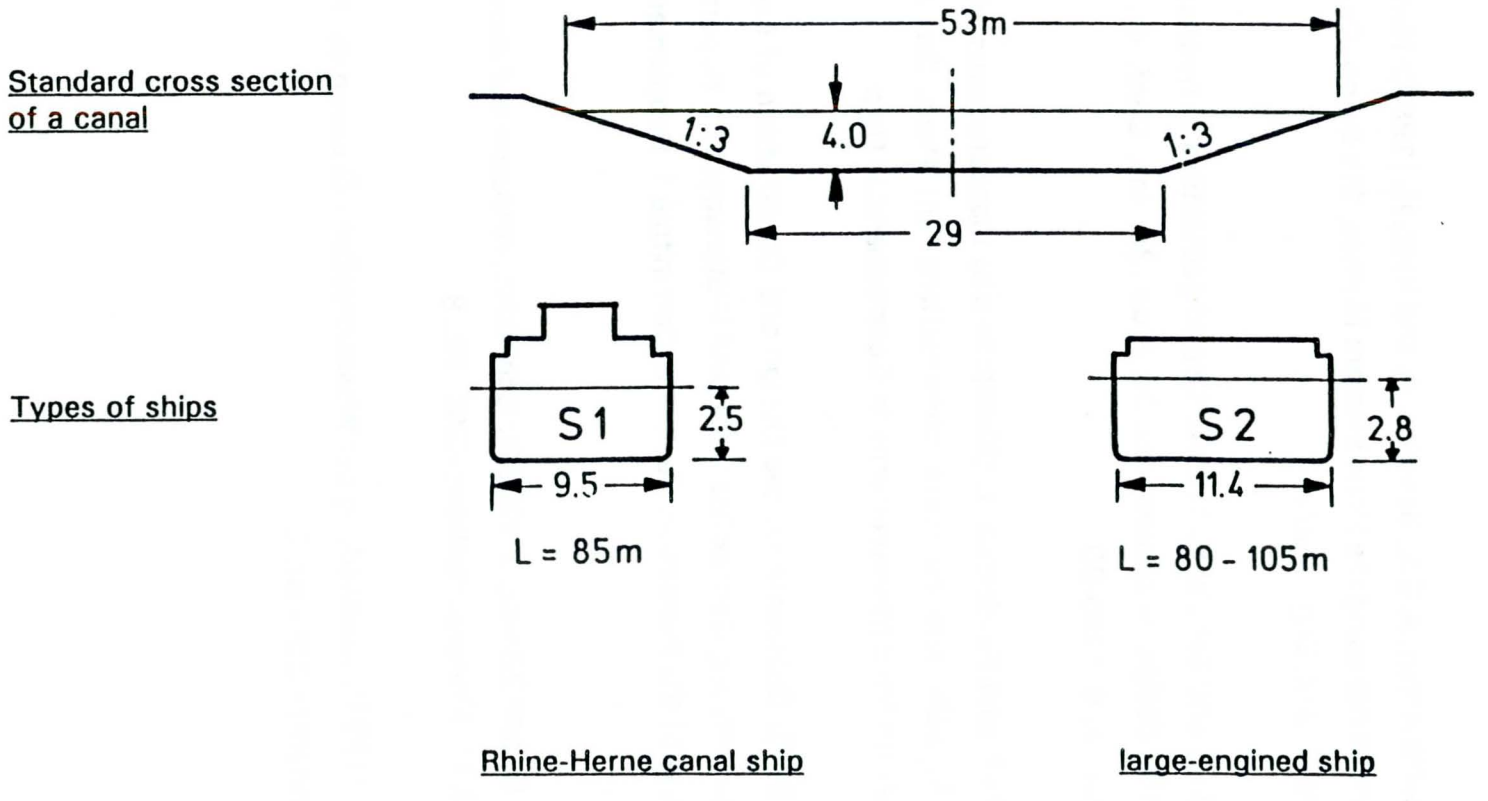

Fig. 1: Cross section of west an northern German waterways

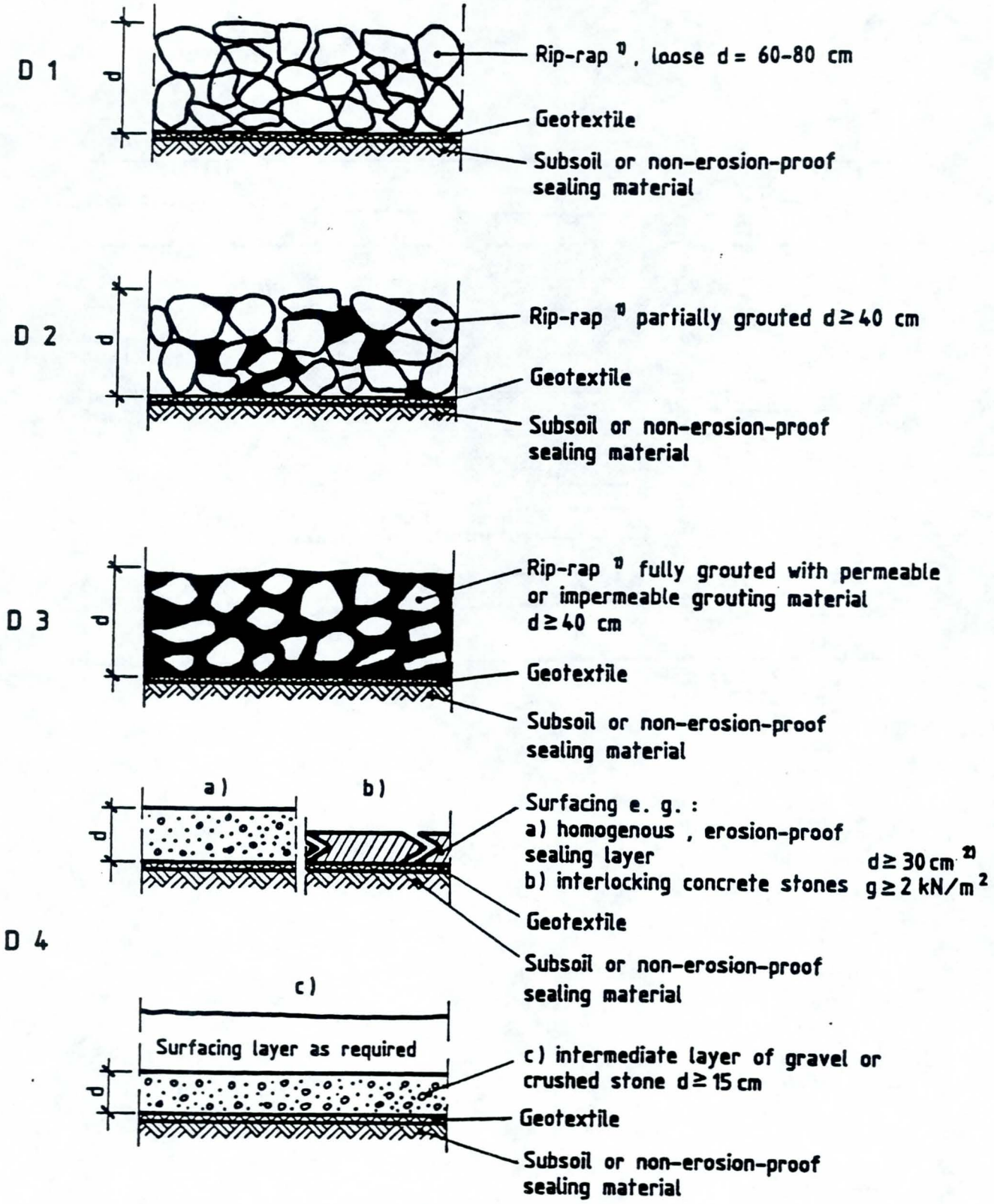

Fig. 2: Standard design forms for permeable revetments

1) Category II or III according to the technical delivery conditions for stones for hydraulic structures (TLW)

2) does not apply in connection with asphalt costructions (see EAAW)

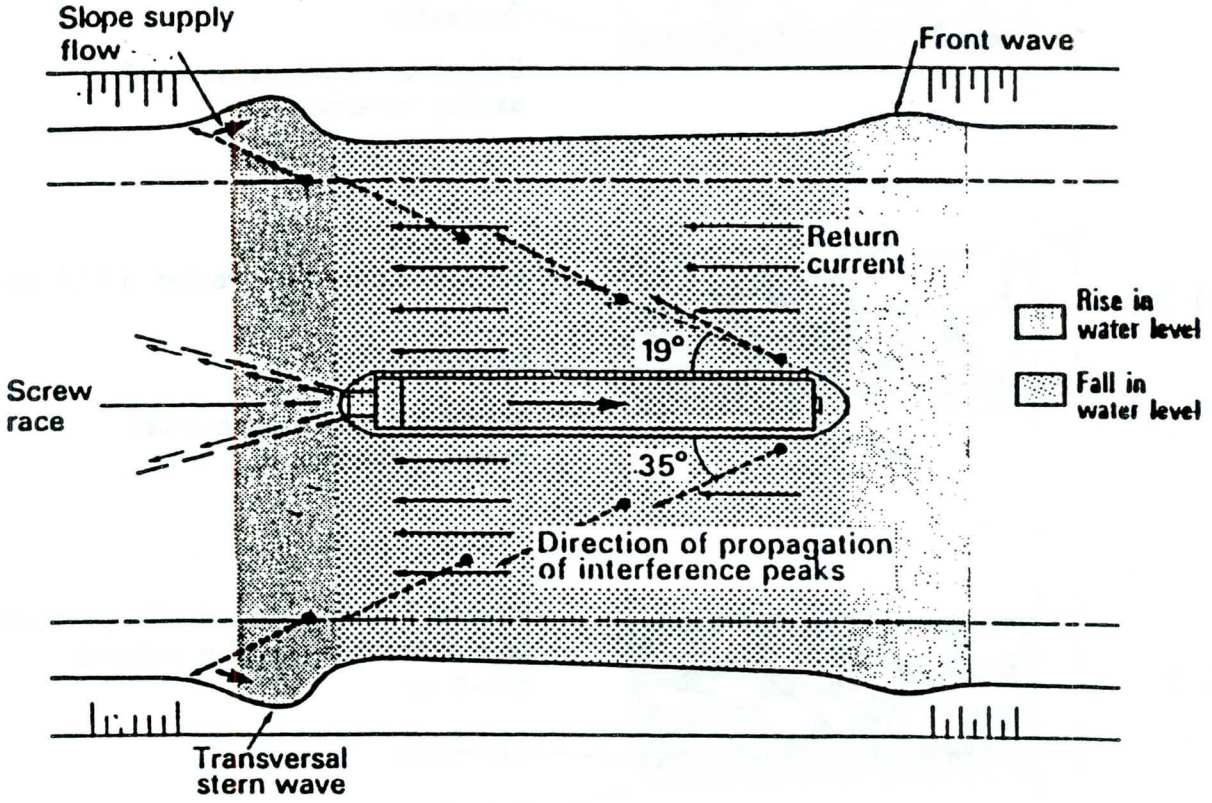

Fig. 3: Hydraulic loads in canals

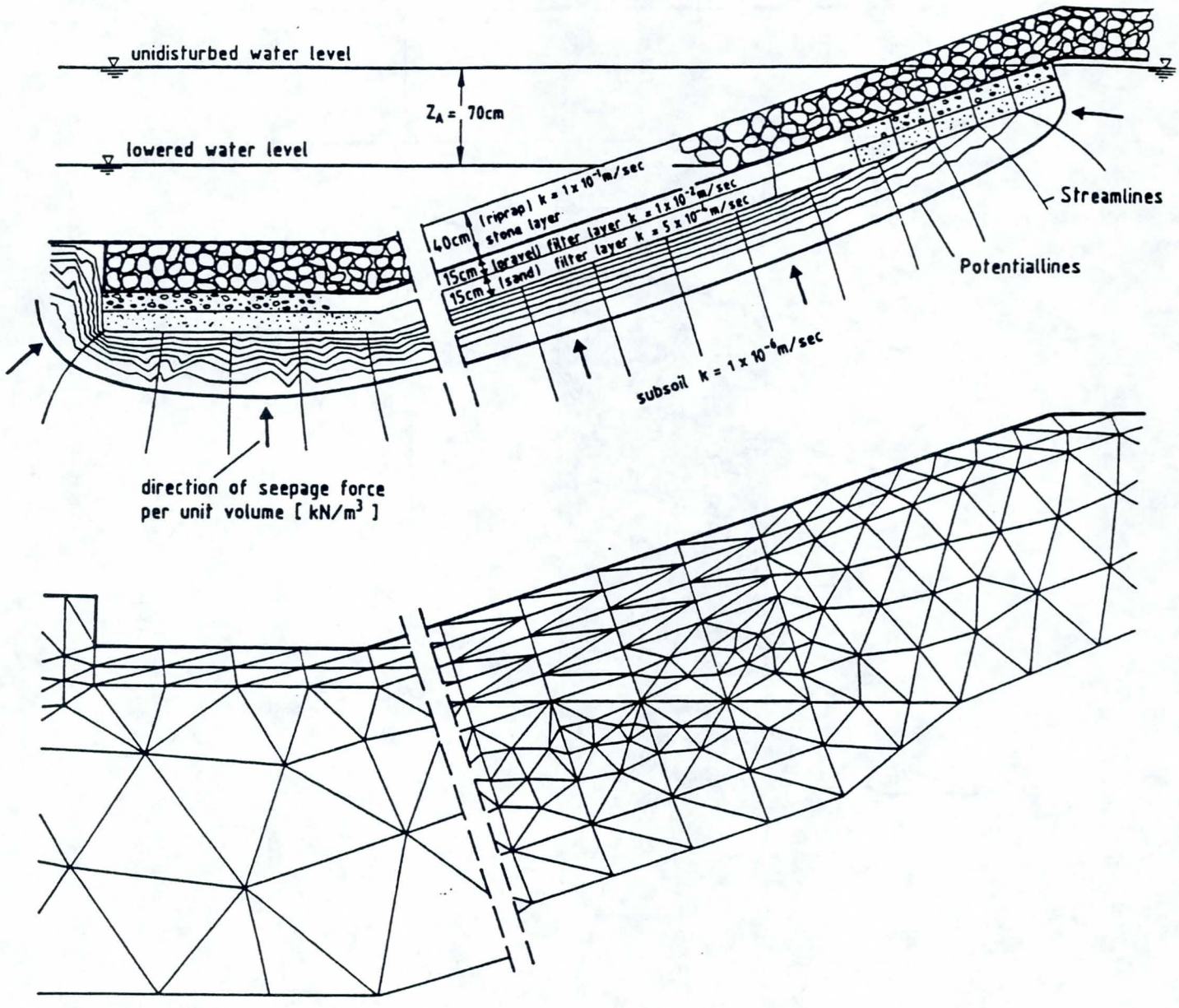

Fig. 4: Net of iso-potential and stream lines for a water table draw down

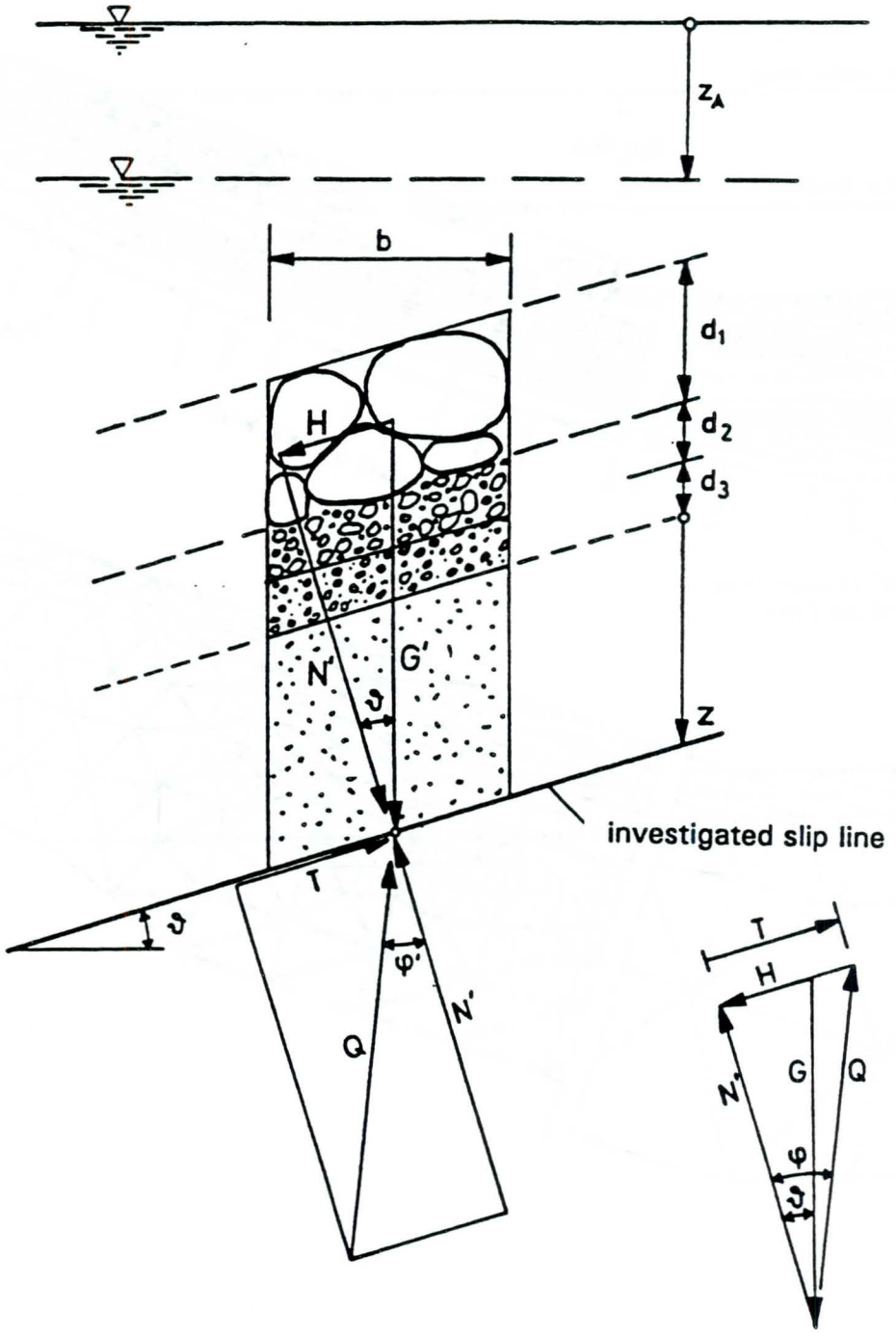

Fig. 5: Element of a revetment including the subsoil with a slip line without water level draw down

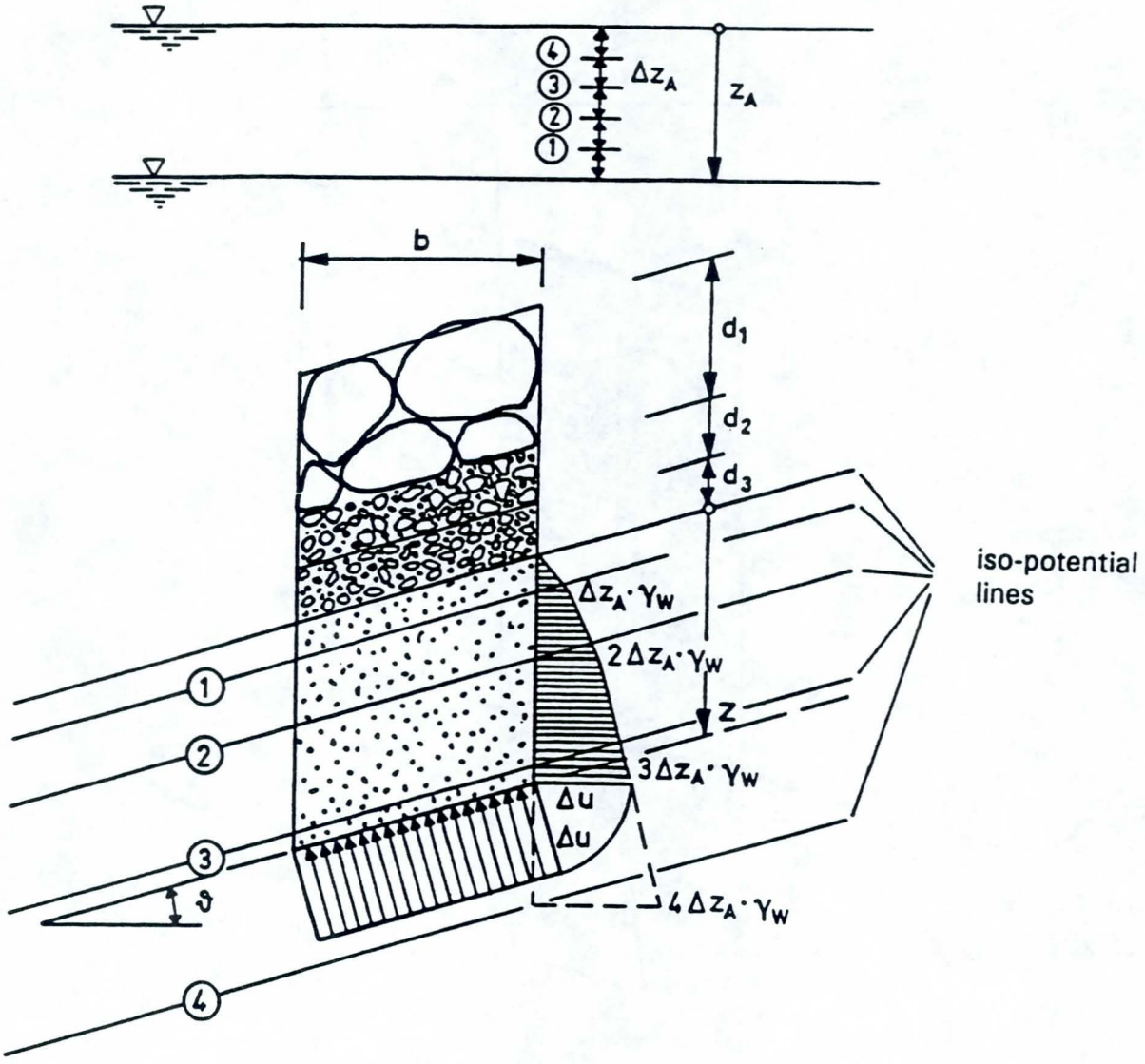

Fig. 6: Revetment including the subsoil with iso-potential lines due to water level draw down

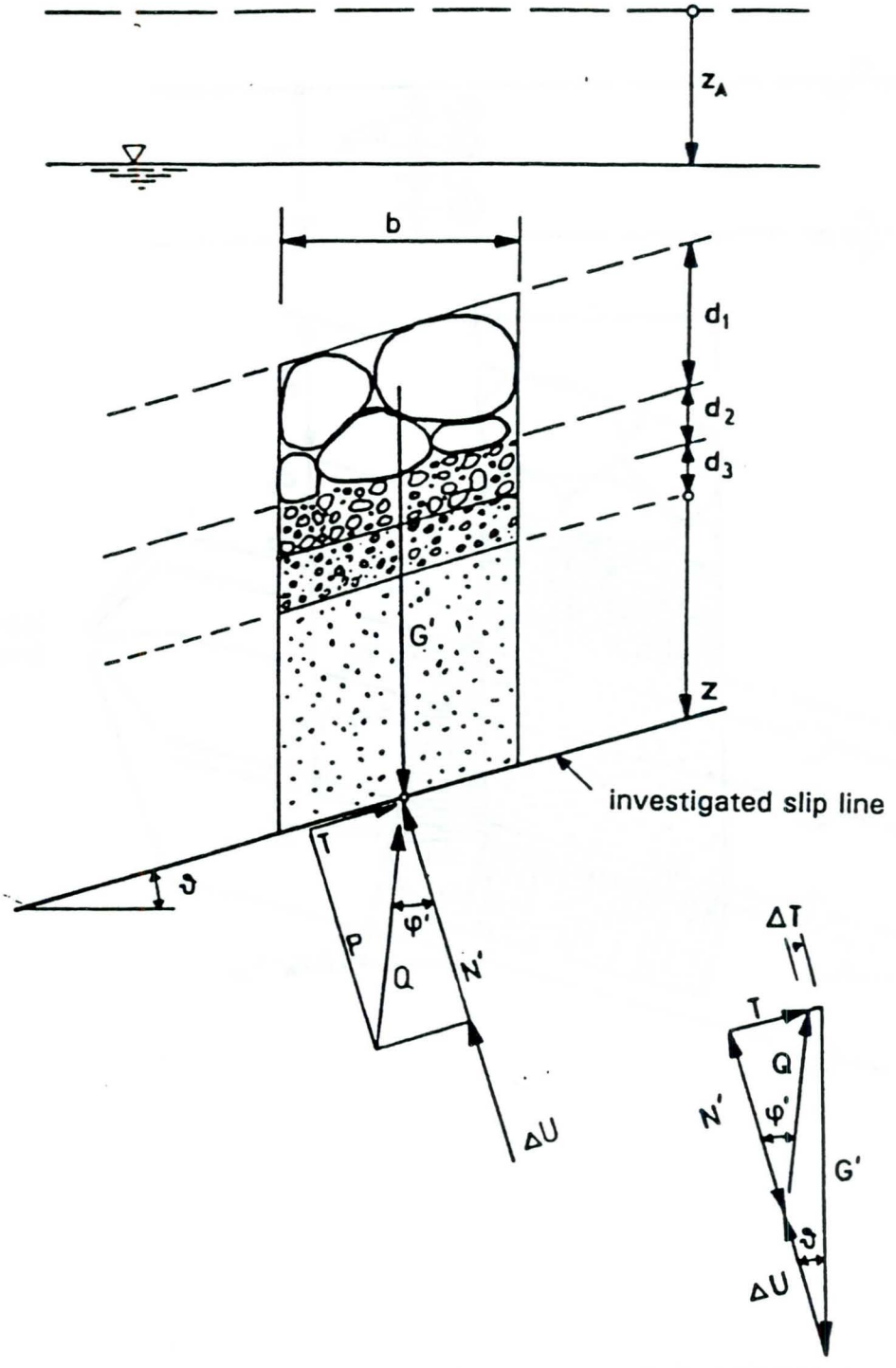

Fig. 7: Revetment element with slip line in the subsoil and force polygon

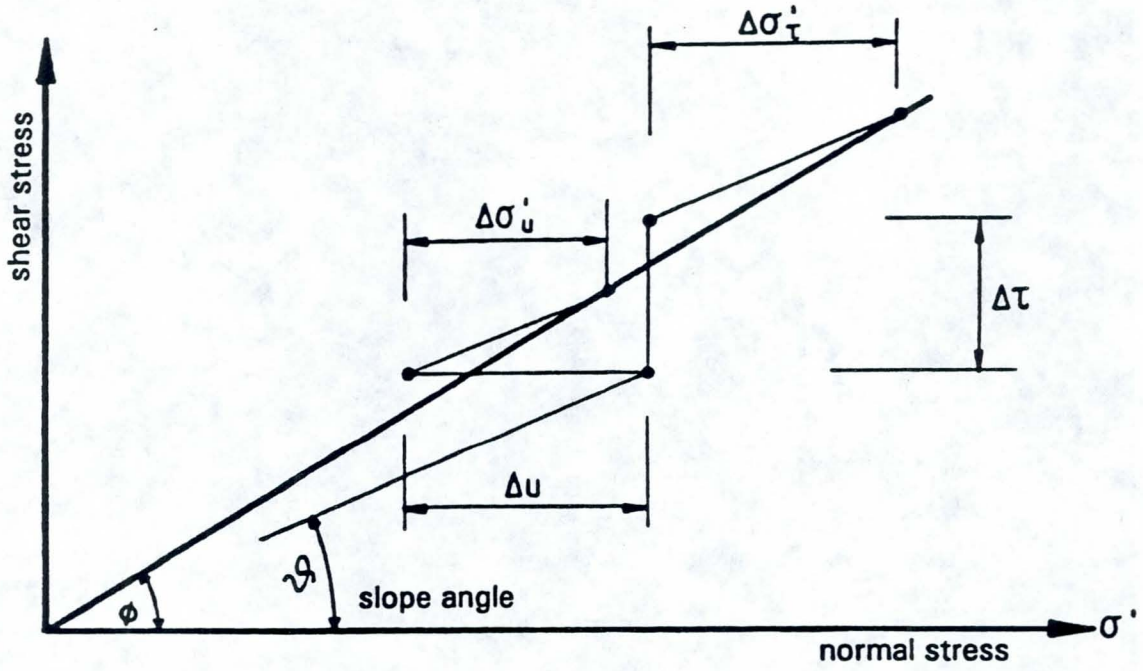

Δ u excess pore water pressure due to draw down

Δ σ_u' necessary surcharge in case of Δ u

Δ τ additional shear stress due to flow of water

Δ σ_τ' necessary surcharge in case of Δ τ

Fig. 8: Stability conditions for the subsoil

Fig. 9: Model test pit for revetment investigations

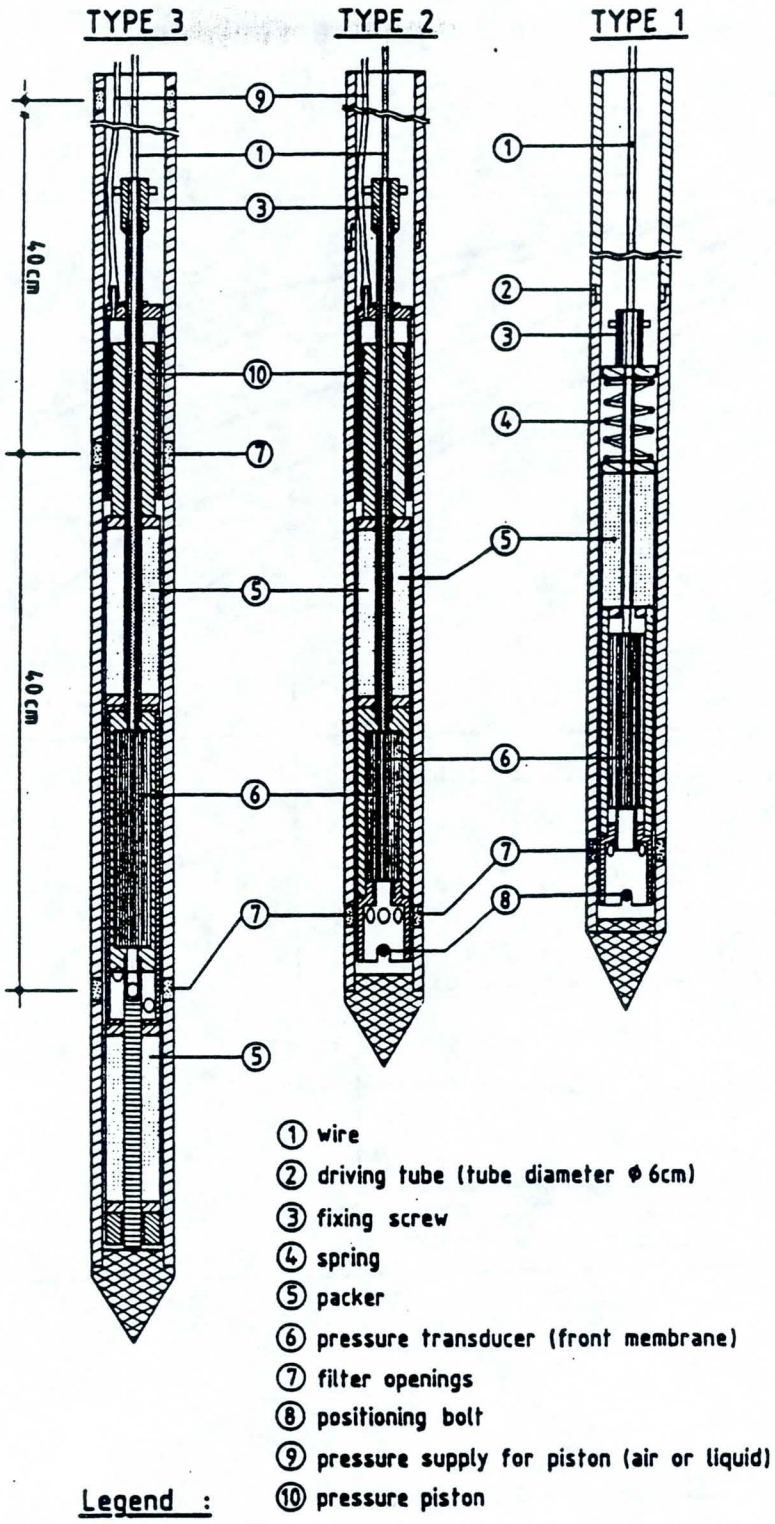

Fig. 10: Pore water pressure measuring device

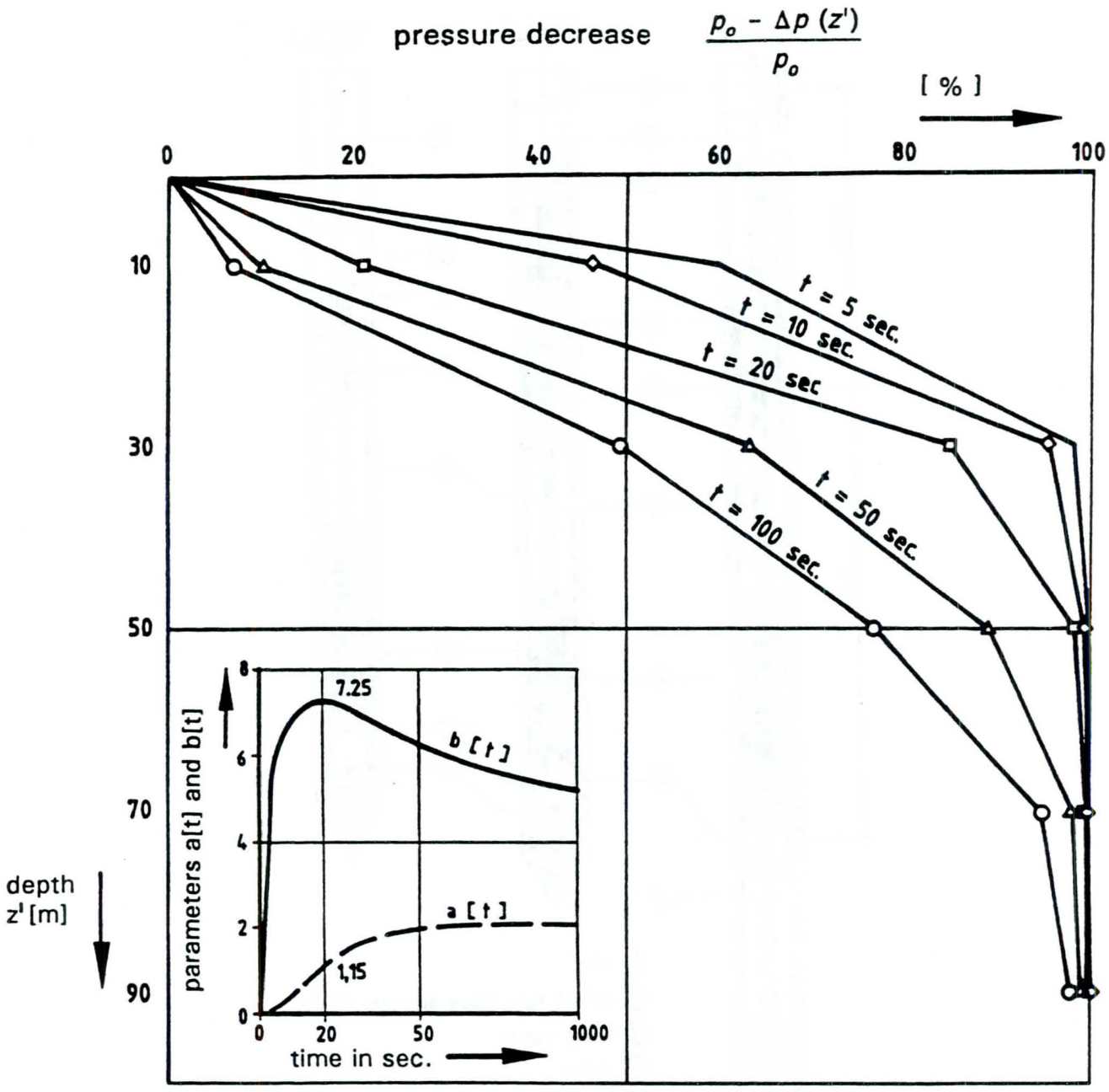

Fig. 11: Relative pore pressure change over depth z'

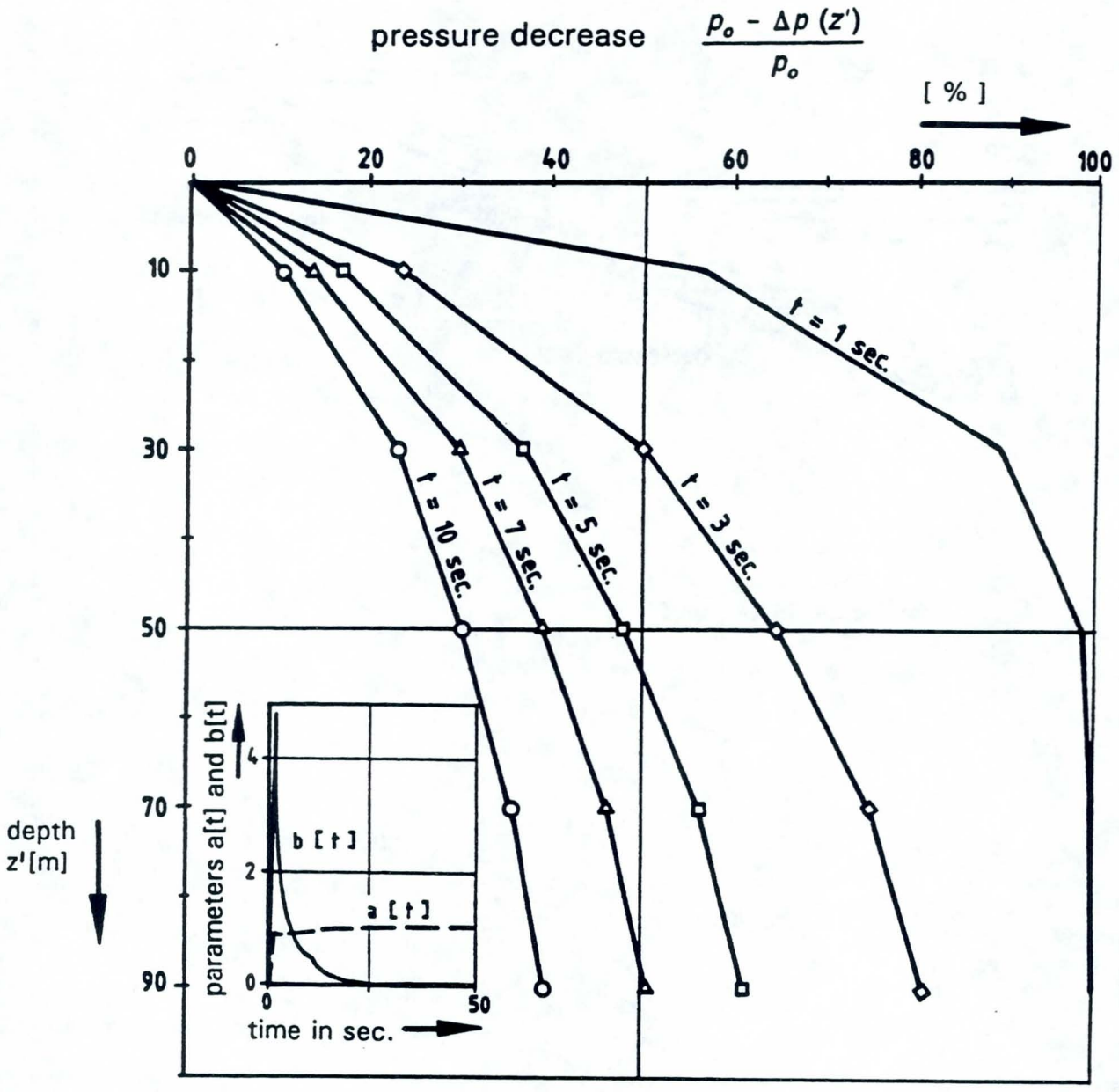

Fig. 12: Relative pore pressure change over depth z'

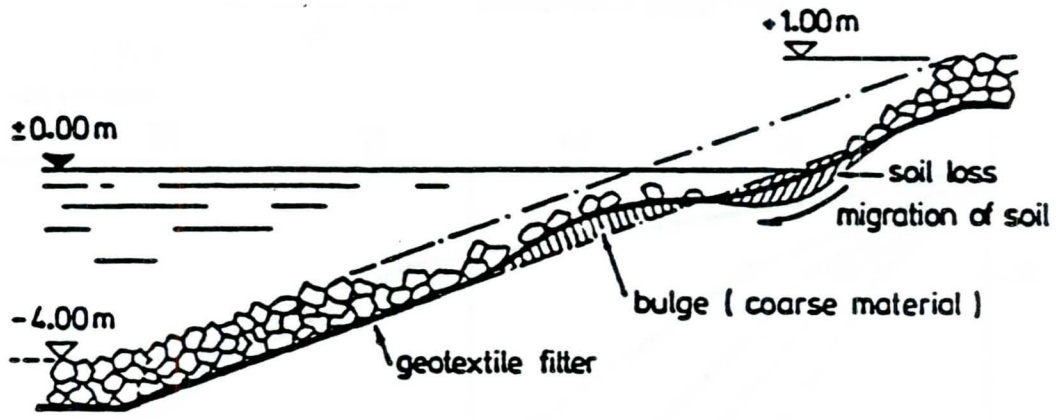

Fig. 13: S-shaped failure profile

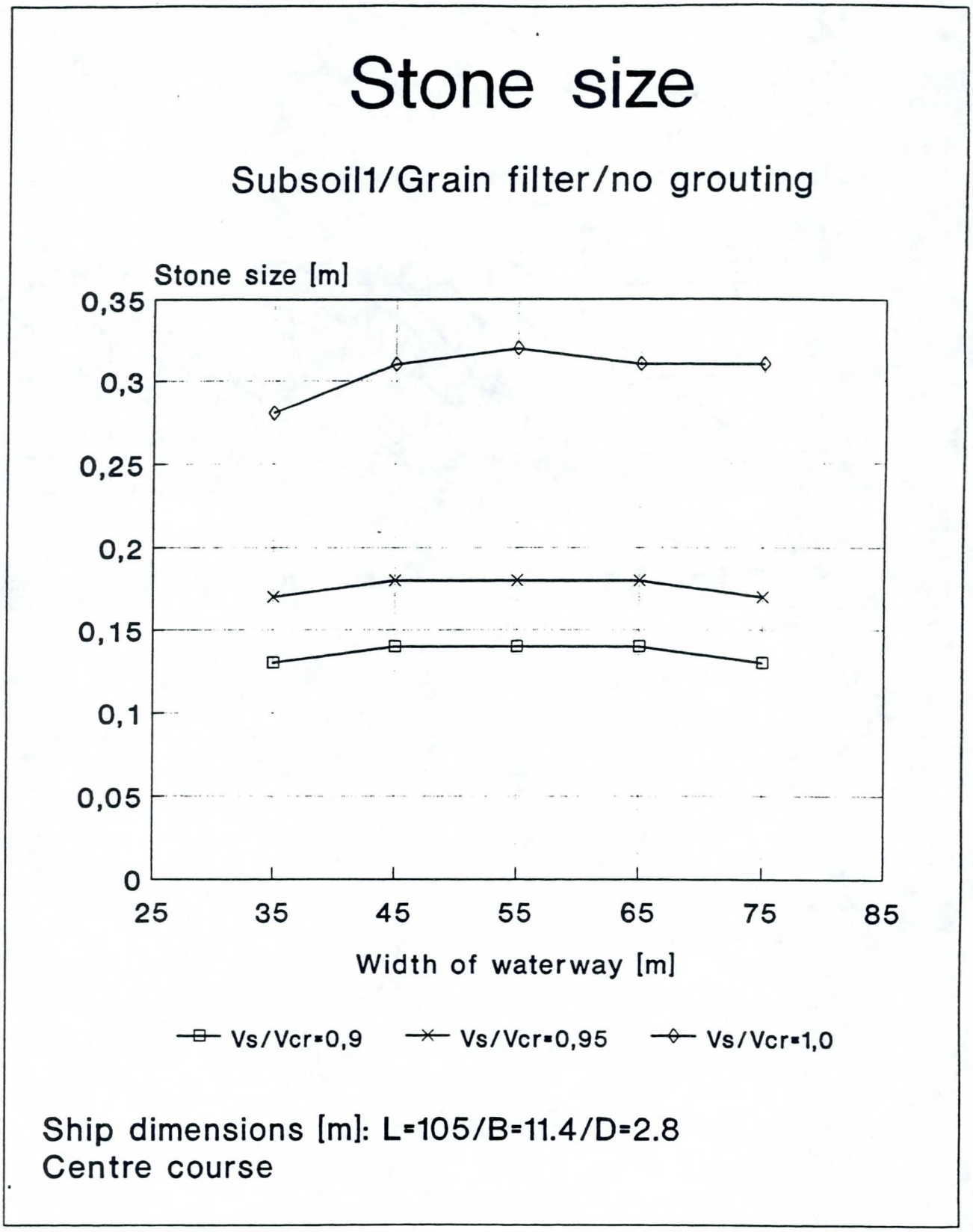

Fig. 14: Stone size D_{N50} as function of the speed of a large-engined ship over the width of a waterway

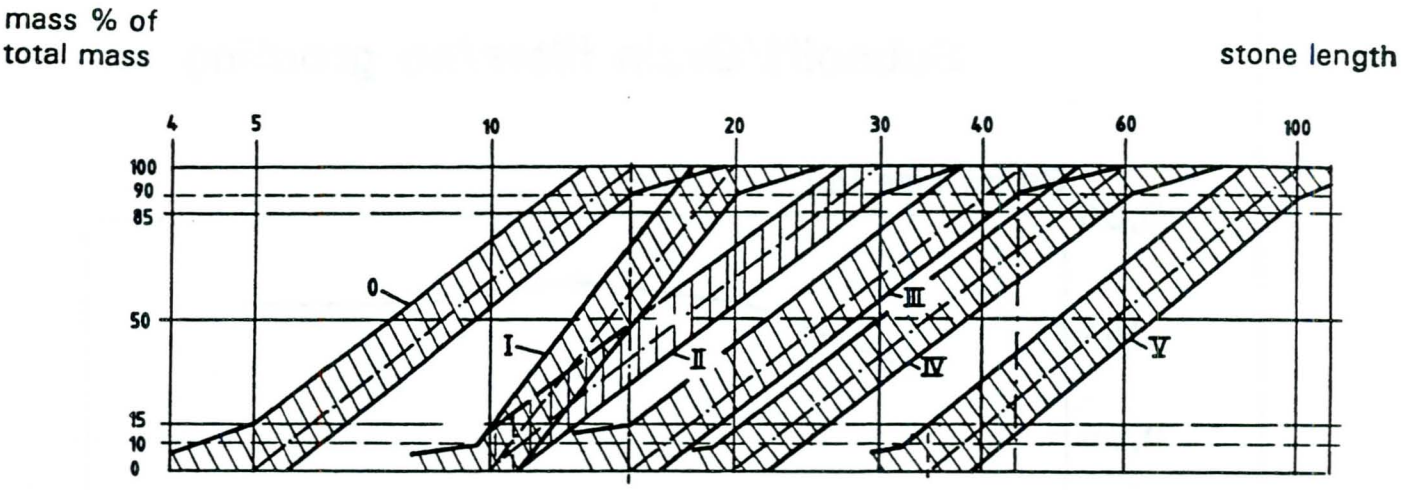

Fig. 15: Stone size classes 0 to V for revetments for German inland waterways

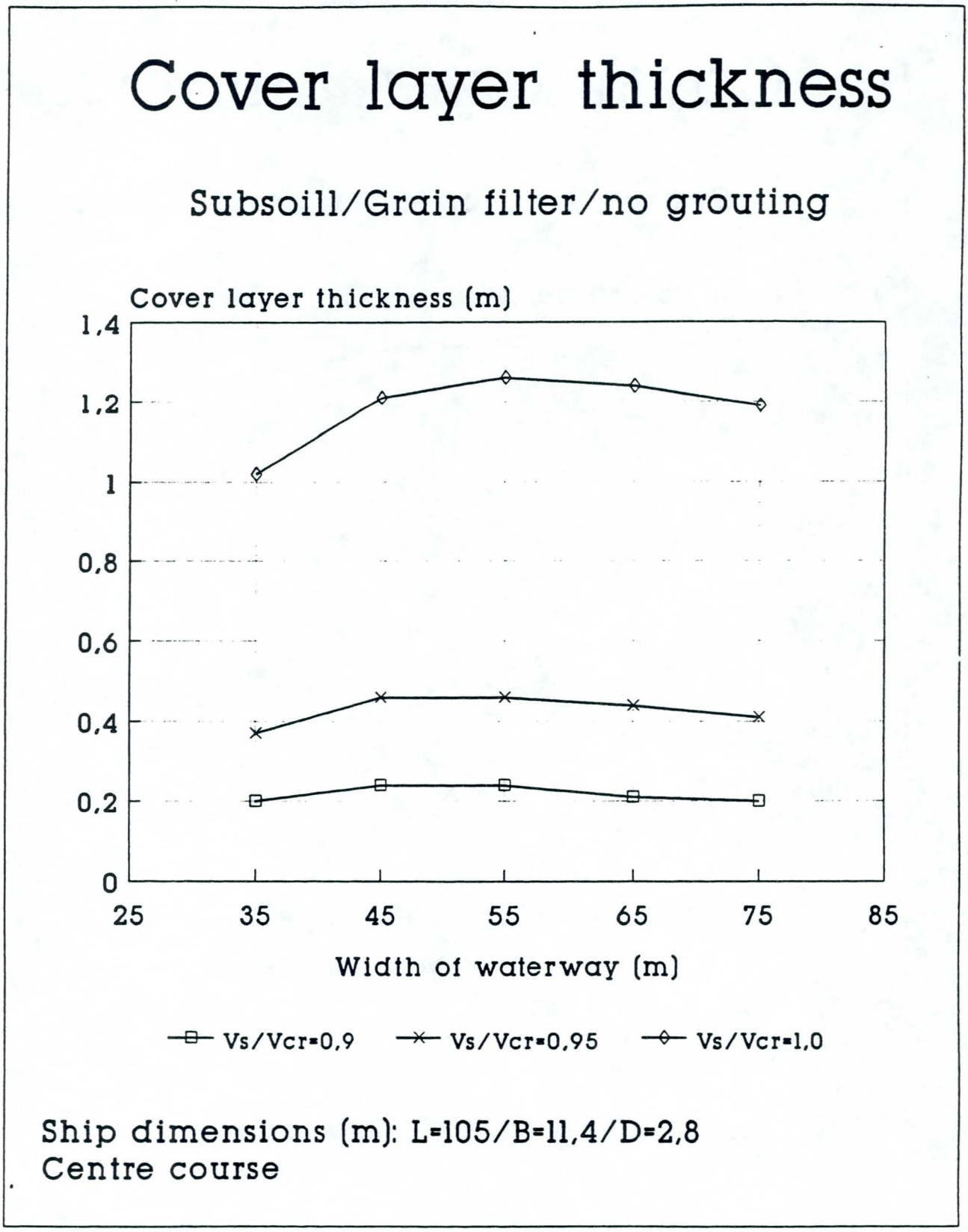

Fig. 16: Thickness of revetment as function of the speed of a large-engined ship over the width of a waterway

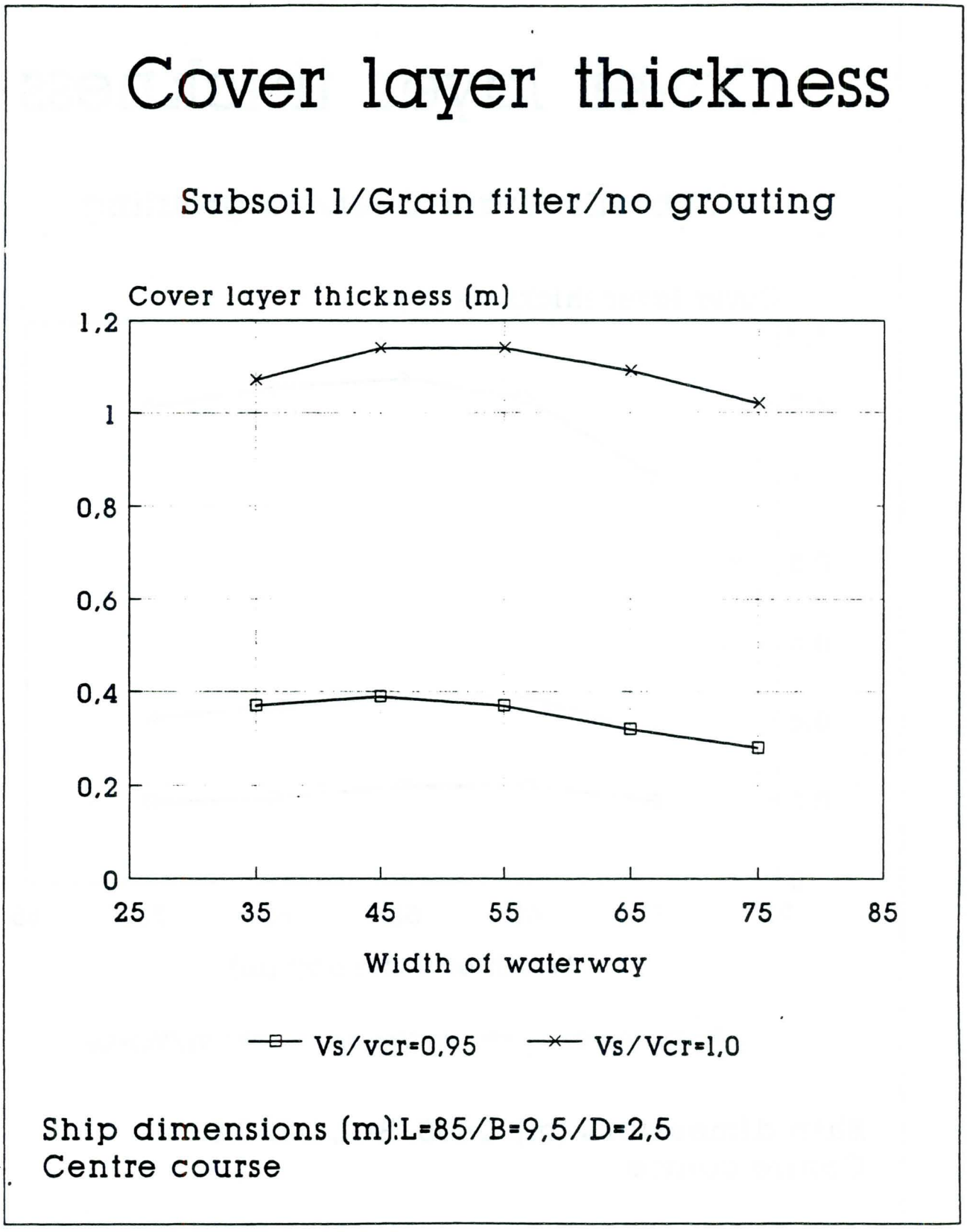

Fig. 17: Thickness of a revetment as function of the speed of a Rhine-Herne canal ship over the width of a waterway

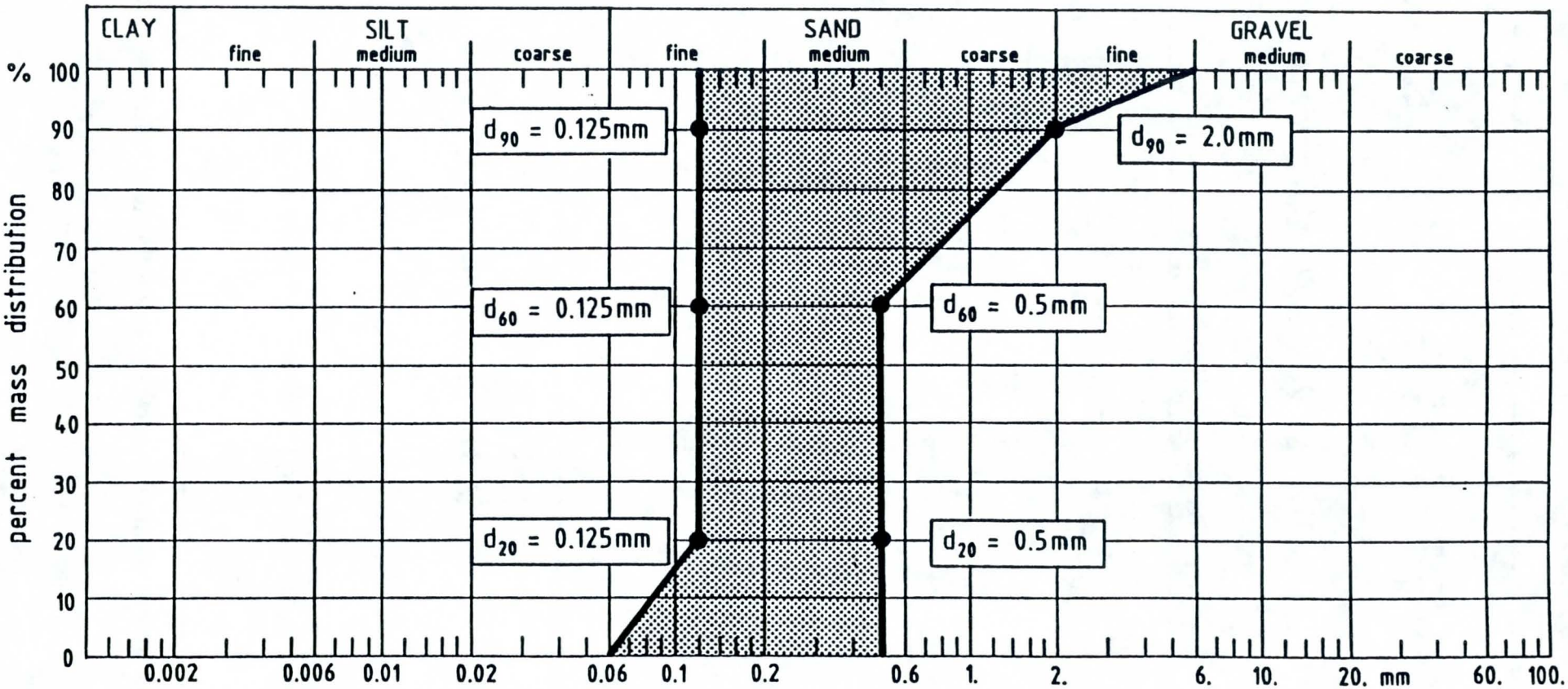

Fig. 18: Grain size band of subsoil 1

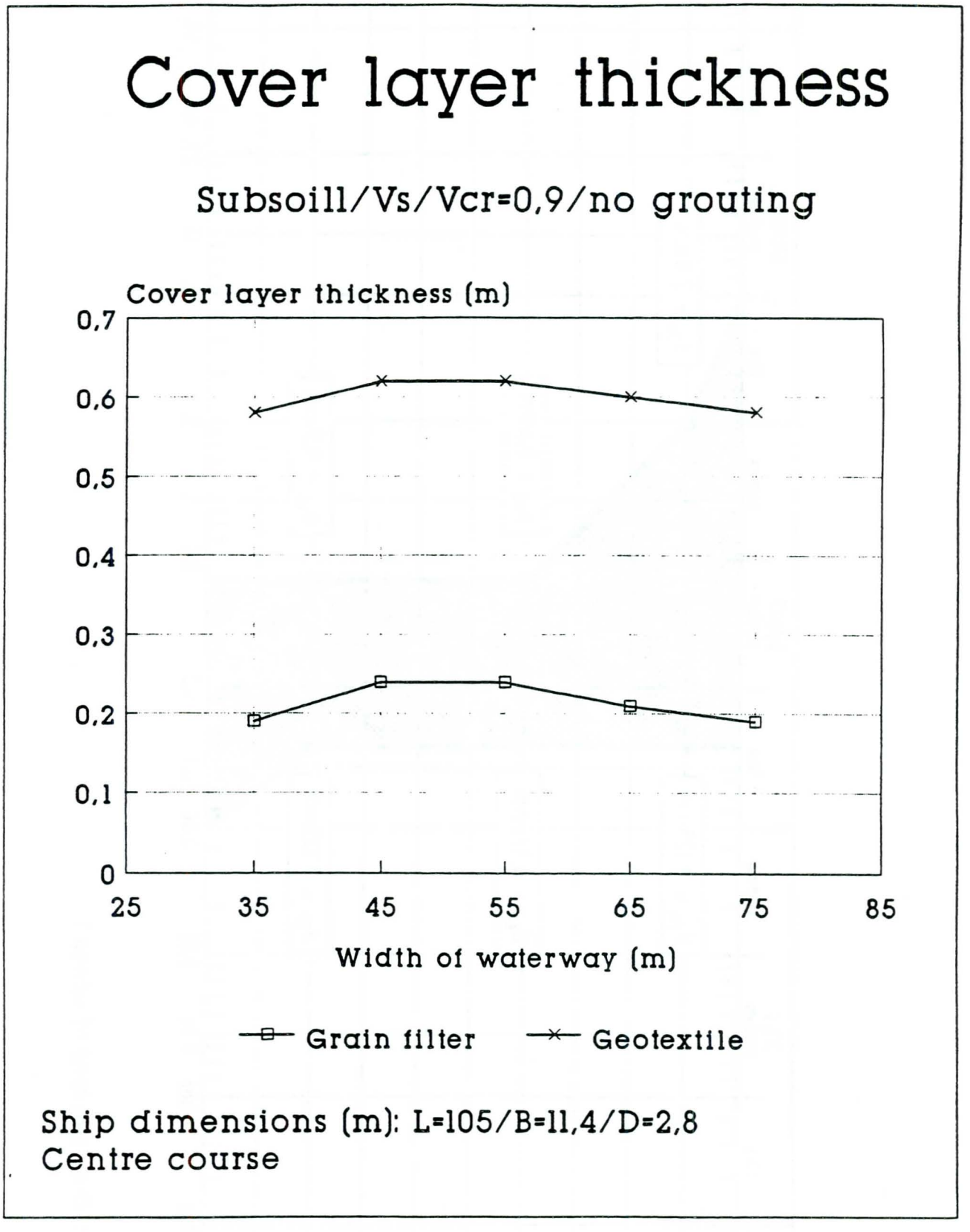

Fig. 19: Comparison of revetment thickness according to different filter types

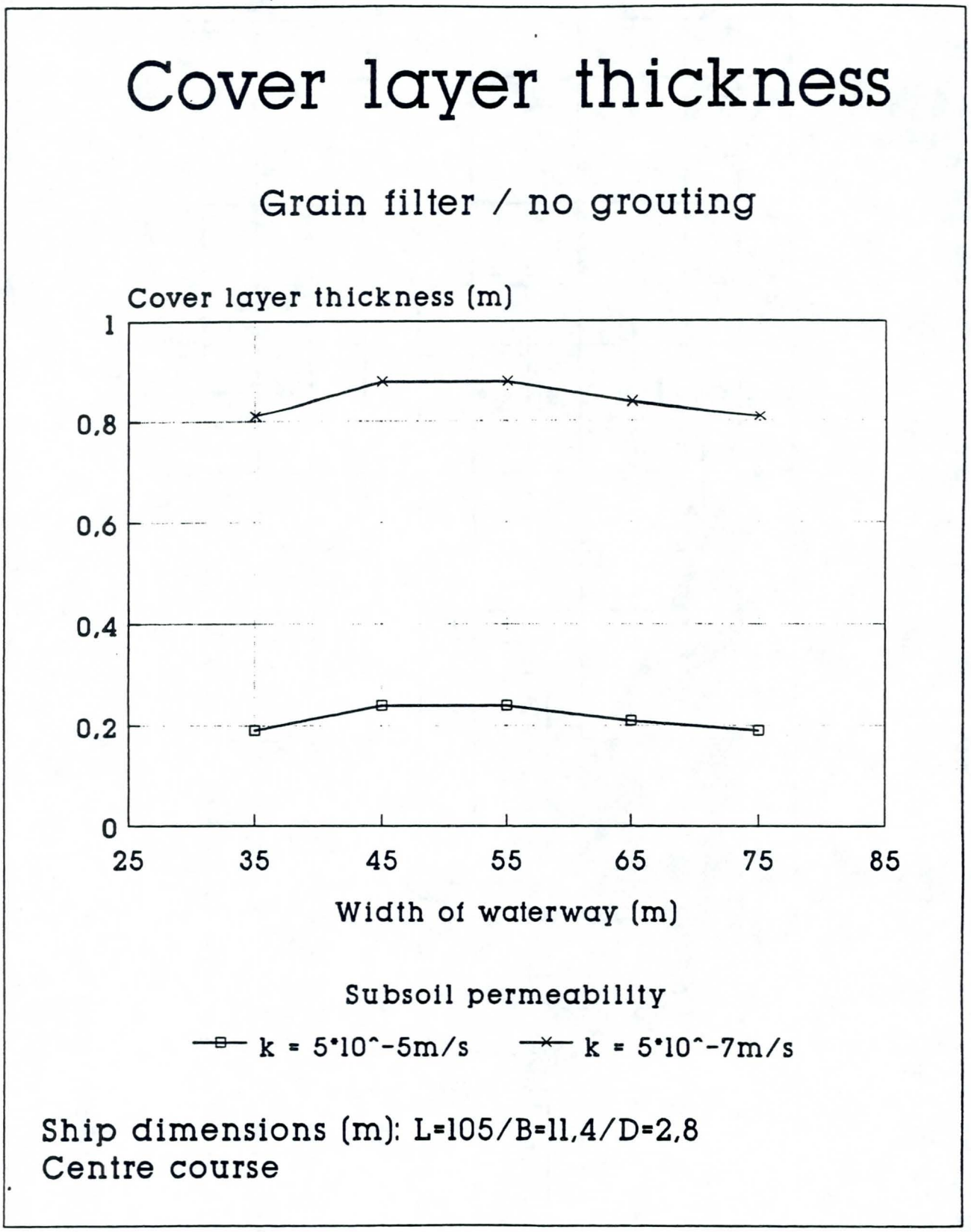

Fig. 20: Comparison of revetment thickness according to different subsoil conditions

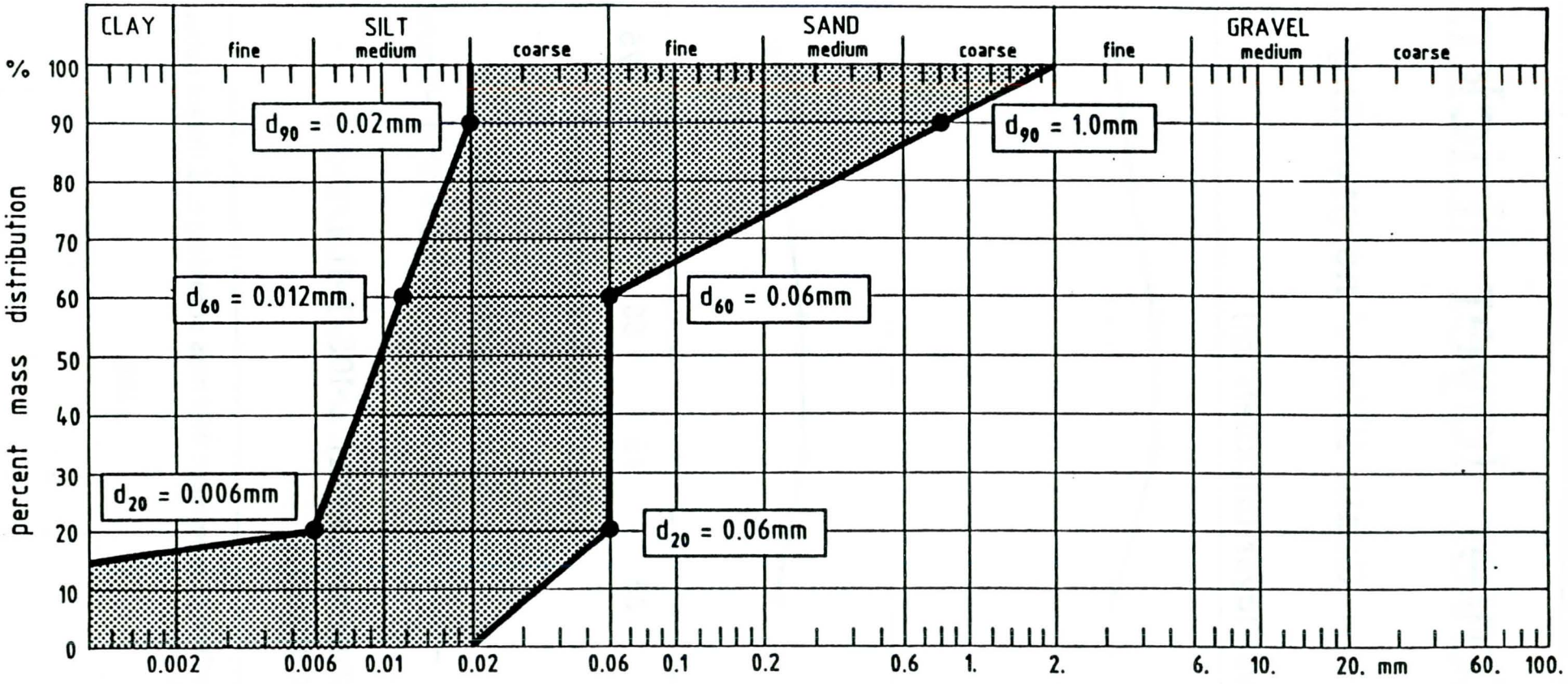

Fig. 21: Grain size band of subsoil 2

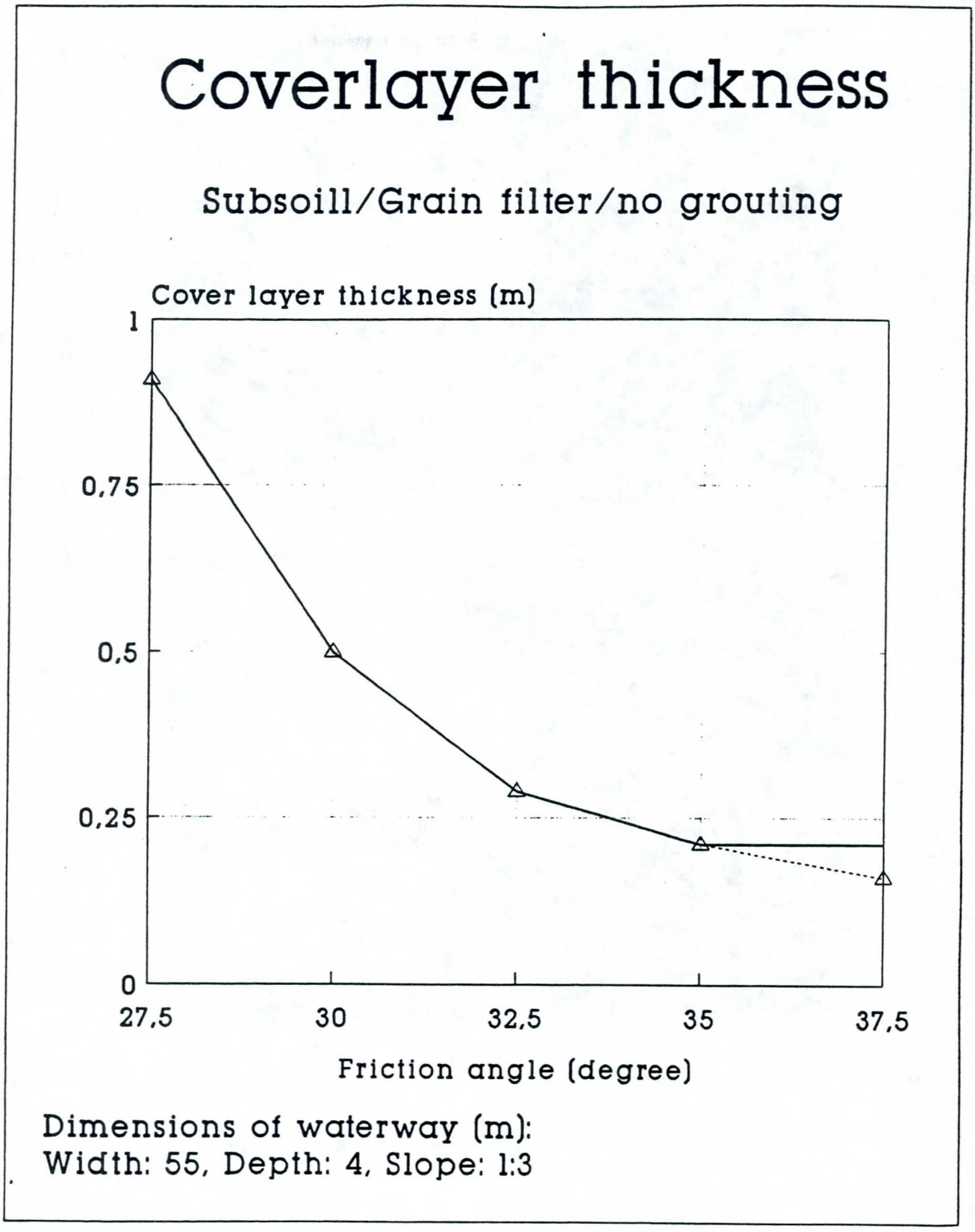

Fig. 22: Revetment thickness over friction angle of subsoil

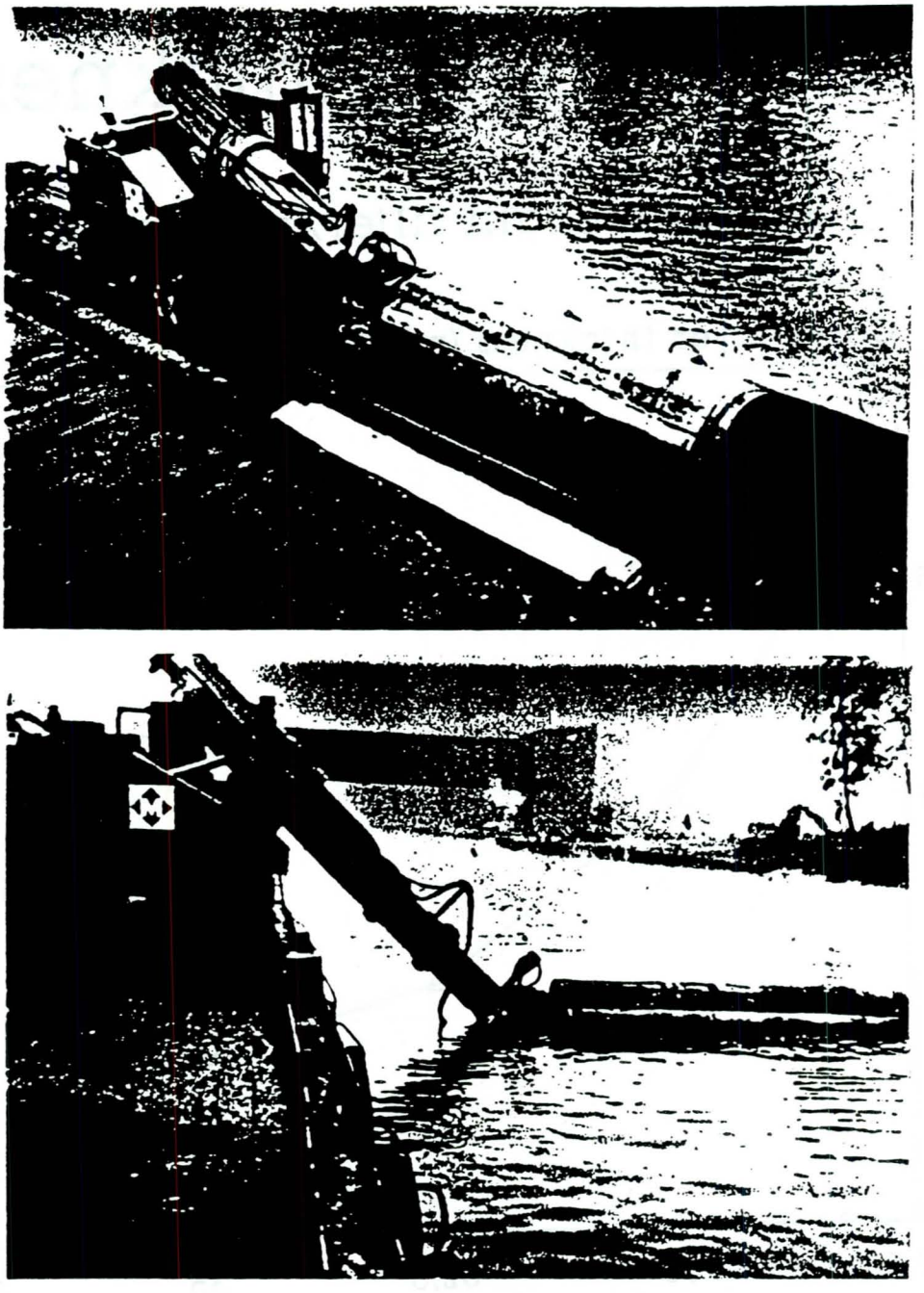

Fig. 23: Roller for placing geotextiles onto the subgrade

TOWARDS GREENER RIPRAP: ENVIRONMENTAL CONSIDERATIONS FROM MICRO- TO MACROSCALE

F.D. Shields, Jr., C.M. Cooper and S. Testa, III
US Department of Agriculture, Agr. Research Service
National Sedimentation Lab, Oxford, USA

ABSTRACT

Effects of riprap on riverine fish and macroinvertebrate habitats are strongly related to spatial scale. Three scales are recognized: areas approximately equivalent to the median stone diameter squared (microscale), areas on the order of the square of the channel width (mesoscale), and channel reaches at least ten or more channel widths long (macroscale). At the microscale, riprap typically supports dense, diverse populations of macroinvertebrates and compares favorably with natural bank sediments and woody debris as invertebrate substrate. Biological density and diversity appear to be positively correlated with the range and maximum of riprap stone size. Available evidence from rivers in the US indicates that mesoscale habitats provided by intermittent structures such as spur dikes are superior to those provided by continuous revetments. Macroscale effects of comprehensive planform stabilization of larger rivers on bed material size and cross-section shape (and thus frequency distributions of depth and velocity) have not been clearly established for all stabilized river systems, but drastic reductions in riverine wetlands and backwaters have been widely observed.

1. INTRODUCTION

Riprap is a fundamental tool of mankind for development and control of rivers, streams, and canals. This paper describes effects of riprap on habitats of macroinvertebrates and fishes in riverine ecosystems. The nature of these effects is strongly related to spatial scale. Three scales are recognized: areas approximately equivalent to the median stone diameter squared (microscale), areas on the order of the square of the channel width (mesoscale), and channel reaches at least ten or more channel widths long (macroscale). Small-scale effects reflect modifications to local hydraulic conditions; as scale increases, impacts on geomorphological processes become important. Below we relate the reported biological effects of riprap to physical phenomena, at least by hypothesis.

The effects of replacing natural vegetation and bank soils in riparian zones with riprap are important at all scales and are manifest in aquatic as well as terrestrial communities. However, we have limited the scope of our discussion primarily to aquatic habitats and species, and therefore, little space is devoted to effects above the water's edge. Obviously, this is an artificial distinction. Natural bank and riprap structure habitats are compared herein; much of the value of natural banks is due to overhanging cover, root wads, woody debris, and coarse particulate organic matter (leaves and twigs) provided by trees and shrubs.

2. MICROSCALE

Flow forces are stressful for many aquatic organisms (Statzner et al., 1988), and consequently, organisms that lack very streamlined body morphology seek out zones of reduced shear stress and turbulence in order to conserve energy. Sheltered microhabitats adjacent to flow fields that transport food and waste products to and from organisms are valuable habitats (e.g., a boundary layer adjacent to or within the surface layers of a riprap revetment). Visual observations indicate that flow adjacent to and within riprap structures in rivers is highly nonuniform. Nonuniformity is important because biological diversity is often associated with physical heterogeneity (e.g., Bournaud and Cogerino, 1986).

Quantification of physical heterogeneity adjacent to riprap is difficult. Data describing velocity fields at riprap blanket surfaces and within voids are scarce due to the difficulties of measurement (A review of techniques for such measurements in gravel stream beds is given by Williams and Hynes, 1974). Several investigators (e.g., Abt et al., 1991 and Jain et al., 1988) report results of flume experiments where interstitial velocities for porous dikes or for rockfills placed on impervious embankments are measured using tracers or computed from head loss. Interstitial velocities are dependent upon hydraulic gradient and stone gradation; empirical relations have been derived from flume data. However, these relations are difficult to apply to bank protection because prediction or estimation of the local hydraulic gradient is problematic. Nevertheless, flow through rockfill voids is highly heterogeneous with laminar, turbulent, and transition regimes present (Jain et al., 1988); and void velocities are much lower than the channel velocities above and adjacent to the revetment. For example, Abt et al. (1991) measured interstitial velocities in flows just submerging riprap on slopes ranging from 1 to 20%. Median stone sizes ranged from 2.6 to 13.0 cm, and riprap layers were 7.6 to 30.5 cm thick. Mean interstitial velocities were 3 to 44.8 cm s^{-1}, which were two to three times lower than computed velocities for wide, open channel flows at similar depths and slopes with Manning's n = 0.3. Williams and Hynes (1974) measured current velocity in a stream of 36 cm s^{-1} but an interstitial velocity 10 cm below the bed surface of only 0.1 cm s^{-1}.

Benthic aquatic species include invertebrates that burrow into soft sediments (infauna) and those that attach themselves to rocky surfaces (epifauna). Some epifaunal species and smaller vertebrates (e.g., juvenile fishes), spend at least part of their life cycle in voids within matrices of noncohesive particles like a riprap structure (Williams, 1984; Hjort et al., 1984, Li et al., 1984). Some evidence suggests that macroinvertebrate populations within a riprap structure are more dense and diverse than those found on its outer surfaces (Mathis et al., 1982).

The number and type of epifaunal organisms on and in a natural sediment deposit in a stream reflects sediment particle size, size gradation, and particle stability (Minshall, 1984). If a riprap structure is stationary relative to natural movable beds, it follows that riprap gradation is the dominant microscale habitat factor for a given set of hydraulic conditions. Results of experiments using uniform artificial stones suggests that the population density and species richness of benthos respond to stone size in a complex fashion: both are higher for small rocks placed alone in the flow, but when aggregate deposits are considered, larger stones support higher densities (Figure 1). Minshall (1984) suggested that this phenomenon was due to the association of larger (and thus possibly more habitable) voids with larger particles. Others have pointed out that physical complexity generally increases with median particle size; physical heterogeneity implies more habitat niches are available, and thus a more diverse biological community may result.

Riprap revetments in sediment-laden streams often become locations for sediment deposition (Tockner, 1991; Fischer et al., 1991; Shields, 1991). Thin layers (~ 1 mm) of fine sediments and algal growth on riprap surfaces provide "secondary substrate" that is utilized by benthic invertebrates. In addition, sediments deposited in riprap interstices can enhance habitat and benthic species diversity (Buress et al., 1982; Mathis et al., 1982), but sand deposits that cover riprap reduce habitat quality (Sanders et al., 1986). When placed in sand-bed systems with little naturally occurring sediment larger than sand, riprap provides an otherwise unavailable or very scarce stable substrate for invertebrate production (Witten and Bulkley, 1975).

Copious literature attests to the ecological value of microscale riprap habitats to invertebrates, and a sample of findings for large US rivers is provided in Table 1a. Riprap substrates compare favorably with natural banks as benthic habitat. The cited authors described the sampled "natural bank" habitats as steep, eroding banks that are typical of the types of habitats replaced by revetment; samples from stable banks and sandbars were not included. Generally, they reported that organisms inhabiting natural bank sediments

were sampled by collecting sediment samples using various types of sampling dredges and returning the sediments to the laboratory for separation and processing of biota. Riprap was sampled using metal baskets filled with riprap and implanted on the riprap structures for a fixed period of time (Sanders et al., 1985), or by collecting all stones enclosed by a rectangular frame placed on the structure at random (Burress et al., 1982; Atchison et al., 1986; Hjort et al., 1984), although less quantitative methods (such as collecting all organisms from a fixed number of riprap stones) have also been used (Sanders et al., 1986; Baker et al., 1988b).

Woody debris is an important invertebrate habitat, particularly in sand-bed rivers. Benke et al. (1985) found that woody debris supported 60% of the total invertebrate biomass, although it accounted for only 4% of the habitat area in a low-gradient sand bed river in Georgia. Baker et al. (1988a) found an average benthic macroinvertebrate density of 3121 m^{-2} representing an average of 21 taxa on large woody debris adjacent to natural banks on the lower Mississippi River. In the streams listed in Table 1, woody debris is usually more common along steep, eroding, natural banks than riprap revetments. Comparisons of habitat values of natural and revetted banks should allow for different woody debris densities. In channelized or unstable sand bed rivers, riprap structures may partially serve the function (stable substrate for macroinvertebrates) that large woody debris does in relatively undisturbed rivers.

Microscale phenomena may also affect utility of riprap as fish habitat. Riprap size heterogeneity rather than mean size has been shown to be an important determinant of benthic fish habitat at artificial reefs in marine environments (Helvey and Smith, 1985). Farabee (1986) found that fish biomass catch per unit effort at a Mississippi River revetment constructed with 0.6-m diameter riprap was more than twice as great as for a similar revetment constructed with riprap fitting a 0.3-0.6-m gradation. Michny and Deibel (1986) and Schaffter et al. reported 30-90% fewer juvenile salmon were found at Sacramento River revetted banks than natural banks, and suggested that the rougher riprap surfaces prevented formation of low-turbulence zones preferred by the juvenile salmon for feeding. However, riprap locations showed higher numbers of fish species that preyed upon and competed with the juvenile salmon (Michny and Hampton, 1984). In another region, placement of riprap revetments created additional spawning sites for lake sturgeon (Folz and Meyers, 1985). Thus by altering near-bank flow fields, riprap revetments can induce shifts in fish species composition and relative abundance.

2. MESOSCALE

2.1 Revetments

At the channel-width scale, hydraulic conditions created by riprap structures can be beneficial or detrimental to habitat quality. Some investigators have suggested that riprap revetment placed on the outside of a bend induces formation of a narrower, deeper baseflow channel; conflicting data from the Sacramento River have been presented by Harvey and Watson (1988) and Buer et al. (1989). The overall biological impact of revetment depends upon the magnitude of channel alteration and the quality of the habitat replaced by the revetment. Knudsen and Dilley (1987) compared summer and fall anadromous fish populations in five western Washington stream reaches before and after construction of riprap revetments. Fishes in smaller streams (mean discharge 0.4-2.4 m^3s^{-1}) were adversely impacted--biomass (in grams m^{-2}) was reduced 26% in the revetted reaches, but increased 54% in unaltered control reaches. Effects were different for larger streams (mean discharge 4.9-11.6 $m^3 s^{-1}$) : revetted reach biomass levels increased 227%, while control reach biomass increased only 30%. Since this study was limited to a short period of time (months), it may simply indicate that large and small stream communities respond over different time scales.

Local effects of revetment construction have also been studied. For example, Li et al. (1984) sampled adult fishes adjacent to natural banks, and continuous riprap revetments along the Willamette River, Oregon, and found 20 species near natural banks but only 10 adjacent to revetments, possibly due to more diverse physical conditions at natural banks. Additional studies that include comparison of fishes at natural and revetted banks are listed in Table 2.

2.2 Spur dikes and other intermittent structures

Studies comparing macroinvertebrate (Table 1b) and fish (Table 2) assemblages adjacent to continuous and intermittent bank protection structures have been performed in a wide variety of stream habitats. Readers unfamiliar with limitations of technology for sampling fish in rivers should be aware that data in Table 2 may reflect differential sampling efficiencies along different bank types, cyclical or climatic effects, etc. Also, species richness and catch per unit effort do not tell the whole story. For example, although investigators studying the Sacramento River found more species along revetments than natural banks, juvenile salmon preferred natural banks in significantly greater numbers (Schaffter et al., 1983; Michny, 1988; US Fish and Wildlife Service, 1992). Nevertheless, the values in Table 2 are all means of data generated by repetitive sampling in time and space and represent the best information available.

Results presented in Tables 1b and 2 indicate that intermittent structures like spur dikes or groins usually provide aquatic habitats superior to continuous revetment and sometimes surpassing natural banks. The superior performance of spur-type structures as fish habitat is related to creation of stable pools (scour holes) at riverward tips (Witten and Bulkley, 1975; Knight and Cooper, 1991; Shields et al., In Press), creation of lentic (still water) habitat connected with the main stream (Backiel and Penczak, 1989), provision of a complex of depth-velocity-bed type combinations not found adjacent to continuous riprap blanket (Li et al., 1984; Beckett et al., 1983; Baker et al., 1988b), and preservation of portions of the natural bankline and associated riparian vegetation and woody debris (Li et al., 1984). Woody debris is an important determinant of mesoscale habitat quality. Higher levels of physical heterogeneity are associated with higher woody debris densities (Shields and Smith, 1992), and fish populations respond negatively to debris removal or absence (Angermeier and Karr, 1984; Hortle and Lake, 1983).

Li et al. (1984) examined the use of natural banks, continuous riprap revetments, and spur dikes in the Willamette River, Oregon, by larval fishes. Continuous revetments were poor habitat for larval fishes relative to natural banks, while spur dikes were of intermediate quality due to the physical heterogeneity generated by the typically complex flow patterns around the spurs. Shallow zones above the gradually sloping bars adjacent to the spur dikes were particularly good habitat. Similar findings were reported by Schiemer and Spindler (1989) for the Danube in Austria. Geometrically complex bank lines along the Danube River that included gravel banks and littoral bays supported higher densities and diversities of juvenile fish than adjacent riprap revetments. Twelve species were captured from gradually sloping gravel banks and 12 species were also found in small bays in the inshore zone, but riprapped banks produced only 3 species.

2.3 Restoration and innovation

Because of the mesoscale effects described above, riprap structures have been widely used to rehabilitate aquatic habitats in streams damaged by channelization and erosion (Swales, 1989; Wesche, 1985). For example, Shields et al. (In Press) described habitat restoration for an incised channel in northwest Mississippi. Previous channel stabilization work (construction of a grade control structure downstream and placement of about 40 riprap groins) had been ineffective in restoring habitat quality. By adding low extensions to every other groin and placing a riprap toe along the opposite bank, scour hole volumes and depths were increased dramatically (Figure 2). For the same water surface elevation, mean maximum depth of scour holes at all 40 groins increased from 40 to 70 cm after restoration, and mean depth increased from 24 to 40 cm. After restoration the mean length of fish, number of fish species, and biomass catch per unit effort of

electrofishing increased 81, 60, and 1142%, respectively (Shields et al., In Press). Favorable results for habitat restoration projects in channelized streams that featured riprap spurs and weirs have also been reported by Swales (1982), Edwards et al. (1984), and Carline and Klosiewski (1985). Design criteria are provided by Wesche (1985).

Innovative concepts for riprap structures--both intermittent and continuous--have been proposed to address economic, environmental, and engineering weaknesses of more orthodox approaches (Table 3). In general, these concepts produce mesoscale habitats superior to those found at more orthodox structures. However, all of them should be viewed as experimental when applied to a setting for which test data are unavailable. Institutional and political factors arising from stabilization of the Sacramento River have led to development of a number of modified revetment designs intended to preserve riparian vegetation and anadromous fish habitat (Mifkovic and Petersen, 1975; US Fish and Wildlife Service, 1992). Most of these concepts are listed in Table 3. Despite development of these innovations, they have not been extensively employed, and declines in riparian habitat and dependent species have been significant (Figure 3).

3. MACROSCALE

Riprap structures are major components of stream corridor management projects. In many cases, stream corridor development demands either preservation of a wide zone for channel migration or comprehensive stabilization of river planform using riprap training structures. The latter course of action has been chosen for many if not most of the major temperate zone rivers (Bayley, 1991). In many cases (e.g., Missouri, Willamette, Rhine, Vistuala) ecologically rich braided rivers have been confined to single channels with slight sinuosity, high velocities, and extremely low levels of habitat diversity. Channel bed degradation that follows channelization isolates the river and its tributaries from floodplain water bodies, often by draining abandoned channels and oxbows (Atchison et al., 1986; Lelek, 1989). Floodplain development requires flood control, and levees have often been constructed so close to river banks that the area of land subject to flooding is nearly eliminated (e.g., Dister et al., 1990). Bank stabilization, usually with riprap revetments, is usually required in order to protect levees.

Comprehensive stabilization of river planform has major, long-term implications for habitat quality and biodiversity because, as currently practiced, it leads to gradual but permanent elimination of lentic (backwater) habitats adjacent to the main channel (Table 4; Petts, 1989). Current thinking in stream ecology emphasizes the importance of periodic exchange of water and the sediments, nutrients, and organisms in it between the main channels of higher order rivers and lentic waters on their floodplains (Junk et al., 1989;

Dister et al., 1990). Bayley (1991) suggested that river-floodplain systems with natural annual flood pulses have multispecies fish yields per unit area several times that of constant water level systems (impoundments or lakes). The area subjected to flood pulses is greatly reduced or even eliminated by orthodox river development projects. Floodplain development facilitated by flood control and channel stabilization projects often exacerbates the process of backwater elimination (Vanderford, 1980; Dister et al., 1990). Long-term effects on ecosystem components and their economic value are hard to estimate because of the paucity of preproject data, but available findings indicate these effects are significant. For example, the commercial fish harvest from the Missouri River in the state of Missouri declined at least 80% between 1947 and 1978 (Figure 4). The actual decline may have been greater than 80% because catch reporting has been more efficient in recent years.

Recorded backwater sedimentation rates for US rivers range from 1 to 18 cm vertical accretion per year (McHenry et al., 1980 and 1984; Shields and Gibson, 1989). The rate of formation of new backwaters is extremely low because channel migration rates have been greatly reduced by impoundment and channel stabilization, usually with riprap structures. For example, along the lower Missouri River, construction of dikes and revetments coupled with closure of upstream reservoirs has resulted in conversion of almost half of the aquatic habitat to terrestrial habitat. Virtually all of the backwater habitat has been lost in some reaches, leaving only the less productive main channel (Sandheinrich and Atchison, 1986). Overall habitat diversity has declined greatly. Conversely, morphologic changes on the lower Mississippi River associated with channel stabilization and upstream flow regulation have been relatively mild (Nunnally and Beverly, 1986). This difference in channel response may be due to the lower historical sediment load and the lower elevation of the training works relative to mean and peak stages on the lower Mississippi relative to the Missouri. Bed degradation along the Missouri has also exacerbated reduction of backwater area.

Comprehensive bank stabilization projects along gravel-bed rivers reduce the movement of gravel from eroding banks into the channel. Although it has been suggested that extensive bank protection might reduce gravel supply enough to adversely impact gravel-spawning fishes, field studies on the Sacramento (Harvey and Watson, 1988) and Willamette (Klingeman, 1989) Rivers have been inconclusive. Even channels with virtually all of their banklines protected receive gravel from bed erosion and tributary reaches.

4. IMPLICATIONS

Designers of streambank erosion control and channel training structures who wish to address environmental concerns are faced with several gaps in the state of the art. Environmental approaches for these efforts typically involve use of intermittent structures, plant materials (alone and in combination with stone), and backwater sediment management (Henderson, 1986). Since experience with these approaches is not as well documented as for orthodox riprap revetment, there are higher levels of uncertainty regarding project performance. We suggest that reward and risk are proportional, and note that at least some orthodox views of environmental measures (i.e., vegetation on revetments) are unrealistically conservative (Shields, 1991).

Use of plant materials alone or in conjunction with riprap is extremely attractive from an environmental (i.e., aesthetic and habitat conservation) standpoint. The state of the art in this area is rapidly expanding, and design textbooks have recently been produced (Schiechtl, 1980; Gray and Leiser, 1982; Coppin and Richards, 1990). The emphasis on biotechnical alternatives to riprap in this volume is interesting and commendable. Although some biotechnical approaches to bank protection are somewhat elaborate and require specialized expertise to design and implement, others are as simple as planting dormant willow posts (e.g., Shields and Cooper, In Review). However, institutional, political, and psychological barriers to widespread adoption of biotechnical approaches by the civil engineering community are deep-seated. Those who believe that riprap specialists will abandon the skills they have spent a lifetime developing to embrace others for the sake of environmental quality have a decidedly more sanguine view of human nature than we do.

Habitat conversion due to backwater sedimentation is one of the most major environmental issues associated with large river channel stabilization. Methods for restoring river corridor habitats degraded by sedimentation are diverse (Schnick et al., 1982; US Army Corps of Engineers, 1990; Patin and Hempfling, 1991) and range from planting aquatic macrophtyes and reflooding leveed floodplains (Sparks, 1990) to excavating notches in existing spur dikes (Shields, 1984). Combinations of dredging and placement of dredged materials to build islands or levees are common (Patin and Hempfling, 1991; Shields, 1987). However, many of these techniques are inordinately costly, marginally effective, and take a piecemeal approach to ecosystem restoration (e.g., Niemi and Strauser, 1991; Shields, 1988). In contrast, Bayley (1991) proposed restoration of natural flooding over a large, contiguous river-floodplain area by purchasing land, removing levees and modifying reservoir operations for a river reach between two navigation dams as an interim first step in "restoring the watershed." Although the ecological benefits of such a project are apparent, the economic and political obstacles appear intractable to us.

ACKNOWLEDGMENTS

John Baker, Steve Maynord, James Gore, James Kushlan, E. A. Dardeau, and Scott Knight read an earlier version of this paper and made many helpful suggestions. Mary Evelyn Barnes provided assistance with preparation of the reference list. P.D. Mitchell prepared Figure 2.

REFERENCE LIST

Abt, S. R., Ruff, J. F., and Wittler, R. J. (1991). Estimating Flow Through Riprap. *Journal of Hydraulic Engineering*, **117**, 670-675.

Angermeier, P. L., and Karr, J. R. (1984). Relationships between Woody Debris and Fish Habitat in a Small Warmwater Stream. *Transactions of the American Fisheries Society*, **113**, 716-726.

Atchison, G. J., Bachmann, R. W., Nickum, J. G., Barnum, J. B., and Sandheinrich, M. B. (1986). Aquatic Biota Associated with Channel Stabilization Structures and Abandoned Channels in the Middle Missouri River. Technical Report E-86-6, US Army Engineer Waterways Experiment Station, Vicksburg, Miss.

Babinski, Z. (1992). Hydromorphological consequences of regulating the lower Vistual, Poland. Regulated Rivers: Research and Management, 7, 337-348.

Backiel, T., and Penczak, T. (1989). The Fish and Fisheries in the Vistula River and its Tributary, the Pilica River, In Dodge, D. P. (ed.) Proceedings of the International Large River Symposium, Special Publication of Fisheries and Aquatic Sciences 106, Department of Fisheries and Oceans, Ottawa, 488-503.

Baker, J. A., Kasul, R. L., Winfield, L. E., Bingham, C. R., Pennington, C. H., Coleman, R. E. (1988a). An Ecological Investigation of Revetted and Natural Bank Habitats in the Lower Mississippi River. Report 9, Lower Mississippi River Enviromental Program, US Army Corps of Engineers, Mississippi River Commission, Vicksburg, Miss.

Baker, J. A., Kasul, R. L., Winfield, L. E., Bingham, C. R., Pennington, C. H., and Coleman, R. E. (1988b). An Ecological Investigation of the Baleshed Landing-Ben Lomond and Ajax Bar Dike Systems in the Lower Mississippi River, River Mile 481 to 494 AHP. Report 12, Lower Mississippi River Enviromental Program, US Army Corps of Engineers, Mississippi River Commission, Vicksburg, Miss.

Baker, J. A., Kilgore, K. J., and Kasul, R. L. (1991). Aquatic Habitats and Fish Communities in the Lower Mississippi River. *Reviews in Aquatic Science*, **3**(4), 313-356.

Bayley, P. B. (1991). The Flood Pulse Advantage and the Restoration of River-Floodplain Systems. *Regulated Rivers: Research and Management*, **6**, 75-86.

Beckett, D. C., Bingham, C. R., and Sanders, L. G. (1983). Benthic Macroinvertebrates of Selected Habitats of the Lower Mississippi River. *Journal of Freshwater Ecology*, **2**(3), 247-261.

Benke, A. C., Henry, R. L., III, Gillespie, D. M., and Hunter, R. J. (1985). Importance of Snag Habitat for Animal Production in Southeastern Streams. *Fisheries*, **10**(5), 8-13.

Bournaud, M., and Cogerino, L. (1986). The aquatic microhabitats of the banks of a large water course: the faunistic approach. *Annales de Limnolgie*, **22**(3), 285-294.

Buer, K. Y., Eaves, J. N., Scott, R. G., and McMillan, J. R. (1984). Basin changes affecting salmon habitat in the Sacramento River, In Hassler, T. J. (ed.) Proceedings of the Pacific Northwest Stream Habitat Management Workshop, Humboldt State University, Arcata, Calif., 14-50.

Buer, K., Forwalter, D., Kissel, M., and Stohlert, B. (1989). The Middle Sacramento River: Human Impacts on Physical and Ecological Processes Along a Meandering River. Proceedings of the California Riparian Systems Conference, Berkeley, California: Pacific Southwest Forest and Range Experiment Station, 22-32.

Burress, R. M., Krieger, D. A., and Pennington, C. H. (1982). Aquatic Biota of Bank Stabilization Structures on the Missouri River, North Dakota. Technical Report no. E-82-6, US Army Engineer Waterways Experiment Station, Vicksburg, Miss.

Carline, R. F., and Klosiewski, S. P. (1985). Responses of Fish Populations to Mitigation Structures in Two Small Channelized Streams in Ohio. *North American Journal of Fisheries Management*, **5**(1), 1-11.

Coppin, N. J. and Richards, I. G.(eds.) (1990). *Use of vegetation in civil engineering*. Construction Industry Research and Information Association, Butterworth Publishers, London.

Davinroy, R. D. (1990). Bendway Weirs, a New Structural Solution to Navigation Problems Experienced on the Mississippi River. *Bulletin of the Permanent International Association of Navigation Congresses*, **69**, 5-19.

Dister, E., Gomer, D., Obrdlik, P., Petermann, P., and Schneider, E. (1990). Water Management and Ecological Perspectives of the Upper Rhine's Floodplains. *Regulated Rivers: Research and Management*, **5**, 1-15.

Edwards, C. J., Griswold, B. L., Tubb, R. A., Weber, E. C., and Woods, L. C. (1984). Mitigating Effects of Artificial Riffles and Pools on the Fauna of a Channelized Warmwater Stream. *North American Journal of Fisheries Management*, **4**, 194-203.

Farabee, G. B. (1986). Fish Species Associated with Revetted and Natural Main Channel Border Habitats in Pool 24 of the Upper Mississippi River. *North American Journal of Fisheries Management*, **6**, 504-508.

Fischer, K. J., Harvey, M. D., and Pridal, D. B. (1991). Deposition on revetments along the Sacramento River, In Proceedings of the Fifth Federal Interagency Sedimentation Conference (FIASC), Federal Energy Regulatory Commission, Washington, DC, 4-102--4-108.

Fletcher, W. B., and Davidson, R. L. (1988). South Santiam River Bank Protection Study: A Pilot Study for the Willamette River Bank Protection Study. U. S. Army Corps of Engineers, Portland District, Portland, Oregon.

Folz, D. J. and Meyers, L. S. (1985). Management of the lake sturgeon, *Acipenser fulvescens*, population in the Lake Winnebago system, Wisconsin, In Binkowski, F. P. and Doroshov, S. I. (eds.) North American Sturgeons, Dr W. Junk Publishers, Dordrecht, Netherlands, 135-146.

Frayer, W. E., Peters, D. D., and Pywell, H. R. (1989). Wetlands of the California Central Valley: Status and Trends, 1939 to mid 1980's, US Fish and Wildlife Service, Portland, Oregon.

Fremling, C. R., Rasmussen, J. L., Sparks, R. E., Cobb, S. P., Bryan, C. F., and Claflin, T. O. (1989). Mississippi River Fisheries: A Case History, In Dodge, D. P. (ed.) Proceedings of the International Large River Symposium, Special Publication of Fisheries and Aquatic Sciences 106, Department of Fisheries and Oceans, Ottawa, 309-351.

Funk, J. L., and Robinson, J. W. (1974). Aquatic Series No. 11. Changes in the Channel of the Lower Missouri River and Effects on Fish and Wildlife. Jefferson City, Missouri: Missouri Department of Conservation.

Gray, D. H. and Leiser, A. T. 1982. *Biotechnical slope protection and erosion control*. Van Nostrand Reinhold, New York.

Harvey, M. D., and Watson, C. C. (1988). Effects of Bank Revetment on Sacramento River, California. Proceedings of the California Riparian Systems Conference, Davis, California, 1988, Berkeley, California: Pacific Southwest Forest and Range Experiment Station, 47-50.

Helvey, M., and Smith, R. W. (1985). Influence of Habitat Structure on the Fish Assemblages Associated with Two Cooling-Water Intake Structures in Southern California. *Bulletin of Marine Science*, 37(1), 189-199.

Henderson, J. E. (1986). Environmental Designs for Streambank Protection Projects. *Water Resources Bulletin*, 22, 549-558.

Hjort, R. C., Hulett, P. L., LaBolle, L. D., and Li, H. W. (1984). Fish and Invertebrates of Revetments and Other Habitats in the Willamette River, Oregon. Technical Report E-84-9, US Army Engineer Waterways Experiment Station, Vicksburg, Miss.

Hortle, K. G., and Lake, P. S. (1983). Fish of Channelized and Unchannelized Sections of the Bunyip River, Victoria. *Australian Journal of Marsh and Freshwater Research*, 34, 441-450.

Jain, S. C., Holly, F. M., and Lee, T. H. (1988). Head loss through porous dikes. *Canadian Journal of Civil Engineering*, 15, 766-775.

Junk, W. J., Bayley, P. B., and Sparks, R. E. (1989). The Flood Pulse Concept in River-Floodplain Systems, In Dodge, D. P. (ed.) Proceedings of the International Large River Symposium, Special Publication of Fisheries and Aquatic Sciences 106, Department of Fisheries and Oceans, Ottawa, 110-117.

Kallemeyn, L. W. and Novotony, J. F. (1977). Fish and fish food organisms in various habitats of the Missouri River in South Dakota, Nebraska, and Iowa. Report No. FWS/OBS-77/25, U. S. Fish and Wildlife Service, Washington, D. C.

Keck, R. A. (1990). Baseline habitat inventory and mapping for Sacramento River Bank Protection Project, California. Third Phase, US Fish And Wildlife Service, Sacramento, Calif.

Klingeman, P. C. (1989). Geomorphic influences on sediment transport in the Willamette River, In Erosion and Sedimentation in the Pacific Rim, IAHS Publication No. 165, International Assocation of Hydrological Sciences, Wahington, DC, 365-374.

Knight, S. S., and Cooper, C. M. (1991). Effects of bank protection on stream fishes, In Proceedings of the Fifth Federal Interagency Sedimentation Conference (FIASC), Federal Energy Regulatory Commission, Washington, DC, 13-34--13-39.

Knudsen, E. E., and Dilley, S. J. (1987). Effects of riprap bank reinforcement on juvenile salmonids in four western Washington streams. *North American Journal of Fisheries Management*, 7, 351-356.

Lelek, A. (1989). The Rhine River and Some of its Tributaries Under Human Impact in the Last Two Centuries, In Dodge, D. P. (ed.) Proceedings of the International Large River Symposium, Special Publication of Fisheries and Aquatic Sciences 106, Department of Fisheries and Oceans, Ottawa, 469-487.

Li, H. W., Schreck, C. B., and Tubb, R. A. (1984). Comparison of habitats near spur dikes, continuous revetments, and natural banks for larval, juvenile, and adult fishes of the Willamette River. Corvallis, Oregon: Water Resources Research Institute, Oregon State University.

Mathis, D. B., Bingham, C. R., and Sanders, L. G. (1982). Assessment of implanted substrate samplers for macroinvertebrates inhabiting stone dikes of the Lower Mississippi River. Miscellaneous Paper No. E-82-1, US Army Engineer Waterways Experiment Station, Vicksburg, Miss.

McHenry, J. R., Ritchie, J. C., and Cooper, C. M. (1980). Rates of recent sedimentation in Lake Pepin. *Water Resources Bulletin*, **16**, 1049-1056.

McHenry, J. R., Ritchie, J. C., Cooper, C. M., and Verdon, J. (1984). Recent rates of sedimentation in the Mississippi, In *Contaminants in the Mississippi River*, Proceedings of the 15th Annual Meeting of the Mississippi River Research Consortium, Butterworth Publishers, Boston, 99-117.

Michny, F. J. (1988). Concluding report, evaluation of palisade bank stabilization, Woodson Bridge, Sacramento River, California, US Fish and Wildlife Service, Sacramento, Calif.

Michny, F. J. and DeHaven, R. W. (1987). Evaluation of primary environmental mitigation measures implemented for the Sacramento River Chico Landing to Red Bluff protection project, US Fish and Wildlife Service, Sacramento, Calif.

Michny, F. J., and Deibel, R. (1986). Sacramento River, Chico Landing to Red Bluff Project, 1985 juvenile salmon study, US Fish and Wildlife Service, Sacramento, Calif.

Michny, F. J., and Hampton, M. (1984). Sacramento River, Chico Landing to Red Bluff Project, 1984 juvenile salmonid study, US Fish and Wildlife Service, Sacramento, Calif.

Mifkovic C. S. and Petersen M. S. (1975). Environmental aspects-Sacramento Bank Protection, *Journal of the Hydraulics Division*, American Society of Civil Engineers, **101**, 543-555.

Minshall, G. W. 1984. Aquatic insect-substratum relationships, Chapter 12, In Resh, V. H. and Rosenberg, D. M. (eds.) *The ecology of aquatic insects.* Praeger Publishers, New York.

Niemi, J. R., and Strauser, C. N. (1991). Environmental river engineering. *Permanent International Association of Navigation Congresses Bulletin*, **73**, 100-106.

Nunnally, N. R., and Beverly, L. B. (1986). Morphologic effects of Lower Mississippi River dike fields. Miscellaneous Paper E-86-2, US Army Engineer Waterways Experiment Station, Vicksburg, Miss.

Patin, J. W. P., and Hempfling, T. E. (1991). Environmental management of the Mississippi. *The Military Engineer*, **83**(541), 9-11.

Reice, S. R. 1980. The role of substratum in benthic macroinvertebrate microdistribution and litter decomposition in a woodland stream. *Ecology* **61**:580-90.

Reynolds, J. and Segelquist, C. Undated. Final report--effects of dike notching on fish and wildlife in the Missouri River. Prepared for US Army Engineer Districts, Kansas City and Omaha, US Fish and Wildlife Service, Office of Biological Services, Columbia, Mo.

Sanders, L. G., Baker, J. A., Bond, C. L., and Pennington, C. H. (1985). Biota of Selected Aquatic Habitats of the McClellan-Kerr Arkansas River Navigation System. Technical Report E-85-6, US Army Engineer Waterways Experiment Station, Vicksburg, Miss.

Petts, G. E. (1989). Historical Analysis of Fluvial Hydrosystems, In Petts, G. E. (ed.), *Historical Change of Large Alluvial Rivers*: *Western Europe,* John Wiley & Sons, Ltd., Chichester, 1-18.

Sanders, L. G., Bingham, C. R., and Beckett, D. C. (1986). Macroinvertebrate Gear Evaluation. Miscellaneous Paper No. E-86-3, US Army Engineer Waterways Experiment Station, Vicksburg, Miss.

Sandheinrich, M. B. and Atchison, G. J. (1986). Environmental effects of dikes and revetments on large riverine systems. Technical Report No. E-86-5, US Army Engineer Waterways Experiment Station, Vicksburg, Miss.

Schaffter, R. G., Jones, P. A., and Karlton, J. G. (1983). Sacramento River and Tributaries Bank Protection and Erosion Control Investigation- Evaluation of Impacts on Fisheries, The Resources Agency, Department of Fish and Game, Sacramento, Calif.

Schiechtl, Hugo M. 1980. *Bioengineering for land reclamation and conservation.* The University of Alberta Press, Hignell Printing Ltd., Winnipeg, Manitoba.

Schiemer, F., and Spindler, T. (1989). Endangered Fish Species of the Danube River in Austria. *Regulated Rivers: Research and Management,* **4**, 397-407.

Schmitt, L. J. (1983). A Method of Improving Aquatic Habitat in the Navigation Channel of the Kaskaskia River, IL. Thesis submitted in partial fulfillment of the requirements for the degree of Master of Science in Environmental Science in Civil Engineering in the Graduate College of the University of Illinois at Urbana-Champaign,

Schnick, R. A., Morton, J. M., Mochalski, J. C., and Bailey, J. T. (1982). Mitigation and enhancement techniques for the Upper Mississippi River System and other large river systems, US Fish and Wildlife Service Research Publication 149, Washington, DC.

Sedell, J. R. and Froggatt, J. L. (1984). Importance of streamside forests to large rivers: The isolation of the Willamette River, Oregon, U.S.A., from its floodplain by snagging and streamside forest removal. *Verhandlung Internationale Vereinigung Limnologie*, **22**, 1828-1834.

Shields, F. D., Jr. (1984). Environmental Guidelines for Dike Fields, In Elliot, C. M. (ed.) *River Meandering*, Proceedings of the Conference Rivers '83, American Society of Civil Engineers, New York, 430-441.

Shields, F. D. ,. Jr. (1987). Management of Environmental Resources of Cutoff Bends along the Tennessee-Tombigbee Waterway. Miscellaneous Paper EL-87-12, US Army Engineer Waterways Experiment Station, Vicksburg, Miss.

Shields, F. D., Jr. (1988). Effectiveness of Spur Dike Notching, In Abt, S. R., and Gessler, J. (eds.), *Hydraulic Engineering*, Proceedings of the 1988 National Conference, American Society of Civil Engineers, New York, 334-339.

Shields, F. D., Jr. (1991). Woody vegetation and riprap stability along the Sacramento River mile 84.5-119. *Water Resources Bulletin*, 27(3), 527-536.

Shields, F. D., Jr., and Cooper, C. M. (In Press.) Initial response to incised channel rehabilitation. Manuscript accepted by *Aquatic Conservation: Marine and Freshwater Ecosystems*.

Shields, F. D., Jr. and Gibson, A. C. (1989). Physical changes in cutoff bends along the Tennessee-Tombigbee Waterway. Miscellaneous Paper No. EL-89-5, US Army Engineer Waterways Experiment Station, Vicksburg, Miss.

Shields, F. D., Jr. and Smith, R. H. (1992). Effects of large woody debris removal on physical characteristics of a sand-bed river, *Aquatic Conservation: Marine and Freshwater Ecosystems*, 2, 145-163.

Shields, F. D., Jr., Cooper, C. M., and Knight, S. S. (1992). Rehabilitation of aquatic habitats in unstable streams. Proceedings, Fifth International Symposium on River Sedimentation, April 6-10, 1992, University of Karlsruhe, Germany, 1093-1102.

Shields, F. D., Jr., Knight, S. S., and Cooper, C. M. In Press. Restoration of an incised stream channel: preliminary results. Manuscript accepted for inclusion in *Advances in Hydro-Science and Engineering*, Proceedings of the 1993 International Conference on Hydro-Science and Engineering, Center for Computational Hydroscience and Engineering, University, Mississippi.

Sparks, R. E. (1990). Disturbance and recovery of large floodplain rivers. *Environmental Management*, 14(5), 699-709.

Statzner, B., Gore, J. A., and Resh, V. H. (1988). Hydraulic stream ecology: observed patterns and potential applications. *Journal of the North American Benthological Society*, 7(4), 307-360.

Storfer, A. (1992). Baseline habitat inventory and mapping for Sacramento River Bank Protection Project, Third Phase, California, US Fish and Wildlife Service, Sacramento, Calif.

Swales, S. (1982). Notes on the Construction, Installation and Environmental Effects of Habitat Improvement Structures in a Small Lowland River in Shropshire. *Fisheries Management*, 13(1), 1-10.

Swales, S. (1989). The Use of instream habitat improvement methodology in mitigating the adverse effects of river regulation on fisheries. Chapter 7, In Gore, J. A. and Petts, G. E. (eds.), *Alternatives in Regulated River Management*, CRC Press, Inc., Boca Raton, Florida.

Tockner, K. (1991). Riprap: an artificial biotope (Impounded area of the River Danube, Altenworth, Austria). *Internationale Vereinigung fuer Theoretische und Angewandte Limnologie*, 24, 1953-1956.

Trush, W. J., Jr. 1979. The effects of area and surface complexity on the structure and formation of stream benthic communities. Unpublished MS thesis, Virginia Polytechnic Institute and State University, Blacksburg.

US Army Corps of Engineers. (1990). Missouri River Bank Stabilization and Navigation Fish and Wildlife Mitigation Project, US Army Engineer Division, Missouri River, Omaha, Neb.

US Army Engineer District, Kansas City. (1980). Potamology investigaton, Missouri River, Rulo, Nebraska to Mouth, MRD Sediment Series No. 22, US Army Engineer Division, Missouri River, Omaha, Neb.

US Fish and Wildlife Service. (1992). Juvenile salmon study, Butte Basin Reach, Sacramento River Bank Protection Project. Final Report prepared for US Army Corps of Engineers, Sacramento, Calif.

Vanderford, M. J., ed. (1980). Fish and wildlife, GREAT I study of the Upper Mississippi River, technical appendices, Vol. 5, Department of Nuclear Engineering Science, University of Florida, Gainesville.

Wesche, T. A. (1985). Stream channel modifications and reclamation structures to enhance fish habitat, Chapter 5, In Gore, J. A. (ed.), *The Restoration of Rivers and Streams: Theories and Experience*, Butterworth Publishers, Boston.

Williams, D. D. (1984). The hyporheic zone as a habitat for aquatic insects and associated arthropods, Chapter 14, In Resh, V. H. and Rosenberg, D. M. (eds.) *The ecology of aquatic insects.* Praeger Publishers, New York.

Williams, D. D., and Hynes, H. B. N. (1974). The Occurrence of Benthos Deep in the Substratum of a Stream. *Freshwater Biology*, **4**, 233-256.

Witten, A. L., and Bulkley, R. V. (1975). A Study of the Effects of Stream Channelization and Bank Stabilization on Warmwater Sport Fish in Iowa. Subproject No. 2: A Study of the Impact of Selected Bank Stabilization Structures on Game Fish and Associated Organisms, Report No. FWS/OBS-76/12, US Fish and Wildlife Service, Columbia, Mo.

Zimpfer, S. P., Kelso, W. E., Bryan, C. F., and Pennington, C. H. (1988). Ecological Features of Eddies Associated with Revetments in the Lower Mississippi River, Report 8, Lower Mississippi River Enviromental Program, US Army Corps of Engineers, Mississippi River Commission, Vicksburg, Miss.

FIGURE CAPTIONS

Figure 1. Effect of rock size on benthic diversity and density. Effect is different for individual rocks and aggregates of rocks, suggesting that voids within aggregate matrix become more habitable as rock (and thus void) size increases. After Minshall (1984).

Figure 2. Modification of short riprap spur dikes at Hotophia Creek, Mississippi to improve mesoscale habitats.

a. Stone added to modify habitat. Existing structures are light, additions are darker.

b. Effect of spur dike extensions on availability of scour hole habitat. Maximum depth of scour holes at dike tips measured at nearly identical stages at midsummer before and after extension of every other dike.

Figure 3. Cumulative length of riprap revetments constructed along the Sacramento River between river kilometer (RK) 311-391 versus decade average of estimated number of fall-run chinook spawners for the reach upstream of RK 391. The decline in fish numbers 1987-1992 was even more rapid, probably due to reduced streamflow. Revetment data are from Schaffter et al. (1983) and Michny and DeHaven (1987). Fish data are from Buer et al. (1984). Decline in fish numbers reflects many influences in addition to river stabilization; however, the loss of juvenile rearing habitat immediately downstream of the spawning reaches is a factor.

Figure 4. Cumulative length of riprap revetments constructed along the Missouri River and annual commercial fish harvest. Revetment data are from US Army Engineer District, Kansas City (1980). Fish catch figures are from Funk and Robinson (1974). Fish harvests are probably lower than actual for years prior to 1945 due to incomplete reporting.

ROCKSIZ.XLS

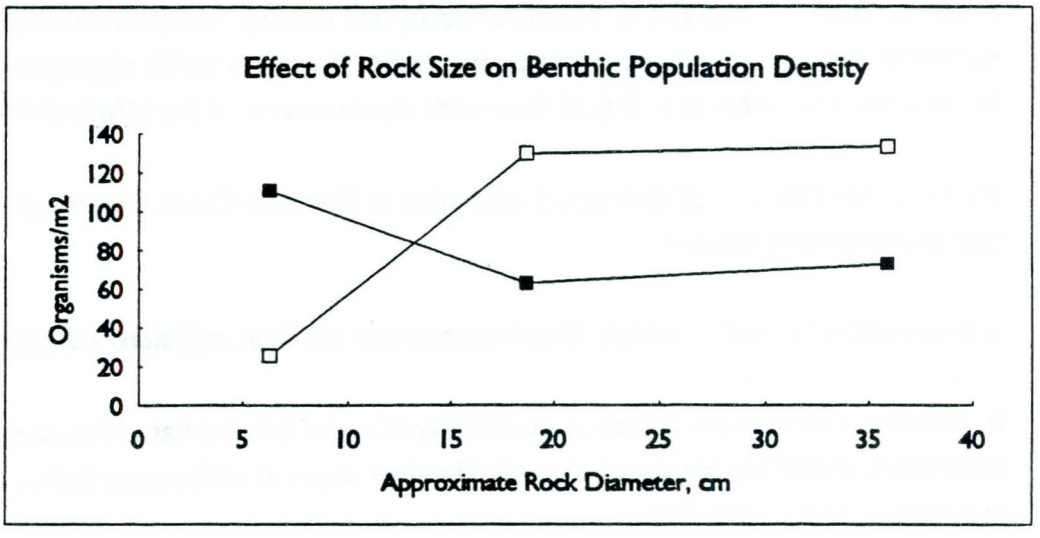

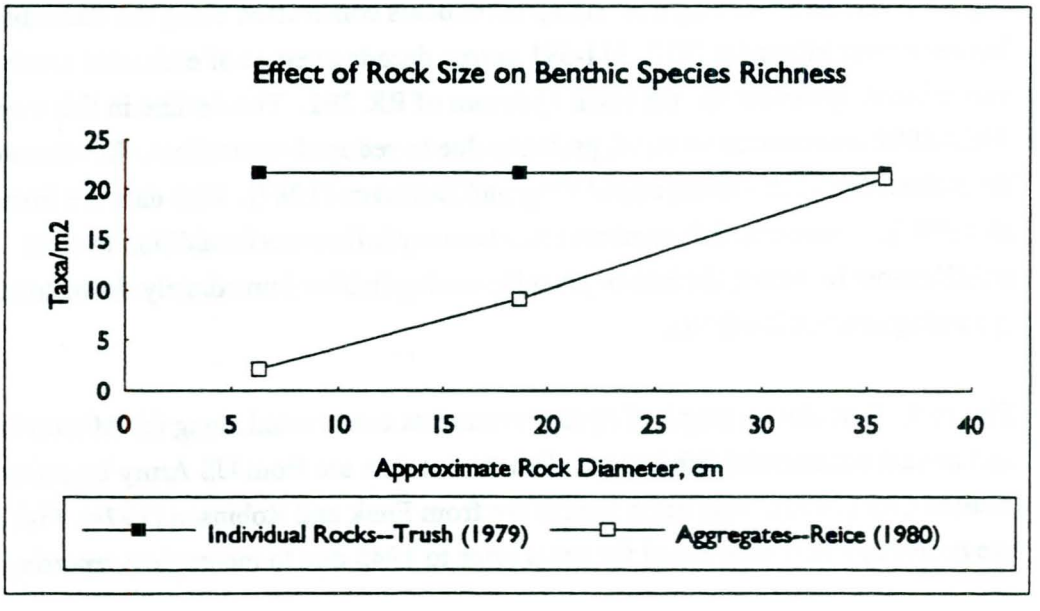

Figure 1.

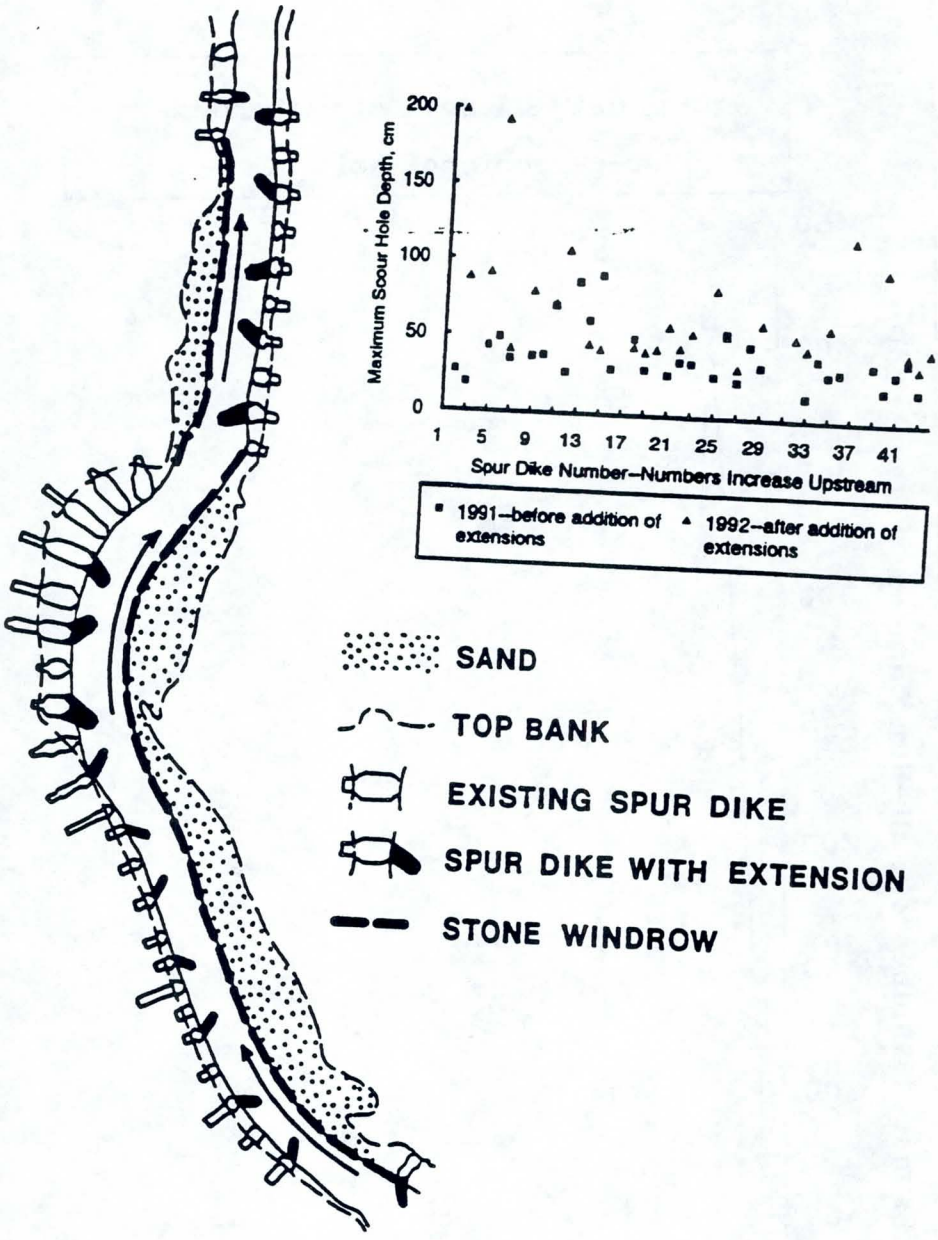
Maximum Scour Hole Depth, cm
200
150
100
50
0
1 5 9 13 17 21 25 29 33 37 41
Spur Dike Number--Numbers Increase Upstream
1991--before addition of extensions
1992--after addition of extensions
SAND
TOP BANK
EXISTING SPUR DIKE
SPUR DIKE WITH EXTENSION
STONE WINDROW

Figure 2.

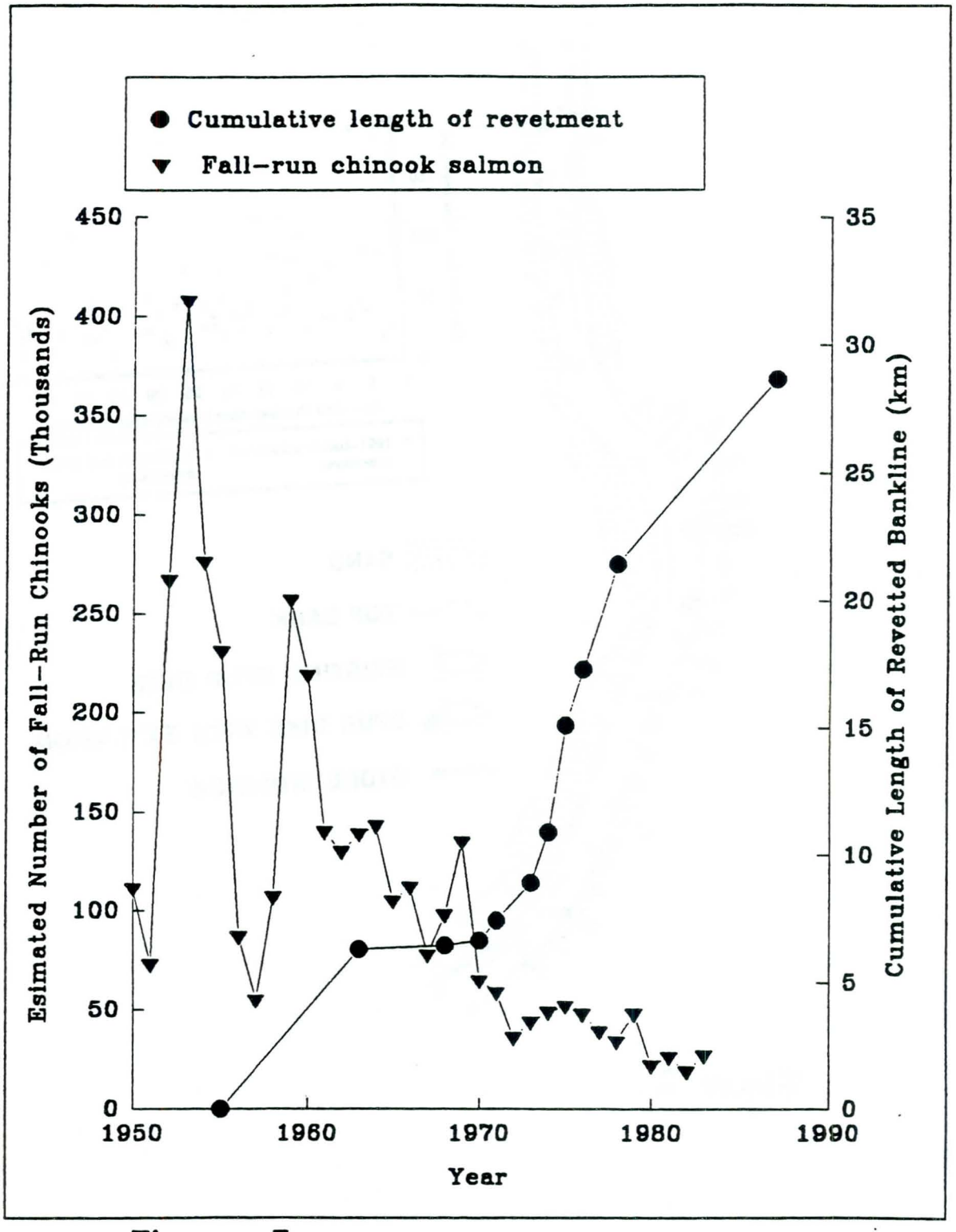
Cumulative length of revetment
Fall-run chinook salmon
Esimated Number of Fall-Run Chinooks (Thousands)
Cumulative Length of Revetted Bankline (km)
Year
0
50
100
150
200
250
300
350
400
450
0
5
10
15
20
25
30
35
1950
1960
1970
1980
1990

Figure 3.

FUNK.XLS

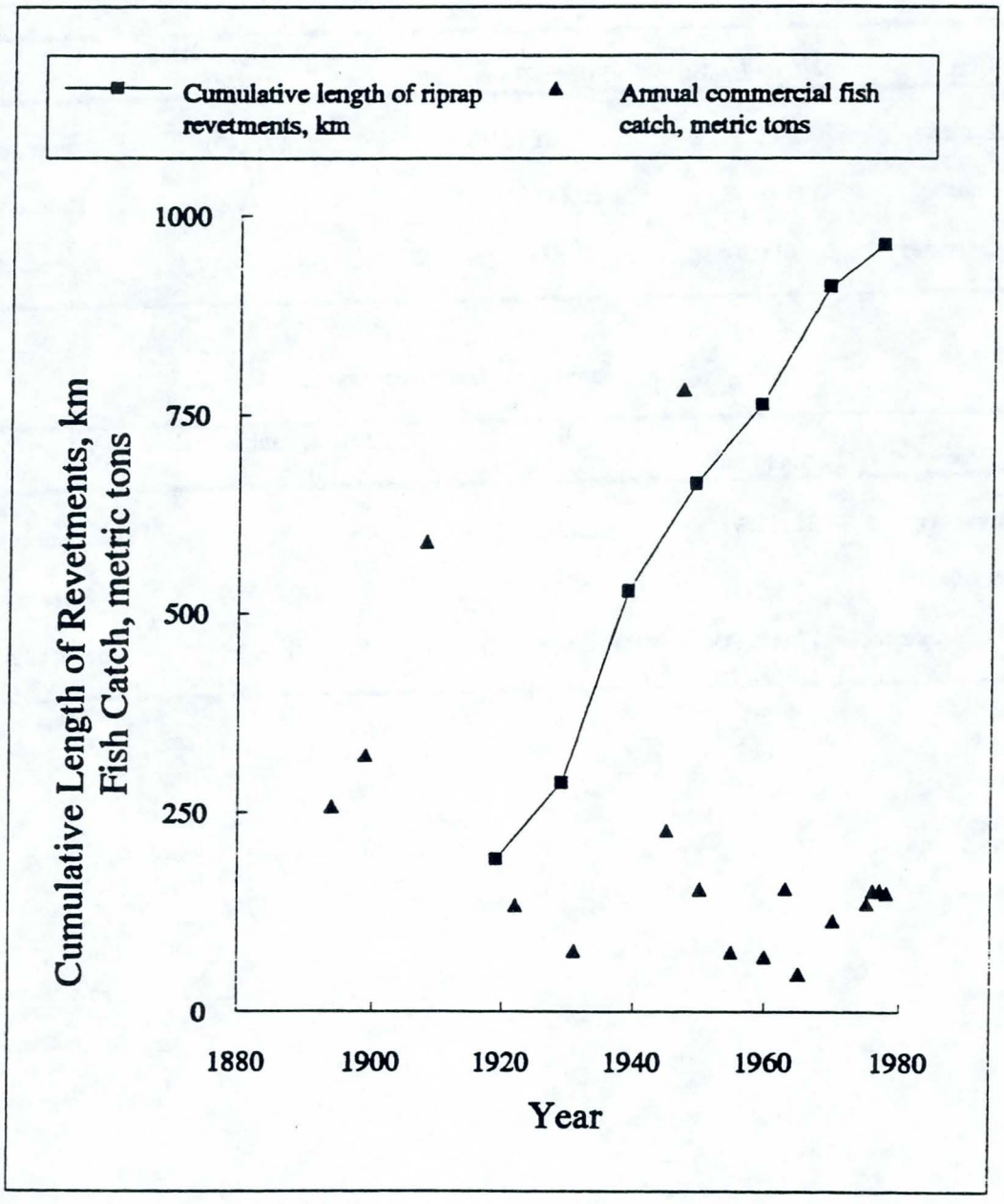

Figure 4.

Table 1. Mean benthic invertebrate species richness (density in numbers per square meter) for natural banks and riprap structures. Species richness and density values are means for a given location and a given time. Mean species richness values in different rows are not directly comparable because different sampling methods were used.

a. Natural banks and riprap revetments

River	Natural Banks	Riprap Revetments	Riprap/Natural Bank (percent)	Source
Arkansas	22 (1737)	38 (853)	172 (49)	Sanders et al. (1985)
Willamette	33 (2043)	48 (19 619)	130 (476)	Hjort et al. (1984)
Upper Missouri	4[1] (68)	6[1] (1570)	150 (2300)	Burress et al. (1982)

b. Natural banks and riprap spur dikes

River	Natural Banks	Riprap Spur Dikes	Riprap/Natural Bank (percent)	Source
Arkansas	22 (1737)	22 (900)	100 (193)	Sanders et al. (1985)
Upper Missouri	4 (68)	8 (3037)	200 (4467)	Burress et al. (1982)
Lower Mississippi	17 (4903)	not given (849-23 462)	—(17-479)	Baker et al. (1988a and 1991)

[1]Taxa enumerated by order only.

Table 2. Mean fish species richness (mean numerical catch per unit effort) for natural banks (usually steep, eroding banks) and riprap revetments. Species richness values are means for a given location and a given time. Mean values in different rows are not directly comparable because different sampling methods were used. However, column-to-column comparisons in the same row are valid. Fishes were sampled by electrofishing unless otherwise noted.

River	Natural Banks	Riprap Spur Dikes	Riprap Revetments	Spur Dike/Revetment (percent)	Source
Willamette	13 (89)	not sampled	11 (281)	–	Hjort et al. (1984)
Willamette	20	9	10	90	Li et al. (1984)[2]
Sacramento	8 (21)	not sampled	10 (26)	—	Michny (1988)
Sacramento	10 (488)	not sampled	12 (330)	—	Schaffter et. al. (1983)
Upper Missouri	8	14	10	140	Burress et al. (1982)[3]
Middle Missouri	not sampled	11 (26)	15 (66)	73 (39)	Atchison et al. (1986)[4]
Upper Mississippi	33 (41)	not sampled	33 (87)[5]	–	Farabee (1986)
Arkansas	10 (98)	13 (225)	13 (110)	100 (205)	Sanders et al. (1985)[6]
Batupan Bogue, Mississippi	25 (360)	25 (410)	18 (196)[7]	139 (209)	Knight and Cooper (1991)
Lower Mississippi	60	68	not sampled[8]	–	Baker et al. (1991)[9]

[2] Cumulative total number of species captured, not mean per site per sampling date.
[3] Electrofishing, hoop netting, seining, gill netting.
[4] Electrofishing. Hoop net results were similar.
[5] Two revetments were sampled. One was constructed with 30-60 cm diameter riprap, the other with riprap "that averaged" > 60 cm diameter. The larger riprap site had mean numerical and biomass catches per unit of effort that were 130% and 250% , respectively, of the same values for the smaller stone revetment.
[6] Electrofishing. Use of additional sampling gears in areas around spur dikes yielded 16 additional species there.
[7] Structures sampled for this study were longitudinal toe dikes (windrows of stone placed parallel to flow along bank toes), and provided habitat similar to riprap blanket revetment placed on a graded bank.
[8] Lower Mississippi River revetments are articulated concrete mattresses (ACM) with riprap and asphalt on upper banks. Species richness for natural banks and those covered with ACM are similar (Pennington et al., 1983).
[9] Numbers shown are total numbers of species reported in literature. Fifty-five species have been reported for articulated concrete mattress revetments.

Table 3. Concepts for riprap structures with potential for providing mesoscale habitats superior to traditional designs.

Concept[12]	Description	Objective	Benefits to Habitat	Testing[13]	Remarks	Source
Bendway weirs	submerged, level-crested spur dikes angled upstream	develop and maintain navigation channel	minimize disturbance of bank (shaping, clearing vegetation, etc.)	model studies and prototype installation on middle Mississippi River; no biological studies	developed expressly for a particular reach; applicability elsewhere may be questionbable	Davinroy (1990)
Off bankline revetments	windrows of riprap placed in shallow water a short distance from eroding bank with periodic gaps	protect bank	create low-velocity habitat created between structure and bank. Bank clearing and shaping eliminated. Gaps allow movement of organisms and recreational craft	biological field studies on Middle Mississippi and Missouri Rivers	may be vulnerable to sedimentation. Stone requirements likely greater than for blanket-type revetment	Niemi and Strauser (1991) Reynolds and Segelquist (undated) Kallemeyn and Novotny (1977)
Using larger stone gradation in traditional revetment	upper end of gradation curve shifted to include a few large (~0.6 m) stones	protect bank	heterogeneity of voids increased. Larger voids available for larger organisms.	biological study at one field site	potential adverse effects on revetment stability	Niemi and Strauser (1991) Farabee (1986) Kallemeyn and Novotny (1977)
Notched spur dikes	gaps constructed or allowed to form in transverse training structures.	reduce sediment deposition in dike fields	develop heterogeneous flow patterns and preserve low-velocity aquatic habitat contiguous with main channel	several biological field studies that include limited physical data	some locations are vunerable to sedimentation or simply create additional high-velocity habitat	Shields (1984 and 1988)
Fish groins	traditional riprap revetment with low ridges of riprap running from top bank to toe perpendicular to channel	create eddies and zones of reduced velocity	provide habitat for juvenile salmonids	biological field study and physical modeling	when combined with plantings of woody vegetation, provides best replacement for natural bank as juvenile salmon habitat	US Fish and Wildlife Service (1992)
Filling interstices with gravel	traditional riprap revetment covered with a layer of gravel	create near-bank hydraulic conditions similar to natural gravel banks	provide habitat for juvenile salmonids	biological field study		US Fish and Wildlife Service (1992)
Rearing bench	gradually-sloping (1V:5H) gravel bench parallel to channel placed at an elevation where it will be inundated at moderate flows	create near-bank hydraulic conditions similar to natural gravel bar	provide habitat for juvenile salmonids	biological field study	juvenile salmonid densities were higher than for riprap but lower than for natural banks	Michny and Deibel (1986)
Indented revetment	traditional riprap revetment with periodic shelf-like indentations.	form shallow pools adjacent to the main channel	provide low-velocity habitat	physical model study and a biological field study of similar concept	may be vulnerable to sedimentation. Quality of habitat provided unstable due to stage variation.	Schmitt (1983) Zimpfer et al. (1988)

[12] Terms used in this column are taken from literature listed in source column.

[13] Testing documented in sources.

Table 4. Revetments and transformation of major rivers. Impacts on habitat and fishery reflect the influence of water quality degradation, impoundment of upstream and tributary reaches, levee construction, woody debris removal, channel straightening, and transverse training structures such as spur dikes.

River	River Kilometer (=0 at mouth)	Revetted Bank (percent)[10]	Impacts on Habitat	Impact on Fishery	Source
Mississippi	0-1570	45	river length shortened 229 km, floodplain reduced 90% by levees	unknown	Baker et al. (1988a) Fremling et al. (1989)
Missouri	0-1181	60[11]	river length shortened 64.4 km, water area reduced 34-66%, 2111 km^2 natural habitat lost from channel and meander belt	commercial fish harvest reduced 80% in reach within state of Missouri	US Army Engineer District, Kansas City (1980), Nunnally and Beverly (1986), US Army Corps of Engineers (1990), Funk and Robinson (1974)
Sacramento	0-311	47	freshwater wetland vegetation acreage in valley reduced 43% between 1939-mid 1980s	mean fall-run chinook salmon numbers upstream of RK 391 reduced 87% between 1950-59 and 1980-85.	Keck (1990), Storfer (1992) Frayer et al. (1989), Buer et al. (1984)
Willamette	0-301	40	four-fold decrease in surface water volume. Elimination of braided reaches. Removal of 550 snags km^{-1}	unknown	Fletcher and Davidson (1988) Sedell and Froggatt (1984)
Rhine	0-1320	unknown	backwaters, braids and side channels greatly reduced. Bed degradation up to 7 m. Area subjected to flooding reduced 85-94%.	'since 1915, a continuous and irreversible decline of catches has occurred.'	Lelek (1989) Dister et al. (1990)
Vistula	0-640	'all stretches'	'...disappearance of islands and braided reaches, particularly in the lower course of the river.' Channel width reduced by 50%, bed lowered 1.3 m (reach from Wloclawek dam to Swiecie)	sharp decline in commercial fish harvest, especially of migratory species	Backiel and Penczak (1989) Babinski (1992)

[10] Estimates generated by dividing total length of revetted bankline by twice the reach length.
[11] For RK 0-802 only.

FUNDAMENTAL CONCEPTS APPLIED TO THE UTILIZATION OF ROCK RIPRAP TO ACHIEVE CHANNEL STABILIZATION

D.B. Simons
Simons and Associates, Fort Collins, Colorado, USA

1. INTRODUCTION

An evaluation of the riverine systems in the United States has documented that there are approximately 3.5 million miles of rivers, creeks, and other channels. The Corps of Engineers in their evaluation of instability of streams reported that erosion is occurring on approximately one-half million miles of bank lines within the system of rivers. This, of course, does not include instability problems associated with lake shore lines, reservoir shore lines and coastal problems. Because of the magnitude of the erosion problem, the River and Harbor Act of 1968 (Title 1 of Public Law 90-483, Section 120) authorized and directed the Secretary of the Army acting through the Chief of Engineers; "*... to make studies of the nature and scope of the damages which result from streambank erosion throughout the United States.*" Based upon an analysis of the total annual damages resulting from streambank erosion, it was estimated that the annual cost of bank protection required to prevent further damage would be on the order of $420,000,000. As a consequence of this background information, the Corps of Engineers recommended a vigorous research and development effort under existing agency authorities to improve and develop the required low-cost remedial measures and to develop a better understanding of the erosional processes and their effects. As an outgrowth of this recommendation, and in recognition of the serious economic losses occurring throughout the U.S. due to bank erosion, the U.S. Congress passed the Streambank Erosion Control Evaluation and Demonstration Act of 1974, Section 32, Public Law 93-251 (as amended by Public Law 94-587, Section 155 and Section 161, October 1976) which authorized a 5-year program related to identification of revetment methodologies, initiation of a test program utilizing a wide variety of revetment materials, and evaluation of their effectiveness. This extensive study included an evaluation of streambank erosion, a literature survey, hydraulic research, geotechnical research, and development and demonstration projects. As a part of the demonstration effort, five work units were established. These groups had the duty of evaluating the usefulness and relative cost of different types of revetment materials utilized throughout the United States. The original act established a funding limit of $25,000,000 for 5 fiscal years ending June 30, 1978. The act was then amended and a funding cap of $50,000,000 was set.

As a consequence of the foregoing amendment, the Corps of Engineers has continued this work to a limited degree. Some ten documents have been prepared reporting the success and failures of different types of revetment materials that were subjected to a wide range of climatological, hydrological, and hydraulic conditions. This information has been reviewed and is a source of background material upon which this report is based. During the initial phases of the COE study, D.B. Simons was serving as a consultant to the Corps of Engineers regarding the foregoing and related work, principally on the Ohio River, the Mississippi River, the Chippewa River, and rivers in the Yazoo River basin.

In order to arrive at the conclusions presented herein, Simons & Associates also personally contacted and communicated with key staff at the following organizations in order to build up a current database regarding the use of widely utilized revetment materials: Waterways Experiment Station, Corps of Engineers, Vicksburg, MS.; Vicksburg District Corps of Engineers; California Department of Transportation; Colorado Department of Transportation; Federal Highway Administration, Washington, D.C.; Highway Research Board, Washington, D.C. (ARC); Tom Fish, Consultant; Colorado State University; Simons, Li & Associates, Consultant; Soil Conservation Service; as well as other engineering and consulting firms and contractors presently engaged in channel revetment work. Based upon data provided by the these sources, it has been determined that the approximate percentages of use of different materials presented in Table 1 is applicable on a national basis.

TABLE 1
Relative Use of Revetment Materials

Item	Percentage of Total Use Nationally
Rock Riprap	55-65
Gabions	5-15
Concrete Surfacing	5
Soil Cement	3
Miscellaneous	12-32
Armorflex	
Articulated Concrete Mattress	
Bituminous Revetment	
Cellular Blocks	
Cellular Soil Stabilization	
Clay Blankets	
Dry Rubble	
Filtercloth	
Geogrid Reinforcement	
Grouted Riprap	
Grouted Rubble	
Kellner Jacks	
Low-Quality Rock	
Plastic Lining	
Sack Revetment	
Slope Mattress	
Soil Stabilization (Cement, Lime)	
Steel Furnish Slag	
Used Autotire Mattress	
Vegetation	

The results of the in-depth analysis presented in Table 1 confirm that rock riprap is still the predominant material of choice for revetment work to stabilize river banks and protect the side slopes of embankments. In the final report to Congress, the Corps of Engineers (1981) concluded that rock will likely continue to be the first choice of bank protection materials where material of sufficient size is available and affordable, because of durability, and other advantages. Considering distribution of construction costs based upon limited 1991 and 1992 data, rock riprap accounted for 31.3% of revetment materials utilized during this period of time (see Fig. 1).

2. STREAMBANK EROSION

Processes of bank erosion are of primary importance in the context of process/response systems involving flowing water as it interacts with bed and bank material. Changes in channel geometry with time are particularly significant during periods when alluvial channels are subjected to high flows. The converse situation exists during relatively dry periods. Erosive forces during high flow periods may have a capacity approximately 100 times greater than those forces acting during periods of intermediate and low flow. In most instances when considering the instability of alluvial rivers, it can be shown that approximately 95 percent of all river changes occur during that small percentage of the time when the discharge exceeds dominant discharge.

Regardless of the fact that the majority of bank changes occur during comparatively short time periods, there may also be regions within a river in which some degree of instability is exhibited for all flow conditions. Raw banks may develop on the outside of bends as a consequence of direct impingement of the flowing water. Sloughing banks may occur as a result of seepage and other secondary forces created by water draining back through the banks into the river. Continuous wave action, generated either naturally or by man's activities, may also perpetuate erosion problems.

2.1 Causes of Streambank Failure

A summary of the variables and factors affecting erosion of river banks is outlined below.

I. Hydraulic Parameters
   - A. Fluid Properties
   - B. Flow Characteristics
     1. Magnitude of Discharge
     2. Duration of Discharge
     3. Velocity Range and Distribution

II. Characteristics of Bed and Bank Material
   - A. Size
   - B. Gradation
   - C. Shape
   - D. Specific Weight

III. Characteristics of the Banks
  A. Noncohesive
  B. Cohesive
  C. Stratified
  D. Rock
  E. Height
IV. Subsurface Flows
  A. Wave Forces
  B. Seepage Forces
  C. Piping
V. Wind Waves and Boat Waves
  A. Wave Forces
  B. Surface Erosion
  C. Piping
VI. Climatic Factors
  A. Freezing
  B. Thawing
  C. Permafrost
VII. Biological Factors
  A. Vegetation
  B. Animal Life
VIII. Man-induced Factors
  A. Pool Fluctuations
  B. Agricultural Activities
  C. Mining
  D. Transportation
  E. Urbanization
  F. Drainage
  G. Flood Plain Development
  H. Recreational Boating

Due to the complex nature of erosional processes and interaction of the variables and forces that cause erosion, the mechanics of erosional patterns of channels and banks are inadequately understood at present. A better understanding of these erosional processes can only be made through a detailed evaluation of adequate data.

2.2 Bed and Bank Material

Resistance of a river bank to erosion is closely related to several characteristics of the bank material. Bank material can be broadly classified as cohesive, noncohesive and composite.

Cohesive material is more resistant to surface erosion and has low permeability which reduces the effects of seepage, piping, frost heaving, and subsurface flow on the stability of the banks. However, such banks when undercut and/or saturated are more likely to fail due to mass wasting processes such as sliding.

Noncohesive bank material tends to be removed grain by grain from the bank line. The rate of particle removal, and hence the rate of bank erosion, is affected by factors such as the direction and magnitude of the velocity adjacent to the bank, the turbulent fluctuations, the magnitude and fluctuations in the shear stress exerted on the banks, seepage force, and piping wave forces, many of which may act concurrently.

Composite or stratified banks are very common on alluvial rivers and generally are the product of past transport and deposition of sediment by the river. More specifically, these types of banks consist of layers of materials of various sizes, permeability, and cohesion. The layers of noncohesive material are subject to surface erosion, but may be partly protected by adjacent layers of cohesive material. This type of bank is also vulnerable to erosion and sliding as a consequence of subsurface flows and piping.

2.3 Subsurface Flow

With flow of water from the river into the adjacent banks, a stabilizing seepage force is generated. Rivers that continuously seep water into the banks tend to have smaller widths and larger depths for a particular discharge. The reverse is true of the rivers that continuously gain water by an inflow through their banks. The inflowing water creates a seepage force that tends to destabilize the banks.

If the water table is higher than river stage, flow will be from the banks into the river. The high water table may result from: (1) a wet period during which water draining from adjacent watersheds saturates the flood plain to a higher level; (2) poor drainage conditions resulting from deterioration or failure of surface drainage systems; (3) increased infiltration resulting from changes in land use causing an increase in water level; (4) irrigated flood plains; and (5) development of the adjacent flood plain for homes and businesses that utilize septic tanks and leach fields to dispose of waste water and sewage.

With a rise in river stage, an outward gradient is developed that induces flow into the banks. This can be caused by: (1) the storage and release of water for pumped storage hydropower generation which causes numerous fluctuations in river stage; and (2) boat and wind waves which cause local variations in stage that introduce inflow and outflow of water from the banks. However, because the duration of the change in stage is small, the inflow and outflow phenomena are usually concentrated locally in the surface of the banks; and (3) the formation and loss of backwater caused by ice flows and ice jams which lead to both seepage into and out of the banks.

The presence of water in the banks of rivers and its movement toward or away from the river affect bank stability and bank erosion in various ways. The related erosion of banks is a consequence of seepage forces, piping, and mass wasting.

2.4 Piping of River Banks

Piping is another phenomenon common to the alluvial banks of rivers. With stratified banks, i.e., lenses of sand and coarser material sandwiched between a layer of fine cohesive materials, flow is induced in more permeable layers by changes in river stage and by wind- and boat-generated waves. If the flow through the permeable lenses is capable of dislodging and transporting particles from the permeable lenses, the material is slowly removed, undermining portions of the bank. Without this foundation material to support the overlying layers, a block of bank material drops down the results in the development of tension cracks. These cracks allow surface flows to enter, further reducing the stability of the affected block of bank material. Bank erosion may continue on a grain-by-grain basis or the block of bank material may ultimately slide downward and outward into the channel, causing bank failure as a result of a combination of seepage forces, piping, and mass wasting.

2.5 Mass Wasting

An alternative form of bank erosion is caused by local mass wasting. If the bank becomes saturated and possibly undercut by flowing water, blocks of the bank may slump or slide into the channel. Mass wasting may be further aggravated by construction of homes on river banks, operation of equipment on the flood plain adjacent to the banks, added gravitational force resulting from tree growth, location of roads that cause unfavorable drainage conditions, saturation of banks by leach fields from septic tanks, and increased infiltration of water into the flood plain as a result of changing land-use practices.

Landslides, the downslope movement of earth and organic materials, result from an imbalance of forces. Various forces are involved in mass wasting. These forces are associated with the downslope gravity component of the slope mass. The forces that resist the downslope gravity component include the shear strength of the earth, the reinforcement provided by vegetation, and any additional stabilizing factors as a consequence of man's activities. When a slope is acted upon by a stream or river, an additional set of forces is added. These forces are associated with removal of material from the toe of the slope, fluctuations in ground water levels, and vibration of the slope. A slope may fail if stable material is removed from the toe. When the toe of a slope is removed, the slope loses more resistance by buttressing than it does by downslope gravitational forces. The slope materials may then tend to move downward into the void in order to establish a new balance of forces or equilibrium. Oftentimes, this equilibrium is a slope configuration with less than original surface gradient. The toe of the failed mass can provide a new buttress against further movements. However, if this buttress is removed by stream erosion, the force equilibrium may again be upset. For slope toes acted upon by erosive stream water, the continual removal of toe material can upset the force balance.

2.6 River Training and Stabilization

Various devices and structures have been developed to control river flow along a preselected path and to stabilize the banks. Most have been developed through trial and error applications, aided in some instances by hydraulic model studies. Specific functions of bank protection and training works include: (1) stabilize eroding river banks and channel location in the case of shifting streams; (2) economize on bridge lengths by constricting the natural waterway; (3) direct flow parallel to piers in order to minimize local scour; (4) improve the hydraulic efficiency of a waterway opening, reducing afflux and scour and facilitating passage of ice and debris; (5) protect road approaches from stream attack and to prevent meanders from folding on to the approaches; (6) permit construction of a square bridge crossing by diverting the channel from a skewed alignment; (7) reduce the overall cost of a road project by diverting the channel away from the base of a valley slope, thereby allowing a reduction in bridge length and height; (8) secure existing works, or to repair damage and improve initial designs; and (9) protect longitudinal encroachments. A comprehensive bank stabilization and channel rectification program to control a river reach completely normally requires extensive work on concave banks in bends, minor work on convex bars, and control on both banks through crossings.

To minimize attack by the stream on stabilization and rectification structures, the river is shaped to an alignment consisting of a series of easy bends, with the flow directed from one bend into the next bend downstream in such a way as to maintain a direction essentially parallel to the channel control line. Straight reaches of very small curvature should be avoided, insofar as practical, because there is a tendency for flows to shift from side to side in such reaches. The optimum bend radius approximates that of relatively stable bends in the general river reach.

- **Fixed Points** - One of the essential requirements in designing a system of stabilization works is that construction start at a stable, fixed point on the bank and continue downstream to another stable location or to some point below which the river can safely be left uncontrolled. Construction of relatively short isolated stabilization work has often proved unsuccessful because eventual changes in the direction of flow inherent in bank caving in the upstream uncontrolled reach either will set up a direct attack against the isolated protective work and severely damage or destroy it or will shift the attack to some other nearby reach of bank, requiring additional work and possible abandonment of the original work. Between fixed points revetments should be constructed on a smooth alignment, with no irregularities, in order to avoid eddies set up by such disturbances to the flow that can lead to local scour and subsequent undermining of the revetment.

- **Radius of Curvature** - The most appropriate radius of curvature for rectification and stabilization varies from river to river and from reach to reach for a given river. It must be determined on the basis of relatively stable natural bends for each stream. The shorter the radius of curvature of a bend, the deeper the channel will be adjacent to the concave bank. The deeper the channel is, the greater the possibility of undermining bank protection work in the bend and the greater the cost of maintaining the structure. Therefore, sharp curvature of bends should be avoided to obtain the most economical control of the river.

Bank stabilization and channel rectification works fall into one of two broad categories, generally defined as follows:

1. **Revetments** - which are structures parallel to the current used for such purposes as stabilizing concave banks of bends.
2. **Flow Control Structures** - which are used for:
   - directing flow from one bend into the next bend downstream,
   - fair out sharp bends to a larger radius of curvature providing a more desirable channel alignment,
   - close off secondary channels and old bendways, and
   - concentrate flow on a limited width within a wider channel.

3. RIPRAP SIZE AND STABILITY ANALYSIS

When available in sufficient size, rock riprap is usually the most economical material for bank protection. Rock riprap has many other advantages over other types of protection. A riprap blanket is flexible and is neither impaired nor weakened by slight movement of the bank resulting from settlement or other minor adjustments. Local damage or loss is easily repaired by the placement of more rock if repair is completed in a timely manner. Construction is not complicated so special equipment or construction practice is not necessary. Riprap is usually durable and recoverable and may be stockpiled for future use. The cost-effectiveness of locally available riprap provides a viable alternative to many other types of bank protection. Riprap stability increases with increasing thickness because more material is available to move to damaged areas and more energy is dissipated before it reaches the filter and streambank supporting the riprap. Although the riprap must be placed to the proper level in the bed to accommodate degradation and local scour, there are no foundation problems. The appearance of rock riprap is natural and after a period of time vegetation may grow between the rocks. Wave run up on rock slopes is usually less than on other types. Finally, when the usefulness of the protection is finished, the rock may be salvageable.

The important factors to be considered in designing rock riprap blanket protection are:

- The durability of the rock.
- The density of the rock.

- The full range of velocities (both magnitude and direction) of the flow in the vicinity of the riprap for the total range of expected discharges.
- The slope of the bed or bank line being protected.
- The angle of repose for the riprap.
- The shape and angularity of the riprap.
- What shape and weight of riprap will be stable in the streamflow?
- What thickness of riprap is required?
- Is a filter needed between the bank and the blanket to allow seepage but to prevent erosion of bank soil through the blanket?
- How far below the existing bed elevation must the riprap be placed to accommodate anticipated general scour, local scour, and incisement of the channel into the average bed of the channel?
- How will the riprap be tied into the bank at its upstream and downstream ends?

3.1 Different Methods

Currently, several design procedures are routinely used to determine the appropriate size of rock riprap for protection of embankments, channels, unprotected slopes, the impact of flowing water, for stabilization of the banks of reservoirs, and for stabilizing coastal erosion problems. Principal methods widely adopted include the following which are discussed in some detail by Simons & Sentürk (1992).

- Application of beginning of motion to practical problems.
- Stability analysis of riprap including:
  - stability of a particle on a sloping surface,
  - horizontal flow on a side slope,
  - flow on a plane sloping bed, and
  - flow on a horizontal bed.

Common methods of determining the size of riprap include:

- Lane's Solution - Stability on a Sloping Surface.
- University of Minnesota Method.
- The U.S. Corps of Engineers Waterways Experiment Station Method.
- California Division of Highways Method.
- ASCE Sedimentation Manual Method.
- Bureau of Reclamation Method.
- Bureau of Public Roads' Method.
- Riprap Design With Factors of Safety.
- Stephenson Method.
- Velocity Method.

In addition to the foregoing methods, additional studies have been completed by agencies and universities worldwide. The important conclusion from analyzing these methodologies is that most methods are empirical to some degree, are based upon limited field data, and in many instances, require data that are difficult to obtain for field application. In summary, to arrive at a proper solution to a particular stabilization problem, it is essential to consider the geomorphology of the system, the causes of streambank failure, the types of bed and bank material, the possibility of subsurface flows, and the potential for piping of river banks. Thereafter, if utilization of riprap provides an acceptable means for achieving channel stability, it is necessary to review and identify workable means of sizing the riprap, determining an acceptable factor of safety for the design in question, properly placing the riprap and thereafter subjecting the site to review and adequate maintenance. Simultaneously, it is necessary to consider the specific characteristics of the system to be stabilized, i.e., stabilization of side slopes of channels in both straight reaches and bends, and the stabilization of groins, abutments, and other structures that may protrude into the flow. A thorough understanding of the impacts of varying geometries in the channel system on velocity distributions and velocity fluctuations is essential to success. In general, in spite of the large number of variables impacting on the design of riprap, an excellent, simple indicator for sizing riprap is knowledge of the velocity field to which the riprap will be subjected.

Considering geomorphic and sediment transport impacts on channel stability, it is essential to document potential changes in stream bed geometry paying particular attention to stream bed elevation fluctuations, and more specifically, to the potential for long-term degradation of the channel bed. The proper utilization of riprap, in general, requires the use of appropriate filters between the rock riprap and the material requiring protection. This issue requires consideration of filters constructed of natural material as well as an evaluation of the acceptability of permeable manufactured filter cloth. As an alternative to filters, the need may be eliminated by the proper choice of gradation of the riprap. Concepts will be presented concerning the adequacy of specifications dictating the criteria for placement of riprap, methods of placing the rock riprap, the impacts of placement techniques on long-term stability, and the essential need for continual surveillance and maintenance of the protected system.

4. RIPRAP GRADATION AND PLACEMENT

The concept of a representative grain size for riprap is simple. A uniformly graded riprap with a median size D_{50} scours to a greater depth than a well-graded mixture with the same median size. The uniformly distributed riprap scours to a depth at which the velocity is less than that required for the transportation of D_{50} size rock. The well-graded riprap, on the other hand, develops an armor plate. That is, some of the finer materials, including sizes up to D_{50} and larger, are

transported under the given flow conditions. Thus, the size of rock representative of the stability of the riprap is determined by the larger sizes of rock. The representative grain size D_m for riprap is larger than the median rock size D_{50}.

The computations of the representative grain size D_m for the recommended gradation are given in Table 2.

TABLE 2
Data for Suggested Gradation

Percent Finer	Sieve Diameter	D_i
0	0.25 D_{50}	
10	0.35 D_{50}	0.28 D_{50}
20	0.5 D_{50}	0.43 D_{50}
30	0.65 D_{50}	0.57 D_{50}
40	0.8 D_{50}	0.72 D_{50}
50	1.0 D_{50}	0.90 D_{50}
60	1.2 D_{50}	1.10 D_{50}
70	1.6 D_{50}	1.50 D_{50}
90	1.8 D_{50}	1.70 D_{50}
100	2.0 D_{50}	1.90 D_{50}

The rock sizes in the last column in Table 2 are used in the following equation (Stevens, 1968) to find the representative grain size D_m. This effective grain size, D_m, of the mixture corresponds to the size D_{65} of the riprap.

$$D_m = \left[\frac{\sum_{i=1}^{10} D_i^3}{10}\right]^{1/3} \cong 1.25 D_{50}$$

When the bed material has a log-normal distribution, the representative size of the bed material based on the weight of the particles is given by Mahmood (1973) as a function of the gradation coefficient G:

$$D_m = D_{50} \exp\left\{\frac{3}{2}(\ln G)^2\right\}$$

For gradation coefficients of 2 and 3, $D_m = 0.72 D_{50}$ and $1.81 D_{50}$ respectively.

With a distributed size range, the interstices formed by the larger stones are filled with the smaller sizes in an interlocking fashion, preventing formation of open pockets. Riprap consisting of angular stones is more suitable than that consisting of rounded stones. Control of the gradation of the riprap is almost always made by visual inspection. If it is necessary, poor gradations of rock can be employed as riprap provided the proper filter is placed between the riprap and the bank or bed material.

Considering the practical problems of quarry production, a gradation band is usually specified by the U.S. Army Corps of Engineers (1983) rather than a single gradation curve, and any stone gradation within the limits is acceptable. The Corps criteria for establishing gradation limits for riprap are as follows:

- The lower limit of D_{50} stone should not be less than the size of stone required to withstand the design shear forces.
- The upper limit of D_{50} stone should not exceed five times the lower limit of D_{50} stone, the size which can be obtained economically from the quarry, or the size that satisfies layer thickness requirements.
- The lower limit of D_{100} stone should not be less than two times the lower limit of D_{50} stone.
- The upper limit of D_{100} stone should not exceed five times the lower limit of D_{50} stone, the size which can be obtained economically from the quarry, or the size that satisfies layer thickness requirements.
- The lower limit of D_{15} stone should not be less than 1/16 the upper limit of D_{100} stone.
- The upper limit of D_{15} stone should be less than the upper limit of the filter material.
- The bulk volume of stone lighter than the D_{15} stone should not exceed the volume of voids in the structure without this lighter stone.

The riprap thickness should not be less than 12 inches for practical placement, less than the diameter of the upper limit of D_{100} stone, or less than 1.5 times the diameter of the upper limit of D_{50} stone, whichever is greater. If riprap is placed under water, the thickness should be increased by 50 percent, and if it is subject to attack by large floating debris or wave action it should be increased 6 to 12 inches.

Riprap placement is usually accomplished by dumping directly from trucks. If riprap is placed during construction of the embankment, rocks can be dumped directly from trucks from the top of the embankment. Rock should never be placed by dropping down the slope in a chute or pushed downhill with a bulldozer. These methods result in segregation of sizes. With dumped riprap there is a minimum of expensive handwork. Poorly graded riprap with slab-like rocks requires more

work to form a compact protective blanket without large holes or pockets. Draglines with orange peel buckets, backhoes, and other power equipment can also be used advantageously to place the riprap.

Hand placed riprap is another method of riprap placement. Stones are laid out in more or less definite patterns, usually resulting in a relatively smooth top surface. This form of placement is used rarely in modern practice because it is usually more expensive than placement with power machinery, and it is more likely to fail than dumped riprap.

Dumped riprap keyed (or plated) by tamping has proved to be effective. Guidelines for placement of keyed riprap have been developed by the Oregon Department of Transportation and distributed by the Federal Highway Administration, Region 14. In the keying of a riprap, a 4,000 pound (1,818 kg) or larger piece of steel plate is used to compact the rock into a tight mass and to smooth the revetment surface. Keyed riprap is more stable than loose riprap revetment because of reduced drag on individual stones, its angle of repose if higher, and its cost is less because a lesser volume of rock per unit area is required. However, the resistance to flow is reduced resulting in somewhat higher velocities.

5. FILTERS FOR RIPRAP

Filters are used under riprap to allow water to drain from the bank without carrying out soil particles. Filters must meet two basic requirements: stability and permeability. The filter material must be fine enough to prevent the base material from escaping through the filter, but it must be more permeable than the base material. There is no standard filter that can be used in all cases. Two types of filters are commonly used: gravel filters and plastic filter cloths.

5.1 Gravel Filters

A layer or blanket of well-graded gravel should be placed over the embankment or riverbank prior to riprap placement. Sizes of gravel in the filter blanket should be from 3/16 of an inch to an upper limit depending on the gradation of the riprap with maximum sizes of about 3 to 3-1/2 inches. Thickness of the filter may vary depending upon the riprap thickness but should not be less than 6 to 9 inches. Filters that are one-half the thickness of the riprap are quite satisfactory.

5.2 Synthetic Filter Cloths

Plastic cloth and woven plastic materials are also used as filters, replacing a component of a graded filter. Numerous plastic filter fabrics are on the market, with a wide variation in size and number of opening and in strength and durability of material. Opening areas of 25 to 30 percent appear desirable to minimize the possibility of clogging and to reduce head loss.

When filter fabric is used, care must be taken not to puncture the fabric during construction. If the filter cloth is placed on top of the base material, gravel can sometimes be placed directly on the cloth, eliminating the need for filter sand. However, if the paving materials are dumped or cast stone it is desirable to place a protective blanket of sand or gravel on the filter -- or to take care in placing the rock -- so that the filter fabric is not punctured. Stones weighing as much as 3,000 pounds have been placed on plastic filters with no apparent damage. If a protective covering is not used, the size and drop of the rock should be limited. The sides and toe of the filter fabric must be sealed or trenched so that base material does not leach out around the filter cloth. Care is also required in joining adjacent sections of soft filter fabric together; sewn, overlapped, and/or welted seams are used. Cloths are generally in 100 foot long rolls, 12 to 18 feet wide. Overlap of 8 to 12 inches is provided with pins at 2 to 3 foot intervals along the seam to prevent separation in case of settlement of the base material.

6. NONCONVENTIONAL APPLICATIONS OF RIPRAP

The complex nature of channel instability problems has made it necessary to develop and investigate special methods of applying riprap because of conditions imposed physically, conditions imposed environmentally, and conditions imposed by economic restraints. In situations where it is difficult to modify the bank to a suitable side slope to receive riprap, it may be necessary to dig a trench in the desired alignment of the river as close to the river and river level as possible considering land ownership, environmental considerations, and the dynamics of the river within which a computed quantity of riprap could be placed to be launched, thus armoring the bank as erosion progressed landward. As another alternative, the rock riprap may be windrowed at the top of the bank in the alignment desired for the channel. Similarly, the riprap would then be launched by the landward movement of the river. For a successful application of riprap utilizing either of these two methods, it is essential to place, in either the trench or the windrow, a sufficient volume of rock so that when launched it will adequately blanket the bank, leaving a reserve of materials as subsequent degradation may lower the bed level requiring additional material to stabilize the bank. This particular methodology was developed by the English as they attempted to cope with the instability of the rivers in India prior to the partition of India. The results of their studies are documented by Inglis (1949). His documentation of methodology was based upon materials presented by an engineer by the name of Bell who developed this methodology based upon large-scale laboratory tests. It is interesting to note that where this type of application has been utilized the resultant side slope adopted by the launched rock is generally 2 horizontal units to 1 vertical unit or flatter. In all cases, the launched riprap adopts and adjusts to a stabilized slope considerably flatter than the angle of repose for the riprap. In instances where rock riprap is not available, it is possible to manufacture soil cement, break it into appropriate sizes, build the windrow or fill the trench with

this material which will subsequently launch due to the lateral movement of the river. This approach was adopted to stabilize the right bank of the Jamuna River in Bangladesh and has been particularly successful for this reach of river.

Another innovative procedure for applying riprap to achieve bank line stability has been developed and tested by the U.S. Corps of Engineers. The technique involves the armoring of approximately the lower one-half of the bank. This results in a considerable reduction in the volume of riprap needed and yet provides good bank line protection for a wide range of discharges. This method is principally applicable to those rivers which run at a small discharge for a long enough period of time to apply the riprap. In the case of very large flows of relatively long duration, the river could erode above the top of the riprap a significant distance enabling an avulsion to occur. The potential for an avulsion and flow conditions seem to be the major limitations in utilizing this particular method of application.

In estuaries, bank stabilization requires careful evaluation of flow phenomena induced by tidal activity. Referring to the Skokomish River in Washington, the tidal range is on the order of 12 feet. As the system experiences high tide a large volume of water is stored in the estuary. Upon the recession of tidal activity, the channel gradient is considerably steepened by the discharge of the stored water from the estuary, which results in relatively high flows and relatively high velocities, thus riprap must be designed for conditions imposed by this complex environment. Similar conditions were observed on the Mad River in California where it discharges into the Pacific Ocean. The geomorphology and hydraulics of the lower end of the Mad River are self-perpetuating and, to some degree, the hydraulic phenomena increases in erosive capability as the Mad River channel paralleling the ocean extends and develops because of combined river flow, tidal activity, and wave wash. This complex condition results because the further the channel geomorphically extends itself to the North, the larger the capacity of the channel to store water during the rising tide, and, on the falling tide, the larger the volume of water that is released. This results in continuing cyclical high velocities in the vicinity of the bend at the extreme north end of the reach adding to the speed with which the channel extends itself northward. This activity is supported by a hydraulic phenomena at the bend at the downstream end of the Mad River where it discharges into the Pacific Ocean. The traverse pressure gradient at the bend causes a secondary flow to exist within the channel which sweeps the bed sediment in the river to the left bank (looking downstream). The combined effect of the transverse currents with the wave action assures the continued development of the strip of sand existing between the channel and the ocean. Furthermore, the development of vegetation on this swath of land significantly limits the supply of wind-blown sediments from the ocean to the land to the channel, adding to the stability of the spit existing between the Mad River and the ocean.

In order to stabilize the channel considering the highly dynamic nature of the system, it was determined that it would be necessary to place the rock riprap material in a trench to subsequently be launched by channel erosion. It was determined that as the material in the trench is launched by erosion, the launching action should be observed and if segregation of sizes is significant at a particular location, adjustment should be made to protect the mixture to conform with a more desirable gradation. The rock classes selected to resist anticipated stream velocity and wave action required an adoption of rock riprap for which 50% of the riprap by weight would be larger than twice the median diameter, and approximately 20% of the material by weight would be smaller in size than one-half the median diameter of the mixture. Any uncertainty regarding the adequacy of the riprap is dependent upon achieving a suitable gradation of sizes so that large voids do not exist in the mixture. In general, the large rock thus selected is adequate and will have a suitable factor of safety against displacement by anticipated water, velocity and/or wave action. However, extreme care must be exercised to assure that the large voids in the launched riprap will be filled with smaller rock ranging in size from the order of the size of the void downward, so that each successive size class has its voids filled with smaller sized particles. To assist in achieving this goal, the contractor was instructed to add the necessary finer material to the specified gradation to achieve a desirable range of sizes prior to placement.

7. SUMMARY

In applying riprap to achieve channel and embankment stability, the following concepts should be used as a guide.

- The slope of the banks should be 1.5 horizontal units to 1 vertical unit or flatter.
- The bank material must be analyzed to determine the necessity, or lack thereof, for placement of a filter beneath the riprap.
- In placing the riprap, it is necessary to recognize the potential for degradation of the channel bed.
- In terms of selecting the size of rock riprap, velocity is the best index, i.e., it can be accurately estimated; it can be measured in the field; the variation of velocity in the cross section can be integrated into the design; the impacts of bends on the velocity distribution can be determined; and if it is necessary to estimate velocity, excellent supporting information regarding selection of roughness coefficients for a wide range of channel conditions was presented by Simons, et al (1989).
- In placing the riprap, segregation by size should be limited, the application of the riprap should be uniform, the riprap should be tied down or windrowed to accommodate possible degradation, and if a filter is required, appropriate selection of filter cloth or a natural filter

should be incorporated into the design. In some instances it is impossible to place a filter of either type. In this case, a proper selection of sizes of material constituting the rock riprap can reduce the need for a filter.

- It is impossible to guarantee perfect placement when using riprap. Therefore, the installation of rock riprap should be carefully inspected annually and immediately after each significant hydrology event. Based upon observed conditions, maintenance should be performed immediately to prevent failure in identified zones of weakness or partial failure.
- The selection and sizing of rock riprap is relatively straight forward and can be performed with reliable accuracy. However, proper placement is much more difficult to achieve. To assure proper placement, specifications properly formulated must be adhered to and thereafter, as emphasized above, a continual maintenance program is required.

Further research regarding the utilization of riprap should be subjected to careful consideration. In order to appropriately apply existing knowledge to the installation of riprap, it is essential to have a thorough knowledge of the physical processes. At best, the accuracy of design using present methods is on the order of plus or minus 25%. Therefore, a factor of safety must be incorporated into any acceptable design and should be supported by an organized maintenance program. In analyzing research needs related to the placement of rock riprap, it is easy to slip into the rut of analyzing trivia. Before launching into research, it is suggested that it would be worthwhile through a sensitivity analysis to estimate the increased accuracy in the design and application of riprap that could be achieved, assuming that the research is successful. On the other hand, even though such research may not contribute to improved design and application of riprap under field conditions, it has the advantage of training those participating in the research regarding the physical processes. However, such an approach to education implies very expensive tuition paid by the taxpayer. He may not be pleased with this approach.

REFERENCES

Inglis, C.C., 1949. "The Behavior and Control of Rivers with Canals (with the Aid of Models)," Parts I and II, Research Publication No. 13 prepared for the Government of India, Central Waterpower Irrigation & Navigation Research Station, Poona.

Mahmood, K., 1973. "Log-normal Size Distribution of Particulate Matter," J. of Sedimentary Petrology, Vol. 43, No. 4, December, pp. 1161-1165.

Richardson, E.V., D.B. Simons and P.Y. Julien, 1990. Highways in the River Environment, Prepared for the U.S. Department of Transportation, Federal Highway Administration.

Simons, D.B. and F. Sentürk, 1992. Sediment Transport Technology (Water and Sediment Dynamics), Second Edition, Water Resources Publications, Littleton, Colorado, January 1992.

Simons, R.K., R.A. Mussetter, P.Y. Julien and D.B. Simons, 1989. "Modeling Resistance to Flow in Open Channels," Channel Erosion and Channel Geomorphology 1989 ASAE Meeting, Quebec City, Canada.

U.S. Army Corps of Engineers, 1983. "Engineers Technical Letter 1110-2-284," 1982 Hydraulic Design Conference.

U.S. Army Corps of Engineers, 1981. "The Streambank Erosion Control Evaluation and Demonstration Act of 1974," Section 32, Public Law 93-251: Final Report to Congress, Main Report and Appendices A through H.

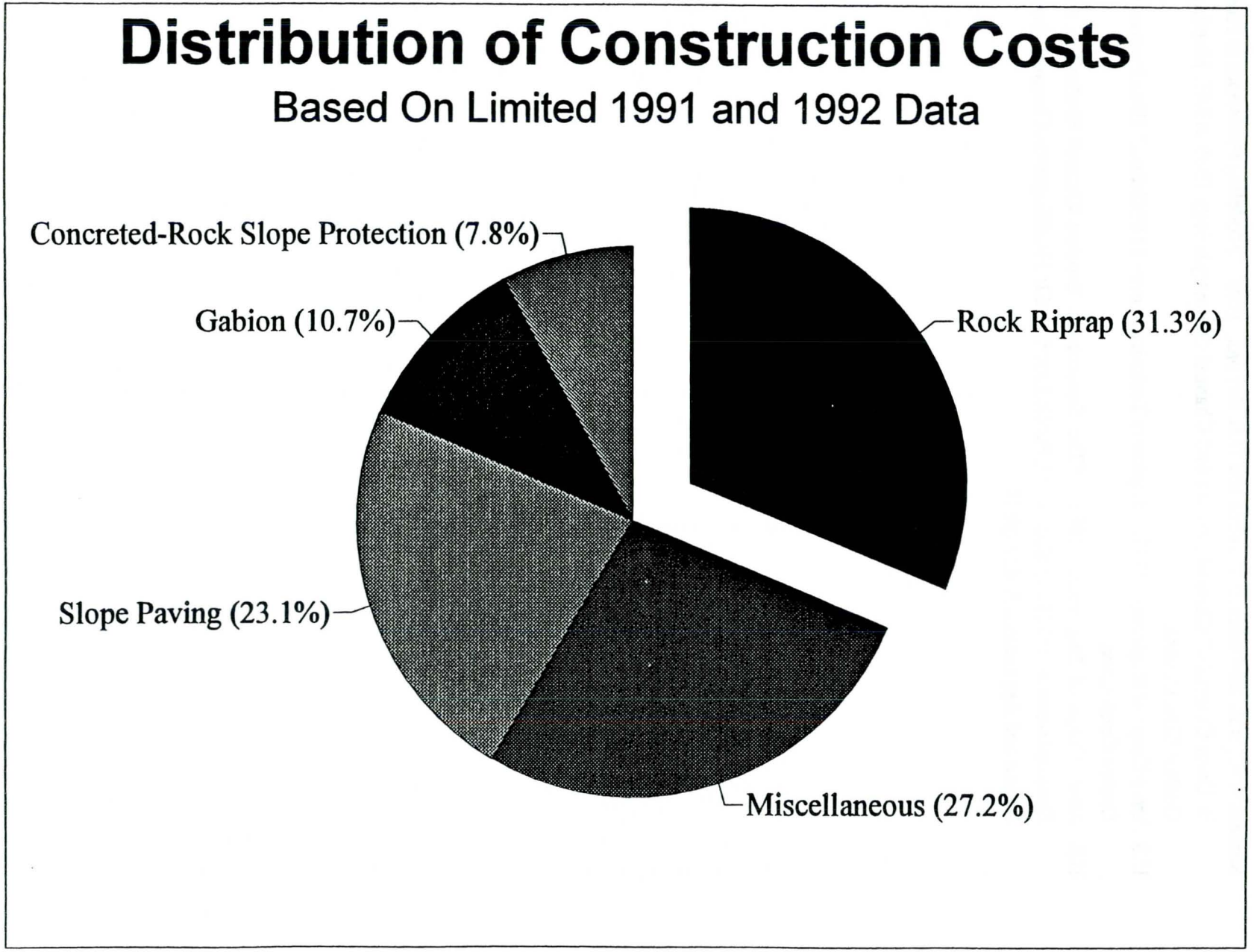
Distribution of Construction Costs
Based On Limited 1991 and 1992 Data
Concreted-Rock Slope Protection (7.8%)
Gabion (10.7%)
Rock Riprap (31.3%)
Slope Paving (23.1%)
Miscellaneous (27.2%)

Figure 1

RIVER TRAINING WORKS FOR A BRIDGE ACROSS THE BRAHMAPUTRA RIVER, BANGLADESH

Bert te Slaa
Haskoning, Royal Dutch Consulting Eng. and Architects,
P.O. Box 151, 6500 AD Nijmegen, The Netherlands

1. OVERVIEW OF THE JAMUNA BRIDGE PROJECT

The Jamuna (the local name for a stretch of the Brahmaputra in Bangladesh), the Ganges and the Padma divide Bangladesh in three parts: East, South West and North West (see figure 1.1). These rivers obstruct the social and economic development of Bangladesh. A bridge across the Ganges, built in 1912 provides a link between the North West and South West. A bridge across the Jamuna would establish the infrastructure for a multipurpose crossing to improve the road and rail communication network and to provide river crossings for electrical cables and a gas pipe.

After various preliminary studies had been executed by others, Rendel Palmer and Tritton (UK), NEDECO and Bangladesh Consultants Ltd. were entrusted in 1987 with a feasibility study, followed by the detailed design of a multipurpose bridge across the Jamuna. NEDECO (HASKONING, Royal Dutch Consulting Engineers and Architects, and Delft Hydraulics Laboratory) was in charge of the river engineering aspects of the project.

The Brahmaputra, being a braided river, has no fixed bed. Instead a multitude of channels move freely within the boundaries of a flood plain. At the selected crossing site the width of the flood plain is approximately **12 km**. Without special provisions the length of a bridge spanning the Jamuna would at least have to match the width of the flood plain. Even then the bridge abutments would have to be set at safe distances from the river's edges to cater for occasional wandering of an individual river channel outside the "normal" boundary of the flood plain.

From a hydraulic and morphological point of view the total width of the bridge opening need not be more than **4 to 5 km**. For this width the backwater effects and construction scour at the bridge site, in case of a major flood, would still not be too large. A "short" bridge requires a system of river training works to guide the river "under the bridge". The primary function of those river training works (RTW) is to protect the approaches to the bridge against erosion by outflanking river channels. It was found that a system of river training works as indicated in figure 1.2 would be adequate for that purpose. The system consists mainly of:

- a pair of guide bunds near the bridge approaches, each approx. 2200m long,
- a pair of "hard points", located upstream of the bridge at the border of the flood plain,

The guide bunds are the largest components of the RTW scheme. They have been conceived as earthen structures with a protection against current and wave attack. The protection has to reach to a depth of approximately 40m below the water level (flood level). This level is substantially deeper than the natural depths in the Jamuna. To reach this depth it is essential to construct the guide bunds beyond the direct influence of the

Jamuna channels. A trench should be dredged during the low water season, without disturbance by river flow. One side of the trench has subsequently to be covered with protective mattresses, thus forming the guide bund; see figures 1.3 and 1.4 for a plan view and a cross section of a proposed guide bund.

For each guide bund approx.12 million m^3 of sandy soil has to be dredged and approx. 750,000 t of riprap has to be provided for slope protection works. The project is at present (March, 1993) in the tendering stage. Cost for the river training works is likely to be in the region of US$ 230 million.

2. THE JAMUNA - HYDROLOGY AND MORPHOLOGY

(a) Hydrology

For various locations along the Jamuna long series of daily recorded water levels are available. For Bahadurabad, 83 km upstream of the bridge site, also a long record of daily discharges is available. Based on the historical record at Bahadurabad, a frequency distribution of the discharge at this station has been computed, assuming a Gumbel distribution for the annual maximum discharge. From this frequency distribution the expected discharge has been determined for various frequencies. The results are presented in table 2.1.

Table 2.1 Discharge and flood levels for various frequencies

Frequency [1/year]	Discharge [m^3/s]	Level [PWD +m]
1:100	91,000	15.08
1:50	87,000	14.85
1:10	76,000	14.29
Average	65,000	13.66

Making use of various statistical methods a stage-discharge relationship at the planned bridge site was derived; this is also indicated in table 2.1.

The gradient of the river near the bridge site during high(er) water is approx. 0.07m/km. A hydrograph of the river near the bridge site is given in figure 2.1. The level of the flood plain near the bridge site is approx. PWD + 12m.

(b) Morphology

Numerous very interesting aspects could be mentioned about the Jamuna, but they are outside the scope of this paper. The most noteworthy are:

- the fairly recent avulsion of the Brahmaputra from its old course, now known as Old Brahmaputra, to its present course, now known as Jamuna (only two centuries ago),
- general tendency of the river to shift in a western direction,
- geologically active area,
- a total yearly sediment transport is approximately 600 million tonnes.

Some features of the braiding character are depicted in figures 2.2 (variation of cross section at the bridge site between 1968 and 1986) and figure 2.3 (satellite imageries taken between 1978 and 1987).

3. BASIC CONCEPTS FOR GUIDING THE RIVER "UNDER THE BRIDGE"

Guide bunds have in the past been widely used in the Indian sub-continent to guide rivers under bridges and towards regulators or weirs. Rules for designing guide bunds are discussed in a famous indian publication: Manual on River Behaviour, Control and Training, 1971 (Publication no. 60 of the Central Board of Irrigation and Power). It should be stressed that the rules discussed in the publication were originally developed for meandering rivers. A concept widely used for determining the lay-out of the guide bunds is that of the "worst possible loop". In the initial study phase the lay-out of the guide bunds was indeed based on the worst possible loop concept. The length of a guide bund was at that time determined at 3700m.

For braiding rivers the application of the "standard" rules leads to very long guide bunds. During the first series of tests in a large physical model in "De Voorst" it was observed that relatively short (3000m, thus shorter than earlier assumed) guide bunds would be adequate to safeguard the approaches to the bridge against outflanking, at least in the model. This was confirmed by subsequent model tests in which the length of the guide bunds was further reduced to 2200m (developed length).

An essential question to be answered was: "Does the model correctly represent the behaviour of an outflanking channel?" To answer that question additional studies and model tests have been carried out, which indicate that the length of the guide bunds of 2200m is "approximately correct".

All considerations formulated and all model tests executed so far were based on the assumption that "hard" or "fixed" points would exist at some distance North of the proposed bridge alignment. On the right bank the "hard" point is formed by the Sirajganj town protection works, consisting of slope protection works along the perimeter of Sirajganj and a groyne just North of Sirajganj. On the left bank the situation is different. East of Bhuapur an area has been identified which apparently has a higher erosion resistance than the surrounding areas. Some soil borings carried out in the area indicate that the "erosion resistant" area contains some clay in the upper strata (10-15m thick). As the degree of erosion resistance cannot be predicted with certainty, it has been proposed to reinforce the banks of the Bhuapur channel over a length of approximately 1500m, so that also at the left bank one could count on the existence of a "hard point".

The two hard points are approximately located on the borders of the present flood plain. Outflanking of the hard points themselves would in principle not be impossible, but the time required for any such outflanking to reach the bridge approaches would be considerable, possibly an order of magnitude larger (longer) than the time required for outflanking near the proposed guide bunds. The line connecting the hard points was assumed as the boundary of the river training scheme.

4. RIVER STUDIES

Apart from studying all available morphological and hydrological information, the following studies and modelling efforts were undertaken to arrive at the final design for the river training structures, particularly for the guide bunds:

4.1 Overall movable bed model

A movable bed model was set up in "De Voorst" laboratory with the aim to simulate the braiding patterns of the Jamuna river and to study the influence of constricting the river width at the bridge site on the river behaviour. The studies revealed that it was not really possible to guide the river channels towards the bridge opening. Though the water was

forced to flow through the opening, the various channels had a tendency to follow their own path and, given enough time to threaten to attack the approaches to the bridge. Figures 4.1 and 4.2 give an impression of two possibilities of attack to be expected. As the guide bunds do not really guide the river flow, the term "river defence structure would be more opportune.

4.2 Flow model

As the overall model was a model with distorted scales, it suffered from scale effects, so that the flow patterns and velocities were not represented correctly. Though the overall model was of considerable help in developing a lay-out for the river training works, it could not be used forthwith for the design of the guide bunds, particularly where such matters as local scour and current velocities were concerned.

To get a better insight in the current patterns and velocities, a two dimensional mathematical model was constructed. Figures 4.3 and 4.4 give an impression as to the results for a particular case.

4.3 Local scour model

To study the scour to be expected in case of attack of the guide bunds, another scale model was used. The tests carried out were rather conventional. The output of the flow model was used to calibrate the local scour model. The most severe case of attack is indicated in figure 4.5, while the time-scour relationship for this case is given in figure 4.6.

5. TYPES OF SCOUR - COMBINATIONS OF SCOUR

5.1 General scour

General scour is the scour one has to anticipate in the long term, irrespective of the construction of the bridge. Factors influencing the general scour are:

- change in sediment supply into the river,
- change in discharge,
- construction of flood embankments,
- diversion of water and/or sediment into other rivers,
- change in sea level.

For a realistic combination of the factors mentioned, a small aggradation of the Jamuna bed has to be expected, whereby the influence of a (predicted) sea level rise exceeds the other influences substantially. Long term (100 years) prediction for aggradation, becoming obvious in a rise of both river bed and water level: approximately 0.50m.

5.2 Constriction scour

Constriction scour has to be expected as a result of the narrowing of the river (viz. channels and flood plain) at the bridge site. Various bridge openings have been investigated. For openings of 5300m to 3500m the maximum constriction scour varies between 0.8m and 3.0m

5.3 Confluence scour

An extensive study of field data revealed that the maximum depth (h_{scour}) at a confluence can be expressed as a function of the average depth ($h_{average}$) of the upstream anabranches and the angle of incidence (θ, in degrees) between anabranches:

$h_{scour} / h_{average} = 2.235 + 0.0308 * \theta$

The confluence scour to be expected during a 1:100 year flood at the confluence of two anabranches carrying each 50 percent of the discharge (during bankfull discharge), meeting at an angle of 50 degrees is approximately 29m (below water level).

5.4 Bend scour

The maximum depth resulting from scour at a natural outer bend (thus not influenced by a local obstruction) can be expressed as a function of the average depth (h_av) of the river. The average depth for a particular discharge in excess of bankfull discharge can be calculated by adding the average depth of "the river" (as opposed to the depth of an individual channel) for bankfull discharge, and the stage difference between actual and bankfull discharge:

$h_{bankfull} = 0.23 * (44{,}000)^{0.32} = 7.04$ m

$h_{average}$ (1:100 yr) = 7.04 + 2.85[1] = 9.89 m

The outer bend scour can then be determined with:

$h_{scour} = k1 * h_{average}$ in which k1 is a factor from measurements in nature, giving the relationship between average depth and scour depth. The maximum scour to be expected in an outer bend during a 1:100 year flood is approximately: 20.8 m (below water level).

5.5 Local scour

For local scour near a guide bund substantially more insight has been gained through the local scour model test. The local scour depth can be determined through the formula:

$h_{scour} = h_{init} + h_{regime} * (k3 - 1)$, in which:

h_{scour} = scour depth (below water level),
h_{init} = initial depth at "commencement" of the local scour,
h_{regime} = "regime" depth, for the guide bund case determined at 18m,
k3 = model factor, as obtained from model tests and literature.

In the initial depth the influence of constriction scour should be taken into account for the guide bunds. For river training works near the border of the flood plain, like the protection works near Bhuapur, this constriction scour need not be taken into account. The maximum local scour, during a 1:100 flood, has been calculated to be approximately 43m below the corresponding flood level. The flow conditions for the local scour model were generated by the mathematical flow model.

5.6 Combination of forms of scour

The design of the river training works and the bridge piers has been based on a combination of the various forms of scour. For physical and statistical reasons due attention has been given to the combined occurrence of the various scour forms, whereby the stochastic nature of the location, orientation, etc. of the various channels in the braiding Jamuna River have been acccunted for. For scour along the guide bunds the following observations can be made:

---

[1] Water depth above floodplain; bankfull discharge corresponds with floodplain level.

(a) The local scour seems to be dominant over all other forms of scour; however it should be realised that the local scour is a function of the "initial" depth, which in turn is a function of scour in an outer bend and constriction scour.

(b) Only general scour (which in this case turns out to be general aggradation) has to be added to the local scour along a guide bund.

With probabilistic design methods the following scour levels along a guide bund were determined:

Table 5.2 SCOUR ALONG GUIDE BUNDS

Level (relative to PWD) [m]	Depth (relative to high water) [m]	Chance (per year)
-28	43	0.050
-30	45	0.023
-32	47	0.008
-34	49	0.002

Confluence scour has to be taken into account for the design of the bridge piers, but not for the guide bunds; moreover all bridge piers will experience local scour as well, but the nature of this local scour is independent from the initial depth.

6. BOUNDARY CONDITIONS FOR DESIGN OF GUIDE BUNDS

6.1 Geotechnical boundary conditions

The soil in/through which the guide bunds have to be constructed consists of predominantly fine, slightly silty sand, of which the upper 10-15m has to be considered as relatively loosely packed. Underlying layers have a higher density, which can be classified as medium dense to dense. The results of an in-situ density test with a nuclear device have been indicated in figure 6.1.

Geotechnical boundary conditions, including dynamic conditions, will determine the stability of the river training works during and after construction, and thereby the gradient of the slopes to be applied.

The selection of a statically stable slope does not imply that no deformation has to be expected during dynamic conditions (earthquakes). Earthquakes could liquefy the loose layers. The liquefiable depth would be considerable. Unless special measures are taken, deformation of the guide bund as a result of an earthquake could be substantial. In order to limit damage as a result of earthquakes, two different measures were proposed:

- to densify the critical zones in the upper 15m of the soil,
- to use gentle slopes.

The slope steepness has in principle no influence on the occurrence of liquefaction, but it does have an influence on the resulting deformation. Even with special precautions, earthquake loadings may lead to "slumping" of a guide bund section. In view of the selected slope steepness of 1:3.5 in the denser layers, and 1:5 in the upper layers, the slump to be expected at the top of the guide bund may be limited to 1-1.5m. Such a slump would not immediately endanger the bridge-system, but would need to be repaired after an earthquake.

6.2 Current velocities

Current velocities were initially determined with the simple relationship of the Chezy ($v = C * \sqrt{(h * I)}$), even for the deepest scour holes. The tests with the local scour model, for which the velocity field was determined with the two dimensional mathematical model, indicated that this led to somewhat exaggerated velocities (10% too high). Maximum average velocities in a vertical are of the order of 3.5 m/s.

6.3 Waves

A study of the wind climate and possible fetch length revealed that the wave heights to be expected are rather moderate: seldom more than 1m, with corresponding wave periods of 4 s.

7. SLOPE PROTECTION

7.1 General

The scour to be expected along a guide bund can be of the order of 40m below the level of the flood plains. The extreme options which can be used to provide protection against current to such depths are:

(a) Provide a sufficient quantity of erosion resistant material along the perimeter of the guide bund, and leave it to "nature" to deposit this material at the anticipated depth during the scour process. If the erosion resistant material is provided at original ground level (flood plain level), no dredging work will be required for the guide bund. The principle discussed is known as the "falling apron" sometimes referred to as the "launched apron".

(b) Dredge a trench to full depth and cover one side of the trench with an erosion resistant protection; the covered slope will become the river side of the guide bund.

A very important aspect associated with a falling apron is of a geotechnical nature. The gradient under which the eroded (and subsequently protected) slope will stabilise is approximately equal to the angle of internal friction of the soil. In case of the Jamuna Bridge this would imply a slope of 1:2 or steeper. This is (far) too steep for the relatively loosely upper soil strata (approximately 15m thick). It is therefore imperative to dredge at least to this depth (PWD +12m - 15m = PWD -3m) and to form the slope at the required minimum gradient of 1:5.

Also below the level of PWD - 3m more gentle slopes are preferred in order to limit any deformation of the subsoil caused in case of an earthquake. Moreover protective elements on steeper slopes will be heavier than on more gentle slopes. Ideally gentle slopes extending till the full expected erosion depth are preferred. Unfortunately in the case of the Jamuna Bridge project dredging to full depth would:

- lead to very large dredging volumes (order of 22 million m^3 per guide bund; such volumes would be very difficult to handle within the short construction time available;
- require very specialised dredging equipment, which is not available in the market;
- be very expensive.

Cost comparisons have been made for combinations of dredging to a certain depth (with proper slope protection on the dredged slope) and a falling apron over the "remaining" height, from which it was concluded that, not surprisingly, the cost for the protection increases with the depth of the falling apron. For this increased cost it is obvious that a higher degree of safety for the guide bund, and thereby for the bridge system, can be achieved. The Consultants proposed to adopt a level of PWD -18m as the initial level of the falling apron for the following reasons:

- the "remaining" falling height for the apron is large (up to 13m), but not too large to implement any additional measures to protect the slope should this become necessary;
- the dredging depth is very substantial (up to 30m, measured from the level of the floodplain), but can be dredged with equipment which is available in the market or which can fairly easily be adapted;
- through requiring a major effort, it is possible to complete an entire guide bund within one working season.

A typical section over the guide bund is given in figure 1.3

7.2 Types of slope protection

So far it has been tacitly assumed that other types than protected soil structures would not be appropriate to function as river training works. In view of the large differential soil levels to be expected at both sides of such a structure (up to 45m, ground level of the flood plain on one side, scoured river bed on the other side), such structures would be prohibitively expensive. For soil structures one could think of "open" or "closed" protection. In view of the large differences in water levels (high ground water levels "behind" the protection and low river level "in front") a closed protection is not preferred. Therefore only open type structures have been dealt with.

For the protection of the guide bunds, the following sections have been distinguished:

- the above water protection (on slope 1:3.5) between levels PWD +16.5 and PWD +9m (approximately), to be applied on slopes, partly formed by excavation, partly by filling;
- the under water protection (on slopes 1:5 and 1:3.5) between levels PWD +9m and PWD - 18m, to be applied on dredged slopes;
- the falling apron section, to be constructed at level PWD - 18m (initial level).

The under water protection on dredged slopes constitutes the most important component of the slope protection works. Most attention was devoted to comparing and selecting alternatives for that section.

The following criteria were included in the comparison:

(a) current resistance (short and long term), (b) complications arising from overlaps, (c) application in curved areas, (d) (aspects of) quality control and (e) (possibility of implementing) repairs

The following alternatives were compared:

(1) riprap on a fascine mattress, (2) concrete block mattress - manufactured "on shore" (3) concrete block mattress - manufactured "over water", (4) cellular geotextile mattress, (5) grouted aggregate mattress (cement and asphalt bonded) and (6) gabion mattress.

On the basis of multi-criteria analyses, the following types of slope protection were selected:

Table 7.1 SELECTED TYPES OF SLOPE PROTECTION

For under water slopes	For above water slopes	For falling apron
fascine mattress with a protective layer of riprap (grade 10 to 60), with a total thickness of 0.50m; locally a slightly heavier grade (10 - 100 kg) to a thickness of 1.0m has been proposed.	open stone asphalt, thick 0.15m, on a geotextile mat	riprap with a wide grading of 1 - 100 kg, at the rate of 26 m^3 per lineal metre (near the position of the bridge increased to 35 m^3 because of the influence of bridge piers on the scour depth)

The following design aspects are noteworthy:

(a) Design of current resistant elements

The slope protection works were designed prior to the publication of Pilarczyk's formula, yet the formulas used and developed for the project contain many of the elements which were later also integrated in Pilarczyk's formula. In essence the well known formula of Isbash was used: $\Delta * D = (0.7 * v_{cr}^2)/(2 * g)$, with corrections for:
- influence of decreasing shear stress for increasing depth
- influence of slopes
- influence of somewhat higher turbulence than "normal".

In the final design use was made of probabilistic methods, whereby the accepted chance of failure for the slope protection works was determined through an extensive risk analysis (making use of fault trees).

(b) The falling apron section

As established in "real" cases and in scale tests, sand tight mattresses lead to very steep slopes at the edges of any (horizontal or sloping) section of the slope protection which has not been installed to the ultimate scour depth. Loose material, such as rip rap would not have a large enough angle of internal friction to remain on the geotextile in case of scour at the edge.

The most secure method to provide coverage of the slope of the scour hole is by using loose granular material. The quantity should be "sufficient" to cover the entire eroded slope. The thickness and the grading of the granular material should be such that at the end of the "falling" process the underlying soil is retained by the protective layer (principle of imperfect filter).

Soil can in principle be retained by a filter built up from granular materials with different grading. The grading closest to the soil to be retained shall be rather fine, while the grading closest to the current shall be large enough to withstand the current forces. In the falling process the filter will not be built up as nicely as necessary for a proper filter function. This can be compensated by providing more granular material than would be required for a "proper" filter. As a rule of thumb an excess quantity of sixty percent of the "proper filter" quantity will be sufficient. This rule is more or less equivalent to another design rule, which indicates that the total thickness of an "all in" filter should be approximately five times the diameter of a single rock which can (just) withstand the current forces. Another excess quantity is required to take account of the circumstance that not all material in the falling apron reaches its intended destination. Here an excess quantity of twenty five percent is recommended, particularly in the indian literature.

"Combination" of the mentioned design rules implies that approximately 1.3m³ of graded rock (0 - 100 kg) has to be "stocked" (in the falling apron) for each m² of slope expected to be exposed as a result of scour; the slope gradient to be expected is approximately 1:2, equivalent to the natural slope of the underlying soil.

(c) Maintenance

From the foregoing it may have become clear that the proposed guide bunds provide protection to the full expected scour depth. However the behaviour of the falling apron is not exactly known. Under certain circumstances some damage cannot be ruled out. It is therefore imperative that regular inspection, particularly of the lower part of the guide bunds takes place, and that damage will be repaired timely. Though it would in principle be possible to design a "maintenance-free" slope protection, the cost would be exorbitant.

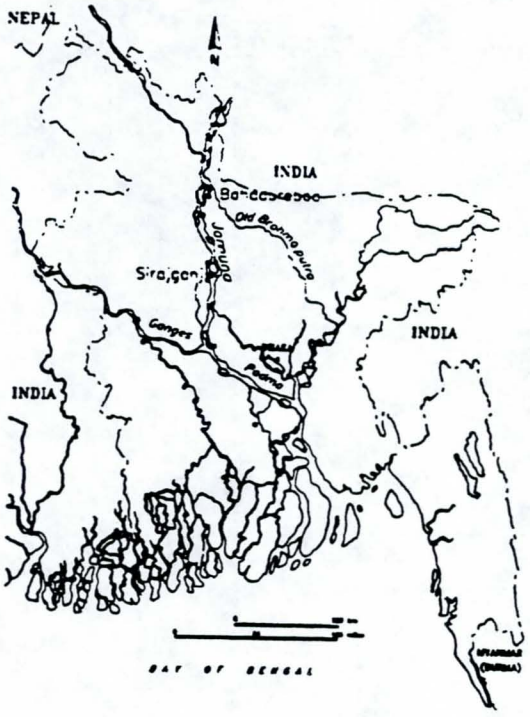

FIGURE 1.1 - MAP OF BANGLADESH WITH JAMUNA RIVER

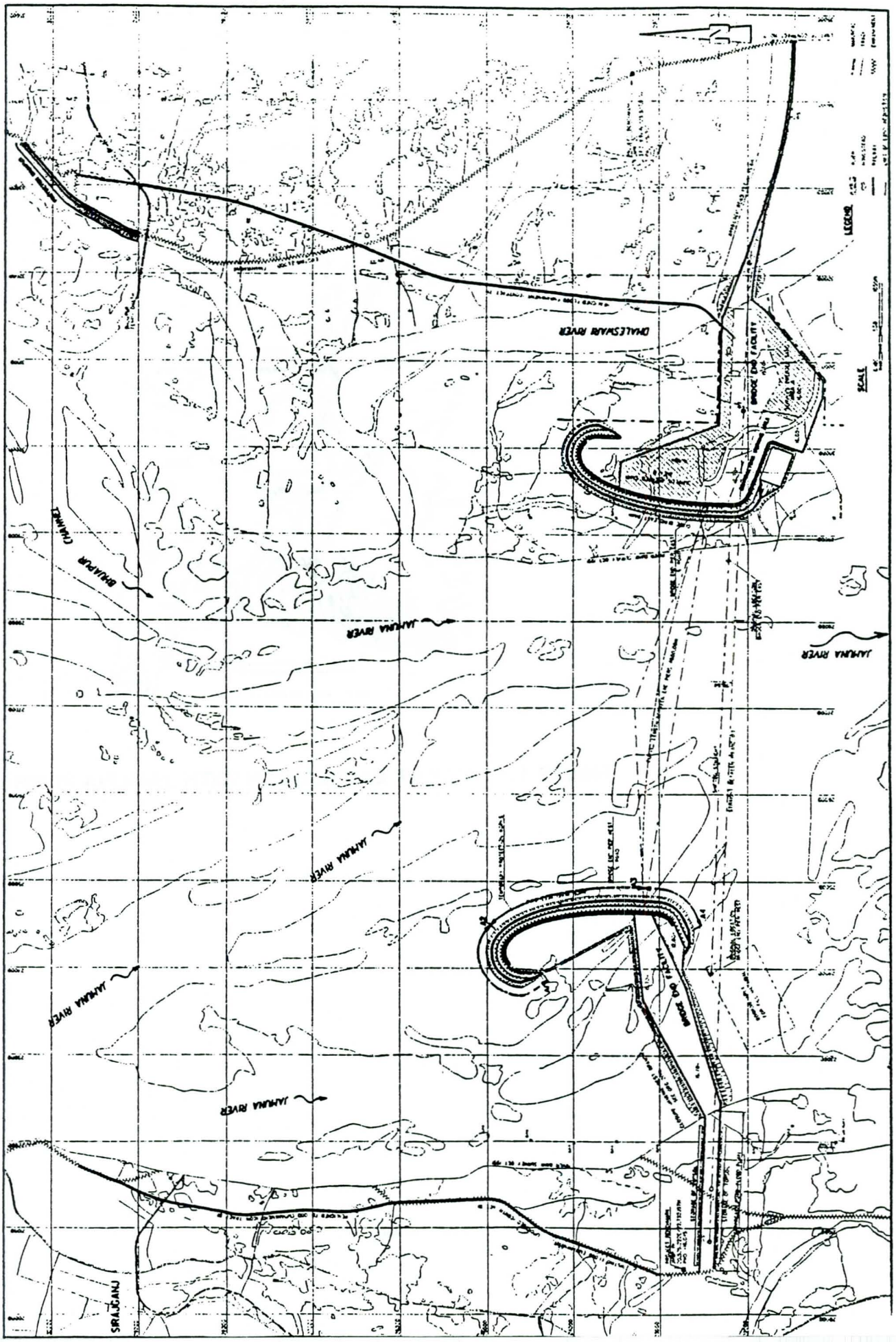
DHALESWAR RIVER
BRIDGE DAM FACILITY
BHAIRAB CHANNEL
JAMUNA RIVER
JAMUNA RIVER
JAMUNA RIVER
JAMUNA RIVER
JAMUNA RIVER
SRAJGANJ
LEGEND
SCALE

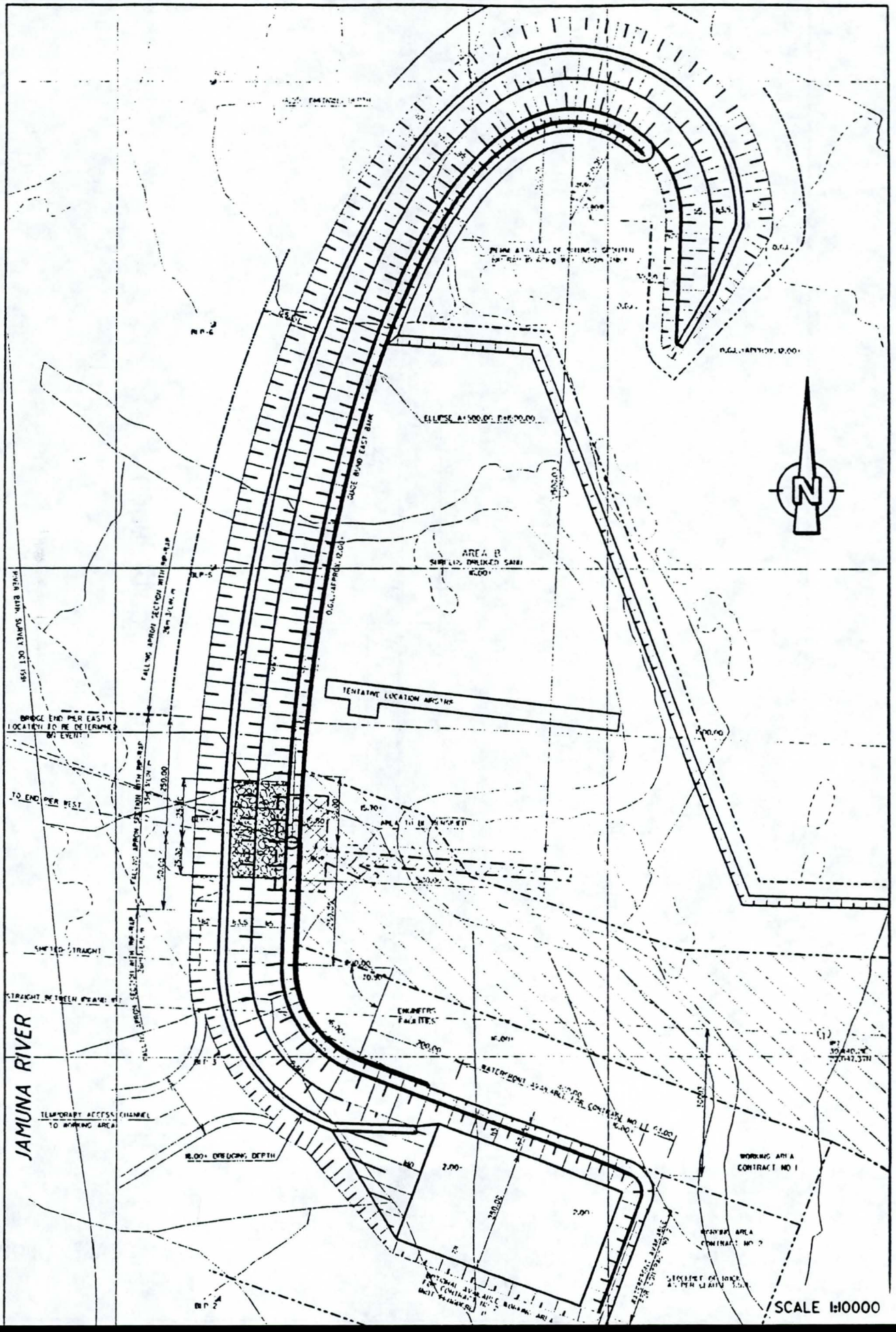
JAMUNA RIVER
AREA B
TENTATIVE LOCATION ARCHES
BRIDGE END PIER EAST
TO END PIER WEST
ENGINEERS FACILITIES
WORKING AREA CONTRACT NO 1
SCALE 1:10000

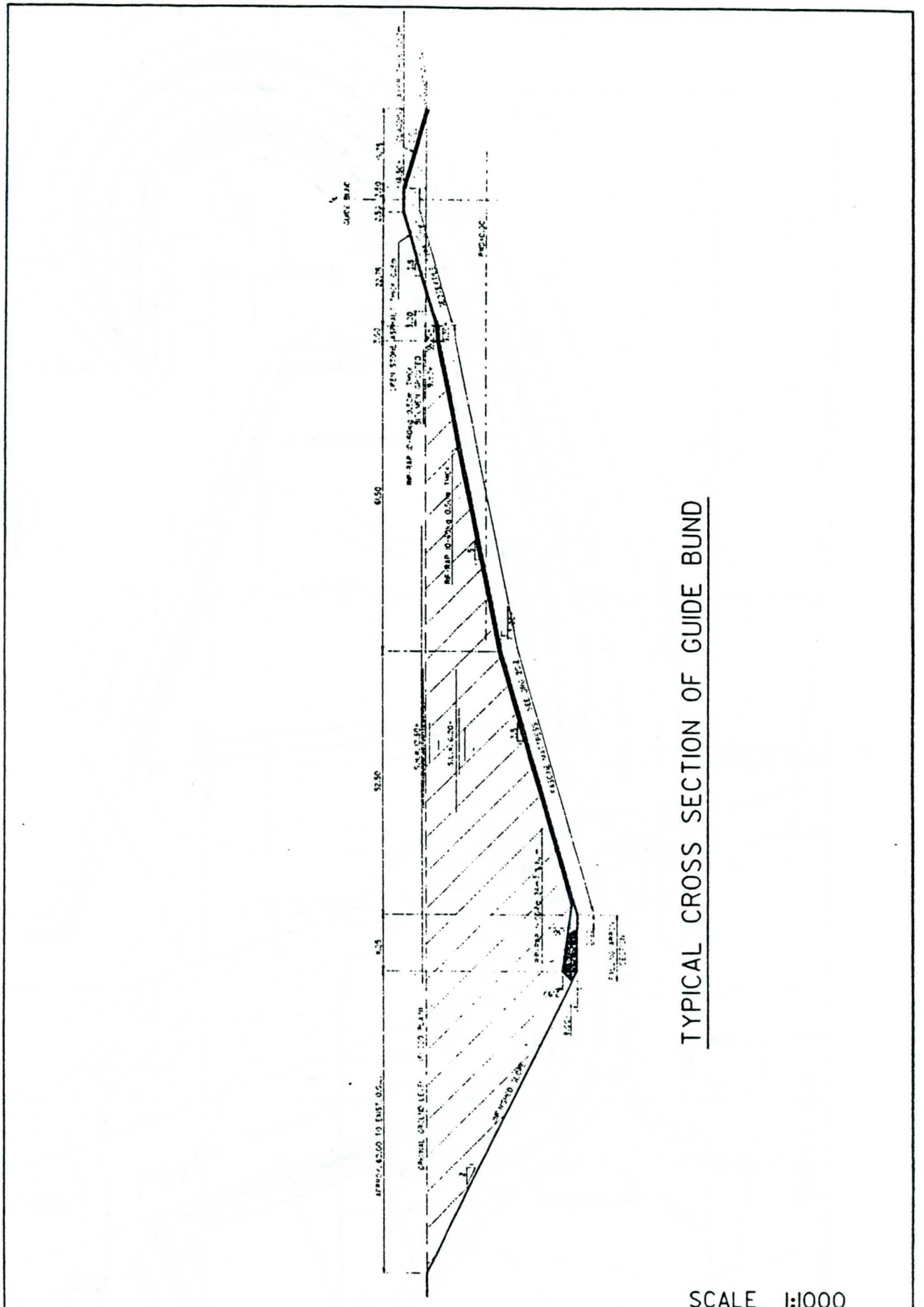

TYPICAL CROSS SECTION OF GUIDE BUND

SCALE 1:1000

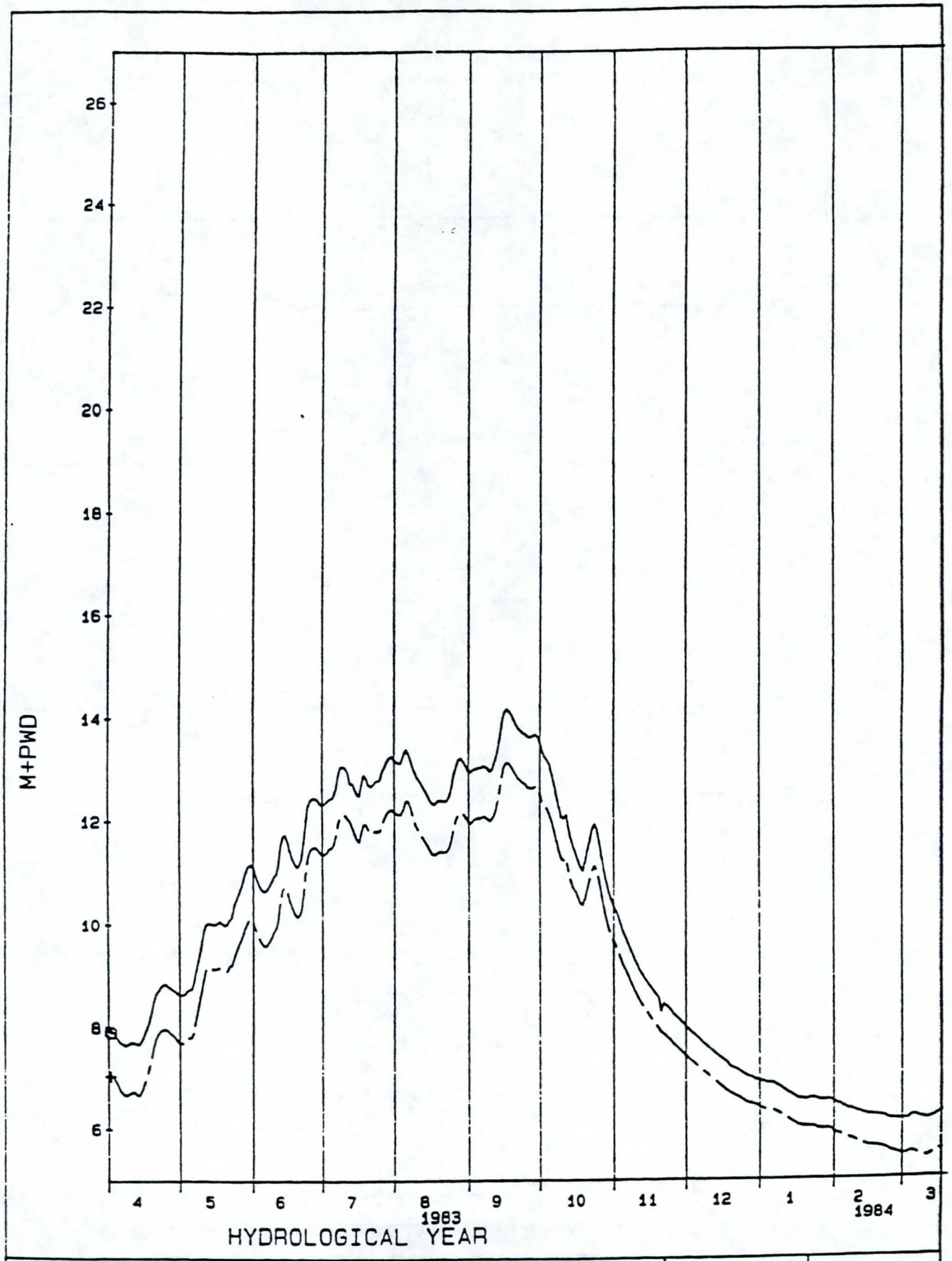

HYDROGRAPHS
STATIONS 49 and 22.JRD

DRT NEDECO BCL

Q553

FIG 2.1

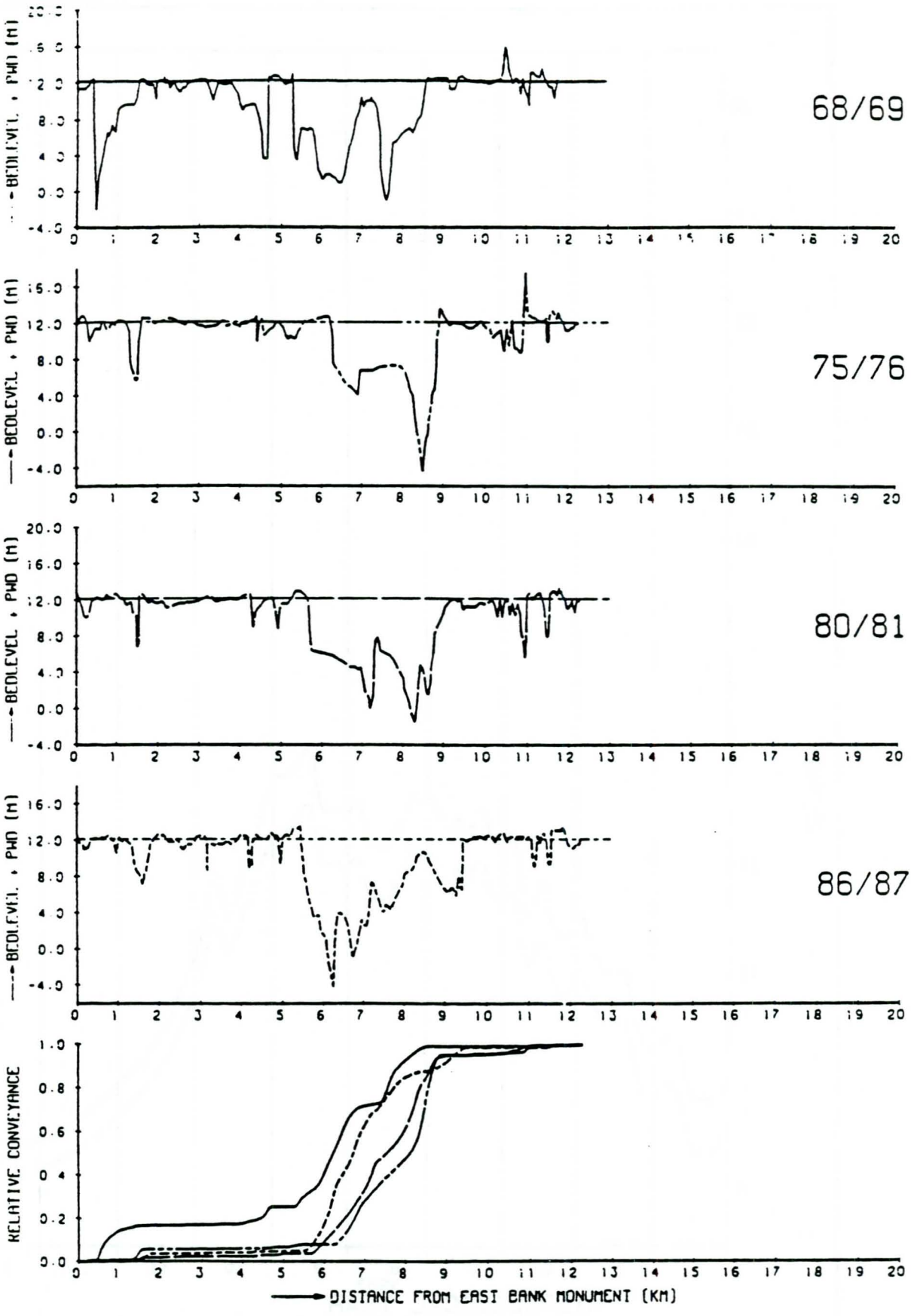

CROSS SECTIONS JAMUNA RIVER BANGLADESH (68/69-75/76-80/81-86/87)	J6-1	
RPT - NEDECO - BCL	Q 0553	FIG 2.2

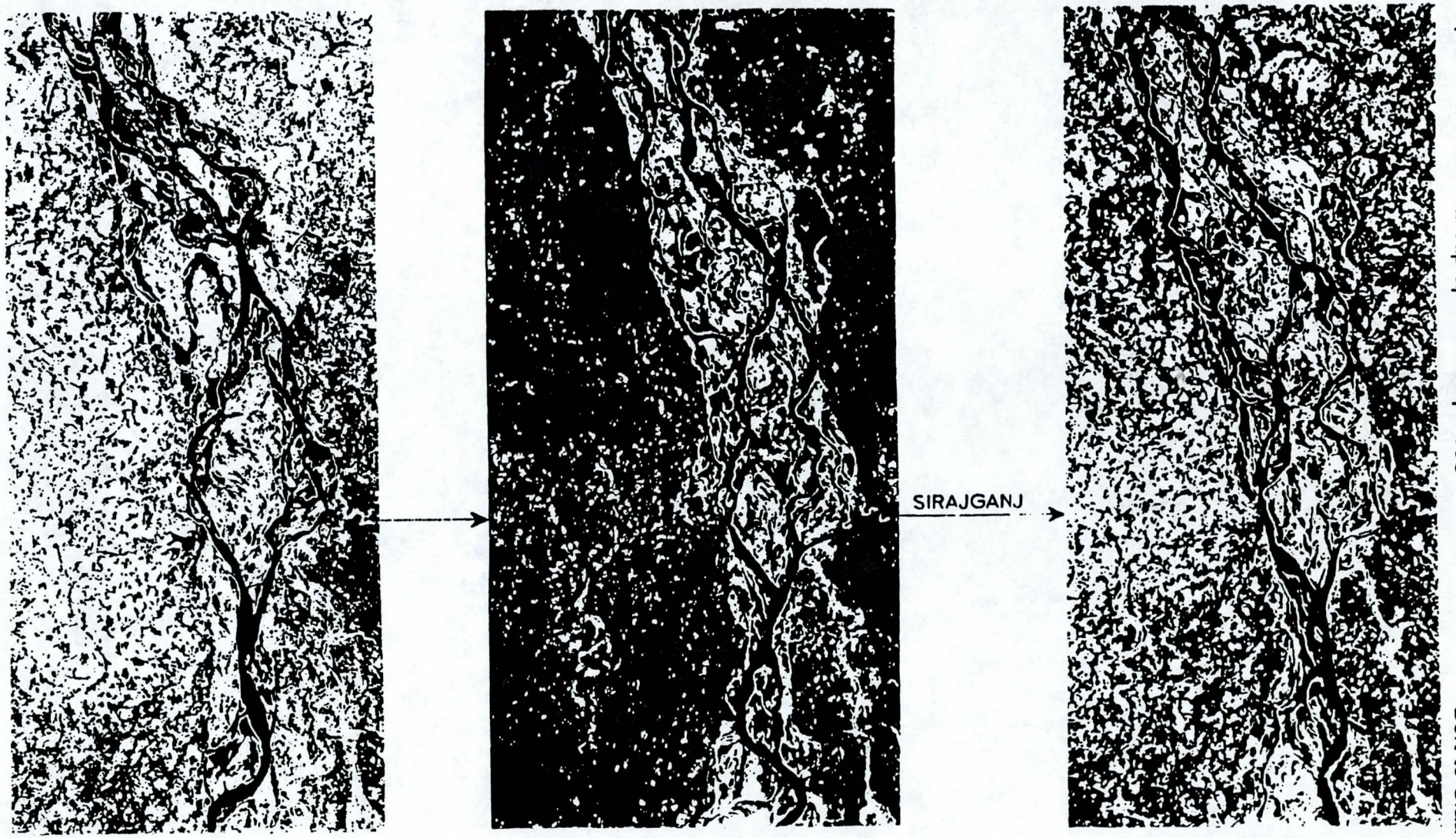

FIGURE 2.3 - SATELLITE IMAGERIES

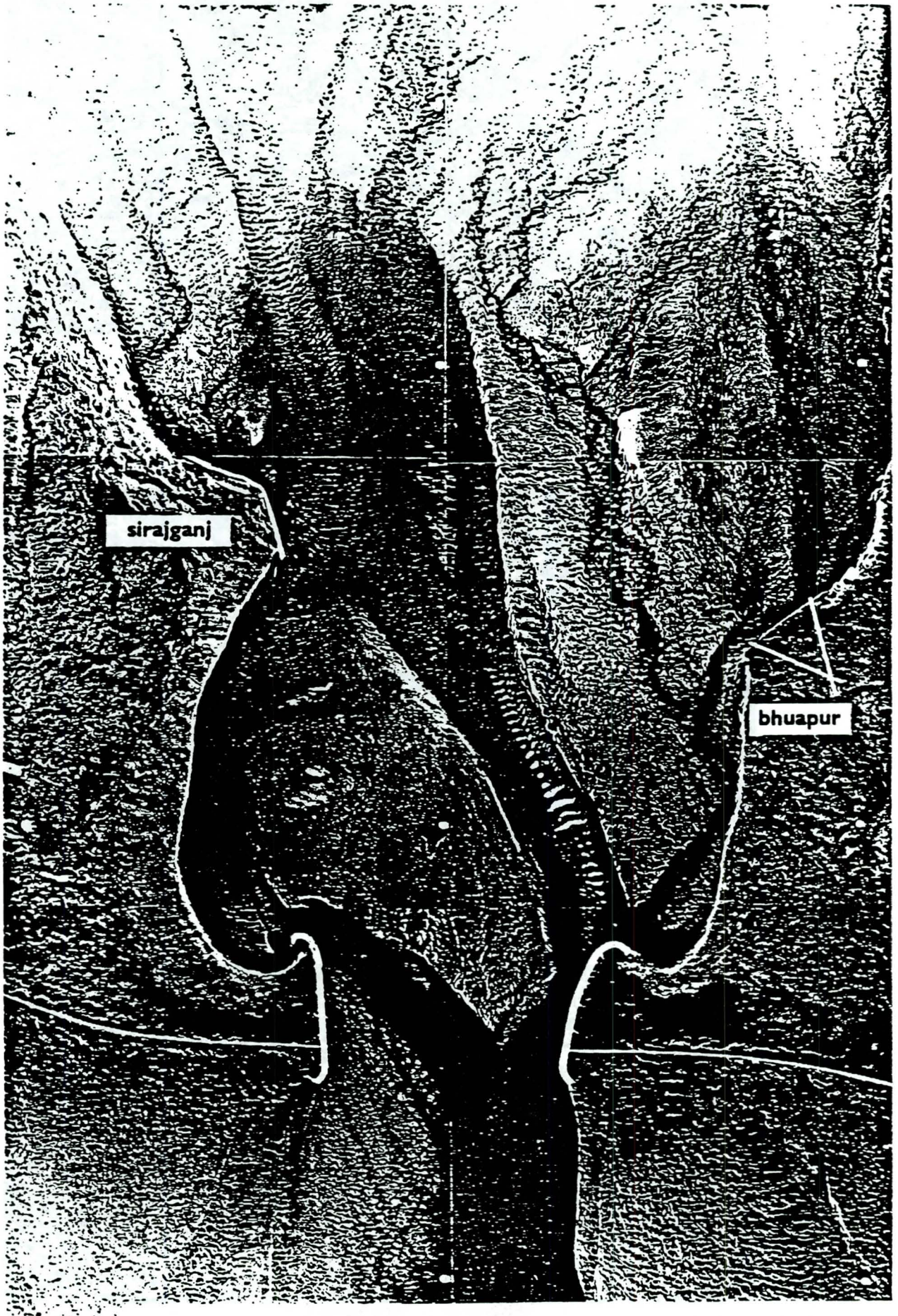

FIGURE 4.1 OVERVIEW OF MOVABLE BED MODEL WITH OBLIQUE ATTACK

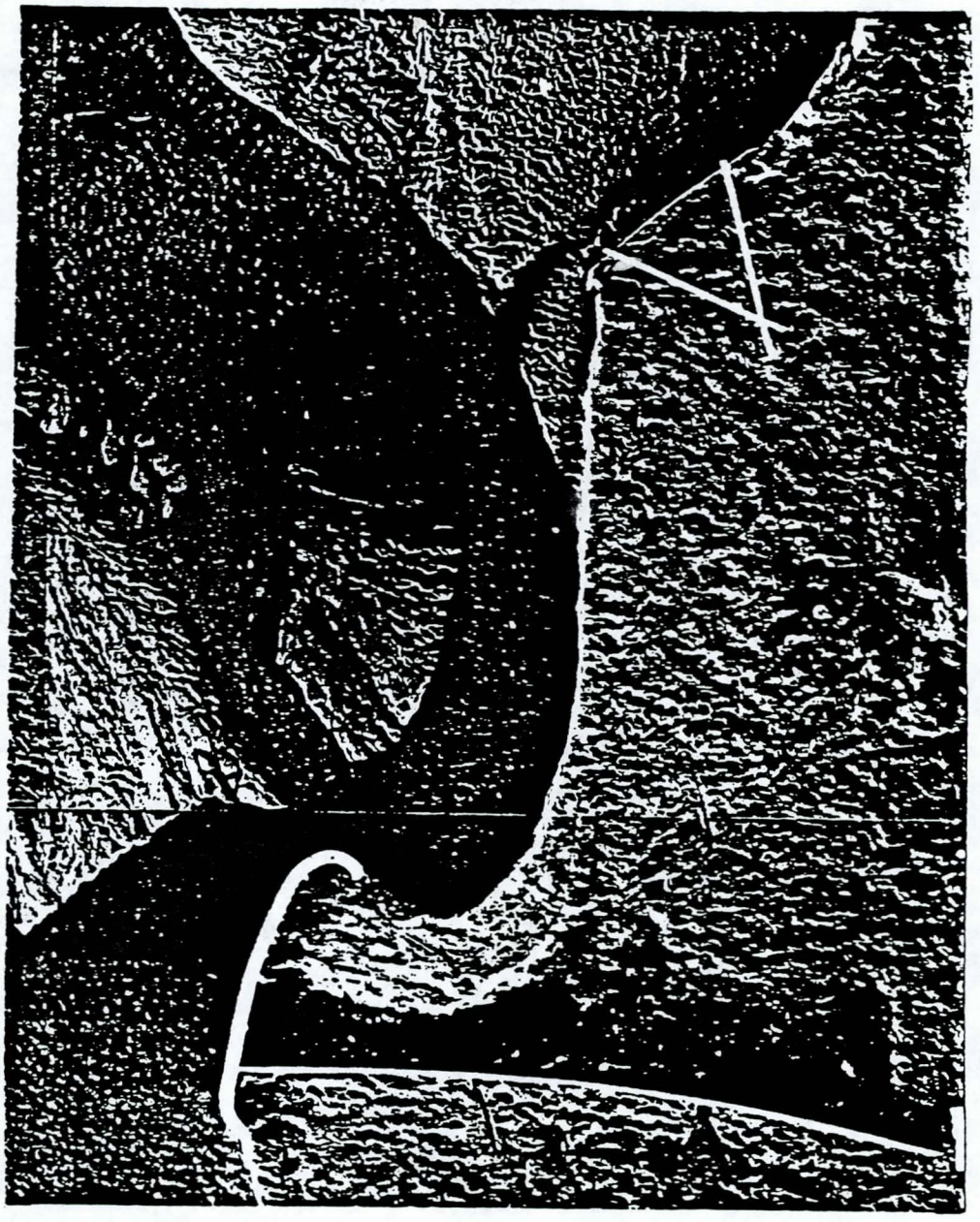

FIGURE 4.2 - DETAIL MOVABLE BED MODEL WITH ATTACK BY OUT-FLANKING CHANNEL

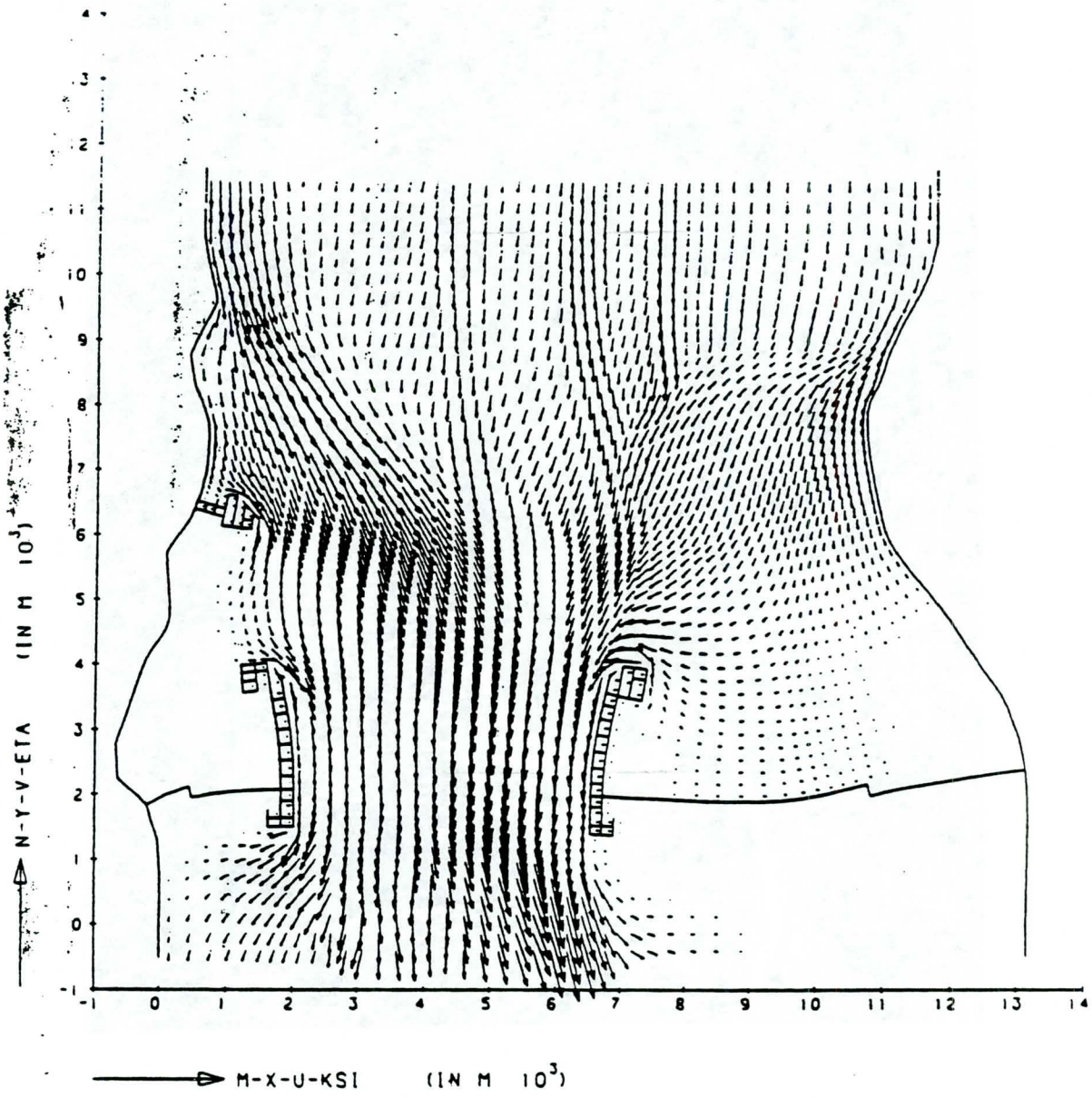

SCALE 1 CM : = 4 M/S

JAMUNA BRIDGE VECTOR FIELD

OPC = J 02

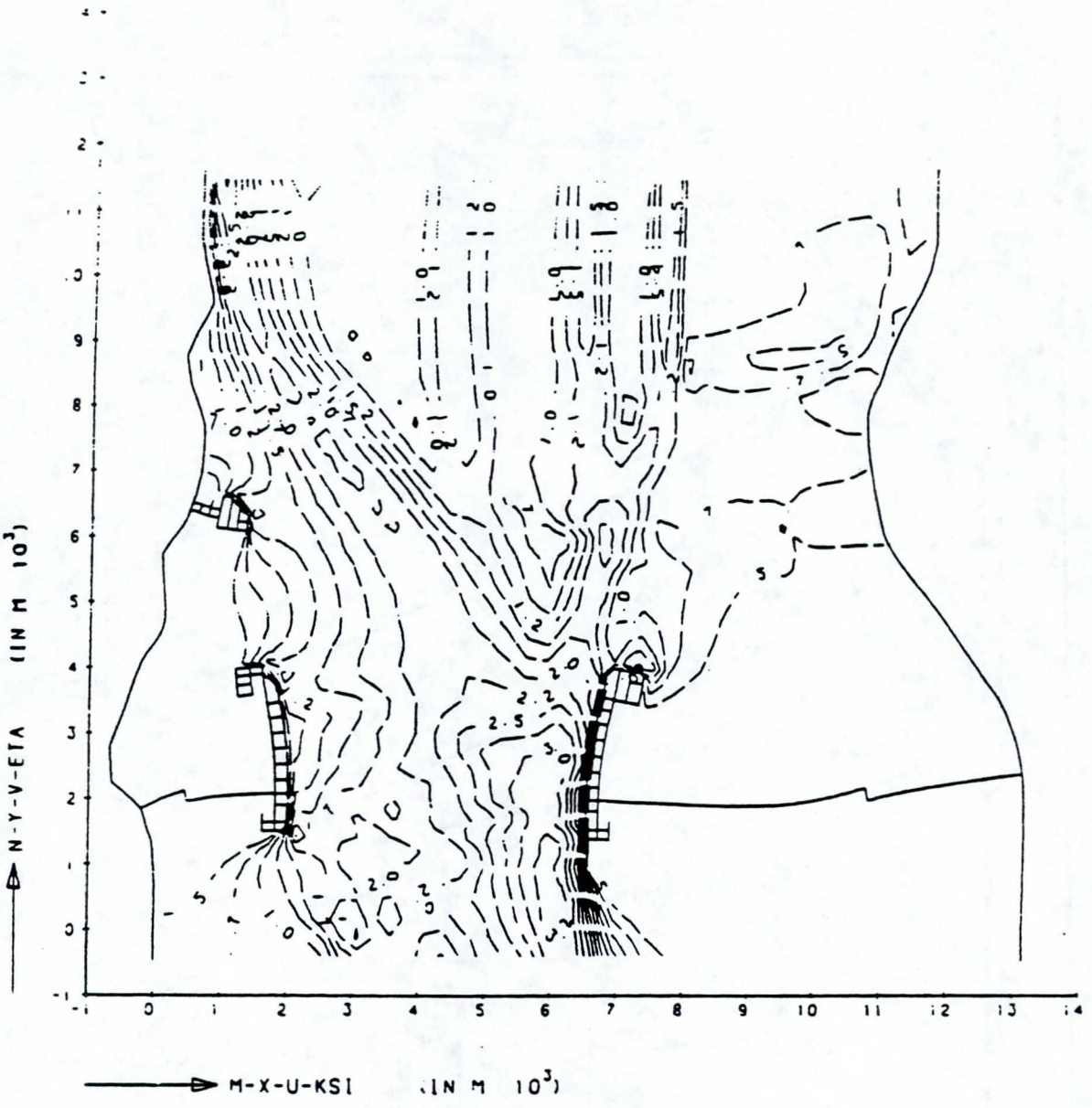

JAMUNA BRIDGE
ISOLINES MAGNITUDE VELOCITIES

OPC = J02

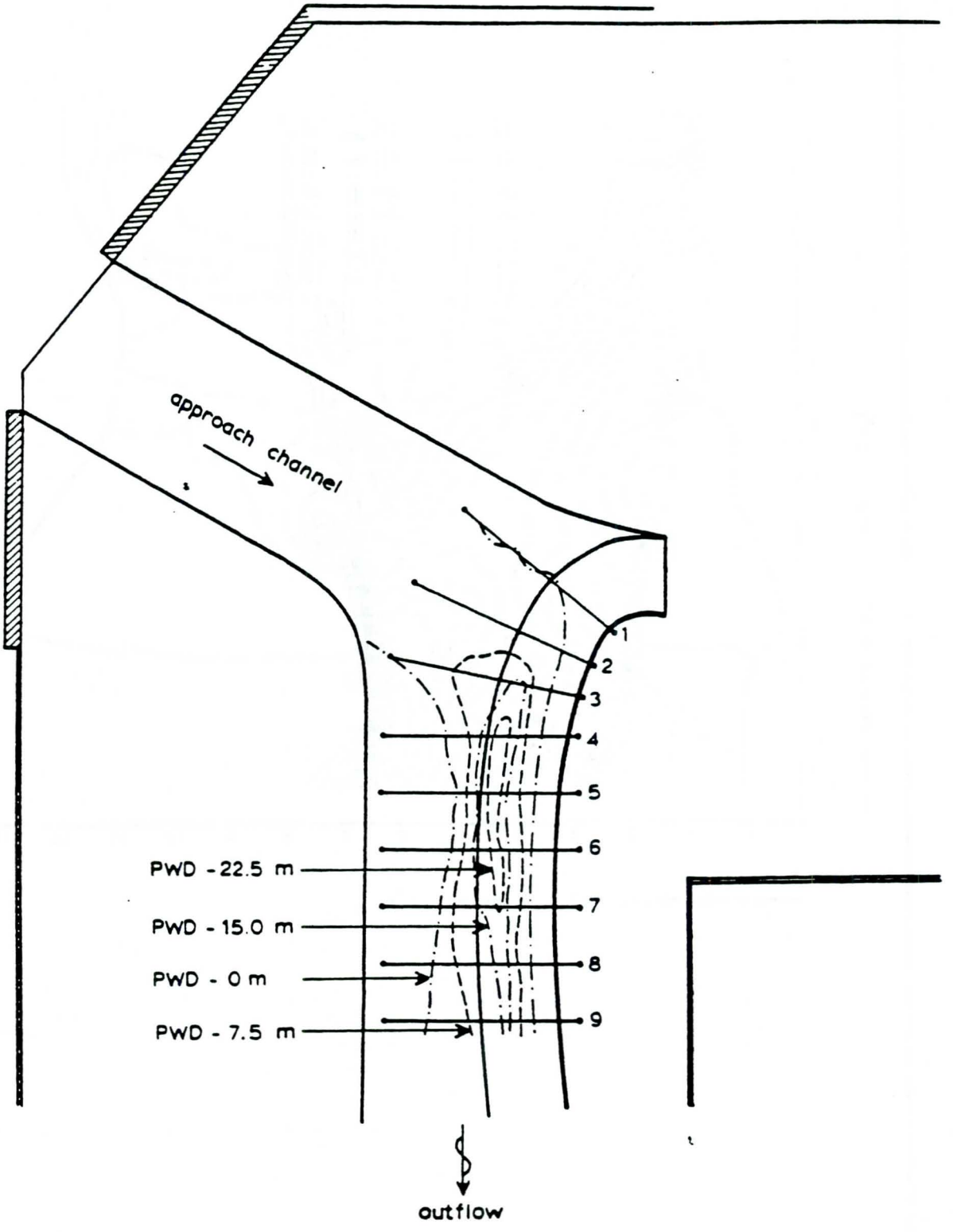

LINES OF EQUAL MEASURED SCOUR DEPTHS
(FLOW DIRECTION 3)

Bert te Slaa

TIME - SCOUR RELATIONSHIP FOR STRAIGHT REACHES OF THE GUIDE BUND

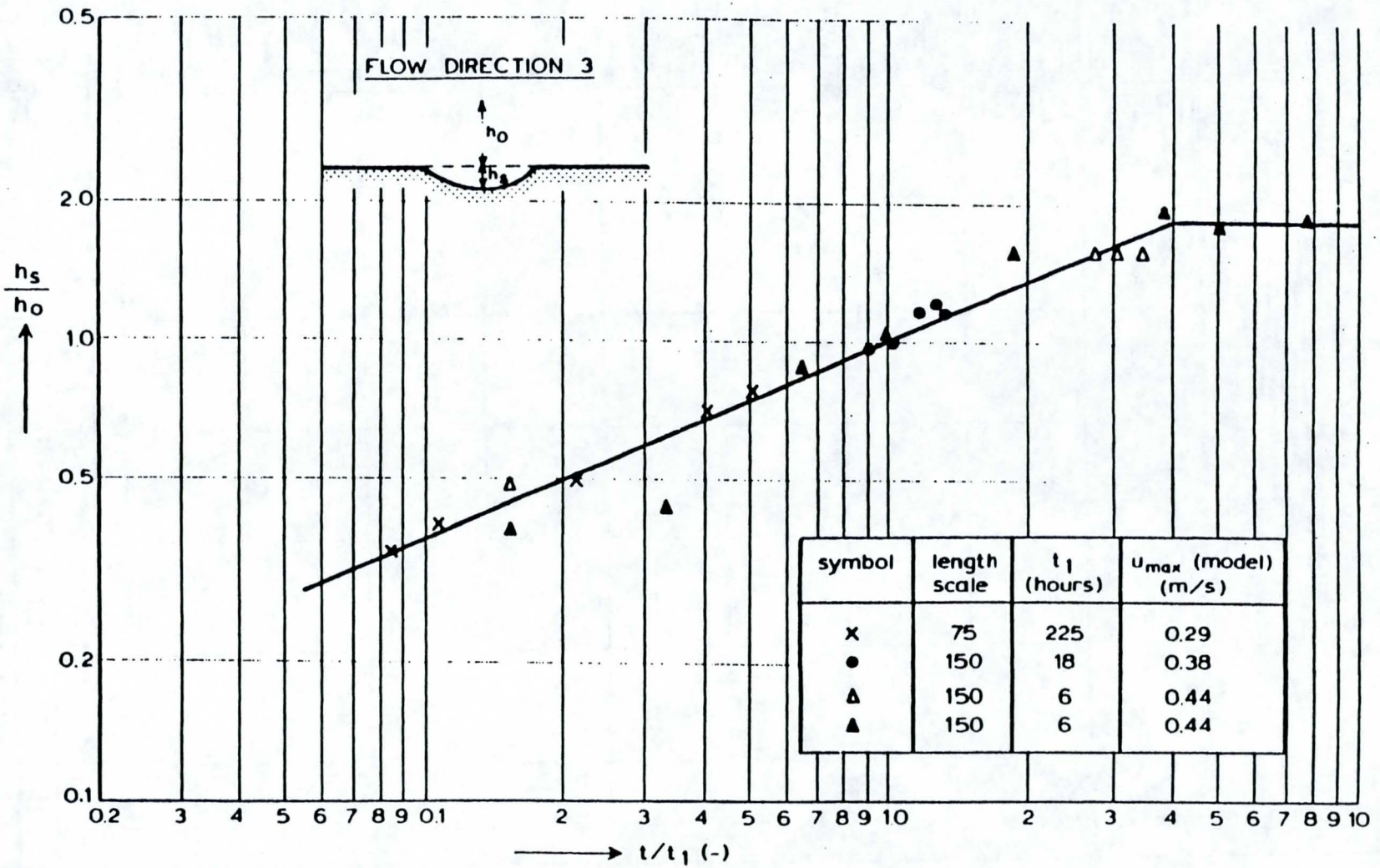

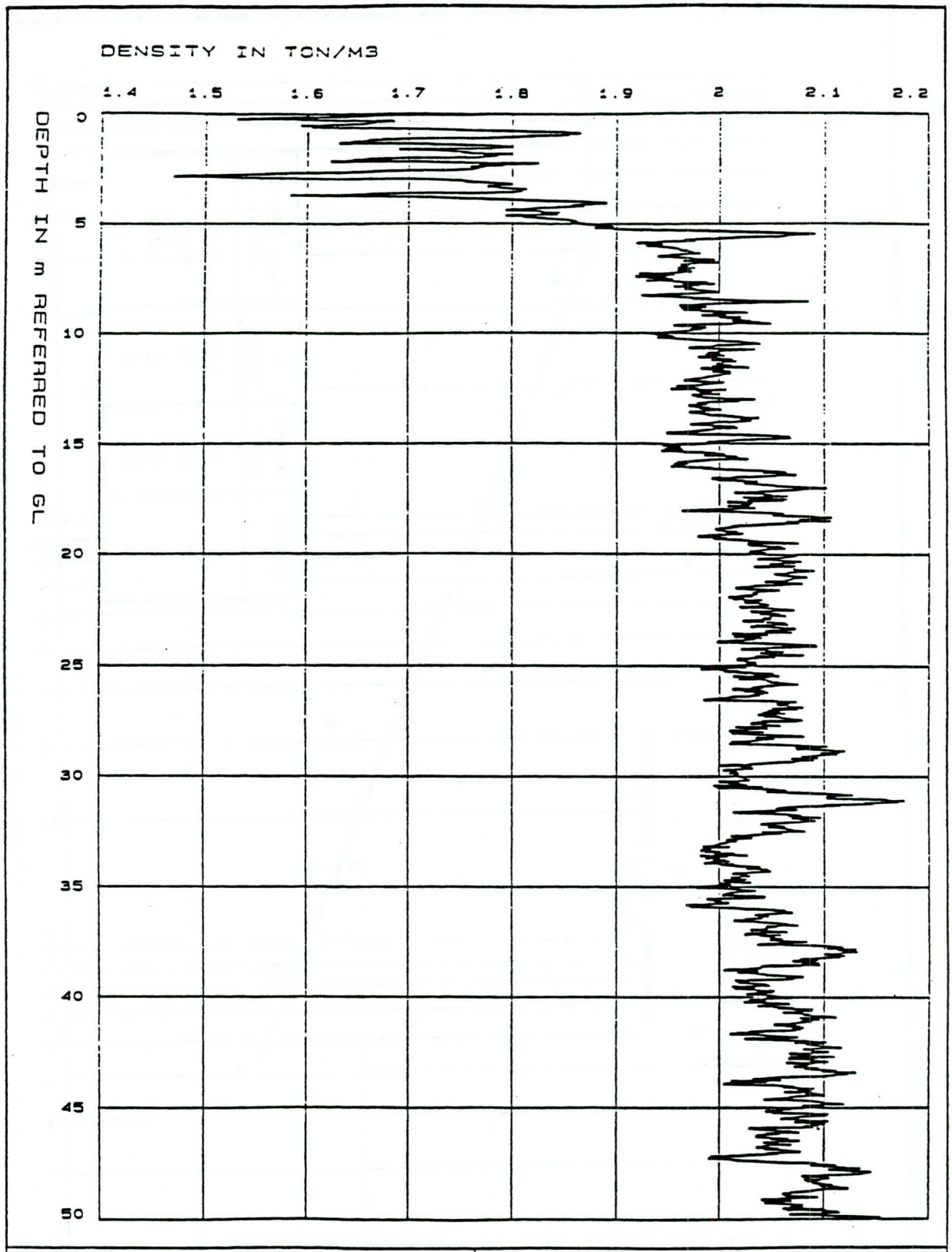

JAMUNA MULTIPURPOSE BRIDGE	CONTINUOUS DENSITY TEST
PHASE II FEASIBILITY STUDY	
JMBA-IBRD-UNDP	
DRAWN RPT / SCALE ——	
RPT / NEDECO / BCL	DATE APRIL 88 / FIGURE No. 6.1

USE OF RIPRAP IN SOIL BIOENGINEERING STREAMBANK PROTECTION

R.B. Sotir and N.R. Nunnally
Robbin B Sotir & Associates, Marietta, Georgia

Introduction

Vegetation is, perhaps, the most important component of a riverine system. The role of vegetation in streambank stability is well known and widely accepted. Woody vegetation slows velocities in the vicinity of the bank, and the root systems help support the bank and reduce scour. On small streams trees and shrubs provide shade that helps prevent solar radiation from increasing water temperatures, and overhanging vegetation provides much needed cover for fish and organic debris that is used for cover and food by aquatic organisms.

Clearly, streambank protection systems that incorporate woody vegetation provide additional benefits over those that do not. Soil bioengineering, a technology developed and refined largely in Europe, and more recently in North America, employs woody vegetation as the major structural component in streambank protection designs. This approach to streambank protection is being accepted increasingly in the United States and Canada, especially in areas where environmental quality is a major concern. Examples include streams in urban areas, parks, scenic locations, and streams with important salmonid fisheries.

Use of Riprap in Soil Bioengineering Systems

In some applications adequate protection against erosion can be provided by vegetative systems alone. Most applications, however, require the use of some rock in conjunction with vegetation to prevent damage to the system that would impair its effectiveness or reduce its environmental benefits. Several examples are provided in this section to illustrate how stone is employed in soil bioengineering designs.

Vegetated dikes

Vegetated dikes, sometimes referred to as live booms, are dikes (or groins) constructed from live fascines, soil, live stakes, and rock. They are built upon a rock foundation that extends from the bed to a depth sufficient to prevent failure by undercutting. Ordinarily, we wrap this rock in Tensar or some other geogrid material. This allows the structure to settle as a unit if any undercutting does occur, and it also permits the use of excavated stream gravels larger than the grid openings, thereby helping to reduce costs.

Beginning at the bed elevation a gridwork of live fascines are constructed, consisting of long fascines placed lengthwise about 30 to 50 centimeters apart and short fascines placed on top and perpendicular to the long live fascines with the same spacing. After securing the fascines by driving wooden stakes through the points of intersection, the grid is backfilled with rock. This process continues until the structure attains a height equivalent to the elevation of the normal high water level (defined as the discharge that is exceeded 5 percent of the time) except that soil is substituted for rock at the mean low water elevation (which is defined as the elevation of the discharge exceeded 50 percent of the time).

Once the desired height is reached, the entire structure is covered with hand placed riprap and is live staked. The 80 to 100 cm long stakes are cut from native dormant plants 2 to 4 cm in diameter and are installed on 30 to 60 cm centers. Typically, willow (salix) species makes the best cuttings for this purpose. Large stone is then dumped around the upstream side and the nose of the structure. See Photographs 1 and 2.

Toe Protection

A number of systems constructed of woody vegetation are placed directly on or parallel to the bank to trap sediment and to protect against scour. Examples include live siltation structures, brushmattress, live fascines, and vegetated geogrids. See Photographs 3, 4, 5 and 6. Although these can be used without toe protection on some streams (such as streams with well armored beds or other non-scouring situations), most applications require toe protection

Photograph 1 Spring, prior to vegetative growth. Note deposition between the live booms.

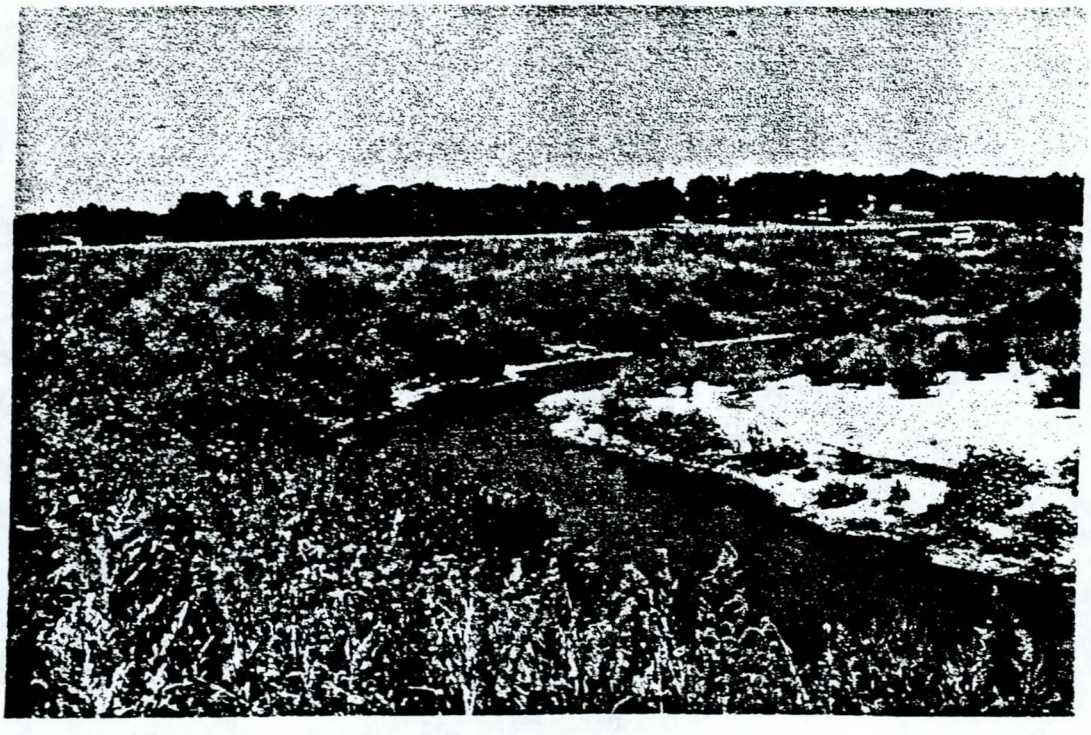

Photograph 2 Fall, vegetative growth within the same year.

to prevent undermining and subsequent failure. Riprap is the most common form of toe protection used when stone of sufficient size and quality is available. Small stone that otherwise would not be stable can be wrapped or placed in gabion cages to provide toe protection.

Vegetated Riprap

Sometimes riprap is the form of bank protection that is preferred by a client for cost or other reasons. Where not prohibited by institutional constraints, environmental benefits of riprap can be enhanced considerably by live staking as described previously. When live stakes are used with riprap the process is called joint planting to distinguish it from live staking without rock. Stakes should be tamped into the soil below the riprap and any filter layer to a depth of at least 50 cm at an angle perpendicular to the slope and angled slightly downstream. Joint planting can provide a considerable amount of shade and cover, as well as trapping sediment, even during the first growing season. See Photograph 7.

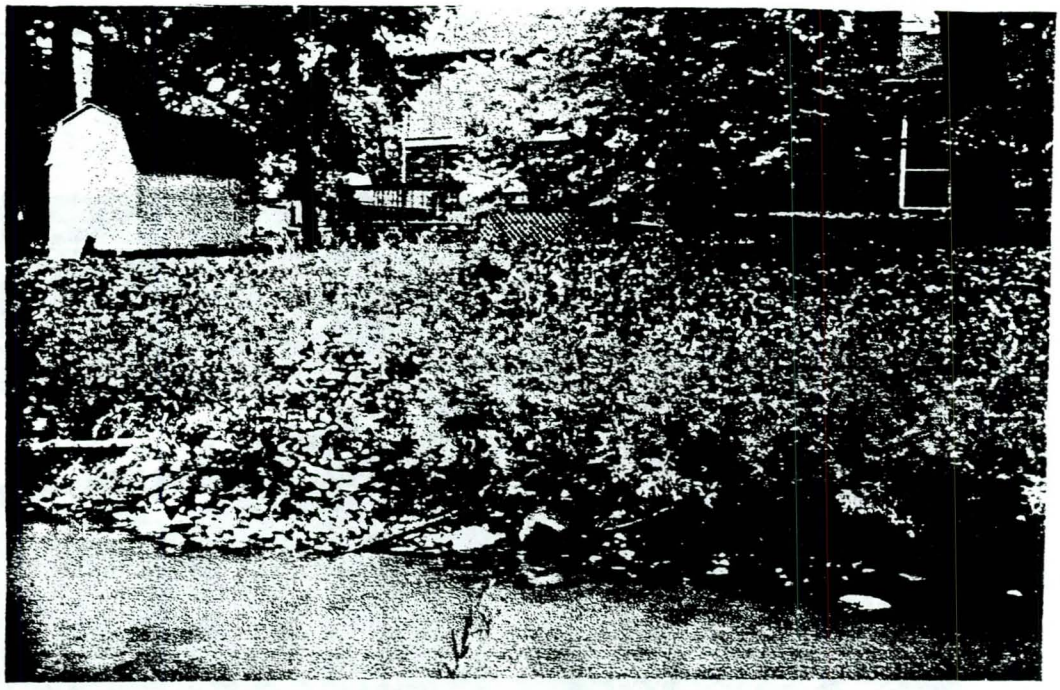

Photograph 3 Live siltation construction and live boom in the early spring.

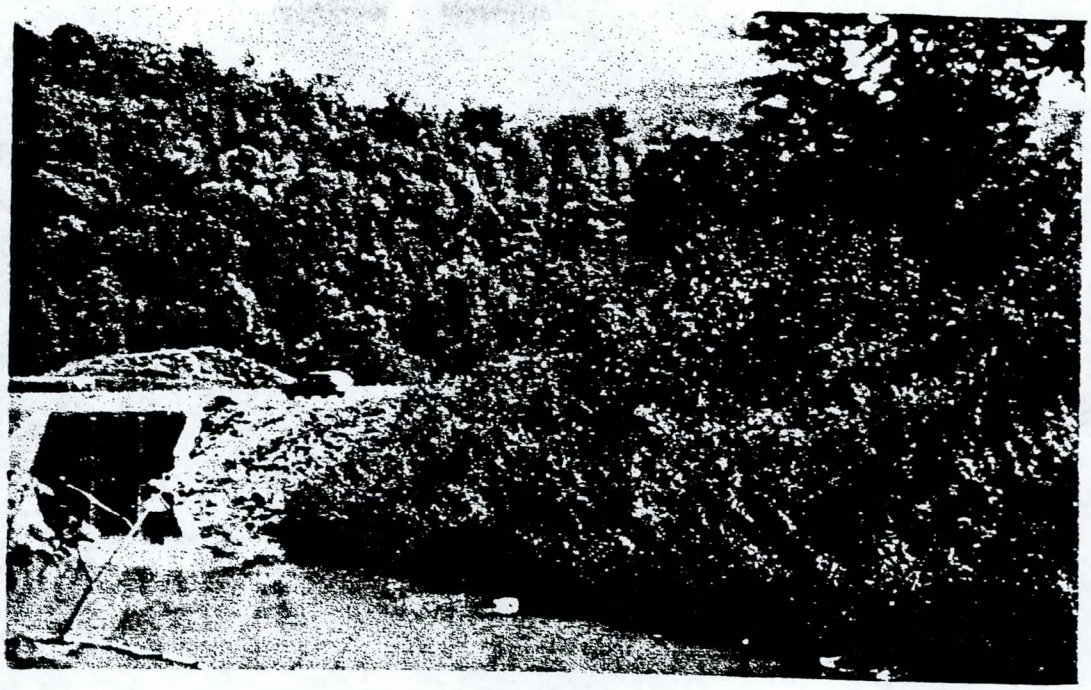

Photograph 4 Brushlayer in the second year of growth.

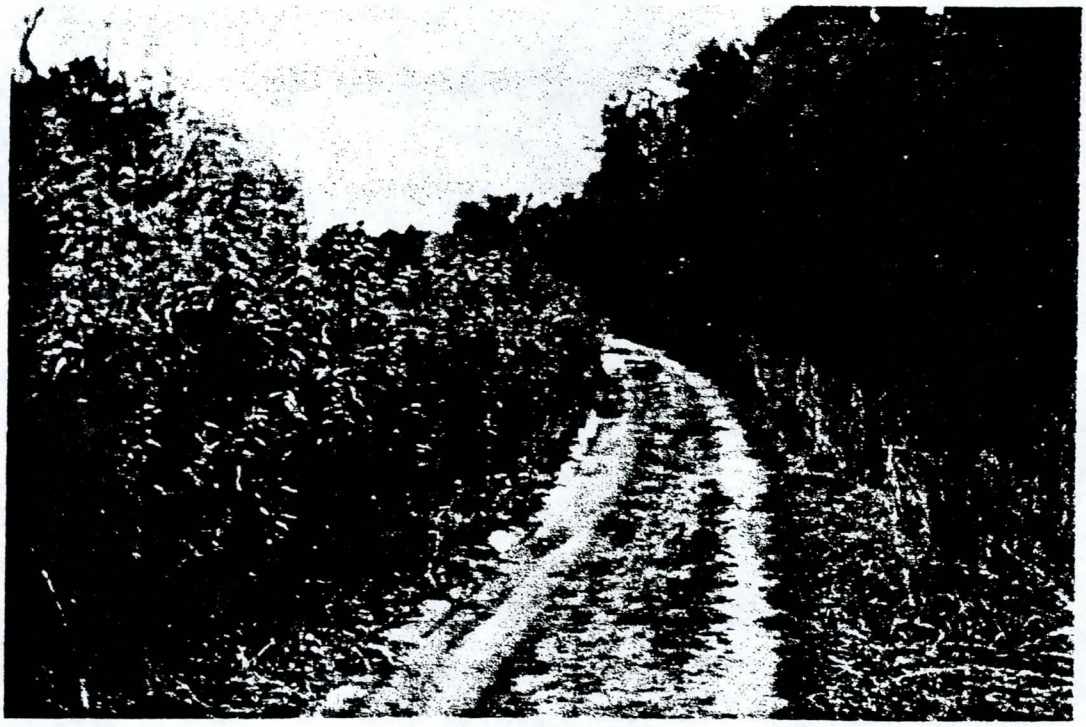

Photograph 5 Live fascine growth two years after construction.

Photograph 6 Vegetated geogrid in its first year of growth.

Major Design Considerations

The major design considerations encountered when using riprap in the situations just described involve issues of stability - bed degradation, scour depth, and appropriate rock size and blanket thickness. Each of these is discussed separately.

Bed Degradation or Bed Scour

Most streambank protection work is performed on streams with inherent instability. This instability can result from channel modifications such as straightening or enlargement; altered rainfall-runoff relationships due to activities such as urbanization, agriculture, or forestry; or to base level changes, just to name some examples. When installing foundations or toe protection for streambank protection it is essential to have some idea whether bed degradation might be occurring, and, if so, what the ultimate depth is likely to be.

Predicting the amount of bed degradation is a difficult and risky business, and one that is likely to tax the skills of even the most innovative and experienced practitioner. Although we are unable to suggest a single approach that works in a majority of situations, we can propose an approach that may have potential when degradation has been going on for several years and reliable measurements of bed elevation have been taken at several time periods. Plotting the elevation data against time and fitting a regression line to the plot as shown in Figure 1 may suggest a limiting depth. The data in Figure 1 apply to a Mississippi stream that has been undergoing bed scour for a number of years.

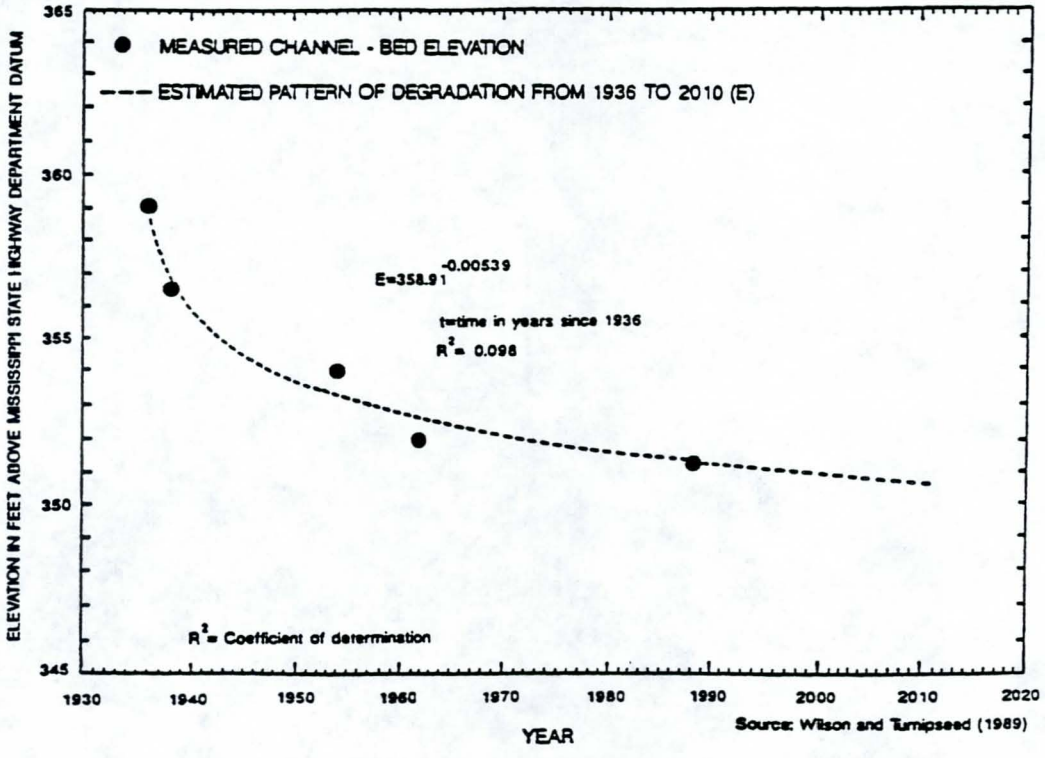

Figure 1 Estimated scour depth for Osborne Creek.

Predicting Scour Depth in Bends and Around Structures

Even in streams with stable beds localized scour caused by secondary currents can undermine streambank protection structures. The two most common situations where this is encountered is along outside meander bends and around the tips of dikes.

Outside meander bends are zones of scour, as indicated by the pools that normally occupy these locations. Streams with beds composed of sand and fine gravel may be scoured to substantial depths during the passage of flood events. Some of the greatest scour occurs in meander bends. On one Mississippi stream where an experimental streambank protection design was tested that consisted of closely spaced posts with overlapping automobile tires, tires came off the bottoms of the posts when the bed was scoured below the ten foot depth to which the posts were installed. Although the pool in a meander bend may refill as the falling limb of the hydrograph passes, any rock placed on the bed would be buried or swept downstream during the scouring event.

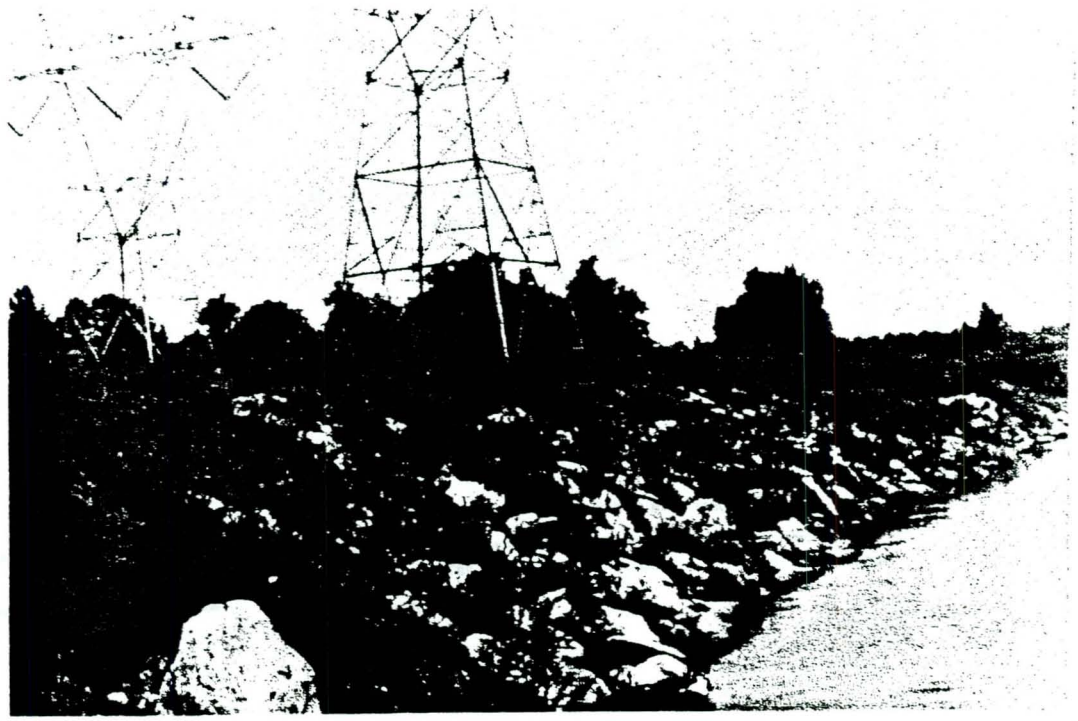

Photograph 7 A joint planted streambank one year after installation.

The authors are presently unaware of any reliable method of predicting scour depth, given the lack of data and the time and cost constraints that are usually encountered in streambank protection work. Accordingly, we have adopted two rules of thumb that we have used. First, we use a minimum key in depth of one meter on small streams (bankfull discharge less than about 15-20 cubic meters per second) and two meters on larger streams. Second, we add additional stone, either as a surface blanket extending away from the buried toe or buried in the toe trench as additional width.

Dikes are used on large rivers to contract flow through a narrower width and scour channels for navigation purposes. These dikes are normally placed in series and are long enough to cause significant channel contraction. Dikes used for streambank protection typically contract the channel very little and cause local scour around the tip of the dike only.

Numerous studies about dikes have been published. Some of them propose empirical formulas for predicting scour depth around the tips of dikes. These relationships are usually derived from studies done with flumes or with movable bed models of large streams. We have had little success with these formulas for various reasons. Some employ empirical constants that do not seem to be applicable to most streams; some require data, such as discharge and bed material size, that are unavailable and too time consuming or expensive to collect; and, some apply only to dikes with specific orientations, heights, relative lengths, or other specific design criteria.

There is significant lack of agreement on how to design dikes to maximize bank protection. When unsubmerged, all flow is forced around the tip of the structure, causing acceleration of flow and scour. Thus, the higher the dike, the deeper the scour hole tends to be. There is evidence from model studies that dikes angled upstream develop deeper scour holes than those perpendicular to the bank or angled downstream. For these reasons we tend to avoid alignments angled upstream and build our structures with sloping crests that intersect the bank at about the same elevation as the natural sedimentary berms present in many streams (about the elevation of the flow that is exceeded five percent of the time). So far, we have experienced few problems with undercutting, except on streams undergoing active degradation.

Rock Size and Blanket Thickness

In sizing rock and determining blanket thickness we prefer the guidance developed by the U.S. Army Corps of Engineers Waterways Experiment Station (WES). Not only do we find this approach to be easy to use and cost effective, but it lends itself readily to hand placement of stones and joint planting in most cases. Sometimes governmental clients have their own guidance for sizing stone that they prefer us to use.

Major Problems

Aside from availability of stone suitable for riprap, which is sometimes a problem, the major threats to successful project performance are improper site assessment, design, installation and lack of monitoring and maintenance. Improper site assessment and design occurs due to failure to consider all pertinent hydraulic, geotechnical, and hydrologic information. Improper installation occurs for a variety of reasons. Contractors employed to do the work are usually general contractors who lack experience in bidding soil bioengineering projects and requirements for handling dormant vegetation. Clients often try to save money by shortening the reach after design or by modifying designs through elimination or substitution of elements.

Monitoring and maintenance are critical to any streambank protection project, but especially so to those employing vegetation. During the first year after installation, projects should be inspected following all high flow events. Thereafter, they should be inspected annually and following all major flood events. Shortly after the growing season commences all vegetative systems should be inspected to identify and correct any problems of vegetative growth.

Summary

Vegetation is an important element in streambank stability and a critical element in aquatic and riparian habitat. Streambank protection that incorporates vegetation offers far more environmental benefits than structural designs without vegetation. Stresses imposed on vegetative systems by the flow of water often necessitate the use of stone in conjunction with

vegetation to protect against undercutting and scour. When used together they can provide effective protection against erosion in addition to environmental benefits. See Photograph 8.

Photograph 8 Rock used in conjunction with vegetated soil bioengineering treatments offering both protection against erosion as well as broad environmental benefits.

PREDICTION OF NEAR-BANK VELOCITY AND SCOUR DEPTH IN MEANDER BENDS FOR DESIGN OF RIPRAP REVETMENTS

C.R. Thorne
University of Nottingham, Nottingham, UK
S.R. Abt
Colorado State University, Fort Collins, USA
S.T. Maynord
US Army Waterways Experiment Station, Vicksburg, USA

ABSTRACT

Most alluvial rivers adopt a sinuous course and locations of serious bank erosion are usually related to the meander planform. Erosion often occurs at the outer bank in a bend, as a result of both elevated near-bank velocities and deep bed scour adjacent to the bank. The magnitudes of both the near bank velocity increase and the additional scour depth due to bend effects are known to be related to the shape and, particularly, the curvature of the bend. When designing riprap for bank protection it is necessary to ensure that the rock is safe against both direct attack by the flow and collapse due to undermining by toe scour. This paper examines empirical and analytical approaches to predicting maximum values of near-bank velocity and toe scour depth at a meander bend for riprap design purposes. Data from a wide range of sizes and types of river are used. It is found that existing empirical curves may be overly conservative in predicting near-bank velocity and that the 'Bendflow' model developed by J S Bridge (1982) may present a more accurate analytical approach. The model is able to predict maximum near-bank velocity to within about +/- 15% for bends with R/w values greater than about 3. In the case of bed scour, the analytical approach is less successful and errors of +/- 100% are liable to occur, but an empirical equation based on data for the Red River, Louisiana is found to generally predict maximum scour depth to within +/- 25%.

INTRODUCTION

Most alluvial rivers have a meandering planform. Such rivers naturally migrate back and forth across their flood plain by a combination of relatively orderly meander loop growth and downstream progression which is interrupted occasionally through abrupt by-passing of acute bends by chute and neck cut-offs. Generally, meander growth and progression occur through retreat of the outer bank and advance of the inner bank of a bend, although in particular cases this pattern may be reversed.

A great deal of engineering work is undertaken each year on rivers of all scales from small creeks up to great rivers like the Lower Mississippi to curtail and control lateral activity due to meandering. This is an essential component of projects to improve navigation, increase flood capacity, stabilize banklines, decrease flood plain destruction and reduce the downstream dredging requirement of the river. Often bank stabilization is achieved using structures made from rock; sometimes alone, but often in combination with other materials and treatments. For example, on the Lower Mississippi River upper bank riprap and lower bank articulated concrete mattress (ACM) are used to protect against the erosive attack of the near bank flow, together with bank regrading and sub-surface drainage control to prevent mass failure. On smaller rivers riprap may be used alone, or increasingly, in combination with other low cost, environmentally friendly alternatives such as vegetation.

Bank stabilization assumes particular significance where a flood embankment (levee) or other important piece of infra-structure is set back only a short distance behind the bank line. At such locations retreat of the bank cannot be allowed because it would put the levee or structure in jeopardy. Yet despite awareness of the potentially damaging impacts of failure, revetments do still occasionally fail, resulting in retreat of the bank line, destruction of areas of the flood plain and, in some cases, the loss of a section of levee.

Riprap failure may be due to under-design of the size of the riprap stone, allowing entrainment of rock from the protective blanket to expose the weaker underlying materials. Hence, it is vital to ensure that the rock size is sufficient to resist the flow attack under all circumstances. However, failures due to under-sized rock are comparatively rare. More often the cause of a revetment failure is scouring of the bend pool adjacent to the outer bank to a greater depth than that allowed for in the design. Scour below the toe of the revetment may trigger mass failure of the whole bank (including, or followed by, the structure behind the bank) by one a variety of mechanisms. Mechanisms identified as being the most critical include: rotational slip, slab-type collapse and retrogressive flow failure (Turnbull et al., 1966; Torrey, 1988). Consequently, it is important to be able to predict the likely maximum scour depth in a bend accurately when designing revetment.

Conversely, given the considerable cost of revetment, it is important to avoid significant over-design of either rock size or toe scour protection. In this regard, design approaches that are overly conservative, and which are therefore not cost effective, are also undesirable.

This paper briefly reviews approaches to near-bank velocity and scour depth prediction at bends based on empirical and analytical methods and then uses extensive data sets obtained from field observation and from the literature to test and evaluate various approaches. The results are used to asses the reliability and accuracy of different methods and to make recommendations for future investigations.

VELOCITY PREDICTION - EMPIRICAL APPROACH

Existing Methods

When using riprap it is necessary to select the appropriate size for the stone on the basis of the intensity of flow attack as represented by either the boundary shear stress on the outer bank or the flow velocity over the toe of the outer bank. Usually, this achieved using empirical diagrams of which those used by the US Army Corps of Engineers are typical (Fig. 1).

Figure 1 predicts the ratio of velocity over the toe of the outer bank to average velocity in the approach channel (V_{toe}/V_{avg}) as a function of the radius of curvature to width ratio for the bend (R_c/w). A logarithmic scale is used for the independent variable (R_c/w) and a linear scale for the dependent variable (V_{toe}/V_{avg}). Two lines are plotted, corresponding to natural channels (with asymmetrical cross-sections) and trapezoidal channels (with symmetrical cross-sections), respectively. The ratio of outer bank to mean velocity is markedly higher in natural than in trapezoidal channels. Plotted as straight lines on a semi-log graph, these lines indicate logarithmic relations for the two types of channel. The equations of the lines are not specified by WES, but analysis of the graph suggests that they approximate to:

Natural Channels

$$\frac{V_{TOE}}{V_{AVG}} = 1.75 - 0.5 \log \left(\frac{R}{w}\right) \quad (1)$$

Trapezoidal Channels

$$\frac{V_{TOE}}{V_{AVG}} = 1.6 - 0.71 \log \left(\frac{R}{w}\right) \quad (2)$$

While the diagram has been found to give safe results when used with sound engineering judgement and with careful consideration of the limits to their applicability, it is nonetheless desirable to develop improved procedures that better account for the parameters of flow hydraulics, boundary roughness and channel geometry that are believed to influence flow intensity at the outer bank in a meander bend. Several other aspects of bend geometry, channel shape and boundary roughness have been shown to influence bend flow patterns significantly on both theoretical and practical grounds (Thorne, 1978; Hooke and Harvey, 1983; Rais, 1984; Lapointe and Carson, 1986; Thorne and Osman, 1988; Odgaard, 1989a and b), and a method which uses only a single parameter to characterize the bend, ignoring all others, cannot hope to account for these effects.

An alternative to the use of near bank velocity as an index of flow attack at the bank is the use of the boundary shear stress. However, this is a particularly difficult parameter to predict accurately and is in fact difficult for non-specialists to visualize. It is desirable to relate the severity of bank attack and toe scour to a less obscure flow descriptor, such as near-bank velocity. Some modelers even prefer to relate bank attack and retreat rates to near bank velocities instead of bank shear stress (Odgaard, 1990). Theory shows that near-bank velocity and boundary shear stress are, in any case, closely related, although the relation between them is neither simple, or easily quantified for real world situations. Hence in this study consideration is given to the prediction of depth-averaged velocity over the toe of the outer bank.

Field Database and Testing

Data were obtained from a number of diverse sources. The primary source was studies undertaken by the first author and colleagues at Colorado State University, London University, UK and the University of East Anglia, UK. Other sources were researchers working independently on bend flow problems who were willing to share their data, and from papers published in academic journals.

The data set which has resulted is not universal in its scope. It does, however, contain only data which the authors know to be sound and complete. The range of sizes and types of channel encompassed is large and there is a sufficient number of independent collected data sets to support the statistical analysis. Consequently, it is probable that the addition of a few further data would be unlikely to materially alter the overall distribution of data or the outcome of the analyses.

The ranges of variables in the database are listed in Table 1. The database includes a range of variables describing the geometry and hydraulics of each bend, in order to allow examination inter-relationships amongst the variables and with the outer bank velocity. The complete database is available in a Colorado State University Report (Thorne and Abt, 1989) and the published and unpublished sources of data are listed in the references. These data were used to derive dimensionless parameters of bend geometry and hydraulic roughness which are believed to affect the pattern of flow through a bend.

The data were plotted in relation to the empirical design curve developed by the US Army

Engineer Waterways Experiment Station (Fig. 2). The design line does not pass through the points, but forms a good upper boundary to the data with the exception of only 3 out of the 34 points. Thus, it may be concluded that the WES design curve represents a reasonable, but rather conservative approach to the estimation of (V_{toe}/V_{avg}) in natural channels. This is essential so that in the final design, the size of riprap specified is always on the safe side. A regression line through the scatter of the points for V_{toe}/V_{avg} could be used, but this would require that a factor of safety be introduced in the relationship between the critical local velocity for entrainment and the size of stone used in a revetment. Present WES preference is to position the design line as an upper bound to the data, so that all of the zone of uncertainty is on one side of the line (N. R. Oswald, personal communication, 1990).

However, there is considerable scatter in the data, and this deserves comment. Partly, it is a result of the methods used to collect the data. Usually, velocities were measured at a finite number of cross-sections around each bend. In some studies many sections were used (up to seven per bend), but in others only a few (three or less) were used. Near bank velocities at intermediate points between sections were not measured. Consequently, there is no guarantee that the *actual maximum* outer bank in a bend would be observed in any study. Indeed, in studies with only a few sections, it is highly probable that the outer bank maximum velocity for a bend would not be measured. It is, therefore, to be expected that field data should plot either close to or below a line defining the maximum possible ratio of outer bank to average velocity. However, even for bends with multiple measured sections, the data often plot well below the WES line. This suggests that there are further variables affecting the velocity ratio which are unaccounted for in the WES analysis.

Points for bends of very low R_c/w values reveal that the monotonic increase in V_{toe}/V_{avg} observed as R_c/w decreases may cease at an R_c/w of about 2. For R_c/w values less than 2, the data show a wide range of V_{toe}/V_{avg} values, but the velocity ratio never exceeds 1.6. This accords with other recent studies of bend flow in very tightly curved bends, which have shown that both outer bank scour pool depth and outer bank retreat rate may actually decrease with decreasing R_c/w for bends with R_c/w less than 2 (Biedenharn et al., 1989; Thorne, 1989). This is not unexpected theoretically, as there is a major discontinuity in the way the pattern of bend flow responds to increasing bend tightness at R_c/w of between 2 and 3 (Bagnold, 1960). Further data and analyses are required to confirm this tentative finding.

Further examination of the data centred on the additional parameters of bend geometry measured in the field. A correlation matrix between the different variables is shown in Table 2. This reveals that the four additional bend descriptors are in fact each strongly correlated with R_c/w, as well as being strongly inter-correlated. On this basis the great strength of R_c/w as a descriptor of bend geometry is demonstrated. It must be concluded that, due to the strong auto-correlation within the bend descriptors, any improvements in prediction gained by adding further variables will be relatively minor. Conversely, initial inspection of the data when split between bends with straight and with meandering approach channels suggested that there was a marked difference in velocity ratios. Therefore, this classification of channel planform geometry was considered in more detail.

Effect of Approach Conditions

Figures 3a and b show the R_c/w versus V_{toe}/V_{avg} relations for natural channel bends with straight and meandering entrance conditions, respectively. Examination of the plots suggests that for the same R_c/w value, bends downstream of straight reaches have higher velocity ratios than those downstream of meandering reaches. The WES design curve forms a reasonable upper bound to the data for bends with straight entrance conditions, but significantly over-estimates the increase in the velocity ratio that accompanies a decrease in R_c/w for bends in meandering reaches. The discrepancy increases as the R_c/w decreases. This is, potentially, an important finding because it suggests that different design approaches might be appropriate for a single, isolated bend rather than a series of consecutive bends in a meandering river.

The difference may arise due to the contrasting transverse distributions of longstream velocity at the entrance of bends with straight and meandering reaches upstream. At the end of a long, straight approach reach the maximum velocity filament is at the channel centerline. It must cross only half the channel width before encountering the outer bank zone to elevate outer bank toe velocities. This is usually achieved just after the bend apex, in the second half of the bend, where skewing of the flow field by the bend is at its strongest.

Conversely, at the exit of an upstream bend the maximum velocity filament is located adjacent to the outer bank for that bend. If the next bend (which is of opposite curvature) is immediately downstream, then at its entrance the maximum velocity filament is located near the inner bank. It must cross the whole channel width before encountering the outer bank zone. This requires fully developed secondary flow and a long bend, and is seldom achieved until downstream of the bend exit, where the strength of skew-induced flow is already declining. As a result, the ratio of outer bank to average velocity in such a bend may be lower than that in an equivalent bend at the end of a straight reach. This preliminary finding is consistent with long-held ideas on the effect of entrance conditions on bend flow (see for example, Chacinski and Francis, 1952) and it merits further research.

Regression Analysis of Field Data

To investigate whether an improvement in the prediction of toe velocity could be made, regression analysis was performed on the empirical data. From the initial examination of the data it was concluded that the log-linear relation between R_c/w and V_{toe}/V_{avg} breaks down for R_c/w values less than 2 due to major changes in flow pattern and associated impinging flow and areas of separation at the outer bank. In view of this, it was decided to limit the curve fitting to bends with R_c/w values equal to or greater than 2.

It was noted earlier that in some studies only a few sections were monitored in each bend, and that consequently the data collected do not represent the absolute maximum ratio of V_{toe}/V_{avg} for that bend. This explains why some points plot low in Fig. 2. Taking this fact together with the recommendation from WES personnel that an upper bound line is preferable to a best-fit line when predicting Vtoe/Vavg for riprap design, it was decided to perform the multiple regression using only points from the upper edge of the scatter. These points turned out to come mostly from bends which were intensively studied (for example, studies by Thorne et al., by Dietrich, and by Bridge). Some data came from single sections too, apparently where those sections happened to have coincided with the highest values of Vtoe/Vavg for the bend. Hence, the correlation co-efficients indicate the linearity of the upper surface of the data cloud, rather than the strength of correlation overall.

Natural Rivers: Straight Approach Conditions

The points used to define the upper boundary are indicated in Fig. 3a. The best-fit regression equation for the upper bound to bends with straight entrance conditions is:

$$\frac{V_{TOE}}{V_{AVG}} = 1.66 - 0.42 \log \left(\frac{Rc}{w}\right) \quad (3)$$

The adjusted coefficient of determination for this equation (r^2) is 0.90, indicating good log-linearity at the upper edge of the data cloud. The resulting line is shown in Fig. 3a.

Natural Channels: Meandering Approach Conditions

The points used to define the upper boundary are shown in Fig. 3b. The resulting equation for rivers with meandering entrance conditions is:

$$\frac{V_{TOE}}{V_{AVG}} = 1.4 - 0.24 \log \left(\frac{Rc}{w}\right) \quad (4)$$

The adjusted coefficient of determination for this equation (r^2) is 0.87, again indicating good linearity at the upper edge of the data cloud. The line produced by this equation is shown in Fig. 3b.

Conclusion

These results indicate that the planform pattern of the approach channel may influence the ratio of the depth averaged velocity over the toe of the outer bank to the average velocity at the bend entrance. Generally, bends with meandering approach channels have lower velocity ratios than bends with straight approach channels. While the WES design curve is very similar to the empirical curve for bends with straight approach channels, it may be overly conservative for bends with meandering approach channels.

VELOCITY PREDICTION - ANALYTICAL APPROACH

Background

During the last decade, many mathematical models for predicting the velocity distribution and bed topography in river bends have appeared in the literature. Most models are intended either for use by sedimentologists interested in reconstructing past environments (eg. Allen, 1970, Bridge, 1976), or river engineers attempting to predict the distribution of scour as an aid in the design of successful channel stabilization schemes (eg Odgaard, 1987). However, many models may be criticized because they are unnecessarily complicated and esoteric for these tasks, and because no attempt is made to specify clearly where, when, and how they should be applied to natural waterways. Some very pertinent remarks were made concerning the role of mathematical models in fluvial hydraulics and river engineering during a discussion by conference participants at the concluding session of the ASCE Rivers '83 conference, New Orleans, 1983 (Elliott, 1983). These are encapsulated by a comment from Charles Neill, a senior practising river engineer from Northwest Hydraulic Consultants, Canada. He said,

> "It is important that mathematical models should have a good familiarity with the range of features encountered. ...It would be a service to the profession if these could be used to produce generalized tables, graphs or programs that would enable reasonable estimates of velocity and shear distributions to be made by practising engineers, without the necessity of access to an elaborate modelling facility" (Neill, 1983)

Difficulties are often encountered when attempting to apply models to natural rivers. If the model requires certain input parameters that need to be known or to be measured in the field (the centerline mean velocity or the mean Darcy-Weisbach friction factor are examples), it is often difficult to assign a value with confidence. Often, field measurements unavailable and estimates are unreliable, and it may be the case that the model output may highly sensitive to incorrect values having been assigned to the input parameters.

Also, many models are written by, and apparently for, researchers. Unless the user is a specialist: expert in programming, three dimensional fluid mechanics, and mathematics, it is virtually impossible to use them for a real world application without some assistance from the author of the computer code.

In this paper we examine two readily available mathematical models as predictors of outerbank velocity in bendways. Before going on to report the results from the models selected, it is relevant to present a short outline of the physical basis for the models.

Basic Principles of Numerical Modelling of Bend Flow

The numerical modelling of flow and sediment processes in river bends is a subject that is receiving ever-increasing attention, and a large number of models are available. There are two components to most models. The first involves a solution to the equations of motion for fluid flow. The second is the interaction between the flow and the bed topography. This requires balancing the different forces acting on bed-material particles to produce an equilibrium bed topography.

All flow models start with the equations of motion for fluid flow. For application to bend flow, the equations are usually written in cylindrical coordinates. Given below are the equations of motion for the steady flow of an incompressible fluid in an orthoganal cartesian coordinate system (Rozovskii, 1957). The velocity components in the s (stream-wise), n (perpendicular to s-axis), and z (vertical upwards from the stream bed) directions are denoted u, v, and w respectively, r = local radius of curvature; p = pressure; and F = friction term in the s, n and z directions respectively:

$$u\frac{\partial u}{\partial s} + v\frac{\partial u}{\partial n} + w\frac{\partial u}{\partial z} + \frac{uv}{r} = -\frac{1}{\rho}\frac{\partial p}{\partial s} + F_s \qquad (5)$$

$$u\frac{\partial v}{\partial s} + v\frac{\partial v}{\partial n} + w\frac{\partial v}{\partial z} - \frac{u^2}{r} = -\frac{1}{\rho}\frac{\partial p}{\partial n} + F_n \qquad (6)$$

$$u\frac{\partial w}{\partial s} + v\frac{\partial w}{\partial n} + w\frac{\partial z}{\partial w} + g = -\frac{1}{\rho}\frac{\partial p}{\partial z} + F_z \qquad (7)$$

The left hand sides of these equations are the convective acceleration terms. There are no local acceleration terms ($\partial/\partial t$) and so strictly speaking the models are not prognostic but diagnostic.

The continuity equation for 3-dimensional, incompressible flow is also specified:

$$\frac{\partial u}{\partial s} + \frac{1}{r}\frac{\partial (vr)}{\partial n} + \frac{\partial w}{\partial z} = 0 \qquad (8)$$

The principal cross-stream and downstream force balances are between: the centrifugal and pressure gradient forces in the cross-stream direction: and the downstream balance between gravitational and frictional forces.

Secondary circulation is usually considered to be the most important effect of curvature on flow, but the tilting of the water surface is also very important, because it alters the downstream slope of the water surface, generating large cross-stream variation in the downstream boundary shear stress and velocity fields.

Flow and bed topography models attempt to simulate the bed morphology of a channel bend by assuming that, at equilibrium, the forces directed inwards and outwards on each bed particle are balanced (Allen, 1970; Bridge,1977). This means that particles of different sizes travel along paths of equal depth along the channel, under the influence of longstream drag. Models that use this scheme differ in the way in which the forces of lift and longstream drag are determined. The balance of forces acting on a particle in the mean flow direction is:

$$F_D \cos\delta = (W - F_L)\cos\alpha \tan\varphi \qquad (9)$$

where F_D = drag force, d = deviation of the bed shear stress vector from the longstream direction, W = submerged weight, F_L = lift force, tanj is the dynamic friction coefficient due to collisions with the bed and other grains, and a = transverse slope of the point bar surface (Bridge, 1977).

The transverse force balance is therefore:

$$F_D \sin \delta = (W - F_L) \sin \alpha \qquad (10)$$

For any given point on the transverse bed profile, the balance of drag and immersed weight components acting on a bed particle is:

$$\pi (D/2)^2 \tau_x \tan \delta = \frac{4}{3} \pi (D/2)^3 (\sigma - \rho) g \sin \alpha \qquad (11)$$

Where D = particle diameter, t_x = longstream bed shear stress, and s and r = the sediment and fluid densities, respectively.

The theory assumes that the particles are moving as contact load. It is also important to note that for suspended particles, forces due to lift and the cross-stream component of particle weight are insignificant.

Another assumption common to many models is that the angular deviation (d) of the shear stress vector from the downstream direction (and therefore the local transverse bed slope) is proportional to the ratio between the depth and radius of curvature:

$$\tan \delta = C \frac{h}{r} \qquad (12)$$

where C is an empirical coefficient. This relation, developed by Rozovskii (1957) from the equations of motion, is actually applicable only to fully-developed secondary flow. Fully-developed flow occurs in the downstream part of long, constant-radius reaches where flow and bed topography remain constant with distance downstream and are independent of upstream conditions. For developing flow where flow and bed topography do not remain constant with distance, the governing equations are more complex and difficult to solve.

As the outward component of gravity is proportional to the cube of the diameter of the grain whilst the inward-acting drag on the particle is proportional to the square of the diameter. This leads to a sorting mechanism, recognized as an important process in meander bends by Allen (1970), Bridge (1977), Dietrich and Smith (1984) and Parker and Andrews (1985), whereby for the same velocity, larger particles will tend to roll, due to gravity, out towards the pool, while smaller ones will tend to be swept inwards by fluid drag. Wilson (1973) used the same principle to propose an explanation for sorting in straight channels.

Models Used

Two models were applied to predict the ratio of outer bank to average velocities in bendways: those of Bridge (1982) and Odgaard (1988). These models were unusual in that their authors were willing to make them fully available to us and assist us in their application. Most modellers do not release their models in this way for a variety of reasons. Others supplied copies of papers reporting their models, but not computer codes. The task of rewriting entire codes for extremely complex models would be burdensome and the chances of faithfully reproducing the author's model would be remote. Consequently, only the models actually provided in full, with documentation were tested. Complete details of the models may be found in papers authored by Bridge (1982) and by Odgaard (1988). These programs were used to produce estimates of the maximum depth averaged velocity over the toe of the outer bank at each of the natural and laboratory channel bends represented by the data in the first of these two papers.

Results of Model Applications

Bridge's model crashed for bends with very low radius to width ratios ($R_c/w < 1$), which caused a fatal computational error. Odgaard's model failed in many more cases. The problem was that in long bends the model predicted negative water depths at the inner bank, leading to its crashing. This problem has been recognised by the author of the program and further work on the model is underway to resolve it (Odgaard, personal communication, 1991).

The results are plotted as observed versus predicted outer bank velocities in Figure 4. The agreement is generally quite good, although systematic errors are apparent in both graphs. In the case of Bridge's model these can be largely explained by a plot of the percent error versus the R_c/w ratio. For this purpose, error is defined by:

$$\text{error} = \frac{(\text{observed } V_{toe} - \text{predicted } V_{toe})}{\text{observed } V_{toe}} \times 100\ \% \qquad (13)$$

The error distributions are plotted in Figure 5. Bridge's model is seen to give generally excellent accuracy for bends with R_c/w values greater than 2, but is inaccurate for tighter bends with R_c/w less than 2. This accords with the theory of bend flow, the results of the empirically based approach and with Bridge's own guidelines on the use of his model. More applications are needed to develop firm conclusions on Odgaard's model, but the preliminary results show that it is prone to underestimating the toe velocity by up to about 30 percent. This occurs because for bends with coarse sand or gravel beds the model does not predict the degree of bed scouring at the outer bank which is actually observed in nature. As discussed later, outer bank depths are only marginally greater than centerline depths, and similarly outer bank velocities are only slightly greater than the centerline velocity. However, the errors do not increase markedly at low Rc/w values, and the model is consistent even in the tightest bend with an Rc/w = 0.8.

Conclusions

On the basis of this test, Bridge's model can be relied upon to predict the outer bank velocity in a bend to within approximately +/-15% for bends with R_c/w greater than 2. This would appear to make it a strong candidate for adoption as a design method. For engineering design purposes it might be desirable to introduce a factor of safety of 1.15 to the predicted velocity so that errors are likely to be on the safe side. However, Bridge's model should definitely not be used for bends with R_c/w is less than 2, where it is prone to large errors. Bridge's model is available in menu driven format for IBM PC computers or compatible machines, and it is relatively easy to use.

Odgaard's model could not be fully tested as it crashed for many of the bends studied. For the bends at which it did work, errors were between 5 and 40 percent, for bends with Rc/w ratios between 0.8 and 5. Further work is needed before Odgaard's 1988 model could be recommended for use as a design method, particularly to prevent it crashing for long bends on large rivers and to increase the depth of outer bank scour in channels with coarse bed sediments. But on the credit side, the fact that Odgaard's model does not fail for short, tight radius bends is very encouraging.

BEND SCOUR DEPTH PREDICTION - EMPIRICAL APPROACH

Existing Methods

The existing empirical approach tested in this paper comes from a project recently completed using data from a 1981 hydrographic survey of the Red River, between Index, Arkansas and Shreveport, Louisiana (Thorne, 1988). Data from 70 bends were used to produce

a regression equation for the prediction of maximum bend scour (d_{max}) on the basis of the mean depth of the approach channel at the crossing upstream of the bend (d_{bar}) and the bend geometry represented by the ratio of bend radius (R_c) divided by width at the upstream crossing (w). Separate regression equations were developed for all meander bends and for those stabilized by the revetments on the outer bank. The regression equations for the empirical method are:

All Meanders

$$\frac{d_{max}}{d_{bar}} = 2.07 - 0.19\log\left(\left(\frac{R_c}{w}\right) - 2\right) \qquad (14)$$

Revetted Bends

$$\frac{d_{max}}{d_{bar}} = 2.15 - 0.27\log\left(\left(\frac{R_c}{w}\right) - 2\right) \qquad (15)$$

The correlation coefficients were 0.8 and 0.83 respectively, and were both statistically significant at the 0.01 level of confidence. The coefficients of determination were 0.64 and 0.69 respectively, indicating that variation in (R_c/w) was able to account for 64% of the variation in (d_{max}/d_{bar}) in all meanders, and 69% in revetted bends. The lower limit to the applicability of the equation is an R_c/w value of 2. This is consistent with the observation that the monotonic increase in scour depth with decreasing R_c/w seems to stop at this value. A complete account of the methodology is available in Thorne (1988).

Field Database and Testing

The data set prepared in this part of the study contains data for 257 bends on natural rivers compiled by Thorne and Abt (1990). It also contains 8 points for laboratory flumes for comparative purposes. The data come from a wide variety of types and sizes of rivers, located in different physiographic regions and from different parts of the world. They were compiled from existing reports and papers supplemented by information solicited in letters sent to researchers known to be actively interested in bend flow. The sources of data are first reviewed briefly. Due to space limitations, the whole database is not listed here, but it is available in hard copy (Thorne and Abt, 1990) and on computer disk, from the authors on request.

Thorne and Abt (1990). The base data for these natural rivers may be found in a Colorado State University Report by Thorne and Abt (1990). It should be noted that as the surveys were based on surveying of a finite number of cross-sections (between three and seven per bend) it cannot not be guaranteed that the recorded maximum scour depth was actually the maximum observed anywhere in the bend. Also it should be noted that measurements correspond to high, in-bank flows in the rivers rather than to 'design flows' of long return period.

Red River Hydrographic Surveys. The second and third sources of data are hydrographic surveys of the Red River between Index, Arkansas and Shreveport, Louisiana made in 1981 and 1969. The river in this reach is highly mobile, with rapid bank erosion, bend migration and planform evolution. Since the bed topography, bend geometry and planform configuration in 1981 bears little relation to that in 1969, it may be concluded that the surveys yield essentially independent data sets on the relationship between bend geometry and bed topography. The base data for 1981 are listed in Thorne (1988). The depths are referenced to the water surface profile for the two year flow, which was identified by Biedenharn et al. (1987) as a good guide to the channel forming discharge for this river. However, no measurements of the discharge corresponding to the two year flow at each bend were recorded by Thorne (1988).

Information on the variations in the volumetric discharge for the two year flow along the study reach were supplied by the Vicksburg District, US Army Corps of Engineers. Also, a large amount of additional information on the meander wavelength and channel sinuosity were required. The first PI, working with the research assistants working on this project, used maps and aerial photographs supplied by the Vicksburg District to make measurements of the relevant planform parameters for the study bends. A similar exercise was performed to compile the data from the 1969 hydrographic survey.

British Gravel-Bed Rivers. The fourth data set comes from a study of stable gravel-bed rivers in the United Kingdom reported by Hey and Thorne (1986). All of the required data for this study were present except the wavelength and radius of curvature for each individual bend. Wavelengths and bend radii could not be measured in the field, as were the other parameters in this Hey and Thorne's data set, but were estimated from available 1:25,000 topographic maps. The scale of the maps and size of some of the channels was such that while measuring wavelengths was straightforward, estimating the bend radius was difficult on the smallest rivers. Thus the accuracy of Rc must be reduced in this data set.

It should also be noted that the observed maximum bend scour depths are based on a single cross-section at each bend and may not necessarily represent the actual maximum for the entire bend. Sections were located in the field specifically with the intention of representing the maximum expression of the pool geometry, however. It would therefore be expected that true maxima be similar to the observed values, but they could be a little larger than those observed in some cases.

River data from other Researchers. The fifth data set consists of river data supplied by various other researchers in response to letters of enquiry. The data cover a wide range of scales of flow but data from the River Ganges proved to be inconsistent with data from all other rivers and was not used in the testing of the methods.

Laboratory Flume Data. The sixth and final data set comprises data from laboratory flume channels with mobile bed materials that have been used to simulate flow and bend scour in river bends. It is felt that real river data present a better vehicle than flume channels for tests of practical scour predictors but, physical modeling using mobile bed sediments demonstrates that flumes can simulate the morphology of real rivers and so the data are included.

BEND SCOUR DEPTH PREDICTION - ANALYTICAL APPROACH

Background

The data-set allowed application of the models for bend flow and bed topography developed by Bridge (1982) and by Odgaard (1990) as described earlier. The data correspond to high, in-bank flows and should meet the requirements for application of the models.

RESULTS OF EMPIRICAL AND ANALYTICAL PREDICTIONS OF SCOUR DEPTH

Figure 6 compares observed and predicted scour depths for all the bends. The data cover maximum scour depths that range from a few centimetres in flume channels up to about seventeen metres in large rivers. This encompasses the likely scour in all but the world's greatest rivers.

Generally, the empirical method produces the best overall agreement. The points cluster around the line of perfect agreement and errors appear to be randomly distributed. Figure 20 shows that practically all the predictions fall with +/- 50% of the observed values across the whole range of scour depths and bend geometries, and the vast majority fall within a band from +30 to -25%. This compares very favourably to the analytical predictions.

Bridge's model produces wide scatter, with a general tendency to over-estimate scour depth. Examination of the distribution of errors a function of bend geometry (Figure 7) confirms the earlier results of Thorne and Abt (1990) in that errors increase markedly as the R_c/w value decreases towards a value of 2. It has been recognised that in such tight bends the flow may strike the outer bank at a steep angle, driving reversed flow upstream of the apex. In this respect, attack of the outer bank is associated with impinging flow, and this has found to be an intractable problem in both single thread and braided rivers.

Based on these findings, the applicability of the Bridge model is limited to relatively long radius bends, with R_c/w ratios greater than about 4. Even in these bends over-estimates of 50%, and occasionally as much as 100%, must be expected.

Odgaard's model systematically under-predicts scour depth. For the smaller rivers points trend around a line of -50%, but the model crashed and produced little further increase in predicted scour depth once the observed depth passed about 10 metres. However, Figure 7 shows that Odgaard's model was consistent even for the tightest bends, and actually did well for cases where R_c/w was around unity. If the problems of bed material mobility and application to large rivers can be solved (which they are being), then Odgaard's model has real potential, especially for tight, short radius bands where the empirical model is inapplicable and the Bridge model is inaccurate.

Conclusions

This study has assembled a large and internally consistent data-set for maximum toe scour at bends. Application of three different approaches to scour prediction has illustrated the present problems of making accurate predictions in bends of different geometry and size. The empirical method produces the best overall agreement, but for longer radius bends Bridge;s model does nearly as well. The empirical method cannot be used for tight bends, with $Rc/w = 2$ being a lower boundary. Although it is capable of producing predictions, Bridge's model should not actually be used for shorter radius bends, as it seriously over-predicts scour depth. Odgaard's model remains consistent in under-estimating scour depth by about 50% over a wide range of bend geometries. Accuracy actually improves for very tight bends. The model, therefore shows promise, but could not be used routinely in its 1988 version.

It should be noted that both Bridge and Odgaard are continuously developing and upgrading their models. The authors understand from both researchers that the problems and difficulties noted in this study are consistent with their experience and that they have been addressed in subsequent editions of the models. The latest versions will be supplied to replace the earlier ones as soon as they are ready, but nothing has appeared as yet (April 1993). Updated predictions will be produced when the new versions arrive.

Prediction of Toe Scour in Revetted versus Free Meanders

It is generally believed that scour depths in revetted bends are deeper than for free meanders of similar geometry. The primary purpose of this part of the study is to assess the capabilities of the models to predict scour in revetted bends, and so this part of the analysis concentrates on bends with revetted outer banks. However, as the data-set includes both revetted and free meanders, the bends were split along those lines, to allow comparison of revetted and free conditions. Bends which were wholly or partially constrained by resistant outcrops of clay, backswamp deposits or Pleistocene materials were excluded. Such bends would be expected to have scour depths intermediate between revetted and free states, and so a clearer picture should emerge.

The observed and predicted results for revetted bends are shown in Figure 8. They are broadly in line with the overall study. Bridge's model produces the most scatter and generally over-predicts scour, Odgaard's model systematically under-predicts and the empirical model does comparatively well. Examination of the distribution of errors (Figure 9) shows how errors in the Bridge model increase for tight bends. His model appears inapplicable to revetted bends with Rc/w less than 4. But for longer bends the model does quite well, with predictions in the

approximate range +15 to - 25%. The empirical model is successful, but as a considerable number of the revetted bends come from the Red River, 1981 hydrographic survey, this is not a stringent test for the method. Errors are evenly distributed fro a range of Rc/w values and fall in the range +25 to -15%. Odgaard's model seriously under-predicts scour in all cases.

In the Red River study of Thorne (1988), a separate empirical analysis was developed for revetted bends. Like the general equation for all bends, this was based on the logarithm of ((Rc/w) - 2) as the x variable. The least squares regression equation was:

$$\frac{d_{max}}{d_{bar}} = 2.15 - 0.27\log\left(\left(\frac{R_c}{w}\right) - 2\right) \qquad (t5)$$

To examine if this equation had potential to better describe the expanded data-set a semi-log plot of (Rc/w) - 2) versus dmax/dbar was plotted (Figure 10). The scatter shows a linear trend to the data with a negative slope. Consequently, the data are consistent with the form of the empirical revetment toe scour equation. Figure 11 shows the observed and predicted scour depths for the empirical and revetment equations. Figure 12 shows the distribution of errors as a function of bend geometry. There is no obvious improvement in prediction for the revetment equation, and it actually does *less well* in the revetted long radius bends of the Missouri River. On the basis of this test it does not appear that the equation for revetted bends is any better than that for all 257 bends.

Figure 13 shows a semi-log plot for the freely migrating meanders. Comparison with the revetted bends in Figure 10 shows that the two data clouds overlap to such a degree that there is no easy way to discriminate between them. This suggests that the empirical analysis based on a semi-log equation is equally applicable to bends of all outer bank types. This finding is in contrast to the findings of the earlier study on the Red River. There are at least two possible explanations for this. Firstly, it comes about because the wider range of conditions in the rivers of the large data set have swamped differences due to bank condition. Thus, while bank effects may be identified on a particular river, they cannot be discerned in a data-set for many different rivers. Secondly, the parameters used in this analysis may tend to collapse data for different bank conditions together. This is the case because the width and mean depth at the crossing are not themselves independent of the bank condition. Rivers with stiff banks tend to be narrower and deeper than those with erodible banks. Hence, in using crossing width and mean depth to scale bend geometry and scour depth, the bank type effects are being implicitly taken into account. Consideration of the impacts of revetments on the regime geometry would help to resolve this issue, but is getting beyond the scope of this study.

It can be concluded though that the empirical method constitutes a robust predictor of scour depth for bends of a variety of bank types and conditions, with errors usually within the range +/- 30%.

CONCLUSIONS

1. The planform pattern of the approach channel may influence the ratio of the depth averaged velocity over the toe of the outer bank to the average velocity at the bend entrance. Bends with meandering approach channels appear to have lower velocity ratios than those with straight approach channels.

2. The WES design curve (Fig. 1) is very similar to the empirical curve for bends with straight approach channels, but it may be overly conservative for bends with meandering approach channels.

3. On the basis of this study equations 3 and 4 may be used to make empirical predictions of the highest depth averaged velocity over the toe of the outer bank encountered at a meander bend.

4. On the basis of this test, Bridge's model can be relied upon to predict the outer bank velocity in a bend to within approximately +/-15% for bends with R_c/w greater than 2. For engineering design purposes a multiplier of 1.15 should be applied to the predicted velocity so that errors are on the safe side.

5. Bridge's model should definitely not be used for bends with R_c/w is less than 2, where it is prone to large errors.

6. Odgaard's model could not be fully tested as it crashed for many of the bends studied. For the bends at which it did work, errors were between 5 and 40 percent, for bends with Rc/w ratios between 0.8 and 5. The fact that Odgaard's model does not fail for short, tight radius bends is very encouraging.

7. The empirical method produces the most reliable scour estimates, with the great majority of predictions being within +/- 25% of the observed maximum bend scour depth.

8. Bridge's bend flow model does nearly as well for long radius bends, but massively over-predicts scour depth for tight bends. Bridge's model should only be used to predict scour for bends with Rc/w ratios greater than 4.

9. The Odgaard model was the least satisfactory for scour prediction. It systematically under-predicted scour depth by about 50% and failed to account for the deep scour holes found in large rivers. Problems with the model center on the entrainment function, which does not predict any scour in bed materials coarser than sand, and on large rivers, where the program crashed due to the prediction of negative depths at the inner bank.

10. There was no evidence that revetted bends suffer deeper scour than free meanders, in terms of the dimensionless scour depth (d_{max}/d_{bar}) scaled on the mean depth at the upstream crossing. This may be because the mean crossing depth is itself a function of bank stiffness, so that bank effects are actually accounted for in its use as a scour scaling parameter. If true, this further strengthens the range of applicability of the empirical approach developed by Thorne (1988).

11. Extrapolation of the approaches tested here to higher flows is limited by the inter-action between in-bank and over-bank components of the flow. If inter-action is negligible, notional walls may be envisaged, separating the channel flow from the flood plain storage and allowing the delineation of geometrical and hydraulic parameters for the in-channel portion of the flow. Hence, provided that the water level associated with the design flood is only slightly above the top of the revetment and remains mostly in-bank, then the methods described here can be used with caution. However, when the overbank flow depth is a significant proportion of the channel depth, the exchange of water between the channel and the flood plain is not negligible. Flow patterns and bed scour will be dominated by water and momentum fluxes which cannot be predicted by these (or any other) in-bank flow models and it would not be wise to attempt to extrapolate the methodology to such flows. If significant out-of bank flows over and behind the revetment are to be allowed for in the design then a model of flood plain water flow and sediment movement is required.

ACKNOWLEDGEMENTS

The work reported here was undertaken at Colorado State University and the University of Nottingham under research funding provided by the US Army Engineer waterways Experiment Station. The support and encouragement of WES staff is gratefully acknowledged.

REFERENCES

Allen, J R L (1970) "Studies in fluviatile sedimentation" Jour. Sediment. Petrol., 40, 298-323.

Bagnold, R.A. 1960. 'Some aspects of the shape of river meanders', USGS Professional Paper, 282E.

Biedenharn, D.S., Combs, P.G., Hill, G.J., Pinkard, C.F. and Pinkstone, C.B. (1989) Relationship between channel migration and radius of curvature on the Red River, In, Sediment Transport Modeling (S.S.Y. Wang, Ed.), ASCE, Proceedings of the International Symposium, New Orleans, August 1989, 536-541.

Bridge, J.S. 1977. 'Flow, bed topography, grain size and sedimentary structure in open-channel bends: a three-dimensional model', Earth Surface Processes, 2, 401-416.

Bridge, J.S. 1984 "Flow and sedimentary process in river bends; comparison of field observations and theory" In, River Meandering, C.M. Elliott (ed.), ASCE, New York, USA, 857-872.

Bridge, J.S. 1982. 'A revised mathematical model and FORTRAN IV program to predict flow, bed topography and grain size in open-channel bends', Computers and Geosciences, 8 (1), 91-95.

Chacinski, T.M. and Francis, J.R.D. 1952. 'Discussion of: On the origin of river meanders, by P.W. Werner', Transactions of the American Geophysical Union, 33 (5), 771-773.

Dietrich, W.E., Smith, J.D. and Dunne, T. 1979 "Flow and sediment transport in a sand-bedded meander" Journal of Geology, 87, 305-315.

Dietrich, W.E., Smith, J.D. and Dunne, T. 1984 "Boundary shear stress, sediment transport and bed morphology in a sand-bedded river during high and low flow" In, River Meandering, C.M. Elliott (ed.), ASCE, New York, USA, 632-639.

Dietrich, W.E. and Whiting, P. 1989 "Boundary shear stress and sediment transport in river meanders of sand and gravel" In, *River Meandering*, S. Ikeda and G. Parker (eds.), American Geophysical Union, Water Resources Monograph 12, 2000 Florida Avenue, Washington D.C., USA, 1-50.

Elliott, C M (1983) River Meandering, ASCE, New York, USA, 632-639.

Engelund, F. 1974 "Flow and bed topography in channel bends" *Journal of the Hydraulics Division*, ASCE, 100(11), 1631-1648.

Hey, R.D. and Thorne, C.R. 1986. 'Stable channels with mobile gravel beds', Journal of Hydraulic Engineering, 12 (8), 671-689.

Hooke, J.M. 1987. 'Discussion of: Lateral migration rates of river bends, by E.J. Hickin and G.C. Nansen', Journal of Hydraulic Engineering, 113 (7), 915-918.

Lapointe, M.F. and Carson, M.A. (1986) "Migration patterns of an asymmetrical meandering river: The Rouge River, Quebec." Water Resources Research, 22, 731-743.

Markham, A.J. 1990. '*Flow and Sediment Processes in Gravel-Bed River Bends*', thesis submitted to the Department of Geography, Queen Mary and Westfield College, London, in complete fulfilment of the requirements of the degree of Doctor of Philosophy, 419p.

Odgaard, A.J. 1986. 'Meander flow model. II: Applications', *Journal of Hydraulic Engineering*, 112 (12), 1137-1150.

Odgaard, A.J. 1989. 'River-meander model. I: Development', Journal of Hydraulic Engineering, Vol. 115,No. 11, 1433-1450.

Odgaard, A.J. 1989. 'River-meander model. II: Applications', Journal of Hydraulic Engineering, Vol. 115,No. 11, 1450-1464.

Odgaard, A.J. and Bergs, M.A. 1988 "Flow processes in a curved alluvial channel" Water Resources Research, 24(1), 45-56.

Parker, G and Andrews, E D (1985) "Sorting of bed load sediment by flow in meander bends" Water Resources Research, 21(9), 1361-1373.

Rozovskii, L.L. 1957. 'Flow of water in bends of open channels', translated by the Israel Programme for Scientific Translation (1961), 233p.

Thorne, C. R. (1978). "Processes of bank erosion in river channels." *unpublished Ph.D. thesis*, Univ. of East Anglia, Norwich, NR4 7TJ, England, 447p.

Thorne, C R (1988) "Bank processes on the Red River between Index, Arkansas and

Shreveport, Louisiana" Final Report to the US Army European Research Office under contract number DAJA45-88-C-0018, Dept. Geography, Queen Mary College, December 1988, 50p

Thorne, C R & Osman, A M (1988) "Riverbank Stability Analysis: II Applications" Journal of Hydraulic Engineering, ASCE, Vol 114, No 2, pp 151-172

Thorne, C.R. and Abt, S.R. (1990) "Estimation of Velocity and shear stress at the outer bank in river bends" Final Report to the US Army Engineers Waterways Experiment Station, under contract number DACW39-89-K-0015, Colorado State University, Ft Collins, Co., May 1990.

Thorne, C R, Zevenbergen, L W Bradley, J C & Pitlick, J C (1985) "Measurements of Bend Flow Hydraulics on the Fall River at Bankfull Stage" Report 85-3, Water Resources Field Support Lab, NPS, Colorado State University, June 1985, 69p

Torrey, V.H. (1988) "Retrogressive failures in sand deposits of the Mississippi River" Waterways Experiment Station, Technical Report GL-88-9.

Turnbull, W. J., Krinitzsky, M. and Weaver, F. J. (1966). "Bank erosion in soils of the lower Mississippi Valley." *J. Soil Mech. Div.*, Proc. ASCE, 92(SM1), 121-136.

U.S. Army Corps of Engineers. (1981). "The stream bank erosion control evaluation and demonstration act of 1974, Section 32, Public Law 93-251. Appendix F - Yazoo River Basin demonstration projects." Final report to congress, Office of the Chief of Engineers, Washington DC., USA.

Tables

Table 1 Ranges of Data for Prediction of depth averaged, outer bank toe velocity (from Thorne and Abt, 1990)

Measured Variables		
Variable	**Units**	**Range**
Radius of Curvature	meters	8 - 4,525
Bend Length	meters	16 - 5,633
Width	meters	4 - 232
Average Depth	meters	0.4 - 5.65
Outer Bank Angle	degrees	21 - 90
Outer Bank Roughness	--	Rough-Intermediate
Median Bed Material Size	millimeters	0.3 - 63
Bedforms	--	Plane - Dunes
Approach Channel	--	Straight-Meandering
Average Velocity	meters/second	0.42 - 1.47
Depth-averaged Toe Velocity	meters/second	0.55 - 1.81
Derived Variables		
R/w	--	0.75 - 21.6
L/w	--	1.45 - 26.9
w/d	--	9.05 - 46.1
d/D50	--	13.8 - 18,833
Vtoe/Vavg	--	1.04 - 1.57

Table 2 Correlation Matrix between derived parameters of bend geometry.

Correlation Matrix for Variables: X_1 ... X_5

	Rc/w	L/w	w/d	d/D50	Bank An...
Rc/w	1				
L/w	.881	1			
w/d	.758	.688	1		
d/D50	.858	.834	.885	1	
Bank Angle	-.775	-.777	-.67	-.86	1

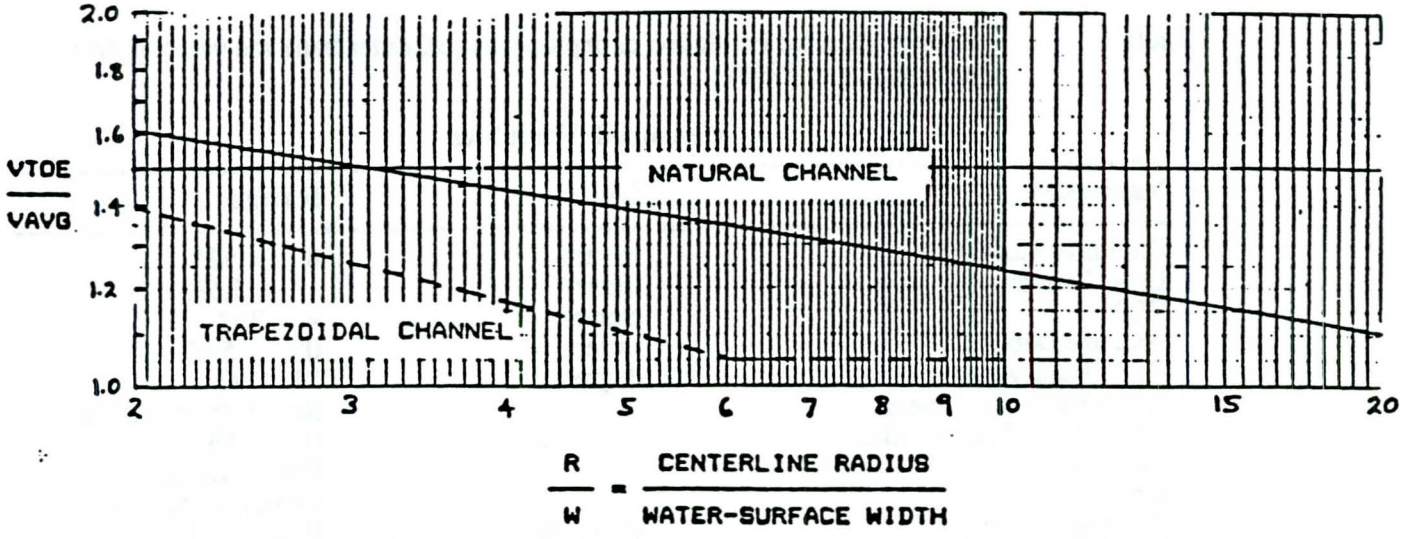

Fig.1 US Army WES curve for prediction of depth averaged velocity over the toe of the outer bank at bendways.

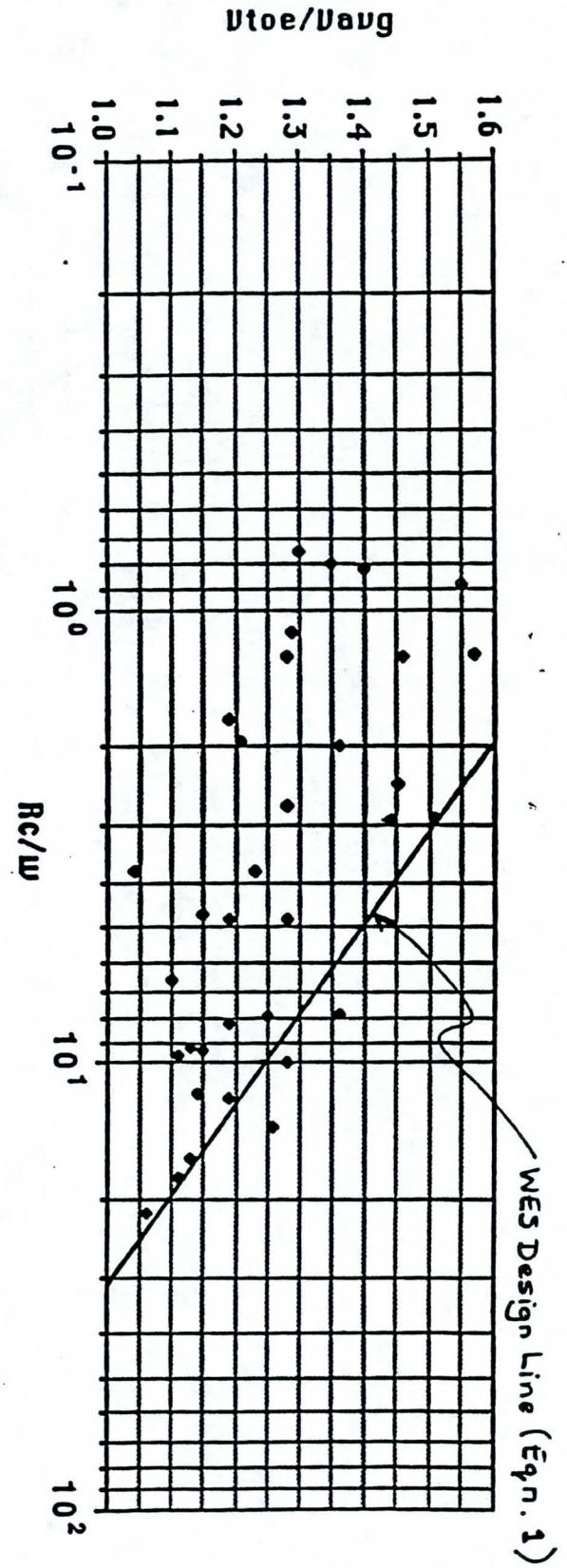

Fig.2 Field data assembled in this study plotted on the WES prediction graph for outer bank, depth averaged toe velocity.

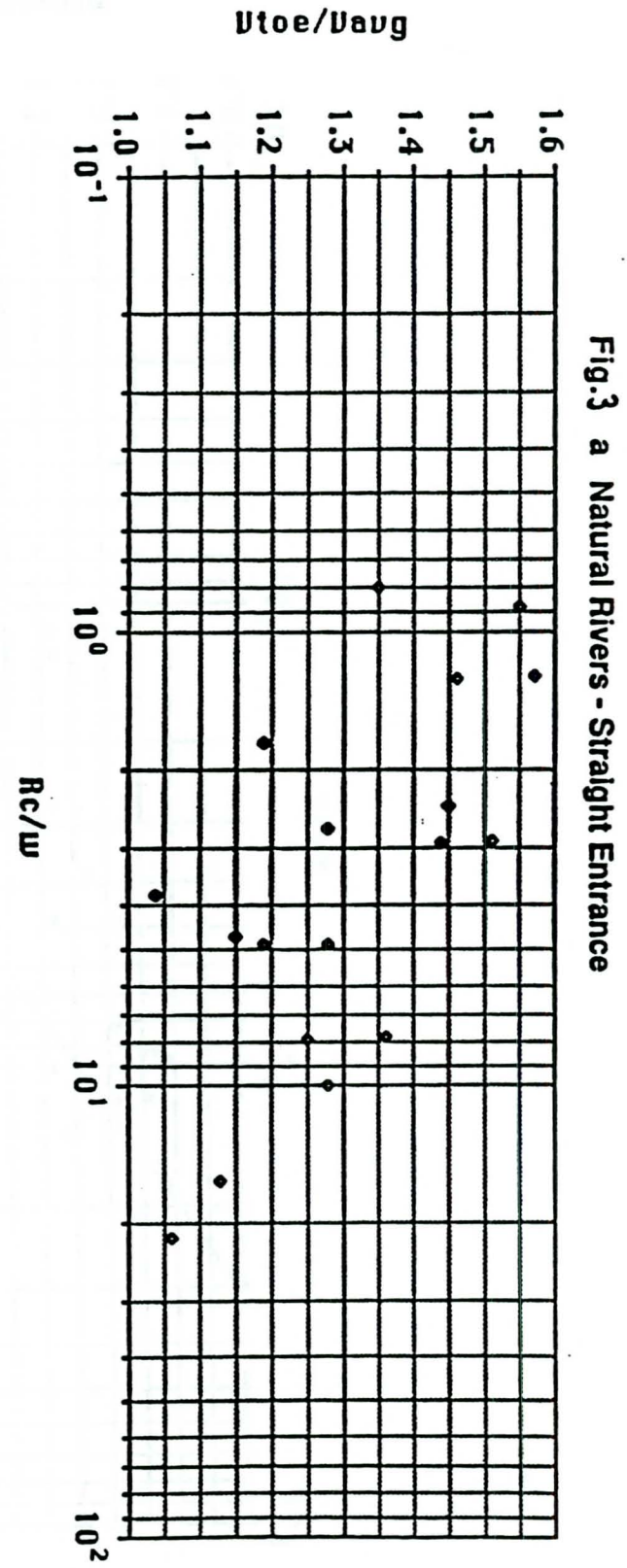

Fig.3 a) Field data for bends with straight approach channels.

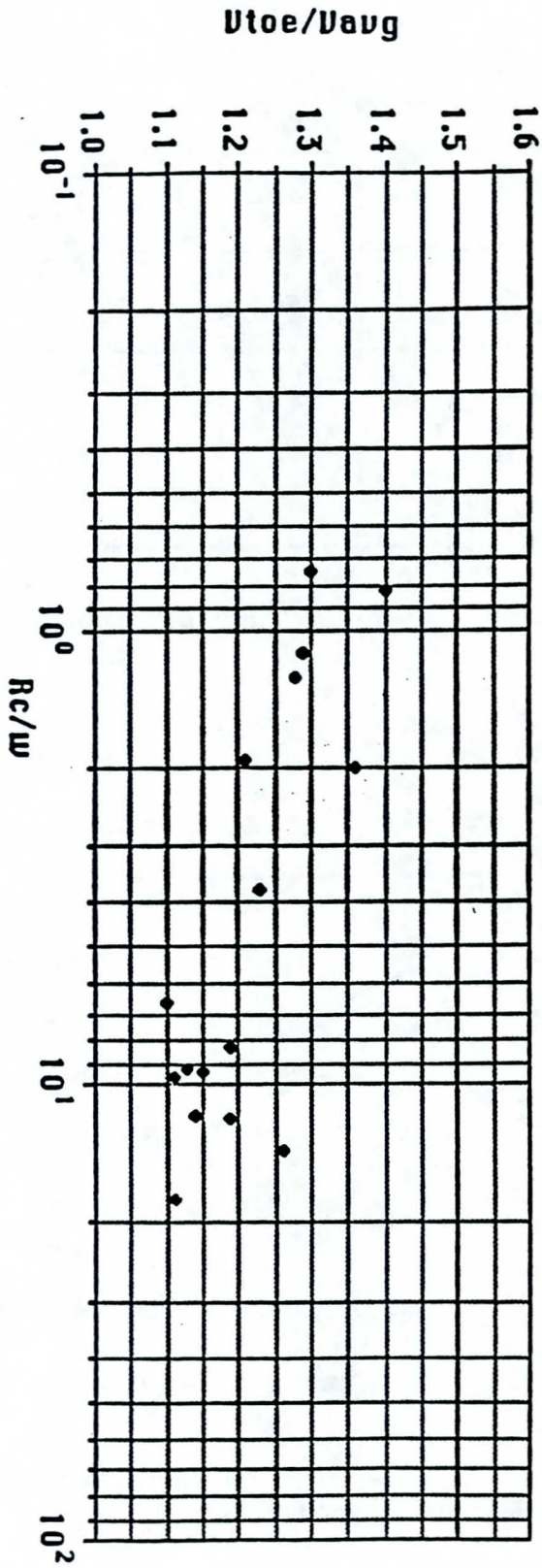

Fig.3 b Natural Rivers - Meandering Entrance

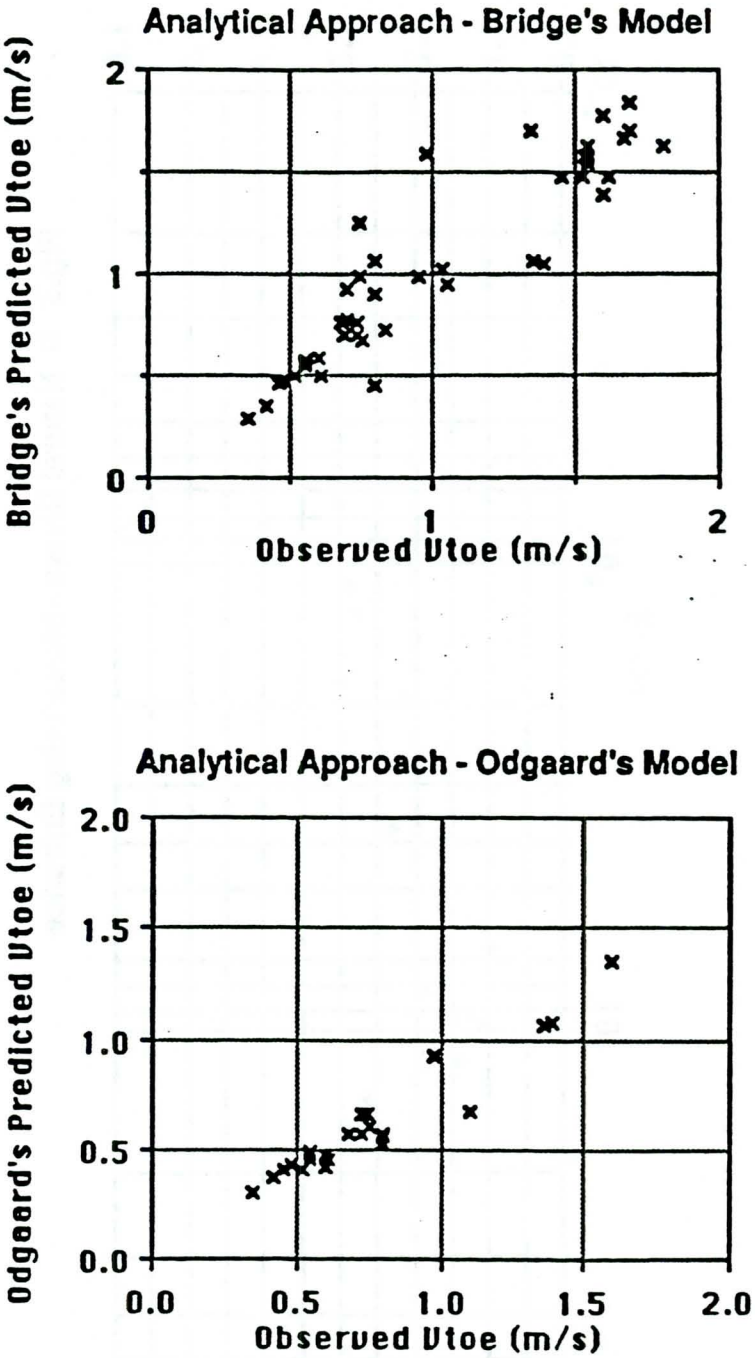

Fig.4 Observed versus predicted outer bank toe velocities for the analytical predictions of Bridge and Odgaard models.

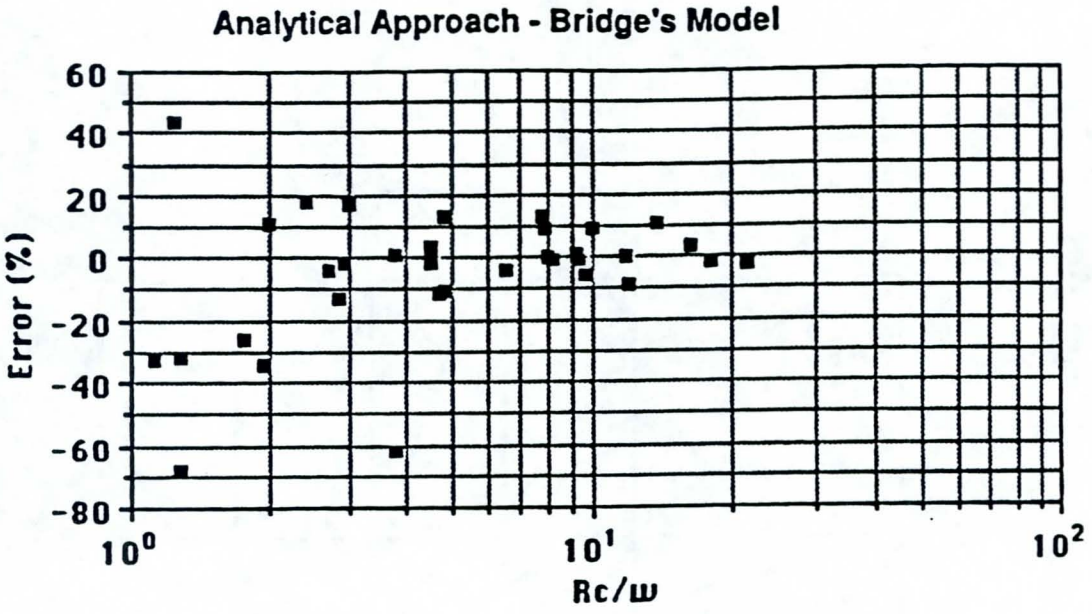

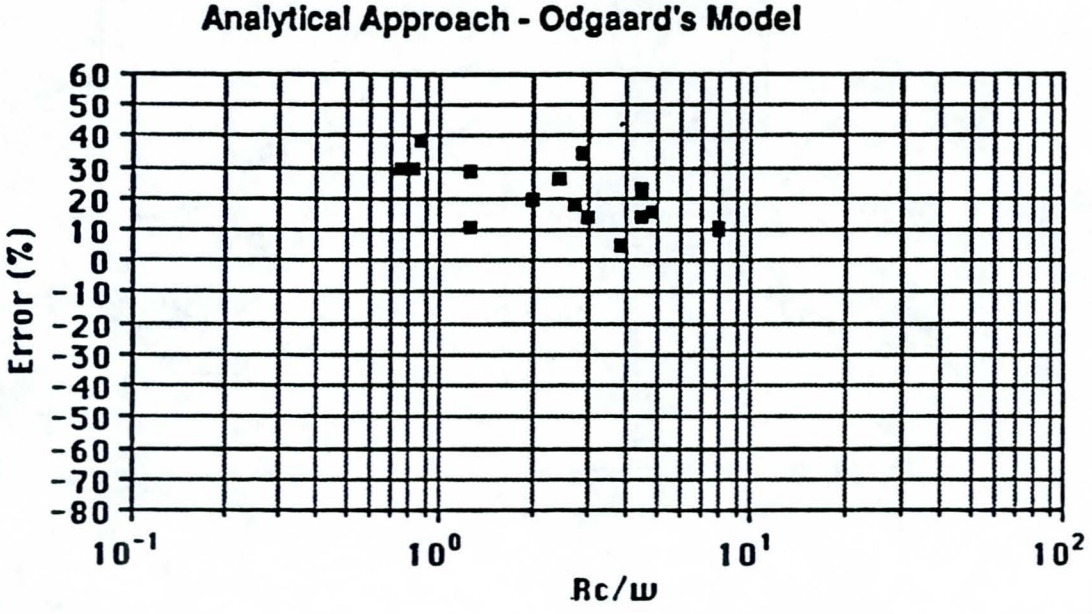

Fig.5 Prediction errors in outer bank velocity as a function of Rc/w for analytical models.

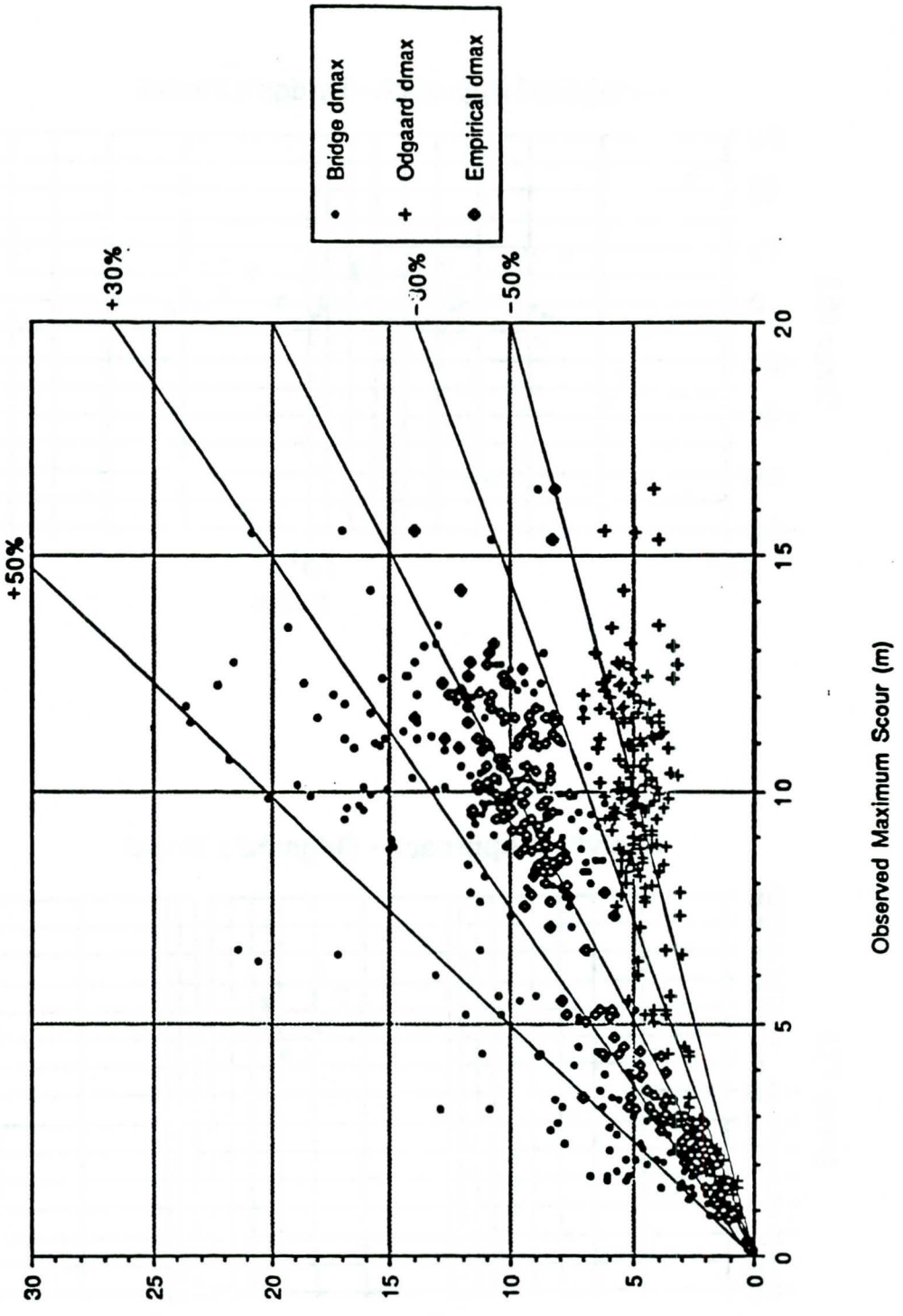

Fig.6 Observed versus predicted bend maximum scour depth for empirical and analytical methods.

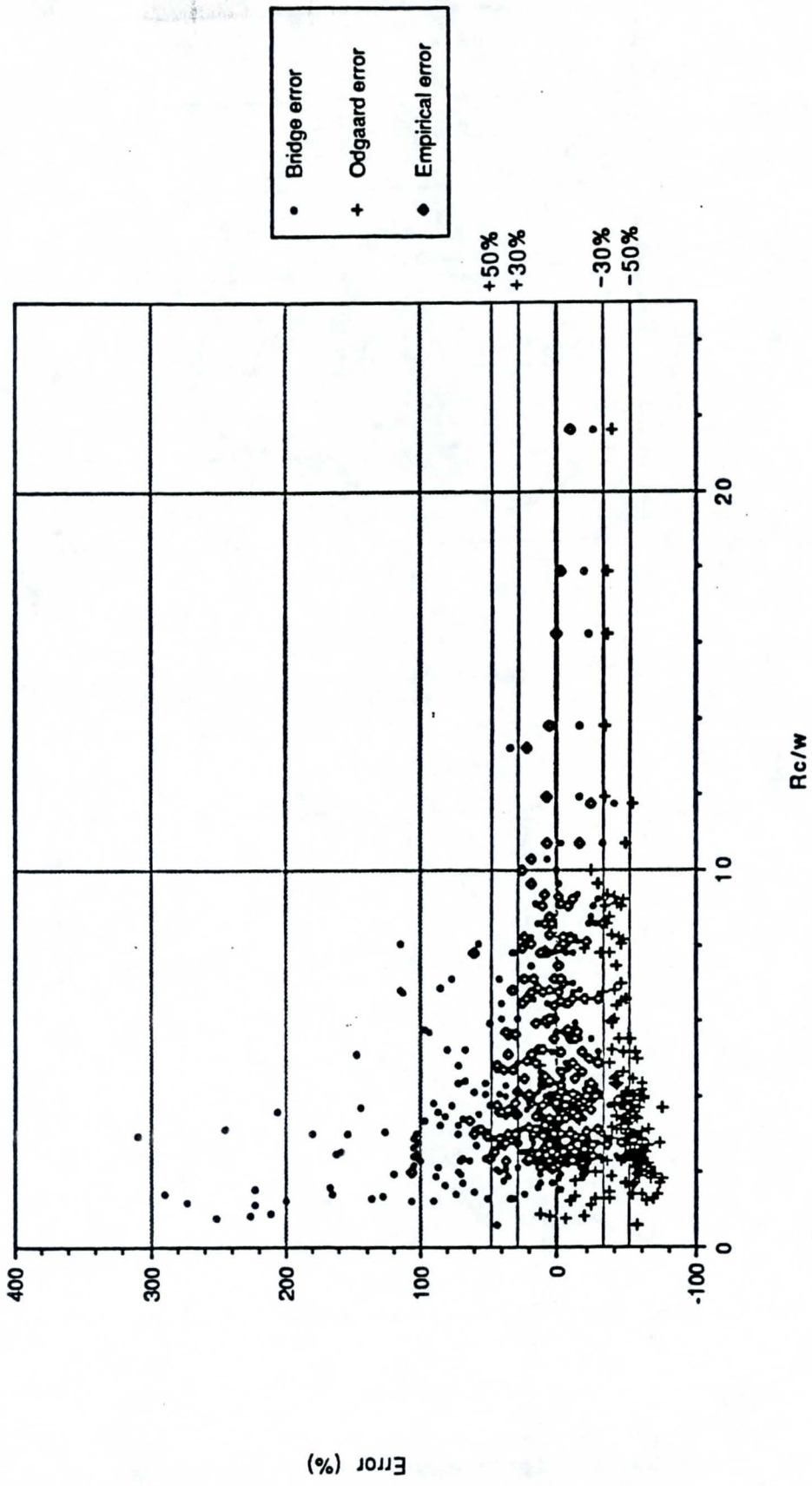

Fig.7 Prediction errors in scour depth versus Rc/w for empirical and analytical methods.

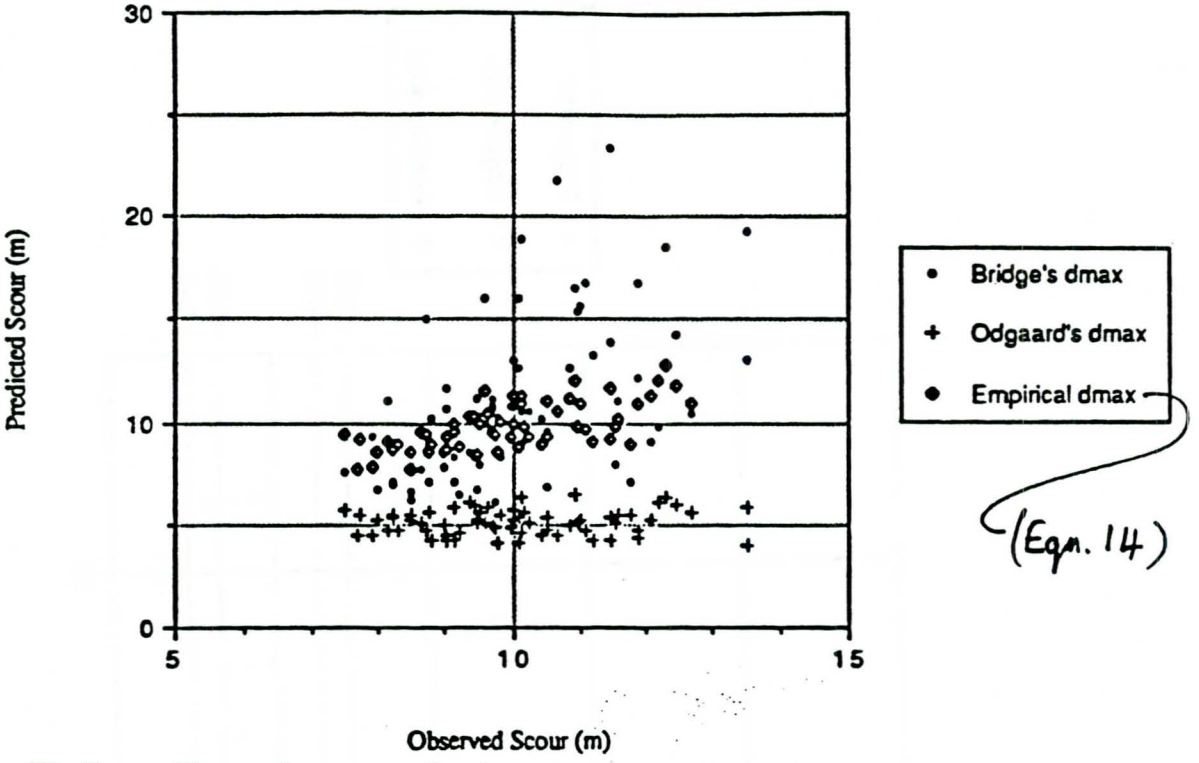

Fig.8 Observed versus predicted maximum scour depths for revetted bends using empirical & analytical prediction methods.

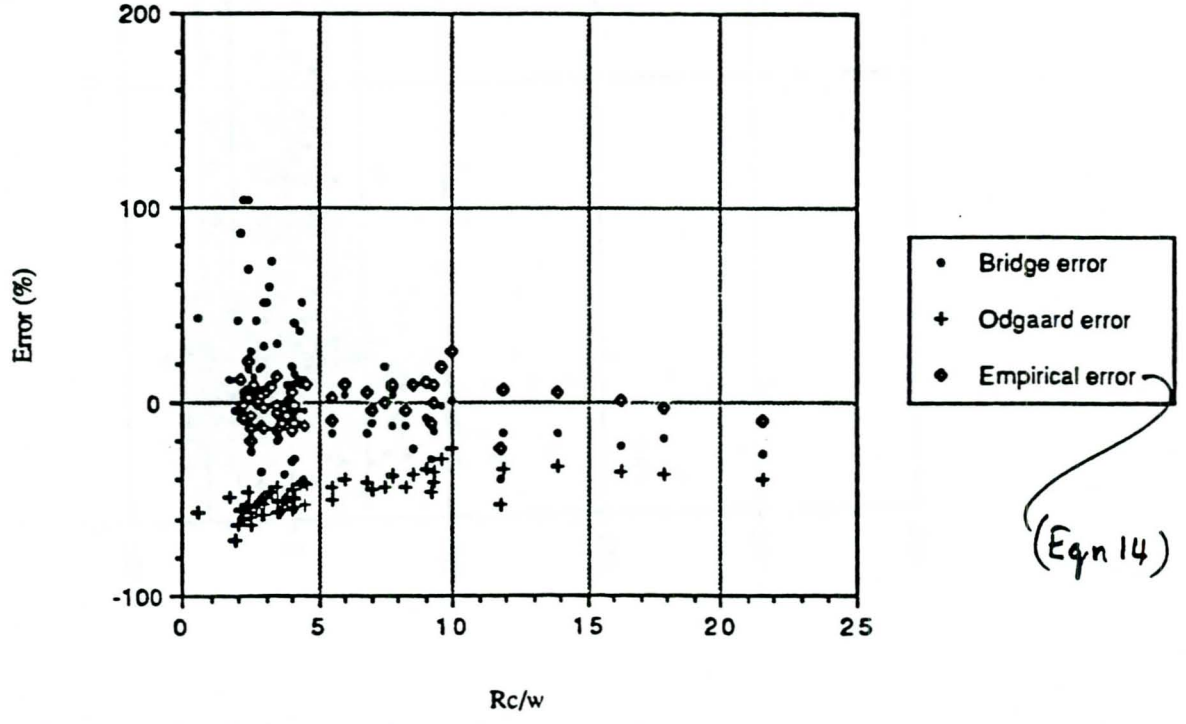

Fig.9 Prediction errors for maximum scour depth at revetted bends using empirical and analytical approaches.

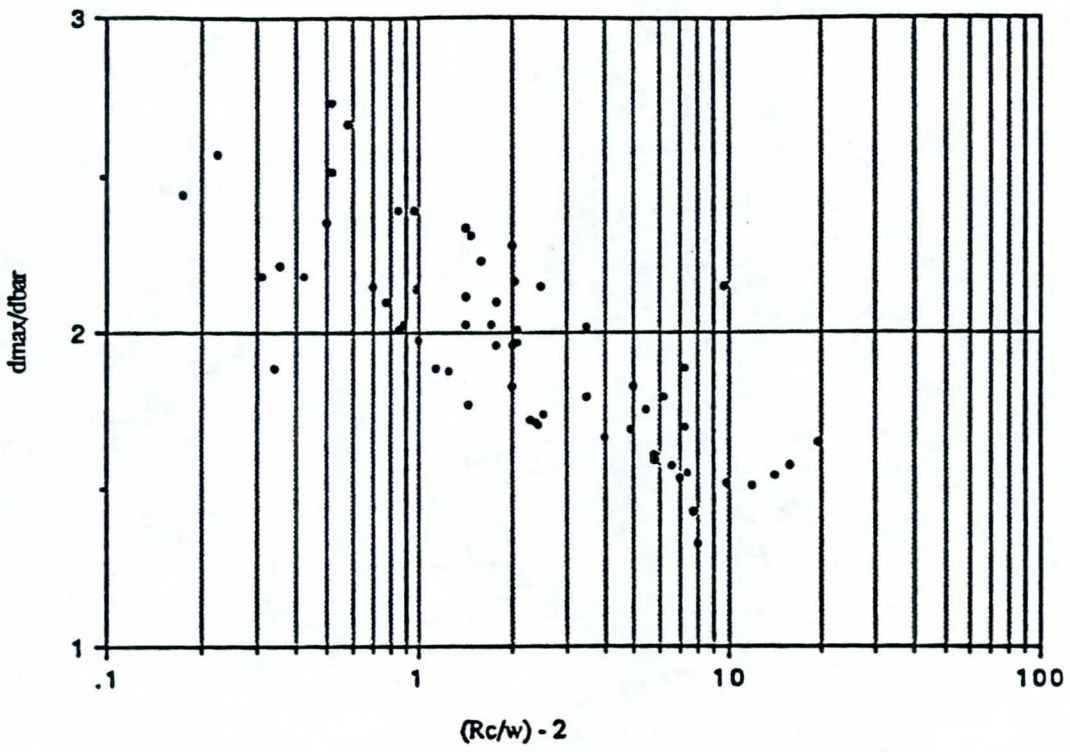

Fig.10 Semi-log plot of dimensionless scour depth in revetted meander bends.

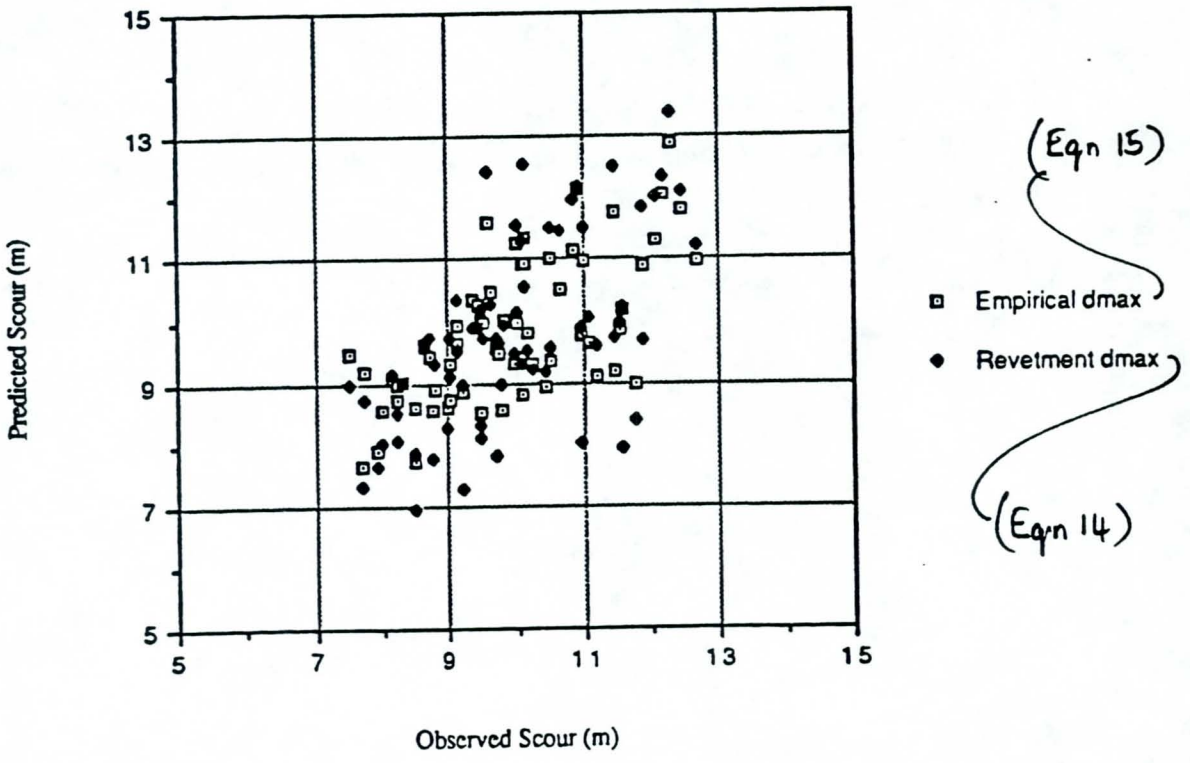

Fig.11 Observed versus predicted maximum scour depths at revetted bends using empirical approach for free alluvial meander bends and for revetted bends.

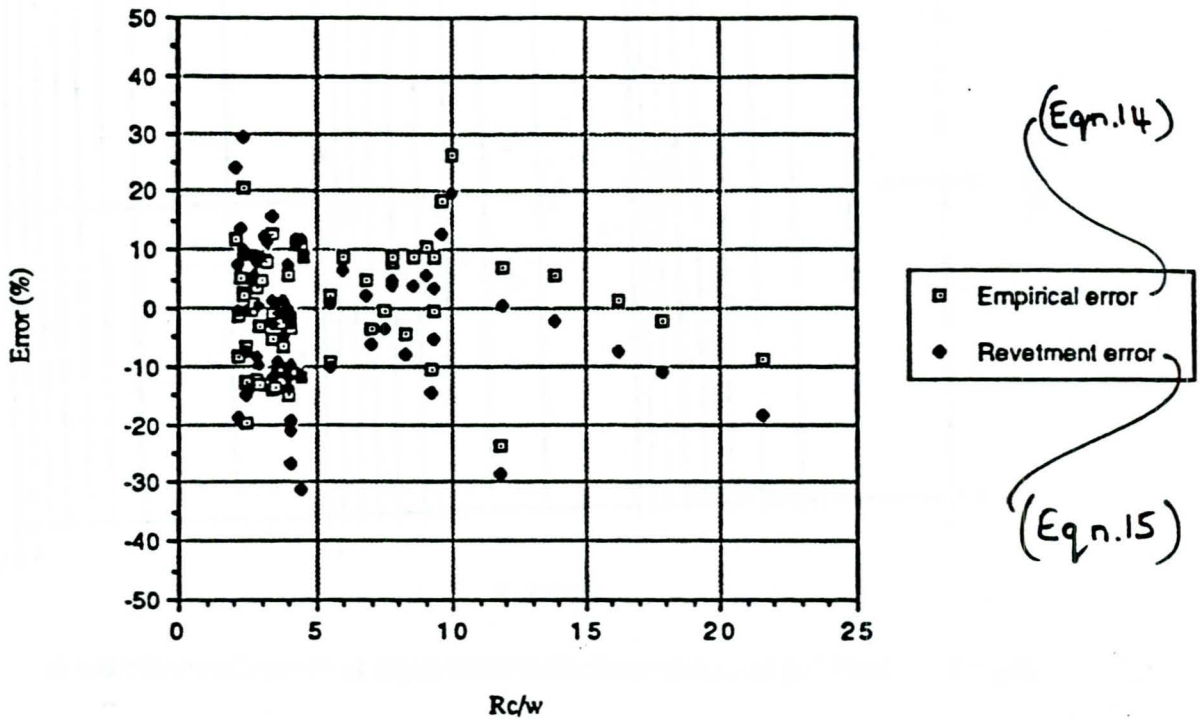

Fig.12 Prediction errors for maximum scour depth at revetted bends as a function of Rc/w.

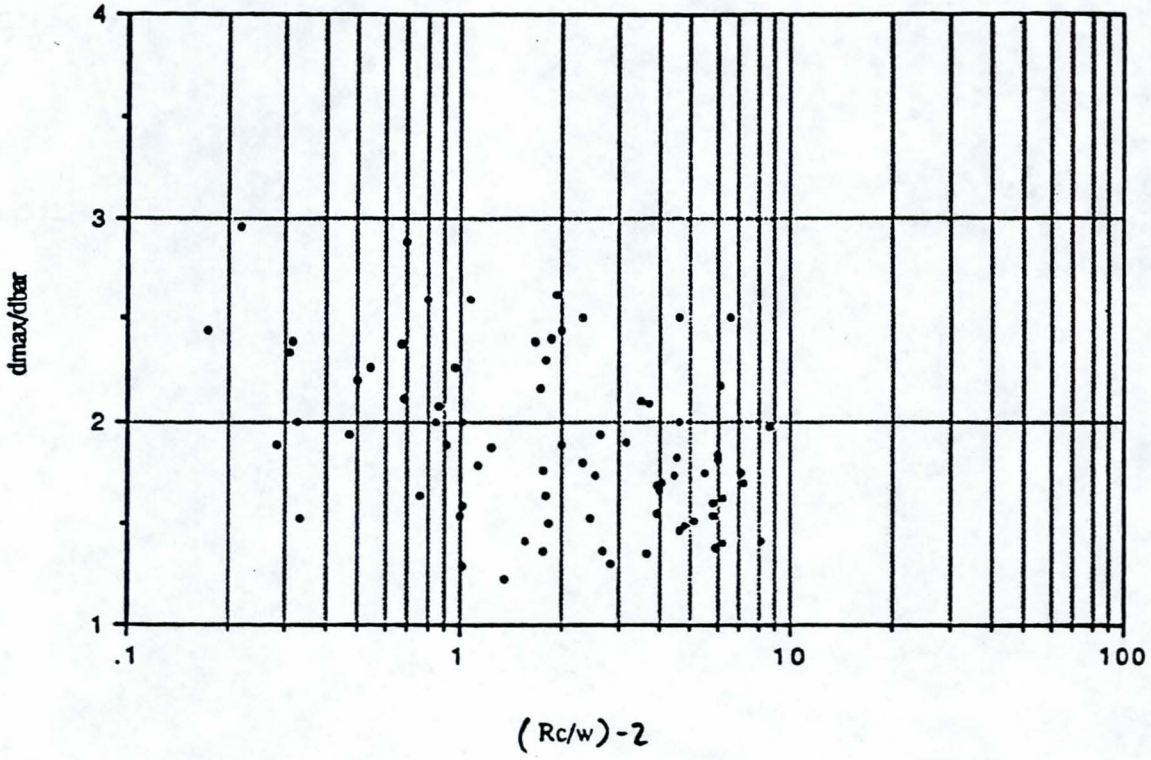

Fig.13 Semi-log plot of dimensionless scour depth at free alluvial meander bends.

FLOW SLIDES IN MISSISSIPPI RIVERBANKS

V.H. Torrey III
US Army Engineer Waterways Experiment station,
Vicksburg, Mississippi, USA

SYNOPSIS

For more than 40 years, the U.S. Army Engineer Waterways Experiment Station has been intermittently investigating the problem of flow slides which occur frequently in mass sand deposits of Mississippi riverbanks. This paper presents some of the more interesting findings of the years of investigations which include the identification of the susceptible bank reaches, explain the unique failure mechanism, and provide a means to assess threat of the failures to stability of mainline flood protection levees.

INTRODUCTION

The U.S. Army Engineer Waterways Experiment Station (WES), as the oldest and largest of the Corps of Engineers (USACE) Research and Development Laboratories, frequently undertakes investigations to solve special problems encountered by USACE District and Division offices or by other governmental agencies. One such problem which WES has been addressing since the mid-1940's is the occurrence of flow slides in significant sand strata of point bar deposits of the Mississippi River from approximately Memphis, Tennessee at river mile 740 (1191 km), to the Delta at river mile zero (Head of Passes) some 100 miles (161 km) downstream of New Orleans, Louisiana. These studies have been conducted under the auspices of the USACE Lower Mississippi Valley Division (CELMV). Justification for the work is the considerable annual damage to the costly articulated concrete revetment mattress used for bank stabilization. A photograph of a typical flow failure scar and the breached revetment is shown in Fig. 1. In addition, and of greater importance, is the threat posed to mainline flood protection levees (dikes) often situated very near the top of the riverbank along the 230-mile (370-km) reach from Baton Rouge, Louisiana, to river mile zero. For example, since 1954, more than 200 flow failures have caused revetment repair expenditures of many millions of dollars. During the great flood of 1973, major failures occurred downstream of Baton Rouge at four locations. Those four failures so threatened the stability of sections of the

levee that emergency construction of new sections (setbacks) further from the top of the riverbank were required. The setback at Montz, Louisiana, gained national news media attention because the major portion of a small community had to be condemned and relocated. In addition, the levee was breached by failures at Marchand and Greenville Bend, Louisiana, in 1983 and 1987, respectively. In general, the necessity of a levee setback below Baton Rouge carries a high probability that relocation of private homes, businesses, and even heavy industry may also be entailed.

EARLIER STUDIES

In 1947, a series of "potamology" studies was initiated by the CELMV to address several subjects pertinent to bank stabilization and channel maintenance. To date, over 60 reports have been published concerning hydraulic model studies of dike configurations, revetment mattress performance, and channel meander; hydraulic and hydrographic studies of channel characteristics and revetment mattress; and geologic and geotechnical investigations of riverbank deposits as related to bank stability.

There are three types of localized riverbank losses. Expert eyewitnesses of failures in progress and underwater contour maps obtained from annual revetment hydrographic surveys confirm two failure modes resulting from mass instability and one which is progressive erosion (scour). Therefore, bank losses are classified as shear failure, flow failure, or erosional. A shear and flow failure can be distinguished one from the other on the basis of differences in both plan and section. The shear failure exhibits a U-shape in plan and usually a rotational sliding surface in section perpendicular to the river, with heave or slide debris often found at the toe. The flow failure (see Fig. 2) exhibits a fan or bulb shape in plan with a narrow neck riverward. Bottom slopes in the flow slide scar transverse to the bank are flatter than 20 degrees to the horizontal and debris is usually swept away. The particular danger posed by the flow slide is that it develops subaqueously during high water without warning and may progress into the bank steadily removing large quantities of soil in a matter of hours. In 1949, a flow failure developed at Wilkinson Point (see Fig. 3) across the river from Baton Rouge which

ultimately involved more than 4 million cubic yards (3,000,000 m^3) of soil and breached the levee which was more than 500 ft (150 m) from the top of the bank.

As a result of Professor Arthur Casagrande's personal consultation relative to the giant Wilkinson Point failure, the mechanism of flow slides was accepted to be that of liquefaction of the thick substratum of fine sands. Associated with that presumed failure mechanism was the necessary added assumption that those sands were relatively loose with respect to their in situ densities.

By 1954, several basic aspects of the flow slide problem had been empirically established. For instance, it was discovered that flow slides had occurred only in point bar deposits. Those deposits exhibiting failures were found to be structured with a somewhat cohesive overburden composed of interbedded clays and silts underlain by fine sands or silty sands which graded with depth into coarse sands and gravels. Further scrutiny of the field data resulted in division of the substrata sand into the "upper sand series" representing finer material and the "lower sand series" consisting of deeper, coarser soils. These two categories reflected a broad observation that flow slides had been restricted to the shallower, finer sand gradations. More thorough examination of case histories coupled with extensive site boring data led to an additional subdivision of the "upper sand series" into "Zone A" sand over "Zone B" sand. In general, the record showed that flow failures had only involved overburden and sands of the Zone A range in gradation. Over the years since, the original gradation criteria were modified only slightly to their current form as given in Table I. In addition, it was determined that flow failures did not occur if the ratio of overburden thickness to Zone A sand thickness was large. Refinement produced additional criteria which indicated potentially unstable conditions with respect to flow failure only if the ratio between overburden thickness and Zone A thickness was less than 0.85 and the Zone A thickness was at least 20 ft (6.1 m).

A study was initiated in 1954 to verify the above empirical criteria. Initially, all riverbank borings in point bar deposits taken in support of revetment construction were cataloged and classified by site as either reflecting susceptible conditions or not. Each boring was assumed to be representative of the stratigraphy for 500 ft (150 m) either side of its location.

Each year, any new revetment borings were added to the catalog. When annual revetment hydrographic surveys revealed a failure, it was first classified as to type using plans and sections. Note here that the conventional revetment mattress does not prevent flow failures and many of the observed failures were entirely contained horizontally and vertically within the limits of the mattress. If the failure was of the flow type, the nearest boring within 500 ft (150 m) was checked for the prediction with respect to flow slide susceptibility. Depending upon that prediction, the empirical criteria were either supported or violated. As of 1977, the final year of the verification studies, a total of 204 flow failures (all within revetted banks) were on record. Only 19 of those occurred in apparent violation of the empirical criteria.

The last concentrated effort under the older potamology study series was completed in the mid-50's. Only the empirical criteria verification reports continued (Torrey and Gann, 1976). Insufficient knowledge had been gained to term any specific bank reach actually unsafe with enough confidence to warrant expenditure of large sums in devising and constructing special bank protection measures. This was especially true because less than one fourth of all the sites predicted to be susceptible had actually suffered a flow failure. Also, as of the end of the former period of study, the riverbanks below Baton Rouge were not considered susceptible because of their stability, at least within the period of formal record going back to the turn of the century. This portion of the stream had been so relatively untroublesome that much of it wasn't revetted and detailed geological mapping of point bar deposits was not done until the mid-60's. However, when that mapping revealed widely distributed point bar containing very thick strata of fine sands, CELMV, fearing for the safety of the mainline levees often located near the top of the bank, reinstigated concentrated studies of the flow slide phenomenon. This decision was also stimulated by the knowledge that extensive channel stabilization activities upstream were beginning to alter the essentially equilibrium conditions along significant portions of the lower river.

RECENT STUDIES

In the late 1960's, CELMV asked WES to renew the study of the problem with focus upon the river reach below Baton Rouge. The objectives were to

identify dangerous reaches using the empirical criteria, determine the conditions which trigger the slides, and devise methods to prevent flow failures.

During 1971, an interesting set of data became available. Durham (1971) performed a series of consolidated undrained triaxial shear tests on reconstituted specimens of Reid-Bedford Zone A sand to determine its steady-state void ratio as a function of consolidation stress. The Reid-Bedford revetment reach (see Fig. 1) not far downstream of Vicksburg, Mississippi, is noted for suffering many flow slides. Durham's test procedures were after those of Castro (1969). The startling result was that the Reid-Bedford Zone A sand would not exhibit liquefaction in the laboratory above a relative density of only 13 percent even under a confining pressure (lateral stress) of 4 tons/ft^2 (386 kPa). The higher the confining pressure, the higher the density (higher the relative density) at which a sand can liquefy. A lateral stress of about 4 tons/ft^2 in the point bar deposit corresponds to a depth below ground surface of about 160 ft (49 m). However, the very largest of the flow slide scars observed along Reid-Bedford revetment were less than 40 ft (12 m) deep. Therefore, if liquefaction was the failure mechanism, the in situ density of the Zone A sands would have to correspond to the very loosest density at which they could be placed in a mold in the laboratory (zero relative density). A very large field investigation program had been conducted along the Reid-Bedford revetment and several other point bar sites under the earlier studies in the 1950's. Undisturbed sampling and Standard Penetration testing at several sites exhibiting flow slides had indicated in situ relative densities of Zone A sands to be above 40 percent. However, in those times, understanding of the phenomenon of liquefaction was very limited and laboratory testing techniques to assess susceptibility were crude.

Fortunately, an extensive bank revetment program had been underway below Baton Rouge so that many revetment boring records were available for applying the empirical criteria developed under the earlier studies. This task had just been completed when the 1973 major spring flood struck. All four of the large flow failures necessitating levee setbacks (previously mentioned) developed within bank reaches designated as susceptible. Now the truth was known. The point bar deposits below Baton Rouge would experience flow slides if subjected to sufficiently severe flood conditions, i.e., river attack on the banks. Therefore, the dearth of flow slides along that reach had apparently

reflected the infrequent occurrence of major floods. Furthermore, because of the greater depth of the river and consequently greater thickness of Zone A sand strata exposed to river attack, the flow failures could be expected to be considerably larger than those of record upriver.

In 1975, it was decided to conduct an intensive in situ testing and undisturbed sampling field investigation to establish the in situ density of the Zone A sands and by laboratory testing of samples to determine whether or not the in situ densities were susceptible to liquefaction. This was considered necessary because the techniques of in situ testing, sampling, and laboratory liquefaction testing had been significantly advanced since the last flow slide field investigations of the 1950's. Two point bar sites located about 35 miles (56 km) upriver of New Orleans were selected. Based on old bank-line surveys, both sites had suffered several failures in the past. The primary site receiving the greater effort was at Montz, Louisiana, where the largest of the four 1973 flow failures had occurred. The secondary site was that of Bonnet Carre' Point located 4 river miles (6.4 km) upstream of the Montz site and on the opposite bank. The Bonnet Carre' location had experienced a flow failure in 1970 which was attributed to the severe localized scour conditions typically observed immediately at the downstream end of a revetted reach. Although interesting differences were found between the two sites, only the findings relative to the primary Montz site will be discussed herein.

The general location of the Montz failure site is shown in Fig. 4. The failure developed rapidly during March 1973 and ultimately involved over 300,000 yd^3 (229,000 m^3) of soil. An isometric drawing of the scar is shown in Fig. 5. The specific position of the detailed investigation site was selected based on two sources of information. First, a reconnaissance split-spoon boring program was conducted in a sweep of the bank from upstream to downstream of the old failure scar to find stratigraphy most conducive to flow failures according to the empirical criteria. The stratigraphy would be the thinnest overburden over the thickest Zone A stratum. This condition was found immediately landward and slightly downstream of the old scar. Secondly, old top of bank line surveys showing a trend in direction into the bank of failures over the years, were used to align the detailed site within the area of the critical stratigraphy. The stratigraphy consisted of about 35 ft

(10.7 m) of clay overburden overlying Zone A sands to a depth of at least 120 ft (36.6 m) which was the maximum depth of exploration and about twice the maximum depth of the 1973 failure scar. The thalweg (deepest point) of the river in front of the site was about 140 ft (43 m) below the average top of bank elevation. During flood stages, the river regularly exceeds bank-full levels.

For the detailed investigation, a grid pattern was laid out at a 20-ft (6.1 m) centerline spacing to mark the location of the various borings or soundings. The layout philosophy was to group Standard Penetration Tests (SPT), electric cone penetration tests (CPT), resistivity cone penetration tests (RCPT), and electric piezocone penetration tests (PCPT) around each of two undisturbed sample borings. Within the grid pattern of overall dimensions of 40 ft by 120 ft (12.2 m by 36.6 m), were two undisturbed sample borings, five SPT borings, four CPT locations, five RCPT locations, and five PCPT locations. The depth of exploration was set at 120 ft (36.6 m).

Undisturbed samples of the Zone A sands were obtained by WES rig employing an Osterberg fixed-piston sampler which accepted 3-in. diameter (7.6 cm) lacquered Shelby tubes. A bentonite slurry was used as a drilling fluid. After each sampling stroke, the sampler was raised slowly out of the hole and a perforated O-ring packer, covered with filter paper, was inserted and secured against the bottom of the sample after first trimming out a small jar specimen. The Shelby tube was carefully removed from the sampler always in a vertical position and then hung vertically on a rack and allowed to drain of groundwater completely. After drainage, a top packer was installed and the sample frozen in a vertical position in an on-site upright freezer. Prior to transport of the frozen samples to WES, they were repacked in sawdust horizontally in a chest-type freezer which was in operation throughout the trip. At WES, the samples were stored vertically in an environmental room maintained at 22° Fahrenheit (-5.6° c). All tubes were x-rayed in the frozen state from two orthogonal directions. The x-ray negatives indicated excellent sample recovery and the absence of disturbance by ice lenses. In addition, there was a surprising absence of structure , i.e., bedding in the samples. The x-rays were used to select tube locations from which specimens for triaxial testing were extracted.

The SPT tests were also performed by WES. The split-spoon was driven by

an automatic trip hammer.

The CPT tests were contracted to Fugro-Gulf, Inc. of Houston, Texas. The electric cone conformed to ASTM Designation D 3441-79 and yielded tip resistance and sleeve friction with depth.

The RCPT tests were performed with the equipment of and by personnel of the Laboratorium Voor Groundmechanica, Delft, the Netherlands, under subcontract to Fugro-Gulf whose cone pushing rig was compatible with the Delft equipment. The RCPT sounding employs two cone devices. The first consists of an electric cone tip and friction sleeve ahead of a 73-cm long insulated section containing two 4-electrode arrays. With the probe in sand, an electrical field is applied across the outermost two electrodes and the potential drop across the innermost two electrodes is measured. In this manner the specific resistivity of the soil-groundwater mixture was obtained at each 20 cm increment of depth. A second cone device having the capability to draw in a specimen of the groundwater, measure its specific resistivity, and then expel the specimen was pushed within about a meter of the resistivity cone hole. Groundwater resistivity was measured at the same depths as the soil-water resistivity. In order to translate the field RCPT readings into values of porosity of the Zone A sands, laboratory correlations had to be developed between porosity and specific resistivity of the water and soil-water mixture. WES shipped samples of the Zone A sands to the Delft laboratories to perform the correlations. The Delft laboratory (Ir. H. Koning) also converted the field data to implied values of porosity. The porosity and the value of specific gravity of the sand solids (G_s) can be used to calculate density.

The PCPT soundings were performed under contract to Ardaman and Associates of Orlando, Florida (Dr. Anwar Wissa). Two piezocones were used; an 18-degree apex angle cone which provided only readings of pore water pressures induced during advance of the cone and a 60-degree apex angle combination pore pressure, tip resistance, and friction sleeve electrical cone. Except for a cylindrical porous stone at the tip, the combination cone also conformed to ASTM standards. The primary value of a piezocone is that it can "see" very thin soil strata on the order of an inch (2.54 cm) by the dynamic pore pressure response. At the time, it was also hoped that pore pressure response could be related to liquefaction susceptibility but that was never achieved.

It is not possible to present details of the results of the field

investigations and the conclusions drawn from them. These are reported by Torrey, Dunbar, and Peterson (1988). Comparisons of all data from both field in situ instruments and laboratory tests on the undisturbed samples resulted in excellent correlation among the methods. Relative densities of the Zone A sands implied from SPT blow counts, undisturbed samples, and CPT were in general agreement. All data indicated a medium, say 50 percent, to dense, say 80 percent, relative density with higher values trending with increasing depth. Densities measured from undisturbed samples were somewhat higher than those interpreted from RCPT readings. All specimens thawed and tested in the triaxial apparatus under consolidated, undrained conditions tended to dilate (increase in volume) during undrained shear loading at confining pressures simulating the sample depth. The liquefaction phenomenon occurs as a result of a looser sand's tendency to contract (decrease in volume) under undrained shear. The higher the confining pressure, the denser a sand may be and still liquefy. However, dilatancy was also observed from undisturbed specimens under confining pressures much higher than those comparable to any depth of sample taken from the site.

Steady-state void ratio testing on the Montz Zone A sands showed that in situ densities implied from the field investigations were entirely too high to support the hypothesis of liquefaction as the flow slide failure mechanism. The same overall results were obtained from the investigations relative to the Bonnet Carre' site where the Zone A sands were found to be consistently more dense than at the Montz site. These findings with respect to the in situ density of point bar Zone A sands were consistent with the field investigations conducted in the 1950's. If not liquefaction, then what might the failure mechanism be?

During 1975, Christopher Padfield, a PhD student under Professor Andrew Schofield, Cambridge University, England, visited the author to familiarize himself with the flow slide problem. He was preparing to perform centrifugal model tests as part of his dissertation to attempt to explain the empirical criteria pertaining to the ratio of overburden thickness to Zone A sand thickness. Even though the centrifuge model tests eventually proved to be partially inconclusive, the Cambridge involvement also introduced Dr. R.G. James to the subject in support of Padfield's studies. It was James who offered Padfield the hypothesis that the failure mechanism could be one of

retrogression in dense (dilatant) sands. The concept is that a locally oversteepened subaqueous slope (perhaps generated by rapid, severe, localized scour, say, as by a vortex) could be sustained by the presence of negative (with respect to hydrostatic) pore water pressure generated by shear stresses immediately behind the steep face. However, the sand at the slope face and under no confinement other than inward seepage gradient would be free to cascade down the face and flow downslope with some of it resedimenting with distance and some of it resuspended and swept away. By this process, the oversteepened slope would remain and also retrogress into the bank. In addition, because the resedimented sand would be steadily building on a very flat slope at the toe of the retreating face, the height of that face would be steadily diminishing. Therefore, the process would "run out" at the upper boundary of the sand, i.e., at its interface with the overburden and along some angle(s) to the horizontal. The basic process is the same as that observed in the Delft laboratories in large hydraulic models pertaining to dredging research. The mechanism is that which feeds a dredging suction pipe as it is advanced into a dense sand. Importantly, flow failure would not be evident at the ground surface unless the thickness and properties of the overburden would not permit it to bridge the cavity beneath. In that case, chunks of the overburden would progressively shear (a process previously reported by eyewitnesses) as underlying support was lost and ride out of the growing scar upon the carpet of fluidized sand. Padfield (1978) mathematically modeled the hypothesized mechanism and successfully fitted it to a failure case history. Padfield showed that as long as properties such as density or permeability of the Zone A sands were relatively consistent that the "run-out" angle to the horizontal would be essentially a constant throughout the process. Padfield calculated a runout angle of about 7 degrees from assumed properties of the sand and its resedimentation traits. Torrey (1988) estimates a run-out angle more like 9 or 10 degrees based on additional case studies. The hypothesized failure mechanism which may be envisioned as by retrogressive, thin-veil fluidization followed by partial resedimentation of the sand can be observed in a small pan of submerged dense sand in the laboratory whereas even centrifugal models employing very loose sand and in situ levels of stress will not allow a true liquefaction mechanism to be observed. Indeed, Padfield concluded that flow failure by retrogressive liquefaction cannot be modelled in the

centrifuge. If retrogression in dense sand is the failure mechanism, it exhibits geometric characteristics, i.e., the "run-out" distance into the bank will be a function of the depth of initiation and the run-out angle. If so, the adequacy of foreshore to protect the stability of the levee may be judged. Even in the work performed years ago, a correlation was seen among the depth, length, and maximum width of flow failures. A series of conceptual drawings of the retrogressive failure mechanism in dilatant sands is shown in Fig. 6.

Concurrent with the geotechnical field investigations at Montz and Bonnet Carre' Point, hydrographic surveys were performed along the Montz and Bonnet Carre' revetted bank reaches and along two unrevetted point bar reaches with susceptible stratigraphies to obtain data relative to river attack. Comparisons of the locations of the four major slides of 1973 had revealed strong similarities with respect to upstream channel alignments in that each was positioned on the inside of a bendway toward the upstream end of the point bar deposit. These similarities are seen in the superimpositions of the failures shown in Fig. 7. The length of bank and position of the surveys within the river bendways were based on those findings. The average length of survey along the bank was 2500 ft (762 m). Surveys were run at each site during rising, crest, and falling river stages for one water cycle. Analyses of these data showed that the underwater angles of repose in the Zone A sands correlated well to the 35° effective angle of internal friction measured for the undisturbed samples from Montz and Bonnet Carre' sites. In addition, over a 400 ft (122 m) reach at one of the unrevetted hydrographic survey sites an underwater slope over 50 ft (15 m) in height with a slope of about 2 vertical to 1 horizontal was seen in a large underwater bar deposited since the previous survey less than six months earlier. It is logical that material deposited in such quantity in that short interval was sand. The only explanation of such steep slopes in a cohesionless soil appears to be that of the dilatant retrogressive mechanism. The survey at the same site only months later showed the bar to be absent.

In addition, historical hydrographic survey data for the entire river reach below Baton Rouge from as early as 1894, reveal that the scope of the point bar problem is probably limited to only bank reaches exhibiting "permanent", secondary, scour pools which have been attacking the bank in the upstream area of bendways slowly but surely in their direction of creep over the

years. The term "secondary" is used to distinguish these smaller and separate pools from the large and lengthy pools typically seen within the bendways of all meandering streams. The secondary pool at Montz has eroded/failed the bank (i.e., the river channel has migrated) over 3000 ft (914 m) in the easterly direction since the 1890's. Trouble at Montz is far from over nor is it for many other point bar sites where the levee is very close to the top of the bank.

Currently, the studies continue under the assumption that retrogression in dense sands is the failure mechanism and that it is triggered by highly intense, localized scour during high water periods when the current is typically against the bank on the inside of bendways. A flow slide levee safety monitoring system has been developed and is being routinely applied by the USACE New Orleans District along reaches identified as susceptible to flow failure. That system presumes an empirically established run-out angle of 10° beginning at the toe of the slope as indicated by annual hydrographic revetment surveys. A minimum factor of safety against mass shear failure is calculated to determine the potential for the levee to be involved in a potential failure of the bank. Of course, if the run-out angle implies that the levee would be undermined by the flow failure itself, there arises great concern for monitoring that site with extra care and making sure that the revetment is well maintained or beefed up.

In 1983, another dimension of the flow slide problem reared its head. On August 23 of that year, a major levee failure occurred along the Marchand, Louisiana, revetted bank during low water. Analysis of that failure (Dunbar and Torrey 1991) indicated that clay overburden in excess of 90 ft (27 m) in thickness had undergone a series of shear failures over the years as the result of gradual loss of underlying deep sands. As each successive round of shear failures year by year removed large chunks of soil, the factor of safety of the bank decreased until finally a massive wedge-type failure occurred with the levee as part of the driving forces. There is every probability that the loss of the sands from beneath the thick overburden resulted from the same retrogressive mechanism as seen in the shallower, much thinner-overburden point bar events. In the case of the very thick clay overburden, a much longer time frame including years of erosion and upper bank shear failures was required to eventually bring about the same result more immediately seen in

the case of the point bar flow slides.

Under the conviction that there is little else that can be done within technology available with respect to strictly geotechnical aspects up on the riverbank, it has been decided to go out into the river and begin to closely monitor river attack along two selected susceptible point bar reaches below Baton Rouge. The two reaches selected are along Montz revetment and along Port Sulphur revetment at about river mile 35 (56.3 km). Over 2000 ft (610 m) of bank at each site are being hydrographically surveyed six times a year based on river stage along survey ranges spaced only 50 ft (15 m) apart transverse to the bank. The surveys are duplicated each time in layout by means of global positioning control. In addition, measurements of current velocities and directions with depth are being taken. These efforts are scheduled to continue indefinitely until more information is obtained regarding the failure mechanism itself and river attack conditions leading to triggering.

Related studies are also underway by geophysicists at WES which are aimed at developing the means to "see" the areal condition of revetment mattress by some rapid indirect means even if it is buried. It appears at this time that such methods will be developed employing self-potential of the steel-wire and steel-cable interlaced mattress as well as special water or airborne high technology now available from the U.S. Navy. Those methods will be indispensible in assessing the relative performances of any new protective measures applied in eventual prototype test installations.

With respect to possible preventative measures, it appears to be the familiar problem of preventing severe localized scour. That is not a simple proposition for a river as deep and powerful as the Mississippi in its lowermost reach. Furthermore, effective and complete armoring of any significant bank reach may produce other problems both upstream and downstream. Contemplation of high population densities, many heavy petro-chemical industries, and even a nuclear power plant totally dependent upon a thin thread of earthen embankment is frightening enough. The additional reality that the thin protective thread is itself vunerable to sudden breach during the worst of high water periods elevates the flow slide problem to the status of national importance. The record proves that the articulated concrete revetment mattress placed in a typical single layer will not prevent flow slides. New forms of

revetment, protective elements or layered applications of the current type may prove adequate. In any case, considerable test sections will be required when the decision to expend such large sums of money to build and observe them appears to be warranted when there is a consensus that the failure mechanism, the triggering river conditions, the most susceptible locations (as opposed to long bank reaches), and the potential effects of protective measures on other bank reaches are all settled issues.

CONCLUSIONS

This paper has been a very broad overview of many years of multi-faceted investigation. A great many interesting tasks and findings could not be addressed nor could all the individuals who made significant contributions along the way be named. Many of those persons are engineers employed by the CELMV in geotechincal, potamological, channel stabilization, and river engineering positions. Their combined expertise relative to the fluvial processes and behavior of the Mississippi River is unparalleled. The author considers it impractical to conclude a paper of this nature with a listing of conclusions save for the obvious one, if not also the most concrete, that the problem is not yet solved. However, it can be stated that the solution is closer than ever before. In the meanwhile, the tried and proven emergency flood fighting operations of the CELMV and its New Orleans District must continue to protect the life and property along the lower reaches of the Mississippi River as they have in the past.

REFERENCES

Castro, G. 1969. "Liquefaction of Sands", Harvard Soil Mechanics Series No. 81, Cambridge, Massachusetts.

REFERENCES (continued)

Dunbar, J. B. and Torrey, V. H. 1991. "Geological, Geomorphological, and Geotechnical Aspects of the Marchand Levee Failure, Marchand, Louisiana", Miscellaneous Paper GL-91-17, U.S. Army Engineer Waterways Experiment Station, Vicksburg, Mississippi.

Durham, G. N. 1971. "A Study of the Liquefaction Phenomena of a Fine Sand Utilizing the Consolidated Undrained Triaxial Compression Test Under Controlled-Stress Loading", Master's Thesis, Mississippi State University, Mississippi State, Mississippi.

Padfield, C. J. 1978. "The Stability of Riverbanks and Flood Embankments", Final Technical Report, U.S. Army European Research Office, London, England.

Torrey, V. H. and Gann, A. R. 1976. Verification of Empirical Method for Determining Riverbank Stability, 1970 and 1971 Data", Potomology Investigations Report No. 12-22, U.S. Army Engineer Waterways Experiment Station, Vicksburg, Mississippi.

Torrey, V. H., Dunbar, J. B., and Peterson, R. W. 1988. "Retrogressive Failures in Sand Deposits of the Mississippi River, Report 1, Field Investigations, Laboratory Studies, and Analysis of the Hypothesized Failure Mechanism", Technical Report GL-88-9, U.S. Army Engineer Waterways Experiment Station, Vicksburg, Mississippi.

Torrey, V. H. 1988. "Retrogressive Failures in Sand Deposits of the Mississippi River, Report 2, Empirical Evidence in Support of the Hypothesized Failure Mechanism and Development of the Levee Safety Flow Slide Monitoring System", Technical Report GL-88-9, U.S. Army Engineer Waterways Experiment Station, Vicksburg, Mississippi.

Fig. 1. Undated Photograph by Dr. M.J. Hvorslev of a Flow Failure Scar, Reid-Bedford Revetment Reach, Mississippi River

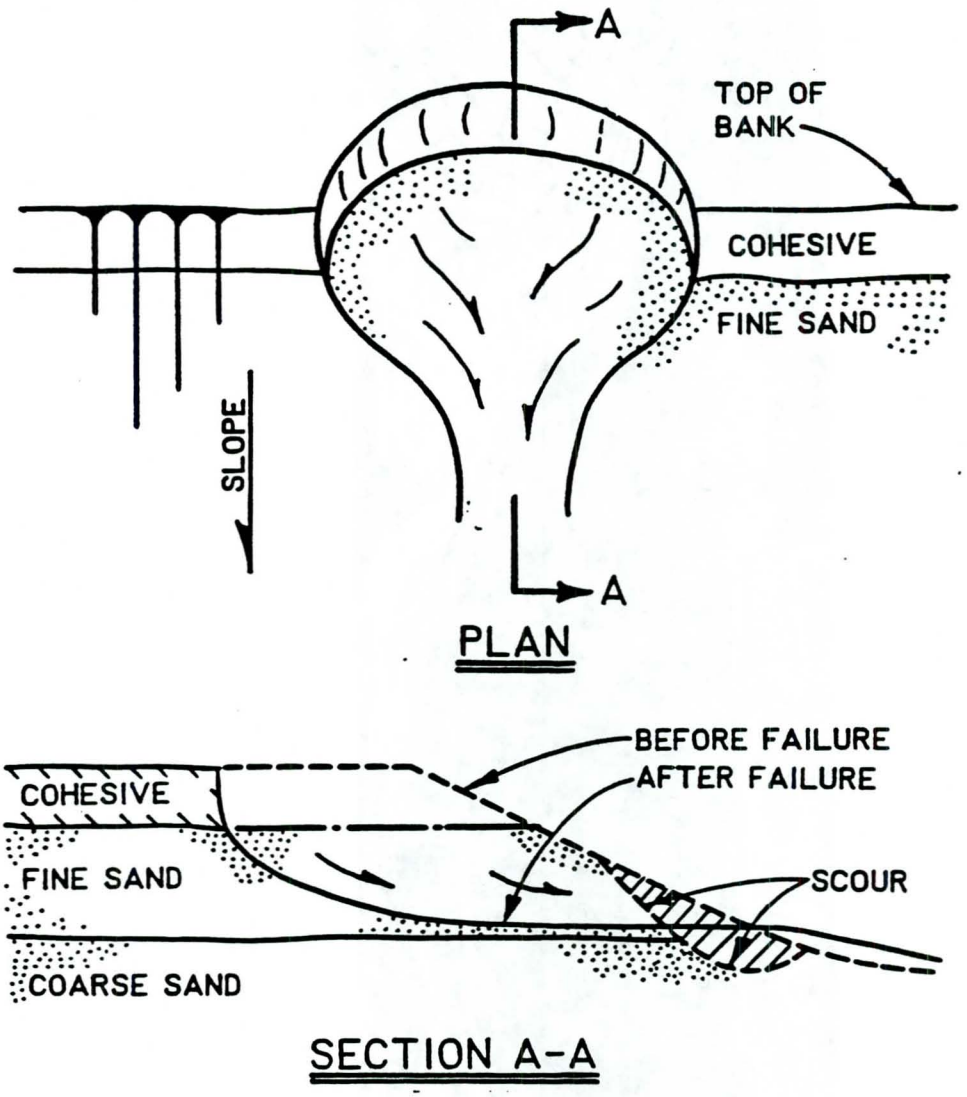

Fig. 2. Typical Plan and Section of a Mississippi Riverbank Flow Failure

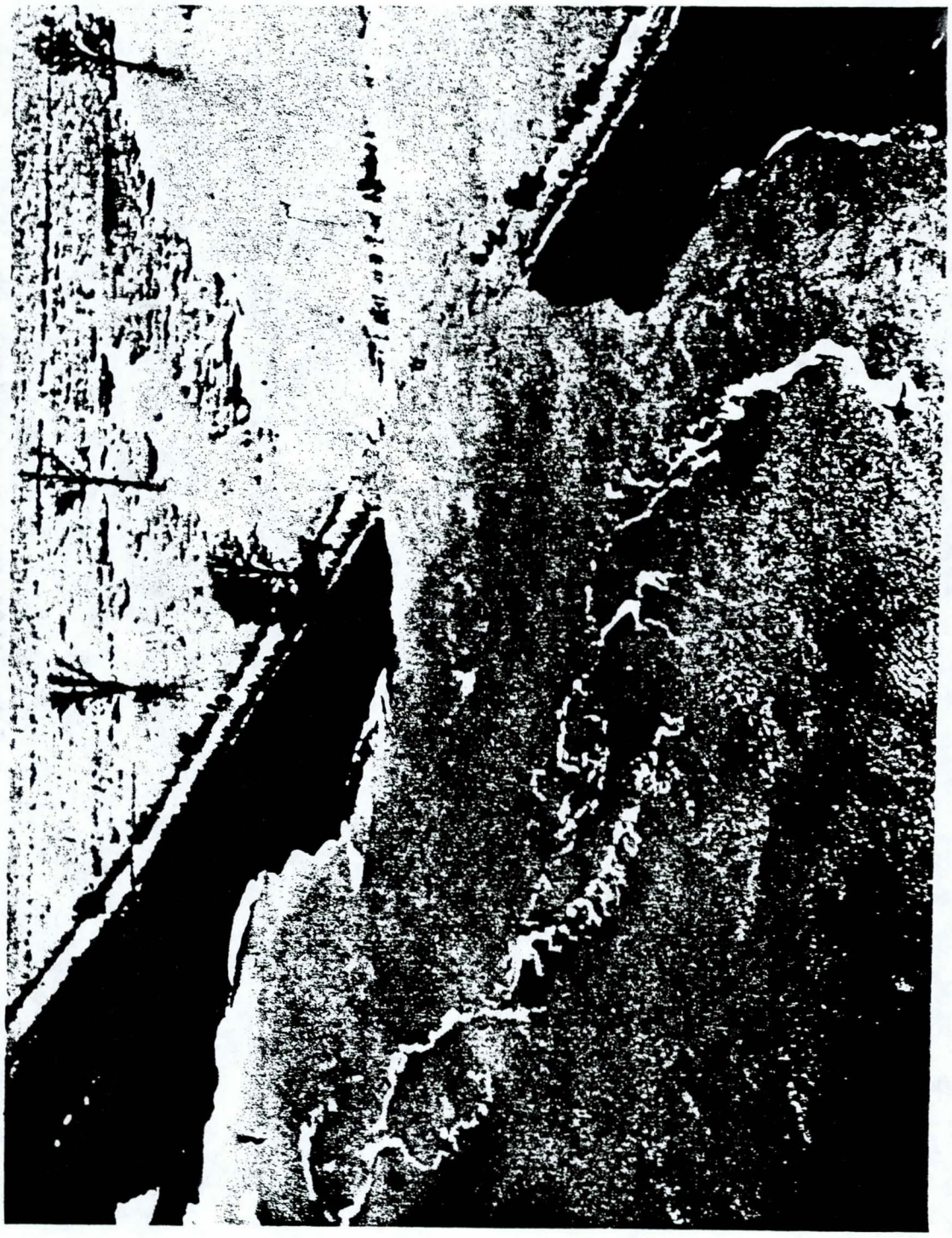

Fig. 3. Aerial Photograph of the Wilkinson Point Flow Failure of 1949

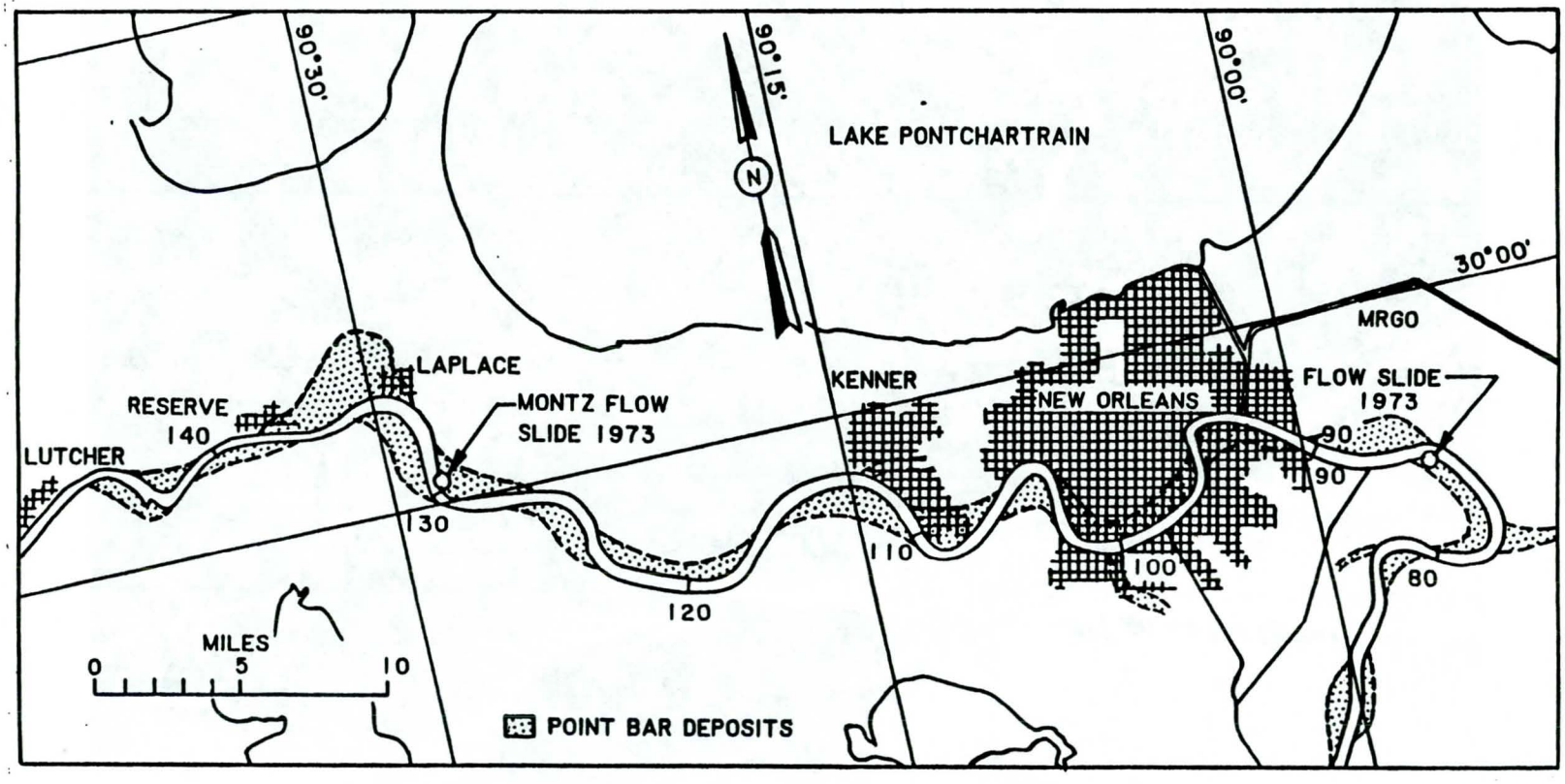

Fig. 4. General Location of the 1973 Flow Failure at Montz, Louisiana

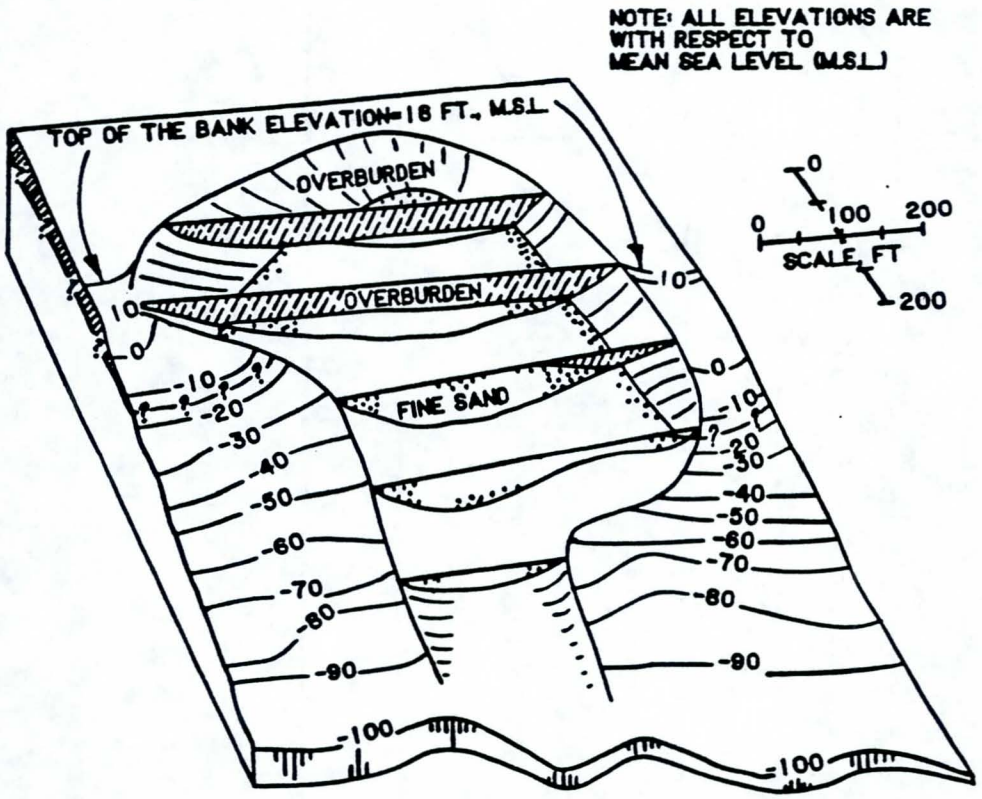

Fig. 5. Isometric Drawing of the 1973 Flow Failure at Montz, Louisiana

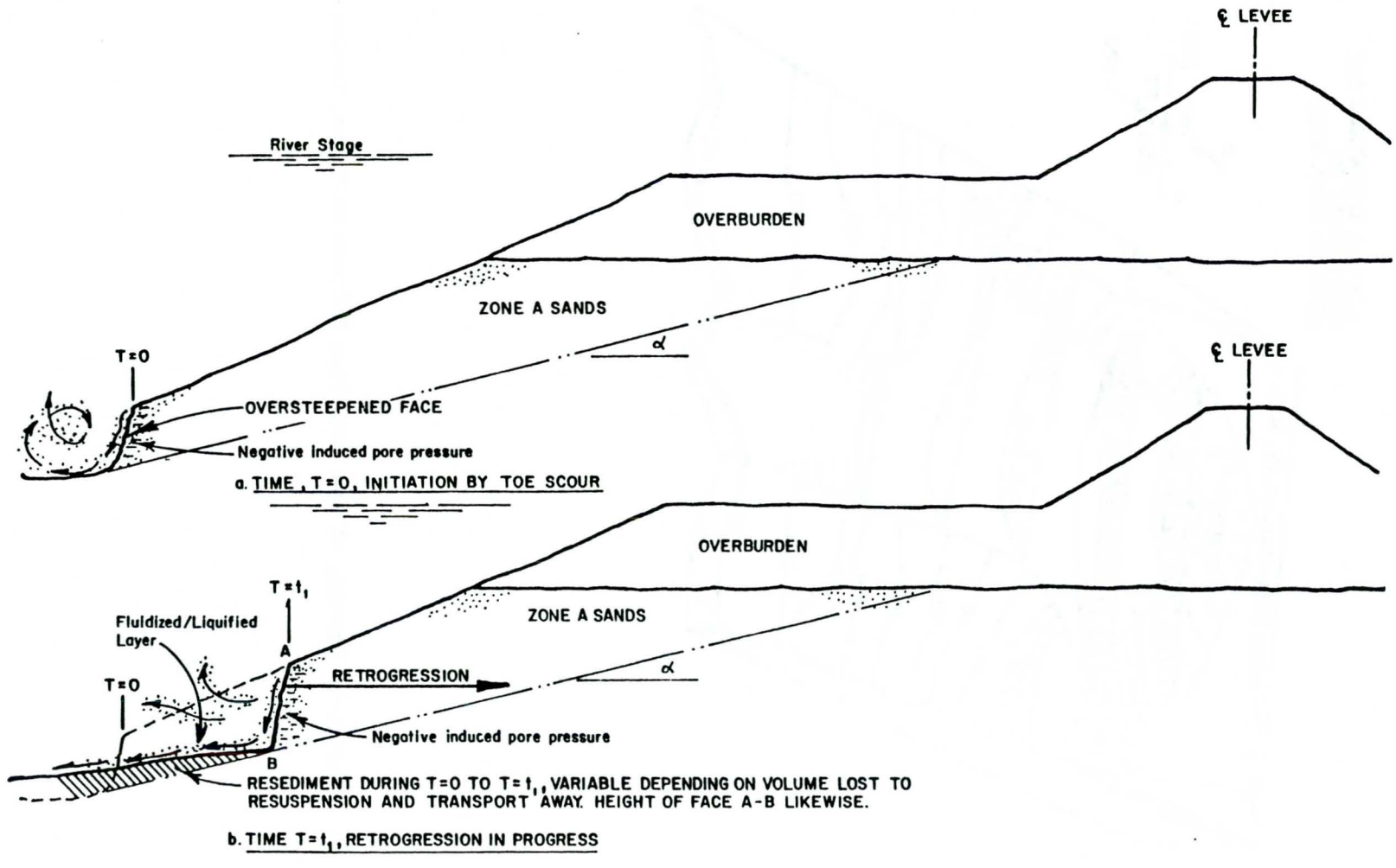

Fig. 6. Sequential Stages of a Retrogressive Flow Slide in Dilatant Sands

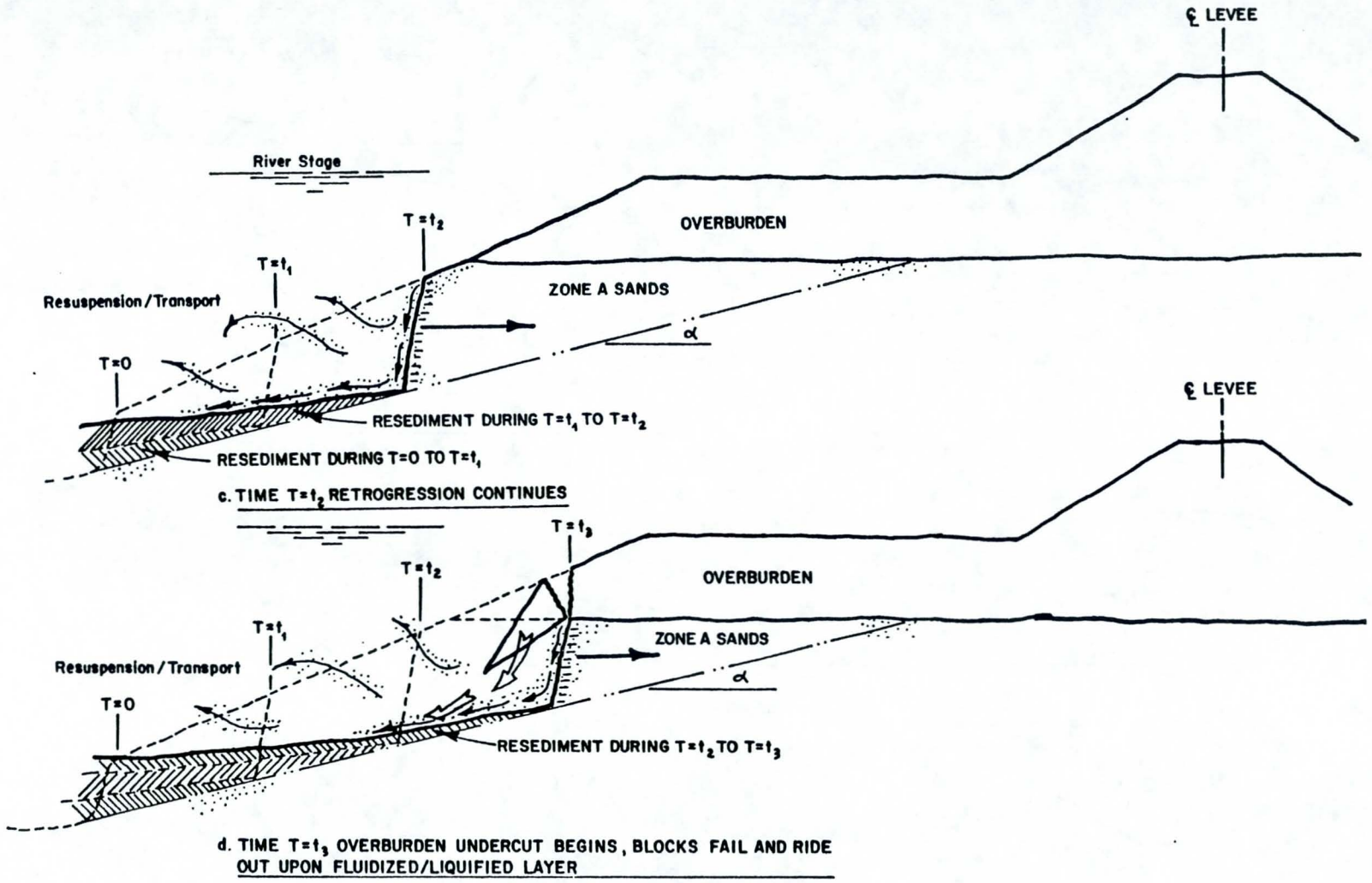

Fig. 6. (continued) Sequential Stages in a Retrogressive Flow Slide in Dilatant Sands

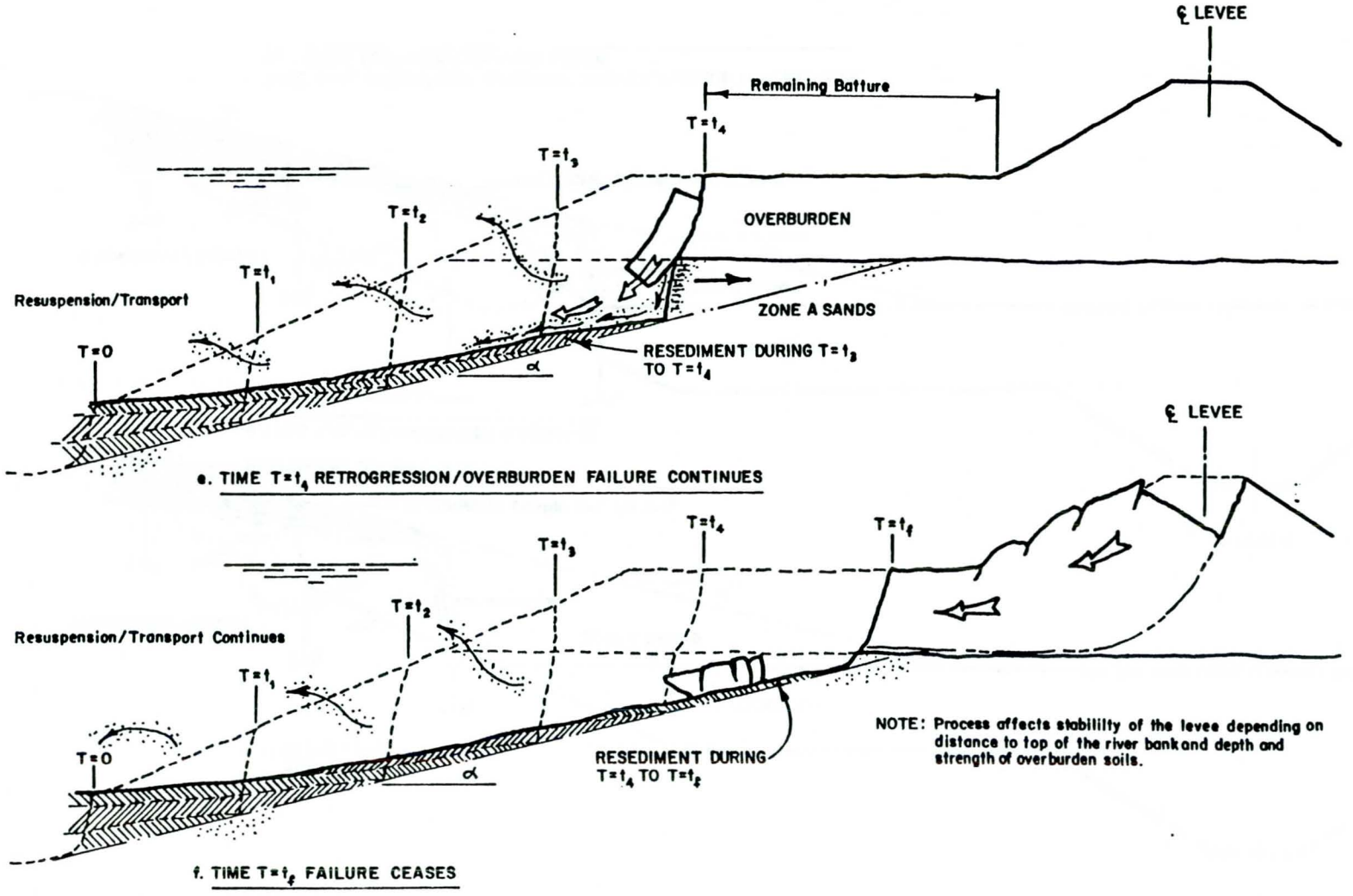

Fig. 6. (concluded). Sequential Stages of a Retrogressive Flow Slide in Dilatant Sands

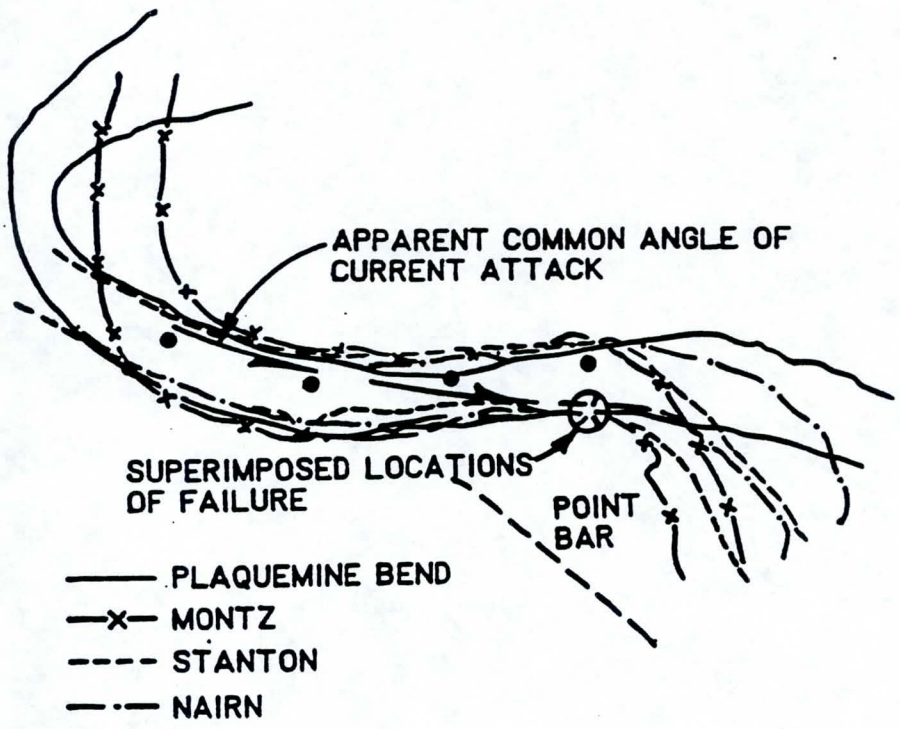

Fig. 7. Illustration of the Similarity of 1973 Flow Failure Positions

NUMERICAL CALCULATION OF RUNUP AND OVERTOPPING ON RIPRAP REVETMENTS

D.L. Ward
US Army Engineers Coastal Engineering Research Center
Vicksburg, Mississippi, USA

INTRODUCTION

Design of revetments for protection against wave attack requires an accurate assessment of the potential for runup and overtopping to determine design height of the structure and estimate damages shoreward of the revetment. These factors clearly have a direct effect on construction costs of the project and affect the project feasibility. Unfortunately, good information on these parameters is difficult to obtain.

Typically, estimates of runup and overtopping are made based on empirical equations or from physical model studies. Both of these methods have serious limitations. Physical model studies are time-consuming and expensive and may be affected by reflected wave energy, parasitic waves, and scale effects. Empirical equations are usually derived from physical model tests and therefore incorporate the problems of physical models. In addition, empirical equations are limited to the range of test conditions from which the data was obtained, including both structure geometry and incident wave conditions. Common prototype conditions such as compound slopes or offshore bars are not included in most empirical equations.

Two computer models, IBREAK (Kobayashi and Wurjanto, 1989a) and RBREAK (Wurjanto and Kobayashi, 1991), have been developed that are capable of determining runup and overtopping for many coastal structures. With IBREAK and RBREAK, performance of revetments with compound slopes, fronting berms, or other irregular profiles may be determined. Maximum wave runup is predicted for sub-aerial structures that are sufficiently high to prevent overtopping, overtopping rates are estimated for lower subaerial structures, and wave transmission is calculated for submerged structures.

IBREAK and RBREAK were developed by Dr. Nobuhisa Kobayashi at the

University of Delaware with funding from the National Science Foundation and the Delaware Sea Grant College Program, then modified and user manuals produced under contract with the US Army Engineers Coastal Engineering Research Center (CERC). The programs were designed for nonporous structures of arbitrary geometry subjected to a normally incident wave field. The programs were written in FORTRAN 77 and are currently running at CERC on a VAX 3600 computer, Cray Y-MP supercomputer, and an HP 9000 workstation.

IBREAK is limited to monochromatic incident waves; RBREAK is a modification of IBREAK to allow the input of spectral waves. RBREAK is currently being tested at CERC, and results of the tests should be available when this paper is presented. Because testing of RBREAK has not been completed, this paper will be limited to discussion of IBREAK, although most of the text is applicable to RBREAK as well.

It should be noted that several other numerical models are available for predicting wave/structure interactions (Allsop et al., 1988; Hölscher et al., 1988; Sulisz and McDougal, 1988; Thompson, 1988). Discussion of these and other numerical models is beyond the scope of this report.

THE MODEL

Overview

Detailed information on the mathematics and numerical methods employed in IBREAK have been presented in several reports, some of which are listed under 'Additional Information' at the end of this paper. This paper will therefore present only a brief overview of the model.

IBREAK uses a numerical flow model to predict flow characteristics on a rough impermeable slope and was developed such that any monochromatic, normally incident wave train could be specified at the toe of the slope. The model is based on conservation of mass and momentum in finite-amplitude shallow-water wave equations in Madson and White (1976) which include the effects of bottom friction. A discretized finite difference grid of constant space and constant time step is solved by an explicit dissipative Lax-Wendroff method.

Incident wave conditions, which must be monochromatic, are specified either by height and period or defined in a separate data file. If height and period are specified, the program calculates incident wave profile by Stokes

second-order wave theory if the Ursell parameter U_r is less than 26, otherwise cnoidal wave theory is used. The Ursell parameter is defined as

$$U_r = \frac{HL^2}{d^3}$$

where H is wave height, L is wave length, and d is depth, all taken at the structure toe. If wave height is known at a depth other than the toe, the program will compute the wave height at the toe. The description of a specific wave profile, such as may be determined from a physical model test, may also be entered as an input.

IBREAK does not compute energy dissipation through porous media, but rather calculates energy losses by a friction coefficient which is based on roughness of the slope. Determination of the friction coefficient for a particular slope under a given incident wave set is described below; calibration of the model is required for cases in which the friction coefficient has not been determined. Calibration of the program may be done with data from laboratory studies given the dimensions and type of armor units, structure slope geometry, and incident wave conditions.

Computed oscillations of the waterline on the slope are used to predict runup and rundown, which are determined at a specified vertical distance above the slope. This measurement is related to the use of a waterline meter that has a given height above the slope. While it is possible to enter several different heights for the calculations, results indicate that wave runup is relatively insensitive to this height, but the wave rundown is very sensitive since a thin layer of water remains on the slope during downrush.

Reflected wave train is computed from wave characteristics advancing seaward. Reflection coefficients are calculated in three ways. The first method is based on the normalized height of the reflected wave train as compared to the normalized height of the incident wave energy. The other two methods are energy methods, comparing the time-averaged reflected wave energy to the time-averaged incident wave energy, with one of the energy methods accounting for the difference between the still water level and the mean water level at the toe.

The program is also written to predict armor unit stability by calculating variation of the local stability number along the slope. The minimum computed value of the stability number corresponds to the critical stability number for initiation of armor movement. Calibration for armor stability and movement requires coefficients for shape, volume, lift, drag, and inertia of the armor units. Little data is currently available for these coefficients, but attempts are currently being made at CERC to develop tables of data for these parameters based on previous research. Use of the program for stability predictions will not be covered in this paper; additional information on the numerical stability model may be found in Kobayashi and Otta (1987).

Although the program is limited to non-porous structures, the geometry is arbitrary and compound slopes, offshore bars, and attached berms are acceptable profiles.

Inputs

Inputs are stored in a datafile which is requested at the beginning of the program. Primary inputs concern structure geometry, incident wave conditions, and roughness of the slope (friction coefficient), plus a set of values to specify the desired run options and computed data to save in files created by the program. Dimensional data for structure geometry and incident wave conditions may be entered in either metric or US customary units, with the system of measurement being specified in the input datafile.

Structure geometry may be input either as a set of coordinate pairs designating the ends of linear segments of slope, or by length and angle of individual linear segments of structure cross-section. As an example, the revetment with a compound slope illustrated in Figure 1 may be input either by the four coordinate points shown or by the horizontal lengths and angles of the three segments of the cross-section, with angles entered as tangent of the slope with the horizontal. If the program is to compute maximum runup, it is necessary that the slope extend far enough above the still water level (swl) to prevent overtopping, and an error message will be returned if the slope is of insufficient length. Alternatively, the program has the option of calculating the overtopping rate for lower structure crests. Depth at the toe

is also required as an input.

Approximately 60 variables are required in the input data file. However, only a few of these are required by an engineer analyzing the performance of a revetment. Generally, given incident wave conditions, structure geometry, and a means of estimating the friction coefficient, it is possible to obtain runup or overtopping estimates from the program.

Outputs

The main output file from IBREAK, named ODOC.DAT, includes the incident wave conditions and slope properties from the input datafile, several computational parameters used by the program, plus the computed results. In addition, the program will store spatial variables of water surface elevation and horizontal velocity during a specified time interval and temporal variations in water depth at specified nodes, if requested.

If wave overtopping calculations are specified, the program estimates the maximum and the average overtopping rates per unit structure length at the crest of the structure, assuming unimpeded flow past the crest. Overtopping is assumed to occur whenever the depth at the crest is greater than a small value used to calculate the moving waterline. No calculations are performed shoreward of the crest of the structure.

Wave transmission calculations over a submerged bar are somewhat limited in that transmitted waves are assumed to propagate shoreward without being reflected from the shoreline, transmitted flow is computed without a return current, and the structure is assumed to remain submerged at all times. Wave transmission over the structure is computed by each of the three methods used to compute reflection coefficients.

DETERMINATION OF FRICTION COEFFICIENTS

In order for IBREAK to be useful on armored slopes, the appropriate friction coefficients must be determined. Friction coefficients were determined by comparing runup predicted by IBREAK to a series of 49 large-scale tests conducted in a wave flume with average stone weights ranging from about 12 to 55 kg, incident wave heights from about 55 to 115 cm, wave periods

from 2.8 to 11.3 sec, and structure slopes including 1:2.5, 1:3.5, and 1:5.0.

The large-scale tests were conducted in 1975 by Mr. John Ahrens at CERC (Ahrens 1975). Wave data and runup values in his report are for the zero-damage wave height determined for the revetment being tested, and are listed here in Table 1.

To estimate friction coefficients, conditions from each of the wave tank tests were input into IBREAK and the model was run with friction coefficients ranging from 0.3 to 0.7 with increments of 0.05. Additional runs of the numerical model were conducted with higher or lower friction coefficients if necessary to obtain results that bracketed the observed runup values. Linear interpolation was used to obtain an estimated friction coefficient that corresponded to measured runup values. Results of the numerical model test runs are shown in Table 2.

In addition to presenting the shallow-water wave equations on which IBREAK is based, Madsen and White (1976) developed empirical equations for determining the friction coefficients. The two empirical equations for friction coefficients in Madsen and White, which differ somewhat due to different data sets being analyzed, are given below.

$$f_w = 0.25\left[\frac{d_{n(50)}}{d}\right]^{-0.74}\left[\frac{d_{n(50)}\ \tan\theta}{R}\right]$$

$$f_w = 0.29\left[\frac{d_{n(50)}}{d}\right]^{-0.5}\left[\frac{d_{n(50)}\ \tan\theta}{R}\right]^{0.7}$$

where f_w is friction coefficient, $d_{n(50)}$ is nominal diameter of the riprap, d is depth at the toe, θ is structure slope, and R is height of the runup above the swl. Friction coefficients computed with these formulae for Ahren's test conditions are shown in Table 3 along with friction cefficients determined in this study. Madsen and White's equations are seen to substantially underpredict friction factors used in IBREAK.

Although both Madsen and White (1976) and IBREAK solve the same shallow-water wave equations, differences in friction factors between the models are not surprising due to differences in other parts of the models. However, the equations for friction coefficients in Madsen and White provide a reasonable

starting point to determine a new empirical equation for friction coefficients in IBREAK.

Equations 2 and 3 are not suitable for design purposes because they require runup to determine friction coefficients, while the purpose of this study is to determine friction coefficients that will allow IBREAK to accurately predict runup. A new equation is therefore sought that will allow determination of the friction coefficient using parameters that should be available to a design engineer.

The factor $d_{n(50)}/d$ in Equation 1 is a relative roughness factor. Ward and Ahrens (1992) use the parameter $d_{n(50)}/L_o$, where L_o is deepwater wavelength, as a relative roughness term, and stone diameter relative to local wavelength or wave height (H) are also logical choices for roughness. Each of these terms will be investigated for use in a regression equation.

A correlation analysis was conducted on each of the four relative roughness terms defined in the preceding paragraph compared to the interpolated friction coefficients in Table 2. Correlation coefficients are given in Table 4 for the roughness terms as well as structure slope and wave steepness.

It is seen in Table 4 that there is very little correlation between friction coefficient and relative roughness defined with wave height or depth at toe of structure. It is noted, however, that this data set was collected at a constant water depth, and only the zero-damage wave height is given in the data set. A more general data set may yield higher correlation between friction coefficients and relative roughness defined either by wave height or water depth.

Table 4 shows a strong correlation between friction coefficient and relative roughness defined by either local or deepwater wavelength, with deepwater wavelength yielding a slightly better correlation. A high correlation is also noted between friction factor and wave steepness, and a weaker negative correlation with cotangent of structure slope.

Regression analysis was used to define the following relationship:

$$f_w = C_o \left[\frac{d_{n(50)}}{L_o} \right]^{C_1} (\tan\theta)^{C_2}$$

where C_0 , C_1 , and C_2 are regression coefficients with the following values:

$$C_0 = 2.3508$$
$$C_1 = 0.5511$$
$$C_2 = 0.6145$$

The model, the best of many that were tried, was determined by linearizing the equation by taking the natural logarithm of each side of the equation, and doing a linear regression analysis on the model

$$\ln f_w = \ln C_0 + C_1 \ln(d_{n(50)}) + C_2 \ln\tan\theta \qquad (5)$$

to obtain approximate coefficients for the model. This linear model had a correlation coefficient of 0.964, however the linear regression analysis provided a best fit for the log of the friction coefficients rather than the friction coefficients themselves. Correlation between friction coefficients determined from the log values in Equation 5 and friction coefficients in Table 2 was 0.938. The coefficients determined from the linear regression analysis were then used as a starting point in the iterations of a nonlinear regression analysis on the model in Equation 4. Nonlinear regression analysis reduced the sum squares of differences between predicted friction coefficients and those in Table 2 by about 11% over results of just the linear regression. Final correlation coefficient between the friction coefficients from Equation 4 and those in Table 2 was 0.944, and the average error was 0.011.

It should be noted that the model does not include wave steepness; including wave steepness reduced the sum squares errors by only 0.25%, and correlation coefficient between friction coefficients from Equation 4 and those in Table 2 remained at 0.944 when rounded to three decimal places. However, wave heights in the data set where restricted to the zero-damage wave

heights; with a more general data set, it is entirely possible that wave steepness or some other parameter with wave height will be significant.

Runup coefficients in IBREAK are determined by water surface elevation above the slope, that is, thickness of the film of water on the slope. Selection of different values for runup thickness will change the calculated runup elevation. Runup values shown in Table 2 determined by IBREAK were calculated with a runup thickness of 6.4 mm. For the basis of comparison, selected tests were rerun with the same friction coefficient but with the runup thickness reduced in half. The change in runup, shown in Table 5, is less than one percent.

USE OF NUMERICAL MODEL

Computational stability of the equations is dependent on the size of the spatial and temporal increments. No guidance is available on the size of the increments that should be used, and is currently being determined on a trial-and-error basis. Similarly, while the program includes an extensive set of error messages that help identify the problem if the program fails, including the time step, location, and condition that caused the failure, there is little guidance available to correct a failure condition. Familiarity with the program is therefore required. A new user interface and more complete user guidance is currently being developed at CERC.

The program exceeds the 640 kilobyte limit imposed by the DOS operating system, and therefore does not run on personal computers (PC's) under DOS. The program has been run on a PC under UNIX, but at present the program is most effective running on a larger computer. CERC is therefore using a VAX 3600, Cyber Y-MP, or HP 9000 to run the program.

Limitations

While IBREAK is extremely powerful and should prove to be a valuable tool for testing various configurations in the early stages of the design process, the program has some obvious limitations. Major limitations include requiring monochromatic incident waves, only allowing input of one roughness coefficient for the structure, and being a one-dimensional model. Each of

these limitations has either been addressed or is being addressed.

Using monochromatic waves greatly simplifies the program, however, waves are random in nature. While RBREAK was written to address this limitation, IBREAK still provides much valuable information. Monochromatic waves are frequently used in laboratory studies where depth-limited breaking waves are expected, or to model a conservative "worst case" situation.

The model for friction coefficients presented in this paper determines friction coefficients from stone size and structure slope. For compound slopes or flow over a beach segment plus a revetment segment, multiple roughness coefficients are required. RBREAK is currently being modified to allow multiple roughness coefficients and should be available with this modification in Fall, 1993.

Since IBREAK is based on a one-dimensional flow model, it is not possible to determine velocities at structure toes (although stability numbers near the toe may be calculated to aid in toe design) or at any particular point on the structure. A two-dimensional model, VBREAK, is therefore being developed and should be available in 1994.

Conclusions

IBREAK has been used to try to reproduce the observed runup on a set of large-scale tests on riprap-covered slopes. The model is capable of predicting runup within a few percent of the measured values.

Other numerical models have also been developed that predict runup and overtopping on riprap slopes. With proper calibration and determination of required coefficients in the models, the models show great potential as an engineering design and analysis tool. Use of numerical models should aid in preliminary design studies, reduction in required physical model testing, analysis of existing structures, and estimation of flooding potential over structures. As existing models are improved and new models are developed, the potential for numerical models in the design and analysis process should continue to increase.

Additional Information

The numerical flow model used in IBREAK was reported in Kobayashi et al. (1986, 1987). Kobayashi and Greenwald (1986, 1988) performed experiments to calibrate and evaluate the model. The numerical flow model was used to predict wave reflection and runup on smooth impermeable slopes in Kobayashi and Watson (1987), and wave transformation and swash oscillation on beaches in Kobayashi et al. (1988, 1989).

The wave overtopping model for subaerial structures was presented in Kobayashi and Wurjanto (1988, 1989b). Wave reflection and transmission over submerged structures was predicted in Kobayashi and Wurjanto (1989c, 1989d) and in Wurjanto and Kobayashi (1989).

A review of the governing equations in IBREAK, listings of input and output formats, examples of inputs and outputs, and a complete listing of the program are found in Kobayashi and Wurjanto (1989a).

Acknowledgement

The work described in this paper was conducted as part of the Coastal Research and Development Program of the US Army Engineers Coastal Engineering Research Center. Permission to publish this paper was granted by the Chief of Engineers.

References

Ahrens, J.P. (1975) Large wave tank tests of riprap stability. *Tech. Memo. No. 51*, US Amy Engineers Coastal Engineering Research Center, Ft. Belvoir, Virginia. 41 pp.

Allsop, N.W.H., Smallman, J.V., and Stephens, R.V. (1988) Development and application of a mathematical model of wave action on steep slopes. *Proc. 21st Coastal Engrg Conf.*, ASCE, 281-291.

Hölscher, P., drGroot, M.B., and van der Meer, J.W. (1988) Simulation of internal water movement in breakwaters. *Modeling Soil-Water-Structure Interactions*, Kolkman et al. (eds), Balkema, Rotterdam, The Netherlands, 427-433.

Kobayashi, N., Roy, I., and Otta, A.K. (1986) Numerical simulation of wave runup and armor stability. OTC Paper 5088, *18th Offshore Tech. Conf.*, 51-56.

Kobayashi, N. and Greenwald, J.H. (1986) Prediction of wave runup and riprap stability. *Proc. 20th Coastal Engrg. Conf.*, ASCE, 1958-1971.

Kobayashi, N. and Otta, A.K. (1987) Hydraulic stability analysis of armor units. *J. Waterway, Port, Coastal, and Ocean Engrg.*, ASCE, 113(2), 171-186.

Kobayashi, N., Otta, A.K., and Roy, I. (1987) Wave reflection and runup on rough slopes. *J. Waterway, Port, Coastal, and Ocean Engrg.*, ASCE, 113(3), 282-298.

Kobayashi, N. and Watson, K.D. (1987) Wave reflection and runup on smooth slopes. *Proc. Coastal Hydrodynamics*, ASCE, 548-563.

Kobayashi, N. and Greenwald, J.H. (1988) Waterline oscillation and riprap movement. *J. Waterway, Port, Coastal, and Ocean Engrg.*, ASCE, 114(3), 281-296.

Kobayashi, N., Strzelecki, M.S., and Wurjanto, A. (1988) Swash oscillation and resulting sediment movement. *Proc. 21st Coastal Engrg. Conf.*, ASCE, 1167-1181.

Kobayashi, N., and Wurjanto, A. (1988) Numerical prediction of wave overtopping on coastal structures. *Res. Rept. No. CE-88-72*, Ocean Engrg. Prog., Univ. of Delaware, Newark, Delaware. 51 pp.

Kobayashi, N., DeSilva, G. S., and Watson, K.D. (1989) Wave transformation and swash oscillation on gentle and steep slopes. *J. Geophys. Res.*, 94(C1), 951-966.

Kobayashi, N., and Wurjanto, A. (1989a) Numerical model for design of impermeable coastal structures. *Research Report No. CE-89-75*, Center for Applied Coastal Research, Dept. Civil Engrg, Univ. of Delaware, Newark, Delaware. 222 pp.

Kobayashi, N., and Wurjanto, A. (1989b) Wave overtopping on coastal structures. *J. Waterway, Port, Coastal, and Ocean Engrg.*, ASCE, 115(2), 235-251.

Kobayashi, N., and Wurjanto, A. (1989c) Numerical prediction of wave transmission over submerged breakwaters. *Research Report No. CE-89-73*, Center for Applied Coastal Research, Dept. Civil Engrg, Univ. of Delaware, Newark, Delaware. 76 pp.

Kobayashi, N., and Wurjanto, A. (1989d) Wave transmission over submerged breakwaters. *J. Waterway, Port, Coastal, and Ocean Engrg.*, ASCE, 115(5), 662-681.

Madsen, O.S., and White, S.M. (1976) Energy Dissipation on a rough slope. *J. Waterways and Harbors Coastal Engrg. Div.*, ASCE, 102 (WW1) 31-48.

Sulisz, W., and McDougal, W.G. (1988) Wave interaction with a composite breakwater. *Computer modeling in Ocean Engineering*, Schrefler and Zienkiewicz (eds), Balkema, Rotterdam, The Netherlands, 715,721.

Thompson, A.C. (1988) Numerical model of breakwater wave flows. *Proc. 21st Coastal Engrg Conf.*, ASCE, 2013-2027.

Ward, D.L., and Ahrens, J.P. (1992) Laboratory study of a dynamic berm revetment. *Tech. Rep. CERC-92-1*, US Amy Engineers Coastal Engineering Research Center, Vicksburg, Mississippi. 74 pp.

Wurjanto, A, and Kobayashi, N. (1989) Wave overtopping and transmission over breakwaters. *Proc. PORTS '89*, ASCE, 247-256.

Wurjanto, A, and Kobayashi, N. (1991) Numerical model for random waves on impermeable coastal structures and beaches. *Research Report No. CACR-91-05*, Center for Applied Coastal Research, Dept. Civil Engrg, Univ. of Delaware, Newark, Delaware. 365 pp.

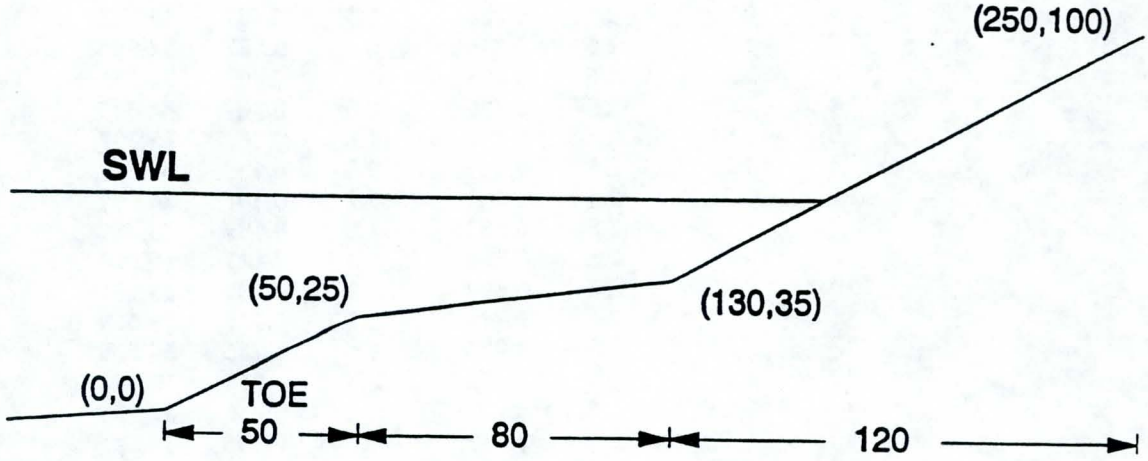

GEOMETRY MAY BE ENTERED BY:

	COORDINATE PAIRS OR		LENGTH AND TANGENT	
n	XBSEG(n)	ZBSEG(n)	WBSEG(n)	TBSLOP(n)
1	0.	0.	50.	.5000
2	50.	25.	80.	.1250
3	130.	35.	120.	.5417
4	250.	100.		

Figure 1. Alternate methods for entering geometry of the structure. XBSEG, ZBSEG, WBSEG, and TBSLOP are names used in IBREAK.

Table 1. Test conditions in Ahrens (1975).

Test No.	Meas R/H	Cot Slope	Wave Height (m)	Wave Period (sec)	Dn(50) (m)	Wave Length (m)
1	0.98	2.5	0.786	2.8	0.167	12.018
2	1.44	2.5	0.646	5.7	0.167	34.559
3	1.21	2.5	0.625	4.2	0.167	23.251
4	1.61	2.5	0.738	8.5	0.167	54.509
5	1.81	2.5	0.811	11.3	0.167	73.867
6	1.62	2.5	0.661	8.5	0.167	54.509
7	1.51	2.5	0.603	5.7	0.167	34.559
8	1.22	2.5	0.555	4.2	0.167	23.251
9	1.01	2.5	0.756	2.8	0.167	12.018
10	1.22	2.5	0.539	4.2	0.167	23.251
11	1.36	2.5	0.744	5.7	0.235	34.559
12	1.61	2.5	0.933	8.5	0.235	54.509
13	1.01	2.5	1.003	2.8	0.235	12.018
14	1.23	2.5	0.792	4.2	0.235	23.251
15	1.69	2.5	1.021	11.3	0.235	73.837
16	1.32	2.5	0.762	5.7	0.235	34.559
17	0.73	3.5	1.155	2.8	0.232	12.018
18	1.06	3.5	1.012	4.2	0.232	23.251
19	1.15	3.5	0.799	5.7	0.232	34.559
20	1.45	3.5	0.920	8.5	0.232	54.509
22	1.56	3.5	1.009	11.3	0.232	73.867
23	1.11	3.5	0.841	5.7	0.232	34.559
24	1.44	3.5	0.896	8.5	0.232	54.509
25	0.91	3.5	0.948	4.2	0.232	23.251
26	1.17	3.5	0.756	5.7	0.232	34.559
27	0.75	3.5	0.859	2.8	0.165	12.018
28	1.06	3.5	0.640	4.2	0.165	23.251
29	1.21	3.5	0.573	5.7	0.165	34.559
30	1.55	3.5	0.640	8.5	0.165	54.509
31	1.78	3.5	0.768	11.3	0.165	73.867
32	1.05	3.5	1.033	5.7	0.272	34.559
33	1.36	3.5	0.969	8.5	0.272	54.509
34	1.50	3.5	1.189	11.3	0.272	73.867
35	0.91	3.5	1.146	4.2	0.272	23.251
36	1.08	3.5	0.902	5.7	0.272	34.559
37	1.42	3.5	0.957	8.5	0.272	54.509
38	0.98	5	0.802	5.7	0.182	34.559
39	1.33	5	0.680	8.5	0.182	54.509
40	0.54	5	1.006	2.8	0.179	12.018
41	0.83	5	0.817	4.2	0.177	23.251
42	1.35	5	0.683	8.5	0.175	54.509
43	1.05	5	0.792	5.7	0.152	34.559
44	1.49	5	0.774	11.3	0.152	73.867
45	0.90	5	0.872	5.7	0.230	34.559
46	1.23	5	0.829	8.5	0.230	54.509
47	1.36	5	0.927	11.3	0.230	73.867
48	1.25	5	0.872	8.5	0.230	54.509
49	0.81	5	1.048	4.2	0.230	23.251
50	0.96	5	0.896	5.7	0.230	34.559

Table 2. Wave runup (R/H) determined by IBREAK for a range of friction coefficients, measured runup, and interpolated friction factor to best fit the measured runup.

Test No.	Friction Coefficients 0.25	0.3	0.35	0.4	0.45	0.5	0.55	0.6	0.65	0.7	0.75	0.8	Interp Friction Coef	Meas R/H
1		1.196	1.157	1.125	1.100	1.074	1.056	1.027	1.010	0.988	0.966		0.718	0.98
2		1.711	1.654	1.604	1.559	1.518	1.482	1.447	1.415	1.387			0.611	1.44
3		1.545	1.489	1.440	1.397	1.359	1.323	1.292	1.263	1.235	1.203		0.739	1.21
4		1.966	1.907	1.858	1.810	1.773	1.734	1.699	1.664	1.633	1.604		0.740	1.61
5		2.007	1.961	1.920	1.881	1.845	1.812	1.780	1.749	1.722			0.553	1.81
6		1.968	1.911	1.867	1.825	1.785	1.746	1.713	1.681	1.649	1.618		0.747	1.62
7		1.731	1.674	1.624	1.579	1.538	1.501	1.467	1.435	1.406			0.538	1.51
8		1.587	1.529	1.480	1.436	1.396	1.360	1.328	1.298	1.270	1.236	1.217	0.792	1.22
9		1.210	1.170	1.136	1.112	1.086	1.060	1.037	1.020	1.004			0.681	1.01
10		1.597	1.539	1.489	1.445	1.405	1.370	1.336	1.307	1.279	1.250	1.220	0.800	1.22
11		1.671	1.614	1.565	1.520	1.480	1.443	1.410	1.378	1.350			0.682	1.36
12		1.871	1.814	1.761	1.714	1.668	1.631	1.591	1.559	1.529			0.576	1.61
13		1.109	1.080	1.055	1.032	1.011	0.990	0.970	0.951	0.937			0.502	1.01
14		1.464	1.414	1.365	1.322	1.285	1.253	1.223	1.193	1.168			0.588	1.23
15		2.014	1.959	1.910	1.865	1.824	1.785	1.750	1.716	1.685			0.692	1.69
16		1.665	1.608	1.558	1.514	1.474	1.437	1.404	1.373	1.344	1.312		0.738	1.32
17		0.790	0.775	0.760	0.745	0.730	0.715	0.702	0.688	0.675			0.500	0.73
18		1.093	1.056	1.023	0.995	0.968	0.944	0.924	0.902	0.881			0.345	1.06
19		1.359	1.308	1.260	1.218	1.180	1.146	1.114	1.086	1.059			0.544	1.15
20		1.569	1.504	1.447	1.399	1.356	1.313	1.276	1.244	1.213			0.397	1.45
22		1.798	1.721	1.654	1.595	1.542	1.494	1.450	1.409	1.374			0.483	1.56
23		1.349	1.295	1.247	1.205	1.168	1.134	1.103	1.075	1.048			0.589	1.11
24		1.576	1.512	1.456	1.405	1.360	1.320	1.283	1.251	1.220			0.416	1.44
25		1.111	1.073	1.039	1.009	0.981	0.960	0.937	0.914	0.893			0.660	0.91
26		1.379	1.323	1.274	1.231	1.193	1.158	1.127	1.097	1.070			0.533	1.17
27		0.861	0.841	0.822	0.804	0.787	0.770	0.753	0.743	0.728			0.615	0.75
28		1.236	1.191	1.149	1.113	1.081	1.054	1.026	1.000	0.977			0.539	1.06
29		1.463	1.404	1.352	1.307	1.266	1.229	1.196	1.165	1.137			0.579	1.21
30		1.718	1.653	1.594	1.543	1.495	1.455	1.416	1.380	1.348			0.443	1.55
31		1.873	1.801	1.736	1.679	1.627	1.581	1.536	1.498	1.461			0.366	1.78
32		1.298	1.247	1.202	1.162	1.127	1.094	1.065	1.037	1.012			0.627	1.05
33		1.556	1.491	1.435	1.387	1.341	1.300	1.266	1.229	1.201			0.479	1.36
34		1.745	1.667	1.599	1.540	1.487	1.439	1.395	1.356	1.319			0.488	1.50
35		1.064	1.029	0.999	0.972	0.947	0.923	0.901	0.881	0.861			0.580	0.91

Table 2 (concluded).

Test No.	Friction Coefficients 0.25	0.3	0.35	0.4	0.45	0.5	0.55	0.6	0.65	0.7	0.75	0.8	Interp Friction Coef	Meas R/H
36		1.331	1.277	1.231	1.190	1.153	1.120	1.089	1.061	1.035			0.616	1.08
37		1.560	1.494	1.437	1.388	1.344	1.305	1.268	1.235	1.203			0.417	1.42
38		1.054	1.012	0.974	0.940	0.909	0.880	0.853	0.827	0.803			0.392	0.98
39		1.354	1.290	1.235	1.187	1.144	1.104	1.069	1.036	1.006			0.319	1.33
40		0.592	0.570	0.549	0.530	0.512	0.494	0.478	0.463	0.448			0.424	0.54
41		0.857	0.829	0.803	0.778	0.755	0.733	0.713	0.693	0.674			0.348	0.83
42		1.353	1.289	1.234	1.186	1.143	1.103	1.068	1.035	1.005			0.302	1.35
43		1.057	1.015	0.977	0.943	0.911	0.881	0.854	0.829	0.805			0.308	1.05
44	1.542	1.464	1.392	1.329	1.275	1.226	1.182	1.143	1.106	1.071			0.283	1.49
45		1.033	0.933	0.957	0.924	0.893	0.864	0.838	0.813	0.786			0.489	0.90
46		1.312	1.250	1.197	1.150	1.108	1.070	1.035	1.003	0.973			0.369	1.23
47		1.402	1.331	1.270	1.217	1.169	1.126	1.087	1.051	1.018			0.330	1.36
48	1.306	1.241	1.182	1.131	1.086	1.046	1.009	0.977	0.946	0.918			0.293	1.25
49	0.814	0.800	0.776	0.752	0.731	0.710	0.690	0.671	0.653	0.636			0.264	0.81
50		1.027	0.987	0.951	0.918	0.888	0.860	0.833	0.808	0.785			0.388	0.96

Table 3. Optimum friction coefficients determined by interpolating IBREA results compared to friction coefficients determined by the empirical equations of Madsen and White (1976).

Test No.	Interp Friction Coef	Eq. 2	Eq. 3
1	0.718	0.605	0.496
2	0.611	0.501	0.435
3	0.745	0.616	0.503
4	0.737	0.392	0.367
5	0.553	0.318	0.316
6	0.745	0.435	0.394
7	0.538	0.511	0.441
8	0.789	0.689	0.544
9	0.681	0.611	0.500
10	0.805	0.708	0.554
11	0.682	0.504	0.439
12	0.576	0.339	0.333
13	0.502	0.503	0.439
14	0.588	0.523	0.451
15	0.692	0.295	0.302
16	0.741	0.506	0.441
17	0.500	0.430	0.393
18	0.345	0.338	0.332
19	0.544	0.395	0.370
20	0.397	0.272	0.285
22	0.483	0.230	0.254
23	0.589	0.388	0.366
24	0.416	0.281	0.292
25	0.660	0.420	0.387
26	0.533	0.410	0.380
27	0.615	0.515	0.443
28	0.539	0.489	0.428
29	0.579	0.479	0.421
30	0.443	0.335	0.328
31	0.366	0.243	0.262
32	0.627	0.348	0.340
33	0.479	0.287	0.297
34	0.488	0.212	0.240
35	0.580	0.362	0.350
36	0.616	0.388	0.367
37	0.417	0.278	0.291
38	0.392	0.303	0.307
39	0.319	0.263	0.278
40	0.424	0.436	0.395
41	0.348	0.349	0.338
42	0.302	0.256	0.272
43	0.308	0.273	0.284
44	0.282	0.197	0.226
45	0.489	0.323	0.322
46	0.369	0.248	0.268
47	0.330	0.201	0.231
48	0.292	0.232	0.256
49	0.279	0.298	0.304
50	0.388	0.294	0.302

Table 4. Pearson correlation coefficients for friction coefficient compared to structure slope, wave steepness, and four relative roughness terms.

	Pearson Correlation Coefficients						
	f_w	$\cot\theta$	H/L	$d_{n(50)}/d$	$d_{n(50)}/L$	$d_{n(50)}/H$	$d_{n(50)}/L_o$
f_w	1.00000	-0.43899	0.82361	-0.07256	0.87023	-0.10664	0.88087

Table 5. Effect of changing thickness of runup film from 6.4 mm to 3.2 mm on IBREAK runup calculations.

Test No.	Friction Coef.	R/H for Thickness of Runup Film: 3.2 mm	6.4 mm	% Greater Runup with 3.2 mm
2	0.65	1.423	1.415	0.57
12	0.60	1.593	1.591	0.13
20	0.40	1.450	1.447	0.21
31	0.40	1.737	1.736	0.06
39	0.35	1.286	1.290	-0.31
47	0.35	1.334	1.331	0.23

SHIELDS PARAMETER IN LOW SUBMERGENCE OR STEEP FLOWS

R.J. Wittler
US Bureau of Reclamation, Denver, USA
S.R. Abt
Colorado State University, Dept. of Civil Eng.,
Fort Collins, USA

INTRODUCTION

Shields parameter is an integral part of riprap design. No other single parameter matches Shields parameter in describing the mechanics of incipient motion, or in riprap terminology, failure. This paper presents three methods for deriving Shields parameter and one method for deriving the boundary or particle Reynolds number. This paper is not a continuation of the spurious correlation argument that seems to arise when discussing Shields parameter. The purpose of this paper is to investigate the behavior of Shields parameter in flow regimes not considered by Shields.

Some investigators assert that Shields parameter is not constant above boundary Reynolds number 10^4. Characteristics of this flow regime are low relative submergence ($d/D_{50} < 5$) and bulked or aerated water. This paper is an attempt to show that Shields parameter is indeed constant in this flow regime.

Background

Shields published "Anwendung der Aehnlichkeitsmechanik und der turbulenzforschung auf die geschiebebewegung: Mitteilung der Preussischen Versuchsanstalt fuer Wasserbau und Schiffbau" in 1936, in the German language. Most papers cite the translated title "Applications of similarity principles and turbulence research to bed-load movements". Quoting from a translation [6], Shields main proposition is:

> "The ratio of the active force of the water parallel to the bed, to the resistance of a grain on the bed is a universal function of the ratio of the grain size to the thickness of the laminar sublayer."

From Gessler [3] the following relationship puts Shields words into mathematical form.

$$T = \frac{\tau_c}{(\gamma_s - \gamma)k} = f_1\left(\frac{k}{\delta_1}\right) = f_2\left(\frac{u_* k}{\nu}\right) \quad (1)$$

T ..... Shields Parameter

τ_c ..... Critical shear stress

γ_s ..... Specific weight of the grain

γ ..... Specific weight of the fluid

δ_1 ..... Thickness of the laminar sublayer

ν ..... Kinematic viscosity

u_* ..... Shear velocity, $u_* = \sqrt{\tau/\rho}$

ρ ..... Density of fluid

τ ..... Bottom shear stress

Shields determined the functions f_1 and f_2 experimentally. Gessler [3] describes the difficulty of defining incipient motion.

> "During the course of the experiments the difficult question of the definition of incipient motion arose; due to various reasons the uniform size grains did not all begin to move at the same time. Shields defined the beginning of motion in the following way: he found in experiments with different bottom shear stresses, that were just above critical, small bedload transport rates per unit time. He extrapolated the function for bedload movement dependent on bottom shear stress obtained in this way in the direction of decreasing bottom shear stress to the point where the bedload transport is zero. He called the corresponding shear stress of this point the "critical shear stress"."

Therefore, in the simplest terms, Shields parameter is a delineator of particle motion and particle stability.

Stevens and Simons [9] analyzed the forces and moments acting on riprap. By balancing the turning forces or moments with the righting forces or moments, they created a stability factor for riprap mixtures based upon a characteristic particle size that was a function of the riprap gradation. A stability factor of 1.0 defines incipient motion. Values less than 1.0 indicate instability and values greater than 1.0 indicate stability. The stability factor functions very much like the safety factors prevalent in engineering design practice. By definition, Stevens and Simons correlate a stability factor of 1.0 to a Shields parameter of 0.047. This

correlation was a convenient method of estimating the forces by water parallel to the bed. Therefore, in more complex terms, Shields parameter is a safety factor.

Shields and others developed data in flows with large relative submergence. The definition of relative submergence, λ_{smb},, is the ratio of water depth to particle size.

$$\lambda_{smb} = \frac{d}{k} \tag{2}$$

d ..... Fluid depth

k ..... Particle size

Stevens and Simons method may be applied to flows that are steep, rough, and with relative submergence much less than tested by Shields. Wittler and Abt [10] show that the stability factor method of Stevens and Simons becomes increasingly conservative as slope increases. Shen [7] [8] proposes that the value of Shields parameter is roughly five times greater at boundary Reynolds numbers greater than 10^4 than the accepted value of 0.047 at boundary Reynolds number $170 < Re_* < 10^4$. This raises the question of the basis of the stability factor, in steep flow conditions, the basis being the value of Shields parameter.

SHIELDS PARAMETER

The following section presents several methods for deriving Shields parameter. Two methods of fractional analysis show that Shields parameter is physically derivable.

Pi

The process for creating dimensionless variable groups is straight forward. The following matrix identifies the pertinent variables.

Variable	Mass	Length	Time
k		1	
g		1	-2
ρ	1	3	
ρ_s	1	3	
u		1	-1

The rank of the matrix is one indicating a single dimensionless variable group.

$$T = f\left(\frac{\rho_w u^2}{\rho_s g k}\right) \Leftrightarrow \frac{\frac{m}{l^3}\frac{l^2}{t^2}}{\frac{m}{l^3}\frac{l}{t^2}l} \tag{3}$$

If u is proportional to u_*, then

$$T = f\left(\frac{\tau}{\gamma k}\right) \tag{4}$$

which is a form of Shields parameter.

Similitude

Similitude is an imaginative comparison of forces, moments, or energy acting on a particle in a flow field. Force similitude is the simplest case, considering magnitude and direction of forces. Moment similitude adds another dimension to force similitude by considering the moment arm through which forces act. Energy supersedes force magnitude and direction by considering potential and mechanical energy.

Forces

There are two primary forces acting on a particle in flowing water: The gravitational force associated with the particle, and the inertial force of the flowing water. The gravitational force is a function of the mass and volume of the particle. The inertial force is a function of the form of the particle, the projected area perpendicular to the direction of flow, and the mass density of the fluid.

$$F_g = mg$$

$$\text{Gravity: } m \propto (\rho_s - \rho)k^3 \tag{5}$$

$$F_g \propto g(\rho_s - \rho)k^3$$

$$F_i = C_d \frac{u^2}{2} A \rho$$

$$\text{Inertia: } A \propto k^2 \tag{6}$$

$$F_i \propto \rho k^2 u^2$$

The velocity term represents the mean local velocity about the particle. The shear velocity, u_*, is proportional to u, so that

$$\frac{F_g}{F_i} \propto \frac{g(\rho_s - \rho)k^3}{\rho k^2 u^2}$$
$$u \propto u_* = \sqrt{\tau/\rho} \tag{7}$$
$$\frac{F_g}{F_i} \propto \frac{(\gamma_s - \gamma)k}{\tau} = \text{constant}$$

The ratio of gravitational and inertial forces is the inverse of Shields parameter. In engineering sense, a safety factor is a ratio of positive to negative. In terms of force, the safety factor is a ratio of the stabilizing or resistive forces to the destabilizing or motivating forces. As shown in Equation 7, Shields parameter is the inverse of a safety factor, if gravitational forces are stabilizing and fluid inertial forces are destabilizing.

Moments

The similitude of moments acting on a particle is very similar to the force similitude. The additional factor in the moment analysis is a moment arm. The line of action of both gravitational and inertial forces is difficult to define. The direction of the gravitational force is well known, but the other component, buoyancy, is not. The line of action of each with respect to the pivot point about which moments are calculated is obviously a factor of the particle diameter, k. The line of action of the inertial components, lift and drag, is even less detectable. However, the line of action must pass within some factor of the particle diameter regardless of the direction of either component.

To write the following equations take the moment about the downstream contact point, and assume that the upstream contact points are zero force at incipient motion.

$$M_g = mgl$$
$$l \propto k$$
$$m \propto (\rho_s - \rho)k^3 \tag{8}$$
$$M_g \propto g(\rho_s - \rho)k^4$$

$$M_i = C_d \frac{u^2}{2} A \rho l$$
$$l \propto k \tag{9}$$
$$A \propto k^2$$
$$F_i \propto \rho k^3 u^2$$

$$\frac{M_g}{M_i} \propto \frac{g(\rho_s - \rho)k^4}{\rho k^3 u^2}$$

$$u \propto u_* = \sqrt{\tau/\rho} \tag{10}$$

$$\frac{M_g}{M_i} \propto \frac{(\gamma_s - \gamma)k}{\tau} = \text{constant}$$

The ratio of the moments causes the extra length dimension to divide out. The same proportionality, which is Shields parameter, therefore exists whether considering ratios of forces or moments. With the uncertainty in direction of forces and lines of action, it helps to explore another facet of the physics of flowing water, a facet that is a scalar, energy.

Energy

The energy required to lift a particle from a position of rest is equal to the potential energy of the particle one particle diameter above it's initial position.

$$E_L = mgk \tag{11}$$

The mass of the particle is equal to the volume times the buoyant mass density of the particle. The volume of the particle is proportional to the diameter cubed. The inertial energy is a function of mass and the local velocity squared.

$$E_L \propto gk(\rho_s - \rho)k^3 = gk^4(\rho_s - \rho) \tag{12}$$

$$E_I = \tfrac{1}{2}mu^2$$

$$E_I \propto (\rho_s - \rho)k^3 u_*^2 \tag{13}$$

Again the assumption is that the shear velocity is proportional to the local particle velocity. The ratio of the inertial energy to the potential energy is Shields parameter.

$$\frac{E_I}{E_L} \propto \frac{\rho k^3 u_*^2}{(\rho_s - \rho)gk^4} = \frac{\tau}{(\gamma_s - \gamma)k} \tag{14}$$

This section shows three methods of deriving Shields parameter. Gessler [2] presents an exhaustive treatise on the derivation of Shields parameter. In following sections the assumptions made in the derivations will help explain the behavior of Shields parameter in flows of boundary Reynolds number greater than 10^4. The next section derives the boundary Reynolds number.

BOUNDARY REYNOLDS NUMBER

Like Shields parameter, the boundary or particle Reynolds number is the ratio of two forces. In this case the two forces are the inertial and viscous forces.

$$F_I \propto \rho k^2 u^2$$
$$F_V \propto k u^2 \mu \frac{du}{dy} \tag{15}$$

Again the assumption is that the shear velocity approximates the local velocity. Also, the differential $\frac{du}{dy}$ is proportional to $\frac{u_*}{k}$. Following these two assumptions, the boundary Reynolds number, Re_* results.

$$\frac{F_I}{F_V} \propto \frac{\rho k^2 u^2}{k^2 \mu \frac{du}{dy}} = \frac{u^2}{\mu \frac{du}{dy}}$$
$$\frac{F_I}{F_V} \propto \frac{u_* k}{\nu} \tag{16}$$
$$\therefore Re_* = \frac{u_* k}{\nu}$$

This completes the background of Shields parameter, T, and the boundary Reynolds number, Re_*. The functional relationship between Shields parameter and the boundary Reynolds number is usually presented in graphical form, Shields diagram.

SHIELDS DIAGRAM

Shields published a diagram [6] showing a functional relationship between what he described as a dimensionless shear stress and the particle Reynolds number. The curve was added later by Rouse [5]. The original curve plots a constant Shields parameter, T_c, of 0.06 at $Re_* > 10^4$. This value is based upon Shields definition of incipient motion, that is zero bedload. Gessler proposes that the correct value of T_c is 0.047. The basis of this assertion is that Shields neglected to account for shear stress due to form drag from ripples and bed forms, thus over estimating the value of the parameter. Therefore, Gesslers correction is based upon a different definition of incipient motion. Gesslers definition [3] is that the particle has a fifty percent probability of motion. Figure 1 shows Shields diagram as corrected by Gessler. The Stability Factors riprap design procedure [9] is based upon the corrected value of T_c.

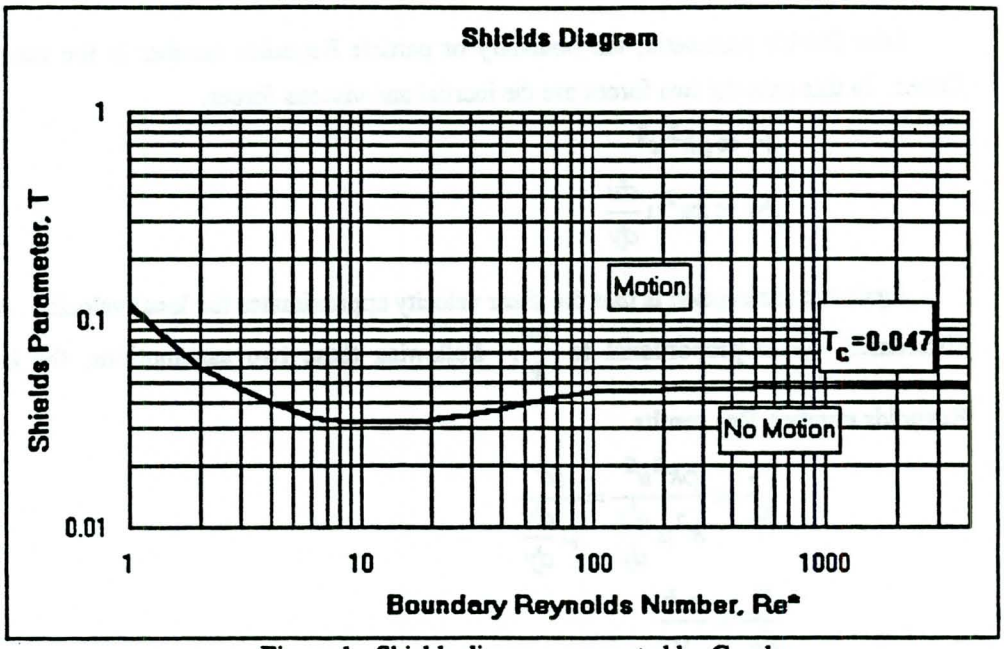

Figure 1. Shields diagram, corrected by Gessler.

BEHAVIOR OF SHIELDS PARAMETER AT $Re_* > 10^4$

Background

Shields diagram can be divided into two phases. The first phase is characterized by the non-constant value of Shields parameter and corresponds to the laminar boundary layer regime characterized by boundary Reynolds number less than roughly 200. The second phase is the range characterized by boundary Reynolds number greater than 200. In this range, the value of Shields parameter is thought to be constant. Shen and others propose that a third phase exists. In this range of boundary Reynolds number greater than 10^4 Shen proposes that the constant value increases from 0.06 (corrected to 0.047 by Gessler) to 0.25, and then remains constant. If riprap design procedures such as Stability Factors are to be applied in steep, low submergence flow regimes, then the knowledge of the behavior of Shields parameter in this type of flow is critical. Two researchers have reported values of Shields parameter much greater than 0.047 in the region where $Re_* > 10^4$.

Shen

Shen and Wang [7] [8] propose that Shields parameter achieves a constant value of 0.25 at $Re_* > 10^4$. They base this proposition on data collected in China in flood channels. The

mean relative submergence of the tests by Shen and Wang is 7.9 and the average energy slope is .047, or 4.7 percent. Shen and Wang explain the increase in Shields parameter as a drag reduction effect. They base their proposition on the drag reduction that occurs at Reynolds number of 10^5 to 10^6. Schlicting [4] reports the drag reduction phenomenon. The median stone size is the basis for k in calculations of Shields parameter. Depth and slope measurement techniques are undocumented.

Abt et al

Abt et al [1] achieved similar results for a wide variety of median riprap sizes and slopes. They report maximum Shields parameter values of 0.12. The median stone size is the basis for k in calculations of Shields parameter. Median rock sizes include 1, 2, 3, 4, and 6 inches. Bed slopes tested include 1%, 2%, 5%, 10%, 15%, and 20%. Relative submergence ranges from 0.48 to 2.01. They report highly aerated flow, periods of instability followed by periods of stability, and ultimate failure of the riprap blanket. Depth is piezometric head measured at the filter-riprap interface corrected to the virtual riprap surface.

Rationale for a Two-phase Shields Parameter

The following sections each address reasoning supporting a two-phase Shields parameter. The basis for analyzing Shields parameter in the large boundary Reynolds number range are the assumptions made in the derivation of Shields parameter and making hypothetical modifications to the force, moment, or energy ratios.

Aeration-Bulking

Aeration or bulking is the process of ingesting air into flowing water. Air is ingested by a mechanism related to the momentum and viscosity of the air-water interface. The practical effect of aeration is an inflated depth of flow and a deflated fluid density. Equation 7 facilitates a hypothetical demonstration of the effects of aeration upon Shields parameter.

$$\frac{F_g}{F_i} \propto \frac{g(\rho_s - \rho)k^3}{\rho k^2 u^2}$$

$$u \propto u_* = \sqrt{\tau/\rho} \qquad (7)$$

$$\frac{F_g}{F_i} \propto \frac{(\gamma_s - \gamma)k}{\tau} = \text{constant}$$

The gravitational force has four components: gravitational acceleration, g, particle mass density, ρ_s, and the . Gravitational acceleration is unaffected by aeration as is the particle

size and particle mass density. Therefore, in the numerator of the force ratio, only the mass density of the fluid is effected by aeration.

The inertial force has three components: fluid mass density, ρ, particle size, k, and the local velocity, u. The particle size is unaffected by aeration. Local velocity may be effected but it is unclear whether aeration increases or decreases the local velocity. The effect of aeration upon velocity is neglected. Only fluid mass density is effected, therefore, by aeration, in the inertial force.

A simplified form of equation 7 shows the modified factors.

$$T_a \propto \frac{(\rho_s - \rho_a)}{\rho_a}$$

$$\rho_a = \text{aerated fluid mass density} \qquad (7.a.)$$

$$T_a = \text{aerated Shields parameter}$$

Let's assume that the air water mixture is 50% air and 50% water.

$$\frac{T_a}{T} = \frac{\dfrac{(\rho_s - \rho)}{\rho}}{\dfrac{\rho_s - \rho_a}{\rho_a}} \qquad (17)$$

$$\frac{T_a}{T} = \frac{\dfrac{(2.65-1)}{1}}{\dfrac{2.65-.5}{.5}} \qquad (18)$$

$$\frac{T_a}{T} = 0.384$$

The result of equation 18 shows that aeration reduces the value of Shields parameter. Clearly, aeration is not a rationale for asserting that Shields parameter increases in any range of boundary Reynolds number.

One effect that aeration has on Shields parameter is the determination of measured factors in laboratory or field measurements. The final form of Shields parameter demonstrates the errors that can creep into field or laboratory measurements.

$$T = \frac{\tau}{(\gamma_s - \gamma)k} = \frac{\gamma RS}{(\gamma_s - \gamma)k} \qquad (19)$$

Again, assuming a 50%-50% air-water mixture, let's examine the effect upon measuring Shields parameter.

In aerated flow, fluid unit weight, γ, is overestimated. It is common to assume that γ has a value of 62.4 pcf, when in actuality, in a 50% air-water solution, it is 31.2 pcf, an error factor of two. The hydraulic radius is similarly overestimated by a factor of two. Meanwhile, the buoyant weight of the particle is underestimated by a factor of 1.3. Therefore, the overall error results in overestimating Shields parameter by a factor of 5.21.

$$T = \frac{\tau}{(\gamma_s - \gamma)k}$$

$$\tau = \gamma RS$$

$$\frac{T}{T_a} = \frac{\dfrac{\gamma RS}{(\gamma_s - \gamma)k}}{\dfrac{\gamma_a R_a S}{(\gamma_s - \gamma_a)k}}$$

$$\frac{T}{T_a} = \frac{\dfrac{62.4(2R)S}{62.4(2.65-1)k}}{\dfrac{31.2RS}{62.4(2.65-0.5)k}} = 5.21 \qquad (20)$$

Recall that Shen reported a four-fold increase in the apparent value of Shields parameter, while Abt reported a two-fold increase using piezometric depth, negating the illusory hydraulic radius factor.

Coefficient of Drag

Recall that Shields parameter is the inverse of the ratio of the gravitational and inertial forces. Or more simply, Shields parameter is the ratio of the inertial and gravitational forces.

$$\frac{F_g}{F_i} \propto \frac{g(\rho_s - \rho)k^3}{\rho k^2 u^2}$$

$$u \propto u_* = \sqrt{\tau/\rho} \qquad (7)$$

$$\frac{F_g}{F_i} \propto \frac{(\gamma_s - \gamma)k}{\tau} = \text{constant} = 1/T$$

The numerator of Shields parameter then is an expression of the inertial force, that before any assumptions is a product of velocity squared, area, fluid density and a coefficient of drag, C_d. Shen bases the increase in Shields parameter upon a corresponding decrease in C_d, as

previously noted by Schlicting. But if C_d decreases, then the numerator of Shields parameter decreases, and therefore, Shields parameter decreases.

$$F_i = C_d \frac{u^2}{2} A \rho \tag{6a}$$

Therefore, drag reduction is not a rationale for asserting that Shields parameter increases in the range of boundary Reynolds number greater than 10^4.

Steep Slope: S or $\sin\theta$?

Engineers often assume the bottom tractive force, or shear stress, τ, to be equal to the unit weight of water, γ, times the hydraulic radius, R, or depth, d, times the slope, S.

$$\tau = \gamma R S \tag{21}$$

The basis of equation 21 rests upon the following assumptions: Normal depth of flow, wide channel such that the hydraulic radius is roughly equal to the depth, and a shallow slope such that S is roughly equal to $\sin\theta$. The tractive force is the resolved weight of a control volume of water. The volume has an area in contact with the wetted perimeter, p, with dimension pl, where l is a unit distance in the stream wise direction while p is perpendicular to the flow. The thickness of the volume is the depth, that is perpendicular to the bed, d. The bed slopes at an angle θ. The flow is uniform so that the hydrostatic forces at the upstream and downstream ends of the control volume negate each other.

$$\begin{aligned} w &= \text{control volume width} \\ A &= wd \\ \tau &= \frac{\gamma A l}{pl} \sin\theta = \gamma R \sin\theta \end{aligned} \tag{22}$$

The basis of τ is the assumption that $\sin\theta$ is roughly equal to S. This assumption is accurate to less than one percent until the slope exceeds roughly 0.15 or fifteen percent. On embankments where slopes approach 33% the error can accumulate quickly.

Relative Submergence

The assumption that the local velocity, u, is proportional to the shear velocity, u_*, bears further investigation. Gessler [2] states "Some of the discussion about effect of relative depth on incipient motion probably reflects the fact that introducing mean velocity instead of shear velocity necessarily leads to such an apparent effect." Shear velocity, u_*, and mean velocity, u, are related by the log-velocity law.

$$\frac{\bar{u}_y}{u_*} = 5.75 \log_{10}\left(30.2 \frac{yx}{k}\right) \tag{23}$$

The logarithmic term contains a relative submergence term, y/k. The effects of relative submergence are not clear. However, in an intuitive sense, the radically differing regimes of flow between Shields and steep, air-entrained, low submergence flows, suggests that some effect may exist. Shields tested millimeter sized materials in flows with slope less than one-hundredth of one percent and greater than a meter in depth. Shen and Abt tested flows with slopes three orders of magnitude greater, material sizes two and one-half orders of magnitude greater, and relative submergence three orders of magnitude greater than Shields. Even though Shields parameter is based upon ratios of forces, the assumptions that allow simple quantification of those forces may not apply to these vastly different regimes of flow.

CONCLUSIONS

The purpose of this paper is to investigate the behavior of Shields parameter at boundary Reynolds number greater than 10^4. The hypothesis of this paper is that Shields parameter is constant in this flow regime. Investigation of the background and derivation of Shields parameter show that there is no reason to expect Shields parameter to increase, and indeed it is more likely that Shields parameter decreases in this regime. The apparent and reported increase in Shields parameter is the result of measuring flow properties upon which Shields parameter calculations are based.

REFERENCES

1. Abt, S.R., Wittler, R.J., Ruff, J.F., LaGrone, D.L., Khattak, M.S., Nelson, J.D., Hinkle, N.E., Lee, D.W., Development of Riprap Design Criteria by Riprap Testing in Flumes: Phase II. Followup Investigations. U.S. Nuclear Regulatory Commission, NUREG/CR-4651, ORNL/TM-10100/V2, Vol. 2. September, 1988.

2. Gessler, J., Beginning and Ceasing of Sediment Motion, River Mechanics, Vol. I., Chapter 7. Edited & Published by H.W. Shen, P.O. Box 606, Fort Collins, CO 80521. 1971.

3. Gessler, J., The Beginning of Bedload Movement of Mixtures Investigated as Natural Armoring in Channels. W.M. Keck Laboratory of Hydraulics and Water Resources, California Institute of Technology, Pasadena, California. 1965-67.

4. Schlicting, H., Boundary Layer Theory. Translated by Dr. J. Kestin, Sixth Ed., McGraw-Hill, New York. 1968. pp. 17.

5. Sedimentation Engineering, ASCE-Manual and Reports on Engineering Practice-No. 54. Edited by Vito A. Vanoni, prepared by the ASCE Task Committee for the Preparation of the Manual on Sedimentation of the Sedimentation Committee of the Hydraulics Division. ASCE, New York, New York. 1975. pp. 97.

6. Shields, Anwendung der Aehnlichkeitsmechanik und der turbulenzforschung auf die geschiebebewegung: Mitteilung der Preussischen Versuchsanstalt fuer Wasserbau und Schiffbau, Heft 26, Berlin.

7. Shen, H.W. and Wang, S., Analysis of Commonly Used Riprap Design Guides Based on Extended Shields Diagram. Second Bridge Engineering Conference, Vol. 2, Transportation Research Record 950, Transportation Research Board, National Research Council, Washington D.C. 1984. pp. 217-221

8. Shen, H.W. and Wang, S., Incipient Sediment Motion and Riprap Design. Journal of Hydraulic Engineering, ASCE, Vol. 111, No. 3, March, 1985. pp. 520-538.

9. Stevens, M.A. and Simons, D.B., Stability Analysis for Coarse Granular Material on Slopes, River Mechanics, Vol. I, Chapter 17. Edited & Published by H.W. Shen, P.O. Box 606, Fort Collins, CO 80521. 1971.

10. Wittler, R.J. and Abt, S.R., Riprap Design by Modified Safety Factor Method, Hydraulic Engineering, Proceedings of the 1988 National Conference, ASCE. Edited by S.R. Abt and J. Gessler, ASCE, New York, New York. pp. 143-148.

SLOPE INSTABILITY DUE TO WAVE-INDUCED LIQUEFACTION IN THE SEABED

K. Zen and H. Yamazaki
Port & Harbour Research Institute, Negase,
Yokosuka, Japan

1. INTRODUCTION

The interaction between propagating ocean waves and seabed has received extensive attention in the field of offshore engineering. The wave-induced liquefaction in porous seabed is one of the significant subjects in considering the stability of offshore structures, since the liquefaction, if it happens, may cause severe damage to offshore structures such as breakwaters, platforms, pipelines and anchors. Furthermore, wave-induced liquefaction is said to be closely related to the scour, rittoral drift and settlement of concrete blocks. Authors (Zen and Yamazaki, 1990a, 1990b, 1991) have already reported that the wave-induced liquefaction easily occurs in actual permeable seabed. They have proposed a procedure to estimate the liquefaction potential on the basis of the laboratory experiment and field observation.

This paper presents a case study on the slope instability of a detached breakwater composed of rock materials, with regards to the wave-induced liquefaction and strength reduction of seabed at the toe of the slope. The wave characteristics, such as wave height and wave period, in front of the slope are statistically evaluated from the observed field wave data. The soil profiles of seabed are modeled with the results of soil investigation and laboratory test. The depths and areas of the liquefaction are numerically calculated. Then, the circular failure analysis was performed to check the safety factor. In this case study, it is demonstrated that the liquefaction in the seabed is very critical against the slope stability of offshore rock structures. A practical procedure for design taking account of the wave-induced liquefaction is presented.

2. THEORETICAL BACKGROUNDS

2.1 Liquefaction Criteria

When the water level is subjected to a rapid change from the initial still water level in accordance with wave propagation, the total stress variation is induced in the deposit. Provided that the pore pressure change from the initial state of the hydro-static pressure in the seabed, $p(z,t)$, is not equal to the pressure change imposed on the seabed surface, $p(0,t)$, the vertical total stress, $\sigma_v(z,t)$, and the pore pressure, $u(z,t)$, in the seabed are given by the following equations, respectively:

$$\sigma_v(z,t) = \sigma_v(z,0) + p(0,t) \tag{1}$$

$$u(z,t) = u(z,0) + p(z,t) \tag{2}$$

where $\sigma_v(z,0)$ is the initial vertical total stress and $u(z,0)$ is the initial pore water pressure. The wave-associated pressures are positive in the direction to which they increase from the initial hydro-static pressure. The vertical effective stress in the seabed, $\sigma'_v(z,t)$, can be derived by subtracting **Eq.(2)** from **Eq.(1)** and setting $\sigma'_v(z,0) = \sigma_v(z,0) - u(z,0)$:

$$\sigma'_v(z,t) = \sigma'_v(z,0) + \{p(0,t) - p(z,t)\} \tag{3}$$

The effective stress change, $\Delta\sigma'_v(z,t)$, is obtained from

$$\Delta\sigma'_v(z,t) = p(0,t) - p(z,t) \qquad (4)$$

Since the pore pressure change, p(z,t), is to be equal to the wave-associated water pressure on the seabed surface, p(0,t), under steady state condition, the difference can be thought to represent an 'excess' component of the pore pressure in the seabed. The excess pore pressure, $u_e(z,t)$ is defined as:

$$u_e(z,t) = -\{p(0,t) - p(z,t)\} \qquad (5)$$

The effective stress variation, $\Delta\sigma'_v(z,t)$ is caused by this excess pore pressure, $u_e(z,t)$. It is noted that no effective stress variations are produced in case the values of p(0,t) and p(z,t) are identical with each other.

The schematic drawings of the pore pressure and effective vertical stress distributions are illustrated in **Fig.1**. The solid curves in **Fig.1(a)** indicate the pore pressure beneath a wave trough and a wave crest. The excess pore pressure expressed by **Eq.(5)** is transient in nature, because the p(0,t) and p(z,t) are oscillatory and periodical in real ocean environment. Consequently, the effective vertical stress expressed by **Eq.(3)** varies periodically in accordance with the change of the {p(0,t)-p(z,t)}. If it attains zero or less at certain depths, the soil skeleton will become a liquefied state there. Thus, the criterion for the wave-

induced liquefaction is easily derived from **Eq.(3)** by setting the vertical effective stress, $\sigma'_v(z,t)$, equal to zero or less:

$$\sigma'_v(z,0) \leq -\{p(0,t) - p(z,t)\} = u_e(z,t) \qquad (6)$$

The solid curves in **Fig.1(b)** show the vertical effective stress distribution drawn by replacing the $\sigma'_v(z,0)$ with $\gamma' z$, {where γ' is the submerged unit weight of deposit. The numbered ① and ② in **Fig.1(b)** correspond to ones numbered ① and ② in **Fig.1(a)**, respectively. In **Fig.1(b)**, the liquefied zone shown by the slant lines where the vertical effective stress becomes zero or less appears near the seabed surface, under wave trough. As the excess pore pressure is positive in this situation, the transient upward seepage flow is generated toward the seabed surface. From another point of view, the liquefaction, namely quick sand, is considered to be induced by the seepage force exerted on the soil skeleton in the seabed.

Whereas, if the vertical effective stress variation, $\Delta\sigma'_v(z,t)$, reaches positive values, say it exceeds the initial vertical effective stress, $\sigma'_v(z,0)$, as shown by the line numbered ② in **Fig.1(b)**, the wave-induced stress exerts a force on the soil skeleton to possibly densify the seabed.

As stated above, the wave-induced liquefaction is governed by the initial vertical effective stress at calm sea, $\sigma'_v(z,0)$, and the oscillatory excess pore pressure,

$-\{p(0,t)-p(z,t)\}$. So, the $\sigma'_v(z,0)$, $p(0,z)$ and $p(z,t)$ are expressed for convenience as: $\sigma'_v(z,0)=\sigma'_{vo}$, $p(0,t)=p_b$ and $p(z,t)=p_m$, hereafter.

2.2 Oscillatory Pore Pressure

Considering a soil element at depth, z, in the seabed and assuming the flow of pore water in the soil element is governed by the steady state form of Darcy's law, Eq.(7) is derived from the conservation of mass of pore water:

$$\frac{k}{\gamma_w}\frac{\partial^2 p_m}{\partial z^2} = -m_v\frac{\partial \sigma'_v}{\partial t} + n\,m_v\frac{\partial p_m}{\partial t} \qquad (7)$$

where, k; the coefficient of permeability, m_v;the coefficient of volume compressibility, n;the porosity, m_w;the compressibility of pore water, γ_w;the unit weight of pore water and t;time. The k and m_v are assumed constant irrespective of time and space. As the effective vertical stress is expressed by Eq.(3) and $\partial\sigma'_{vo}/\partial t$ is equal to 0, we obtain,

$$\frac{\partial \sigma'_v}{\partial t} = \frac{\partial (p_b - p_m)}{\partial t} \qquad (8)$$

which may be introduced into Eq.(10) to yield:

$$\frac{k}{\gamma_w m_v}\frac{\partial^2 p_m}{\partial z^2} = \left(1 + \frac{n\,m_w}{m_v}\right)\frac{\partial p_m}{\partial t} - \frac{\partial p_b}{\partial t} \qquad (9)$$

Replacing,

$$C_v = \frac{k}{\gamma_w\, m_v} \qquad (10)$$

$$\alpha = 1 + \frac{n\, m_w}{m_v} \tag{11}$$

Eq.(9) may be written in the form:

$$C_v \frac{\partial^2 p_m}{\partial z^2} = \alpha \frac{\partial p_m}{\partial t} - \frac{\partial p_b}{\partial t} \tag{12}$$

where the C_v is the coefficient of consolidation and the α is a parameter which controls the water pressure propagation. In that sense, the α is referred to as the coefficient of propagation, hereafter. The α is represented by the following equation:

$$\alpha = 1 + \frac{n}{m_v}\left(m_{wo} S_r + \frac{1 - S_r}{p_{mg}}\right) \tag{13}$$

where the m_{wo} is the compressibility of pore water at fully saturated state, the S_r is the degree of saturation and the p_{mg} is the pore pressure by means of absolute value.

The boundary conditions and initial condition are written as:

$$p_m = p_b \qquad \text{at} \quad z = 0 \tag{14}$$

$$\frac{\partial p_m}{\partial z} = 0 \qquad \text{at} \quad z = \ell \tag{15}$$

$$p_m = 0 \qquad \text{at} \quad t = 0 \tag{16}$$

where the ℓ is the thickness of permeable seabed.

It is noted that the p_m does not mean the 'excess' pore pressure but denotes the oscillatory nature of pore pressure. The governing equation on the excess pore pressure is derived from Eq.(12) by using Eq.(5):

$$C_v \frac{\partial^2 u_e}{\partial z^2} = \alpha \frac{\partial u_e}{\partial t} + (\alpha - 1) \frac{\partial p_b}{\partial t} \qquad (17)$$

When the compressibility of pore water is negligible, say the coefficient, α, is equal to 1.0, Eq.(17) becomes identical with the consolidation equation.

3. VERIFICATION OF THEORY WITH FIELD DATA

3.1 Propagation Characteristics of wave-associated Pressures

In the derivation of **Eq.s(1) and (2)**, the wave-associated pressures on the seabed surface were assumed not to propagate fully into the seabed. **Fig.2** shows the relationship between the pressure ratio, p_b/p_m, and the wave period, T, at the non-dimensional depth of $z/l \fallingdotseq 0.45$ (Zen and Yamazaki, 1990a). It is found from **Fig.2** that the p_b/p_m is strongly dependent of the wave period. The ratio

becomes (less than 1.0) in proportion to the decrease of wave period. This means that the ~~wave-associated~~ water pressure (induced) by the rapid lowering of water level does not propagate completely into the seabed.

3.2 Comparison of Oscillatory Pore Pressures

The oscillatory pore pressure in the seabed, p_m, is one of the dominant factors in evaluating the liquefaction potential. In order to examine the validity of the governing equation expressed by **Eq.(12)**, the theoretical results are compared with the observed data. The details of the field observation are presented elsewhere (Zen and Yamazaki, 1991). The input data for the analysis are tabulated in **Table 1**. The coefficient of consolidation, C_v, was determined from the permeability, k, and the coefficient of compressibility, m_v, which were measured in the laboratory with Hazaki sand taken from the observation site. The coefficient of propagation, α, was decided from the laboratory model test using the same sample

(Zen and Yamazaki, 1991).

In the solution of Eq.(12), the finite difference technique is adopted (Zen and Yamazaki, 1990b). As the wave-associated bottom pressure has irregular forms, the observed p_b is directly introduced into Eq.(12) as the surface boundary condition. The thickness of permeable layer, ℓ, is determined by calculating the minimum depth below which the effect of the thickness on the p_m distribution disappears. The thickness thus obtained was 2.3 m.

Fig.3 shows the comparisons of the trains of the oscillatory pore pressures and vertical effective stress ratios between the theory and observation. Fig.4 shows the comparison of the distribution curves of the oscillatory pore pressures between the theory and observation at the typical phases of the period of a wave. The theoretical results shown in Figs.3 and 4 indicates that the proposed equation can successfully estimate the oscillatory pore pressures and effective stress variations in the seabed.

3.3 Occurence of Liquefaction

The maximum oscillatory excess pore pressures, u_{emax}, are presented in Fig.5 to compare with the vertical effective stress at calm, σ'_{vo}. According to the liquefaction criterion expressed by Eq.(6), the liquefaction is considered to occur at the depths where the u_{emax} exceeds the σ'_{vo}. Fig.5(a) is an example of the results in which no liquefaction is observed, because the oscillatory excess pore pressures are less than the σ'_{vo}. Whereas, in Fig.5(b) the oscillatory excess pore pressures to Wave: Nos.27 28, 29 and 30 exceed the σ'_{vo}. This demonstrates that the liquefaction ~~takes place~~ has occurred near the surface of the seabed.

3.4 Liquefaction due to Seepage Flow

The wave-induced liquefaction in the seabed is closely related to the transient seepage flow. The seepage force, j, the hydraulic gradient, i, and the flow velocity, v, are respectively given by Eqs. (18) to (20):

$$j = -\frac{\partial p_m}{\partial z} \tag{18}$$

$$i = \frac{j}{\gamma_w} \tag{19}$$

$$v = \frac{kj}{\gamma_w} \tag{20}$$

Therefore, the j, i and v are easily calculated from the distribution curves of the oscillatory pore pressure, p_m. The solid circles shown in Fig. 6 are calculated from the curve numbered d in Fig. 4 which reveals the most rapid reduction of the p_b (see the wave form of the p_b in Fig. 4). The hydraulic gradient and seepage force become remarkably large near the seabed surface. Especially, the hydraulic gradient attains more than 1.0 in absolute value near the surface of the seabed. This upward seepage flow is considered to cause the quick sand, (that is) the liquefaction, in the seabed. The liquefaction near the seabed surface creates a large potential for the transportation of suspended sand particles. This has been actually confirmed by the field measurement done by Tsuruya and Korezumi(1990). Meanwhile, the flow velocity in Fig. 6 appears too small to bring about {boiling} of the liquefied sand deposit. The flow velocity of the suspension in the liquefied zone might be far more larger than that evaluated from Darcy's law.

The increment of the vertical effective stress is represented under one dimensional conditions by:

$$\frac{\partial \sigma_v'}{\partial z} = j + \gamma' \qquad (21)$$

The vertical effective stress is derived by integrating **Eq.(21)**:

$$\sigma_v' = \int_0^z j \, dz + \gamma' z \qquad (22)$$

where γ' is the submerged unit weight of deposit. **Eq.(22)** is equivalent to **Eq.(3)** when the σ'_{vo} is identical with $\gamma' z$. Both the vertical effective stresses obtained from **Eqs.(3) and (22)** are drawn in **Fig.6** in which the solid line is estimated from **Eq.(3)** and the open circles are calculated from **Eq.(22)**. In either cases, the vertical effective stresses compare quite well with each other. Thus, it can be concluded that the wave-induced liquefaction is a kind of quick sand caused by the transient seepage flow induced by ocean waves.

4. PROCEDURE FOR ASSESSING LIQUEFACTION POTENTIAL

4.1 Two Types of Liquefaction

Wave-induced liquefaction is classified into two categories by the mechanism of the excess pore pressure build-up (Zen and Yamazaki, 1990a). The differences of the excess pore pressure are schematically illustrated in Fig. 7. Liquefaction due to the oscillatory excess pore pressures occurs transiently and appears periodically so many times during a storm wave, responding to each wave. Whereas, liquefaction due to the residual nature of excess pore pressures (referred to as the residual excess pore pressure in Fig. 7), happens at once after certain numbers of cyclic wave loading. This type of liquefaction is similar to that induced by earthquakes in the mechanism of the excess pore pressure build-up. The total excess pore pressure to cause liquefaction should be the superposition of both the oscillatory and residual excess pore pressures. In this study, however, only liquefaction (caused by) (oscillatory excess pore pressure is treated. The liquefaction due to residual excess pore pressure is reported elsewhere (Zen et al., 1986).

4.2 Influential Factors on Liquefaction

The wave-associated pressures on the seabed surface can be evaluated using the linear wave theory, (by) (in which a) (small amplitude of waves is assumed. This assumption has been used in most of previous works (Henkel, 1970; Bjerrum, 1973 among others). The linear wave theory gives the wave-associated pressure, p_b, (on the seabed surface) as:

$$p_b = p_o \sin\left(\frac{2\pi}{L}x - \frac{2\pi}{T}t\right) \qquad (23)$$

where the amplitude of the bottom pressure, p_o, is:

$$p_o = \left(\frac{\gamma_w H}{2}\right) \frac{1}{\cosh(2\pi h/L)} \qquad (24)$$

γ_w ; the unit weight of water, h; the water depth, H; the wave height, T; the wave period, L; the wave length, t; time and x; the coordinate axis in the direction of the progress of waves.

Referring to Eqs.(7), (23) and (24), the influential factors on the oscillatory pore pressure, p_m, are expressed by a function, F:

$$p_m = F(H, L, T, m_v, k, n, \gamma_w, m_w, h, z, l, t, S_r, N_c) \qquad (25)$$

Among these factors, the H, L, T and N_c are the factors depending on the wave characteristics. The m_v and n are ones related to the soil properties, and the γ_w and m_w depends on the properties of pore water. The h, l and z are the geometrical factors. The k and S_r are related to the properties both of soils and pore water. Although the number of waves, N_c, is not included in Eq.(7), it is an important factor to be considered.

When a small amplitude of waves is assumed and non-dimensional parameters expressed by Eqs.(26) to (29) are introduced:

$$\bar{P} = \frac{p_m}{p_o} \qquad (26)$$

$$\bar{Z} = \frac{z}{\ell} \quad (27)$$

$$\bar{T} = \frac{t}{T} \quad (28)$$

$$C = \frac{C_v T}{\ell^2} \quad (29)$$

Eq.(12) is rewritten in the form:

$$C \frac{\partial^2 \bar{P}}{\partial \bar{Z}^2} = \alpha \frac{\partial \bar{P}}{\partial \bar{T}} - 2\pi \cos(2\pi \bar{T}) \quad (30)$$

Therefore, Eq.(25) can be represented by the following function, G:

$$\bar{P} = G(\bar{T}, \bar{Z}, C, \alpha, N_c) \quad (31)$$

When the $\bar{T}$ and $\bar{Z}$ are given, the influential factors on the $\bar{P}$ are represented in terms of the C, α and N_c. According to the laboratory model tests, the effect of the N_c on the $\bar{P}$ was so small as to be disregarded (Zen et al., 1987) .

4.3 Evaluation Procedure

The liquefaction criteria expressed by Eq.(6) includes three parameters; the wave-associated pressure at the seabed surface, P_b, the oscillatory pore pressure (P_m) and the effective vertical stress at calm sea (σ'_{vo}). These parameters can be assessed by the procedure presented in Fig.8 . As the waves are irregular in their forms in real ocean, it is quite difficult to determine the forms in advance. So, the small amplitude of waves is assumed as a first approximation. The wave height, wave period and wave length during a storm are estimated statistically every one or two hours with data collected by observation or by wave hindcasting.

Introducing wave characteristics and the water depth into Eqs.(23) and (24), the p_b is evaluated. The p_b is used for the calculation of the p_m as a boundary pressure condition. The coefficient of drainage, C, and the coefficient of propagation, α, are determined from the laboratory tests performed by using the sample taken from the site. The p_m is calculated using Eq.(12) or Eq.(30) by giving the p_b or p_o, C, α and ℓ. When the p_b and p_m are obtained, the oscillatory excess pore pressure, u_e, is calculated by Eq.(5). The liquefaction is assessed by Eq.(6) by comparing the oscillatory excess pore pressure with the effective vertical stress at calm sea.

4.4 Application to Practical Problem

An extensive local scour at the edge of a detached breakwater foundation has been observed. A large number of concrete blocks, which had composed the detached breakwater in Niigata coast, were found widely and deeply spread in the seabed. These phenomena are supposed closely related to the wave-induced liquefaction of seabed sands, because once liquefaction occurs in the seabed, the seabed loses its shear strength and suspended sand particles are very easily transported by currents.

The procedure presented in the previous section was applied to the evaluation of the liquefaction potential in a permeable seabed beneath detached breakwaters shown in Fig.9 . The p_b is estimated from the wave characteristics observed near the site using the linear wave theory. The p_m is calculated from Eq.(12). and the liquefaction depth is assessed by using Eq.(6). The input data for the analysis are: the wave height, H_{max}, is 7.2m, the wave period, T, is 11.8s, (the water depth, h, is 8.5 m,) the coefficient of propagation, α, is 2.0, the coefficient of consolidation, C_v, is $0.71 m^2/s$, the submerged unit weight of deposits is 0.9 t/m^3 and the thickness of permeable seabed is 20.5m.

Fig.10 shows the oscillatory excess pore pressures and the effective vertical stresses beneath the toe and center of the breakwater. It is obvious from Fig.10 that the liquefaction occurs at the toe. No liquefaction, however, takes place in the seabed beneath the center of the breakwater because of the large overburden pressure produced by the rubble mound. (Fig.11 denotes the liquefied zone in the seabed in front of the breakwater. The liquefaction depth at the toe attains 1.25m in maximum under wave trough. Fig.12 shows

the circular failure of the sloping breakwater after liquefaction. The safety factor during calm sea was more than 1.3, but it decreases to 0.90 due to the liquefaction in seabed sands. The submergence of concrete blocks into the seabed reported so far can be attributed to such a liquefaction-related instability of seabed.

The liquefied zone shown in Fig.11 is computed for only one wave. Provided that the liquefied sand particles are completely transported after the liquefaction and no sand particles are supplied there, the scoured area gradually spreads widely and deeply in the seabed until no liquefaction occurs in the seabed. Thus, the wave-induced liquefaction is considered one of the significant reasons related to the scouring of seabeds. The accuracy of the existing estimation methods of scouring zone will be improved if the transport mechanics of liquefied sand particles are properly evaluated.

Fig.13 is the relationship between the wave height H and maximum liquefied depth dl. The depth increases when the wave height becomes larger. No liquefaction, however, occurs in this case study in case the wave height is less than about 4m.

5. CONCLUSION

The mechanism of wave-induced liquefaction in permeable seabed is discussed in terms of excess pore pressure which is an important parameter in considering the liquefaction problems. It is shown that the excess pore pressure is defined as the difference between the wave-associated pressure on the seabed surface and the wave-associated oscillatory pore pressure in the seabed. The liquefaction potential can be estimated by comparing the wave-induced oscillatory excess pore pressure with the initial vertical effective stress during calm sea. According to the criteria, the liquefaction occurs in the seabed where the oscillatory excess pore pressure becomes greater than the initial vertical effective stress during calm sea.

A procedure to estimate the wave-induced liquefaction in permeable seabed is presented to apply to practical problems. By means of a case study, it is demonstrated that the liquefaction of seabed ~~is~~ easily occurs and is very critical against the slope stability. ~~The proposed procedure is extended to prepare a liquefied area map in coastal zone which may be utilized for the evaluation of liquefaction in the planning, construction and maintenance of offshore structures.~~ The liquefaction should be appropriately taken into account in design of offshore structures on permeable seabed.

REFERENCES

Bjerrum, L.(1973):"Geotechnical Problem Involved in Foundations of Structures in the North Sea", Geotechnique, Vol.23, No.3, pp.319-358.

Henkel, D.J.(1970):"The Role of Waves in Causing Submarine Landslides", Geotechnique, Vol.20, No.1, pp.75-80.

Tsuruya, K. and Korezumi, T.(1990): "Liquefaction and Resuspension of Sands in a Surf Zone", Proceedings of the Coastal Engineering, JSCE, pp.289-293 (in Japanese).

Zen, K., Umehara, Y. and Finn, W.D.L.(1986a): "A Case Study of the Wave-induced Liquefaction of Sand Layers under the Damaged Breakwater", Proceedings of the 3rd Canadian Conference on Marine Geotechnical Engineering, Vol.2, pp.505-520.

Zen, K., Yamazaki, H. and Watanabe, A.(1987):"Wave-induced Liquefaction and Densification in Seabed", Report of the Port and Harbour Research Institute, Vol.26, No.4, pp.125-180 (in Japanese).

Zen, K. and Yamazaki, H.(1990a): "Mechanism of Wave-induced Liquefaction and Densification in Seabed", Soils and Foundations, Vol.30, No.4, pp.90-104.

Zen, K. and Yamazaki, H.(1990b): "Oscillatory Pore Pressures and Liquefaction in Seabed Induced by Ocean Waves", Soils and Foundations, Vol.30, No.4, pp.147-161.

Zen, K. and Yamazaki, H.(1991): "Field Observation and Analysis of Wave-induced Liquefaction in Seabed", Soils and Foundations, Vol.31, No.4, pp.161-179.

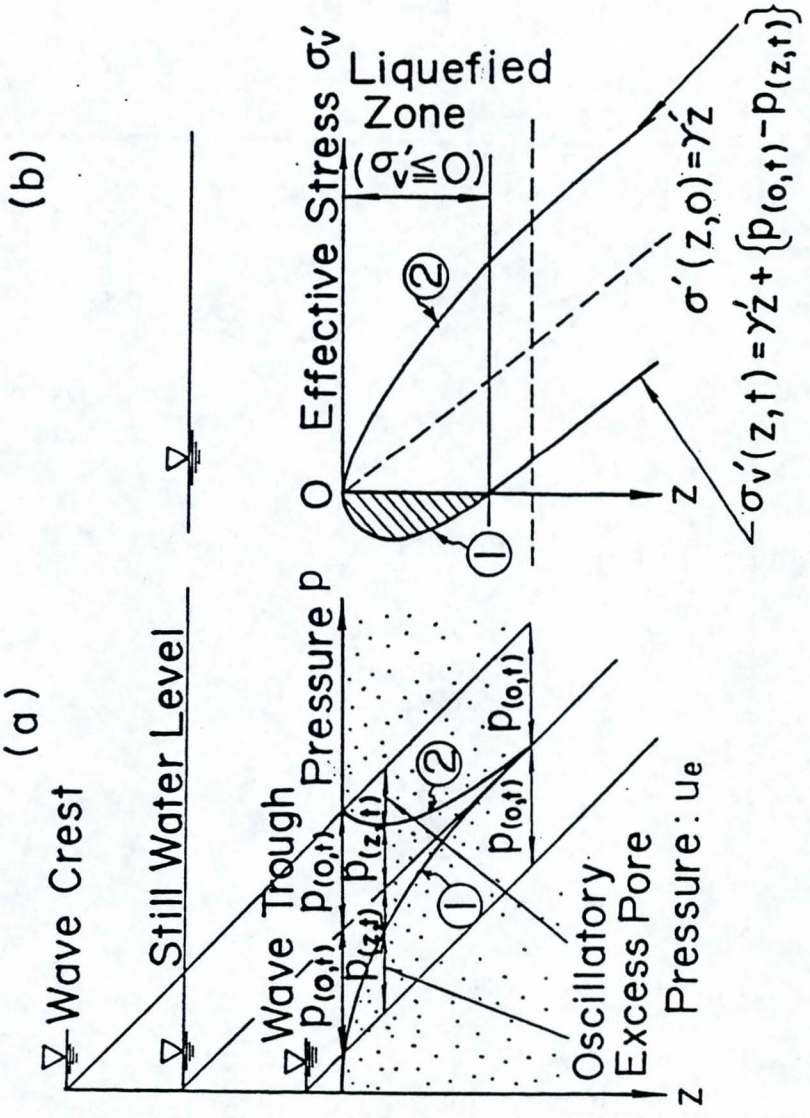

Fig.1 Concept of wave-induced liquefaction and densification; a)Oscillatory excess pore pressure, (b)Effective vertical stress

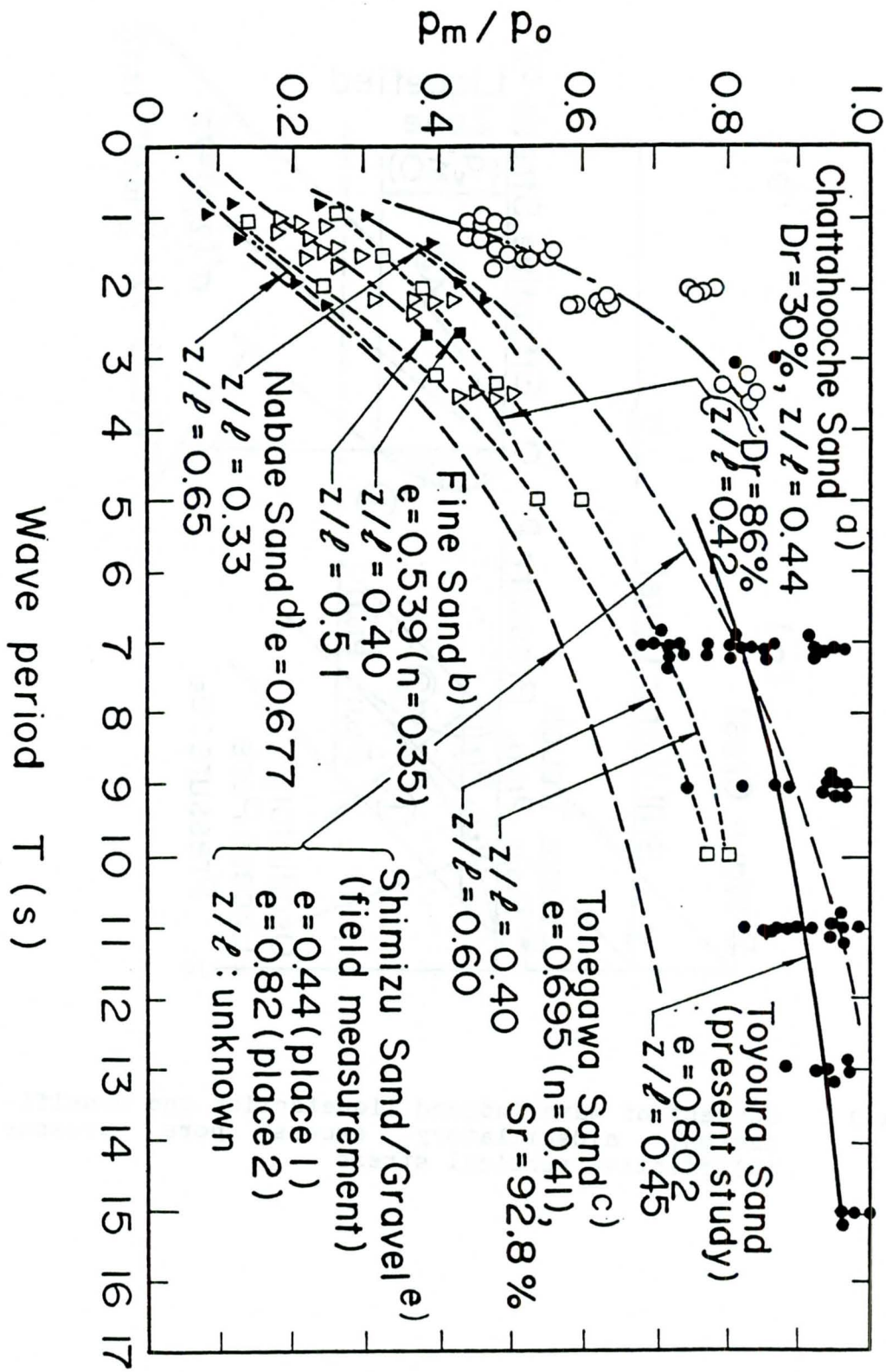

Fig.2 Pressure ratio against wave period

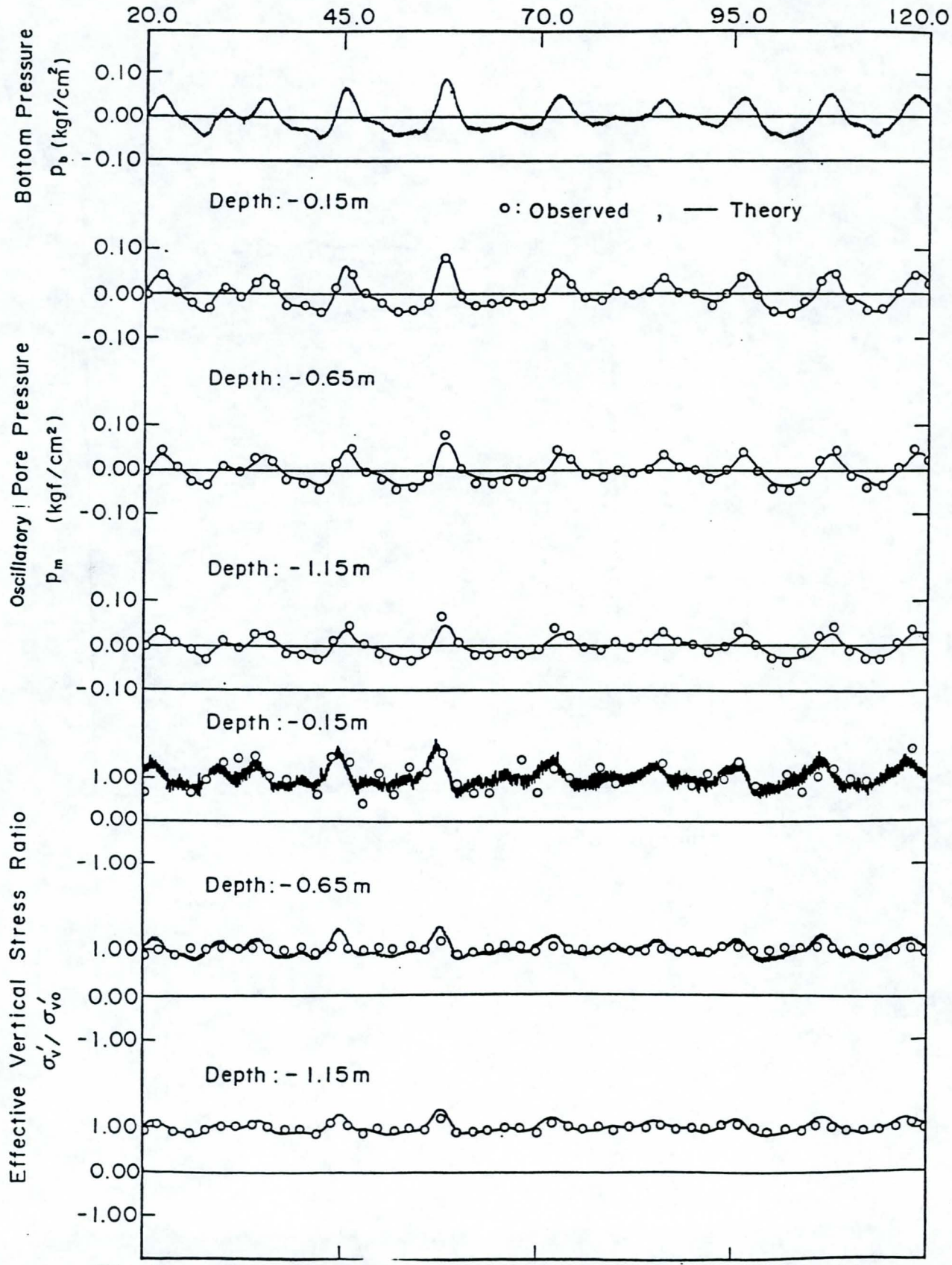

Fig.3 Comparison of oscillatory pore pressure and effective stress variation between theory and observation

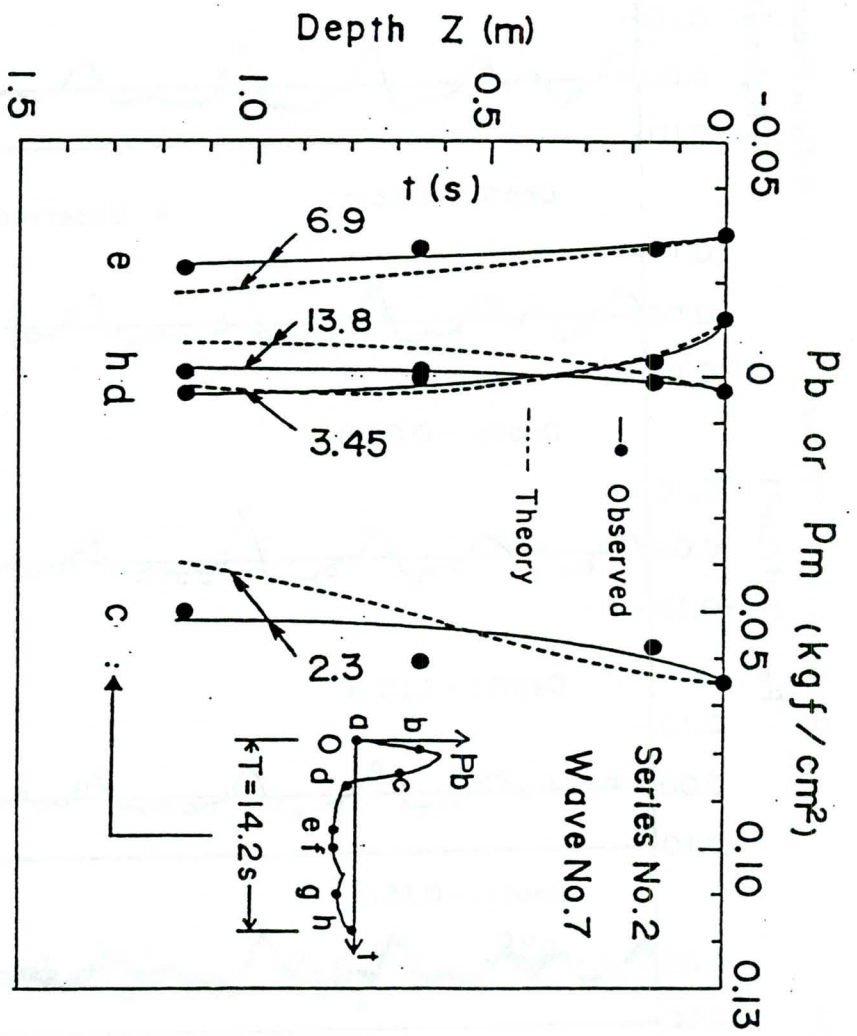

Fig.4 Distribution of oscillatory pore pressure

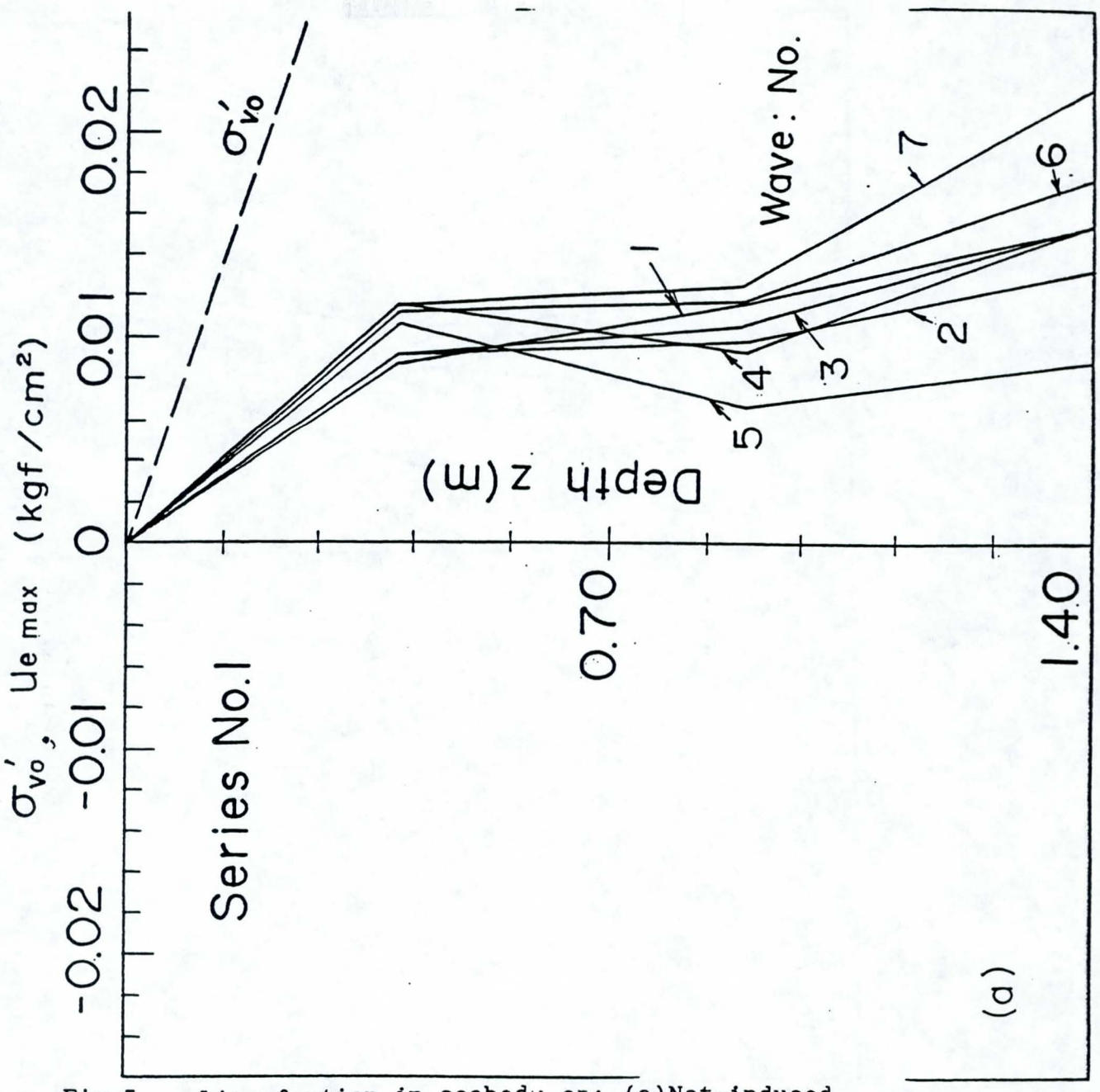

Fig.5 Liquefaction in seabed : (a)Not-induced, (b)Induced

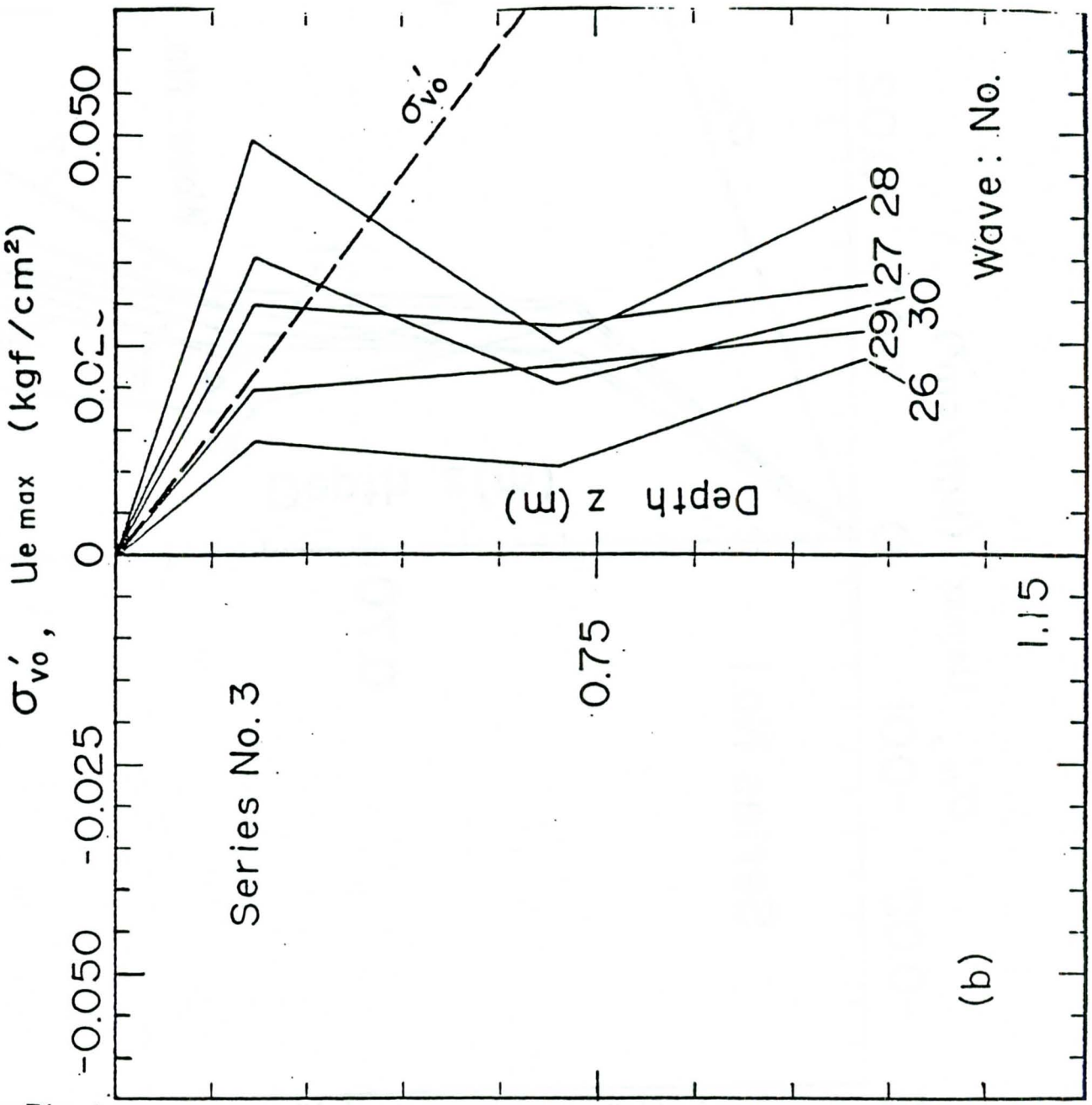

Fig.6 Liquefaction due to seepage flow

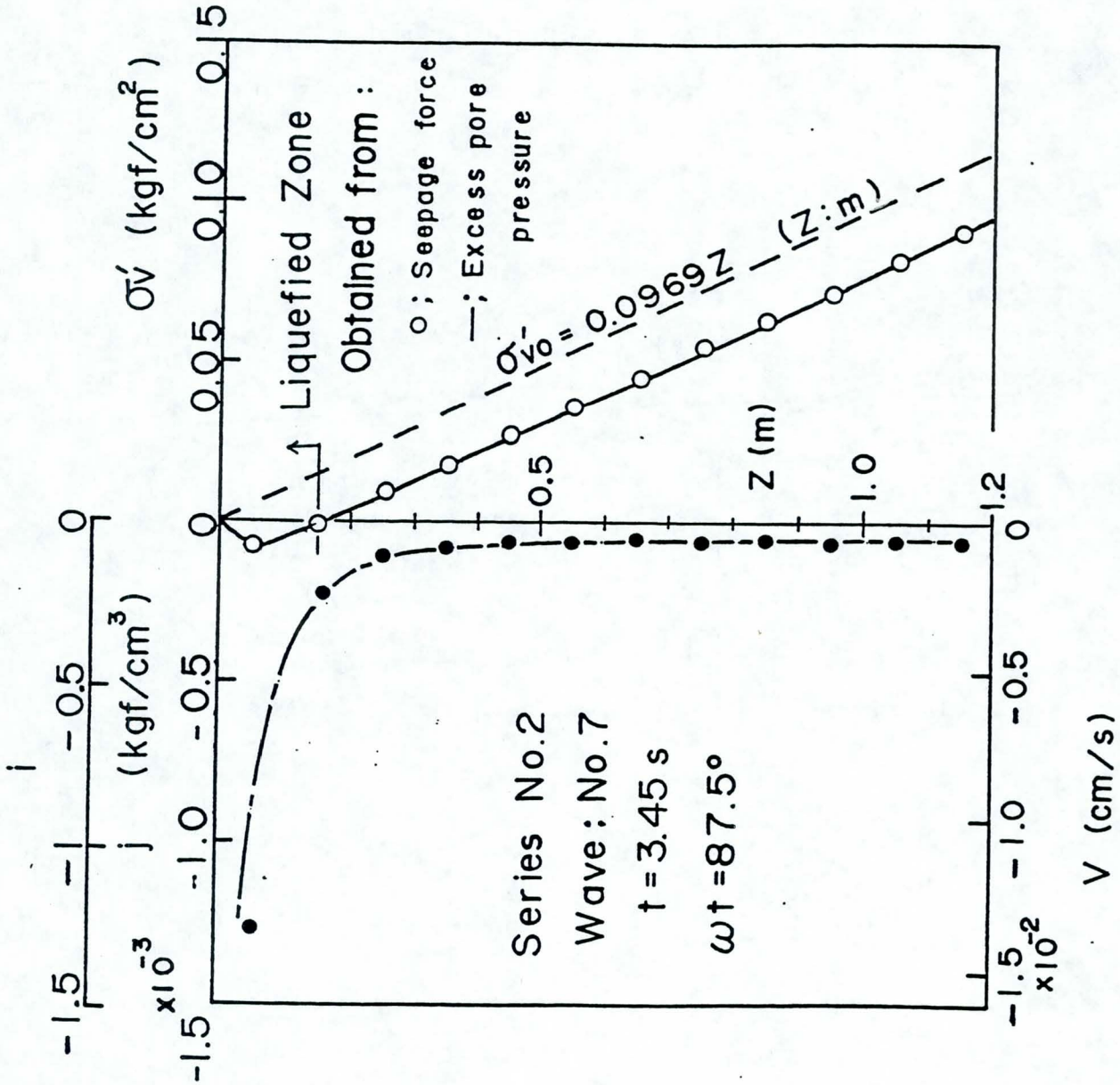

Fig.7 Two types of liquefaction

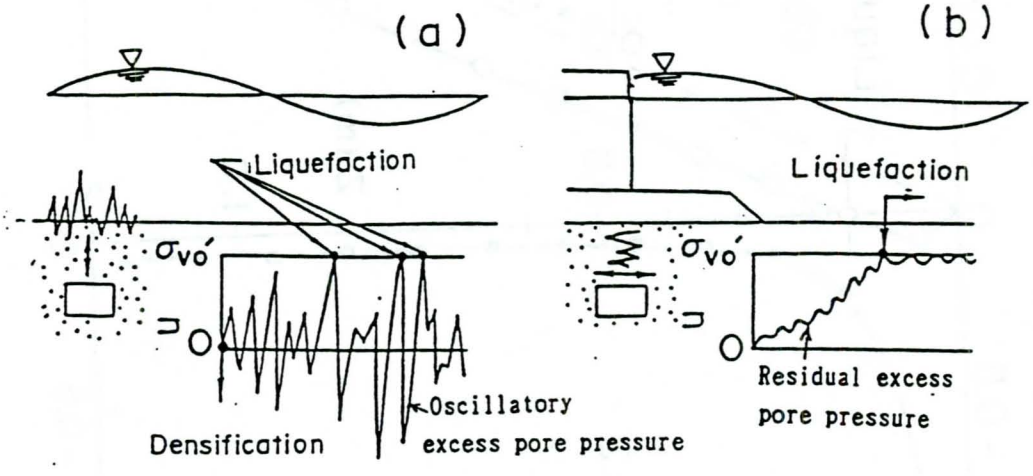

Fig.8a Flow chart

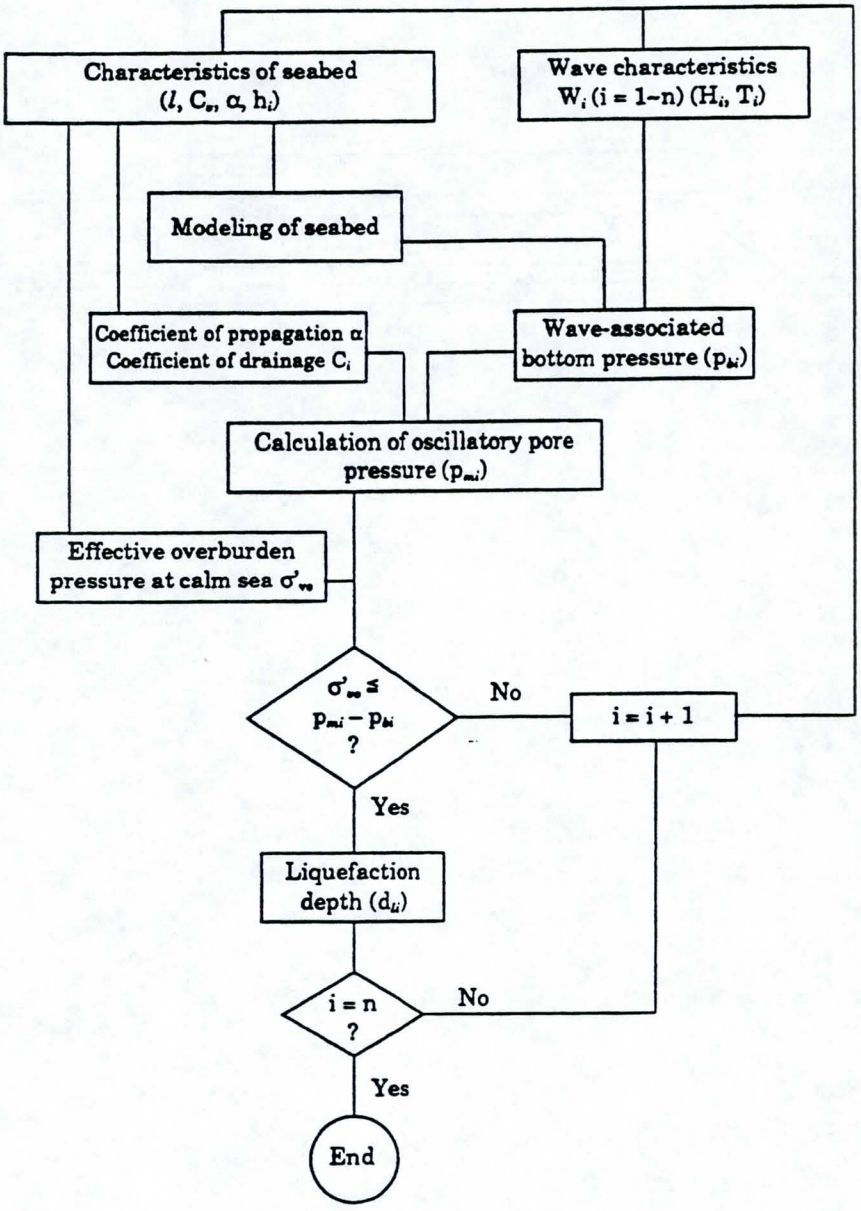

Fig. 8b Flow chart

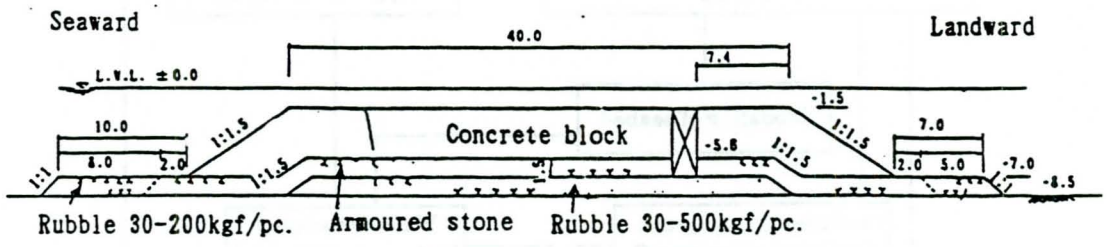

Fig.9 Detached breakwater

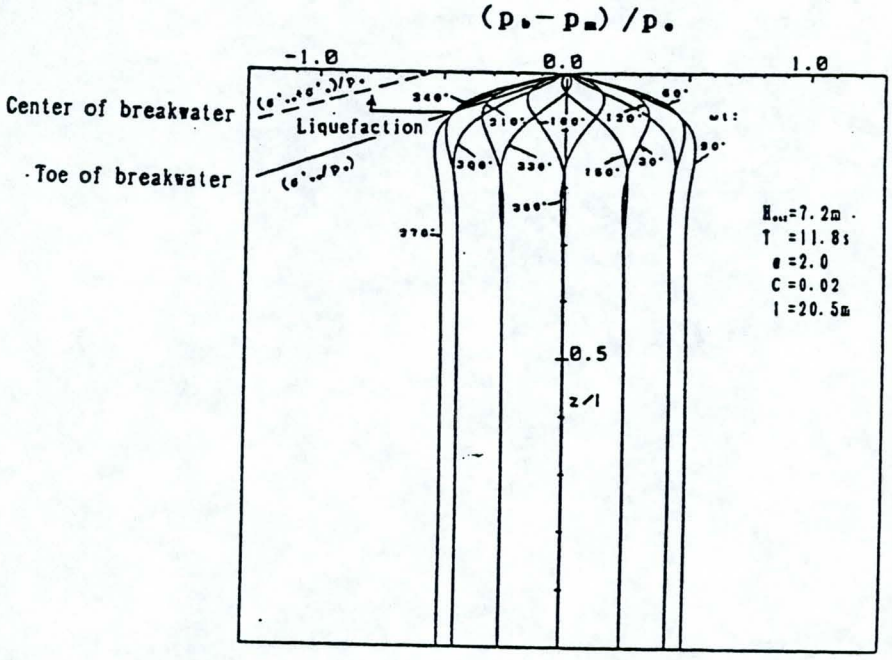

Fig.10 Effective stress variation and liquefaction

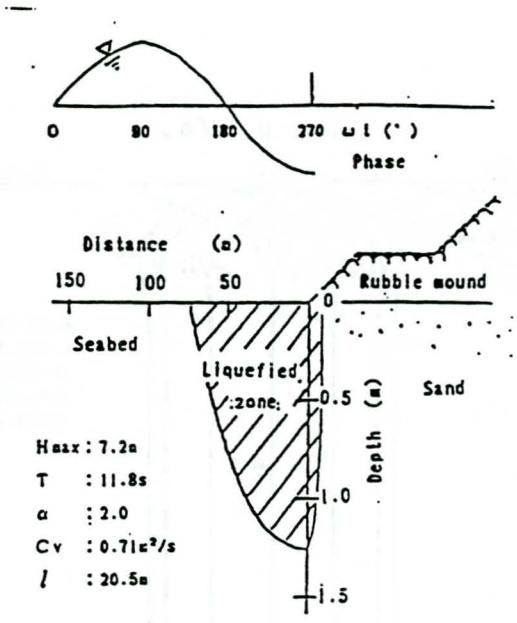

Fig.11 Liquefied zone

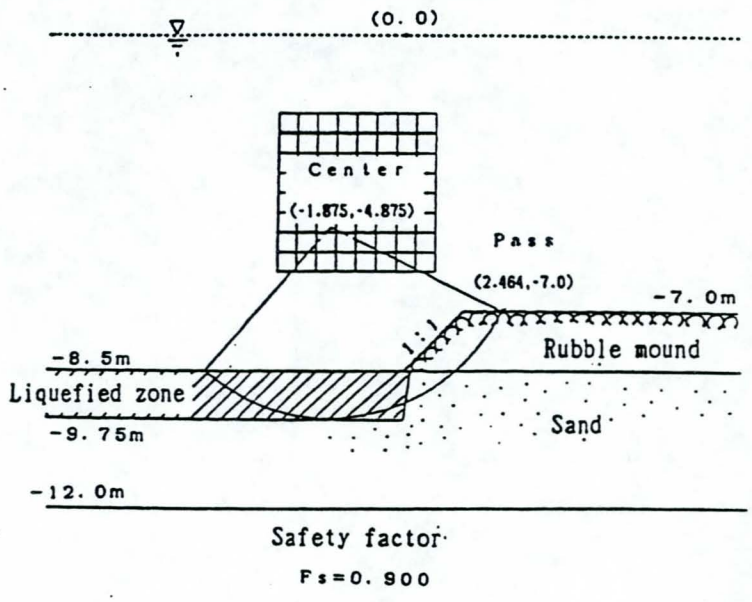

Fig.12 Circular failure

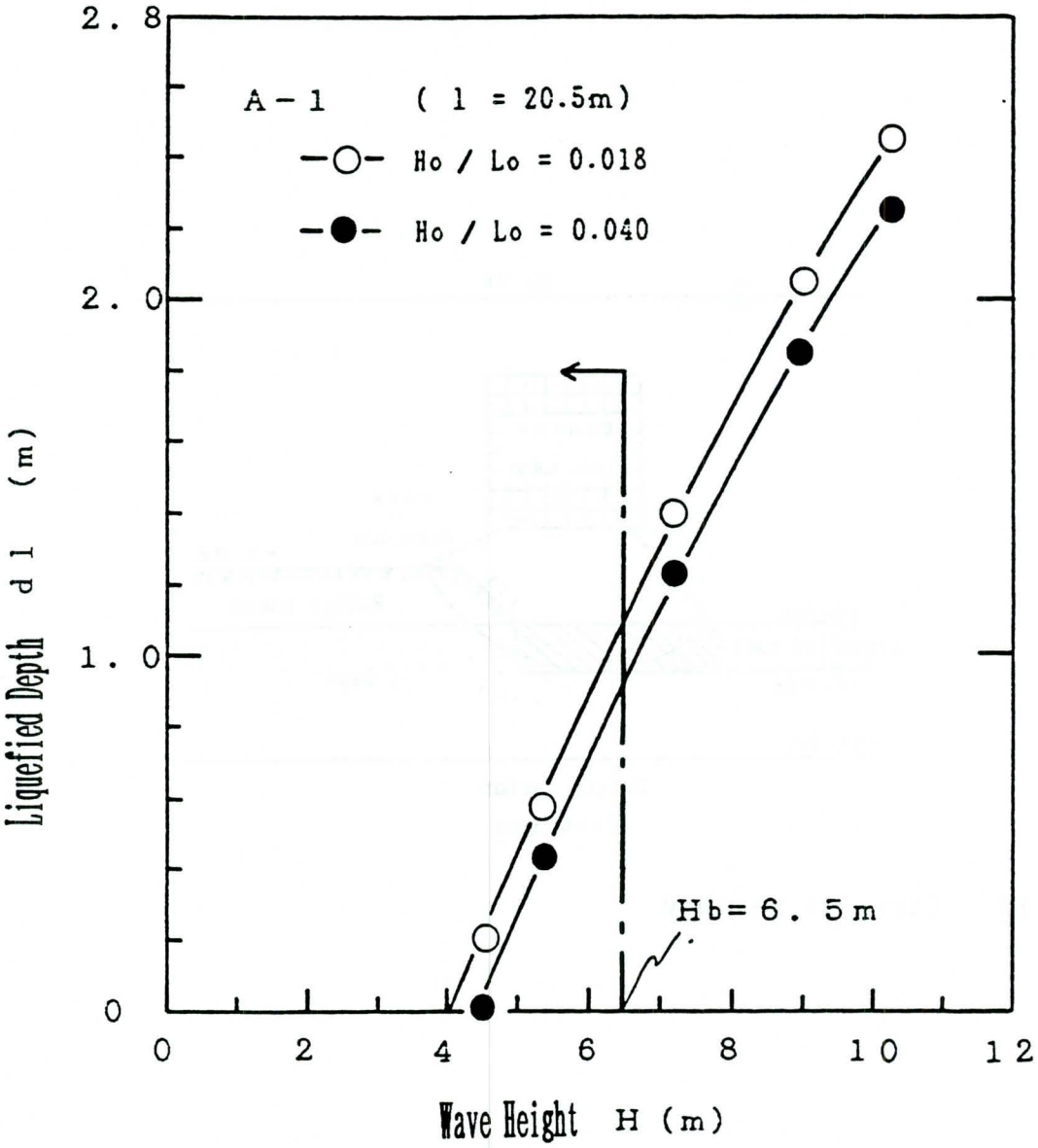

Fig.13 Relationship between liquefied depth and wave height

Submerged unit weight	γ' (gf/cm³)	0.969
Coefficient of permeability	k (cm/s)	1.12×10^{-2}
Coefficient of volume compressibility	m_v (cm²/kgf)	1.56×10^{-3}
Coefficient of consolidation	C_v (cm²/s)	7.18×10^{3}
Degree of saturation	S_r (%)	99.45
Thickness of permeable layer	l (cm)	230
Coefficient of propagation	α	2.0

* 1 kgf/cm² = 98 kN/m², 1 gf/cm³ = 9.8 kN/m³

LIST OF TABLE

Table 1 Input data for analysis

DESIGN OF A RIPRAP STILLING BASIN FOR OVERHANGING PIPE

M. Shafai-Bajestan
Shahid-Chamran University, Ahwaz, Iran
M.L. Alberston
CSU, Dept. of Civil Engineering, Fort Collins, USA

Abstract

In this paper the criteria for designing of a simple and economic dissipator structure, a riprap stilling basin, which could be used below an overhanging pipe are presented. These are: riprap size, riprap thickness, riprap gradation, required gravel filter and the basin dimensions. A numerical example to illustrate the design methodology also is presented.

Introduction

Overhanging pipe refers to a situation where the tailwater into which the pipe discharges is below the inverted of the pipe. Under these situation the pipe discharges occurs as a free Jet. For the case of unprotected pipe outlets the removal of alluvial material from the base through the action of high local velocity produces a hole which may eventually cause extensive damage to the surrounding area.

The stone basin is the most common and economical method of handling the problem at pipe outlet. The advantage of the method is speed of construction absence of the need for skilled labour, and utilization of inexpensive local deposits of stone.

The most important step for designing the stone basin is to determine the riprap criteria including: 1) Proper stone size large enough to withstand under the action of the Jet and small enough from economic point of view. 2) Proper size distribution (gradation), 3) Proper thickness layer and 4) Proper filter beneath the stone layer. Development of such criteria, is the main purpose of this paper.

To accompolish these goals, first starting from the basic

principles, and with a knowledge of previous studies, a general relationship describing the incipient motion of the bed material downstream of a circular Jet in general and below a pipe outlet in particular were developed. Then to supply the neccessary coefficient, of this general relationship and to clarify the riprap criteria, a series of experimental tests were performed and conducted in the Hydraulic laboratory of the Engineering Research Center of Colorado state University. For visual observation of sediment movement the haff + Jet technique was used. This technique also allows to conduct a large number of tests in a relatively short period of time. The experimental set-up, procedures and the criteria for threshold conditions can be see in detail in refernce No.[2]. In this paper, the resuts of the experimental tests for the design of stone bas in will be presented.

Summary of Experimental Program

The experimental facilities utilized through this study consisted of a basin 8 ft(2.44m) in length, 4ft.(1.22m) in width and 5ft(1.52m) in height. For visual observation the basin wall on the side of pipe was made of plexi-glass. The overhanging pipes 2 inches(5.08 Cm) & 4 inches(10.16 Cm) were placed at three different elevation 48 inches (1.22 m), 24 inches(0.61 m), and 16 inches (0.41 m) from the stone surface. Four different sizes of uniform riprap material and three different sizes of graded riprap material were used. The riprap layer varies from $1D_{100}$ to $3D_{100}$ and five series of tests were made to study the filter criteria used beneath the riprap layer. The flow dicharge were selected on the basis of the value of the stability number. The stability number was defined as: $\frac{v}{\sqrt{g(G_s-1)D_{50}}}$.

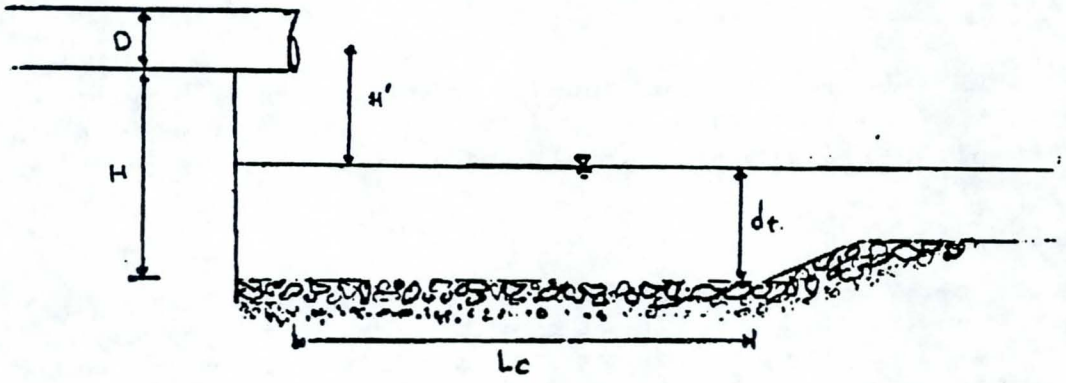

The range of non dimensional parameters in this study are as follows:

Parameter	Definition	Values
Stability Number	$\frac{v}{\sqrt{g(G_s-1)D_{50}}}$	1-12

Dicharge Intensity	$\frac{Q}{D^2\sqrt{gD}}$	0.4-5.7
Relative height	H/D	4-24
Standard deviation of riprap material	$\sigma=\sqrt{\frac{D_{84}}{D_{16}}}$	1.2-3.0

Combination of the foregoing ratios led to 146 separate tests. At the beginingof each test the tailwater level gradually was lowered from high level to where the riprap layer removed. During each test when the first movement of the bed material, the first movement of the riprap material, and the general movement of the riprap layer was observed, the tailwater level was recorded.

Path of the Jet in the Water

The experimental observation made clear that once the Jet enters the water in the basis, the Jet tended to follow a straight line inclined fromwater surface to the rock surface. The inclination angle β is called peneration anlge. The distance from the water surface to the rock surface, along the Jet centerline, is called penetration length P_e. The theoretical and experimental results showed that these values can be obtained from the following equations:

$$\beta = \cos^{-1}\left(\frac{v}{v_p}\right) \qquad (1)$$

$$P_e = \frac{d_t}{\sin(\beta)} \qquad (2)$$

in which v is the exit pipe velocity and v_p is the velocity of Jet at the water surface which is equal to $(2gH'+v^2)^{1/2}$ in which H' is the vertical distance from the center of pipe to the tailwater surface.

Design of rock size

To obtaine a relationship for the purpose of sizing riprap at pipe outlet, a rock particle was considered attacked by hydrodynamic forces. The hydrodynamic forces was determined based on the concept of Jet diffusion (Albertson et al 1950). Therefore a general relationship in the following form was developed:(for detail see [2]).

$$\frac{v}{[g(G_s-1)D_s]^{1/2}} = C_u\left(\frac{P_e}{D}\right) \qquad (3)$$

To obtained the value of Cu, the experimental data were used and the stability number were plotted versus $\frac{P_e}{D}$. The value of P_e were calculated using the tailwater at incipient motion and also the tailwater

at incipient failure. For the incipient motion, it was found that when D_{30} of the rock material is used in calculation of stability number, data from both uniform and graded riprap material are more closer, on the other hand for the case of incipient failure, the D_{90} of the rock material should be applied in the calculation of the stability number. The criteria for sizing riprap are as follow:

For incipient motion:

$$\frac{v}{[g(G_s-1)D_{30}]^{1/2}} = 0.382\left(\frac{y_e}{D}\right) \qquad r^2=0.91 \qquad (4)$$

For incipient failure:

$$\frac{v}{[g(G_s-1)D_{90}]^{1/2}} = 0.422\left(\frac{y_e}{D}\right) \qquad r^2=0.88 \qquad (5)$$

these equations are valid when $\frac{y_e}{D} > 3.3$

Riprap thickness

A total of 13 tests were conducted to determine the effect of blanket thickness on stone stability. The main conclusion from the tests were that thickness has no effect on movement of the stone, however, when the riprap size distribution is uniform and no gravel filter is used the minimum thickness of riprap blanket should be $3D_{100}$. For thickness of less than $3D_{100}$, leaching of the bed material occurs, which causes failure of blanket. For graded riprap and when filter is used, the thickness of $1D_{100}$ was found to be adequate.

Gravel filter

To prevent the fine material beneath the riprap blanket from whashing out through the interstices between particles, it is often necessary to place some type of filter, synthetic or gravel filter. The gravel filter is the most common filter uses with riprap.

The size distribution of the gravel filter depends on the size distribution of the bed and riprap materials. For riprap in open channel the criteria proposed by the Corps of Engineers(1970)is used. To investigate the applicability of those criteria, five series of tests, were conducted. The results and the general observations from the tests conducted showed that those criteria are not adequate for use with riprap below a pipe outlet because of the impact of the Jet. It was found that the size distribution of the filter, D_{85}, should be closer to the size D_{15} of riprap. Therefore the following criteria is reccommended:

more restrictive than Corp regmts

$$D_{15}(\text{riprap})/D_{85}(\text{filter})<2 \qquad (6)$$

$$D_{15}(\text{filter})/D_{85}(\text{bed material})<2.5 \qquad (7)$$

If the size distribution of the riprap material is relatively large

compare to the bed material, more than one layer of filter should be placed. The thickness of filter should be one-half of the riprap layer.

Length of the basin

The basin length should be at least $\frac{3}{2} L_c$, in which L_c is the horizental distance from the end of pipe to the Place where the Jet strike the riprap surface. This length can be obtained by combining the free Jet path and the penetration length, which gives the following equation:

$$L_c = v\left(\frac{2H'}{g}\right)^{1/2} + P_e \cos\beta \qquad (8)$$

In which v is the pipe exit velocity, H' is the vertical distance from the center of pipe to the tailwater surface and d_t is the tailwater depth.

Plunge pool

The theoretical and experimental study clearly indicated that the tailwater has a greate affect in the require riprap size. Therefore it is advise that the rock basin be depressed below the original bed level of the downstream channel. Formation of such a plunge pool is needed if the available riprap material are small or the exit velocity is relatively high.

Numerical example

To illustrate the use of methodology presented in this paper, a numerical example on the design of a riprap stilling basin will be provided. Consider a horizontal pipe, 0.5 diameter, spillway flowing water into an alluvial channel. The center of pipe is 4.5 meter above the channel bed. The channel bed consist of fine sand to medium gravel with D_{50}=3.0 mm and D_{85}=8 mm. The estimated peak dicharge through the pipe is 0.5 m^3/sec which produces a normal depth of 1.5 meter at the channel downstream.

Design First using the information given calculate the hydraulic parameters which gives exit velocity v=2.5 m/sec, H'=3.0 m, velocity at the tailwater surface, v_p=8.07 m/sec, penetration angle, Eq.(1), $\beta = 7.95^0$, penetration length Eq.(2), P_e= 1.5/Sin 71.95=1.58 m, and the stability number at incipient motion is, Eq.(4), $SND_{30} = 0.342\left(\frac{1.58}{0.5}\right) = 1.21$

Then determine the D_{30} of riprap wich is required, from:

$\frac{v}{\sqrt{g(G_s-1)D_{30}}} = 1.21$ for g=9.81 m/sec^2 and G_s=2.65 this gives D_{30}=0.26m.

If the riprap for this size is not available then it is advisable to provide a plunge pool at pipe outlet. For example excavate a plunge pool 0.5 meter deep (below channel bed), then the penetration length will be $p_e = \frac{1.5+0.5}{\text{Sin } 71.95} = 2.10$ and the critical stability number SND_{30}

will be: $SND_{30} = SND_{30} = 0.382(\frac{2.10}{0.5}) = 1.61$ and from $\frac{v}{\sqrt{g(G_s-1)D_{30}}} = 1.61$ the D_{30} will be equal to 0.15 m. By increasiy the plunge pool deeper, the smaller D_{30} will be required. Graded material with D_{30} equal to 0.15m should be placed. Assume the available riprap material has D_{15}=80 mm, D_{50}=0.25 m and D_{85}=0.45 m. Determine the filter size distribution to be used.

First the need for gravel filter should be checked using Eq.(6) & Eq.(7):

$$\frac{D_{15}(\text{riprap})}{D_{85}(\text{bed material})} = \frac{60}{8} = 15$$

Which is greater than 2, thus layer of gravel filter should be placed prior to riprap placement. The D_{15} and D_{85} of the filter can be obtained from Eq.(6) & Eq.(7): From Eq.(6), D_{85}(filter)>30 mm and from Eq.(7), D_{15}(filter)<20 mm.

References

1. Alberston, M.L., Dai, Y.B., Jensen, R.A., and Rouse, H.(1950). *"Diffusion of submerged Jets."* Transaction, SDCE, Vol. 115, pp. 637-697.

2. Sahfai-Bajestan, M. and M.L. Alberston. *"Riprap criteria at pipe outlet."* Journal of Hydraulic Engineering, ASCE, Vol. 119, No. 2

3. U.S. Army Engineering(1970). *"Stone stability-velocity versus stone diameter."* Sheet 712-1, Civil works Investigations, Hydraulic design criteria, Water-ways Experiment Station, vicksburg, Miss.

Notations

C_u=coefficient

D =pipe diameter

D_{15}, D_{30}, D_{50}, D_{85}, D_{90}, D_{100}=particle size of which 15%, 30%, 50%, 85%, 90%, and 100%, respectively, is finer by weight.

d_t=tailwater depth(flow depth in basin)

G_s=specific gravity of riprap material

g =accelaration of gravity

H'=vertical distance from the center of pipe to the basin water surface

H =vertical distance from the pipe to the bed surface

L_c=the horizontal distance from the pipe to the center of the ecour hole

DETERIORATION OF CARBONATE BREAKWATER STONES ON LAKE MICHIGAN SHORELINE

K.R. Stank and M.M. Baig
Army Corps of Engineers, Geotechnical and Coastal Branch,
Chigaco District, USA

The U.S. Army Corps of Engineers has been inspecting and providing maintenance of breakwaters along the southern Lake Michigan shoreline since the late 19th century. During the last 100 years significant changes have been made in breakwater structure designs and construction materials. Rubble mound breakwater commonly in use today allow for reduced construction costs through quick placement of low cost locally produced materials. However, maintenance costs have increased due to rapid deterioration of the materials. In some cases the entire structures were required to be rehabilitated after only 10 years. The alternative is to use higher cost materials and tighten the QA and QC criteria.

Lake Michigan is located on the western flank of the Michigan Basin. Silurian aged rocks subcrop beneath glacial sediments on the west side of Lake Michigan, gently dipping 10-15° east into the Michigan Basin. Some of these rocks, such as dolomite have been utilized in breakwater construction.

During the early part of the 20th century the large expansion of the steel industry created a need for sources of steel flux. the subcrops of Silurian aged carbonate rocks (dolomite) provided excellent flux material to the steel industry. As a result the economics eventually shifted, favoring purchase of less expensive dolomite stone for breakwaters. Dolomite quarries are now providing the bulk of material being used to rehabilitate old breakwaters utilizing rubble mound designs, and to build new rubble mound structures.

The selection of breakwater stone sources is driven by two factors; cost and supply. A number of problems have been encountered with the use of Silurian dolomite stone because of premature deterioration caused by brittle behavior, and thin interbedded laminations. Delamination, cracking and disintegration have been observed in dolomite stones after only 3 years of service. The quarry operators generally do not have adequate quality control measures to exclude such stones from delivery. It is also difficult to convince quarry operators to perform adequate quality control, in the absence of having a clear definition of unsuitable stones. Laboratory durability tests are costly and limited and therefore do not give a statistically accurate picture of durability from a particular source as a whole. There are sources of highly durable stone, but high cost and an inadequate supply have prevented these sources from being utilized.

Premature stone deterioration has created a maintenance problem for those areas where highly durable stone cannot compete with less durable locally produced stone. Accurate maintenance costs are being developed to evaluate the economic feasibility of using more expensive materials. If expensive materials are not warranted, the design life of the rubble mound structures should be reduced to 10 years. New breakwater designs specifying durable materials in the freeze thaw environment and less durable materials below the water line, may provide an alternative solution to this problem.